

Some pages of this thesis may have been removed for copyright restrictions.

If you have discovered material in AURA which is unlawful e.g. breaches copyright, (either yours or that of a third party) or any other law, including but not limited to those relating to patent, trademark, confidentiality, data protection, obscenity, defamation, libel, then please read our [Takedown Policy](#) and [contact the service](#) immediately

THE UNIVERSITY OF ASTON IN BIRMINGHAM

THE ANTIOXIDANT ROLE OF VITAMIN E IN POLYOLEFINS

SYLVIE ISSENHUTH

Doctor of Philosophy

May 1996

Polymers are subject to oxidation throughout their lifecycle. Antioxidants are generally incorporated in polymers to inhibit or minimise oxidative degradation. Hindered phenolic antioxidants are important stabilisers for polyolefins. However, hindered phenols undergo chemical transformations while performing their antioxidant function during processing and fabrication. In addition, antioxidants are subject to loss from polymers during processing, or subsequently in-service. Migration of antioxidants is a major concern in applications involving polymers in direct contact with food and human environment. This concern is compounded by the realisation that very little is known about the nature and the migration behaviour of antioxidant transformation products. In this work, the antioxidant role of the biological antioxidant α -tocopherol (Vitamin E), which is structurally similar to many synthetic hindered phenols, is investigated in low density polyethylene (LDPE) and polypropylene (PP).

The melt stabilising effectiveness of α -tocopherol (Toc) was found to be very high, higher than that of commercial hindered phenol antioxidants, such as Irganox 1076 (Irg 1076) and Irganox 1010 (Irg 1010), after multiple extrusions, especially at very low concentrations. The high antioxidant activity of Toc was shown to be due, at least in part, to the formation of transformation products during processing. The main products formed are stereoisomers of dimers and trimers, as well as aldehydes and a quinone, the relative concentration of each was shown to depend on the processing severity, the initial antioxidant concentration and oxygen availability. These transformation products were shown to impart better, similar or lower melt stability to the polymer than the parent antioxidant. The nature of the products formed from Toc during processing was compared with those formed during processing of Irg 1076 and Irg 1010 with LDPE and a mechanism for the melt stabilisation of Toc was proposed and compared with the stabilisation mechanisms of the synthetic antioxidants Irg 1076 and Irg 1010. The antioxidant role of Toc as a long-term stabiliser was studied by subjecting the polymer to accelerated thermal and UV ageing tests. Toc was shown to be a good thermal stabiliser at temperatures below 120°C, but like other hindered phenols, Toc offered limited UV stability to the polymer, due to its rapid loss from the polymer during UV irradiation. The mechanism of stabilisation of Toc during thermal ageing in PP was shown to be similar to that observed during processing. However, the formation of coloured transformation products during processing of Toc with LDPE and PP lead to discolouration of the polymer. This could be prevented by adding a hindered aromatic phosphite, Ultrinox 626, during processing, as a consequence of the antioxidant activity of the phosphite.

Migration characteristics of Toc from LDPE films into various food simulants were investigated and compared with those of Irg 1076. It was shown that the extent of migration of Toc and its transformation products was highest in fatty food simulants (e.g. olive oil) and similar to commercial hindered phenols. Therefore the use of the non-toxic Toc has a clear advantage over commercial antioxidants.

KEY WORDS: Tocopherol, Oxidation, Polymer, Degradation, Stabiliser

**PAGE
MISSING
IN
ORIGINAL**

Acknowledgements

I am deeply grateful to S. Al-Malaika for her supervision throughout my research work and for all the help and useful advice she offered.

I wish to thank Hoffmann-La Roche (Basel, Switzerland, and New Jersey, USA) for their financial support and for supplying samples of α -tocopherol and derivatives, as well as polymer samples. I am very grateful to M. Gmünder (Hoffmann-La Roche, Basel) for the useful discussions and help in running MS spectra.

I am also very thankful to M. Perry for his help and advice with the NMR spectra. I would like to thank A. Leaf for his contribution on the migration work, as part of his final year Degree project. I am grateful to L. Castle from the UK Ministry of Agriculture, Food and Fisheries (MAFF) for his help in running MS spectra. I also wish to thank Ciba-Geigy (Switzerland) and BP (UK) for samples of Irganox (1076 and 1010) and polyethylene, respectively. I am grateful to T. Henman (Cambridge Polymer Consultants) for supplying polymer samples (CPC789 series).

I would like to thank all the research and technical staff in the Department of Chemical Engineering and Applied Chemistry for their help and support throughout my work.

LIST OF CONTENTS

<u>Subject</u>	<u>Page</u>
THESIS TITLE	1
SUMMARY	2
ACKNOWLEDGEMENTS	3
LIST OF CONTENTS	4
LIST OF SCHEMES	14
LIST OF TABLES	16
LIST OF FIGURES	24
ABBREVIATIONS	34
<u>CHAPTER ONE</u>	
INTRODUCTION	
1.1 GENERAL INTRODUCTION	35
1.2 DEGRADATION OF POLYOLEFINS	35
1.2.1 General overview	35
1.2.2 Thermal oxidative degradation	36
1.2.3 Photooxidative degradation	41
1.3 STABILISATION OF POLYOLEFINS	45
1.3.1 General mechanisms of antioxidant action	45
1.3.1.1 Autoxidation and antioxidant classification	45
1.3.1.2 The chain-breaking mechanism	46
1.3.1.3 Photostabilisation	48
1.3.2 Hindered phenols as antioxidants	49
1.3.2.1 Structure and antioxidant activity of hindered phenols	49
1.3.2.2 Transformation products of hindered phenols	51
1.3.3 Synergistic effects of hindered aromatic phosphites	56
1.3.3.1 General mechanisms of antioxidant action of organic phosphites	56
1.3.3.2 Synergistic effects of organic phosphites with hindered phenols	58
1.3.3.3 Mechanisms of colour stabilisation of polymers by organic phosphites	58
1.3.4 Ecological acceptability of phenolic antioxidants	60

1.4	VITAMIN E AS A CHAIN-BREAKING ANTIOXIDANT	62
1.4.1	Structure and antioxidant activity of α-tocopherol	62
1.4.2	Nature of oxidation products and mechanism of oxidation of Vitamin E in model system	65
1.4.3	Stabilising effect of α-tocopherol in polymers	75
1.4.3.1	Stabilising activity	75
1.4.3.2	Effect of organic phosphites on the melt stability and colour of polyolefins stabilised with Toc	76
1.4.3.3	Importance of transformation products of Toc in polymers	77
1.5	OBJECTIVES OF THE PRESENT WORK	78

CHAPTER TWO
EXPERIMENTAL

2.1	MATERIALS	80
2.2	OXIDATION OF TOC IN MODEL SYSTEMS AND SYNTHESIS OF TOC DERIVATIVES	84
2.2.1	Oxidation of Toc with lead dioxide	84
2.2.1.1	Reaction procedure and isolation of products	84
2.2.1.2	Analysis of products	84
2.2.2	Purification and isolation of oxidation products of Toc with PbO₂	89
2.2.2.1	Purification of TRI A, B, C and SPD, D by column chromatography	89
2.2.2.2	Further separation of TRI A, B, C and purification of SPD, D by NP-HPLC	92
2.2.2.3	Isolation of DHD, E, ALD 1 and Toc	92
2.2.3	Preparation of DHD of Toc	93
2.2.3.1	Reaction procedure and isolation of products	93
2.2.3.2	Analysis and purification of the DHD product	94
2.2.4	Characterisation of oxidation products of Toc	96
2.2.4.1	Characterisation of synthesised and purified dimers and trimers of Toc	96
2.2.4.2	Characterisation of isolated products	96
2.3	POLYMER COMPOUNDING	98
2.3.1	Multiple extrusion of polymer samples	98
2.3.2	Processing of polymer samples in an internal mixer	99
2.3.3	Film preparation	101

2.4	STABILISING ACTIVITY TESTS	101
2.4.1	Measurement of Melt Flow Index (MFI)	101
2.4.2	Thermal ageing of polymer films	102
2.4.3	Ultraviolet irradiation of polymer films	103
2.5	MEASUREMENT OF TIME TO BRITTLE FRACTURE OF POLYMER FILMS	104
2.6	EXTRACTION OF ANTIOXIDANTS AND THEIR TRANSFORMATION PRODUCTS FROM POLYMER FILMS	105
2.6.1	General procedure	105
2.6.2	Extraction efficiency	106
2.6.3	Extent of extraction of low molecular weight polymer (LMWP)	111
2.7	ISOLATION AND CHARACTERISATION OF TOC TRANSFORMATION PRODUCTS FROM POLYMER EXTRACTS	113
2.7.1	Isolation and characterisation of products extracted from PP stabilised with 39% Toc, pass 4 (CPC789 series, single screw extruder, 270°C)	113
2.7.1.1	Isolation of products	113
2.7.1.2	Characterisation of products	113
2.7.2	Isolation and characterisation of products extracted from LDPE stabilised with 0.2% and 10% Toc, pass 4 (single screw extruder, 180°C)	115
2.7.2.1	Isolation of products	115
2.7.2.2	Characterisation of products	115
2.8	ISOLATION AND CHARACTERISATION OF IRG 1076 AND IRG 1010 TRANSFORMATION PRODUCTS FROM POLYMER EXTRACTS	117
2.8.1	Isolation and characterisation of Irg 1076 transformation products extracted from LDPE stabilised with 10% Irg 1076, pass 4 (single screw extruder, 180°C)	117
2.8.1.1	Isolation of products	117
2.8.1.2	Characterisation of products	117
2.8.2	Isolation and characterisation of Irg 1010 transformation products extracted from LDPE stabilised with 10% Irg 1010, pass 4 (single screw extruder, 180°C)	119
2.8.2.1	Isolation of products	119
2.8.2.2	Characterisation of products	120
2.9	THIN LAYER CHROMATOGRAPHIC TECHNIQUE	122

2.10	HIGH PERFORMANCE LIQUID CHROMATOGRAPHIC TECHNIQUES	122
2.10.1	Analytical High Performance Liquid Chromatography (HPLC)	122
2.10.2	Semi-preparative HPLC	123
2.11	DETERMINATION OF THE CONCENTRATIONS OF THE ANTIOXIDANTS AND THEIR OXIDATION PRODUCTS	123
2.11.1	Determination of the concentrations of Toc and its oxidation products	123
2.11.1.1	Determination of the concentrations	123
2.11.1.2	Examples	128
2.11.1.3	Errors on the concentrations	134
2.11.2	Determination of the concentrations of Irg 1076, Irg 1010 and their transformation products	136
2.12	MIGRATION CHARACTERISTICS OF TOC AND IRG 1076 FROM LDPE FILMS INTO VARIOUS FOOD SIMULANTS	139
2.12.1	General procedure	139
2.12.2	Static migration tests	140
2.12.3	Dynamic migration tests	
2.13	SPECTROSCOPIC TECHNIQUES	142
2.13.1	Ultraviolet spectroscopy	142
2.13.2	Fourier Transform Infrared (FTIR) spectroscopy	143
2.13.3	Proton, carbon-13 and phosphorous-31 nuclear magnetic resonance spectroscopy	143
2.14	MASS SPECTROMETRIC TECHNIQUES	144
2.14.1	Electron-Impact Ionisation	144
2.14.2	Fast Atom Bombardment	144
2.14.3	Gas chromatography- mass spectrometry	145
	LIST OF TABLES FOR THE CHARACTERISATION OF TOC, TOC DERIVATIVES, U-626, IRG 1076 AND IRG 1010 AND THEIR OXIDATION PRODUCTS	146
	FIGURES	181

CHAPTER THREE

STABILISATION EFFICIENCY OF TOC, TOC DERIVATIVES AND COMMERCIAL HINDERED PHENOLS IN LDPE AND PP AND EFFECT OF HINDERED ARYL PHOSPHITES ON THEIR ANTIOXIDANT ACTION

3.1	OBJECT AND METHODOLOGY	277
3.2	RESULTS	284
3.2.1	Melt stabilising efficiency of Toc and commercial hindered phenols during multiple extrusions with LDPE	284
3.2.2	Melt stabilising efficiency of Toc, Toc derivatives and commercial hindered phenols, and effect of hindered aryl phosphites, during processing with PP in an internal mixer	287
3.2.2.1	Effect of processing severity and oxygen concentration on the melt stabilising efficiency of Toc	287
3.2.2.2	Melt stabilising activity of Toc and commercial antioxidants in PP, at low concentrations	288
3.2.2.3	Melt stabilising activities of Toc derivatives	290
3.2.2.4	Effect of hindered aryl phosphites U- 626 and Irgf 168 on the stabilisation efficiency of antioxidants in PP	291
3.2.3	Thermal stabilising activity of Toc, Toc derivatives and commercial hindered phenols, and effect of hindered aryl phosphites in PP processed in an internal mixer	294
3.2.3.1	Thermal stabilising activity of Toc and commercial hindered phenols	294
3.2.3.2	Effect of initial Toc concentration	295
3.2.3.3	Thermal stabilising activity of Toc derivatives	296
3.2.3.4	Effect of hindered aryl phosphites on the stabilising activity of Toc, Toc derivatives and Irg 1010	297
3.2.4	UV stabilising efficiency Toc, Toc derivatives and commercial hindered phenols, in PP processed in an internal mixer	299
3.2.4.1	UV stabilising activity of antioxidants	299
3.2.4.2	Effect of initial concentration of Toc and Irg 1010	300
3.2.4.3	Effect of hindered aryl phosphites on the UV stabilising activity of Toc, Toc derivatives and Irg 1010	300
3.3	DISCUSSION	302
3.3.1	Melt stabilising efficiency of Toc and commercial hindered phenols during multiple extrusions with LDPE	302

3.3.2	Melt stabilising efficiency of Toc, Toc derivatives and commercial hindered phenols during processing with PP in an internal mixer	303
3.3.2.1	Effect of processing severity and oxygen concentration on the melt stabilising activity of Toc	303
3.3.2.2	Effect of initial Toc concentration in PP on the melt stability	304
3.3.2.3	Melt stabilising activity of Toc derivatives in PP	304
3.3.3	Development and prevention of colour during processing of LDPE and PP with antioxidants	305
3.3.4	Thermal stabilising efficiency of Toc, Toc derivatives and commercial antioxidants, in PP processed in an internal mixer	306
3.3.4.1	Comparison of the thermal stabilising activity of Toc with commercial hindered phenols	306
3.3.4.2	Thermal stabilising activity of Toc derivatives	307
3.3.5	UV stabilising efficiency of Toc, Toc derivatives and commercial antioxidants, in PP processed in an internal mixer	308
3.3.5.1	Comparison of the UV stabilising activity of Toc and Toc derivatives with commercial antioxidants	308
3.3.6	Effect of hindered aromatic phosphites on the melt, thermal and UV stabilising activity of Toc, in PP processed in an internal mixer	309
3.3.6.1	Effect of hindered aromatic phosphites on the melt stabilising activity of Toc and Irg 1010	310
3.3.6.2	Effect of hindered aromatic phosphites on the thermal stabilising activity of Toc and Irg 1010	310
3.3.6.3	Effect of hindered aromatic phosphites on the UV stabilising activity of Toc and Irg 1010	310
FIGURES		311

CHAPTER FOUR

NATURE OF TRANSFORMATION PRODUCTS FORMED DURING PROCESSING OF POLYOLEFINS WITH TOC, TOC DERIVATIVES, IRG 1076 AND IRG 1010

LIST OF FIGURES-CHAPTER FOUR	320
4.1	OBJECT AND METHODOLOGY
	324

4.2	RESULTS	334
4.2.1	Nature of transformation products and mechanism of oxidation of Toc in model systems	334
4.2.1.1	Isolation and identification of oxidation products of reactions of Toc with lead dioxide	334
4.2.1.2	Effect of PbO ₂ concentration on the nature of the oxidation products	350
4.2.2	Isolation and characterisation of transformation products of Toc from PP stabilised with 39% Toc	352
4.2.3	Nature of transformation products and mechanism of melt stabilisation of Toc in LDPE, during multiple extrusion	356
4.2.3.1	Extraction efficiency	356
4.2.3.2	Identification and extent of extraction of LMWP	358
4.2.3.3	Isolation and identification of transformation products of Toc	359
4.2.3.4	Effect of extrusion severity and Toc initial concentration on the nature of the transformation products	364
4.2.4	Nature of transformation products formed from Toc and Toc derivatives during processing with PP in an internal mixer	366
4.2.4.1	Extraction efficiency	366
4.2.4.2	Identification and extent of extraction of LMWP	369
4.2.4.3	Effect of O ₂ concentration and processing severity on the nature of products in PP stabilised with 0.2% Toc	371
4.2.4.4	Effect of initial Toc concentration on the nature of its transformation products	373
4.2.4.5	Nature of transformation products in PP stabilised with Toc derivatives	375
4.2.5	Effect of hindered aryl phosphite U-626 on the nature of transformation products of Toc and derivatives during processing with PP in an internal mixer	377
4.2.5.1	Extent of extraction of Toc, Toc derivatives, U-626 and their transformation products	377
4.2.5.2	Nature of transformation products of U-626	379
4.2.5.3	Nature of transformation products of Toc and Toc derivatives	382
4.2.6	Isolation and characterisation of transformation products of Irg 1076 and Irg 1010 from polymer extracts	383
4.2.6.1	Isolation of transformation products of Irg 1076 and Irg 1010	383
4.2.6.2	Characterisation of transformation products of Irg 1076	385
4.2.6.3	Characterisation of transformation products of Irg 1010	389

4.2.7	Effect of extrusion severity on the nature of the transformation products of Irg 1076 in LDPE	392
4.2.8	Effect of extrusion severity on the nature of the transformation products of Irg 1010 in LDPE	395
4.3	DISCUSSION	398
4.3.1	Mechanism of oxidation of Toc with lead dioxide in hexane	398
4.3.1.1	Isolation and identification of oxidation products	398
4.3.1.2	Mechanism of oxidation	400
4.3.2	Isolation and characterisation of transformation products of Toc from polymer extracts	403
4.3.3	Mechanism of melt stabilisation of Toc during multiple extrusions with LDPE	403
4.3.4	Mechanism of melt stabilisation of Toc during processing with PP in an internal mixer	406
4.3.4.1	Effect of processing severity and oxygen concentration on the nature of the transformation products	406
4.3.4.2	Effect of initial Toc concentration on the nature of the transformation products	409
4.3.4.3	Antioxidant activity of Toc derivatives	409
4.3.5	Effect of hindered aryl phosphite U-626 on the antioxidant activity of Toc during processing with PP in an internal mixer	412
4.3.6	Mechanism of melt stabilisation of Irg 1076 during multiple extrusions with LDPE	414
4.3.6.1	Isolation and characterisation of transformation products of Irg 1076	414
4.3.6.2	Effect of initial Irg 1076 concentration and extrusion severity on the nature of the transformation products	415
4.3.7	Mechanism of melt stabilisation of Irg 1010 during multiple extrusions with LDPE	419
4.3.7.1	Isolation and characterisation of transformation products of Irg 1010	419
4.3.7.2	Effect of initial Irg 1010 concentration and extrusion severity on the nature of the transformation products	419
FIGURES		423

CHAPTER FIVE

NATURE OF TRANSFORMATION PRODUCTS FORMED DURING THERMAL AND UV AGEING OF PP STABILISED WITH TOC AND MIGRATION CHARACTERISTICS OF TOC FROM LDPE FILMS INTO FOOD SIMULANTS

LIST OF FIGURES-CHAPTER FIVE	456
5.1 OBJECT AND METHODOLOGY	457
5.2 NATURE OF TRANSFORMATION PRODUCTS OF TOC FORMED IN PP DURING THERMAL AGEING AT 140°C	463
5.2.1 Physical loss of Toc during ageing	463
5.2.2 Nature of transformation products formed during thermal ageing of PP stabilised with Toc	466
5.3 NATURE OF TRANSFORMATION PRODUCTS OF TOC FORMED IN PP DURING UV AGEING	
5.3.1 Physical loss of Toc during ageing	468
5.3.2 Nature of transformation products formed during UV ageing of PP stabilised with Toc	471
5.4 MIGRATION OF TOC AND IRG 1076 AND THEIR TRANSFORMATION PRODUCTS FROM LDPE FILMS INTO FOOD SIMULANTS	473
5.4.1 Static migration tests	473
5.4.2 Dynamic migration tests	474
5.5 DISCUSSION	477
5.5.1 Mechanism of stabilisation of Toc in PP during thermal ageing at 140°C	477
5.5.1.1 Effect of initial Toc concentration in PP on the degradation of the polymer and the loss of the antioxidant during ageing	477
5.5.1.2 Effect of thermal ageing on the nature of the transformation products of Toc	478
5.5.2 Mechanism of stabilisation of Toc in PP during UV ageing	479
5.5.2.1 Effect of initial Toc concentration in PP on the degradation of the polymer and the loss of the antioxidant during ageing	479
5.5.2.2 Effect of UV ageing on the nature of the transformation products of Toc	481
5.5.3 Migration of Toc and its transformation products from LDPE films into various food simulants	482
5.5.3.1 Static migration characteristics of Toc	482
5.5.3.2 Dynamic migration characteristics of Toc	483

FIGURES	485
<u>CHAPTER SIX</u>	
CONCLUSION AND RECOMMENDATIONS FOR FURTHER WORK	491
6.1 CONCLUSION	492
6.1.1 Stabilising efficiency of Toc in polyolefins	492
6.1.2 Development and prevention of colour during processing of LDPE and PP with antioxidants	494
6.1.3 Effect of hindered aryl phosphite on the melt, thermal and UV stabilising activities of Toc	494
6.1.4 Mechanism of melt, thermal and UV stabilisation of Toc in LDPE and PP	495
6.1.4.1 Synthesis, isolation and characterisation of oxidation products of Toc from model systems and polymer extracts	495
6.1.4.2 Mechanism of melt stabilisation of Toc in LDPE and PP	496
6.1.4.3 Effect of hindered aryl phosphite U-626 on the melt stabilisation activity of Toc	498
6.1.5 Mechanism of melt stabilisation of Irg 1076 in LDPE	498
6.1.6 Mechanism of melt stabilisation of Irg 1010 in LDPE	499
6.1.7 Mechanism of thermal stabilisation of Toc in PP	500
6.1.8 Mechanism of UV stabilisation of Toc in PP	500
6.1.9 Migration characteristics of Toc from LDPE films into various food simulants	501
6.2 RECOMMENDATIONS FOR FURTHER WORK	502
REFERENCES	503
<u>APPENDIX</u>	
PUBLISHED WORK	510

LIST OF SCHEMES

<u>Scheme</u>	<u>Title</u>	<u>Page</u>
1.1	Basic mechanism of hydrocarbon oxidation	36
1.2	Chain scission of PP during processing	39
1.3	Competing cross-linking and chain scission in LDPE during processing	40
1.4	Photolysis of PE (the Norrish reactions)	44
1.5	Mechanisms of antioxidant action	46
1.6	Formation of photosensitisers from phenolic antioxidants	48
1.7	Transition state in the formation of phenoxy radicals	50
1.8	Mechanism of oxidation of propionate-type antioxidants with peroxy radicals	53
1.9	Mechanism of chain-breaking antioxidant action of organic phosphites	57
1.10	Mechanism of oxidation of Toc with peroxy radicals in unpolar solvents	74
2.1	Flowchart for the oxidation of Toc with PbO ₂ and the identification and isolation of oxidation products of Toc	86
2.2	Flowchart for the preparation, purification and analysis of DHD, E	95
3.1	Methodology for the determination of the colour and the melt stability of LDPE films stabilised with various concentrations of each of the antioxidants Toc, Irg 1076 and Irg 1010	282
3.2	Methodology for the determination of the colour and the melt, thermal and UV stabilities of PP films stabilised with various concentrations of Toc, Irg 1076, Irg 1010, BHT, Toc derivatives, U-626 and Irgf 168	283
4.1	Methodology for the determination of the nature and concentration of the products of oxidation of Toc with PbO ₂	327
4.2	Methodology for the isolation and identification of transformation products of Toc from PP stabilised with 39% Toc, pass 4 (CPC789 series) and LDPE stabilised with 0.2, 1 and 10% Toc	328
4.3	Methodology for the isolation and identification of transformation products of Irg 1076 and Irg 1010 from LDPE stabilised with 0.2, 1 and 10% of each stabiliser	329
4.4	Mechanism of oxidation of Toc with PbO ₂ in hexane	404
4.5	Mechanism of melt stabilisation of Toc in LDPE and PP	411
4.6	Mechanism of melt stabilisation of U-626 in PP	413

4.7	Suggested mechanism of melt stabilisation of Irg 1076 in LDPE	418
4.8	Suggested mechanism of melt stabilisation of Irg 1010 in LDPE	422
5.1	Methodology for the determination of the loss of total products and of the nature and concentrations of the transformation products formed during thermal and UV ageing of PP stabilised with Toc	462

LIST OF TABLES

<u>Table</u>	<u>Description</u>	<u>Page</u>
1.1	Typical commercial hindered phenol antioxidants	51
1.2	Nature of transformation products of Irganox 1076 formed during processing and thermal ageing with PE and PP	54
1.3	Nature of transformation products of Irganox 1010 formed during processing with PE and PP	55
1.4	Chemical structures of organic phosphites industrially used	56
1.5	Products of oxidation of all-rac-Toc, RRR-Toc and Toc model, with various oxidising agents	67
1.6	Products of oxidation and reduction of transformation products of all-rac-Toc and RRR-Toc, with various agents	69
1.7	Chemical structures of oxidation products of all-rac-Toc, RRR-Toc and Toc model	70
1.8	Melt stability after processing and embrittlement time of PP foils after thermal and light ageing	76
2.1	Chemical structures of antioxidants used	82
2.2	UV and FTIR characteristics of Toc, ALD 1 and TQ (supplied)	148
2.3	¹ H-NMR characteristics of Toc, ALD 1 and TQ (supplied)	149
2.4	¹³ C-NMR characteristics of Toc, ALD 1 and TQ (supplied)	150
2.5	EI-MS analysis of Toc (supplied)	151
2.6	EI-MS analysis of ALD 1 (supplied)	152
2.7	UV characteristics of Irg 1076, Irg 1010 and U-626 (supplied) and ³¹ P-NMR analysis of U-626	153
2.8	¹ H-NMR characteristics of Irg 1076 and Irg 1010 (supplied)	153
2.9	EI-MS analysis of Irg 1076 (supplied)	154
2.10	EI-MS analysis of Irg 1010 (supplied)	154
2.11	Chemical structures, highest yields and colour of products of reactions of Toc with PbO ₂	87
2.12	Reaction yields, colour and major products of reactions of Toc with PbO ₂ and conditions for their isolation	88
2.13	HPLC retention times of Toc and its products of reaction with PbO ₂	89
2.14	HPLC analysis of TRI, A, B, C and SPD, D isolated by column chromatography and semi-preparative HPLC from the products of reaction of Toc with PbO ₂	92

2.15	HPLC analysis of crude and purified DHD, E, obtained from the reaction of SPD, D with LiAlH ₄	94
2.16	UV and FTIR analysis of synthesised DHD, E, SPD, D and TRI, A, B, C	155
2.17	¹ H-NMR characteristics of synthesised DHD, E and SPD, D	156
2.18	¹ H-NMR characteristics of synthesised TRI, A, B, C	157
2.19	¹³ C-NMR characteristics of synthesised DHD, E and SPD, D	158
2.20	¹³ C-NMR characteristics of synthesised TRI, A, B, C	160
2.21	EI-MS analysis of synthesised DHD, E before silylation	162
2.22	EI-MS analysis of synthesised DHD, E after silylation	162
2.23	EI-MS analysis of synthesised SPD, D before and after silylation	163
2.24	FAB-MS analysis of synthesised TRI, A, B, C	163
2.25	¹ H-NMR characteristics of DHD, E and ALD 1, isolated from the products of reaction of Toc with PbO ₂ , ratios 1:1 and 1:40 in Toc:PbO ₂	164
2.26	Extinction coefficients, peak areas and concentrations of products in PP stabilised with 0.2% Toc (CM/N ₂ , 20min, 200°C)	110
2.27	Extent of extraction of LMWP from unstabilised LDPE, unstabilised PP and PP stabilised with 0.2% Toc	112
2.28	Chemical structures and NP-HPLC Rt of products isolated from the extract of PP stabilised with 39% Toc, pass 4 (CPC789 series)	114
2.29	UV analysis of ALD 1, ALD 2, ALD 3 and compound I, isolated from the extract of PP stabilised with 39% Toc, pass 4 (CPC789 series) and FTIR analysis of ALD 1 and ALD 2	165
2.30	¹ H-NMR characteristics of ALD 1, ALD 2, ALD 3 and compound I, isolated from the extract of PP stabilised with 39% Toc, pass 4 (CPC789 series)	166
2.31	¹³ C-NMR characteristics of ALD 1, isolated from the extract of PP stabilised with 39% Toc, pass 4 (CPC789 series)	167
2.32	EI-MS analysis of ALD 1, isolated from the extract of PP stabilised with 39% Toc, pass 4 (CPC789 series)	168
2.33	UV analysis of DHD, E, SPD, D, TRI, A, B, C, ALD 1 and ALD 2, isolated from the extracts of LDPE stabilised with 0.2 and 10% Toc, passes 4	169
2.34	¹ H-NMR characteristics of DHD, E and SPD, D isolated from the extract of LDPE stabilised with 10% Toc, pass 4	170
2.35	¹ H-NMR characteristics of TRI, A, B, C, isolated from the extract of LDPE stabilised with 10% Toc, pass 4	171
2.36	¹ H-NMR characteristics of ALD 1 and ALD 2, isolated from the extract of LDPE stabilised with 0.2% Toc, pass 4	172

2.37	GC-MS analysis of SPD, D, isolated from the extract of LDPE stabilised with 10% Toc, pass 4	173
2.38	GC-MS analysis of TRI, A, B, C, isolated from the extract of LDPE stabilised with 10% Toc, pass 4	173
2.39	GC-MS analysis of ALD 1, isolated from the extract of LDPE stabilised with 0.2% Toc, pass 4	174
2.40	Chemical structures and RP-HPLC Rt of the products isolated and extracted from LDPE stabilised with 10% Irg 1076, pass 4	118
2.41	UV analysis of Irg 1076-1, cinnamate of Irg 1076 (C-Irg 1076) and biscinnamate of Irg 1076 (BC-Irg 1076), isolated from the extract of LDPE stabilised with 10% Irg 1076, pass 4	175
2.42	UV analysis of compounds 2-11, 13 and 14 (Irg 1076-2 to -11 and -13 to -14), extracted from LDPE stabilised with 10% Irg 1076, pass 4	175
2.43	¹ H-NMR characteristics of C-Irg 1076, isolated from the extract of LDPE stabilised with 10% Irg 1076, pass 4	176
2.44	GC-MS analysis of compound 1 (Irg 1076-1), isolated from the extract of LDPE stabilised with 10% Irg 1076, pass 4	176
2.45	GC-MS analysis of cinnamate of Irg 1076 (C-Irg 1076), isolated from the extract of LDPE stabilised with 10% Irg 1076, pass 4	177
2.46	GC-MS analysis of biscinnamate of Irg 1076 (BC-Irg 1076), isolated from the extract of LDPE stabilised with 10% Irg 1076, pass 4	177
2.47	Chemical structures and RP-HPLC Rt of the products extracted from LDPE stabilised with 10% Irg 1010, pass 4	121
2.48	UV analysis of compounds 3 and 6 (Irg 1010-3 and -6), isolated from the extract of LDPE stabilised with 10% Irg 1010, pass 4	178
2.49	UV analysis of compounds 1, 2, 4, 5 and 7-13 (Irg 1010-1, -2, -4, -5 and -7 to -13), extracted from LDPE stabilised with 10% Irg 1010, pass 4	178
2.50	¹ H-NMR analysis of compounds 3 and 6 (Irg 1010-3 and -6), isolated from the extract of LDPE stabilised with 10% Irg 1010, pass 4	179
2.51	GC-MS analysis of Irg 1010-3, isolated from the extract of LDPE stabilised with 10% Irg 1010, pass 4	179
2.52	GC-MS analysis of Irg 1010-6, isolated from the extract of LDPE stabilised with 10% Irg 1010, pass 4	180
2.53	Extinction coefficients of Toc and its oxidation products	127
2.54	Extinction coefficients of TRI, A1, A2, B and C	128
2.55	Integration results obtained for the products of reaction of Toc with PbO ₂ , ratio 1:10 in Toc:PbO ₂ ; hexane:1,4-dioxane = 100:4, v/v; 290nm	129
2.56	Integration results obtained for the products of reaction of Toc with PbO ₂ , ratio 1:10 in Toc:PbO ₂ ; hexane:1,4-dioxane = 100:0.5, v/v; 290nm	130

2.57	Peak areas of the products of reaction of Toc with PbO ₂ , ratio 1:10 in Toc:PbO ₂ ; 290nm	130
2.58	Concentrations of the products of reaction of Toc with PbO ₂ , ratio 1:10 in Toc:PbO ₂ , 290nm, excluding the unknown products	131
2.59	Integration results obtained for the products extracted from PP stabilised with 0.2% Toc (CM/N ₂ , 20min, 200°C); hexane:1,4-dioxane = 100:4, v/v; 290nm	132
2.60	Integration results obtained for the products extracted from PP stabilised with 0.2% Toc (CM/N ₂ , 20min, 200°C); hexane:1,4-dioxane = 100:0.5, v/v; 290nm	132
2.61	Peak areas of the products extracted from PP stabilised with 0.2% Toc (CM/N ₂ , 20min, 200°C); 290nm (excluding LMWP)	133
2.62	Concentrations of the products extracted from PP stabilised with 0.2% Toc (CM/N ₂ , 20min, 200°C) (excluding LMWP and TQ)	133
2.63	Peak areas and extinction coefficients of Toc and TQ extracted from PP stabilised with 0.2% Toc (CM/N ₂ , 20min, 200°C); 275nm	134
2.64	Concentrations of the products extracted from PP stabilised with 0.2% Toc (CM/N ₂ , 20min, 200°C) (excluding LMWP)	134
2.65	Estimated errors on the peak areas	135
2.66	Extinction coefficients of identified transformation products of Irg 1076, isolated from the extract of LDPE stabilised with 10% Irg 1076, pass 4	137
2.67	Food simulants used for the migration tests of LDPE films stabilised with 0.2% Toc and Irg 1076	139
2.68	Test conditions used for the migration tests of LDPE stabilised with 0.2% Toc, according to the conditions of actual use	140
3.1	Chemical structures and description of antioxidants used	280
3.2	Effect of extrusion severity on the MFI and colour of LDPE extruded in the absence and presence of Toc, Irg 1010 and Irg 1076	286
3.3	ΔMFI of LDPE extruded in the absence and presence of Toc, Irg 1010 and Irg 1076	287
3.4	Effect of processing severity on the MFI and colour of PP processed with 0.2% Toc and of a PP control (OM, CM and CM/N ₂)	288
3.5	MFI and colour of PP processed with 0.2% Toc, Irg 1010, Irg 1076 and BHT (CM, 10min)	289
3.6	Effect of concentration on the MFI and colour of PP processed with Toc and Irg 1010 (CM, 10min)	290
3.7	MFI and colour of PP processed with 0.2% Toc derivatives and Toc (CM, 10min)	291

3.8	MFI and colour of PP processed with varying concentrations of Toc and U-626 (CM, 10min)	293
3.9	MFI and colour of PP processed with varying concentrations of Irg 1010, U-626 and Irgf 168 (CM, 10min)	293
3.10	MFI and colour of PP processed with 0.4% U-626 in combination with 0.2% Toc and 0.2% Toc derivatives (CM, 10min)	293
3.11	Effect of temperature on the stability of PP films processed in the absence and presence of 0.2% Toc, Irg 1010, Irg 1076 and BHT (CM, 10min)	295
3.12	Effect of temperature on the stability of PP films processed with varying initial concentrations of Toc and Irg 1010 (CM, 10min)	296
3.13	Thermal stability of PP films processed with 0.2% Toc and 0.2% Toc derivatives (CM, 10min)	297
3.14	Thermal stability of PP films processed with combinations of Toc with U-626 and Irg 1010 with U-626 and Irgf 168 (CM, 10min)	298
3.15	Thermal stability of PP films processed with combinations of Toc derivatives and U-626 (CM, 10min)	298
3.16	UV stability of PP films processed in the absence and presence of 0.2% Toc, Toc derivatives and commercial hindered phenols (CM, 10min)	299
3.17	UV stability of PP films processed with varying concentrations of Toc and Irg 1010 (CM, 10min)	300
3.18	UV stability of PP films processed with Toc, Irg 1010 and U-626 and combinations of U-626 with each of the antioxidants Toc, Toc derivatives and Irg 1010 and Irg 1010 with Irgf 168 (CM, 10min)	301
4.1	Chemical structures and description of oxidation products of Toc and the hindered aryl phosphite U-626	330
4.2	Chemical structures and description of transformation products of Irg 1076	332
4.3	Chemical structures and description of transformation products of Irg 1010	333
4.4	HPLC Rt and conditions for isolation of oxidation products of Toc	335
4.5	Comparison of the spectral characteristics of Toc and its products of oxidation with PbO ₂ , DHD, SPD, TRI and ALD 1	349
4.6	Extinction coefficients of Toc and its products of oxidation with PbO ₂	350
4.7	Concentrations of the products of the oxidations of Toc with PbO ₂	351
4.8	Comparison of the spectral characteristics of ALD 1, ALD 2 and ALD 3, isolated from the extract of PP stabilised with 39% Toc (CPC789 series)	356

4.9	Total concentration of Toc and its transformation products recovered from LDPE films stabilised with 0.2, 1 and 10% Toc	358
4.10	Extraction of LMWP from unstabilised LDPE and LDPE stabilised with 0.2% Toc	359
4.11	HPLC Rt of transformation products of Toc and LMWP extracted from LDPE stabilised with 0.2, 1 and 10% Toc	360
4.12	Concentration of products extracted from LDPE stabilised with 0.2, 1 and 10% Toc	365
4.13	Total concentration of Toc and its transformation products recovered from PP films stabilised with 0.2% Toc (CM, 10min)	368
4.14	Total concentration of Toc and its transformation products recovered from PP films stabilised with 0.2-0.01% Toc (CM, 10min)	368
4.15	Total concentration of Toc derivatives and their transformation products recovered from PP films stabilised with 0.2% Toc derivatives (CM, 10min)	369
4.16	HPLC Rt and UV characteristics of LMWP products extracted from unstabilised PP and PP stabilised with Toc (CM, 10min)	370
4.17	Extent of extraction of LMWP from unstabilised PP and PP stabilised with 0.2% and 0.01-0.05% Toc (CM/N ₂ , CM and OM, 10-30min)	370
4.18	HPLC Rt and UV characteristics of transformation products of Toc and LMWP extracted from PP stabilised with 0.2%Toc (CM/N ₂ , CM and OM, 10min)	372
4.19	Concentration of products extracted from PP stabilised with 0.2% Toc (CM/N ₂ , CM and OM, 10min)	373
4.20	Concentration of products extracted from PP stabilised with 0.01-0.2% Toc (CM, 10min)	375
4.21	Concentration of products extracted from PP stabilised with 0.2% Toc derivatives (CM, 10min)	376
4.22	Extent of recovery of U-626 from PP stabilised with 0.4% U-626 (CM, 10min)	378
4.23	HPLC Rt and UV characteristics of LMWP and U-626 decomposition and transformation products extracted from PP stabilised with Toc, Toc derivatives and U-626 (CM, 10min)	380
4.24	HPLC peak areas of U-626 and its decomposition and transformation products extracted from PP stabilised with Toc, Toc derivatives and U-626 (CM, 10min)	380
4.25	Relative signal intensities and chemical shifts in ¹³ P-NMR of U-626 and its transformation products extracted from PP stabilised with Toc, Toc derivatives and U-626 (CM, 10min)	381

4.26	Concentration of Toc and Toc derivatives and their transformation products extracted from PP stabilised with Toc and Toc derivatives and U-626 (CM, 10min)	383
4.27	HPLC Rt and UV characteristics of the products extracted from LDPE stabilised with 10% Irg 1076, pass 4	384
4.28	HPLC Rt and UV characteristics of the products extracted from LDPE stabilised with 10% Irg 1010, pass 4	385
4.29	Comparison of the main spectral characteristics of Irg 1076-1, C-Irg 1076 and BC-Irg 1076, isolated from the extract of LDPE stabilised with 10% Irg 1076, pass 4	389
4.30	Comparison of the main spectral characteristics of Irg 1010-3 and Irg 1010-6, isolated from the extract of LDPE stabilised with 10% Irg 1010, pass 4	392
4.31	HPLC peak areas at 282nm of the products extracted from LDPE stabilised with Irg 1076	394
4.32	Relative concentrations of Irg 1076, C-Irg 1076 and BC-Irg 1076 extracted from LDPE stabilised with Irg 1076	395
4.33	HPLC peak areas at 282nm of the products extracted from LDPE stabilised with Irg 1010	397
5.1	Chemical structures and UV characteristics of the transformation products formed during thermal and UV ageing of Toc in PP films	460
5.2	Chemical structures and UV characteristics of the commercial hindered phenols Irganox 1076 and Irg 1010	461
5.3	Total concentration of Toc and its transformation products recovered from PP films stabilised with 0.05% Toc (CM, 10min), after thermal ageing at 140°C	465
5.4	HPLC Rt and UV characteristics of transformation products of Toc and LMWP extracted from PP films stabilised with 0.05% Toc (CM, 10min) and thermal aged at 140°C	467
5.5	Concentration of products extracted from PP stabilised with 0.05% Toc (CM, 10min) and thermal aged at 140°C	467
5.6	Total concentration of Toc and its transformation products recovered from PP films stabilised with 1% Toc (CM, 10min), after UV ageing	470
5.7	Concentration of products extracted from PP stabilised with 1% Toc (CM, 10min) and UV aged	472
5.8	Effect of time on the extent of migration, M, of Toc and its transformation products from LDPE films stabilised with 0.2% Toc into various food simulants	475

5.9	Effect of time on the extent of migration, M, of Irg 1076 and its transformation products from LDPE films stabilised with 0.2% Irg 1076 into various food simulants	476
-----	---	-----

LIST OF FIGURES

<u>Figure</u>	<u>Description</u>	<u>Page</u>
1.1	Chemical structures of typical UV absorbers and light stabilisers	49
1.2	Stereochemical structures of natural Vitamin E	62
1.3	Chemical structures of α -tocopherol, its model and BHT	63
1.4	p-orbital orientation in the puckered tocopheroxyl radical compared to the flatter dihydrobenzofuran phenoxyl radical	64
1.5	Chemical structures of analogous α -tocopherol derivative antioxidants	64
2.1.a	HPLC chromatograms of Toc	181
2.1.b	UV spectrum of Toc	182
2.1.c	IR spectrum of Toc	182
2.1.d	^1H -NMR spectrum of Toc	183
2.1.e	^{13}C -NMR spectrum of Toc	184
2.1.f	^1H , ^{13}C -NMR correlation spectrum of Toc	185
2.1.g	EI-MS spectrum of Toc	186
2.2.a	HPLC chromatograms of supplied ALD 1	187
2.2.b	UV spectrum of supplied ALD 1	188
2.2.c	IR spectrum of supplied ALD 1	188
2.2.d	^1H -NMR spectrum of supplied ALD 1	189
2.2.e	^{13}C -NMR spectrum of supplied ALD 1	190
2.2.f	^1H , ^{13}C -NMR correlation spectrum of supplied ALD 1	191
2.2.g	EI-MS spectrum of supplied ALD 1	192
2.3.a	HPLC chromatograms of TQ	193
2.3.b	UV spectrum of TQ	194
2.3.c	IR spectrum of TQ	194
2.3.d	^1H -NMR spectrum of TQ	195
2.3.e	^{13}C -NMR spectrum of TQ	196
2.3.f	^1H , ^{13}C -NMR correlation spectrum of TQ	197
2.4.a	HPLC chromatograms of Irg 1076	198
2.4.b	UV spectrum of Irg 1076	199
2.4.c	^1H -NMR spectrum of Irg 1076	199
2.4.d	EI-MS spectrum of Irg 1076	200
2.5.a	HPLC chromatograms of Irg 1010	201
2.5.b	UV spectrum of Irg 1010	202
2.5.c	^1H -NMR spectrum of Irg 1010	202
2.5.d	EI-MS spectrum of Irg 1010	203

2.6.a	HPLC chromatograms of U-626	204
2.6.b	UV spectrum of U-626	205
2.6.c	³¹ P-NMR spectrum of U-626	205
2.7	HPLC chromatograms of the products of reaction of Toc with PbO ₂ , ratio 1:10, mol/mol, in Toc:PbO ₂	206
2.8	HPLC chromatograms of the products of reaction of Toc with PbO ₂ , ratio 1:40, mol/mol, in Toc:PbO ₂	207
2.9	HPLC chromatograms of the products isolated by column chromatography of the mixtures of products obtained from the oxidations of Toc with PbO ₂	208
2.10	HPLC chromatograms of TRI, A1, A2, B and C, isolated by semi-preparative HPLC of the mixture of TRI, A, B, C obtained by CC of the products of reaction of Toc with PbO ₂	209
2.11	HPLC chromatograms of the products of reaction of SPD, D with LiAlH ₄ , before and after purification by semi-preparative HPLC of DHD, D	210
2.12	Typical HPLC chromatogram of DHD, E obtained from the reaction of SPD, D with LiAlH ₄ during the isolation of DHD, E1, E2 and E3+E4	211
2.13.a	HPLC chromatograms of synthesised DHD, E	212
2.13.b	UV spectrum of synthesised DHD, E	213
2.13.c	IR spectrum of synthesised DHD, E	213
2.13.d	¹ H-NMR spectrum of DHD, E1	214
2.13.e	¹ H-NMR spectrum of DHD, E2	215
2.13.f	¹ H-NMR spectrum of DHD, E3+E4	216
2.13.g	¹³ C-NMR spectrum of DHD, E1	217
2.13.h	¹³ C-NMR spectrum of DHD, E2	218
2.13.i	¹³ C-NMR spectrum of DHD, E3+E4	219
2.13.j	¹ H, ¹³ C-NMR correlation spectrum of synthesised DHD, E	220
2.13.k	EI-MS spectrum of synthesised DHD, E	221
2.13.l	EI-MS spectrum of synthesised DHD, E, after silylation with TMS	222
2.14.a	HPLC chromatograms of synthesised SPD, D	223
2.14.b	UV spectrum of synthesised SPD, D	224
2.14.c	IR spectrum of synthesised SPD, D	224
2.14.d	¹ H-NMR spectrum of synthesised SPD, D	225
2.14.e	¹³ C-NMR spectrum of synthesised SPD, D	226
2.14.f	¹ H, ¹³ C-NMR correlation spectrum of synthesised SPD, D	227
2.14.g	EI-MS spectrum of synthesised SPD, D	228
2.15.a	HPLC chromatograms of synthesised TRI, A, B, C	229
2.15.b	UV spectrum of synthesised TRI, A, B, C	230
2.15.c	IR spectrum of synthesised TRI, A, B, C	230

2.15.d	¹ H-NMR spectrum of TRI, A1	231
2.15.e	¹ H-NMR spectrum of TRI, A2	232
2.15.f	¹ H-NMR spectrum of TRI, B	233
2.15.g	¹ H-NMR spectrum of TRI, C	234
2.15.h	¹³ C-NMR spectrum of TRI, A1	235
2.15.i	¹³ C-NMR spectrum of TRI, A2	236
2.15.j	¹³ C-NMR spectrum of TRI, B	237
2.15.k	¹ H, ¹³ C-NMR correlation spectrum of TRI, A1	238
2.15.l	FAB-MS spectrum of synthesised TRI, A, B, C	239
2.16	Schematic representation of the Humboldt single screw extruder	100
2.17	Schematic representation of the internal mixing chamber of the Hampden-Rapra torquerheometer	100
2.18	UV spectra of a PP film stabilised with 0.2% Toc before and after extraction with dichloromethane	107
2.19	UV spectrum of the products extracted from PP stabilised with 0.2% Toc	109
2.20	HPLC analysis of the extract of PP stabilised with 39% Toc, pass 4	240
2.21 (a-b)	HPLC and UV analysis of ALD 1, isolated from the extract of PP stabilised with 39% Toc, pass 4 (CPC789 series)	241
2.21.c	¹ H-NMR spectrum of ALD 1, isolated from the extract of PP stabilised with 39% Toc, pass 4 (CPC789 series)	242
2.21.d	¹³ C-NMR spectrum of ALD 1, isolated from the extract of PP stabilised with 39% Toc, pass 4 (CPC789 series)	243
2.22 (a-b)	HPLC and UV analysis of ALD 2, isolated from the extract of PP stabilised with 39% Toc, pass 4 (CPC789 series)	244
2.22 (c-d)	IR and ¹ H-NMR spectra of ALD 2, isolated from the extract of PP stabilised with 39% Toc, pass 4 (CPC789 series)	245
2.22.e	EI-MS spectrum of ALD 2, isolated from the extract of PP stabilised with 39% Toc, pass 4 (CPC789 series)	246
2.23 (a-b)	HPLC and UV analysis of ALD 3, isolated from the extract of PP stabilised with 39% Toc, pass 4 (CPC789 series)	247
2.23.c	¹ H-NMR spectrum of ALD 3, isolated from the extract of PP stabilised with 39% Toc, pass 4 (CPC789 series)	248
2.24 (a-b)	HPLC and UV analysis of compound I, isolated from the extract of PP stabilised with 39% Toc, pass 4 (CPC789 series)	249
2.24.c	¹ H-NMR spectrum of compound I, isolated from the extract of PP stabilised with 39% Toc, pass 4 (CPC789 series)	250
2.25	HPLC chromatograms of the products extracted from LDPE stabilised with 0.2 and 10% Toc, passes 4	251

2.26 (a-b)	HPLC and UV analysis of DHD, E, isolated from the extract of LDPE stabilised with 10% Toc, pass 4	252
2.26.c	¹ H-NMR spectrum of DHD, E, isolated from the extract of LDPE stabilised with 10% Toc, pass 4	253
2.27 (a-b)	HPLC and UV analysis of SPD, D, isolated from the extract of LDPE stabilised with 10% Toc, pass 4	254
2.27.c	¹ H-NMR spectrum of SPD, D, isolated from the extract of LDPE stabilised with 10% Toc, pass 4	255
2.27.d	GC-MS spectrum of SPD, D, isolated from the extract of LDPE stabilised with 10% Toc, pass 4	256
2.28 (a-b)	HPLC and UV analysis of TRI, A, B, C, isolated from the extract of LDPE stabilised with 10% Toc, pass 4	257
2.28.c	¹ H-NMR spectrum of TRI, A, B, C, isolated from the extract of LDPE stabilised with 10% Toc, pass 4	258
2.28.d	GC-MS spectrum of TRI, A, B, C, isolated from the extract of LDPE stabilised with 10% Toc, pass 4	259
2.29 (a-b)	HPLC and UV analysis of ALD 1, isolated from the extract of LDPE stabilised with 0.2% Toc, pass 4	260
2.29.c	¹ H-NMR spectrum of ALD 1, isolated from the extract of LDPE stabilised with 0.2% Toc, pass 4	261
2.29.d	GC-MS spectrum of ALD 1, isolated from the extract of LDPE stabilised with 0.2% Toc, pass 4	262
2.30 (a-b)	HPLC and UV analysis of ALD 2, isolated from the extract of LDPE stabilised with 0.2% Toc, pass 4	263
2.30.c	¹ H-NMR spectrum of ALD 2, isolated from the extract of LDPE stabilised with 0.2% Toc, pass 4	264
2.31	HPLC chromatograms of the products extracted from LDPE stabilised with 10% Irg 1076, pass 4	265
2.32	HPLC, UV and GC-MS analysis of Irg 1076-1 isolated from the extract of LDPE stabilised with 10% Irg 1076, pass 4	266
2.33 (a-c)	HPLC, UV and ¹ H-NMR analysis of C-Irg 1076 isolated from the extract of LDPE stabilised with 10% Irg 1076, pass 4	267
2.33.d	GC-MS analysis of C-Irg 1076 isolated from the extract of LDPE stabilised with 10% Irg 1076, pass 4	268
2.34	HPLC, UV and GC-MS analysis of BC-Irg 1076 isolated from the extract of LDPE stabilised with 10% Irg 1076, pass 4	269
2.35	Diode array UV analysis of Irg 1076-11, -13 and -14 extracted from LDPE stabilised with 10% Irg 1076, pass 4	270

2.36	HPLC chromatograms of the products extracted from LDPE stabilised with 10% Irg 1010, pass 4	271
2.37 (a-c)	HPLC, UV and ¹ H-NMR analysis of Irg 1010-3 isolated from the extract of LDPE stabilised with 10% Irg 1010, pass 4	272
2.37.d	GC-MS analysis of Irg 1010-3 isolated from the extract of LDPE stabilised with 10% Irg 1010, pass 4	273
2.38 (a-c)	HPLC, UV and ¹ H-NMR analysis of Irg 1010-6 isolated from the extract of LDPE stabilised with 10% Irg 1010, pass 4	274
2.38.d	GC-MS analysis of Irg 1010-6 isolated from the extract of LDPE stabilised with 10% Irg 1010, pass 4	275
2.39	Diode array UV analysis of Irg 1010-4 and -14 extracted from LDPE stabilised with 10% Irg 1010, pass 4	276
2.40	Calibration graph and equation of the regression line for the determination of the extinction coefficient of Toc at 290nm	127
2.41	Measurement of the net absorbance of the products in polymer films	142
3.1	Effect of initial Toc concentration in LDPE and extrusion severity on the MFI and ΔMFI of LDPE	311
3.2	Effect of extrusion severity on the MFI and initial antioxidant concentration on the ΔMFI of LDPE extruded in the absence and presence of Toc, Irg 1010 and Irg 1076	311
3.3	Effect of processing severity on the MFI of PP, processed in the absence and presence of 0.2% Toc, and effect of oxygen concentration in the internal mixer on the MFI of PP processed with 0.2% Toc	312
3.4	Effect of initial antioxidant concentration on the MFI of PP and comparison of the melt stabilising activity of Toc with those Irg 1076, Irg 1010 and BHT, in PP (CM, 10min)	312
3.5	MFI of PP processed with 0.2% Toc, Toc derivatives and Irg 1010 (CM, 10min)	313
3.6	Effect of U-626 and Irgf 168 on the melt stabilising activities of Toc and Irg 1010 in PP (CM, 10min)	313
3.7	Thermal stability of PP films processed in the absence and presence of 0.2% Toc and commercial antioxidants (CM, 10min)	314
3.8	Effect of initial Toc concentration and temperature on the thermal stability of PP films processed with Toc (CM, 10min)	314
3.9	Thermal stability of PP films processed with 0.2% Toc and 0.2% Toc derivatives (CM, 10min)	315
3.10	Effect of U-626 and Irgf 168 on the thermal stability of PP films processed with Toc and Irg 1010 (CM, 10min)	316

3.11	UV stability of PP films processed in the absence and presence of 0.2% Toc, Toc derivatives, Irg 1010, Irg 1076 and BHT (CM, 10min)	317
3.12	Effect of initial antioxidant concentration on the UV stability of PP films stabilised with Toc and Irg 1010 (CM, 10min)	317
3.13	Effect of hindered aryl phosphites U-626 and Irgf 168 on the UV stabilising efficiencies of Toc, Toc derivatives and Irg 1010 in PP (CM, 10min), at varying initial concentrations of the stabilisers	318
4.1	HPLC chromatogram of compound E at 300nm and UV spectra of compounds E1, E2, E3 and E4	336
4.2	Chemical structure of Toc and suggested configurations of DHD, E1, E2, E3 and E4 (E)	338
4.3	HPLC chromatogram of compound D at 301nm and UV spectra of compounds D1, D2 and D3	339
4.4	Chemical structures and configurations of SPD, D1, D2 and D3	341
4.5	HPLC chromatograms of compounds A1, A2, B and C at 292nm and UV spectra of A1, A2, B1, B2, B3, B4, C1, C2, C3 and C4	342
4.6	¹ H-NMR spectra of TRI, A1, A2, B (B1-B4) and C (C1-C4); region 1.0 to 1.55ppm	345
4.7	Chemical structures and configurations of TRI, A1, A2, B and C	346
4.8	HPLC chromatogram at 290nm and UV spectrum of ALD 1, isolated from the products of reaction of Toc with PbO ₂ , ratio 1:40, mol/mol, in Toc:PbO ₂	347
4.9	Chemical structure of ALD 1, F	348
4.10	Effect of lead dioxide concentration on the nature and concentrations of the products of oxidation of Toc in hexane	351
4.11	HPLC chromatograms and UV spectra of ALD 1, F, ALD 2, G and ALD 3, H	354
4.12	Chemical structures of ALD 1, F, ALD 2, G and ALD 3, H	355
4.13	UV spectra of LDPE films (0.25mm thick) stabilised with 0.2% and 1% Toc, passes 4, before and after extraction with dichloromethane	357
4.14	HPLC analysis of the extracts of unstabilised LDPE, pass 1 and LDPE (a-b) stabilised with 0.2% Toc, pass 4 (LMWP)	423
4.14.c	Diode array UV analysis of the extract of unstabilised LDPE, pass 1	424
4.15	HPLC analysis of the extract of LDPE stabilised with 0.2% Toc, passes 1 and 4 (a-d)	425
4.15	HPLC analysis of the extract of LDPE stabilised with 10% Toc, passes 1 and 4 (e-h)	426

4.16	Effect of initial Toc concentration in LDPE on the concentrations of Toc and its transformation products after multiple extrusions	427
4.17	Effect of initial Toc concentration in LDPE on the concentration of the transformation products, after the first extrusion pass	428
4.18	Effect of initial Toc concentration in LDPE and extrusion severity on the added concentrations of retained Toc and DHD, E, after multiple extrusions	428
4.19	Effect of initial Toc concentration in LDPE and extrusion severity on the nature and distribution of its transformation products	429
4.20	UV spectra of PP films (0.25mm thick) stabilised with 0.2% Toc (CM/N ₂ and OM, 30min), 0.05% and 0.02% Toc (CM, 10min) and 0.2% SPD, D (CM, 10min), before and after extraction with dichloromethane	367
4.21 (a-d)	HPLC analysis of the extracts of unstabilised PP and PP stabilised with 0.2% Toc (CM, 10min, 200°C) (LMWP)	430
4.21 (e-f)	Diode array UV analysis of the extract of unstabilised PP and FTIR analysis of unstabilised PP film (0.25mm thick) (CM, 10min, 200°C)	431
4.22	HPLC analysis of the extracts of PP processed with 0.2% Toc (CM/N ₂ , 200°C) for 5min and 30min	432
4.23	HPLC analysis of the extracts of PP processed with 0.2% Toc (OM, 200°C) for 5min and 30min	433
4.24	Diode array UV analysis of ALD 4 and ALD 5, extracted from PP stabilised with 0.2% Toc (OM, 10min, 200°C)	434
4.25	Effect of oxygen concentration in the internal mixing chamber and processing severity on the concentration of Toc and its transformation products in PP stabilised with 0.2% Toc (OM, CM and CM/N ₂ , 200°C)	435
4.26	Effect of oxygen concentration in the internal mixing chamber on the concentration of Toc and its transformation products in PP stabilised with 0.2% Toc (OM, CM, CM/N ₂ , 5min, 200°C)	436
4.27	Effect of oxygen concentration on the concentration of ALD 1-5 compared to other products in PP stabilised with 0.2% Toc (CM/N ₂ , CM and OM, 200°C)	436
4.28	Effect of processing severity on the concentration of transformation products of Toc in PP stabilised with 0.2% Toc (OM, CM and CM/N ₂ , 200°C)	437
4.29	HPLC analysis of the extracts of PP stabilised with 0.01% and 0.05% Toc (CM, 10min, 200°C)	438
4.30	Effect of initial Toc concentration in PP on the nature and concentrations of its transformation products (CM, 10min, 200°C)	439

4.31	Effect of initial Toc concentration in PP on the distribution of its oxidation products (CM, 10min, 200°C)	440
4.32	HPLC analysis of the extracts of PP stabilised with 0.2% DHD, E and 0.2% TRI, A, B, C (CM, 10min, 200°C)	441
4.33	Nature of transformation products in PP stabilised with 0.2% of each of the Toc derivatives DHD, E, SPD, D and TRI, A, B, C (CM, 10min, 200°C)	442
4.34	UV spectra of PP films (0.25mm thick) stabilised with 0.4% U-626, 0.05% Toc + 0.1% U-626, 0.2% SPD, D + 0.4% U-626 and 0.2% TRI, A, B, C + 0.4% U-626 (CM, 10min, 200°C), before and after extraction with dichloromethane	378
4.35	³¹ P-NMR spectra of U-626 and the extracts of PP stabilised with 0.4% U-626, 0.4% U-626 + 0.2% Toc, 0.1% U-626 + 0.05% Toc, 0.4% U-626 + 0.2% SPD, D and 0.4% U-626 + 0.2% TRI, A, B, C (CM, 10min, 200°C)	443
4.36 (a-d)	HPLC analysis of the extracts of PP stabilised with 0.4% U-626 and 0.05% Toc + 0.1% U-626 (CM, 10min, 200°C)	444
4.36 (e-h)	HPLC analysis of the extracts of PP stabilised with 0.2% SPD, D + 0.4% U-626 and 0.2% TRI, A, B, C + 0.4% U-626 (CM, 10min, 200°C)	445
4.37	Effect of U-626 in PP containing Toc, SPD, D and TRI, A, B, C on the nature and concentration of their transformation products (CM, 10min, 200°C)	446
4.38	Possible chemical structure of the peak at 344 in the MS spectrum of compound 1, Irg 1076-1	386
4.39	Possible chemical structures of compounds 2-10, Irg 1076-2 to Irg 1076-10	386
4.40	Chemical structure of compound 12, C-Irg 1076	387
4.41	Chemical structure of compound 13, BC-Irg 1076	388
4.42	Possible chemical structures of compounds 11 and 14, QM-Irg 1076 and CBQM-Irg 1076	388
4.43	Chemical structure of compound 3, Irg 1010-3	390
4.44	Chemical structure of compound 6, Irg 1010-6	390
4.45	Possible chemical structures of compounds 1, 2, 5 and 7 to 13, Irg 1010-1, -2, -5 and Irg 1010-7 to -13	391
4.46	Possible chemical structures of compounds 4 and 14, Irg 1010-4 and -14	392
4.47 (a-d)	HPLC analysis of the products extracted from LDPE stabilised with 0.2% Irg 1076, passes 1 and 4	447
4.47 (e-h)	HPLC analysis of the products extracted from LDPE stabilised with 10% Irg 1076, passes 1 and 4	448

4.48	Effect of extrusion severity and initial Irg 1076 concentration on the nature and peak areas (282nm) of the transformation products of Irg 1076 in LDPE and concentrations of C-Irg 1076 and BC-Irg 1076, relative to Irg 1076	449
4.49	Effect of extrusion severity on the peak areas (282nm) and distribution of the transformation products of Irg 1076 in LDPE	450
4.50	HPLC analysis of the products extracted from LDPE stabilised with	
(a-d)	0.2% Irg 1010, passes 1 and 4	451
4.50	HPLC analysis of the products extracted from LDPE stabilised with	
(e-h)	10% Irg 1010, passes 1 and 4	452
4.51	Effect of initial Irg 1010 concentration and extrusion severity on the nature and peak areas (282nm) of its transformation products in LDPE	453
4.52	Effect of extrusion severity on the nature and peak areas (282nm) of the transformation products of Irg 1010 in LDPE	454
5.1	Changes in the UV spectra of PP films, unstabilised and stabilised with 0.02, 0.05 and 0.1% Toc, in an internal mixer (CM, 10min) during thermal ageing at 140°C	464
5.2	Decrease in the relative net absorbance at 290nm of Toc and its transformation products in PP films stabilised with 0.02 to 0.2% Toc and yield of total products extracted from PP stabilised with 0.05% Toc (CM, 10min), during thermal ageing at 140°C	465
5.3	HPLC analysis of the extracts of PP stabilised with 0.05% Toc (CM,	
(a-d)	10min) after thermal ageing at 140°C	485
5.3	HPLC analysis of the extracts of PP stabilised with 0.05% Toc (CM,	
(e-h)	10min) after thermal ageing at 140°C	486
5.4	Effect of thermal ageing at 140°C on the concentration of the transformation products of Toc in PP stabilised with 0.05% Toc (CM, 10min)	487
5.5	Changes in the UV spectra of PP films (0.25mm thick), unstabilised and stabilised with 0.2 and 1% Toc, in an internal mixer (CM, 10min, 200°C) during UV ageing	469
5.6	Decrease in the relative net absorbance at 290nm of Toc and its transformation products in PP films stabilised with 0.2 and 1% Toc and yield of total products extracted from PP stabilised with 1% Toc (CM, 10min) during UV ageing	470
5.7	HPLC analysis of the extracts of PP stabilised with 1% Toc (CM, 10min)	
(a-d)	after UV ageing	488

5.7 (e-h)	HPLC analysis of the extracts of PP stabilised with 1% Toc (CM, 10min) after UV ageing	489
5.8	Effect of UV ageing on the concentration of the transformation products of Toc in PP stabilised with 1% Toc (CM, 10min)	490
5.9	Extent of migration of Toc and its transformation products from LDPE stabilised with 0.2% Toc, pass 1, into various food simulants under different conditions	474
5.10	Rate of migration of Toc and Irg 1076 from LDPE stabilised with 0.2% of each antioxidant, pass 1, into various food simulants	476

ABBREVIATIONS

abbreviation	name
ALD 1, 2 and 3	5-formyl- γ -tocopherol, 5-formyl- γ -tocopherol-3en and 7-formyl- β -tocopherol, respectively [@]
BC-Irg 1076	biscinnamate of Irganox 1076*
BHT	2,6-di- <i>t</i> -butyl-4-methylphenol
CB-A and CB-D	chain-breaking acceptor and chain-breaking donor
CBQM-Irg 1076	conjugated bisquinone methide of Irganox 1076*
C-Irg 1076	cinnamate of Irg 1076*
CM, CM/N ₂	closed mixer, closed mixer with prior N ₂ flushing
DHD	dihydroxydimer of Toc ^{\$}
EI-, FAB- and GC-MS	electron-impact-, fast atom bombardment- and gas-chromatography-mass spectrometry
HDPE	high density polyethylene
HPLC, NP- and RP-	high performance liquid chromatography, normal phase and reverse phase
IR	infrared
Irg 1076 and Irg 1010	Irganox 1076 and Irganox 1010 [#]
Irgf 168	Irgafos 168 [#]
LDPE	low density polyethylene
LMWP	low molecular weight polymer
MFI, MM	melt flow index, molecular mass
NMR	nuclear magnetic resonance
OM	open mixer
PD-C, PD-S	catalytic and stoichiometric peroxidolytic
PE, PP	polyethylene, polypropylene
QM	quinone methide
Rt	retention time
SPD	spirodimer of Toc ^{\$}
TQ	α -tocoquinone of Toc [#]
TRI	trimer of Toc ^{\$}
U-626	Ultranox 626 [#]
UV	ultraviolet

[@] See p. 114 for structures

* See p. 118-119 for IUPAC name and structure

^{\$} See p. 87 for IUPAC name and structure

[#] See p. 82-83 for IUPAC name and structure

1.1 GENERAL INTRODUCTION

Polyolefins represent a commercially important class of bulk thermoplastics due to their low price, versatility, ease of processing and low weight to volume ratio [1]. Low density polyethylene and polypropylene are the most widely used food packaging materials [2]. A major drawback, however, is their extreme sensitivity to heat and light [3]. For example, the polymers will rapidly lose most of their mechanical properties after severe processing or periods of thermal and light exposure. To overcome these problems, a range of antioxidants have been developed. Phenolic antioxidants maintain an important position in the stabilisation of polyolefins and were subject to intensive commercial testing and theoretical investigations in the last forty years [4]. A major concern for synthetic antioxidants is the potential hazards arising from their use in food packaging materials, as a consequence of their migration into the foodstuff. Hence, the antioxidant role of biological antioxidants (e.g. Vitamin E) were recently investigated in polyolefins [5-9].

1.2 DEGRADATION OF POLYOLEFINS

1.2.1 General overview

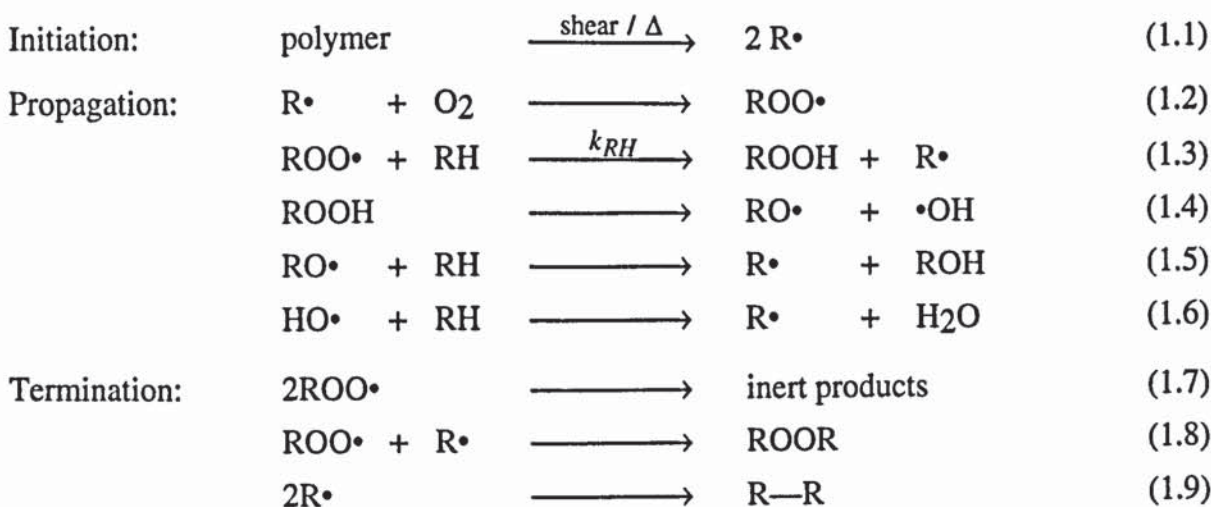
The degradation process of hydrocarbon polymers occurs, to varying extent, during all phases of the polymer lifecycle. Both stages of converting monomers to polymers (polymerisation) and polymers to finished products (processing / fabrication) contribute significantly to accelerating the oxidative degradation process of polymers due to the presence of adventitious chemical impurities. In the former case, for example, residues of metal ions from polymerisation catalysts play a main role in accelerating oxidation, while in the latter case the effect of high processing temperatures, shearing forces and small oxygen concentrations contribute mainly to undesirable chemical changes in the polymer (such as cross-linking and chain scission). These chemical changes, together with the effects of aggressive service environments (e.g. sunlight, heat, leaching solvents and

detergents) lead to premature oxidation of the polymer products with concomitant loss of useful properties.

1.2.2 Thermal oxidative degradation

Polyolefins undergo thermal degradation during processing, where the polymer is normally subjected to temperatures ranging between 180 and 280°C for a relatively short period of time and usually under restricted air access. However, thermal degradation can also occur during service of polyolefin articles, where the temperatures are lower but applied for extended time periods under atmospheric conditions.

All organic compounds are susceptible to attack by molecular oxygen. A basic autoxidation scheme based on the classical free radical chain theory (see scheme 1.1) was developed in the forties by researchers at the British Rubber Producers Association [10-12]. The process of autoxidation was described in terms of a complex set of elementary reaction steps during the stages of initiation, propagation and termination. Extension of these concepts and models to cover applications in polymers is relatively recent [13-15]. In general, the mechanism of degradation of polyolefins has been shown to be very similar to that of low molecular weight hydrocarbons shown in scheme 1.1.



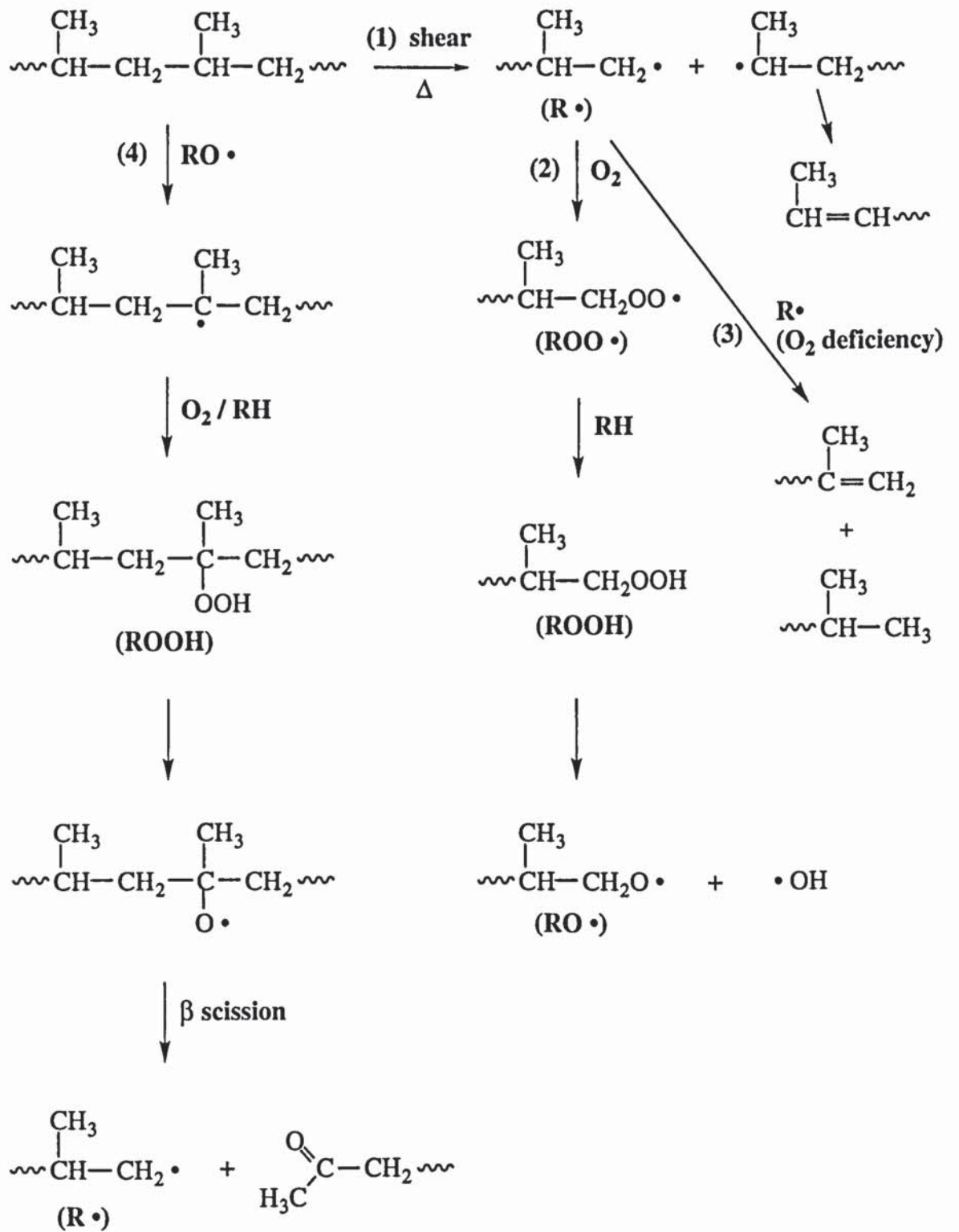
Scheme 1.1: Basic mechanism of hydrocarbon oxidation

The temperature and shear employed in processing cause some of the polymer chains to undergo homolytic chain scission leading to the formation of macroalkyl radicals, R^\bullet (see scheme 1.1, reaction 1.1). For most organic polymers, alkyl radicals react rapidly with oxygen, at normal oxygen pressure, to give alkyl peroxy radicals, ROO^\bullet (reaction 1.2), followed by hydrogen abstraction (rate determining step) from the polymer substrate to yield hydroperoxides, $ROOH$ (reaction 1.3). Primary and secondary peroxy radicals were found to be several times as reactive as tertiary radicals for hydrogen abstraction [16,17]. The formation of hydroperoxides in the chain sequence is the most important source of initiating radicals (reactions 1.5 and 1.6). In the absence of oxygen or other radical trapping agents, the macroalkyl radicals may recombine or slowly disproportionate with little initial change in molar mass. The termination of the radical chain is due to combinations of free radicals with each other, in which inactive products are formed (reactions 1.7 to 1.9). Extensive mechano-oxidation at the processing stage is detrimental to the service performance and durability of the polymer.

The nature and structure of the base polymer exert a profound effect on the mechano-chemistry of the system [18-21]. Polypropylene (PP) undergoes a high rate of chain scission in the initial stage of the processing operation (see scheme 1.2, reaction (1)) leading to the production of macroalkyl radicals in the presence of oxygen (path (2)). Under oxygen deficient conditions (which coexist in an extruder) disproportionation reactions of alkyl radicals take place to yield carbon-carbon double bonds (reaction (3)). The macrohydroperoxides formed lead to the formation of ketones resulting in chain scission (path (4)), i.e. a decrease in the molecular weight of the polymer. In low density polyethylene (LDPE), alkyl radicals are also initially produced during processing by mechanical shear of the polymer backbone, probably primarily at an allylic carbon atom (see scheme 1.3, reaction (1)). These alkyl radicals can react rapidly with oxygen to form hydroperoxides (path (2)), which are responsible for the formation of secondary macroalkyl radicals along the polymer chain, again at allylic hydrogen (reaction (4)). However, LDPE is less prone to attack by peroxy radicals than PP as they abstract tertiary bonded hydrogens in preference to secondary or primary hydrogens [16,17,22]. Which of the

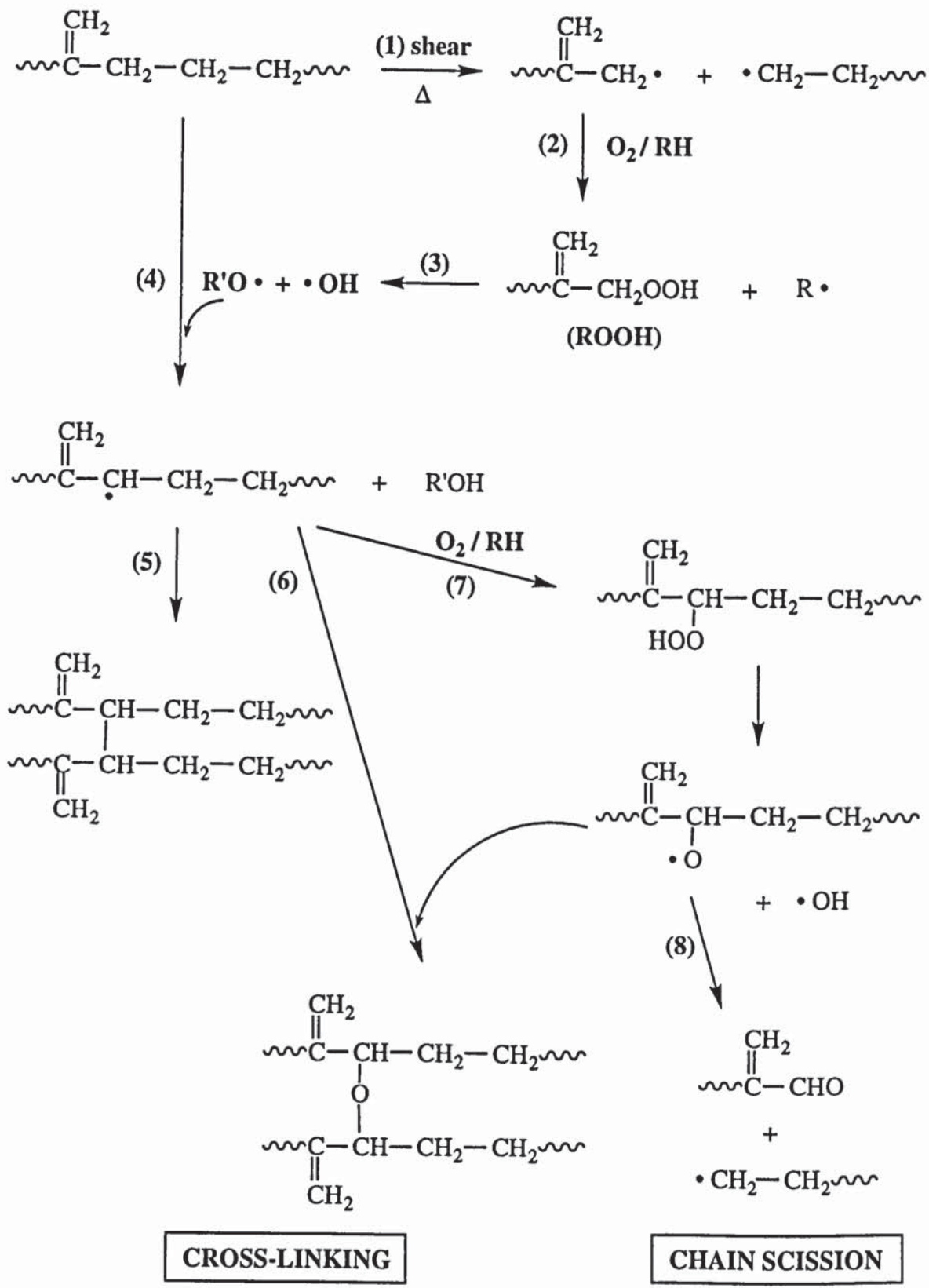
alternative reactions (5) and (6) or (7) and (8) of macroalkyl radicals then occurs is critically dependent on the oxygen availability [23]. In an oxygen deficient medium, cross-linking occurs (reactions (5) and (6)), i.e. molecular enlargement, whereas in an oxygen rich environment, scission of β C-C bonds of an in-chain alkyl radical is favoured (reactions (7) and (8)). In general molecular enlargement is favoured over chain scission under normal commercial extrusion conditions, as a small amount of oxygen is present [19,24,25].

After processing, thermal degradation is highly dependent on the extent of degradation of the polymer suffered during processing and on the concentration of hydroperoxides formed. The polyolefins are also subject to oxidation at room temperature and below, as described earlier in scheme 1.1. Autoxidation commences slowly, then increases in rate and eventually subsides, producing a sigmoid curve as a function of time.



CHAIN SCISSION

Scheme 1.2: Chain scission of PP during processing



Scheme 1.3: Competing cross-linking and chain scission in LDPE during processing

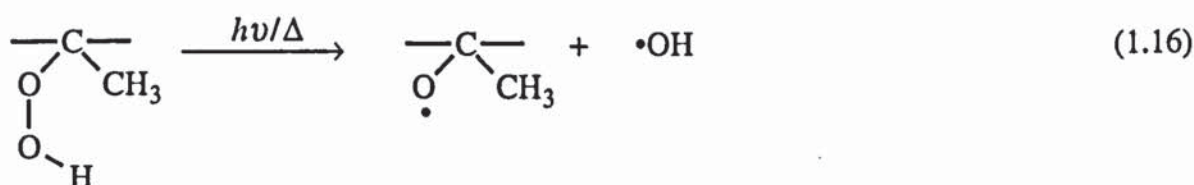
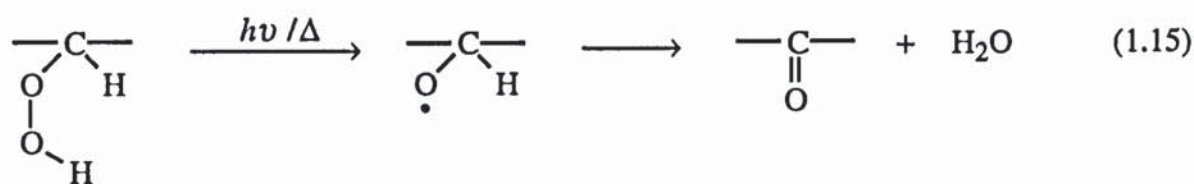
1.2.3 Photooxidative degradation

Most polyolefins are, in their pure state, insensitive to sunlight, since they do not strongly absorb the shorter wavelengths of the sun spectrum ($> 290\text{nm}$) [26]. However, the presence of light absorbing impurities, e.g. hydroperoxides, peroxides, carbonyl compounds and trace levels of metals, arising from commercial production processes, are responsible for the inherent photooxidative shortcomings of commercial polymers such as PE and PP [27]. It is a general consensus that hydroperoxides are by far the most important photoinitiators during the early stages of UV irradiation [26,28]. Since the latter are initially formed during the processing operation (see section 1.2.2), the thermal history of the polymer will be reflected in the outdoor performance of the polymer and will be particularly evident in recycled products. It is generally accepted [26,28] that the chemical processes involved in the photooxidation of polymers and model compounds are basically similar to those occurring during thermal oxidation. The main difference lies in the much more rapid formation of hydroperoxides which are the common initiators of both processes. This is caused by the higher oxygen concentrations present during photooxidation compared to oxidation during processing, where oxygen is excluded as far as practically possible. A consequence of this is an initial higher ratio of alkylperoxyl to alkyl radicals during photooxidation, and at a later stage, the ratio depends on the rate of O_2 diffusion in the solid polymer, i.e. the thickness of the polymer material.

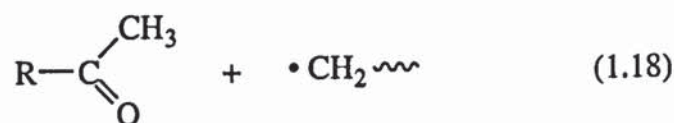
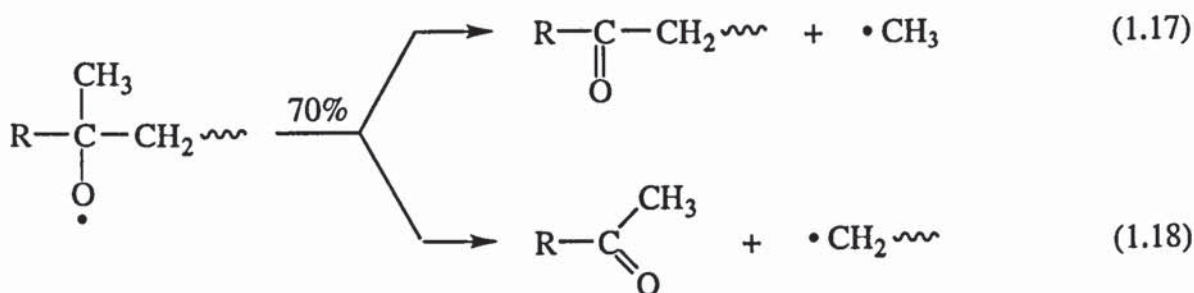
Hydroperoxides undergo photolysis to alkoxy and hydroxyl radicals with concomitant chain scission of the polymer chain and subsequently a build up in carbonyl functions in the polymer (see reactions 1.10 to 1.14).



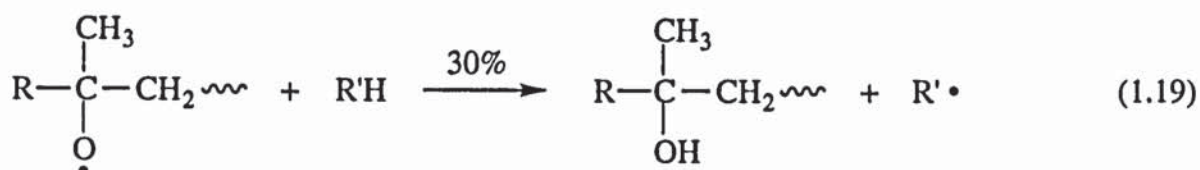
However, hydroperoxides are likely to play a far less prominent role in polyethylene (PE) than they do in PP because secondary hydroperoxides are less stable than tertiary ones. Photo-oxidising PE is therefore found to contain only a very low concentration of hydroperoxides, whereas the concentration of hydroperoxides in PP steadily increases [29]. Furthermore, it has been suggested [30] that chain-branching in PE is counteracted by a fast reaction between the radicals produced by the photocleavage of hydroperoxides with the formation of carbonyl groups (see reaction 1.15).



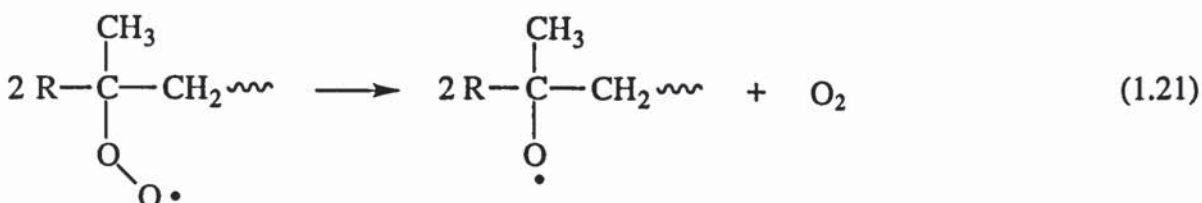
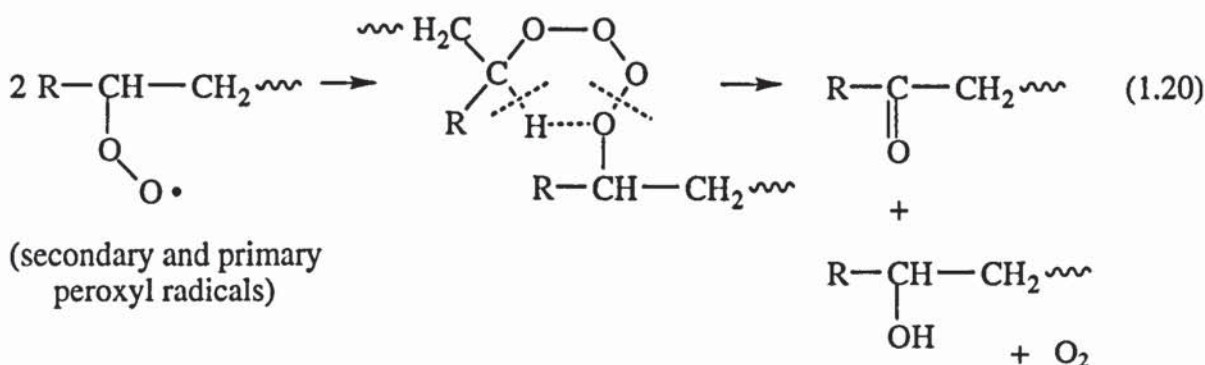
The tertiary hydrogen of the macroalkoxyl radical in reaction 1.15 is assumed to be highly labile. No such labile hydrogen is present in the tertiary hydroperoxides formed in PP, so the radicals cannot destroy each other (reaction 1.16). In the photooxidation of PE, hydroperoxides therefore play a minor part compared with that of carbonyl compounds, which act as initiators upon undergoing the Norrish type I reaction (see scheme 1.4). In PP, the reactive macroalkoxyl radicals formed via reaction 1.16 undergo scission of a β C-C bond to form carbonyl compounds (see reactions 1.17 and 1.18) [31,32].



The reactive PP alkoxy radical may also abstract hydrogen from the PP matrix (reaction 1.19) to form an alcohol [31].



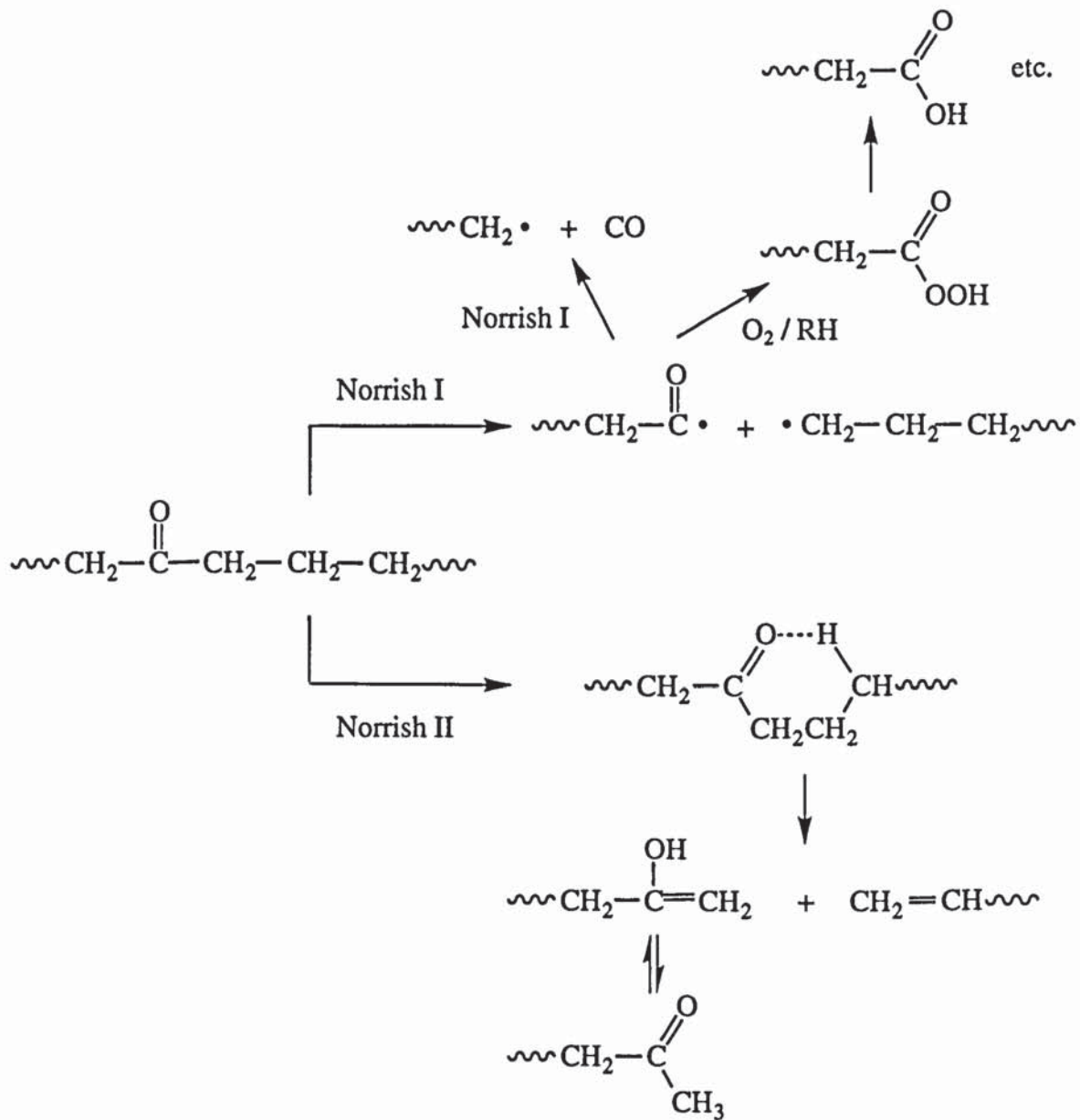
Since oxygen concentrations are initially high during photooxidation, especially in thin films (e.g. for food packaging), the bimolecular termination reaction 1.7 (scheme 1.1) is likely to occur to form ketones and alcohols (see reactions 1.20 and 1.21).



(tertiary peroxy radicals)

In polyolefins hydroxyl groups are formed, for instance, by reactions 1.19 and 1.20, while reactions 1.15, 1.17, 1.18, 1.20 and 1.21 lead to the formation of carbonyl groups. As the concentration of carbonyl compounds builds up in the polymer, they in turn become the centre for further chain scission reactions by carbonyl photolysis. Carbonyl groups can undergo two important photoreactions, the Norrish type I and the Norrish type II processes (scheme 1.4) which both result in chain cleavage [28]. However, in the type I reaction macroalkyl or methyl radicals are formed, whereas the Norrish type II process does not

generate free radicals. Further reactions of the carbonyl radical resulting from the type I process may result in the formation of aldehyde, carboxylic acid and ester, while a second Norrish type I reaction of that radical results in the formation of carbon monoxide (CO).



Scheme 1.4: Photolysis of PE (the Norrish reactions)

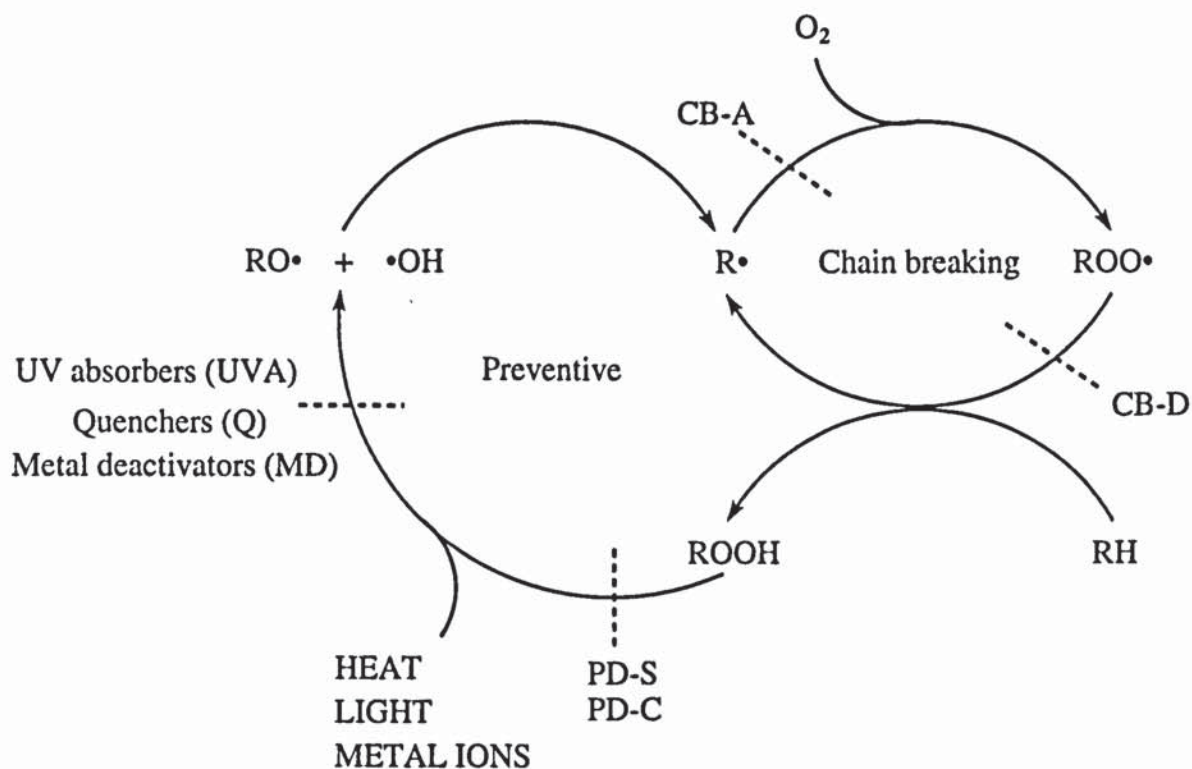
1.3 STABILISATION OF POLYOLEFINS

1.3.1 General mechanisms of antioxidant action

1.3.1.1 Autoxidation and antioxidant classification

The inhibition of polymer oxidation can be achieved by incorporating antioxidants into the polymer system before or during the processing operation. Antioxidants may be classified by the way in which they interfere with the process of autoxidation, i.e. according to their mechanism of action [13,33] as outlined in scheme 1.5. Autoxidation involves two interrelated cyclical processes. In the primary cycle oxygen and hydrocarbons react to give hydroperoxides, which, by homolysis, give rise to new radicals which feed the main cycle. The primary cycle can be interrupted by antioxidants which operate by a chain-breaking mechanism by removing the main propagating radicals $R\cdot$ and $ROO\cdot$. Chain-breaking antioxidants can be further subdivided between electron (and hydrogen) donors (to reduce $ROO\cdot$ to $ROOH$, CB-D), e.g. hindered phenols, and electron acceptors (to oxidise or spin trap $R\cdot$ in the absence of O_2 , CB-A), e.g. quinones.

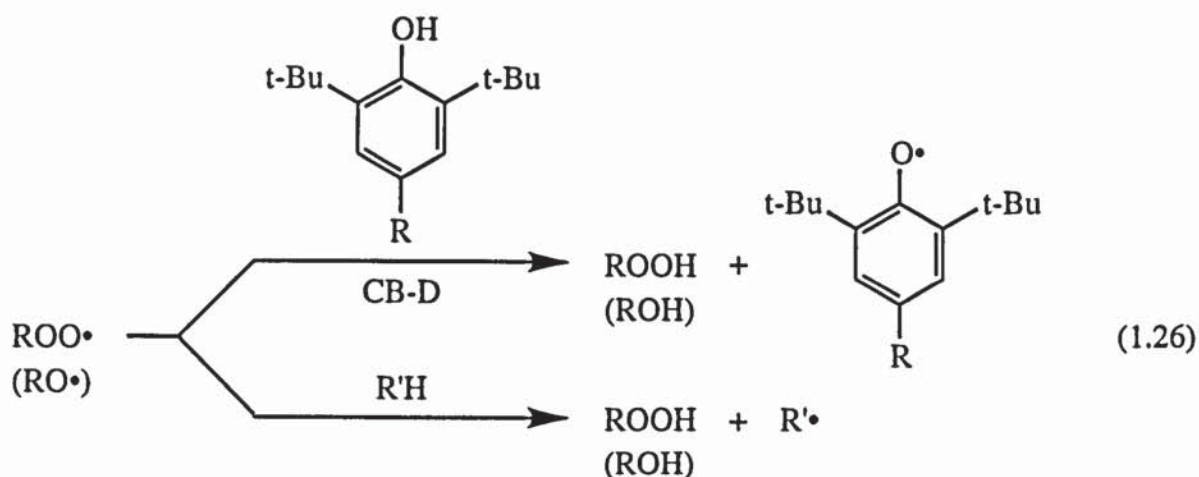
Preventive antioxidants, on the other hand, act by preventing the introduction of the chain-initiating radicals into the polymer system. The most important preventive mechanism, both theoretically and practically, is hydroperoxide decomposition by peroxidolytic antioxidants, in a process which does not involve the formation of free radicals. Peroxidolytic antioxidants fall into two main classes; stoichiometric peroxide decomposers (PD-S), such as phosphite esters which are reagents for the reduction of hydroperoxides to alcohols (see section 1.3.3), and catalytic peroxide decomposers (PD-C) which include a variety of sulphur compounds, as well as cyclic catechol phosphites.



Scheme 1.5: Mechanisms of antioxidant action

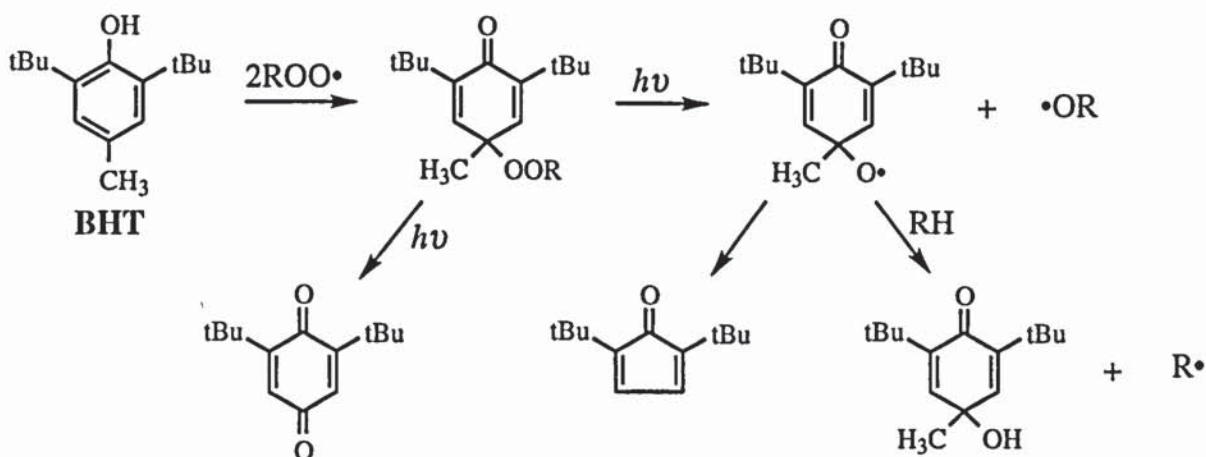
1.3.1.2 The chain-breaking mechanism

The chain-breaking acceptor (CB-A) mechanism has been shown to operate in oxygen deficient systems in polymers where alkyl radicals in the substrate are the reducing species [34]. A variety of quinones, e.g. benzoquinone (UBQ) and diphenoquinone (DPQ) are effective CB-A antioxidants and fall into the same category as polymerisation inhibitors by virtue of their ability to trap alkyl radicals [35]. CB-A antioxidants are therefore in direct competition with oxygen, in reaction with the substrate radical (see reactions 1.22 and 1.23) [36]. The efficiency of reaction 1.22.a depends on the $[R\cdot] / [ROO\cdot]$ ratio, which depends on the oxygen pressure and the oxidisability of the substrate. A high ratio is expected in solid polymers, where the rate of diffusion of oxygen is much slower than in liquid hydrocarbons, i.e. during processing [37]. Because of their structures, benzoquinones also participate to a considerable extent in photochemical processes.



1.3.1.3 Photostabilisation

The major processes in photooxidation involve mainly the formation of hydroperoxides, carbonyl groups, as well as chain scission of the polymer backbone. Conventional thermal antioxidants such as hindered phenols, e.g. BHT (see scheme 1.6 below), are not very effective UV stabilisers. This is because the rapid photodecomposition of the stabiliser is accompanied by the formation of photosensitising products [41] as shown in scheme 1.6 for BHT.



Scheme 1.6: Formation of photosensitisers from phenolic antioxidants

However, they can be protected from photolytic destruction by UV absorbers (UVA), e.g. 2-hydroxybenzophenones and benzotriazoles (see figure 1.1 for structures), which operate primarily by absorbing UV light and dissipating it harmlessly as thermal energy, or

hindered piperidine light stabilisers (HALS), e.g. Tinuvin 770 (see figure 1.1), resulting in powerful synergistic effects [42].

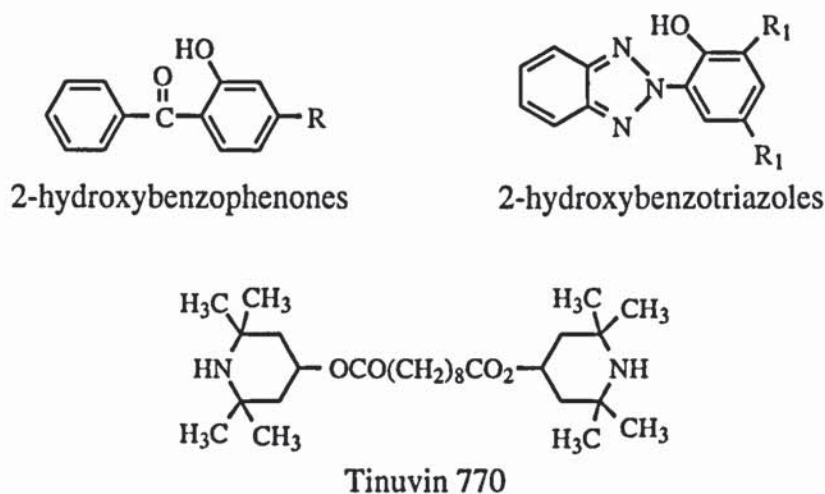
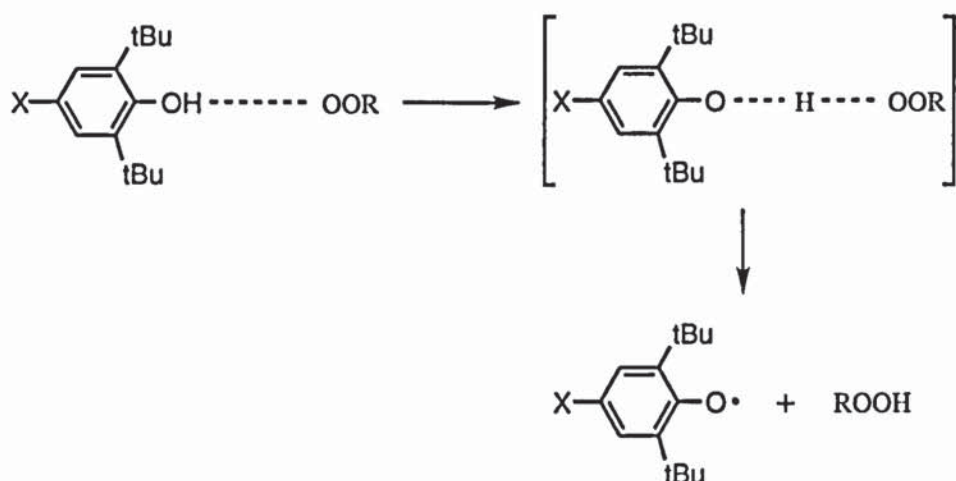


Figure 1.1: Chemical structures of typical UV absorbers and light stabilisers

1.3.2 Hindered phenols as antioxidants

1.3.2.1 Structure and antioxidant activity of hindered phenols

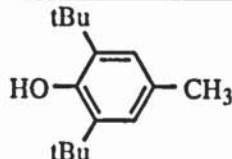
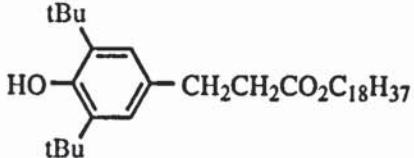
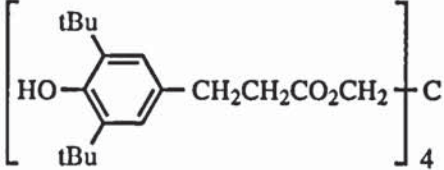
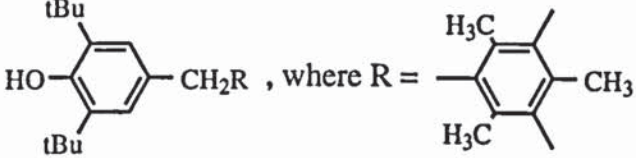
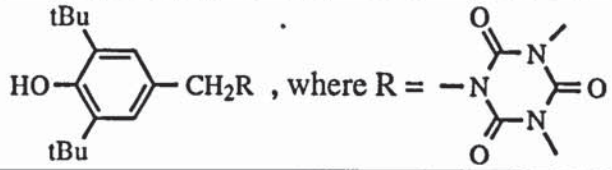
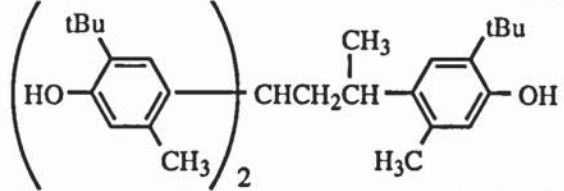
Hindered phenols are an important class of CB-D antioxidants for polyolefins (see reaction 1.26) due to their effective processing and long-term heat stabilising action. The stabilising activity of phenolic antioxidants is strongly dependent on their structure. In general, the transition state for the formation of the phenoxyl radical (reaction 1.26) involves both electron delocalisation and charge separation (see scheme 1.7) [43]. Consequently, groups in the 2, 4 and 6 positions which extend the delocalisation of the unpaired electron (e.g. phenyl or methyl) increase activity. In the *para* position, electron-releasing groups (e.g. R_2N , RNH , RO , R) decrease the energy of the transition state and consequently increase antioxidant activity, whereas electron-attracting groups (e.g. CN , $COOH$, NO_2) decrease activity. The presence of at least one tertiary alkyl group in the *ortho* position is necessary for high antioxidant activity. This steric enhancement is due to the increased stability of the derived phenoxyl radical which reduces the chain transfer reaction.



Scheme 1.7: Transition state in the formation of phenoxy radicals

The simplest substituted phenol meeting the above requirements is BHT (I, see table 1.1 for structure). However, the latter is a relatively volatile antioxidant and is therefore not used in polymers at high temperatures due to its rapid physical loss. To overcome this problem, a variety of higher molecular weight hindered phenols have been developed. Most commercialised phenols have structures of 4-substituted derivatives of 2,6-di-*t*-butyl- or 2-*t*-butyl-6-methylphenol [4], as shown in table 1.1. Systems containing substituted 4-hydroxybenzyl (e.g. Ionox 330, IV, Shell Chemicals, see table 1.1) or 3-(4-hydroxyphenyl)-propionate moieties (e.g. Irganox 1010, III, Ciba Geigy) are favoured.

Table 1.1: Typical commercial hindered phenol antioxidants

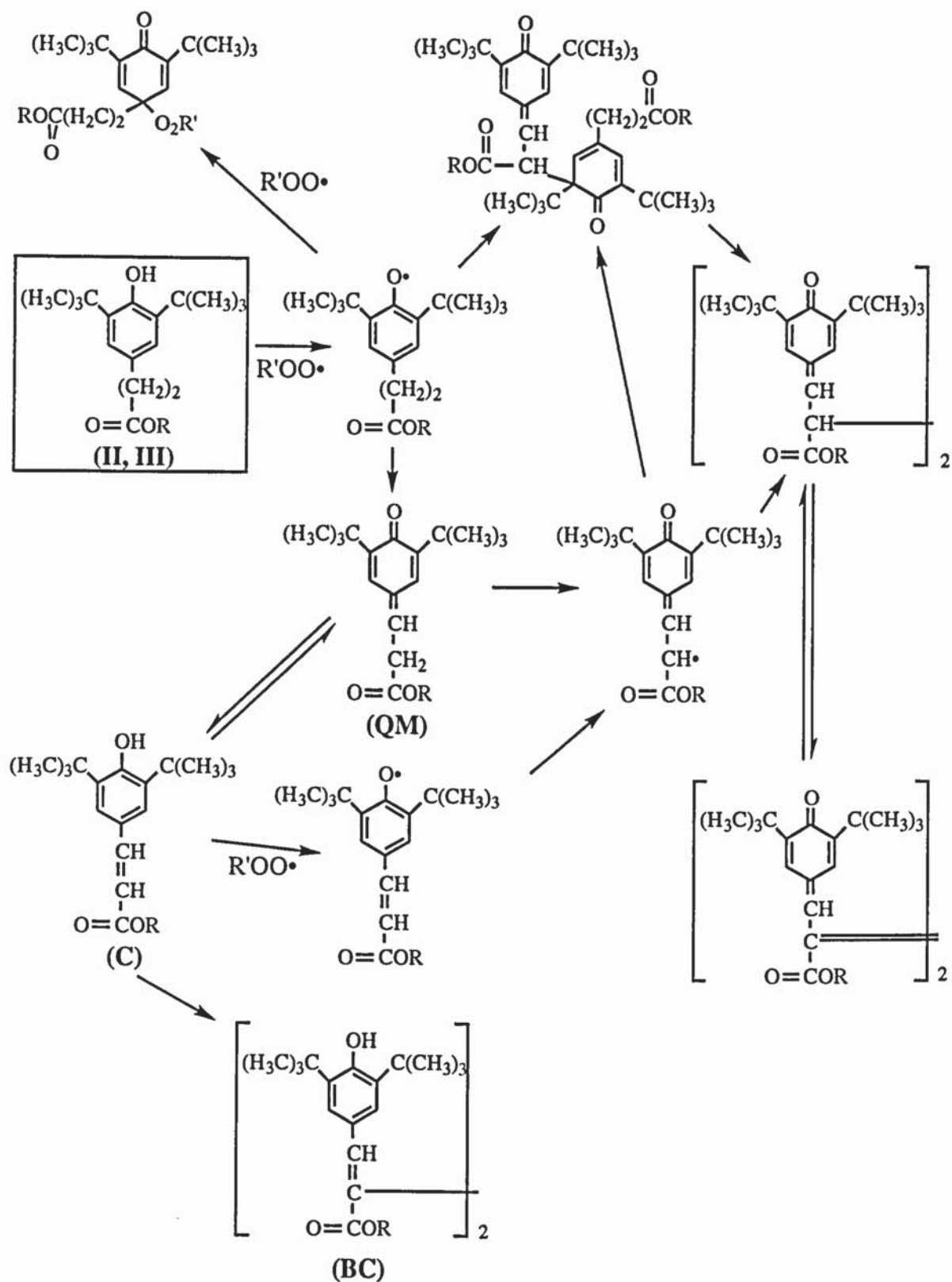
chemical structure	commercial name	code
	BHT	I
	Irganox 1076	II
	Irganox 1010	III
	Ionox 330	IV
	Good-rite 3114	V
	Topanol CA	VI

1.3.2.2 Transformation products of hindered phenols

The high efficiency of systems containing the 4-hydroxyphenyl propionate moiety (e.g. structures II and III in table 1.1) was attributed to the formation of quinone methide (QM) and products of molecular rearrangement and dimerisation [44-49]. Scheme 1.8 shows the mechanism of oxidation of propionate-type phenolic antioxidants [4,50], based on isolated products [44-46] and products formed during processing of PP and PE with Irganox 1076 and Irganox 1010 [47,50,51]. Rearrangements of quinonemethinoid to phenolic structures, e.g. the cinnamate (C) and biscinnamate (BC) structures, having themselves a chain-

breaking action, were used for an explicit explanation of the high efficiency of mono- (e.g. II) and polynuclear (e.g. III) propionate-type phenolic antioxidants [50,52].

A number of transformation products of Irganox 1076 (II) and Irganox 1010 (III) formed during processing and thermal ageing of PP and PE were characterised [47,50,51] and tables 1.2 and 1.3 show some of their structures and MS and UV characteristics if available.



Scheme 1.8: Mechanism of oxidation of propionate-type phenolic antioxidants with peroxy radicals [4,50]

Table 1.2: Nature of transformation products of Irganox 1076 (Irg 1076) formed during processing and thermal ageing with PE and PP

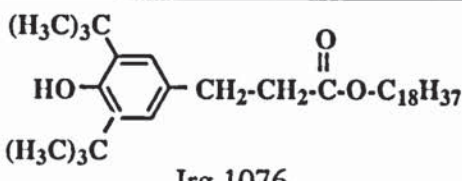
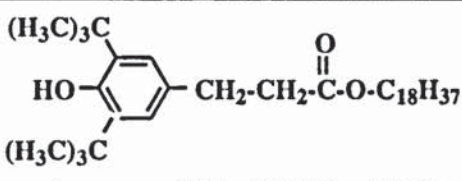
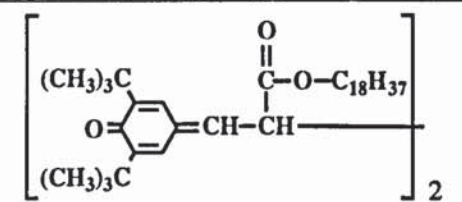
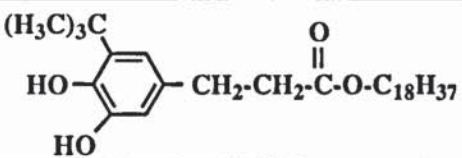
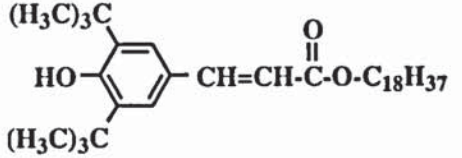
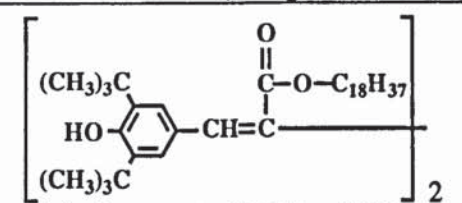
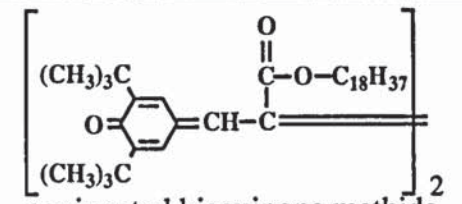
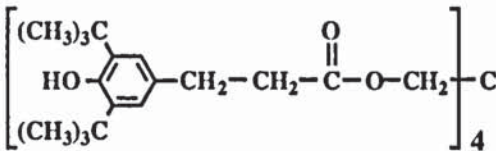
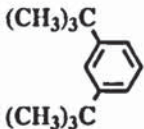
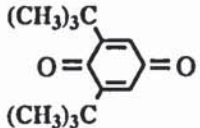
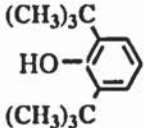
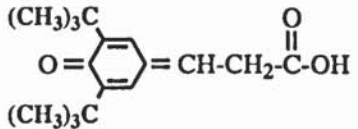
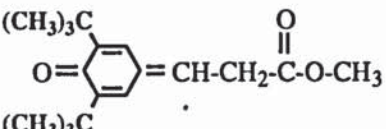
chemical structures and name	oxidation conditions	λ_{\max} , nm (ϵ , l.mol ⁻¹ .cm ⁻¹) M ⁺ , m/z [ref]
 <p>Irg 1076</p>	-	282 (2010) (CHCl ₃) [20] M ⁺ = 530 [53]
 <p>quinone methide (QM-Irg 1076)</p>	PP stabilised with 0.5% Irg 1076 in a Brabender plastograph for 2h at 200°C [51]	316 (26915), 295 (16218) (heptane) [54] M ⁺ = 528 [51]
 <p>unconjugated bisquinone methide (UBQM-Irg 1076)</p>		314 (44870) (CHCl ₃) [20] M ⁺ = 1054 [51]
		M ⁺ = 490 [51]
 <p>cinnamate (C-Irg 1076)</p>	thermal ageing during 1 day at 180°C in an air circulating oven of extruded HDPE stabilised with Irg 1076 [50]	320 [50]
 <p>biscinnamate (BC-Irg 1076)</p>		305 (35400) (CHCl ₃) [20,50]
 <p>conjugated bisquinone methide (CBQM-Irg 1076)</p>		322 (34800) (CHCl ₃) [20,50]

Table 1.3: Nature of transformation products of Irganox 1010 (Irg 1010) formed during processing with PE and PP

chemical structures and name	oxidation conditions	λ_{\max} , nm M^+ , m/z [Ref]
 <p>Irg 1010</p>	-	282 [49] $M^+ = 1176$ [53]
	commercial PP and PE samples containing Irg 1010 and other additives [47]	$M^+ = 162$ [47]
		254 (9100) [20] $M^+ = 220$ [47]
		$M^+ = 206$ [47]
		$M^+ = 276$ [47]
		$M^+ = 292$ [47]

1.3.3 Synergistic effects of hindered organic phosphites

1.3.3.1 General mechanisms of antioxidant action of organic phosphites

Organic phosphites are used on a large scale for the stabilisation of polymers against degradation during processing and long term applications, with the ability to preserve original colour of the polymer. Generally, phosphorous antioxidants are used in combination with hindered phenols and other stabilisers (synergistic effect), but the sterically hindered aryl phosphites are, under some conditions active by themselves. Table 1.4 lists some of the main phosphites industrially used [55].

Table 1.4: Chemical structures of organic phosphites industrially used

chemical structure	code
$P(OPh)_3$	VII
$i-C_{10}H_{21}OP(OPh)_2$	VIII
$(i-C_{10}H_{21}O)_2POPh$	IX
$P\left(O-\text{C}_6\text{H}_4-\text{C}_9\text{H}_{19}\right)_3$	X
$P\left(O-\text{C}_6\text{H}_3(\text{C}(\text{CH}_3)_3)_2-\text{C}(\text{CH}_3)_3\right)_3$	XI (Irgafos 168)
$C_{18}H_{37}O-P\left(O\right)_2-O-C(CH_2)_2-C(CH_2)_2-O-P\left(O\right)_2-OC_{18}H_{37}$	XII
$(H_3C)_3C-C_6H_3(C(CH_3)_3)_2-O-P\left(O\right)_2-O-C(CH_2)_2-C(CH_2)_2-O-P\left(O\right)_2-O-C_6H_3(C(CH_3)_3)_2-C(CH_3)_3$	XIII (Ultranox 626)
$\text{C}_6\text{H}_4\text{O}_2-P\left(O\right)_2-O-C_6H_3(C(CH_3)_3)_2-CH_3$	XIV

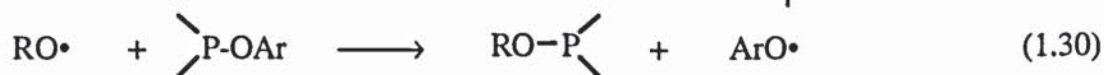
Phosphites are peroxidolytic antioxidants which primarily decompose hydroperoxides stoichiometrically (PD-S) in a non-radical process [56] (see reaction 1.28), suppressing the chain-branching step (1.4) in the familiar radical chain mechanism of autoxidation depicted in scheme 1.1. The phosphite reduces hydroperoxides to give alcohols and the corresponding phosphate.



The reactivity of the phosphites towards peroxides is governed mainly by polar and steric effects of the groups bound to phosphorus [55,57,58], decreasing with increasing electron-acceptor ability and bulk of substituent group in the order:



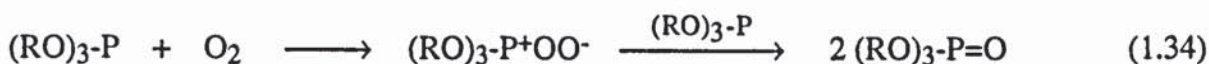
Depending on their structure, aryl phosphites may also act as chain-breaking antioxidants [55], competing with steps (1.3) and (1.5) in scheme 1.1 by trapping RO_2^\cdot and RO^\cdot radicals, hence terminating the oxidative chain reaction, as shown in scheme 1.9.



Scheme 1.9: Mechanism of chain-breaking antioxidant action of organic phosphites

Phosphites with open-chain sterically hindered aryl groups (e.g. structures X, XI and XIII in table 1.4) can act as chain-breaking antioxidants [55,56] by reducing alkyl peroxy radicals to alkoxy radicals (step 1.29 in scheme 1.8), which further react with the

phosphites by substitution, releasing aryloxy radicals (step 1.30) which terminate the oxidation chain reaction (step 1.31). Alkyl phosphites, on the other hand, are not able to react in that way because they are oxidised by alkoxy radicals giving alkyl radicals which propagate the chain reaction (steps 1.32 and 1.33). Phosphites can also react with oxygen at high temperatures [59] as shown in reaction 1.34.



Some phosphite esters which are derived from catechol (e.g. structure XIV in table 1.4) were shown to act by a catalytic mechanism (PD-C) [55,57].

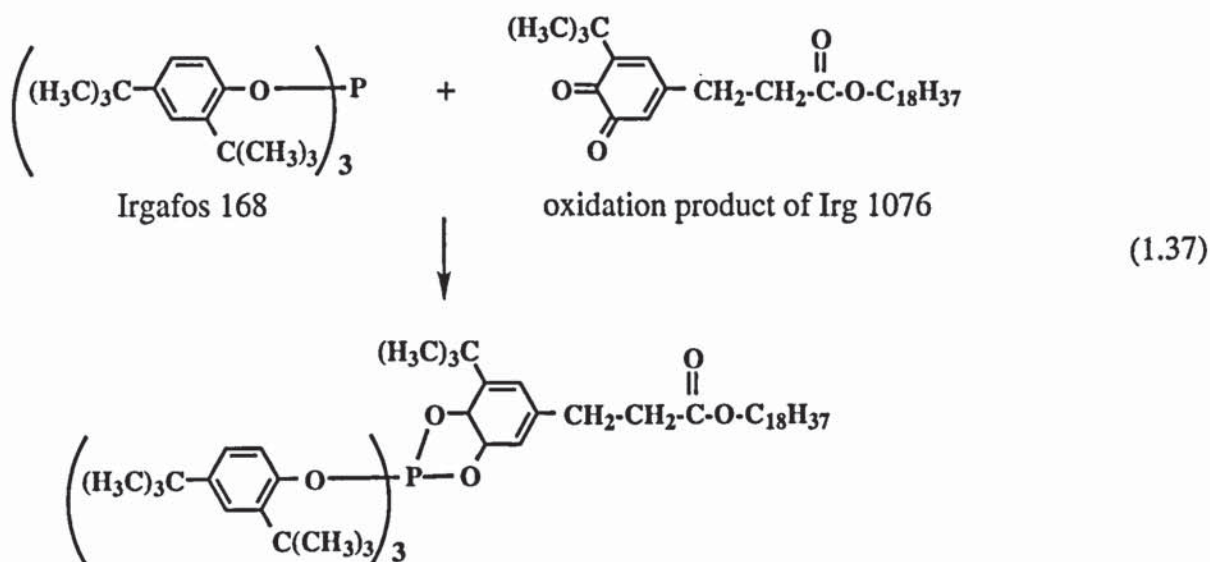
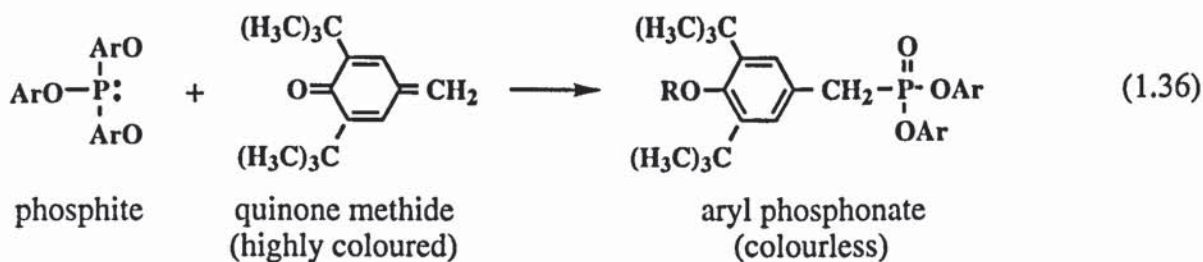
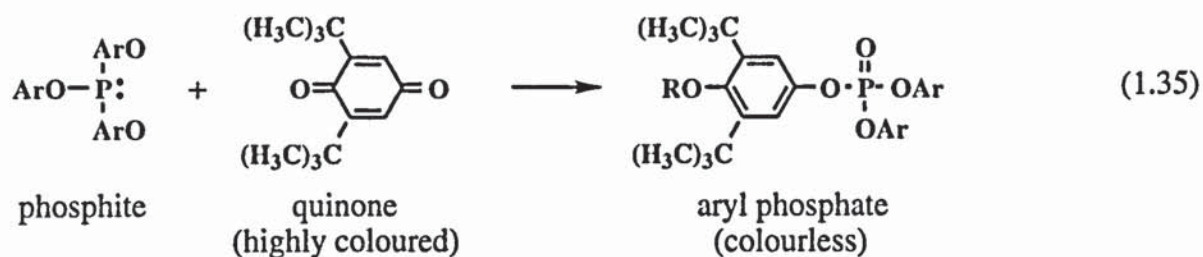
1.3.3.2 Synergistic effects of organic phosphites with hindered phenols

Organic phosphites enhance the antioxidant effect of phenols and reduce discolouration of polymers caused by phenol transformation products. It was reported [25] that the optimum ratio of a phenolic antioxidant like Irg 1076 or Irg 1010 (II and III, see table 1.1 for structures) to tris-(2,4-di-*tert*-butylphenyl)-phosphite (Irgafos 168, XI) in melt stabilisation was 1:4 in HDPE and LDPE and 1:2 in PP. It was shown [25] that during processing of HDPE with an added phenolic antioxidant at 220°C, in the absence of a phosphite stabiliser, as much as 45% of the phenolic antioxidant was consumed after one extrusion pass. In contrast, in the presence of a phosphite stabiliser, only 20% of the antioxidant was consumed after the first extrusion pass. Therefore, one of the major roles of the phosphite is the preservation of the hindered phenol. Mechanistic product studies with these synergistic combinations are mostly lacking.

1.3.3.3 Mechanisms of colour stabilisation of polymers by organic phosphites

Organic phosphites are known to have a substantial advantage over typical stabilisers (e.g. phenols) in preserving the initial colour of the polymer throughout the process of degradation. Various oxidation products (generally with a quinonoidal structure) of

phenolic antioxidants play a significant part in the process of discolouration of polyolefins. The phosphites disrupt the conjugated π -electron systems of the quinone derivatives rendering them colourless [50,51]. Reactions 1.35 and 1.36 show the reactions of an aromatic phosphite with quinone and quinone methide (both of which are highly coloured) to produce the colourless aryl phosphate and colourless aryl phosphonate, respectively [50]. Reaction 1.37 shows the reaction of Irgafos 168 (see table 1.4 for structure) with an oxidation product of Irg 1076 formed during thermal ageing of PP at 150°C [51].



It has also been suggested that the phosphite stabilisers can react with unsaturation and thus disrupt the polyene sequences in the backbone of oxidised PE and hence minimise colour [60].

1.3.4 Ecological acceptability of phenolic antioxidants

A steadily increasing public pressure requiring the removal of hazards arising from the toxicity and/or biological activity of our chemical environment also involves phenolic stabilisers. The latter may be administered to human beings after extraction from stabilised packaging materials (e.g. food packaging plastics, children's toys, packaging materials for pharmaceuticals and other medical applications). In the case of food packaging applications, migration of antioxidants and their transformation products into food represents a major source of contamination of the packaged food. Health authorities in Europe, USA and many other countries have strict regulations to control the use of additives (e.g. antioxidants) in plastics used for food packaging [61-63]. Existing regulations stipulate that packaging materials must not alter the quality of food and that additives must have toxicity clearance and approval of their use. However, the shortcomings of these regulations lie in the fact that although parent antioxidants may have toxicity clearance, the chemical nature, migration behaviour and toxicity effects of their transformation products (mainly formed during processing) still remain either unknown or uncertain.

An increase in the physical persistence of stabilisers expressed as a drastic reduction of extractability into the surrounding environment represents one possibility of the solution of toxicity problems., e.g. macromolecular stabilisers and antioxidants bound to the polymer [64]. Another potential approach consists of application of suitable phenolic substances of plant origin or their synthetic analogues, considered to be "environment friendly". The excellent antioxidant properties of Vitamin E in biological systems triggered the serious interest in its application in polymer stabilisation. Unlike commercial hindered phenols, synthetic Vitamin E can be considered as a safe and non-toxic stabiliser and is therefore

ideally suited for food packaging plastics, e.g. polyolefins. α -tocopherol, the most biologically active form of Vitamin E, is a permitted food antioxidant (E346).

1.4 VITAMIN E AS A CHAIN-BREAKING ANTIOXIDANT

1.4.1 Structure and antioxidant activity of α -tocopherol

Vitamin E, a well known biological antioxidant in living systems [65,66], is a mixture of closely related tocopherols which differ from one another only in the number and positions of the methyl groups in the aromatic ring (see figure 1.2), and it is mainly found in vegetable oil [65,67]. In living systems, Vitamin E, present in cell membranes, protects polyunsaturated lipids and fatty acids from the damaging effects of peroxidation. The biological activity of α -tocopherol is known to be the highest.

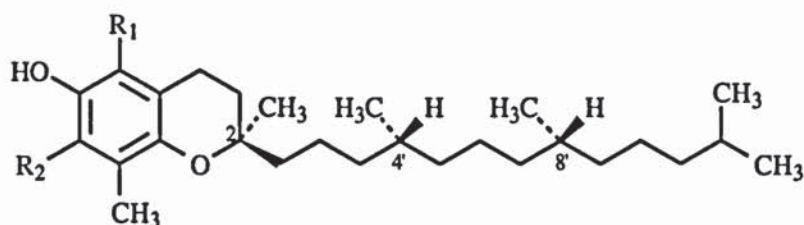


Figure 1.2: Stereochemical structures of natural Vitamin E

RRR- α -tocopherol: R₁ = CH₃, R₂ = CH₃

RRR- β -tocopherol: R₁ = CH₃, R₂ = H

RRR- γ -tocopherol: R₁ = H, R₂ = CH₃

RRR- δ -tocopherol: R₁ = H, R₂ = H

On the other hand, synthetic Vitamin E [68], also called all-rac- α -tocopherol or dl- α -tocopherol, exists as a mixture of equal amounts of all eight possible optical isomers of α -tocopherol [69]. The synthesis is based on the acid-catalysed condensation of 2,3,6-trimethyl-hydroquinone with all-rac-isophytol [70]. The isomers are four pairs of diastereomeric enantiomers with the following structures:

1) 2R, 4'R, 8'R- and 2S, 4'S, 8'S- α -tocopherol

2) 2R, 4'R, 8'S- and 2S, 4'S, 8'R- α -tocopherol

3) 2R, 4'S, 8'R- and 2S, 4'R, 8'S- α -tocopherol

4) 2R, 4'S, 8'S- and 2S, 4'R, 8'R- α -tocopherol

In living systems, lipid peroxidation is a phenomenon of liquid phase oxidation which involves the same elementary reaction steps as hydrocarbon oxidation, i.e. initiation,

propagation and termination [65,71], as described in section 1.2.2 (see scheme 1.1). The initial free radicals are produced from a precursor molecule, e.g. a metal ion catalysed decomposition of a lipid hydroperoxide [65]. Rate constants of antioxidant activity for α -tocopherol, which is structurally similar to many hindered phenols, tocopherol derivatives and commercial hindered phenols have been extensively evaluated in vitro [65,72-78] showing that α -tocopherol is of the best chain-breaking antioxidant known, and far better than commercial antioxidants, e.g. BHT (see figure 1.3 for structures).

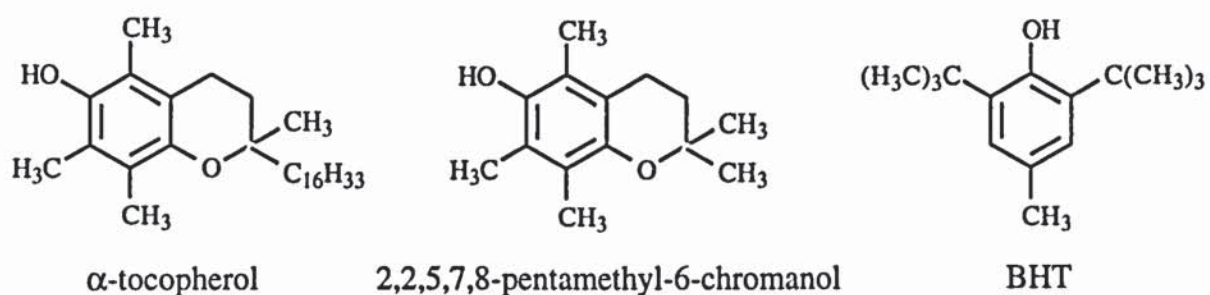


Figure 1.3: Chemical structures of α -tocopherol, its model and BHT

On the basis of X-ray structural determinations carried out on the α -tocopherol model, 2,2,5,7,8-pentamethyl-6-chromanol (see figure 1.3 for structure), the high reactivity of α -tocopherol for trapping peroxy radicals was attributed to stereoelectronic effects [72,73,79]. The heterocyclic ring ensures that the 2p-type lone pair of electrons on the ring oxygen adopts an orientation more or less perpendicular to the plane of the aromatic ring, stabilising the tocopheroxyl radical (see figure 1.4, A). This effect was enhanced with the five-membered ring in 2,3-dihydro-2,2,4,6,7-pentamethylbenzofuran where the nearly flat ring provides better overlap of the ring oxygen p orbital with the aromatic system (see figure 1.4, B) [65,77-79]. Indeed, X-ray analysis showed that the deviation from perfect coplanarity in the phenoxyl was only 6° as opposed to 16° in the α -tocopherol model.

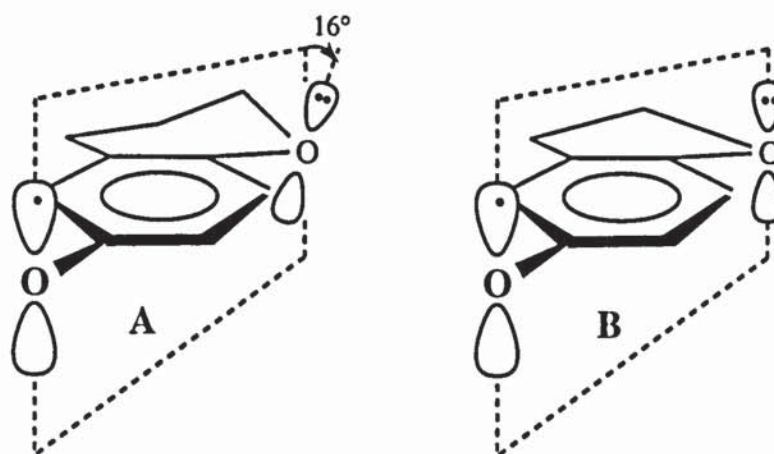
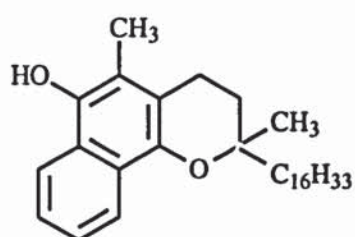
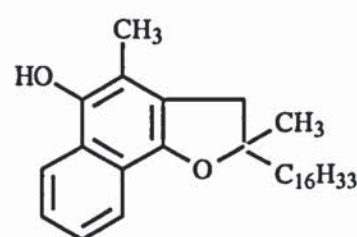


Figure 1.4: p-orbital orientation in the puckered tocopheroxyl radical (A) compared to the flatter dihydrobenzofuran phenoxyl radical (B)

Furthermore, the vitamin K₁ chromanol, 6-hydroxy-2,5-dimethyl-2-phytyl-7,8-benzochroman (see figure 1.5 for structure), was found to be 4 times more active than α -tocopherol [78-79]. It was suggested that the fused aromatic ring further delocalises the unpaired electron in the aryloxy radical and hence raises the antioxidant activity. Finally the antioxidant activity of the five membered analogous α -tocopherol derivative with a fused aromatic ring, 2,3-dihydro-5-hydroxy-2,4-dimethyl-2-phytylnaphtho[1,2-*b*]furan (see figure 1.5 for structure), was found to be 2.5 times better than the vitamin K₁ chromanol and 10 times better than α -tocopherol [79].



6-hydroxy-2,5-dimethyl-2-phytyl-7,8-benzochroman (Vitamin K₁ chromanol)



2,3-dihydro-5-hydroxy-2,4-dimethyl-2-phytylnaphtho[1,2-*b*]furan

Figure 1.5: Chemical structures of analogous α -tocopherol derivative antioxidants

The higher reactivity of α -tocopherol compared to β , γ and δ -tocopherol was attributed to the aromatic *o*-methyl groups which stabilise the phenoxyl [65,73,75-76]. The antioxidant activity was found to decrease in the order α - > β - \geq γ - > δ -tocopherol.

1.4.2 Nature of oxidation products and mechanism of oxidation of Vitamin E in model systems

Unlike commercial hindered phenol antioxidants like Irganox 1076 and Irganox 1010 (see table 1.1), the mechanism of oxidation of α -tocopherol in hydrocarbon polymers has not been investigated. However, considerable interest in the antioxidant action of Vitamin E in food, e.g. oils, and cell membranes has led to numerous investigations. α -tocopherol and its model compound 2,2,5,7,8-pentamethyl-6-chromanol (see figure 1.3) have been oxidised with various oxidising agents and a number of oxidation products have been identified and examined themselves for their antioxidant activity. Two main classes of antioxidants were used. The first class consisted of strong oxidising agents like FeCl_3 , AgNO_3 and $\text{K}_3\text{Fe}(\text{CN})_6$, whereas the second class included generated alkylperoxyl radicals. Tables 1.5 and 1.6 show the reaction conditions for the oxidations or reductions of all-*rac*- α -tocopherol (all-*rac*-Toc), RRR- α -tocopherol (RRR-Toc), their model 2,2,5,7,8-pentamethyl-6-chromanol (Toc model) and identified α -tocopherol and Toc model oxidation products. Table 1.7 reveals the corresponding structures, code names and UV characteristics of the identified products.

Tables 1.5 and 1.6 show that the nature and distribution of oxidation products varies dramatically with the reaction conditions. Table 1.5 shows that under the influence of metal ions like Ag^+ and Fe^{3+} , in the presence of polar solvents, Toc (all-*rac*, RRR and Toc model) yielded mainly quinonoid products, whereas $\text{K}_3\text{Fe}(\text{CN})_6$ under alkaline conditions and in a non-polar solvent oxidised Toc to dimers and trimers as major products. On the other hand, peroxyl radicals derived from the thermolysis of azobis(isobutyronitrile) (AIBN) or azobis(2,4-dimethylvaleronitrile) (AMVN), in protic solvents (e.g. ethanol),

oxidised Toc to 8 α -substituted epoxides and tocopherones, whereas the same radicals in unpolar solvents lead also to dimers of Toc. The influence of the solvent on the distribution of oxidation products of Toc model with peroxy radicals derived from AMVN was studied [80] and it was found that the least polar solvent (cyclohexane) favoured the formation of dimers, whereas the most polar solvent (acetonitrile) lead mainly to 8 α -substituted chromanones and epoxychromanones. Methyl linoleate on its own, at slightly elevated temperatures (37°C) lead to two trimers of RRR- α -tocopherol [81] (TRI 1 and TRI 2), which are diastereomers, differing in the configurations at chiral centres 21 and 22 (see table 1.7 for structure and positions). Under the influence of oxygen and heat, in unpolar solvents, dimers, trimers, as well as quinones and aldehydes are formed [82,83]. Reactions on oxidation products of Toc (All-rac, RRR and model, see table 1.6) [84,85] have shown that SPD can be formed from DHD with $K_3Fe(CN)_6$ and that interconversion between SPD, Toc and TRI, DHD can take place under the influence of heat. It was suggested that SPD and TRI can be formed, as depicted in scheme 1.9, via a quinone methide (QM) or via DHD or both pathways simultaneously. ESR measurements have shown that the formation of the α -tocopheroxyl radical is the first step in the oxidation of Toc with PbO_2 in toluene (see scheme 1.10) [86,87].

Table 1.5: Products of oxidation of all-rac-Toc, RRR-Toc and Toc model, with various oxidising agents (see table 1.7 for structures and code names)

substrate	oxidising agent	conditions	products	reference
all-rac-Toc (1g)	FeCl ₃ (10g)	CH ₃ OH, 50°C, 2h	TQ, TR, TP	88, 89
Toc model	FeCl ₃	CH ₃ OH, reflux, 5h	TAQ, TRI, Toc	82
all-rac-Toc (1.1g)	FeCl ₃ (5g)	CH ₃ OH, 18-20°C, 30min	TQ (92%)	83
all-rac-Toc (25g)	AgNO ₃ (32g)	C ₂ H ₅ OH + H ₂ O, RT, 40min,	TQ (25.3g, 98%)	90
Toc model (105mg, 0.48mmol)	AgNO ₃ (358mg, 2.11mmol)	C ₂ H ₅ OH, 65°C, 2h	TP, TRD, TR, HM-TR	91
Toc model (50mg)	AgNO ₃ (500mg)	C ₂ H ₅ OH, 60°C, 3h	TQ, TR, EM-γ-Toc	92
all-rac-Toc (11g)	K ₃ Fe(CN) ₆ (32.6g) in KOH	isooctane, RT, 3min	TRI, 1 and 2, SPD	84
Toc model	K ₃ Fe(CN) ₆ (3 equivalent) in KOH	isooctane, RT, 10min	TRI, SPD	
Toc model	K ₃ Fe(CN) ₆ (3 equivalent) in NaOH	hexane, RT, 30min	TAQ, ALD 1, TRI, SPD, DHD	82
all-rac-Toc (1.1g)	K ₃ Fe(CN) ₆ (3g) in KOH	hexane, 18-20°C, 1h	SPD (68%)	83
Toc model (560mg)	K ₃ Fe(CN) ₆ (3.26g) in KOH	hexane, RT, 10min	SPD	80
Toc model (1g)	Zn(CN) ₂ (2g), 6N HCl	dry ether, dry HCl gas, 24h	ALD 1	93
RRR-Toc (22mg)	Ag ₂ O (1g)	methyl iodide	SPD (95%)	94
all-rac-Toc (1g)	TMAO (500mg)	liquid paraffin, N ₂ , 180°C, 2h	ALD 1, ALD 2, ALD 3, DHD, Toc	95
all-rac-Toc (2g)	AIBN (1g)	benzene, reflux, 16h	AIBN-Toc adduct, DHD, Toc	96
Toc model (1g)	AIBN (0.5g)	benzene, reflux, 17h	AIBN-Toc adduct, DHD, Toc	
RRR-Toc (1.29g, 3mmol)	AMVN (3.72g, 15mmol)	C ₂ H ₅ OH, 37°C, 34h, air	CR 1, AMVN-Toc adduct 1, ECR 1, ECR 2	97

Table 1.5: continued

substrate	oxidising agent	conditions	products	reference
Toc model (10mg, 45.5 μ mol)	AMVN (40mg, 161 μ mol)	60°C, cyclohexane, C ₆ H ₆ , isopropyl ether, ethyl acetate, tetrahydrofuran, acetonitrile	AMVN-Toc adduct 1, ECR 3, SPD, DHD, TQ	80
RRR-Toc (1.0g)	methyl linoleate (3.0g)	37°C, 30h, dark	TRI 1 and 2	81
Toc model (0.60g)			TRI	
RRR-Toc (0.2g, 0.46mmol)	methyl linoleate (10g 34mmol), AMVN (2.0g, 8.1mmol)	37°C, 30h, dark	AMVN-Toc adduct 2, ML-Toc adducts 1 and 2, SPD, TRI	98
Toc model (20g)	O ₂ bubbling (50ml.min ⁻¹)	heptane, 90°C, 40 days	TAQ, ALD 1, DHD, SPD, TRI, Toc	82
	O ₂ atmosphere (air bubbling, 100ml.min ⁻¹)	nonane, 50°C, dark, 40 days	TQ, TQ-Toc dimer, SPD, TRI	83

Table 1.6: Products of oxidation or reduction of transformation products of all-rac-Toc and RRR-Toc, with various agents (see table 1.7 for structures and code names)

substrate	oxidising/ reducing agent	conditions	products	reference
all-rac-SPD (860mg)	LiAlH ₄ (1.5g)	diethylether, reflux, 30min	DHD	84
all-rac-SPD + Toc (equimolar mixture)	-	isooctane, reflux, 2h	TRI, DHD, Toc	
SPD model (150mg)	ascorbic acid (1g)	C ₂ H ₅ OH + H ₂ O, RT, overnight	DHD (110mg)	
SPD + Toc models (equimolar mixture)	-	benzene, RT, overnight	TRI, DHD	
DHD model (15mg)	K ₃ Fe(CN) ₆ (90mg) in NaOH	petroleum ether, RT, 10min	SPD	
RRR-TRI 1 and 2	5% HCl in CH ₃ OH	benzene, 100°C, 3h, sealed tube	DHD, MM-γ-Toc	81
all-rac-SPD (0.43g)	conc. HCl in 10ml C ₂ H ₅ OH	C ₂ H ₅ OH, 40°C, 30min	TQ-Toc dimer (65%)	83
all-rac-TQ (1.1mmol)	ZnCl ₂ (2.2moles)	toluene, reflux, 3h	TAQ (70%)	

Table 1.7: Chemical structures of oxidation products of all-rac-Toc, RRR-Toc and Toc model

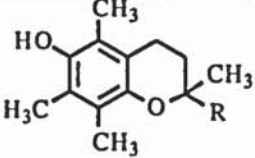
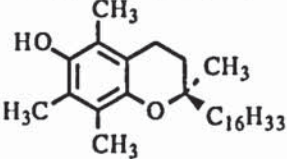
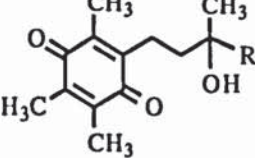
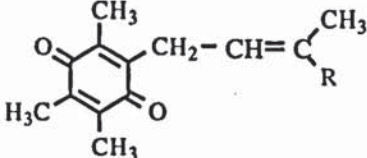
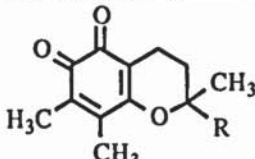
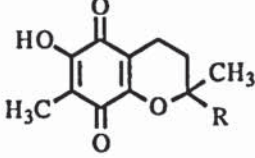
code name	chemical structure / name	λ_{\max} , nm (ϵ , l.mol ⁻¹ .cm ⁻¹) / solvent / colour [Ref]
all-rac-Toc (R = C ₁₆ H ₃₃) Toc model (R = CH ₃)	 <p>all-rac-α-tocopherol (R = C₁₆H₃₃) 2,2,5,7,8-pentamethyl-6-chromanol (R = CH₃)</p>	R = C ₁₆ H ₃₃ : 298 (3650) / hexane [99], R = CH ₃ : 295 (3420) / hexane [81]
RRR-Toc	 <p>RRR-α-tocopherol</p>	298 (3650) / hexane [99]
TQ	 <p>all-rac-α-tocoquinone (R = C₁₆H₃₃) 2-(3-hydroxy-3-methylbutyl)-3,5,6-trimethyl-1,4-benzoquinone (R = CH₃)</p>	R = C ₁₆ H ₃₃ : 268 (15340), 260 (14990) / methanol / yellow oil [83]
TAQ	 <p>all-rac-α-allyl-tocoquinone (R = C₁₆H₃₃) 3,5,6-trimethyl-2-(2-butene-3-methyl)-1,4-benzoquinone (R = CH₃)</p>	R = C ₁₆ H ₃₃ : 265.9 (486.0), 257.5 (483.0) / methanol / yellow oil [82]
TR	 <p>all-rac-α-tocored (R = C₁₆H₃₃) 2,2,7,8-tetramethylchroman-5,6-dione (R = CH₃)</p>	R = C ₁₆ H ₃₃ : 270, 438 / hexane / dark red oil [91]
TP	 <p>all-rac-α-tocopurple (R = C₁₆H₃₃) 2,2,7-trimethyl-6-hydroxy-5,8-chromanquinone (R = CH₃)</p>	R = C ₁₆ H ₃₃ : 295 (14400) / methanol / orange oil [91]

Table 1.7: continued

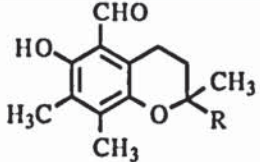
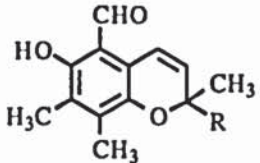
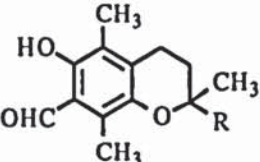
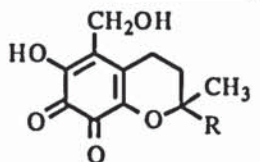
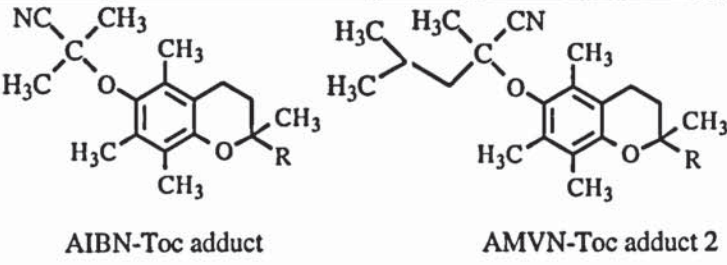
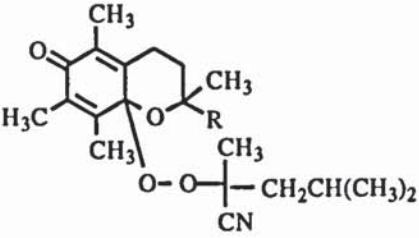
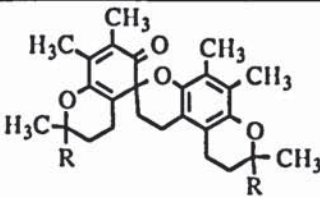
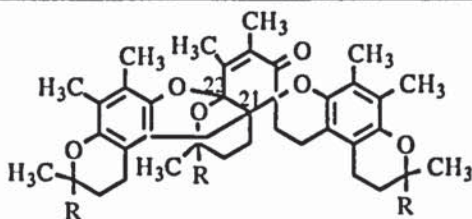
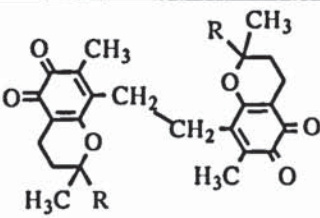
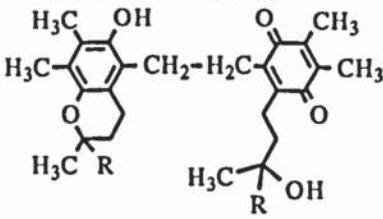
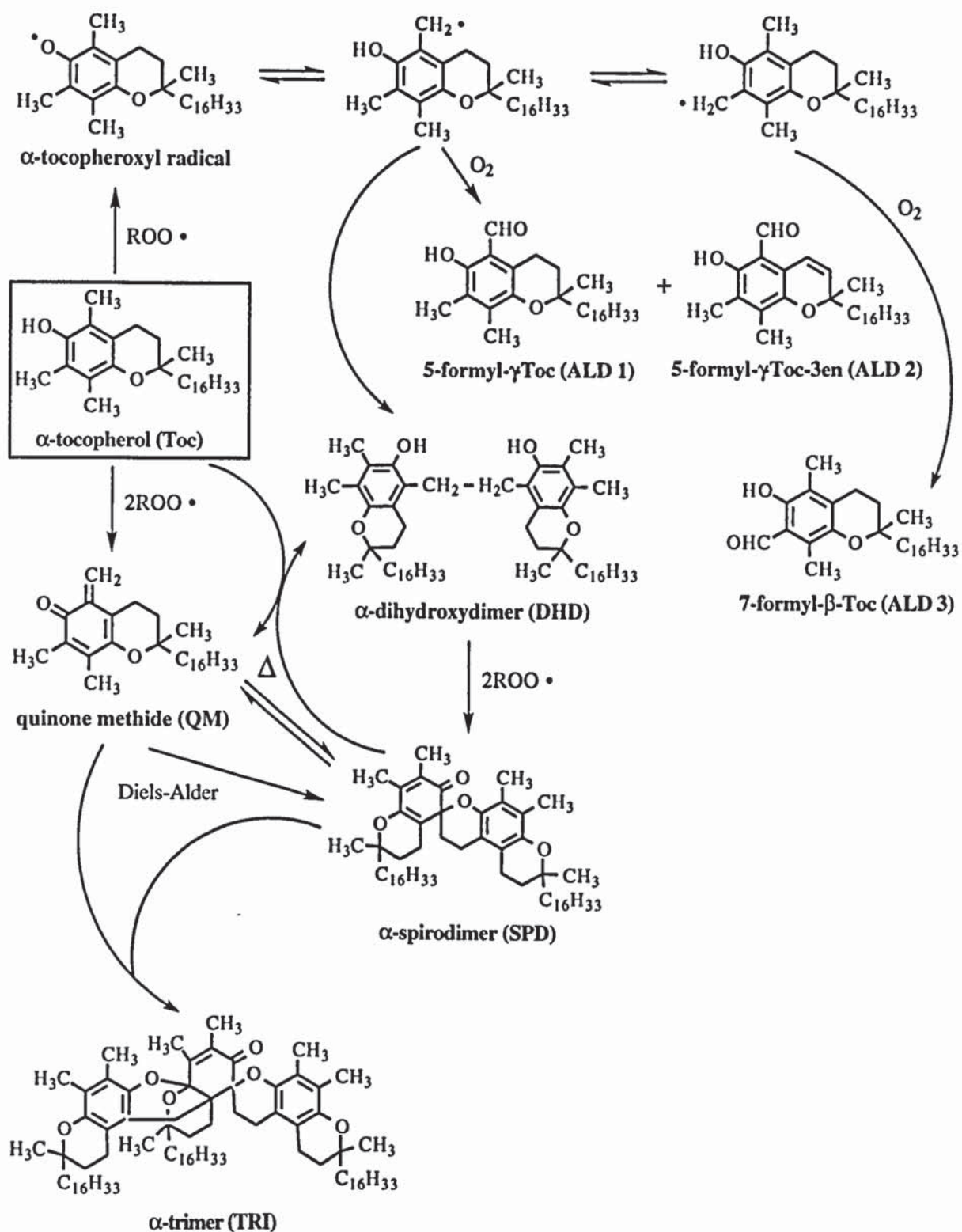
code name	chemical structure / name	λ_{\max} , nm (ϵ , l.mol ⁻¹ .cm ⁻¹) / solvent / colour [Ref]
ALD 1	 <p>all-rac-5-formyl-γ-tocopherol (R = C₁₆H₃₃) 2,7,8-pentamethyl-5-formyl-6-chromanol (R = CH₃)</p>	R = C ₁₆ H ₃₃ : 239, 287 (13610), 391 (4200) / ethanol / orange oil [95]
ALD 2	 <p>all-rac-5-formyl-γ-tocopherol-3en (R = C₁₆H₃₃) 2,7,8-pentamethyl-3en-5-formyl-6-chromanol (R = CH₃)</p>	R = C ₁₆ H ₃₃ : 243, 249, 289~296 (11560), 412 (3720) / ethanol [95]
ALD 3	 <p>all-rac-7-formyl-β-tocopherol (R = C₁₆H₃₃) 2,5,8-pentamethyl-7-formyl-6-chromanol (R = CH₃)</p>	R = C ₁₆ H ₃₃ : 241, 283 (10670), 395 (2870) / ethanol [95]
HM-TR		268, 434 / hexane [91]
AIBN-Toc, AMVN-Toc 1 and 2 adducts	 <p>AIBN-Toc adduct AMVN-Toc adduct 2</p>  <p>AMVN-Toc adduct 1</p>	

Table 1.7: continued

code name (commercial name)	chemical structure / name	λ_{\max} , nm (ϵ , l.mol ⁻¹ .cm ⁻¹) / solvent / colour [Ref]
SPD	 <p>α-spirodimer (R = C₁₆H₃₃, all-rac and RRR) 1,8,9,10-tetrahydro-2',2',5,6,7',8,8,8'-octamethyl-spiro [benzo[1,2-<i>b</i>:4,3-<i>b'</i>] dipyrano-3(2<i>H</i>),5'(6'<i>H</i>)-chroman]-6'-one (R = CH₃)</p>	R = C ₁₆ H ₃₃ (all-rac): 300 (4800), 337 (2400) / isooctane [84], R = C ₁₆ H ₃₃ (RRR): 300 (4600), 337 (1900) / isooctane [100], 301 (4600), 338 (1970) / hexane [94] / yellow oil
TRI	 <p>α-trimer (R = C₁₆H₃₃, all-rac and RRR) 1,1',2',3',8,9,9',10,10',12'-decahydro-3',3',5,5',6,6',8,8,10',10',13',14'-dodecamethyl-spiro [benzo[1,2-<i>b</i>:4,3-<i>b'</i>] dipyrano-3(2<i>H</i>),16'(11<i>a</i>,7<i>a</i>) [1]buteno[8<i>H</i>]dipyrano[3,2-<i>b</i>:3',2'-<i>f</i>] [1]benzopyran]-chroman]-6'-one (R = CH₃)</p>	R = C ₁₆ H ₃₃ (all-rac): TRI 1 (21,22:RR): 294 (7600), TRI 2 (21,22:SS): 294 (6900) / isooctane [84], R = C ₁₆ H ₃₃ (RRR): TRI 1 (21,22:RR): 293 (6100), TRI 2 (21,22:SS): 293 (6200) / hexane [81] / pale yellow oils
TRD	 <p>1,2-bis(2,2,7-trimethylchroman-5,6-dione-8)ethane (R = CH₃) (Tocored dimer)</p>	287, 468 / hexane [91]
TQ-Toc dimer	 <p>1-(2,2,7,8-tetramethyl-6-chroman-5-yl)-2-[2-(3-methyl-3-hydroxybutyl)-5,6-dimethyl-1,4-benzoquinone-3-yl]ethane (R = CH₃)</p>	263, 270, 294 / hexane [83]



Scheme 1.10: Mechanism of oxidation of Toc with peroxy radicals in unpolar solvents

1.4.3 Stabilising effect of α -tocopherol in polymers

1.4.3.1 Stabilising activity

The antioxidant activity of vitamin E in lipidic systems has been attributed to its very high chain-breaking donor activity, surpassing commercial antioxidants like BHT (see section 1.4.1). Applications of Toc in melt stabilisation of polyolefins [5-8, 91] showed that Toc is an excellent melt stabiliser in PP and PE during multiple extrusions, when applied in concentrations lower than those of conventional synthetic phenolic antioxidants like Irg 1076, Irg 1010 and BHT (see table 1.1 for structures) (0.025% and 0.01% for PP and PE, respectively). The thermal stabilising efficiency of Toc is lower than that of conventional materials at high temperatures (>120°C). However, although testing of stabiliser performance is still often requested at 150°C (far removed from actual service conditions), evaluation is increasingly being carried out at temperatures much nearer to those used in practice. Hence, although the performance of Toc alone cannot match that of conventional materials, it is quite apparent that, with an oven life of 28 days at 120°C in PP (0.025% Toc, 0.5mm thick film) [6] (roughly equivalent to 6 years at 60°C), Toc can provide more than adequate 'reallife' heat stability. Like commercial hindered phenols, Toc only possesses limited UV stabilisation activity and added UV stabilisers are required for extreme conditions, which however, usually do not apply in the case food packaging materials. Table 1.8 compares the melt, thermal and UV stabilising activity of Toc with commercial antioxidants in PP [9].

Table 1.8: Melt stability (melt flow index, MFI, 230°C, 2.16kg) after processing (10min, closed mixer, 190°C) and embrittlement time of PP foils (0.25mm thick) after thermal (140°C) and light ageing [9]

stabiliser	concentration, % weight	MFI, g.10min ⁻¹	embrittlement time, h	
			thermal ageing	light ageing
none		0.68	1.5	90
Toc	0.002	0.48	2	50
	0.005	0.34	6	70
	0.02	0.31	55	60
	0.05	0.31	55	55
	0.2	0.34	105	100
	1.0	0.32	260	150
	2.5	0.35	570	145
	5.0	0.38	760	150
	10.0	0.54	260	110
BHT, I	0.2	0.33	3.5	240
	1.0	0.33	12.5	140
Irg 1076, II	0.2	0.39	350	250
	1.0	-	> 250	210
Irg 1010, III	0.2	0.41	> 620	210
Tinuvin 770 (see figure 1.1)	0.2	0.58	10	> 620

1.4.3.2 Effect of organic phosphites on the melt stability and colour of polyolefins stabilised with Toc

Similar to commercial hindered phenols (e.g. Irg 1076, Irg 1010 and BHT), oxidation of Toc, which is a consequence of its stabilising action, will lead to discolouration, most likely due to the formation of quinones [6,8]. However, colour stability can be greatly enhanced by synergistic use of phosphites (see also section 1.4.3). Concentrations as low as 0.01% Toc + 0.04% Ultrinox 626 (U-626, XIII) gave excellent melt stabilisation in HDPE (equivalent to 0.015% Toc alone) and colour retention, even after five extrusion passes [8]. In PP, combinations of 0.01% Toc + 0.02% U-626 gave similar effects [8],

suggesting synergism between the two stabilisers. Furthermore, melt stabilisation and colour retention were higher than in Irg 1076/Irgafos 168 and Irg 1010/Irgafos 168 blends under the same conditions [8]. However, lower levels of Toc (e.g. 0.025% in PP), when used on its own, also provide improved colour results and still imparted good melt flow characteristics [8]. Hence, Toc seems fully acceptable for stabilisation of packaging materials for foods, where a slight discolouration is not a critical factor.

1.4.3.3 Importance of transformation products of Toc in polymers

As a consequence of their antioxidant action during processing (and possibly during in-service), hindered phenols are partly oxidised to various transformation products (see scheme 1.8) which, in general, exhibit unknown or uncertain migration behaviour and toxicity effects in packaging materials. Current regulations are concerned only with the 'safety' of parent antioxidants and specification of their migration limits, they do not address the risks associated with migration of transformation products into food. Therefore, although Toc can be considered as a safe migrant, the behaviour and migration characteristics of the derived transformation products is essential to defining the safe limits incumbent on its use (this is equally important in the case of synthetic antioxidants) in food packaging.

Extensive studies on the effect of hindered phenols, e.g. Irg 1076 and Irg 1010, on melt stabilisation of polyolefins have confirmed the important role of oxidative transformation products, including dimers, trimers and quinonoid structures, in this process (see section 1.3.2.2). Dimers, trimers and tocoquinonoid structures have also been shown to be formed during oxidation of Toc by different oxidants in model compounds (see section 1.4.2). However, there has been no systematic work reported on the nature of transformation products formed during the antioxidant action of Toc in polymers.

1.5 OBJECTIVES OF THE PRESENT WORK

The objectives of the present work are:

1. To determine the stabilising efficiency of Toc in LDPE and PP during high temperature multiple extrusions and processing conditions, as well as during accelerated ageing tests (thermal and UV), and to compare the results with those obtained for commercial hindered phenol antioxidants, e.g. Irg 1076 and Irg 1010.
2. To identify the transformation products formed from Toc during multiple extrusions and processing with LDPE and PP, and also, to examine the products formed from Irg 1076 and Irg 1010 during processing with these polymers.
3. To determine the antioxidant role of the transformation products of Toc during melt processing in PP.
4. To establish the mechanism of melt stabilisation of Toc during multiple extrusions and processing with LDPE and PP, compared to the mechanism of melt stabilisation of Irg 1076 and Irg 1010 in LDPE.
5. To determine the mechanism of stabilisation of Toc during accelerated ageing tests (thermal and UV) in PP.
6. To study the effect of the hindered aryl phosphite Ultrinox 626 on the overall stability (melt, thermal, colour) of PP containing Toc, compared with the effect of the phosphites Ultrinox 626 and Irgafos 168 on the overall stabilising efficiency of Irg 1010, and to examine the mechanism of melt stabilisation of Toc during processing with PP and Ultrinox 626.
7. To investigate the migration characteristics of Toc from LDPE films into various food simulants, and to compare them with those of Irg 1076.

CHAPTER TWO

EXPERIMENTAL

2.1 MATERIALS

Unstabilised low density polyethylene pellets (Novex) were supplied by B.P. Chemicals and unstabilised polypropylene powder (Propathene HF-26) was obtained from I.C.I (Plastic Division) Ltd.

Polypropylene (PP), stabilised with 39% all-rac- α -tocopherol (Toc, Ronotec 201, min. 92%, provided by Hoffmann-La Roche, Switzerland) was donated by Cambridge Polymer Consultants (CPC789 series). The series is a mixture of 56% CPC613 (50% Toc in PP) and 44% CPC612 (25% Toc in PP), resulting in a mixture containing 39%Toc. CPC612 was prepared by stirring Toc at room temperature into Accurel porous PP granules (type EG100, supplied by Akzo) resulting in the absorption of R202 in the polymer. The mixture obtained was then extruded in a twin screw extruder into granules using a melt temperature of 220°C. CPC613 was prepared in a similar way but Toc was mixed with Accurel porous PP powder (type EP100 from Akzo) (the powder material was found to have a higher capacity for absorbing liquids, hence the higher concentration). CPC789 (mixture of CPC612 and CPC613) was extruded four times in a single screw extruder (nominal melt temperature 270°C).

All-rac- α -tocopherol (Ronotec 202, min. 97%), 2,5,7,8-tetramethyl-2RS-(4'RS,8'RS,12'-trimethyltridecyl)-6-chromanol, was kindly donated by Hoffmann-La Roche (Vitamins and Fine Chemicals Division), Switzerland. Commercial antioxidants Irganox 1076, n-octadecyl-3-(3',5'-di-*t*-butyl-4'-hydroxy-phenyl) propionate, Irganox 1010, pentaerythrityl tetrakis-3-(3',5'-di-*t*-butyl-4'-hydroxyphenyl) propionate and Irgafos 168, tris-(2,4-di-*t*-butylphenyl)phosphite, were donated by Ciba-Geigy. The commercial melt stabiliser BHT, 2,6-di-*t*-butyl-4-methylphenol, was provided by Aldrich. The commercial antioxidant Ultrinox 626, bis-(2,4-di-*t*-butylphenyl)pentaerythrityl diphosphite, and the all-rac- α -tocopherol derivatives 5-formyl- γ -tocopherol and α -tocoquinone were kindly donated by Hoffmann-La Roche (Vitamins and Fine Chemicals Division), New Jersey, USA. Table 2.1 shows the chemical structures and code names of the above compounds used

throughout this work. The starting materials were analysed and characterised using various spectroscopic and spectrometric techniques and the results are displayed in form of tables (2.2-2.10, p. 148-154) and figures (2.1-2.6, p. 181-205) at the end of this chapter.

Lead dioxide (min. 97%) was supplied by BDH. Anhydrous sodium sulphate (min. 99%) and lithium aluminium hydride (min. 97%) were obtained from Aldrich. Glass microfibre filter paper (GF/F) was supplied by Whatmann. Aluminium oxide, Brockmann activity 1, and thin layer chromatographic plastic sheets (20x20cm), precoated with silica gel 60 A, of 0.25mm thickness and fluorescent at 254nm, were supplied by Macherey-Nagel.

Dichloromethane, hexane, 1,4-dioxane, diethylether, methanol, chloroform, iso-octane, heptane and water supplied by Fisons, were all HPLC grade and used without further purification. Petroleum ether (b.p. 40-60°C) and absolute ethanol were obtained from Fisons. Rectified olive oil was supplied by Leon Frenkel Ltd and was certified to conform to the CEC specification laid down in EC Directives 85/572/EEC and 82/711/EEC [62]. Acetic acid, analytical grade, was provided by Fisons.

Table 2.1: Chemical structures of antioxidants used

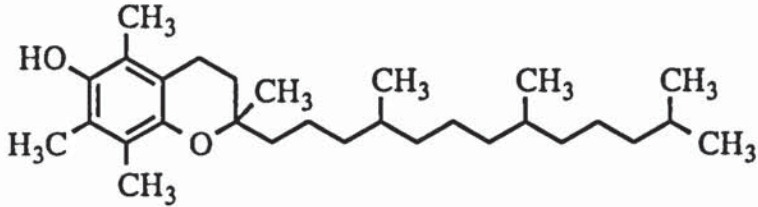
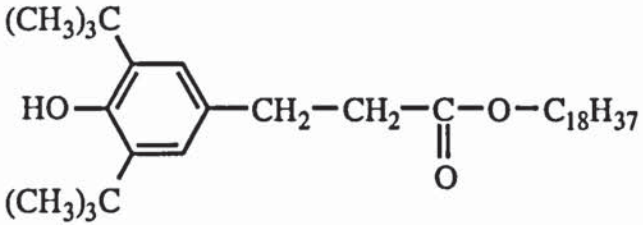
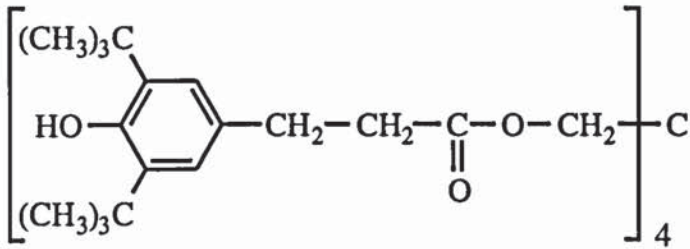
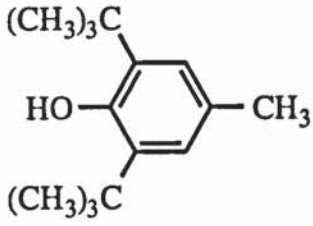
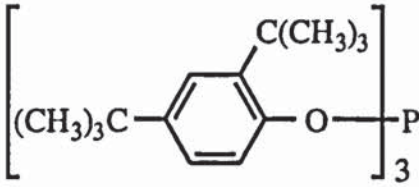
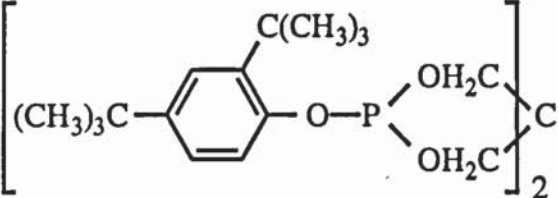
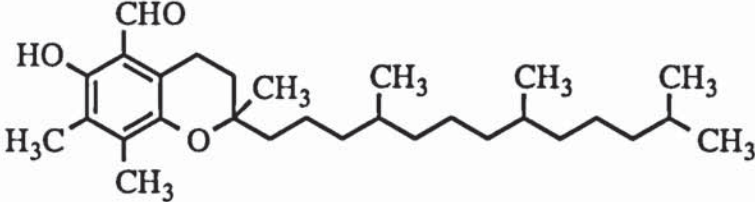
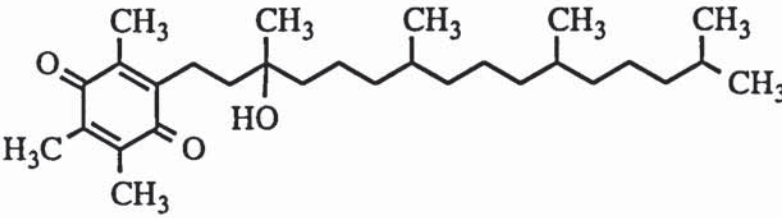
Chemical structure and name (commercial name)	code name (MM, state, m.p.) λ_{\max}	Origin
 <p>2,5,7,8-tetramethyl-2RS-(4'RS,8'RS,12'-trimethyltridecyl)-6-chromanol (all-rac-α-tocopherol, Ronotec 202)</p>	<p>Toc (430g, orange-brown oil) 298nm</p>	<p>Hoffmann-La Roche, Switzerland</p>
 <p>n-octadecyl-3-(3',5'-di-<i>t</i>-butyl-4'-hydroxy-phenyl) propionate (Irganox 1076)</p>	<p>Irg 1076 (530g, white powder, 51.6-52.0°C) 282, 276nm</p>	<p>Ciba-Geigy, Switzerland</p>
 <p>pentaerythrityl tetrakis-3-(3',5'-di-<i>t</i>-butyl-4'-hydroxyphenyl) propionate (Irganox 1010)</p>	<p>Irg 1010 (1177g, white powder, 118-119°C) 282, 276nm</p>	<p>Ciba-Geigy, Switzerland</p>
 <p>2,6-di-<i>t</i>-butyl-4-methylphenol (BHT)</p>	<p>BHT (220g, white powder, 69.6-70.2°C)</p>	<p>Aldrich</p>

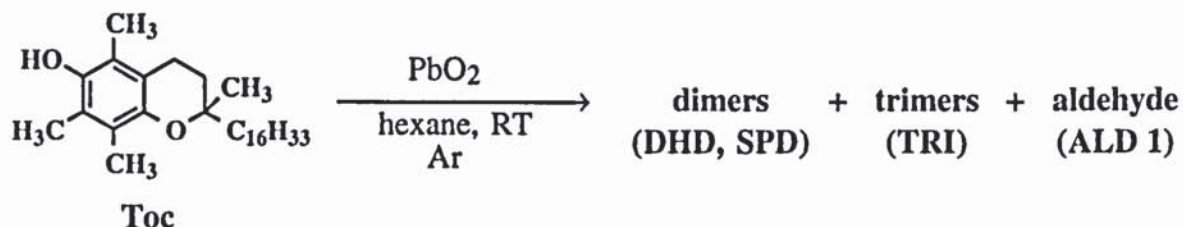
Table 2.1: continued

Chemical structure and name (commercial name)	code name (MM, state, m.p.) λ_{\max}	Origin
 <p>tris-(2,4-di-<i>t</i>-butylphenyl)phosphite (Irgafos 168)</p>	<p>Irgf 168 (646g, white powder, 188-189°C)</p>	<p>Ciba-Geigy, Switzerland</p>
 <p>bis-(2,4-di-<i>t</i>-butylphenyl)pentaerythrityl diphosphite (Ultrinox 626)</p>	<p>U-626 (604g, white powder, 177-178°C) 271, 278nm</p>	<p>Hoffmann-La Roche, USA</p>
 <p>2,7,8-trimethyl-5-formyl-2RS-(4'RS,8'RS,12'-trimethyltridecyl)-6-chromanol (all-rac-5-formyl-γ-tocopherol)</p>	<p>ALD 1 (444g, dark yellow-orange oil) 290, 282, 386nm</p>	<p>Hoffmann-La Roche, USA</p>
 <p>2RS-[3-(4'RS,8'RS,12'-trimethyltridecyl)-3'-butanol]-3,5,6-trimethyl-1,4-benzoquinone (all-rac-α-tocoquinone)</p>	<p>TQ (446g, orange oil) 260, 268nm</p>	<p>Hoffmann-La Roche, USA</p>

2.2 OXIDATION OF TOC IN MODEL SYSTEMS AND SYNTHESIS OF TOC DERIVATIVES

2.2.1 Oxidation of Toc with lead dioxide

2.2.1.1 Reaction procedure and isolation of products

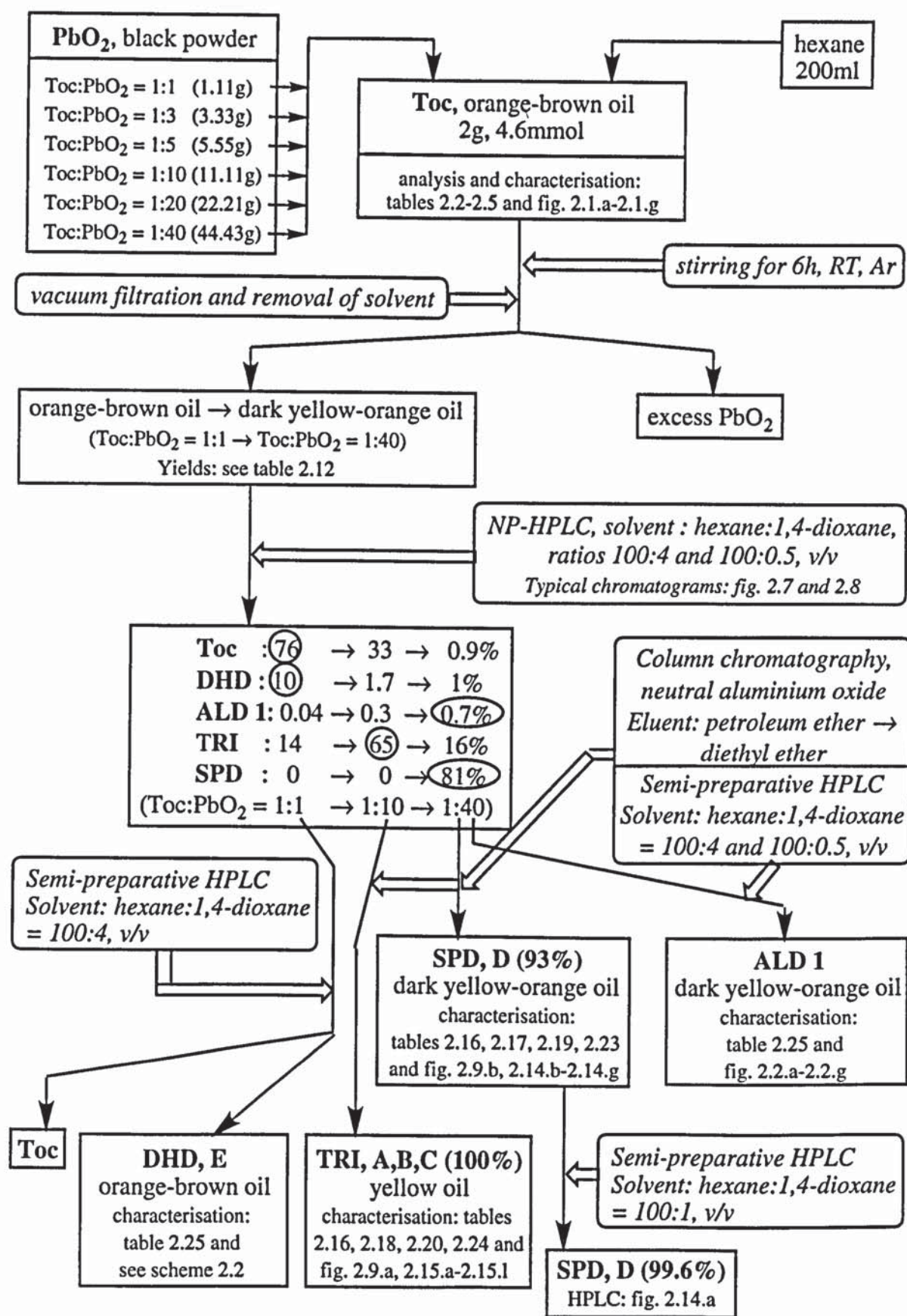


Toc (2g, 4.64 mmol) was dissolved in hexane (200ml) and various amounts of PbO₂ were added, corresponding to each of the molar ratios of 1:1, 1:3, 1:5, 1:10, 1:20 and 1:40 in Toc:PbO₂ (see scheme 2.1 for amounts used). Each of the resulting solutions was stirred under continuous argon bubbling for 6h at room temperature (RT). The reaction products were isolated by filtering the solutions under vacuum, using microfibre filter papers (to remove excess PbO₂), and the solvent was removed in vacuo to leave orange-brown to dark yellow-orange oils.

2.2.1.2 Analysis of products

The reaction products were dissolved in hexane and analysed by normal phase high performance liquid chromatography (NP-HPLC) (see section 2.10.1 for technical details and procedure) using the solvent system hexane:1,4-dioxane = 100:4, v/v, to detect products with high retention times (i.e. DHD E), followed by the ratio 100:0.5, for further separation of products with low retention times (e.g. TRI, A, B, C, ALD 1 and SPD, D), at 290nm (see figures 2.7 and 2.8, p. 206, for typical chromatograms). The concentration of each product was determined from its peak area at 290nm using both chromatograms (solvent ratios 100:4 and 100:0.5) (see section 2.11.1). Scheme 2.1 describes the procedures for the reactions of Toc with PbO₂ and for the isolation and analysis of the

products and tables 2.11 and 2.12 show the structures of the oxidation products formed and the concentrations of the major products obtained for each ratio of PbO_2 used, respectively. Table 2.13 reveals the HPLC retention times (R_t) of the oxidation products of Toc obtained and of the supplied Toc and Toc derivatives samples (ALD 1 and TQ) under all HPLC conditions used (ratios 100:4, 100:3 and 100:0.5, v/v, in hexane:1,4-dioxane).



Scheme 2.1: Flowchart for the oxidation of Toc with PbO₂ and the identification and isolation of oxidation products of Toc

Table 2.11: Chemical structures, highest yields and colour of products of reactions of Toc with PbO₂

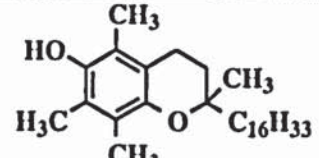
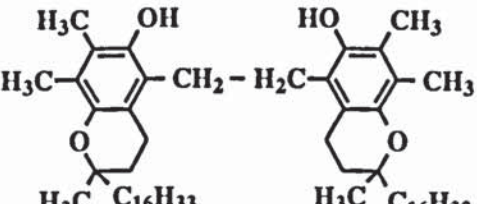
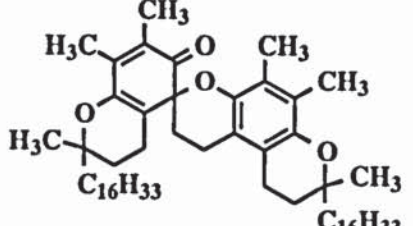
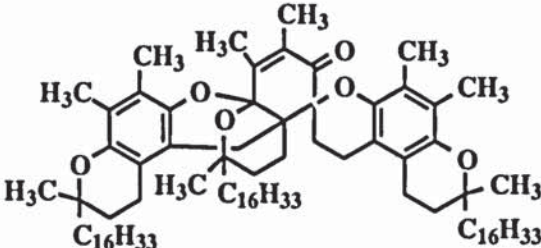
code and HPLC peak names	chemical structure, name and commercial name (MM)	Yield (Toc:PbO ₂ ratio)	colour (λ_{max})
Toc	 <p>2,5,7,8-tetramethyl-2RS-(4'RS,8'RS,12'-trimethyltridecyl)-6-chroman-3-ol α-tocopherol (430g)</p>	-	orange-brown (298nm)
DHD, E (E1, E2, E3, E4, stereoisomers)	 <p>1,2-bis[2,7,8-trimethyl-2RS-(4'RS,8'RS,12'-trimethyltridecyl)-6-chroman-5-yl]ethane dihydroxydimer (859g)</p>	10% (1:1)	orange-brown (300nm)
SPD, D (D1, D2, D3, stereoisomers)	 <p>1,8,9,10-tetrahydro-2',5,6,7',8,8'-hexamethyl-2RS,18RS-bis(4'RS,8'RS,12'-trimethyltridecyl)-spiro[benzo[1,2-b:4,3-b']dipyran-3(2H),5'(6H)-chroman]-6'-one spirodimer (857g)</p>	81% (1:40)	dark yellow-orange (301, 339nm)
TRI, A, B, C (A1, A2, B1-B4, C1-C4, stereoisomers)	 <p>1,1',2',3',8,9,9',10,10',12'-decahydro-3',3',5,5',6,6',8,8',10',10',13',14'-nonamethyl-2RS,18RS,28RS-tris(4'RS,8'RS,12'-trimethyltridecyl)-spiro[benzo[1,2-b:4,3-b']dipyran-3(2H),16'(11a,7a)[1]buteno[8H]dipyrano[3,2-b:3',2'-f][1]benzopyran]-chroman]-6'-one trimer (1286g)</p>	65% (1:10)	yellow (292nm)

Table 2.11: continued

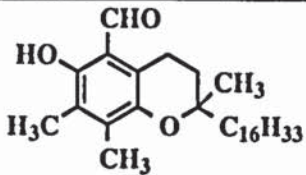
code and HPLC peak names	chemical structure, name and commercial name (MM)	Yield (Toc:PbO ₂ ratio)	colour (λ_{\max})
ALD 1, F	 <p>2,7,8-trimethyl-5-formyl-2RS-(4'RS,8'RS,12'-trimethyltridecyl)-6-chromanol 5-formyl-γ-tocopherol (444g)</p>	0.7% (1:40)	dark yellow-orange (239, 290, 282, 386nm)

Table 2.12: Reaction yields (% weight), colour of products and major products of reactions of Toc with PbO₂ and conditions for their isolation (see scheme 2.1)

Toc:PbO ₂ ratio	Yield and colour of reaction products	major products (yield)	isolated products	method for isolation of products
1:1	98%, orange-brown	Toc (76%), TRI (14%), DHD (10%)	DHD, E Toc	semi-preparative HPLC
1:3	98%, orange-brown	Toc (75%), TRI (23%)	-	-
1:5	98%, orange	Toc (65%), TRI (33%)	-	-
1:10	98%, dark orange	TRI (65%), Toc (33%)	TRI, A, B, C	column chromatography
1:20	96%, dark yellow-orange	SPD (64%), TRI (34%)	-	-
1:40	95%, dark yellow-orange	SPD (81%), TRI (16%) ALD 1 (0.7%)	SPD, D	column chromatography
			ALD 1, F	semi-preparative HPLC

Table 2.13: HPLC retention times (Rt) of Toc and its products of reaction with PbO₂ (290nm) (solvent ratios are in hexane:1,4-dioxane, v/v)

compound		Rt, min:sec		
		100:4	100:3	100:0.5
TRI, A, B, C	A1, A2	3:00-5:00	3:30-6:00	9:30, 9:50
	B1, B2, B3, B4			14:30 (B1), 15:40 (B2+B3), 17:30 (B4)
	C1-C4			30-40
ALD 1, F		5:10	6:30	13:00
SPD, D	D1, D2, D3	3:35, 4:40, 4:55	4:40, 5:20, 6:10	20-30 (broad)
Toc		11:00	16:00	45
DHD, E	E1, E2, E3, E4	14:40 (E1), 15:00 (E2), 15:30 (E3+E4)	22:00, 23:30, 25:00, 26:00	180

2.2.2 Purification and isolation of oxidation products of Toc with PbO₂

2.2.2.1 Purification of TRI, A, B, C and SPD, D by column chromatography

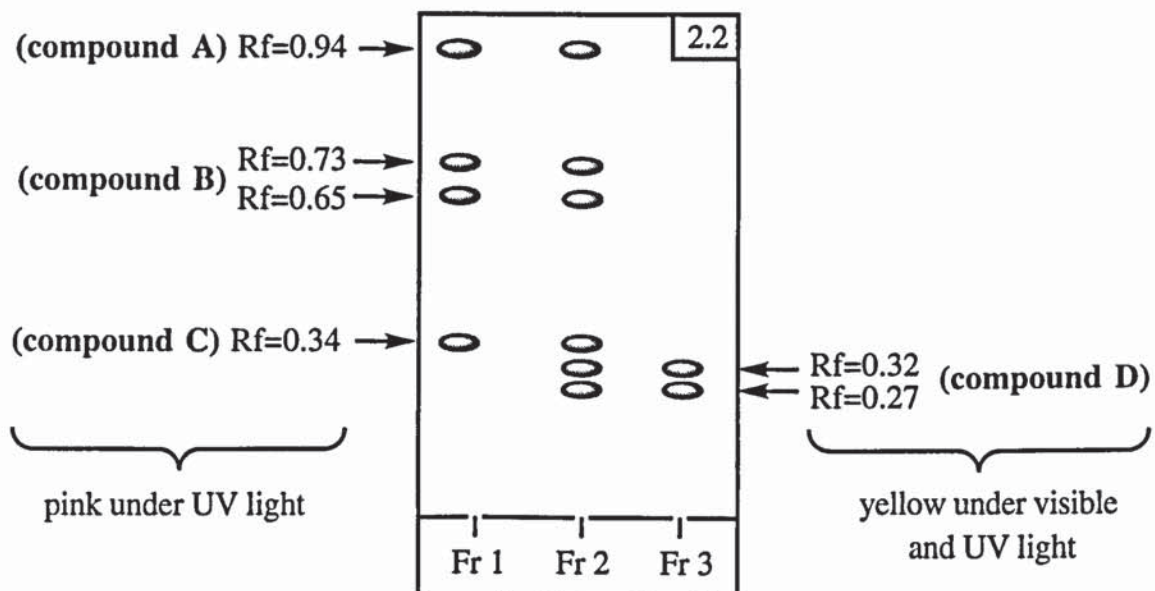
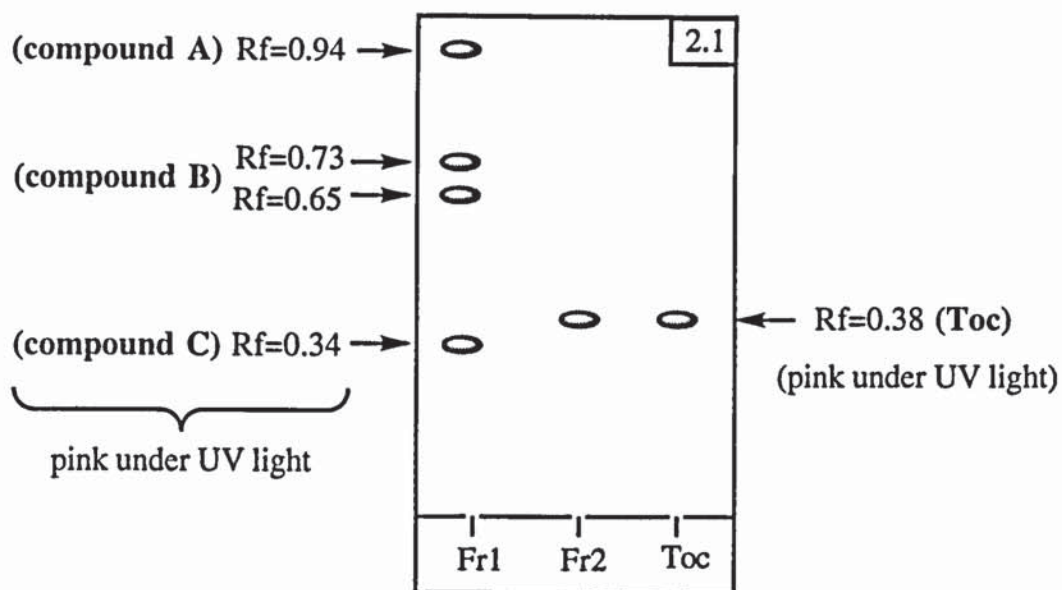
The crude mixtures of TRI, A, B, C (A1, A2, B1-B4 and C1-C4, stereoisomers) and SPD, D (D1, D2, D3, stereoisomers), obtained from the oxidation of Toc with PbO₂, molar ratios 1:10 and 1:40 in Toc:PbO₂, respectively (see table 2.12 and scheme 2.1), were purified by column chromatography. Crude TRI, A, B, C (1.96g) and SPD, D (1.90g) were each dissolved in 15ml petroleum ether (b.p. 40-60°C) and separated on columns of neutral aluminium oxide developed with petroleum ether. The eluates were fractionated using 8ml vials and each fraction was analysed by thin layer chromatography (TLC) (see section 2.9 for procedure).

Elution of the column containing crude TRI, A, B, C with 96ml petroleum ether, followed by 56ml of the solvent mixture petroleum ether:diethylether = 9:1, v/v, yielded 1.23g (63%) of a yellow oil (fraction 1, Fr1, see TLC plate 2.1). Continuing elution with 90ml

diethylether yielded 442mg (23%) Toc (fraction 2, Fr2, TLC plate 2.1). The total column recovery consisted of 1.67g (85%) of oily products.

The column containing the crude SPD, D was first eluted with 96ml petroleum ether, followed by 128ml of the solvent mixture petroleum ether:diethylether = 100:2, v/v, and 136ml of the solvent ratio 10:1 to yield 150mg (8%) of a yellow oil (Fr1, see plate 2.2). Continuing elution with 64ml of the same solvent ratio yielded 231mg (12%) of a yellow-orange oil (Fr2, plate 2.2). Finally, elution with 160ml diethylether gave 1.26g (66%) of a dark yellow-orange oil (Fr3, plate 2.2). The total column recovery was 1.64g (86%).

The purified TRI, A, B, C (1.23g, Fr1, plate 2.1) and SPD, D (1.26g, Fr3, plate 2.2) were analysed by NP-HPLC using the solvent systems hexane:1,4-dioxane, ratios 100:0.5 and 100:3, v/v, respectively (see figure 2.9), and the purity of each mixture of products was determined from their peak areas at 290nm (see table 2.14 and section 2.11.1 for procedure). TRI, A, B, C were characterised by UV, IR, $^1\text{H-NMR}$ and FAB-MS and SPD, D were characterised by UV, IR, $^1\text{H-NMR}$, $^{13}\text{C-NMR}$, $^1\text{H},^{13}\text{C-NMR}$ correlation and EI-MS (see section 2.2.4).



Plates 2.1 and 2.2: TLC analysis of fractions collected by column chromatography of the products of reaction of Toc with PbO_2 , ratios 1:10 (2.1) and 1:40 (2.2) in Toc: PbO_2 (see scheme 2.1)

2.2.2.2 Further separation of TRI, A, B, C and purification of SPD, D by NP-HPLC

TRI, A, B, C (500mg) were further separated by semi-preparative NP-HPLC, using the solvent system hexane:1,4-dioxane = 100:0.5, v/v, at 290nm (see section 2.10.2) to obtain compounds A1 (34mg), A2 (26mg), B (66mg) and C (16mg). Each TRI was analysed by HPLC at 290nm, using the same solvent system as above (see figure 2.10) and characterised by UV, IR and ¹H-NMR. TRI A1, A2 and B were also characterised by ¹³C-NMR and a ¹H,¹³C-NMR correlation was carried out for TRI A1 (see section 2.2.4).

SPD, D (263mg) was further purified by semi-preparative NP-HPLC using the solvent system hexane:1,4-dioxane = 100:1, v/v, at 290nm and the pure SPD was reanalysed by HPLC using the solvent ratio 100:3, to check its purity (see table 2.14 and figure 2.14.a).

Table 2.14: HPLC analysis of TRI, A, B, C and SPD, D isolated by column chromatography (CC) and semi-preparative HPLC (SPD, D only) from the products of reaction of Toc with PbO₂, ratios 1:10 and 1:40, respectively

	TRI A, B, C isolated by CC	SPD D	
		isolated by CC	isolated by CC and purified by semi-preparative HPLC
Purity (% weight)	100 (A: 30, B: 63, C: 7)	92.8	99.6
Other products (% weight)	-	TRI (4.4), Toc (2.8)	Toc (0.4)
Figure	2.9.a, p. 208	2.9.b, p. 208	2.14.a, p. 223

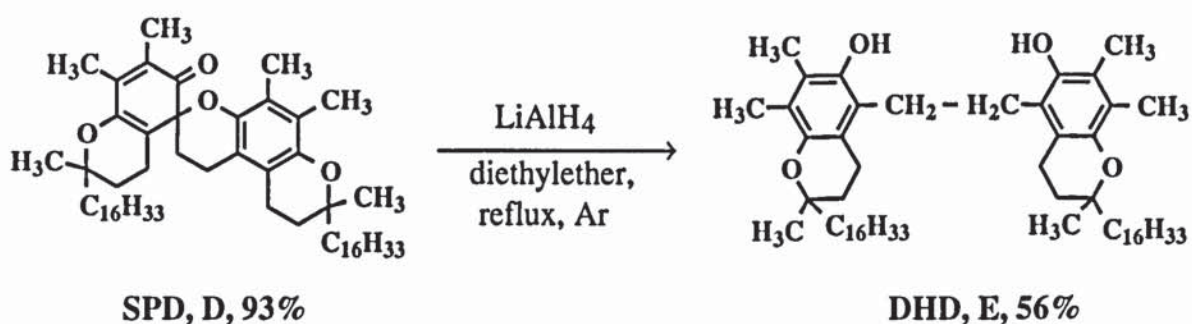
2.2.2.3 Isolation of DHD, E, ALD 1 and Toc

The mixture of DHD, E (E1, E2, E3, E4, stereoisomers) and Toc were isolated from the products of reaction of Toc with PbO₂, ratio 1:1 in Toc:PbO₂ (see table 2.12), by semi-preparative NP-HPLC using the solvent system hexane:1,4-dioxane = 100:4, v/v, at 290nm. ALD 1 was isolated from the products of reaction of Toc with PbO₂, ratio 1:40, using the same conditions as above and a solvent ratio of 100:4 (see figure 2.8.a), to

exclude Toc and DHD, followed by 100:0.5 (see figure 2.8.b), for further purification. The DHD, ALD 1 and Toc were characterised by UV and $^1\text{H-NMR}$ (see section 2.2.4) and the results were compared with those of an authentic synthesised sample of the dihydroxydimer and with supplied samples of Toc and ALD 1 (see sections 2.2.3 and 2.2.4).

2.2.3 Preparation of DHD of Toc

2.2.3.1 Reaction procedure and isolation of products



The DHD was prepared from SPD, D which was isolated by column chromatography from the reaction products of Toc with PbO_2 , ratio 1:40 in Toc: PbO_2 (see table 2.12 and scheme 2.1). The SPD (1g, 1.17mmol) was dissolved in diethylether (150ml) and lithium aluminium hydride (2.21g, 58.3mmol) was added. The resulting mixture was stirred under reflux and argon atmosphere for 2h. The excess LiAlH_4 was decomposed with water and the mixture was filtered under vacuum using a microfibre filter. The organic phase was separated from the aqueous phase which was washed twice with 30ml portions of diethylether. The diethylether layers were combined, dried over anhydrous sodium sulphate and the solvent was evaporated under vacuum to leave 943mg (94%) of a yellow oil. Scheme 2.2 describes the procedures for the reaction and the isolation and analysis of the products.

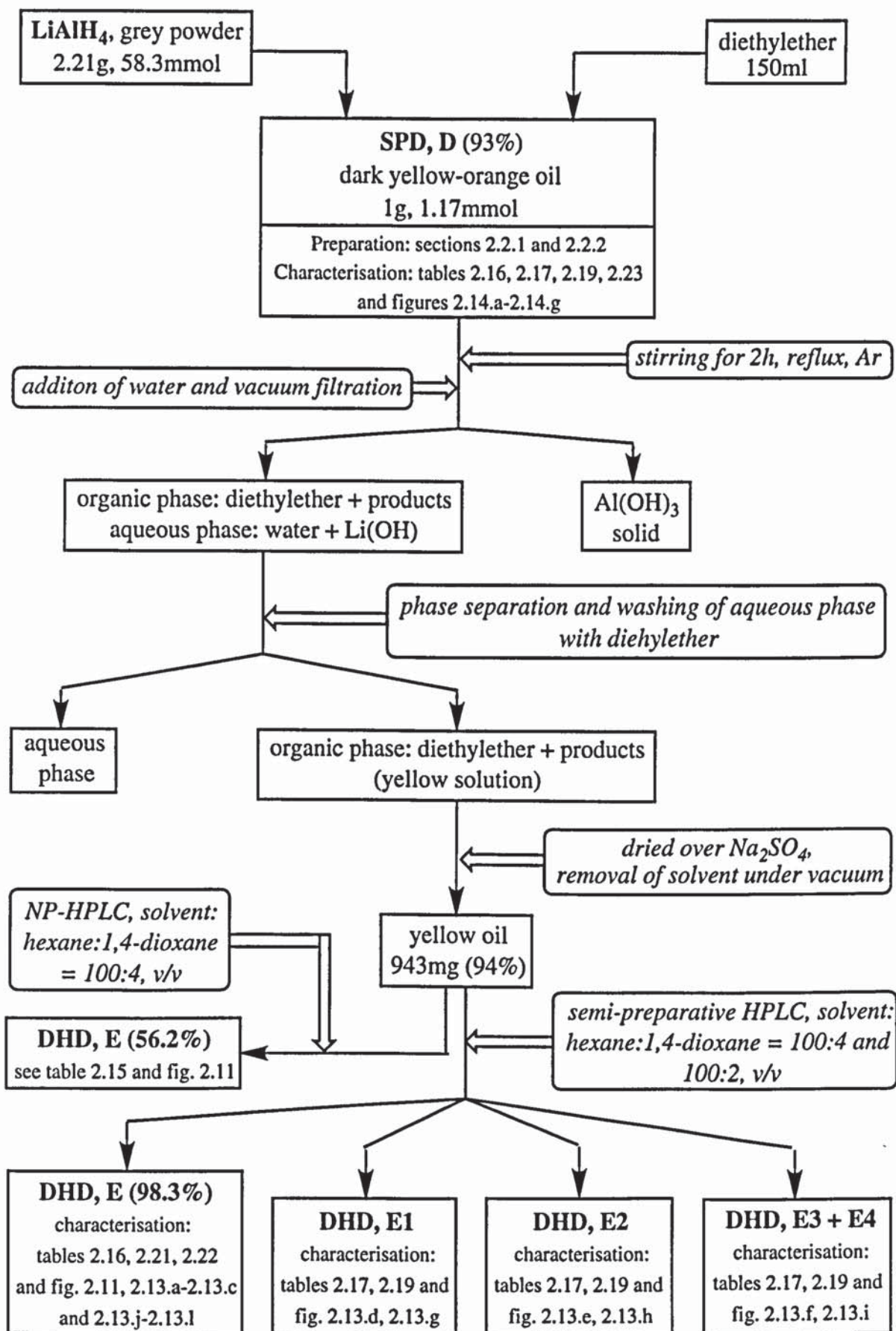
2.2.3.2 Analysis and purification of the DHD product

The crude DHD was dissolved in hexane and analysed by NP-HPLC (see section 2.10.1) using the solvent system hexane:1,4-dioxane = 100:4, v/v (see figure 2.11.a-b). The chromatograms were viewed at wavelengths of 290 and 265nm, the latter permitting the detection of α -tocoquinone (TQ, see table 2.1 for structure and absorption characteristics). Table 2.15 shows the nature of the products and their concentrations, the latter being determined from the peak areas at 290 and 275nm (see section 2.11.1 for procedure). Crude DHD (943mg) was purified by semi-preparative NP-HPLC (see section 2.10.2), using the solvent system hexane:1,4-dioxane = 100:4, v/v, and a wavelength of 265. The purified DHD (269mg) was reanalysed by HPLC using the same solvent system as above (see figure 2.11.c-d) and its purity was determined by integrating the peak areas at 290nm, as TQ was not present after purification (see table 2.15). DHD, E was characterised by UV, IR and $^1\text{H-NMR}$ (see section 2.2.4).

DHD, E (150mg) was further separated into compounds E1, E2 and E3+E4 by semi-preparative HPLC, using the same conditions as above and the solvent system hexane:1,4-dioxane = 100:2, v/v, at 300nm. E1, E2 and E3+E4 were reanalysed by HPLC, using the solvent system hexane:1,4-dioxane = 100:2, v/v, and characterised by UV, $^1\text{H-NMR}$ and $^{13}\text{C-NMR}$ (see section 2.2.4).

Table 2.15: HPLC analysis of crude and purified DHD, E, obtained from the reaction of SPD, D with LiAlH_4

	crude DHD, E	purified DHD, E
Purity (% weight)	56.2	98.3
Other products (% weight)	TRI (11.5), SPD (9.4), Toc (3.2), TQ (19.7)	1.7 (SPD), 0.02 (Toc)
Figure	2.11.a-b, p. 210	2.11.c-d, p. 210



Scheme 2.2: Flowchart for the preparation, purification and analysis of DHD, E

2.2.4 Characterisation of oxidation products of Toc

2.2.4.1 Characterisation of synthesised and purified dimers and trimers of Toc

DHD, E, SPD, D and TRI, A, B, C, which were synthesised and purified by column chromatography and/or preparative HPLC (see sections 2.2.2 and 2.2.3), were characterised using different spectroscopic and spectrometric techniques, as described below (see sections 2.13 and 2.14 for technical and experimental details). The results are shown in tables 2.16-2.24 (p. 155-163) and figures 2.13-2.15 (p. 212-239) at the end of this chapter as follows.

DHD, E (E1, E2, E3 and E4, stereoisomers) and SPD, D (D1, D2 and D3, stereoisomers) were analysed by ultraviolet (UV), Fourier Transform infrared (FTIR) (see table 2.16 and figures 2.13.b to 2.13.c and 2.14.b to 2.14.c), ^1H -NMR (table 2.17 and figures 2.13.d to 2.13.f and 2.14.d), ^{13}C -NMR (table 2.19 and figures 2.13.g to 2.13.i and 2.14.e) and $^1\text{H},^{13}\text{C}$ -NMR correlations (see figures 2.13.j and 2.14.f) spectroscopy and by EI-MS in the absence and presence of tetramethylsiloxane (TMS) (tables 2.21 to 2.23 and figures 2.13.k to 2.13.l and 2.14.g). In the case of SPD, D, the MS results were identical before and after silylation.

TRI, A, B, C (A1, A2, B and C, stereoisomers) were characterised by UV, IR (see table 2.16 and figures 2.15.b to 2.15.c), ^1H -NMR (table 2.18 and figures 2.15.d to 2.15.g), ^{13}C -NMR (table 2.20 and figures 2.15.h to 2.15.j) spectroscopy and a $^1\text{H},^{13}\text{C}$ -NMR correlation was carried out for TRI A1 (see figure 2.15.k). TRI, A, B, C were also analysed by fast atom bombardment mass spectrometry (FAB-MS) (table 2.24 and figure 2.15.l).

2.2.4.2 Characterisation of isolated products

DHD E, Toc and ALD 1, isolated from the products of reaction of Toc with PbO_2 , ratios 1:1 and 1:40 in Toc: PbO_2 (see section 2.2.2.3), were characterised by UV (diode array system) and ^1H -NMR (see table 2.25, p. 164) and the results were compared with those

obtained from supplied (Toc, ALD 1) and synthesised (DHD E) samples. The isolated products had identical UV characteristics to the supplied and synthesised samples (see tables 2.2 and 2.16) and the isolated Toc sample had identical $^1\text{H-NMR}$ characteristics to the supplied sample (see table 2.3).

2.3 POLYMER COMPOUNDING

2.3.1 Multiple extrusion of polymer samples

Low density polyethylene (LDPE) pellets were mixed with the appropriate concentration of the antioxidant in a small amount of dichloromethane. The total weight of the polymer sample was kept constant (1000g), to fully charge the extruder. After exhaustive vacuum evaporation at room temperature of the solvent, the polymer sample was introduced in a Humboldt single screw extruder via the hopper and extruded into thin films. The single screw extruder consisted of a barrel equipped with a screw ($\text{Ø} = 45\text{mm}$, length = 90cm) rotating at a fixed speed and divided into three screw zones and a die head at fixed temperatures (see figure 2.16, below). Extrusions carried out in this work were realised at a screw speed of 50 rotations per minute (RPM), screw zone temperatures of 140°, 150° and 170°C and a die head temperature of 180°C. The molten polymer was extruded through the die into a thin film (0.1-0.5mm) at room temperature by placing it on rolls rotating at a fixed speed (30RPM). A sample of the extruded polymer from the first pass was cut off for melt flow index (MFI) and colour measurements and for product analysis. The remaining sample was re-extruded under the same conditions. A sample was taken off for analysis after this second extrusion pass while the rest was re-extruded for a third time. This was repeated for a fourth time (four extrusion passes in total). The resulting polymer samples were stored in a cold dark place for future investigations including MFI and spectroscopic measurements and product analysis. The extruder was cleaned before each set of four extrusions by processing LDPE only once. LDPE was processed in the absence and presence of each of the antioxidants Toc, Irg 1010 and Irg 1076 at various initial concentrations (0.2-10%, w/w).

2.3.2 Processing of polymer samples in an internal mixer

Polypropylene (PP) powder was mixed with the appropriate concentration(s) of the antioxidant(s) in a small amount of dichloromethane, keeping the total weight of the polymer sample constant (35g) to charge the full capacity of the processing chamber. After evaporation of the solvent under vacuum, at room temperature, the polymer sample was processed in a Hampden-Rapra torquerheometer fixed on Brabender motor and equipped with a digital torque recording motor. Figure 2.17 below describes the internal mixing chamber of the torquerheometer. The chamber comprises two mixing screws contrarotating at a fixed speed. The processing of the polymer sample may be conducted in the presence of excess oxygen (open mixer) or under restricted oxygen access by sealing the chamber with a pneumatic ram (closed mixer). The chamber may also be flushed with nitrogen before closing it, to further restrict the presence of oxygen. Processing carried out in this work was done under open mixing, closed mixing and closed mixing with prior nitrogen flushing (OM, CM and CM/N₂, respectively) conditions, for various times at 200°C (oil temperature) and a rotor speed of 60 RPM. After processing, the sample was removed from the internal mixer, quenched in cold water to avoid further thermal oxidation and stored in a cold dark place for future analysis including MFI and colour measurements, thermal and ultraviolet ageing tests, spectroscopic measurements and product analysis. The processing chamber was cleaned before each experiment by processing PP containing a few styrene beads (total weight of about 35g) for about 5min in a CM. PP was processed in the absence and presence of various antioxidants including Toc, Toc derivatives (DHD, SPD, TRI, ALD 1 and TQ), Irg 1010, Irg 1076, BHT, Irg 168 and U-626, at different initial concentrations (0.01-0.4%, w/w) and using varying processing times (2.5-30min).

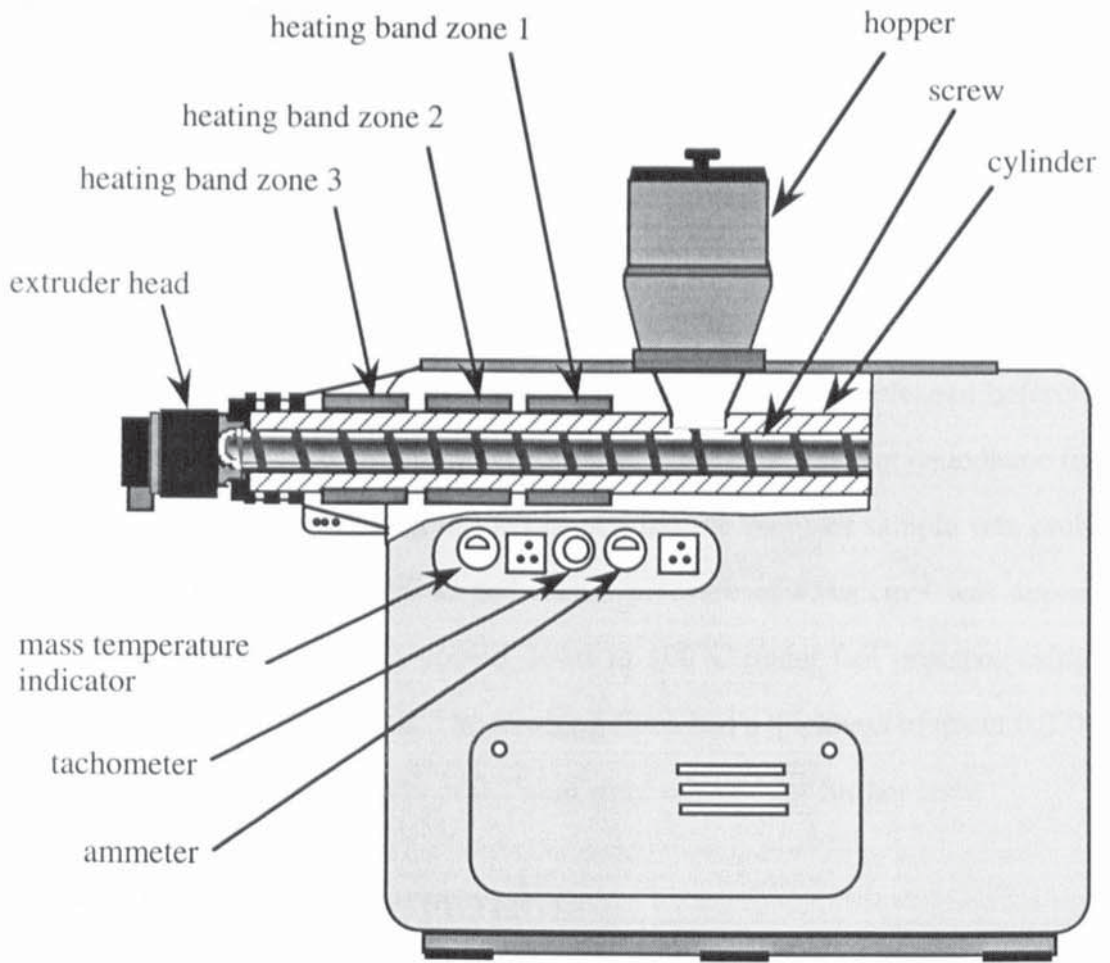


Figure 2.16: Schematic representation of the Humboldt single screw extruder

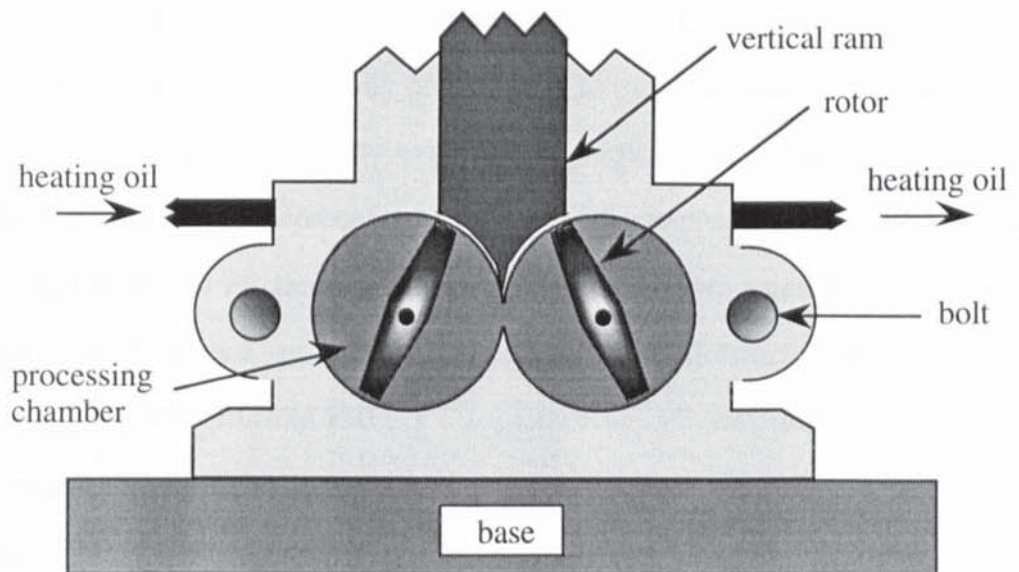


Figure 2.17: Schematic representation of the internal mixing chamber of the Hampden-Rapra torquerheometer

2.3.3 Film preparation

The PP samples, processed in the torquerheometer, were pressed to films for thermal and UV stability tests. The films were prepared by compression moulding, using an electric Daniels press machine. About 5g of the processed PP sample was placed between a paper spacer of 15 x 15 cm² surface and 0.25mm thickness. The resulting preparation was placed between two polished stainless steel plates, which were thoroughly cleaned before use to ensure a smooth surface and laminated with special grade heat resistant cellophane films to prevent the polymer from sticking to the plates. First the polymer sample was preheated for 3min without pressure at 180°C and then a pressure of 85kg.cm⁻² was applied for 1.5min. Finally, the sample was cooled down to 100°C under full pressure using cold running water, before taking it out. The resulting films had a thickness of about 0.2-0.3mm and sections of a uniform thickness of 0.25mm were selected for further tests.

2.4 STABILISING ACTIVITY TESTS

2.4.1 Measurement of melt flow index (MFI)

The melt flow index (MFI) is defined as the mass (g) of the molten polymer extruded through a standard die in a given time (normally 10min). The measurement of the melt viscosity of the polymer is inversely proportional to the molecular weight of the polymer, hence its MFI is a measure of its extent of degradation after processing, i.e. its melt stability. The MFI of all the processed LDPE and PP samples was examined. About 2g of each of the LDPE and PP samples (unpressed) were cut into small pieces and their melt viscosity was measured on a Davenport Melt Flow Indexer at constant extrusion temperatures of 190 ± 5°C and 230 ± 5°C for LDPE and PP, respectively. The barrel of the indexer was charged with the cut material with the heater in the 'boost' position using a charging tool to exclude air and, at that moment the stop watch was started (t = 0min). The charging time should not exceed one minute. A piston was placed on top of the sample and after t = 2min, the heater was reset to the required temperature and the sample was left for

3min to reach an equilibrium temperature ($t = 5\text{min}$). A load of 2.16kg was then placed on top of the piston to extrude the molten polymer through a small die ($\varnothing = 0.1181\text{cm}$). The time interval for the first extrudate or cut-off was 60s and discarded, then five successive cut-offs were taken, each after 60s. All the extrudates were weighed and an average MFI was calculated from the amount of polymer melt (g) which passed through the die within 10min (see equation 2.1). Every sample was carried out in triplicate to establish the experimental error which was calculated from the standard deviation of the weights of the extrudates of all three samples (see equation 2.2). The % error was found to be between 3-5%.

$$\text{MFI} = \frac{10\bar{m}}{T} \quad (2.1)$$

$$s = \sqrt{\sum_i (m_i - \bar{m})^2 / (n - 1)} \quad (2.2)$$

Where,

- \bar{m} = average weight of all extrudates (g)
- T = time of extrusion (1min)
- s = standard deviation of measurements
- m_i = weight of extrudate i (g)
- n = number of measurements

The difference between the MFI of the first pass and the fourth pass (for LDPE samples only) was also determined as shown in equation 2.3.

$$\Delta\text{MFI} (\%) = [(MFI_1 - MFI_4) \times 100] / MFI_1 \quad (2.3)$$

Where, MFI_1 and MFI_4 are the values of MFI after the first and fourth extrusion passes, respectively.

2.4.2 Thermal ageing of polymer films

The long term stability of polymer samples towards oxygen and heat can be evaluated by subjecting the polymer, pressed to a thin film of a fixed thickness, to an accelerated

thermal ageing test. Thermal ageing tests of processed PP samples, pressed to films, were carried out in single cell Wallace ovens at various temperatures (100-140°C) under circulating air atmosphere. Films of 5 x 1cm² surface and 0.25mm thickness were suspended in the oven cells at the required temperature. Films from different samples were placed in a separate cell to prevent cross contamination of the additives by volatilisation and were subjected to an air flow of 85 l.hour⁻¹. The thermal stability of a polymer film was evaluated by measuring its embrittlement time (h) (see section 2.5). All tests were carried out in quadruplicate to establish the experimental error and the average embrittlement time, with its standard deviation, was determined. The % error on the embrittlement time was less than 10%.

2.4.3 Ultraviolet irradiation of polymer films

The long term stability of the processed PP samples towards light was evaluated by placing them in an accelerated ultraviolet (UV) light ageing cabinet. Films of 5 x 1cm² surface and 0.25mm thickness were irradiated with fluorescent sun lamps and black lamps. The UV cabinet consists of a chamber equipped with a concentric circular rotating sample drum in its centre, which is surrounded by 28 fluorescent tube lamps. The lamps are composed of a 1 to 3 combination of sun lamps and black lamps of 20W power each and mounted alternately around a metallic cylindrical board whose periphery is 15cm from the circumference of the sample drum. The rotation of the sample drum allowed an identical amount of total radiation to fall on each sample. The cabinet was open to the atmosphere on both the lower and upper sides and the circulation of air in the cabinet was ensured by driven ventilation situated under the rotating frame. The polymer films were mounted vertically on the circumference of the rotating drum, so that the light beam fell perpendicularly on the surface of the films. The distance of the polymer films from the light source was 10cm and the temperature inside the cabinet with the lamps on was around 30°C. In order to maintain long term uniform spectral distribution inside the cabinet, the lamps were replaced sequentially every 300h of operation. The UV stability of the polymer films was determined by measuring their embrittlement times (h) (see section

2.5). All tests were carried out in quadruplicate to establish the experimental error and the average embrittlement time with its standard deviation was determined. The % error was less than 10%.

2.5 MEASUREMENT OF THE BRITTLE FRACTURE TIME OF POLYMER FILMS

The brittle fracture time or embrittlement time of a polymer film is a measure of its stability under fixed conditions. Unstabilised and stabilised PP films of 0.25mm thickness which were subjected to thermal or UV ageing, were periodically checked for their flexibility by bending them back on themselves 180° manually. Their embrittlement time was reached when the film split during bending.

2.6 EXTRACTION OF ANTIOXIDANTS AND THEIR TRANSFORMATION PRODUCTS FROM POLYMER FILMS

2.6.1 General procedure

The most used extractants for phenolic antioxidants in polyolefins are chloroform, dichloromethane, n-hexane and diethylether [101]. The use of low boiling point solvents is advantageous in order to minimise stabiliser degradation during extraction and for subsequent concentration of the extract. However, most of these solvents extract a certain amount of low molecular weight polymer (LMWP) which is more soluble than the parent polyolefin, hence leading to contamination of the extract. Dichloromethane was found to be a particularly good solvent for PP extractions because of the small amount of atactic material extracted from the polymer compared with other solvents [101]. Therefore, dichloromethane was used in all the extractions experiments.

Stabilised and unstabilised LDPE and PP films of about 0.25mm thickness and 1 x 4 cm² in size were extracted to recover the antioxidants and their transformation products for future UV and HPLC analysis (for the preparation of PP films, see section 2.3.3). The amount of polymer films used was varied according to the initial concentration of the hindered phenol antioxidant in the polymer. For concentrations up to 0.02%, 0.05% to 0.2% and 1% to 10%, about 5g, 2g and 1g of polymer films were used, respectively. When several polymer samples containing the same mixture of antioxidants were processed, i.e. in the case of low concentrations, all the individually processed samples were extracted, to reduce experimental errors. Before extraction, the films were cleaned with ethanol to remove any impurities from their surface. Each polymer sample was then weighed accurately and Soxhlet extracted with 140ml of dichloromethane for 8 hours, which was shown to be sufficient to extract all the products (see section 2.6.2). Three of the films for each sample were marked and analysed by UV spectroscopy before and after extraction to check the extraction efficiency (see section 2.6.2). Unstabilised LDPE and PP films (5g) were also Soxhlet extracted under the same conditions to determine the extent of extraction of LMWP (see section 2.6.3).

After extraction, the solvent was removed from the extracted products under vacuum. The resulting extracts were weighed, dissolved in hexane (Toc and Toc derivatives) or dichloromethane (Irg 1076 and Irg 1010) (about 10ml), filtered using microporous filters (0.2 μ m), to remove LMWP, and the solvent was removed under vacuum. The resulting extracts were stored in a cool dark place for future UV and HPLC analysis. The polymer films were dried under vacuum at RT after extraction and their weight was compared with that measured before extraction, to determine the extent of extraction of LMWP (see section 2.6.3). The marked polymer films were analysed by UV spectroscopy to determine the extraction efficiency (see section 2.6.2).

Stabilised polymer granules (CPC789 series) were extracted in a similar manner to the films but were placed in porous thimbles during the extraction.

2.6.2 Extraction efficiency

The extraction efficiency was checked for each film sample using two different methods. The first quick method consisted of measuring three films by UV spectroscopy before and after extraction. For example, figure 2.18 reveals the change in the UV spectra of PP stabilised with 0.2% Toc, after 20min processing in a CM/N₂, before and after 8 hours extraction with dichloromethane. The second method involved the extracts which were analysed by UV spectroscopy, using hexane as a solvent and blank, but was only applied to extracts containing Toc, Toc derivatives and U-626, as not all the transformation products of Irg 1076 and Irg 1010 could be identified. Each extract was dissolved in a known volume of hexane, v , and the absorbance was determined at a wavelength at which the antioxidant and its transformation products absorb. The concentration, c' , of the products in the extract could then be determined using the Beer-Lambert law, according to equations 2.4 and 2.5.

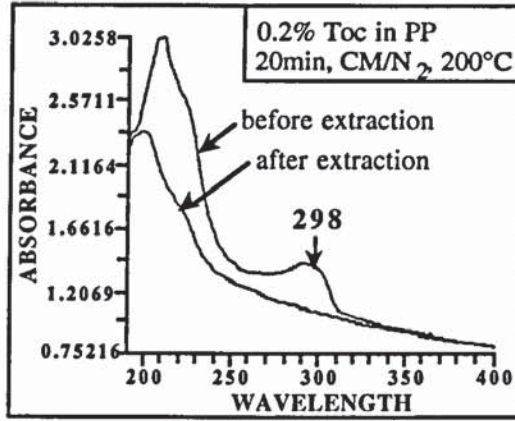


Figure 2.18: UV spectra of a PP film (0.25mm thick) stabilised with 0.2% Toc (internal mixer, CM/N₂, 20min, 200°C) before and after 8 hours extraction with dichloromethane

$$A = \epsilon c l \quad (2.4)$$

$$\Rightarrow A = \bar{E} c' l \text{ with } \bar{E} = \frac{\epsilon}{MM} \quad (2.5)$$

Where,

A = absorbance

ϵ = molar extinction coefficient of extract (l.mol⁻¹.cm⁻¹)

c = concentration of extract (mol.l⁻¹)

l = pathlength of cell (cm)

\bar{E} = extinction coefficient of extract (l.g⁻¹.cm⁻¹)

c' = concentration of extract (g.l⁻¹)

MM = average molar mass of extract (g)

The extinction coefficient \bar{E} is dependent on the individual extinction coefficients of each product in the extract. Therefore it was necessary to know the peak area of each product in the mixture. \bar{E} could then be calculated as shown in equation 2.6 and the weight percentage of the antioxidant and its transformation products in the polymer, m'_{AO} , was determined according to equation 2.7. The wavelength used to determine \bar{E} and m'_{AO} was 290nm, as Toc and its products all absorb strongly at 290nm, apart from TQ which has λ_{max} at 262 and 268nm. Hence, if TQ was present in the extract its concentration was added to the value of c' as shown in equation 2.8.

$$\bar{E} = \frac{\sum_i (A_p E')}{\sum_i A_p} \quad (2.6)$$

$$m'_{AO} = \frac{c' v}{m_i} \times 100 \quad \text{with} \quad c' = \frac{A}{\bar{E} l} \quad (2.7)$$

$$\text{If TQ is present: } c' = \frac{\frac{A}{\bar{E} l} \times c_{TQ}}{100} + \frac{A}{\bar{E} l} \quad (2.8)$$

Where,

\bar{E} = extinction coefficient of the extract ($\text{l.g}^{-1}.\text{cm}^{-1}$)

A_p = peak areas of products in the extract (%)

E' = extinction coefficients of individual products in the extract ($\text{l.g}^{-1}.\text{cm}^{-1}$)

m'_{AO} = weight of extract in the polymer (%)

c' = concentration of extract (g.l^{-1})

v = volume of solvent (l)

m_i = weight of polymer films before extraction (%)

A = absorbance of extract

l = pathlength of cell (cm)

c_{TQ} = concentration of TQ in the extract (% weight)

The errors on the average extinction coefficient, \bar{E} , and the weight of extract, m'_{AO} , in the polymer were estimated as described in equations 2.9 to 2.11 (see table 2.65, p. 135, for errors on peak areas). The errors on A , l and m_i are negligible compared to those on A_p , E' and v .

$$\frac{\Delta \bar{E}}{\bar{E}} = \frac{\sum_i (E' \Delta A_p + A_p \Delta E')}{\sum_i (A_p \times E')} \quad (2.9)$$

$$\frac{\Delta m'_{AO}}{m'_{AO}} = \frac{\Delta A}{A} + \frac{\Delta \bar{E}}{\bar{E}} + \frac{\Delta l}{l} + \frac{\Delta v}{v} + \frac{\Delta m_i}{m_i} + \frac{\Delta c'}{c'} \approx \frac{\Delta \bar{E}}{\bar{E}} + \frac{\Delta v}{v} + \frac{\Delta c'}{c'} \quad (2.10)$$

$$\text{If TQ is present: } \frac{\Delta c'}{c'} = \left[\frac{(A/\bar{E}l)\Delta c_{TQ} + c_{TQ} \times \Delta(A/\bar{E}l)}{100} + \Delta(A/\bar{E}l) \right] \times \frac{1}{c'} \quad (2.11)$$

$$\text{with } \frac{\Delta(A/\bar{E}l)}{(A/\bar{E}l)} = \frac{\Delta\bar{E}}{\bar{E}}$$

As an example, the weight of extract recovered from PP stabilised with 0.2% Toc, after 20min processing in an internal mixer (CM/N₂, 200°C) (see figure 2.19) was calculated as follows (see table 2.26 and equations 2.12-2.17). For errors on individual extinction coefficients and peak areas, see tables 2.53 and 2.65, respectively, and section 2.11.1.3).

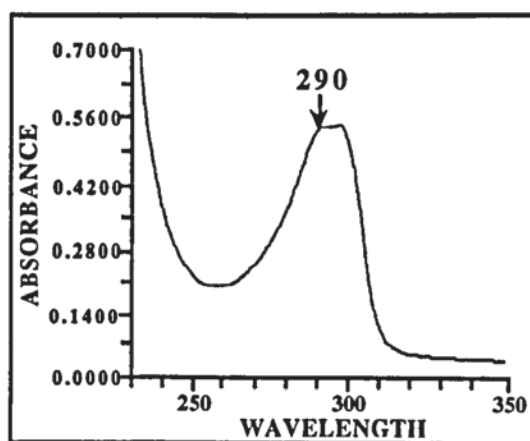


Figure 2.19: UV spectrum, in 6ml hexane, of the products extracted from PP stabilised with 0.2% Toc (internal mixer, CM/N₂, 20min, 200°C)

Table 2.26: Extinction coefficients, peak areas and concentrations of products in PP stabilised with 0.2% Toc in an internal mixer (CM/N₂, 20min, 200°C)

Product	E' ± ΔE' (g ⁻¹ .l.cm ⁻¹), 290nm	E' ± ΔE' (g ⁻¹ .l.cm ⁻¹), 275nm	A _p ± ΔA _p (%), 290nm	c (% weight)
Toc	8.1 ± 0.2	3.3 ± 0.1	86.6 ± 0.43	87.9
DHD, E	7.9 ± 0.5	-	2.1 ± 0.21	2.2
TRI, A, B, C	4.98 ± 0.07	-	3.1 ± 0.31	5.1
ALD 1	20.5 ± 0.5	15.2 ± 0.4	5.3 ± 0.27	2.1
ALD 2	17.7 ± 0.9	-	1.4 ± 0.14	0.7
ALD 3	15.6 ± 0.8	-	0.84 ± 0.084	0.4
ALD 4	18	-	0.27 ± 0.027	0.2
ALD 5	18	-	0.34 ± 0.034	0.2
TQ	-	11.9 ± 0.5	0	1.2
		Total	99.95	100

$$\bar{E} = \frac{\sum_i (A_p E')}{\sum_i A_p} \quad (2.12)$$

$$= \frac{86.6 \times 8.1 + 2.1 \times 7.9 + 3.1 \times 4.98 + 5.3 \times 20.5 + 1.4 \times 17.7 + 0.84 \times 15.6 + (0.27 + 0.34) \times 18}{100}$$

$$= 8.9 \text{ g}^{-1} \cdot \text{l} \cdot \text{cm}^{-1}$$

$$\frac{\Delta \bar{E}}{\bar{E}} = \frac{\sum_i (E' \Delta A_p + A_p \Delta E')}{\sum_i (A_p E')} \quad (2.13)$$

$$= \frac{(8.1 \times 0.43) + (86.6 \times 0.2) + (7.9 \times 0.21) + (2.1 \times 0.5) + (4.98 \times 0.31) + (3.1 \times 0.07) + \text{etc...}}{8.9}$$

$$= 4.5\%$$

$$c' = \frac{A}{\bar{E}l} \times c_{TQ} + \frac{A}{\bar{E}l} = \frac{0.53134}{8.9 \times 0.1} \times 1.2 + \frac{0.53134}{8.9 \times 0.1} = 0.60 \text{ g} \cdot \text{l}^{-1} \quad (2.14)$$

$$\frac{\Delta c'}{c'} = \left[\frac{(A/\bar{E}l)\Delta c_{TQ} + c_{TQ} \times \Delta(A/\bar{E}l)}{100} + \Delta(A/\bar{E}l) \right] \times \frac{1}{c'} \quad (2.15)$$

$$= \left[\frac{[0.53134 / (8.9 \times 0.1)] \times 0.12 + 1.2 \times 0.045}{100} + 0.045 \right] \times \frac{1}{0.60} = 7.7\%$$

$$m'_{AO} = \frac{c'v}{m_i} \times 100 = \frac{0.60 \times 6.10^{-3}}{2.3135} \times 100 = 0.16\% \quad (2.16)$$

$$\frac{\Delta m'_{AO}}{m'_{AO}} = \frac{\Delta \bar{E}}{\bar{E}} + \frac{\Delta v}{v} + \frac{\Delta c'}{c'} = \frac{0.4}{8.9} + \frac{0.03}{6} + \frac{0.046}{0.60} = 13\% \quad (2.17)$$

It was found that 8 hours were sufficient to extract all the antioxidants and their products from the polymer films.

2.6.3 Extent of extraction of low molecular weight polymer (LMWP)

The extent of extraction of LMWP was determined by measuring the weight of the films before and after extraction. The weight of LMWP extracted, m_{LMWP} , could then be calculated as shown in equation 2.18.

$$m_{LMWP} (\%) = \left[\left(\frac{m_i - m_f}{m_i} \right) - m_{AO} \right] \times 100 \quad (2.18)$$

Where,

m_{LMWP} = percentage weight of LMWP extracted (%)

m_i = weight of films before extraction (g)

m_f = weight of films after extraction (g)

m_{AO} = percentage weight of antioxidant (e.g. 0.2%)

As a control, unstabilised LDPE and PP films were extracted and their difference in weight before and after extraction was measured. Table 2.27 shows the results obtained for

unstabilised LDPE (extruded at 180°C) and PP (internal mixer, CM, 200°C), and PP stabilised with 0.2% Toc (internal mixer, CM/N₂, 200°C).

Table 2.27: Extent of extraction of LMWP from unstabilised LDPE (extruded at 180°C), unstabilised PP (internal mixer, CM, 200°C) and PP stabilised with 0.2% Toc (internal mixer, CM/N₂, 200°C)

	unstabilised LDPE (extrusion pass)	unstabilised PP, CM (processing time)	PP + 0.2% Toc, CM/N ₂ (processing time)
weight of films before extraction (m _i , g)	1.5293 (pass 1) 2.3670 (pass 2) 1.7600 (pass 3) 1.6196 (pass 4)	1.6561 (10min) 2.0049 (20min) 1.3596 (30min)	2.3135 (20min) 1.3464 (30min)
weight of films after extraction (m _f , g)	1.5109 (pass 1) 2.3421 (pass 2) 1.7421 (pass 3) 1.6039 (pass 4)	1.6493 (10min) 1.9950 (20min) 1.3522 (30min)	2.2985 (20min) 1.3344 (30min)
weight of antioxidant (m _{AO} , %)	0	0	0.2
weight of LMWP (%) (m _{LMWP} , %)	1.2 (pass 1) 1.1 (pass 2) 1.0 (pass 3) 1.0 (pass4)	0.41 (10min) 0.49 (20min) 0.54 (30min)	0.45 (20min) 0.69 (30min)

2.7 ISOLATION AND CHARACTERISATION OF TOC TRANSFORMATION PRODUCTS FROM POLYMER EXTRACTS

2.7.1 Isolation and characterisation of products extracted from PP stabilised with 39% Toc, pass 4 (CPC789 series, single screw extruder, 270°C)

2.7.1.1 Isolation of products

4.0g of the stabilised polymer granules were placed in a porous thimble and Soxhlet extracted for 8 hours with 140ml dichloromethane (see section 2.6 for procedure). About 15mg of the resulting extract, dissolved in 10ml hexane, was analysed by NP-HPLC (see section 2.10.1 for technical details) using the solvent systems hexane:1,4-dioxane = 100:4 and 100:0.5, v/v, at 290nm (see figure 2.20, p. 240). The group of products with short RT (0-8min), when the solvent ratio 100:4 was used (see figure 2.20.a), were separated from the other products (Toc, DHD, E and TQ) by semi-preparative NP-HPLC using the solvent ratio 100:4. The collected products were then further separated by semi-preparative NP-HPLC using the solvent ratio 100:0.5 (see figure 2.20.b) and the isolated products, including ALD 1, ALD 2, ALD 3 and compound I, were reanalysed by analytical NP-HPLC using the solvent ratio 100:0.5 to check their purity (see figures 2.21.a, 2.22.a, 2.23.a and 2.24.a, respectively).

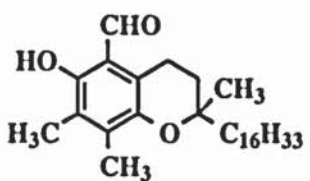
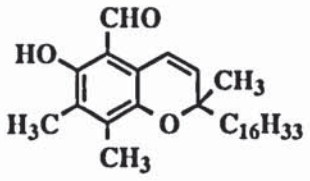
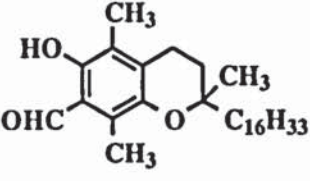
2.7.1.2 Characterisation of products

ALD 1, ALD 2, ALD 3 and compound I (see table 2.28 for structures and HPLC Rt) were characterised using different spectroscopic and spectrometric techniques as described below (see sections 2.13 and 2.14 for experimental details) and the results are displayed in form of tables 2.21-2.32 (p. 165-168) and figures 2.21-2.24 (p. 241-250) at the end of this chapter as follows.

ALD 1, ALD 2, ALD 3 and compound I were characterised by UV and ¹H-NMR and ALD 1 and 2 were also analysed by FTIR (see tables 2.29 and 2.30 and figures 2.21.b to 2.21.c, 2.22.b to 2.22.d, 2.23.b to 2.23.c and 2.24.b to 2.24.c). Furthermore, ALD 1 was

characterised by ^{13}C -NMR (see table 2.31 and figure 2.21.d) and ALD 2 was analysed by EI-MS (see table 2.32 and figure 2.22.e). The results obtained for ALD 1 were compared with those acquired for the supplied ALD 1 (see tables 2.29, 2.30 and 2.31).

Table 2.28: Chemical structures and NP-HPLC Rt (290nm, solvent ratio in hexane:1,4-dioxane, v/v) of products isolated from the extract of PP stabilised 39% Toc, pass 4 (CPC789 series, single screw extruder, 270°C) (figure 2.20, p. 240)

code name	chemical structure and name (MM)	λ_{max} , nm (ϵ , $\text{mol}^{-1}\cdot\text{l}\cdot\text{cm}^{-1}$)	NP-HPLC RT, min:sec (solvent ratio)
ALD 1, F	 5-formyl- γ -tocopherol (444g)	239 290 (9116), 282 (8761), 386 (2846)	4:50 (100:4) 13 (100:0.5)
ALD 2, G	 5-formyl- γ -tocopherol-3en (442g)	250 285 (8234) 297 (7393) 404 (2166)	4:20 (100:4) 11 (100:0.5)
ALD 3, H	 7-formyl- β -tocopherol (444g)	283 (7115), 395 (1912) [102]	4:20 (100:4) 9 (100:0.5)
compound I	?	275, 310, 350	3:20 (100:4) 7:30 (100:0.5)

2.7.2 Isolation and characterisation of the products extracted from LDPE stabilised with 0.2% and 10% Toc, pass 4 (single screw extruder, 180°C)

2.7.2.1 Isolation of the products

9.5g and 5.6g of LDPE films stabilised with 0.2% and 10% Toc (single screw extruder, passes 4, 180°C), respectively, of about 0.25mm thickness, were each extracted for 8 hours with dichloromethane (see section 2.6 for procedure). The resulting extracts, dissolved in 2ml (0.2% Toc in LDPE) and 50ml (10% Toc in LDPE) hexane were analysed by NP-HPLC (see section 2.10.1) using the solvent systems hexane:1,4-dioxane = 100:4 and 100:0.5, v/v, at 275 (ratio 100:4) and 290nm (ratios 100:4 and 100:0.5) (see figure 2.25, p. 251). The group of products with short RT (0-8min), when the solvent ratio 100:4 was used (see figure 2.25.a, c), were separated from the other products (Toc, DHD, E and TQ) by semi-preparative NP-HPLC using the solvent ratio 100:4. The collected products were then further separated by semi-preparative NP-HPLC using the solvent ratio 100:0.5. DHD, E, SPD, D and TRI, A, B, C were isolated from the extract of LDPE stabilised with 10% Toc, whereas ALD 1 and ALD 2 were obtained from the extract of LDPE stabilised with 0.2% Toc. The isolated products were reanalysed by NP-HPLC to check their purity (see figures 2.26.a, 2.27.a, 2.28.a, 2.29.a and 2.30.a for DHD, E, SPD, D, TRI, A, B, C, ALD 1 and ALD 2, respectively).

2.7.2.2 Characterisation of products

DHD, E, SPD, D, TRI, A B, C, ALD 1 and ALD 2 (see tables 2.11p and 2.28p for structures) were characterised using various spectroscopic and spectrometric techniques as described below (see sections 2.13 and 2.14) and the results were compared with those of known oxidation products of Toc, obtained from oxidations of Toc with PbO₂ (see section 2.2.4), products isolated from PP stabilised with 39% Toc (CPC789 series, see section 2.7.1) and supplied samples (ALD 1 and TQ). The results are displayed in form of tables 2.33-2.39 (p. 169-174) and figures 2.26-2.30 (p. 252-264) at the end of this chapter as follows.

DHD, E, SPD, D, TRI, A, B, C, ALD 1 and ALD 2 were characterised by UV and ¹H-NMR (see tables 2.33 to 2.36 and figures 2.26.b to 2.26.c, 2.27.b to 2.27.c, 2.28.b to 2.28.c, 2.29.b to 2.29.c and 2.30.b to 2.30.c). SPD, D, TRI, A, B, C and ALD 1 were also analysed by GC-MS (see tables 2.37 to 2.39 and figures 2.27.d, 2.28.d and 2.29.d). The results were compared with those obtained for synthesised SPD, D, TRI, A, B, C and supplied ALD 1.

2.8 ISOLATION AND CHARACTERISATION OF IRG 1076 and IRG 1010 TRANSFORMATION PRODUCTS FROM POLYMER EXTRACTS

2.8.1 Isolation and characterisation of Irg 1076 transformation products extracted from LDPE stabilised with 10% Irg 1076, pass 4 (single screw extruder, 180°C)

2.8.1.1 Isolation of products

9.98g of LDPE films stabilised with 10% Irg 1076, pass 4, of about 0.25mm thickness, were extracted for 8 hours with dichloromethane (see section 2.6 for procedure). The resulting extract, dissolved in 50ml CH₂Cl₂, was analysed by RP-HPLC (see section 2.10.1) using the solvent system methanol:dichloromethane = 90:10, v/v, at 235nm (see figure 2.31, p. 265, for chromatograms). It was found that at least 15 different transformation products of Irg 1076 were formed. Some of the major products, compounds 1, 12 and 15, were isolated by semi-preparative RP-HPLC (see section 2.10.2) using methanol as a solvent, at 235nm (see figure 2.31.c). The isolated compounds were analysed by RP-HPLC to check their purity (see figures 2.32.a, 2.33.a and 2.34.a for compounds 1, 12 and 15, respectively).

2.8.1.2 Characterisation of products

Compounds 1 to 15 were characterised by UV, using the diode array system (see section 2.10.1), and the isolated compounds, 1, 12 and 15 (see table 2.40 for structures), were analysed by GC-MS (see section 2.14.3 for technical details). Compound 12 was also analysed by ¹H-NMR (see section 2.13.3). The results are displayed in form of tables 2.41-2.46 (p. 175-177) and figures 2.32-2.35 (p. 266-270) at the end of this chapter as follows.

The results of UV analysis of the isolated compounds, 1, 12 and 15, are shown in table 2.41 and figures 2.32.b, 2.33.b and 2.34.b, respectively. The UV characteristics of the other compounds are revealed in table 2.42 and figure 2.35 shows the UV spectra of compounds 11, 13 and 14. The ¹H-NMR characteristics of compound 12 (C-Irg 1076), are

shown in table 2.43 and figure 2.33.c. The MS characteristics of compounds 1, 12 and 15 (BC-Irg 1076) are shown in tables 2.44 to 2.46 and figures 2.32.c, 2.33.c and 2.34.c, respectively.

Table 2.40: Chemical structures and RP-HPLC RT (235nm, solvent systems CH₃OH and CH₃OH:CH₂Cl₂ = 90:10, v/v) of the products isolated and extracted from LDPE stabilised with 10% Irg 1076, pass 4 (single screw extruder, 180°C) (figure 2.31, p. 265)

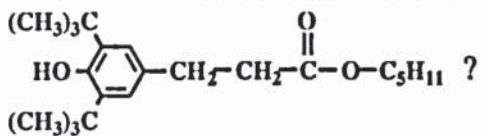
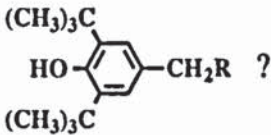
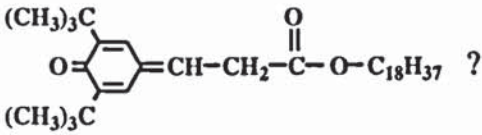
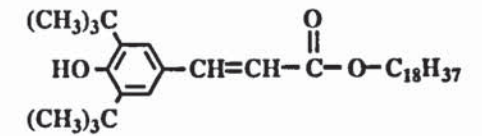
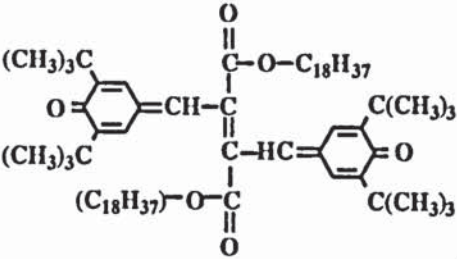
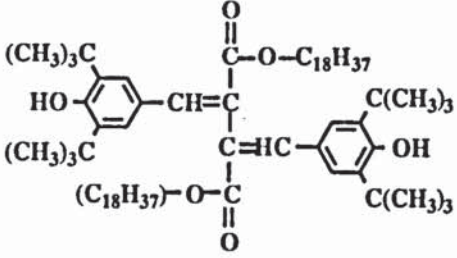
chemical structure and name (MM)	code name (HPLC peak)	λ_{\max} , nm (ϵ , l.mol ⁻¹ .cm ⁻¹)	HPLC Rt, min:sec
 <chem>CC(C)(C)c1cc(O)c(C(C)(C)C)c1CC(=O)OCCCC</chem> ?	Irg 1076-1 (isolated)	282 (broad)	2:40 (CH ₃ OH:CH ₂ Cl ₂), 2:50 (CH ₃ OH)
 <chem>CC(C)(C)c1cc(O)c(C(C)(C)C)c1C[R]</chem> ?	Irg 1076-2-10	282	2:50-11:05 (CH ₃ OH:CH ₂ Cl ₂), 3:05-19:05 (CH ₃ OH)
 <chem>CC(C)(C)c1cc(=O)c(C(C)(C)C)c1C=CC(=O)OCCCCCCCCCCCCCCCCCC</chem> ? n-octadecyl-3-(3',5'-di- <i>t</i> -butyl-4'-oxo-2,5-cyclohexadiene-1-ylidene)-propionate (528g)	QM-Irg 1076 (11)	315 (broad) (26915) [54], 238	13:15 (CH ₃ OH:CH ₂ Cl ₂), 25:30 (CH ₃ OH)
 <chem>CC(C)(C)c1cc(O)c(C(C)(C)C)c1C=CC(=O)OCCCCCCCCCCCCCCCCCC</chem> n-octadecyl-3-(3',5'-di- <i>t</i> -butyl-4'-hydroxy-phenyl) 2,3-dehydro-propionate (528g)	cinnamate, C-Irg 1076 (12, isolated)	240 320 (21230)	14:40 (CH ₃ OH:CH ₂ Cl ₂), 29:10 (CH ₃ OH)
contains cinnamate or quinonoid structure	Irg 1076-13	282, 320 (broad)	16:40 (CH ₃ OH:CH ₂ Cl ₂), 32:50 (CH ₃ OH)

Table 2.40: continued

chemical structure and name (MM)	code name (HPLC peak)	λ_{\max} , nm (ϵ , l.mol ⁻¹ .cm ⁻¹)	HPLC Rt, min:sec
 <p>1,4-bis-(3',5'-di-<i>t</i>-butyl-4'-oxo-2,5-cyclohexadiene-1-ylidene)-2,3-bis-(n-octadecyl-methanoate)-2-butene (1053g)</p>	CBQM-Irg 1076 (14)	320 (broad) (34800) [20], 240	19:30 (CH ₃ OH:CH ₂ Cl ₂), 35:00 (CH ₃ OH)
 <p>1,4-bis-(3',5'-di-<i>t</i>-butyl-4'-hydroxy-phenyl)-2,3-bis-(n-octadecyl-methanoate)-1,3-butadiene (1055g)</p>	biscinnamate, BC-Irg 1076 (15)	308 (35400) [20] 240	23:30 (CH ₃ OH:CH ₂ Cl ₂), 45:00 (CH ₃ OH)

2.8.2 Isolation and characterisation of Irg 1010 transformation products extracted from LDPE stabilised with 10% Irg 1010, pass 4 (single screw extruder, 180°C)

2.8.2.1 Isolation of products

8.90g of LDPE films stabilised with 10% Irg 1010, of about 0.25mm thickness, were extracted for 8 hours with dichloromethane (see section 2.6 for procedure). The resulting extract, dissolved in 50ml CH₂Cl₂, was analysed by RP-HPLC (see section 2.10.1) using the solvent system methanol:dichloromethane = 90:10, v/v, at 235nm (see figure 2.36, p. 271). It was found that at least 14 different transformation products of Irg 1010 were formed. The major products, compounds 3 and 6, were isolated by semi-preparative RP-

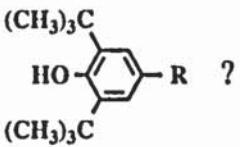
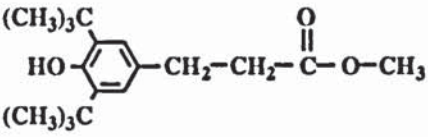
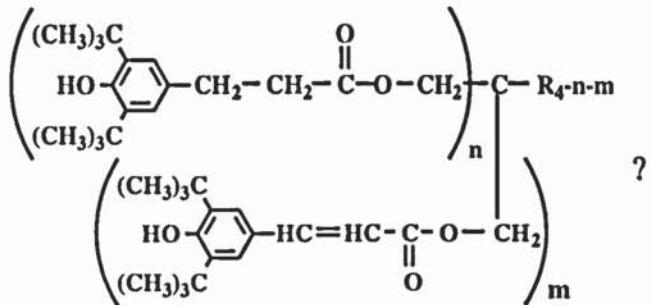
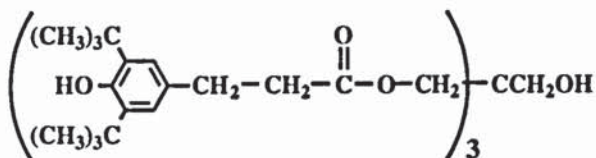
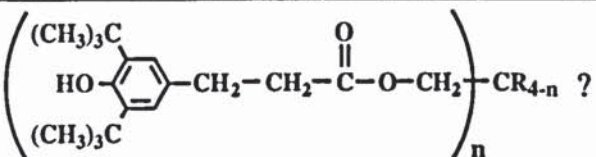
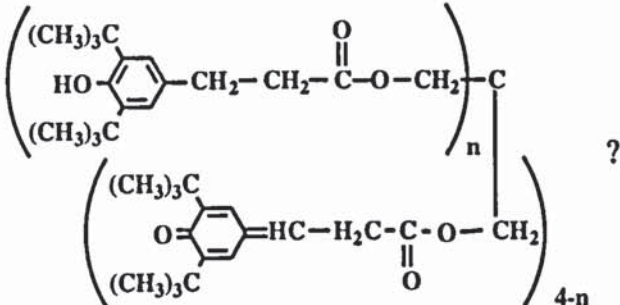
HPLC (see section 2.10.2) using methanol as a solvent, at 235nm (see figure 2.36.b). The isolated compounds were analysed by RP-HPLC to check their purity (see figures 2.37.a and 2.38.a for compounds 3 and 6, respectively).

2.8.2.2 Characterisation of products

Compounds 1 to 14 were characterised by UV, using the diode array system (see section 2.10.1), and the isolated compounds, 3 and 6 (see table 2.47 for structures), were also analysed by $^1\text{H-NMR}$ and GC-MS (see sections 2.13.3 and 2.14.3). The results are displayed in form of tables 2.48-2.52 (p. 178-180) and figures 2.37-2.39 (p. 272-276) at the end of this chapter as follows.

The results of UV analysis of the isolated compounds 3 and 6, are shown in table 2.48 and figures 2.37.b and 2.38.b, respectively. The UV characteristics of the other compounds are revealed in table 2.49. Figure 2.39 shows the UV spectra of compounds 4 and 14. The $^1\text{H-NMR}$ results of compounds 3 and 6 are shown in table 2.50 and figures 2.37.c and 2.38.c, respectively. The MS characteristics of compounds 3 and 6 are shown in tables 2.51 and 2.52 and figures 2.37.d and 2.38.d, respectively.

Table 2.47: Suggested chemical structures and RP-HPLC RT (282nm, solvent system: CH₃OH) of the products isolated and extracted from LDPE stabilised with 10% Irg 1010, pass 4 (single screw extruder, 180°C) (figure 2.36, p. 271)

chemical structure and name (MM)	code name	λ_{\max} , nm	HPLC Rt, min:sec
 <p style="text-align: center;">(CH₃)₃C HO--R ? (CH₃)₃C</p>	Irg 1010-1, -2	282	2:40, 3:00
 <p style="text-align: center;">(CH₃)₃C HO--CH₂-CH₂-C(=O)-O-CH₃ (CH₃)₃C</p> <p style="text-align: center;">methyl-3-(3',5'-di-<i>t</i>-butyl-4'-hydroxy-phenyl) propionate (292g)</p>	Irg 1010-3	282	3:10
 <p style="text-align: center;"> $\left(\begin{array}{c} \text{(CH}_3\text{)}_3\text{C} \\ \text{HO-} \langle \text{phenyl ring} \rangle \text{-CH}_2\text{-CH}_2\text{-C(=O)-O-CH}_2\text{-} \\ \text{(CH}_3\text{)}_3\text{C} \end{array} \right)_n \text{-C-} R_{4-n-m}$ $\left(\begin{array}{c} \text{(CH}_3\text{)}_3\text{C} \\ \text{HO-} \langle \text{phenyl ring} \rangle \text{-HC=HC-C(=O)-O-CH}_2\text{-} \\ \text{(CH}_3\text{)}_3\text{C} \end{array} \right)_m$ </p> <p style="text-align: center;">?</p>	Irg 1010-4	320 (broad), 282	3:20
 <p style="text-align: center;"> $\left(\begin{array}{c} \text{(CH}_3\text{)}_3\text{C} \\ \text{HO-} \langle \text{phenyl ring} \rangle \text{-CH}_2\text{-CH}_2\text{-C(=O)-O-CH}_2\text{-} \\ \text{(CH}_3\text{)}_3\text{C} \end{array} \right)_3 \text{-C-CH}_2\text{OH}$ </p> <p style="text-align: center;">tris-[methylene-(3,5-di-<i>t</i>-butyl-4-hydroxy-phenyl)propionate]-hydroxymethylmethane (916g)</p>	Irg 1010-6	282	3:50
 <p style="text-align: center;"> $\left(\begin{array}{c} \text{(CH}_3\text{)}_3\text{C} \\ \text{HO-} \langle \text{phenyl ring} \rangle \text{-CH}_2\text{-CH}_2\text{-C(=O)-O-CH}_2\text{-} \\ \text{(CH}_3\text{)}_3\text{C} \end{array} \right)_n \text{-CR}_{4-n}$ </p> <p style="text-align: center;">?</p>	Irg 1010-5 and -7- 11	282	3:40, 4:05-5:25
 <p style="text-align: center;"> $\left(\begin{array}{c} \text{(CH}_3\text{)}_3\text{C} \\ \text{HO-} \langle \text{phenyl ring} \rangle \text{-CH}_2\text{-CH}_2\text{-C(=O)-O-CH}_2\text{-} \\ \text{(CH}_3\text{)}_3\text{C} \end{array} \right)_n \text{-C}$ $\left(\begin{array}{c} \text{(CH}_3\text{)}_3\text{C} \\ \text{O-} \langle \text{phenyl ring} \rangle \text{=HC-H}_2\text{C-C(=O)-O-CH}_2\text{-} \\ \text{(CH}_3\text{)}_3\text{C} \end{array} \right)_{4-n}$ </p> <p style="text-align: center;">?</p>	Irg 1010-14	312 (broad), 288	9:30

2.9 THIN LAYER CHROMATOGRAPHIC TECHNIQUE

All chromatograms were prepared by the ascending method in a solvent saturated atmosphere, using the mixture hexane:chloroform = 1:3, v/v, as the solvent system. The compounds in solution were placed 3cm from the bottom of the plate which was submerged in solvent to a depth of about 1cm and the solvent was allowed to run a distance of 10cm. The products were detected by UV light at 254nm.

2.10 HIGH PERFORMANCE LIQUID CHROMATOGRAPHIC TECHNIQUES

2.10.1 Analytical high performance liquid chromatography (HPLC)

Analytical HPLC was performed with a Philips PU4100 liquid chromatograph equipped with a PU4120 diode array detector. The diode array detector was controlled by a PU6003 diode array software system. The system consisted of a software that controlled and collected data from the diode array detector and displayed and analysed it. Using these facilities, a 3D representation of the sample could be built and both chromatographic and spectral information could be obtained from it. The spectrum information permitted to check on the purity of chromatographic peaks and to find optimum detection of each peak. UV spectra could be displayed for each individual peak. Peak areas, for concentration determinations, were determined using the PU6000 integration software. Normal phase HPLC (NP-HPLC) was realised with a Zorbax SIL column (4.6mm x 25cm) developed with varying ratios of hexane:1,4-dioxane at a flow rate of $1\text{ml}\cdot\text{min}^{-1}$. Reverse phase HPLC (RP-HPLC) was realised with a Zorbax ODS column (4.6mm x 25cm) developed with mixtures of methanol with dichloromethane or methanol only, at a flow rate of $1\text{ml}\cdot\text{min}^{-1}$.

2.10.2 Semi-preparative HPLC

Semi-preparative HPLC was carried out on a Gilson liquid chromatograph comprising a Gilson 305 piston pump equipped with a Gilson 806 manometric module and a Dynamax UV-1 variable wavelength UV/visible absorbance detector. NP-HPLC was realised with a Zorbax SIL column (9.4mm x 25cm), developed with varying ratios of hexane:1,4-dioxane at a flow rate of 3.5mlmin⁻¹. RP-HPLC was realised with a Zorbax ODS column (9.4mm x 25cm), developed with methanol at a flow rate of 3.5mlmin⁻¹. The spectra were recorded on a TYP 2041 Linseis chart recorder at 290, 275 or 235nm and the different fractions were collected by a Gilson FC203 fraction collector in a manual mode.

2.11 DETERMINATION OF THE CONCENTRATIONS OF THE ANTIOXIDANTS AND THEIR OXIDATION PRODUCTS

2.11.1 Determination of the concentrations of Toc and its oxidation products

2.11.1.1 Determination of the concentrations

The concentrations of Toc and its oxidation products were determined from the HPLC chromatograms of the mixtures, by integrating the peak areas at a fixed wavelength, using the PU6100 integration software. Mixtures of products include products of reaction of Toc with PbO₂ before and after purification, products of reaction of SPD, D with LiAlH₄ (see section 2.2), extracted products of oxidation of Toc and Toc derivatives after processing of the antioxidants with LDPE and/or PP (section 2.3) and extracted products of oxidation of Toc formed during thermal and UV ageing of the stabilised PP films (section 2.4).

As a UV detector was used in HPLC analysis, the magnitude of the absorption signal is proportional to the concentration of the product according to the Beer-Lambert law and directly dependent on the extinction coefficient ϵ at the wavelength of detection (see equation 2.4, p. 107). The absorbance A of the product is proportional to its peak area A_p at a fixed wavelength, hence its concentration c is proportional to its peak area (equation 2.19). As the quantification of the products was only required in percentage weights, c

could be directly determined from the peak area of the product and the peak areas of the other products present in the mixture, according to equation 2.20.

$$c = \frac{A}{\epsilon l} \Rightarrow c = k \frac{A_p}{E l} \quad \text{with} \quad E = \frac{\epsilon}{MM} \quad (2.19)$$

(Beer-Lambert law)

$$\Rightarrow c_i = \frac{A_{p_i} / E_i}{\sum_i (A_p / E)} \quad (2.20)$$

Where,

- | | |
|---|---|
| <p>c = concentrations (% weight);</p> <p>A_p = peak areas (%);</p> <p>E = extinction coefficients ($\text{l.g}^{-1}.\text{cm}^{-1}$);</p> <p>$A$ = absorbance</p> <p>ϵ = extinction coefficient ($\text{l.mol}^{-1}.\text{cm}^{-1}$)</p> <p>$MM$ = molar mass of product (g)</p> <p>k = constant ($k = A/A_p$)</p> <p>l = pathlength of cell (cm)</p> | <p>c_i = concentration of product i (% weight)</p> <p>A_{p_i} = peak area of product i (%)</p> <p>E_i = extinction coefficient of product i ($\text{l.g}^{-1}.\text{cm}^{-1}$)</p> |
|---|---|

The integrations of the chromatograms were carried out at 290nm, at which wavelength all products absorb strongly, except TQ which has λ_{max} of 260 and 268nm. If TQ was present in the mixture, a second integration was carried out at 275nm and the peak area of TQ was compared with that of Toc, DHD or ALD 1, at the same wavelength, depending which was the major product (see equation 2.21). The final concentrations of the products, c'_i , were then recalculated using equation 2.22.

$$c_{\text{TQ}} = \frac{A_{\text{PTQ}} / E_{\text{TQ}}}{A_{\text{PToc}} / E_{\text{Toc}} \quad \text{(DHD, ALD 1)}} \times c_{\text{Toc}} \quad \text{(DHD, ALD 1)} \quad (2.21)$$

$$c'_i = \frac{1}{c_{\text{TQ}} + 100} \times c_i \times 100 \quad (2.22)$$

Where,

c_{TQ} = relative concentration of TQ, compared to that of Toc (%)

A_{pTQ} = peak area of TQ at 275nm (%)

E_{TQ} = extinction coefficient of TQ at 275nm ($l.g^{-1}.cm^{-1}$)

A_{pToc} = peak area of Toc (DHD, ALD 1) at 275nm (%)
(DHD, ALD 1)

E_{Toc} = extinction coefficient of Toc (DHD, ALD 1) at 275nm ($l.g^{-1}.cm^{-1}$)
(DHD, ALD 1)

c_{Toc} = concentration of Toc (DHD, ALD 1), excluding TQ (%)
(DHD, ALD 1)

c'_i = final concentration of product i (%)

c_i = concentration of product i, excluding TQ (%)

The integration report gave the peak areas which were expressed in absorbance units (AU, added peak heights from the start to the end of the peak) and % (total area of 100%). After the determination of the peak areas, the extinction coefficient of each product was calculated by UV spectroscopy (see section 2.13.1 for technical details), from the Beer-Lambert law (see equation 2.4, p. 107). A calibration of the absorbance versus the concentration was carried out for Toc and each of the isolated oxidation products including DHD, E, SPD, D, TRI, A, B, C and the provided products ALD 1, ALD 2 and TQ (see tables 2.11 and 2.28 for structures), using hexane as a solvent and blank. A typical calibration involved 8 to 10 standard solutions with concentrations ranging from 0.02 to $1.5g.l^{-1}$. However, in the case of ALD 2, isolated from polymer extracts (see section 2.7.1), only three measurements were carried out as only a small quantity of the product was present. ALD 3 was assigned a literature value for its extinction coefficient as it was not pure enough (see table 2.53) [102]. Furthermore, the extinction coefficients of ALD 4 and ALD 5 were given an arbitrary value of $18g^{-1}.l.cm^{-1}$, as the latter could not be isolated in large enough quantities.

The extinction coefficient was determined from the slope (b) of the linear range of the calibration graph which was the line of regression of the absorbance on the concentration, calculated by the method of least squares using computer facilities (see equation 2.23). The

intercept of the equation of the regression line (a) was considered to be equal to zero (when $c = 0, A = 0$). As an example, figure 2.40 shows the calibration graph and the equation of the regression line for Toc. Table 2.53 gives the highest concentration and corresponding absorbances at 290 and/or 275nm, checked to be within the linear range, as well as the extinction coefficients of each product at 290 and/or 275nm.

In the case of TRI, A, B, C, the extinction coefficients of A1, A2, B and C were determined individually, but because only small amounts of the trimers were available (see section 2.2.2.2), only three measurements could be taken for each trimer (see table 2.54). Considering that the values of the extinction coefficients for each trimer are all very similar, the extinction coefficient of the mixture of TRI, A, B, C, which has a much lower experimental error, was used for all the calculations.

$$\text{Equation of the regression line: } y = a + bx \quad (2.23)$$

Where, y = absorbance

x = concentration

a = intercept of line ($a \rightarrow 0$)

b = slope of line ($b \approx \epsilon l$)

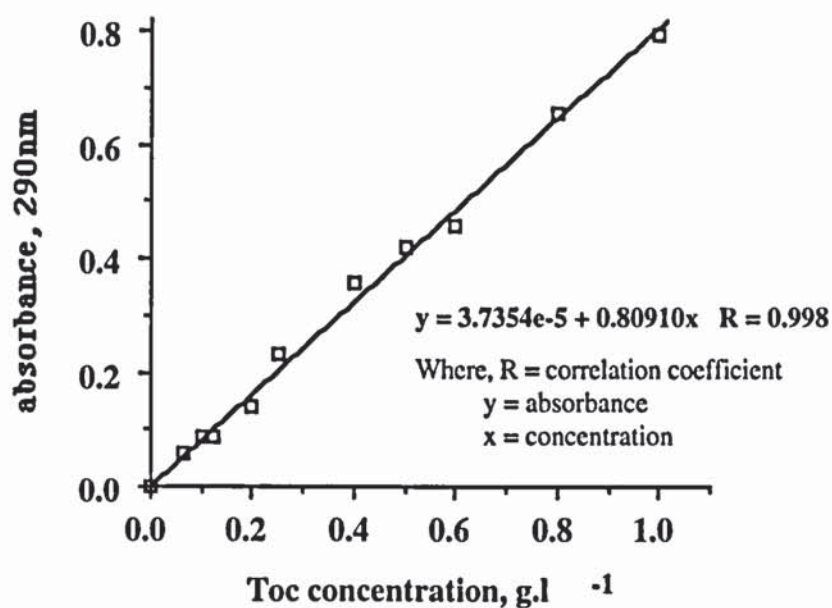


Figure 2.40: Calibration graph and equation of the regression line for the determination of the extinction coefficient of Toc at 290nm

Table 2.53: Extinction coefficients of Toc and its oxidation products

product	highest concentration used in linear range (g.l ⁻¹)	absorbance		E ± s _E (l.g ⁻¹ .cm ⁻¹)	
		290nm	275nm	290nm	275nm
Toc	1	0.8		8.1 ± 0.2	3.3 ± 0.1
DHD E	1.2	0.9	0.35	7.9 ± 0.5	3.0 ± 0.2
SPD D	1	0.45	-	4.3 ± 0.2	-
TRI A, B, C	1.5	0.7	-	4.98 ± 0.07	-
ALD 1	1	2.0	1.52	20.5 ± 0.5	15.2 ± 0.4
ALD 2	0.7	1.2	-	17.7 ± 0.9	-
ALD 3				15.6 ± 0.8	-
ALD 4	-	-	-	18	-
ALD 5	-	-	-	18	-
TQ	0.6	-	0.7	-	11.9 ± 0.5

Table 2.54: Extinction coefficients of TRI, A1, A2, B and C at 290nm

Trimer	$E \pm s_E$ ($l \cdot g^{-1} \cdot cm^{-1}$)
A1	4.7 ± 0.5
A2	4.6 ± 0.5
B	5.2 ± 0.2
C	4.9 ± 0.6

2.11.1.2 Examples

The first example of chromatographic integration report and its interpretation is shown in tables 2.55 to 2.58 which give the results obtained for the mixture of products obtained from the oxidation of Toc with PbO_2 , ratio 1:10 in Toc: PbO_2 (see section 2.2 and figure 2.7, p. 206). When the solvent system hexane:1,4-dioxane = 100:4, v/v was used (see figure 2.7.a), the peak areas of Toc, DHD, E and the mixture of products TRI, A, B, C, ALD 1 and the unknown could be determined, as shown in table 2.55. The peak areas of the products in the latter mixture were revealed by the integration report of the chromatogram when the solvent ratio 100:0.5 in hexane:1,4-dioxane was used (see figure 2.7.b), as shown in table 2.56. The peak areas in table 2.56 only indicate the ratio between TRI, A, B, C, ALD 1 and the unknown products, as DHD, E is not present, and Toc usually shows a broad peak when using the above solvent ratio. The peak areas of TRI, A, B, C, ALD 1 and the unknown were therefore recalculated using the total area of 54.3% found previously, when the solvent ratio 100:4 was used (see table 2.55) and the results are displayed in table 2.57. Finally, the concentration of each known product was calculated from its extinction coefficient (see table 2.53) and the peak areas shown in table 2.57, according to equation 2.20 (see table 2.58). As an example, the determination of the concentration of Toc (c_{Toc}) is described in equation 2.24. The unknown products, present in small amounts, were not taken into consideration in the calculations.

The second example, displayed in tables 2.59 to 2.64, shows the results obtained for the products extracted from PP stabilised with 0.2% Toc, processed for 20min in an internal

mixer (CM/N₂, 200°C). The concentrations of Toc, DHD, E, TRI, A, B, C, ALD 1, 2, 3, 4 and 5 were determined at 290nm as described in the first example (see tables 2.59-2.62). Equation 2.25 describes the calculation of the concentration of TRI, A, B, C as an example. On the other hand, the concentration of TQ was determined by comparing its peak area with that of Toc at 275nm, when the solvent system hexane:1,4-dioxane = 100:4, v/v, was used (see table 2.63 and equation 2.26). The final concentrations of all the products, c'_i , were then recalculated using equation 2.22 (see table 2.64).

Table 2.55: Integration results obtained for the products of reaction of Toc with PbO₂, ratio 1:10 in Toc:PbO₂; solvent system hexane:1,4-dioxane = 100:4, v/v; wavelength: 290nm (figure 2.7.a, p. 206)

peak name	retention time (min)	Peak area (AU)	peak area (%)		Products
1	2.767	0.145	0.109	54.3	unknown + TRI A, B, C + ALD 1
2	3.033	6.825	5.133		
3	3.283	15.989	12.026		
4	3.617	9.405	7.073		
5	4.017	19.857	14.934		
6	4.300	9.934	7.471		
7	4.633	10.009	7.527		
8	10.200	57.826	43.490	43.5	Toc
9	12.917	1.076	0.809	2.2	DHD E
10	13.533	1.896	1.426		
		Total	99.998	100	

Table 2.56: Integration results obtained for the products of reaction of Toc with PbO₂, ratio 1:10 in Toc:PbO₂; solvent system hexane:1,4-dioxane = 100:0.5, v/v; wavelength: 290nm (figure 2.7.b, p. 206)

peak name	retention time (min)	Peak area (AU)	peak area (%)		Products
1	2.883	6.685	0.213	0.60	unknown
2	4.050	11.969	0.382		
3	9.417	224.77	7.173	17.3	TRI A
4	9.817	318.233	10.155		
5	12.383	42.438	1.354	1.4	ALD 1
6	14.100	211.909	6.762	37.6	TRI B
7	15.400	424.387	13.542		
8	17.450	541.550	17.281		
9	31.500	31.779	1.015	11.0	TRI C
10	33.617	121.622	3.881		
11	35.350	191.425	6.109		
12	46.483	1006.968	32.133	32.1	Toc
		Total	100	100	

Table 2.57: Peak areas (%) of the products of reaction of Toc with PbO₂, ratio 1:10 in Toc:PbO₂, at 290nm

chromatogram source (solvent ratio)	peak area	(%)	product
100:4, 100:0.5	0.476	0.48	unknown
100:4, 100:0.5	13.857	52.7	TRI A
100:4, 100:0.5	30.057		TRI B
100:4, 100:0.5	8.801		TRI C
100:4, 100:0.5	1.083	1.1	ALD 1
100:4	43.490	43.5	Toc
100:4	2.235	2.2	DHD E
Total	99.999	100	

$$c_{\text{Toc}} = \frac{A_{\text{PToc}} / E_{\text{Toc}}}{\frac{A_{\text{PToc}}}{E_{\text{Toc}}} + \frac{A_{\text{PTRI, A,B,C}}}{E_{\text{TRI, A,B,C}}} + \frac{A_{\text{PALD 1}}}{E_{\text{ALD 1}}} + \frac{A_{\text{PDHD, E}}}{E_{\text{DHD, E}}}} = 33.0\% \quad (2.24)$$

Where,

c_{Toc} = concentration of Toc (% weight)

A_{PToc} = peak area of Toc = 43.5%

E_{Toc} = extinction coefficient of Toc at 290nm = 8.11.g⁻¹.cm⁻¹

$A_{\text{PTRI, A,B,C}}$ = peak area of TRI, A, B, C = 52.7%

$E_{\text{TRI, A,B,C}}$ = extinction coefficient of TRI, A, B, C at 290nm = 4.981.g⁻¹.cm⁻¹

$A_{\text{PALD 1}}$ = peak area of ALD 1 = 1.1%

$E_{\text{ALD 1}}$ = extinction coefficient of ALD 1 at 290nm = 20.51.g⁻¹.cm⁻¹

$A_{\text{PDHD, E}}$ = peak area of DHD, E = 2.2%

$E_{\text{DHD, E}}$ = extinction coefficient of DHD, E at 290nm = 7.91.g⁻¹.cm⁻¹

Table 2.58: Concentrations (%) of the products of reaction of Toc with PbO₂, ratio 1:10 in Toc:PbO₂, at 290nm, excluding the unknown products

Product	concentration (% weight)
TRI, A, B, C	65.0
ALD 1	0.3
Toc	33.0
DHD, E	1.7

Table 2.59: Integration results obtained for the products extracted from PP stabilised with 0.2% Toc and processed for 20min in an internal mixer (CM/N₂, 200°C); solvent system hexane:1,4-dioxane = 100:4, v/v; 290nm

peak name	retention time (min:sec)	Peak area (AU)	peak area (%)		Products
1	3:50	4.490	0.393	0.39	LMWP
2	3:55	2.622	0.569	11.29	TRI A, B, C + ALD 1, 2, 3, 4, 5
3	4:10	3.818	0.965		
4	5:24	9.296	2.370		
5	5:42	14.555	3.680		
6	6:30-9	8.201	2.073		
7	9-11:30	6.440	1.628		
8	11:32	341.193	86.259	86.26	Toc
9	15-18:30	8.153	2.061	2.06	DHD, E
		Total	99.998	99.98	

Table 2.60: Integration results obtained for the products extracted from PP stabilised with 0.2% Toc and processed for 20min in an internal mixer (CM/N₂, 200°C); solvent system hexane:1,4-dioxane = 100:0.5, v/v; 290nm

peak name	retention time (min)	Peak area (AU)	peak area (%)		Products
1	3-6	10.064	1.110	1.1	LMWP
2	8:00	1.795	0.198	0.30	TRI A
3	9:49	1.096	0.102		
4	9:18	3.33	0.389	0.39	ALD 3
5	10:19	5.7	0.666	0.67	ALD 2
6	12:10	21.011	2.454	2.45	ALD 1
7	17:45	1.069	0.125	0.13	ALD 4
8	18:30-20	0.790	0.504	0.50	TRI B
9	22:47	1.325	0.155	0.16	ALD 5
11	38-42	5.704	0.628	0.63	TRI, C
12		848.58	93.497	93.5	Toc
		Total	99.828	99.83	

Table 2.61: Peak areas of the products extracted from PP stabilised with 0.2% Toc and processed for 20min in an internal mixer (CM/N₂, 200°C); 290nm (excluding LMWP)

chromatogram source (solvent ratio)	peak area (%)	product
100:4, 100:0.5	3.108	TRI, A, B, C
100:4, 100:0.5	0.844	ALD 3
100:4, 100:0.5	1.445	ALD 2
100:4, 100:0.5	5.326	ALD 1
100:4, 100:0.5	0.271	ALD 4
100:4, 100:0.5	0.336	ALD 5
100:4	86.60	Toc
100:4	2.070	DHD E
Total	100	

Table 2.62: Concentrations of the products extracted from PP stabilised with 0.2% Toc and processed for 20min in an internal mixer (CM/N₂, 200°C) (excluding LMWP and TQ)

Product	concentration (% weight)
TRI, A, B, C	5.20
ALD 3	0.45
ALD 2	0.68
ALD 1	2.16
ALD 4	0.13
ALD 5	0.16
Toc	89.04
DHD, E	2.18

$$c_{\text{TRI}} = \frac{A_{\text{pTRI}} / E_{\text{TRI}}}{\frac{A_{\text{pTRI}}}{E_{\text{TRI}}} + \frac{A_{\text{pALD3}}}{E_{\text{ALD3}}} + \frac{A_{\text{pALD2}}}{E_{\text{ALD2}}} + \frac{A_{\text{pALD1}}}{E_{\text{ALD1}}} + \frac{A_{\text{pALD4}}}{E_{\text{ALD4}}} + \frac{A_{\text{pALD5}}}{E_{\text{ALD5}}} + \frac{A_{\text{pALD6}}}{E_{\text{ALD6}}} \text{ etc...}} \quad (2.25)$$

$$c_{\text{TRI}} = 5.20\%, \text{ w/w}$$

Table 2.63: Peak areas and extinction coefficients of Toc and TQ, extracted from PP stabilised with 0.2% Toc (processed for 20min in a CM/N₂, 200°C) at 275nm; solvent system: hexane:1,4-dioxane = 100:4, v/v

	peak area, %	E, l.g ⁻¹ .cm ⁻¹
Toc	69.595	3.3
TQ	3.593	11.9

$$c_{TQ} = \frac{A_{PTQ} / E_{TQ}}{A_{PToc} / E_{Toc}} \times c_{Toc} = \frac{3.6 / 11.9}{69.6 / 3.3} \times 89.04 = 1.28\%, \text{ w/w} \quad (2.26)$$

Table 2.64: Concentrations of the products extracted from PP stabilised with 0.2% Toc and processed for 20min in a CM/N₂ at 200°C (excluding LMWP)

Product	concentration (% weight)
TRI, A, B, C	5.1
ALD 3	0.4
ALD 2	0.7
ALD 1	2.1
ALD 4	0.2
ALD 5	0.2
Toc	87.9
DHD, E	2.2
TQ	1.2
Total	100

2.11.1.3 Errors on the concentrations

According to equation 2.19, p. 124, two major sources of errors affect the value of the concentration: the integration of the chromatographic peaks and the calculation of the extinction coefficient. The error on the peak areas was determined according to its value (see table 2.65) and the standard deviation of the extinction coefficient, s_E , was calculated

from the standard deviation of the slope b , s_b , of the regression line (see equation 2.23) of the calibration graph (see equations 2.27 and 2.28).

Table 2.65: Estimated errors on the peak areas

Peak area (%)	error (%)
0 - 5	10
5 - 10	5
10 - 50	1
50 - 100	0.5

$$s_b = \frac{s_{y/x}}{\left\{ \sum_i (x_i - \bar{x})^2 \right\}^{1/2}} \quad \text{with} \quad s_{y/x} = \left\{ \frac{\sum (y_i - \hat{y}_i)^2}{n-2} \right\}^{1/2} \quad (2.27)$$

$$s_E = \frac{s_b}{l} \quad (2.28)$$

Where,

s_b = standard deviation of the slope b

y_i = absorbance of solution i

\hat{y}_i = absorbance of solution i calculated from the regression equation ('fitted' y_i value)

n = number of measurements

x_i = concentration of solution i

\bar{x} = mean of concentration values

s_E = standard deviation of the extinction coefficient

l = pathlength of cell (0.1cm)

Thus, armed with the values of the error on the peak areas and the standard deviations of the extinction coefficients (see table 2.40), the error on the concentrations was evaluated using equation 2.29.

$$\frac{\Delta c_i}{c_i} = \frac{\Delta E_i}{E_i} + \frac{\Delta A_{p_i}}{A_{p_i}} \quad (2.29)$$

Where,

c_i = concentration of product i (% weight)

A_{p_i} = peak area of product i (%)

E_i = extinction coefficient of product i at 290nm ($l.g^{-1}.cm^{-1}$)

As an example, equation 2.30 described the determination of the error on the concentration of Toc, extracted from PP stabilised with 0.2% Toc, processed for 20min in an internal mixer (CM/N₂, 200°C) (see tables 2.53 and 2.59).

$$\frac{\Delta c_{Toc}}{c_{Toc}} = \frac{\Delta E_{Toc}}{E_{Toc}} + \frac{\Delta A_{pToc}}{A_{pToc}} = \frac{0.2}{8.1} + \frac{0.5}{86.3} = 3\% \quad (2.30)$$

2.11.2 Determination of the concentrations of Irg 1076, Irg 1010 and their transformation products

LDPE was stabilised with various concentrations (0.2, 1 and 10%) of each of the antioxidants Irg 1076 and Irg 1010 (single screw extruder, 4 passes, 180°C) and the extracted products were analysed by RP-HPLC after each extrusion pass.

In LDPE stabilised with Irg 1076 at least 15 transformation products of Irg 1076 were formed (see figure 2.31, p. 265, for HPLC chromatograms). However, only two of the products could be fully identified. One of them, C-Irg 1076, was the major transformation product, whereas the other one, BC-Irg 1076, was present in smaller quantities (see table 2.40, p. 118, for structures). Two other products, Irg 1076-11 and Irg 1076-14, were suggested to be the QM-Irg 1076 and CBQM-Irg 1076, respectively but their structures remain uncertain. Most of the other products had very similar UV characteristics to Irg 1076 and were suggested to contain intact phenolic groups without further conjugation. Hence, it was not possible to determine the exact concentrations of the products in the extracts of LDPE stabilised with Irg 1076. However, their peak areas were determined at

282nm using the PU6100 integration software. Furthermore, the concentrations of C-Irg 1076 and BC-Irg 1076, relative to Irg 1076, were determined from their extinction coefficients and HPLC peak areas at 282nm using equation 2.5. BC-Irg 1076 was given a literature value for its extinction coefficient [20] as it was isolated in very small quantities (see table 2.66).

Table 2.66: Extinction coefficients of identified transformation products of Irg 1076, isolated from the extract of LDPE stabilised with 10% Irg 1076 pass 4 (single screw extruder, 180°C)

products	$E \pm s_E, \text{l.g}^{-1}.\text{cm}^{-1}, 282\text{nm}$
Irg 1076	3.8 ± 0.1
C-Irg 1076	14.6 ± 0.9
BC-Irg 1076	14.7 [20]

RP-HPLC analysis of the extracts of LDPE stabilised with 10% Irg 1010 (see figure 2.36, for chromatograms) lead to the separation of at least 14 transformation products of Irg 1010. Two of them, Irg 1010-3 and Irg 1010-6 (major products) were isolated and identified (see table 2.47, p. 121, for structures). Most of the transformation products had very similar UV characteristics to Irg 1010, suggesting intact phenolic groups without further conjugation. Only two compounds, Irg 1010-4 and -14 suggested the presence of cinnamate and quinonoid structures. Because the exact structures of many of the transformation products could not be determined, it was not possible to determine their concentrations. However, their peak areas were determined at 282nm using the PU6100 integration software. Considering that most of the products are likely to contain one to four Irg 1010 sub-units, their extinction coefficients ($\text{l.g}^{-1}.\text{cm}^{-1}$) are likely to be similar, i.e. the concentrations are likely to be similar to the peak areas at 282nm.

Errors on the peak areas are shown in table 2.65. Errors on the concentrations were evaluated from the errors on the peak areas, as shown in equation 2.29. Errors on the extinction coefficients of Irg 1076 and C-Irg 1076 were determined from the standard

deviation of the slope of the regression line of the absorbance on the concentration (see equation 2.27). Dichloromethane was used as a solvent and blank for the UV analysis of the products.

2.12 MIGRATION CHARACTERISTICS OF TOC AND IRG 1076 FROM LDPE FILMS INTO VARIOUS FOOD SIMULANTS

2.12.1 General procedure

The migration characteristics of Toc and Irg 1076 from LDPE films stabilised with 0.2% of each of the antioxidants in a single screw extruder (one pass, 180°C) into various food simulants were investigated. The type of food simulant and the conditions of migration are specified by the European Community (EC) and the Food and Drugs Administration (FDA, USA) Directives [61-63]. The conditions depend on the time and temperature of contact of the polymer with the food. Due to the difficulty of separating polymer additives from natural foodstuffs, specific food simulants are recommended. The food simulants and conditions used in this work are shown in tables 2.67 and 2.68, respectively, and are in accordance with EC and FDA Directives.

Table 2.67: Food simulants used for the migration tests of LDPE films stabilised with 0.2% of each of the antioxidants Toc and Irg 1076 (single screw extruder, one pass, 180°C), according to the type of food, as specified by EC Directives (unless otherwise stated)

Type of food	Food simulant
aqueous food	distilled water (or of equivalent quality)
acidic aqueous food	3%, w/v, aqueous acetic acid
alcoholic food	15%, v/v, aqueous ethanol
fatty food	rectified olive oil
fatty food	iso-octane
fatty food	n-heptane (recommended by FDA)

Table 2.68: Test conditions used for the migrations tests of LDPE stabilised with 0.2% Toc (single screw extruder, one pass, 180°C), according to the conditions of actual use, as specified by EC Directives

Condition of actual use	Test condition
contact time: $t > 24$ hours temperature: $5^{\circ}\text{C} < T \leq 40^{\circ}\text{C}$	10 days at 40°C
contact time : $t < 2$ hours temperature: $40^{\circ}\text{C} < T \leq 70^{\circ}\text{C}$	2 hours at 70°C

Before migration, the LDPE films (2cm x 9cm, 0.25mm thick) were cleaned with ethanol to remove any impurities from their surface, and were analysed by UV spectroscopy using air as a blank, at both ends of the film, to determine the initial net absorbance, A_i , at 290nm, of the antioxidant and its transformation products (see section 2.13.1 for procedure). Each film was then immersed into 100ml of food simulant contained in a 250ml flask which was fitted with a condenser, and was placed into a thermostatically controlled water bath at the required temperature. After (static tests) or during (dynamic tests) the migration test, the films were removed from the food simulant, cleaned with ethanol and analysed by UV spectroscopy to determine their net absorbance at 290nm, at both ends of the film. The extent of migration, M , of the antioxidant and its transformation products was calculated as shown in equation 2.31.

$$M(\%) = \frac{A_i - A_f}{A_f} \quad (2.31)$$

Where,

A_i = initial net absorbance of the polymer film (before migration)

A_f = net absorbance after migration (static tests) or during migration (dynamic tests)

M = extent of migration (%)

2.12.2 Static migration tests

Static migration tests were carried out with LDPE films stabilised with 0.2% Toc, using the food simulants and test conditions shown in tables 2.67 and 2.68, respectively. The extent of migration, M , was then determined for each test, using equation 2.31.

2.12.3 Dynamic migration tests

Dynamic migration tests were conducted with LDPE films (2cm x 9cm, 0.25mm thick) stabilised with 0.2% of each of the antioxidants Toc and Irg 1076, using the fatty food simulants (olive oil, iso-octane and heptane) and the acidic aqueous food simulant (3%, w/v, aqueous acetic acid), at 40°C. The decrease in net absorbance at 290nm of the antioxidant and its transformation products from the polymer films into the food simulants after increasing times was followed by UV spectroscopy of the film, until a constant value of the extent of migration, M , was obtained.

2.13 SPECTROSCOPIC TECHNIQUES

2.13.1 Ultraviolet spectroscopy

Ultraviolet (UV) spectra of polymer films and solutions were recorded on a Hewlett Packard 8452A diode array spectrophotometer. The magnitude of the absorption signal is proportional to the concentration of the product according to the Beer-Lambert law and directly dependent on its extinction coefficient at the wavelength of detection (see equation 2.4, p. 107).

The spectra of polymer films, including stabilised LDPE and PP films of 0.25mm thickness, were measured to assess the extraction efficiency of antioxidants and their transformation products from the films and to determine the loss of antioxidants during ageing (thermal, UV) and migration experiments. For all the measurements, air was used as a blank. To overcome the problem of the absorption of the polymer in the range 190-400nm, the UV characteristics of the antioxidants and their transformation products were determined by measuring their net absorbance at a maximum wavelength, as shown in figure 2.41.

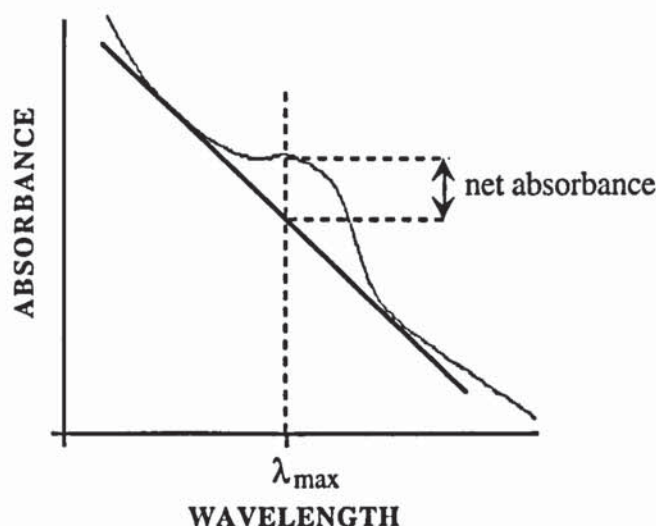


Figure 2.41: Measurement of the net absorbance of the products (antioxidant + transformation products) in polymer films (0.25mm thick)

Solution spectra were conducted for synthesised and isolated oxidation products of Toc, Irg 1076 and Irg 1010, to determine their extinction coefficients and the concentration of total products extracted from polymer films after processing operations and ageing experiments. The solvent (e.g. hexane, dichloromethane) was also used as a blank.

2.13.2 Fourier transform infrared (FTIR) spectroscopy

Infrared spectroscopy was carried out on a Perkin Elmer 1710 Fourier Transform spectrophotometer. FTIR spectra of synthesised and isolated oxidation products of Toc were measured by using KBr windows, to contribute to their identification. The FTIR spectrum of an unstabilised PP film (0.25mm thick), after processing in an internal mixer, was measured directly, to observe the carbonyl group region ($1600-1800\text{cm}^{-1}$) corresponding to degradation products.

2.13.3 Proton, carbon-13 and phosphorus-31 nuclear magnetic resonance spectroscopy

Nuclear magnetic resonance (NMR) spectroscopy was carried out on a Bruker AC300 High Resolution spectrometer. All the spectra were measured in solution state using CDCl_3 as a solvent and internal standard.

^1H -NMR and ^{13}C -NMR were carried out at 300MHz and 100MHz, respectively, to contribute to the identification of synthesised and isolated oxidation products of Toc, Irg 1076 and Irg 1010. ^{13}C -NMR spectra were run using the J-modulated spin echo (JMOD) method which provides a useful way of separating the methyl and tertiary peaks (positive values) from the methylene and quaternary ones (negative values). ^1H , ^{13}C -NMR shift correlation spectra were also carried out for Toc oxidation products. In this method the ^1H signals, which appear on one axis, are correlated with ^{13}C signals which are displayed on the other axis. These spectra were used to assign the ^{13}C signals if the corresponding ^1H assignments are known, or vice versa. ^{31}P -NMR spectra were measured for extracts of PP stabilised with the diphosphite U-626, at 120MHz.

2.14 MASS SPECTROMETRIC TECHNIQUES

2.14.1 Electron-Impact ionisation

Electron-Impact ionisation mass spectrometry (EI-MS) is the most commonly used mass spectrometric technique and allows the analysis of volatile or volatilisable (via derivatisation procedures) substances. The sample is vaporised outside the ion source. This is followed by ionisation in the gas phase by a beam of electrons emitted from a glowing filament.

EI-MS spectra of synthesised and isolated (from stabilised PP samples) oxidation products of Toc were kindly recorded by Hoffmann-La Roche (Basel, Switzerland) on a Finnigan MAT CH7 mass spectrometer, using ethyl acetate as the solvent. Derivatisation of the Toc dimers, dihydroxydimer (DHD) and spirodimer (SPD) with tetramethylsiloxane (TMS) permitted to distinguish between the two dimers, as their mass spectra were very similar ($M^+ = 858$, i.e. MM of DHD). Unlike SPD, the silylation of DHD (presence of two hydroxyl groups) was successful and confirmed its structure. The samples were heated at 4°C per minute from 250 to 350°C.

2.14.2 Fast Atom Bombardment

Fast Atom Bombardment mass spectrometry (FAB-MS) is usually applied to substances which are not volatile or thermally unstable at the temperatures of vaporisation in EI-MS, and when the interest is primarily to determine the molecular weight of a compound. The sample, which is dissolved in a suitable solvent (which does not evaporate in a vacuum), is bombarded by an ionised beam of argon, in the condensed phase. The latter ionises the solvent which reacts with the sample to produce molecular ions.

A FAB-MS spectrum of the trimers of Toc (TRI, A, B, C) was kindly measured by Hoffmann-La Roche (Basel, Switzerland). The trimers were shown to fragment to SPD during EI-MS before they reach the analyser.

2.14.3 Gas chromatography-mass spectrometry

The mass spectrometer is a universal detector for gas chromatographs, since any compound that can pass through a gas chromatograph is converted into ions in the mass spectrometer. Gas chromatography is an ideal separator, whereas mass spectrometry is excellent for identification. Hence, gas chromatography coupled to mass spectrometry (GC-MS) is ideally suited for substances which are not pure or their purity is unknown.

GC-MS spectra were measured for transformation products of Toc, Irg 1076 and Irg 1010, isolated from the extracts of LDPE stabilised with each of the antioxidants in a single screw extruder. The products were obtained in relatively small quantities and their purity was uncertain. The analysis was kindly carried out by the UK Ministry of Agriculture, Food and Fisheries (MAFF) on a VG7070EQ instrument without the use of the tandem facility. Sample introduction was by solid probe, in chloroform. The probe was heated at 50°C per minute to a temperature of 400°C.

LIST OF TABLES FOR THE CHARACTERISATION OF TOC , TOC DERIVATIVES, U-626, IRG 1076 AND IRG 1010 AND THEIR OXIDATION PRODUCTS

Table	Description	Page
2.2	UV and FTIR characteristics of Toc, ALD 1 and TQ (supplied)	148
2.3	¹ H-NMR characteristics of Toc, ALD 1 and TQ (supplied)	149
2.4	¹³ C-NMR characteristics of Toc, ALD 1 and TQ (supplied)	150
2.5	EI-MS analysis of Toc (supplied)	151
2.6	EI-MS analysis of ALD 1 (supplied)	152
2.7	UV characteristics of Irg 1076, Irg 1010 and U-626 (supplied) and ³¹ P-NMR analysis of U-626	153
2.8	¹ H-NMR characteristics of Irg 1076 and Irg 1010 (supplied)	153
2.9	EI-MS analysis of Irg 1076 (supplied)	154
2.10	EI-MS analysis of Irg 1010 (supplied)	154
2.16	UV and FTIR analysis of synthesised DHD, E, SPD, D and TRI, A, B, C	155
2.17	¹ H-NMR characteristics of synthesised DHD, E and SPD, D	156
2.18	¹ H-NMR characteristics of synthesised TRI, A, B, C	157
2.19	¹³ C-NMR characteristics of synthesised DHD, E and SPD, D	158
2.20	¹³ C-NMR characteristics of synthesised TRI, A, B, C	160
2.21	EI-MS analysis of synthesised DHD, E before silylation	162
2.22	EI-MS analysis of synthesised DHD, E after silylation	162
2.23	EI-MS analysis of synthesised SPD, D before and after silylation	163
2.24	FAB-MS analysis of synthesised TRI, A, B, C	163
2.25	¹ H-NMR characteristics of DHD, E and ALD 1, isolated from the products of reaction of Toc with PbO ₂ , ratios 1:1 and 1:40 in Toc:PbO ₂	164
2.29	UV analysis of ALD 1, ALD 2, ALD 3 and compound I, isolated from the extract of PP stabilised with 39% Toc, pass 4 (CPC789 series) and FTIR analysis of ALD 1 and ALD 2	165
2.30	¹ H-NMR characteristics of ALD 1, ALD 2, ALD 3 and compound I, isolated from the extract of PP stabilised with 39% Toc, pass 4 (CPC789 series)	166
2.31	¹³ C-NMR characteristics of ALD 1, isolated from the extract of PP stabilised with 39% Toc, pass 4 (CPC789 series)	167
2.32	EI-MS analysis of ALD 1, isolated from the extract of PP stabilised with 39% Toc, pass 4 (CPC789 series)	168

2.33	UV analysis of DHD, E, SPD, D, TRI, A, B, C, ALD 1 and ALD 2, isolated from the extracts of LDPE stabilised with 0.2 and 10% Toc, passes 4	169
2.34	¹ H-NMR characteristics of DHD, E and SPD, D isolated from the extract of LDPE stabilised with 10% Toc, pass 4	170
2.35	¹ H-NMR characteristics of TRI, A, B, C, isolated from the extract of LDPE stabilised with 10% Toc, pass 4	171
2.36	¹ H-NMR characteristics of ALD 1 and ALD 2, isolated from the extract of LDPE stabilised with 0.2% Toc, pass 4	172
2.37	GC-MS analysis of SPD, D, isolated from the extract of LDPE stabilised with 10% Toc, pass 4	173
2.38	GC-MS analysis of TRI, A, B, C, isolated from the extract of LDPE stabilised with 10% Toc, pass 4	173
2.39	GC-MS analysis of ALD 1, isolated from the extract of LDPE stabilised with 0.2% Toc, pass 4	174
2.41	UV analysis of Irg 1076-1, cinnamate of Irg 1076 (C-Irg 1076) and biscinnamate of Irg 1076 (BC-Irg 1076), isolated from the extract of LDPE stabilised with 10% Irg 1076, pass 4	175
2.42	UV analysis of compounds 2-11, 13 and 14 (Irg 1076-2 to -11 and -13 to -14), extracted from LDPE stabilised with 10% Irg 1076, pass 4	175
2.43	¹ H-NMR characteristics of C-Irg 1076, isolated from the extract of LDPE stabilised with 10% Irg 1076, pass 4	176
2.44	GC-MS analysis of compound 1 (Irg 1076-1), isolated from the extract of LDPE stabilised with 10% Irg 1076, pass 4	176
2.45	GC-MS analysis of cinnamate of Irg 1076 (C-Irg 1076), isolated from the extract of LDPE stabilised with 10% Irg 1076, pass 4	177
2.46	GC-MS analysis of biscinnamate of Irg 1076 (BC-Irg 1076), isolated from the extract of LDPE stabilised with 10% Irg 1076, pass 4	177
2.48	UV analysis of compounds 3 and 6 (Irg 1010-3 and -6), isolated from the extract of LDPE stabilised with 10% Irg 1010, pass 4	178
2.49	UV analysis of compounds 1, 2, 4, 5 and 7-13 (Irg 1010-1, -2, -4, -5 and -7 to -13), extracted from LDPE stabilised with 10% Irg 1010, pass 4	178
2.50	¹ H-NMR analysis of compounds 3 and 6 (Irg 1010-3 and -6), isolated from the extract of LDPE stabilised with 10% Irg 1010, pass 4	179
2.51	GC-MS analysis of Irg 1010-3, isolated from the extract of LDPE stabilised with 10% Irg 1010, pass 4	179
2.52	GC-MS analysis of Irg 1010-6, isolated from the extract of LDPE stabilised with 10% Irg 1010, pass 4	180

Table 2.2: UV and FTIR characteristics of Toc, ALD 1 and TQ (supplied)

compound		Toc	ALD 1	TQ
λ_{\max} , nm (ϵ , l.mol ⁻¹ .cm ⁻¹)		298 (3687)	239, 290 (9116), 282 (8761), 386 (2846)	260 (17422), 268 (17154)
ν , cm ⁻¹	O-H str	3457 (broad)	3374 (weak, broad)	3508 (broad)
	C-H str	2951, 2926, 2868	2952, 2926, 2868, 2850	2954, 2927, 2868
	C=O str	-	1636	1644
	C=C str arom.	1618, 1582	1617, 1581	-
	C-H def	1461, 1422, 1378, 1340	1462, 1415, 1397, 1378, 1311	1463, 1376, 1308
	C-O-C str chroman	1262, 1159, 1112, 1086, 1008	1265, 1242, 1159, 1136, 1097, 1061, 1029	-
	C-O str / O-H def	1213		
Figures		2.1.b (UV) 2.1.c (IR)	2.2.b (UV) 2.2.c (IR)	2.3.b (UV) 2.3.c (IR)

Table 2.3: ¹H-NMR characteristics of Toc, ALD 1 and TQ (supplied)

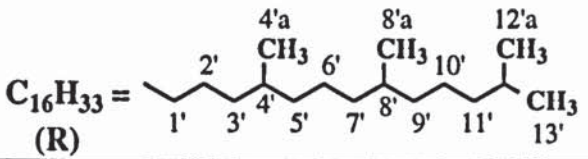
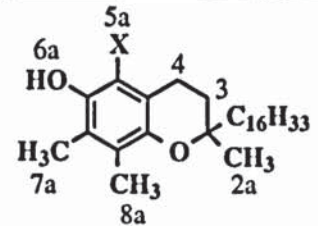
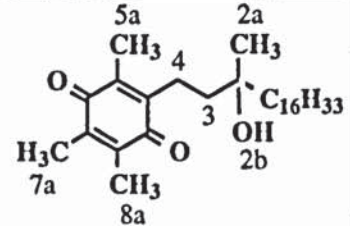
		δ , ppm (multiplicity) (s=singlet, t=triplet, m=multiplet)		
				
group	position			
		Toc (X = CH ₃)	ALD 1 (X = CHO)	TQ
CH ₃ of R	4'a, 8'a, 12'a, 13'	0.85-1.0	0.75-0.85	0.75-0.9
CH ₃ , sat.	2a	1.27 (s)	1.24 (s)	1.20 (s)
CH ₂ of R	3', 5', 7', 9'	1.05-1.4	1.0-1.4	1.0-1.3
	11'	1.05-1.25	1.0-1.2	1.05-1.15
	6', 10'	1.3-1.4	1.15-1.3	1.2-1.3
CH ₂ , CH of R	2', 4', 8'	1.4-1.55	1.3-1.45	1.25-1.4
CH of R	1', 12'	1.55-1.7	1.45-1.55	1.4-1.55
CH ₂ , β unsat.	3	1.75-1.95 (m)	1.75-1.9 (m)	1.4-1.5 (m)
CH ₃ , unsat.	5a	2.16 (s)	-	2.0 (s)
	7a	2.20 (s)	2.15 (s)	1.97 (s)
	8a	2.17 (s)	2.13 (s)	
CH ₂ , α unsat.	4	2.6-2.7 (t)	2.9-3.1 (t)	2.45-2.6 (m)
O-H	6a, 2b	4.3 (s)	12.09 (s)	1.66 (broad, s)
CHO	5a	-	10.17 (s)	-
Figure		2.1.d	2.2.d	2.3.d

Table 2.4: ^{13}C -NMR characteristics of Toc, ALD 1 and TQ (supplied)

		δ , ppm (multiplicity)		
group	position (sign) (+): 1°, 3° C (-): 2°, 4° C			
		Toc (X = CH ₃)	ALD 1 (X = CHO)	TQ
CH ₃ , arom.	5a (+)	11.23 (1)	193.98 (1)	11.94 (1)
+ α , β unsat.	8a (+)	11.75 (1)	11.01 (1)	12.26 (1), 12.34 (1)
+ CHO	7a (+)	12.16 (1)	13.18 (1)	
R	4'a, 8'a (+)	19.58, 19.67, 19.73 (≥ 3)	19.65, 19.72 (≥ 3)	19.63 (>1)
	2' (-)	21.03 (1)	20.94 (1)	21.27 (1)
	12'a, 13' (+)	22.62, 22.71 (2)	22.62, 22.72 (2)	22.59, 22.69 (2)
	6' (-)	24.43 (1)	24.42 (1)	24.45 (1)
	10' (-)	24.80 (1)	24.80 (1)	24.77 (1)
	12' (+)	27.96 (1)	27.96 (1)	27.92 (1)
	4', 8' (+)	32.66, 32.76 (2)	32.64, 32.77 (2)	32.74 (1)
	3' (-)	37.27, 37.32,		37.55, 37.65 (2)
	5', 7', 9' (-)	37.38, 37.44, 37.55 (≥ 5)	37.36 (≥ 3)	37.23, 37.35 (2)
	11' (-)	39.35 (1)	39.34 (1)	39.31 (1)
	1' (-)	39.76, 39.84 (2)	39.49, 39.58 (2)	40.17 (1)
CH ₂ , α , β unsat.	4 (-)	20.73 (1)	18.40 (1)	21.38 (1)
CH ₃ , sat.	2a (+)	23.74 (1)	23.60 (1)	26.53 (1)
CH ₂ , β unsat.	3 (-)	31.46, 31.52 (2)	30.73 (2)	42.22 (1)
Figure		2.1.e	2.2.e	2.3.e

Table 2.4: continued

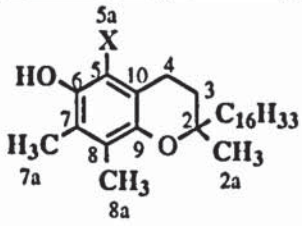
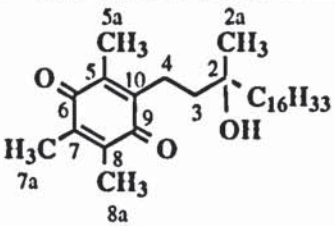
group	position (sign) (+): 1°, 3° C (-): 2°, 4° C	δ , ppm (multiplicity)		
				
		Toc (X = CH ₃)	ALD 1 (X = CHO)	TQ
C, sat	2 (-)	74.44 (1)	75.11 (1)	72.60 (1)
C, unsat	5 (-)	117.25 (1)	124.18 (1)	140.12, 140.36, 140.47 (3)
	7 (-)	118.54 (1)	117.51 (1)	
	8 (-)	121.09 (1)	138.40 (1)	
	10 (-)	122.53 (1)	114.44 (1)	144.38 (1)
	6 (-)	144.49 (1)	143.98 (1)	187.19, 187.64 (2)
	9 (-)	145.51 (1)	155.77 (1)	
Figure		2.1.e	2.2.e	2.3.e

Table 2.5: EI-MS analysis of Toc (supplied) (figure 2.1.g)

Peak mass (g)	possible fragment	possible pathway	name of fragment
430	C ₂₉ H ₅₀ O ₂	molecular ion	M ⁺
431	C ₂₉ H ₅₀ O ₂	molecular ion	M ⁺ + 1
205	C ₁₃ H ₁₇ O ₂	M ⁺ - C ₁₆ H ₃₃	M1
175	C ₁₁ H ₁₁ O ₂	M1 - C ₂ H ₃ - 3H	M2
165	C ₁₀ H ₁₃ O ₂	M2 - CH ₂	M3
164	C ₁₀ H ₁₂ O ₂	M3 - H	M4

Table 2.6: EI-MS analysis of ALD 1 (supplied) (figure 2.2.g)

Peak mass (g)	possible fragment	possible pathway	name of fragment
444	$C_{29}H_{48}O_3$	molecular ion	M^+
445	$C_{29}H_{48}O_3$	molecular ion	$M^+ + 1$
426	$C_{29}H_{46}O_2$	$M^+ - H_2O$	M1
220	$C_{13}H_{16}O_3$	$M^+ - C_{16}H_{33} + H$	M2
201 (100%)	$C_{13}H_{13}O_2$	$M1 - C_{16}H_{33}$	M3
202	$C_{13}H_{14}O_2$	$M3 + H$	M4
192	$C_{11}H_{12}O_3$	$M2 - C_2H_4$	M5
179	$C_{10}H_{11}O_3$	$M5 - CH_2 + H$	M6
151	$C_9H_{11}O_2$	$M4 - C_4H_3$	M7

Table 2.7: UV characteristics of Irg 1010, Irg 1076 and U-626 (supplied) and ³¹P-NMR analysis of U-626

compound	Irg 1076	Irg 1010	U-626
λ_{\max} , nm (ϵ , l.mol ⁻¹ .cm ⁻¹)	282 (2039) 276 (2017)	282 (7537) 276 (7443)	271 (2413) 278 (2250)
³¹ P-NMR chemical shift, ppm	-	-	112.8
Figure	2.4.b (UV)	2.5.b (UV)	2.6.b (UV) 2.6.c (³¹ P-NMR)

Table 2.8: ¹H-NMR characteristics of Irg 1076 and Irg 1010 (supplied)

group	position	δ , ppm (multiplicity)	
		Irg 1076	Irg 1010
		<p style="text-align: center;"> $\text{C}_{18}\text{H}_{37} = \text{CH}_2 - \text{CH}_2 - (\text{CH}_2)_{15} - \text{CH}_3$ (R) </p>	
CH ₃ of R	13	0.85-0.95 (t)	-
CH ₂ of R	12	1.15-1.4	-
	11	1.6-1.75 (m)	-
	10	4.05-4.15 (t)	4.1 (s)
CH ₃ of <i>t</i> -butyl	3b, 5b	1.45 (s)	1.48 (s)
CH ₂ , sat.	7	2.55-2.65 (t)	2.55-2.7 (t)
	8	2.85-2.95 (t)	2.85-2.95 (t)
O-H	4a	5.1 (s)	5.1 (s)
C-H, arom.	2, 6	7.02 (s)	7.0 (s)
Figure		2.4.c	2.5.c

Table 2.9: EI-MS analysis of Irg 1076 (supplied) (figure 2.4.d)

Peak mass (g)	possible fragment	possible pathway	name of fragment
530 (100%)	$C_{35}H_{62}O_3$	molecular ion	M^+
531	$C_{35}H_{62}O_3$	molecular ion	$M^+ + 1$
528	$C_{35}H_{60}O_3$	$M^+ - 2H$	M1 (C-Irg 1076)
515	$C_{34}H_{59}O_3$	$M^+ - CH_3$	M2
501	$C_{33}H_{57}O_3$	$M2 - CH_3 + H$	M3
474	$C_{31}H_{54}O_3$	$M2 - C(CH_3)_3 + H$	M4
278	$C_{17}H_{26}O_3$	$M^+ - C_{18}H_{37} + H$	M5
232	$C_{16}H_{24}O$	$M5 - CO_2H - H$	M6
219	$C_{15}H_{23}O$	$M5 - CH_2CO_2H$	M7
57	C_4H_9	$C(CH_3)_3$	M8

Table 2.10: EI-MS analysis of Irg 1010 (supplied) (figure 2.5.d)

Peak mass (g)	possible fragment	possible pathway	name of fragment
1176	$C_{73}H_{108}O_{12}$	not present	M^+
1009	$C_{61}H_{84}O_{12}$	$M^+ - 3[C(CH_3)_3] + 3H$	M1
952	$C_{57}H_{76}O_{12}$	$M1 - C(CH_3)_3 + H$	M2
916	$C_{56}H_{84}O_{10}$	$M^+ - C_{17}H_{25}O_2 + H$	M3
899	$C_{56}H_{83}O_9$	$M3 - OH$	M4
860	$C_{52}H_{76}O_{10}$	$M3 - C(CH_3)_3 + H$	M5
806	$C_{50}H_{62}O_9$	$M4 - 6(CH_3) - 6H + 3H$	M6
751	$C_{46}H_{55}O_9$	$M6 - C_3H_6 - CH_3 + 2H$	M7
692	$C_{41}H_{56}O_9$	$M3 - C_{15}H_{23}O - 6H + H$	M8
638	$C_{39}H_{58}O_7$	$M3 - C_{17}H_{26}O_3 - H + H$	M9
582	$C_{35}H_{50}O_7$	$M9 - C(CH_3)_3 + H$	M10
544	$C_{31}H_{44}O_8$	$M5 - C(CH_3)_3 - C_{17}H_{25}O_2 + 2H$	M11
488	$C_{27}H_{36}O_8$	$M11 - C(CH_3)_3 + H$	M12
378	$C_{20}H_{26}O_7$	$M12 - C_7H_7O - 4H + H$	M13
346	$C_{22}H_{34}O_3$	$M10 - C_{13}H_{18}O_4 + 2H$	M14
219	$C_{15}H_{23}O$	$M3 - M8 - 5H$	M15

Table 2.16: UV and FTIR analysis of synthesised DHD, E, SPD, D and TRI, A, B, C
(see section 2.2 and schemes 2.1 and 2.2)

compound		DHD, E	SPD, D	TRI, A, B, C
λ_{\max} , nm (ϵ , l.mol ⁻¹ .cm ⁻¹)		300 (7649)	301 (4459) 339 (2144)	292 (6585)
ν , cm ⁻¹	O-H str	3445 (broad)	-	-
	C-H str	2952, 2926, 2868	2951, 2926, 2868	2926, 2868, 2722
	C=O str	-	1677	1693
	C=C str arom.	1583, 1618	not visible	1619, 1588
	C=C str	-	1598, 1657	1648
	C-H def	1462, 1422, 1378,	1462, 1418, 1377, 1322	1462, 1420, 1377
	C-O-C str chroman	1261, 1160, 1109, 1087	1257, 1165, 1125, 1097	1261, 1158, 1094
	C-O-C str ether	-	1018, 968	1136, 1019, 976
Figure		2.13.b (UV) 2.13.c (IR)	2.14.b (UV) 2.14.c (IR)	2.15.b (UV) 2.15.c (IR)

Table 2.17: ¹H-NMR characteristics of synthesised DHD, E and SPD, D
(see section 2.2 and schemes 2.1 and 2.2)

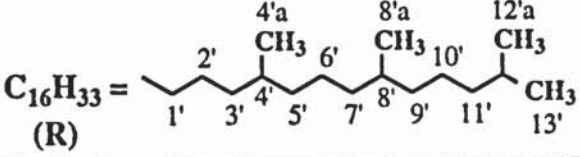
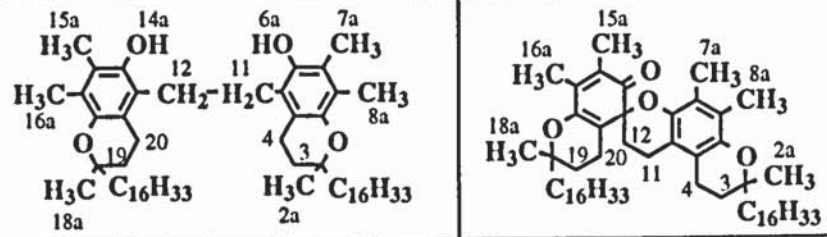
		δ, ppm (multiplicity) (s=singlet, m=multiplet)			
					
group	position				
		DHD			SPD, D
		E1	E2	E3+E4	
CH ₃ of R	4'a, 8'a, 12'a, 13'	0.75-0.95	0.8-0.95 (broad)	0.75-0.95	0.8-0.95
CH ₃ , sat.	2a, 18a	1.22 (s)	1.22 (s)	1.22 (s)	1.20 (s), 1.25 (s), 1.26 (s)
CH ₂ of R	3', 5', 7', 9'	0.95-1.45	0.95-1.45	0.95-1.45	1.0-1.45
	11'	0.95-1.15	0.95-1.15	0.95-1.15	1.0-1.15
	6', 10'	1.15-1.3	1.15-1.3	1.15-1.3	1.15-1.2
CH ₂ , CH of R	2', 4', 8'	1.3-1.45	1.3-1.45	1.3-1.45	1.15-1.45
CH of R	1', 12'	1.45-1.65	1.45-1.7	1.45-1.65	1.45-1.6
CH ₂ , β unsat.	3, 19	1.7-1.9 (m)	1.7-1.9 (m)	1.7-1.9 (m)	1.65-1.80
CH ₃ , unsat.	16a	2.11 (s)	2.11 (s)	2.11 (s),	1.84 (s)
	8a			2.12 (s)	2.09 (s), 2.13 (s)
	7a	2.16 (s)	2.15 (s),	2.16 (2s)	
	15a		2.16 (s)		1.97 (s)
CH ₂ , α unsat.	4, 11, 20	2.65-2.8	2.65-2.75	2.65-2.8	2.3-2.7
	12				2.65-2.8
O-H	6a, 14a	5.43 (s)	5.46 (s)	5.43 (s)	-
Figure		2.13.d	2.13.e	2.13.f	2.14.d

Table 2.18: ¹H-NMR characteristics of synthesised TRI, A, B, C
(see section 2.2 and scheme 2.1)

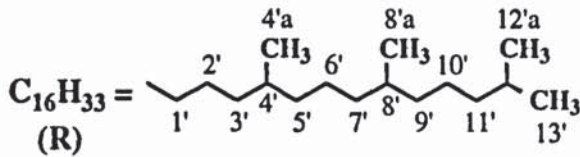
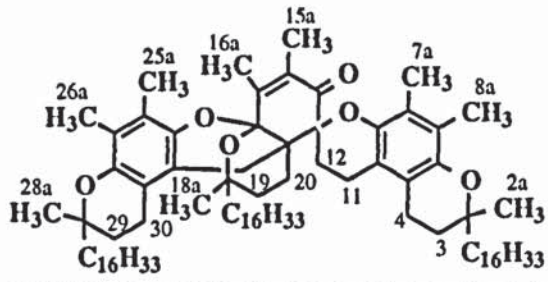
		δ , ppm (multiplicity) (s=singlet)			
		 <p style="text-align: center;">$C_{16}H_{33}$ = </p>			
group	position	A1	A2	B	C
CH ₃ of R	4'a, 8'a, 12'a, 13'	0.8-0.9	0.8-0.95	0.8-0.9	0.8-0.95
CH ₃ , sat.	2a, 28a	1.17 (s), 1.20 (s)	1.18 (s), 1.20 (s)	1.19 (s), 1.21 (s)	1.19 (s)
	18a	1.43 (s)	1.25 (s)	1.26 (s), 1.43 (s)	1.25 (s), 1.43 (s)
CH ₂ of R	3', 5', 7', 9'	1.0-1.45	1.0-1.45	1.0-1.45	1.0-1.45
	11'	1.0-1.15	1.0-1.15	1.0-1.2	1.0-1.2
	6', 10'	1.15-1.3	1.15-1.3	1.2-1.35	1.2-1.35
CH ₂ , CH of R	2', 4', 8'	1.3-1.4	1.3-1.4	1.35-1.45	1.35-1.45
CH of R	1', 12'	1.45-1.65	1.45-1.65	1.45-1.65	1.45-1.6
CH ₂ , β unsat.	3, 12, 29	1.7-1.8	1.7-1.8	1.7-1.9	1.65-1.85
CH ₃ , unsat.	16a	1.67 (s)	1.66 (s)	1.67, 1.68	1.66 (s), 1.68 (s)
	15a	1.99 (s)	1.98 (s)	1.97, 1.98	1.96 (s), 1.97 (s)
	7a, 8a	2.07 (s), 2.11 (s)	2.08 (s), 2.11 (s)	2.09 (s), 2.13 (s)	2.09 (s), 2.12 (s)
	25a, 26a	2.16 (s), 2.21 (s)	2.17 (s), 2.21 (s)	2.17 (s), 2.23 (s)	2.18 (s), 2.22 (s)
CH ₂ , α unsat.	4, 11, 30, 34	2.25-2.9	2.3-2.95	2.3-2.95	2.3-2.95
Figure		2.15.d	2.15.e	2.15.f	2.15.g

Table 2.19: ^{13}C -NMR characteristics of synthesised DHD, E and SPD, D
(see section 2.2 and schemes 2.1 and 2.2)

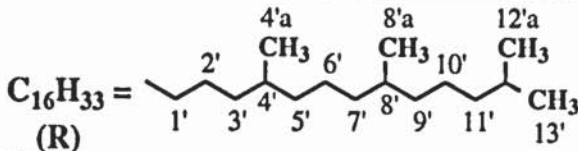
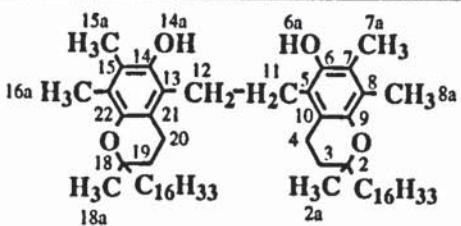
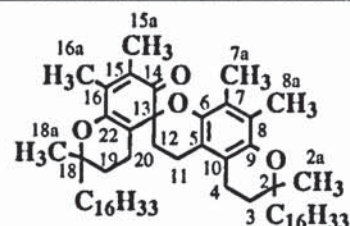
		δ , ppm (multiplicity)			
					
group	position (sign) (+): 1°, 3° C (-): 2°, 4° C				
		E1	E2	E3+E4	SPD, D
CH ₃ , arom. + α , β unsat.	16a (+)	11.90 (1)	11.90 (1)	11.06 (2)	11.11 (1)
	8a (+)				11.64, 11.79 (2)
	7a (+)	12.12 (1)	12.12 (1)	11.62 (1)	
	15a (+)			11.84 (1)	13.82 (2)
R	4'a, 8'a (+)	19.67, 19.74 (≥ 2)	19.67, 19.73 (≥ 4)	19.40, 19.47, 19.73 (≥ 3)	19.53, 19.59, 19.66 (≥ 3)
	2' (-)	21.04 (1)	21.03 (1)	20.53, 20.79 (2)	21.08 (1)
	12'a, 13' (+)	22.62, 22.72 (2)	22.61, 22.71 (2)	22.35, 22.45 (2)	22.54, 22.63 (2)
	6' (-)	24.44 (1)	24.43 (1)	24.16 (1)	24.29 (1)
	10' (-)	24.80 (1)	24.80 (1)	24.52 (1)	24.72 (1)
	12' (+)	27.97 (1)	27.97 (1)	27.70 (1)	27.89 (1)
	4', 8' (+)	32.76 (1)	32.76 (1)	32.49 (≥ 2)	32.69 (1)
	3', 5', 7', 9' (-)	37.38 (≥ 3)	37.27, 37.38 (≥ 4)	36.99, 37.11 (≥ 4)	37.20, 37.31, 37.49 (≥ 3)
	11' (-)	39.35 (1)	39.35 (1)	39.07 (1)	39.28 (1)
1' (-)	39.95, 40.07 (2)	39.97, 40.10 (2)	39.63 (2)	40.61 (1)	
Figure		2.13.g	2.13.h	2.13.i	2.14.e

Table 2.20: ^{13}C -NMR characteristics of synthesised TRI, A, B, C
(see section 2.2 and scheme 2.1)

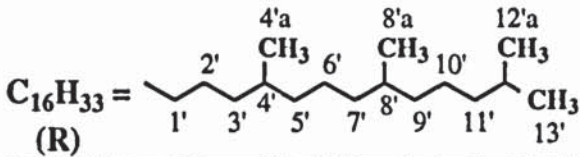
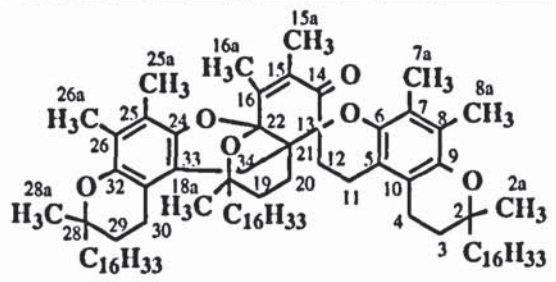
		δ , ppm (multiplicity)		
				
group	position (sign) (+): 1°, 3° C (-): 2°, 4° C			
		A1	A2	B
CH ₃ , arom. + α , β unsat.	16a (+)	11.71 (1)	11.71 (1)	11.70 (1)
	7a, 8a (+)			
	25a, 26a (+)	11.90, 12.07 (2)	12.07 (1)	11.89, 12.06 (2)
	15a (+)	14.07 (1)	14.34 (1)	14.06, 14.32 (2)
R	4'a, 8'a (+)	19.66 (1)	19.66 (1)	19.66, 19.72 (2)
	2' (-)	20.99 (1)	20.99 (1)	21.00, 21.22 (≥ 2)
	12'a, 13' (+)	22.61, 22.70 (2)	22.62, 22.71 (2)	22.61, 22.70 (2)
	6' (-)	24.45 (1)	24.44 (1)	24.43 (1)
	10' (-)	24.79 (1)	24.80 (1)	24.79 (1)
	12' (+)	27.96 (1)	27.96 (1)	27.95 (1)
	4', 8' (+)	32.76 (1)	32.76, 32.97 (2)	32.75 (1)
	3', 5', 7', 9' (-)	37.27, 37.39 (≥ 2)	37.40 (≥ 2)	37.26, 37.37, 37.56 (≥ 2)
	11' (-)	39.35 (1)	39.34 (1)	39.34 (1)
	1' (-)	40.62, 41.19 (2)	40.60, 41.15 (2)	40.60, 41.19 (2)
CH ₂ , α & β unsat.	4, 30, 11, 34 (-)	19.35, 19.99 (2)	19.35, 21.63 (≥ 2)	19.35, 19.99 (2)
	3, 29 (-)	30.87, 31.13 (2)	30.88, 31.10 (2)	30.86, 31.10 (≥ 2)
CH ₂ , sat.	12 (-)	33.65 (1)	34.03 (1)	33.60 (1)
	19 (-)	41.43 (1)	42.45 (1)	41.44, 42.47 (2)
	20 (-)			
CH ₃ , sat.	2a, 18a, 28a (+)	23.05, 23.55 (2)	23.07, 23.51, 27.14 (3)	23.07, 23.54, 24.01 (3)
Figure		2.15.h	2.15.i	2.15.j

Table 2.20 continued

group	position (sign) (+): 1°, 3° C (-): 2°, 4° C	δ, ppm (multiplicity)		
		A1	A2	B
C, sat	21 (-)	44.88 (1)	44.07 (1)	44.07, 44.89 (2)
	2, 28 (-)	74.31, 74.71 (2)	74.32, 74.74 (2)	74.29, 74.43, 74.69, 74.73 (4)
	18 (-)	76.16 (1)	77.13 (1)	76.15, 77.12 (2)
	13 (-)	85.51 (1)	85.54 (1)	85.48 (1)
	22 (-)	99.25 (1)	100.05 (1)	99.24, 100.07, 100.18 (3)
C, unsat	8, 26, 10, 31 (-)	114.84, 115.13, 115.56, 115.75 (4)	115.16, 115.51, 115.78 (3)	114.84, 114.93, 115.12, 115.47, 115.62, 115.74 (4)
	7, 25, 5, 33 (-)	121.91, 122.24, 123.51 (3)	121.92, 122.26, 123.51 (3)	121.90, 122.25, 123.47 (3)
	15 (-)	129.23 (1)	129.69 (1)	129.26, 129.72 (2)
	6, 9, 24, 32 (-)	141.98, 144.68, 145.56 (≥3)	142.37, 144.71, 145.44, 145.69 (4)	141.96, 142.01, 142.37, 142.43, 144.68, 145.48, 145.54, 145.68 (8)
	16 (-)	150.64 (1)	150.28 (1)	150.19, 150.60 (2)
	14 (-)	198.75 (1)	198.90 (1)	198.70, 198.80 (2)
Figure		2.15.h	2.15.i	2.15.j

Table 2.21: EI-MS analysis of synthesised DHD, E before silylation (figure 2.13.k)
(see section 2.2 and scheme 2.2)

Peak mass (g)	possible fragment	possible pathway	name of fragment
858	$C_{58}H_{98}O_4$	molecular ion	M^+
856	$C_{58}H_{96}O_4$	$M^+ - 2H$	M1
631	$C_{42}H_{63}O_4$	$M1 - C_{16}H_{33}$	M2
428	$C_{29}H_{50}O_2$	$M^+ - C_{29}H_{49}O_2 - H$	M4 (QM)
317	$C_{21}H_{33}O_2$	$M4 - C_8H_{17}$	M5
203	$C_{13}H_{15}O_2$	$M4 - C_{16}H_{33} - 2H$	M6
177	$C_{11}H_{13}O_2$	$M6 - C_2H_2$	M7
165 (100%)	$C_{10}H_{13}O_2$	$M7 - CH_2 + 2H$	M8
151	$C_9H_{11}O_2$	$M8 - CH_3 + H$	M9

Table 2.22: EI-MS analysis of synthesised DHD, E after silylation (figure 2.13.l)
(see section 2.2 and scheme 2.2)

Peak mass (g)	possible fragment	possible pathway	name of fragment
1002	$C_{64}H_{114}O_4Si_2$	molecular ion	M^+
777	$C_{48}H_{82}O_4Si_2$	$M^+ - C_{16}H_{33}$	M1
501	$C_{32}H_{57}O_2Si$	$M^+ - C_{32}H_{57}O_2Si$	M2
389	$C_{24}H_{41}O_2Si$	$M1 - C_8H_7 + H$	M3
249	$C_{14}H_{22}O_2Si$	$M1 - C_{16}H_{33} - C_2H_2$	M4
237 (100%)	$C_{13}H_{21}O_2Si$	$M3 - CH_2 + H$	M5
113	C_8H_{17}	$M1 + H - M2$	M6
73	C_3H_9Si	silylating agent - CH_3	TMS

Table 2.23: EI-MS analysis of synthesised SPD, D before and after silylation
(see section 2.2 and scheme 2.1) (figure 2.14.g)

Peak mass (g)	possible fragment	possible pathway	name of fragment
858	$C_{58}H_{98}O_4$	$M^+ + 2H$	M1 (DHD)
856	$C_{58}H_{96}O_4$	molecular ion	M^+
631	$C_{42}H_{63}O_4$	$M^+ - C_{16}H_{33}$	M2
443	$C_{30}H_{51}O_2$	$M1 - C_{28}H_{47}O_2$	M3
430	$C_{29}H_{50}O_2$	$M1 - C_{29}H_{49}O_2 + H$	M4 (Toc)
217	$C_{14}H_{17}O_2$	$M3 - C_{16}H_{33} - H$	M5
203	$C_{13}H_{15}O_2$	$M4 - C_{16}H_{33} - 2H$	M6
177	$C_{11}H_{13}O_2$	$M6 - C_2H_2$	M7
165 (100%)	$C_{10}H_{13}O_2$	$M7 - CH_2 + 2H$	M8
151	$C_9H_{11}O_2$	$M8 - CH_3 + H$	M9

Table 2.24: FAB-MS analysis of synthesised TRI, A, B, C (figure 2.15.l)
(see section 2.2 and scheme 2.1)

Peak mass (g)	possible fragment	possible pathway	name of fragment
1284.9	$C_{87}H_{144}O_6$	molecular ion	M^+
856.6	$C_{58}H_{96}O_4$	$M^+ - C_{29}H_{48}O_2$	M1 (SPD)
859.6	$C_{58}H_{98}O_4$	$M1 + 2H$	M2 (DHD)
631.4	$C_{42}H_{63}O_4$	$M1 - C_{16}H_{33}$	M3
428.3	$C_{29}H_{48}O_2$	$M2 - C_{29}H_{49}O_2 - H$	M4 (QM)
306.7	$C_{20}H_{34}O_2$	$M4 - C_9H_{19} + 5H$	M5
228.7	$C_{16}H_{36}$	$C_{16}H_{33} + 3H$	M6
216.6	$C_{14}H_{17}O_2$	$M2 - C_{28}H_{47}O_2 - C_{16}H_{33} - H$	M7
188.7	$C_{12}H_{13}O_2$	$M2 - C_{30}H_{51}O_2 - C_{16}H_{33}$	M8
174.7	$C_{11}H_{11}O_2$	$M4 - C_{16}H_{33} - C_2H_2 - 2H$	M9
164.7 (100%)	$C_{10}H_{13}O_2$	$M9 - CH_2$	M10
153.7	$C_9H_{13}O_2$	$M10 - CH_2 + 2H$	M11
135.7	$C_8H_7O_2$	$M11 - CH_3 - 3H$	M12

Table 2.25: ¹H-NMR characteristics of DHD, E and ALD 1, isolated from the products of reaction of Toc with PbO₂, ratios 1:1 and 1:40 in Toc:PbO₂ (see section 2.2.2.3)

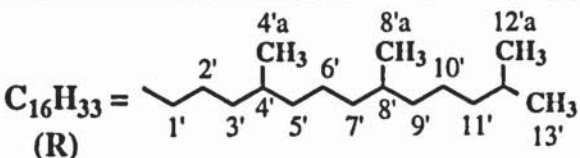
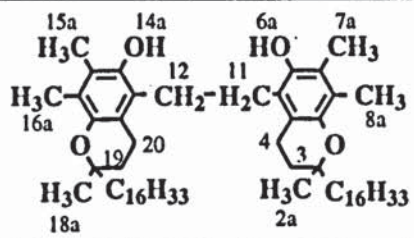
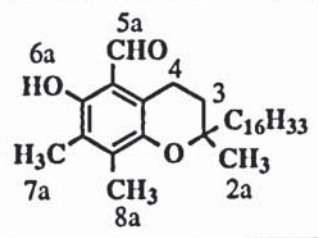
		δ, ppm (multiplicity) (s=singlet, t=triplet, m=multiplet)			
					
group	position				
		E1+E2+ E3, isolated	E1, synthesised	ALD 1, isolated	ALD 1, supplied
CH ₃ of R	4'a, 8'a, 12'a, 13'	0.75-0.95	0.75-0.95	0.7-0.9	0.75-0.85
CH ₃ , sat.	2a	1.23 (s)	1.22 (s)	1.24 (s)	1.24 (s)
	18a	-	-	-	-
CH ₂ of R	3', 5', 7', 9'	0.95-1.45	0.95-1.45	0.95-1.45	1.0-1.4
	11'	0.95-1.2	0.95-1.15	0.95-1.2	1.0-1.2
	6', 10'	1.2-1.3	1.15-1.3	1.2-1.3	1.15-1.3
CH ₂ , CH of R	2', 4', 8'	1.3-1.45	1.3-1.45	1.3-1.45	1.3-1.45
CH of R	1', 12'	1.45-1.65	1.45-1.65	1.45-1.65	1.45-1.55
CH ₂ , β unsat.	3	1.7-1.9	1.7-1.9	1.7-1.9 (m)	1.75-1.9 (m)
	19	(m)	(m)	-	-
CH ₃ , unsat.	8a	2.12 (s)	2.11 (s)	2.14 (s)	2.13 (s)
	16a	-	-	-	-
	7a	2.17 (s)	2.16 (s)	2.15 (s)	2.15 (s)
	15a	-	-	-	-
CH ₂ , α unsat.	4	2.65-2.85	2.65-2.8	2.95-3.1 (t)	2.9-3.1 (t)
	11, 20, 12	-	-	-	-
O-H	6a	5.43 (s)	5.43 (s)	12.10 (s)	12.09 (s)
	14a	-	-	-	-
CHO	5a	-	-	10.18 (s)	10.17 (s)
Figure		-	2.13.d	-	2.2.d

Table 2.29: UV analysis of ALD 1, ALD 2, ALD 3 and compound I, isolated from the extract of PP stabilised with 39% Toc, pass 4, (CPC789 series, single screw extruder, 270°C) and FTIR analysis of ALD 1 and ALD 2 (see section 2.7.1)

compound	isolated ALD 1	supplied ALD 1	ALD 2	ALD 3	compound I	
λ_{\max} , nm (ϵ , l.mol ⁻¹ .cm ⁻¹)	239, 290, 282, 386	239, 290 (9116) 282 (8761) 386 (2846)	250, 285 (8234) 297 (7393) 404 (930?)	283 (7115) 395 (1912)	275, 310, 350	
ν , cm ⁻¹	O-H str	3375 (weak, broad)	3374 (weak, broad)	3400 (weak, broad)		
	C-H str	2952, 2926, 2868, 2850	2952, 2926, 2868, 2850	2953, 2925, 2868, 2850		
	C=O str	1636	1636	1638		
	C=C str arom.	1617, 1581	1617, 1581	1599, 1550, 1513	-	-
	C-H def	1462, 1415, 1396, 1378, 1311	1462, 1415, 1397, 1378, 1311	1462, 1418, 1378, 1307		
	C-O-C str chroman	1265, 1242, 1159, 1136, 1096, 1061, 1029	1265, 1242, 1159, 1136, 1096, 1061, 1029	1261, 1156, 1095, 1023		
Figure	2.21.b (UV)	2.2.b (UV) 2.2.c (IR)	2.22.b (UV) 2.22.c (IR)	2.23.b (UV)	2.24.b (UV)	

Table 2.30: ¹H-NMR characteristics of ALD 1, ALD 2, ALD 3 and compound I, isolated from the extract of PP stabilised with 39% Toc, pass 4, (CPC789 series, single screw extruder, 270°C) (see section 2.7.1)

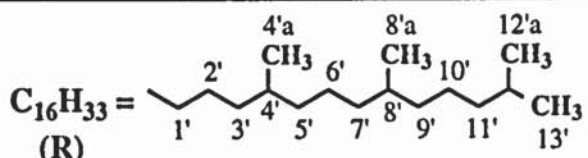
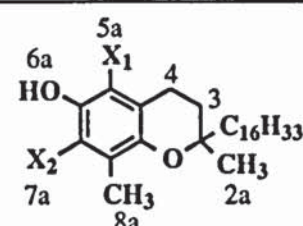
		δ, ppm (multiplicity) (s=singlet, t=triplet, m=multiplet)			
					
group	position			ALD 2	compound I
		ALD 1 (X ₁ = CHO, X ₂ = CH ₃)	ALD 3 (X ₁ = CH ₃ , X ₂ = CHO)		
CH ₃ of R	4'a, 8'a, 12'a, 13'	0.75-0.9	0.7-0.95	0.75-0.9	0.75-0.9
CH ₃ , sat.	2a	1.24 (s)	1.23 (s)	1.23 (s)	1.23 (s)
CH ₂ of R	3', 5', 7', 9'	1.0-1.45	1.0-1.45	1.0-1.45	0.95-1.4
	11'	1.0-1.15	1.0-1.15	1.0-1.2	0.95-1.15
	6', 10'	1.15-1.3	1.15-1.45	1.2-1.3	1.15-1.45
CH ₂ , CH of R	2', 4', 8'	1.3-1.45		1.3-1.45	
CH of R	1', 12'	1.45-1.55	1.4-1.6	1.45-1.6	1.45-1.6
CH ₂ , β unsat. / α unsat.	3	1.7-1.9 (m)	1.7-1.9 (m)	5.76, 5.79 (d)	1.7-1.9 (m)
CH ₃ , unsat.	5a	-	2.10 (s)	-	2.11 (s),
	7a	2.15 (s)	-	2.15 (s), 2.18 (s)	2.12 (s)
	8a	2.14 (s)	2.39 (s)		
CH ₂ , α unsat. / α, β unsat.	4	2.95-3.1 (t)	2.95-3.1 (t)	6.85, 6.89 (d)	2.9-3.1
O-H	6a	12.09 (s)	11.81 (s)	11.90 (s)	6.22 (s)
CHO	5a	10.16	-	10.24 (s)	-
CHO	7a	-	10.27 (s)	-	-
Figure		2.21.c	2.23.c	2.22.d	2.24.c

Table 2.31: ^{13}C -NMR characteristics of ALD 1, isolated from the extract of PP stabilised with 39% Toc, pass 4, (CPC789 series, single screw extruder, 270°C) (see section 2.7.1)

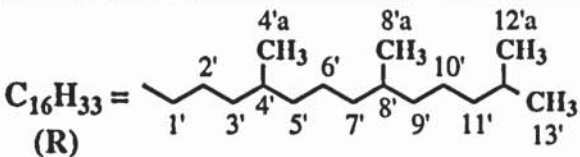
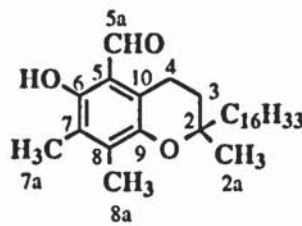
		δ , ppm (multiplicity)	
			
group	position (sign) (+): 1°, 3° C (-): 2°, 4° C		
		isolated ALD 1	supplied ALD 1
CH ₃ , arom.	8a (+)	11.02 (1)	11.01 (1)
	7a (+)	13.20 (1)	13.18 (1)
R	4'a, 8'a (+)	19.66 (2)	19.65, 19.72 (≥3)
	2' (-)	20.94 (≥1)	20.94 (1)
	12'a, 13' (+)	22.62, 22.71 (2)	22.62, 22.72 (2)
	6' (-)	24.41 (1)	24.42 (1)
	10' (-)	24.79 (1)	24.80 (1)
	12' (+)	27.97 (1)	27.96 (1)
	4', 8' (+)	32.76 (2)	32.64, 32.77 (2)
	3', 5', 7', 9' (-)	37.37 (≥2)	37.36 (≥3)
	11' (-)	39.34 (1)	39.34 (1)
1' (-)	39.48, 39.78 (2)	39.49, 39.58 (2)	
CH ₂ , α, β unsat.	4 (-)	18.41 (1)	18.40 (1)
CH ₃ , sat.	2a (+)	23.60 (1)	23.60 (1)
CH ₂ , β unsat.	3 (-)	30.69 (1)	30.73 (2)
C, sat.	2 (-)	75.13 (1)	75.11 (1)
Figure		2.21.d	2.2.e

Table 2.31: continued

group	position (sign) (+): 1°, 3° C (-): 2°, 4° C	δ , ppm (multiplicity)	
		isolated ALD 1	supplied ALD 1
C, unsat	10 (-)	114.5 (1)	114.44 (1)
	7 (-)	117.5 (1)	117.51 (1)
	5 (-)	124.27 (1)	124.18 (1)
	8 (-)	138.6 (1)	138.40 (1)
	6 (-)	144.21 (1)	143.98 (1)
	9 (-)	156.0 (1)	155.77 (1)
Figure		2.21.d	2.2.e

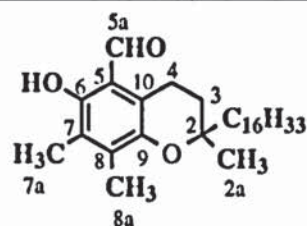


Table 2.32: EI-MS analysis of ALD 2 isolated from the extract of PP stabilised with 39% Toc, pass 4, (CPC789 series, single screw extruder, 270°C) (see section 2.7.1) (figure 2.22.e)

Peak mass (g)	possible fragment	possible pathway	name of fragment
442	$C_{29}H_{46}O_3$	molecular ion	M^+
444	$C_{29}H_{48}O_3$	$M^+ + 2H$	M1
427	$C_{28}H_{43}O_3$	$M^+ - CH_3$	M2
217 (100%)	$C_{13}H_{13}O_3$	$M^+ - C_{16}H_{33}$	M3

Table 2.33: UV analysis of DHD, E, SPD, D, TRI, A, B, C, ALD 1 and ALD 2, isolated from the extracts of LDPE stabilised with 0.2% and 10% Toc, passes 4 (single screw extruder, 180°C) (see section 2.7.2)

compound		DHD, E	SPD, D	TRI, A,B,C	ALD 1	ALD 2
λ_{\max} (nm)	isolated	300	301, 339	292	239, 290, 282, 386	250, 285, 297, 404
	supplied or synthesised (section)	300 (2.2.3)	301, 339 (2.2.1)	292 (2.2.1)	290, 282, 386 (2.1)	285, 297, 404 (2.7.1)
Figure		2.26.b	2.27.b	2.28.b	2.29.b	2.30.b

Table 2.34: ¹H-NMR characteristics of DHD, E and SPD, D, isolated from the extracts of LDPE stabilised with 10% Toc, pass 4 (single screw extruder, 180°C) (see section 2.7.2)

		δ, ppm (multiplicity) (s=singlet, m=multiplet)			
group	position				
		DHD, E		SPD, D	
		isolated	synthesised, E1 (see section 2.2)	isolated	synthesised (see section 2.2)
CH ₃ of R	4'a, 8'a, 12'a, 13'	0.75-0.95	0.75-0.95	0.8-0.9	0.8-0.95
CH ₃ , sat.	2a, 18a	1.23 (s)	1.22 (s)	1.23 (s)	1.20 (s), 1.25 (s), 1.26 (s)
CH ₂ of R	3', 5', 7', 9'	0.95-1.45	0.95-1.45	0.95-1.45	1.0-1.45
	11'	0.95-1.2	0.95-1.15	0.95-1.15	1.0-1.15
	6', 10'	1.2-1.3	1.15-1.3	1.15-1.45	1.15-1.2
CH ₂ , CH of R	2', 4', 8'	1.3-1.45	1.3-1.45		1.2-1.45
CH of R	1', 12'	1.45-1.65	1.45-1.65	1.45-1.85	1.45-1.6
CH ₂ , β unsat.	3, 19	1.7-1.9 (m)	1.7-1.9 (m)		1.65-1.80
CH ₃ , unsat.	16a	2.12 (s)	2.11 (s)	1.83 (s)	1.84 (s)
	8a			2.09 (s),	2.09 (s),
	7a	2.17 (s)	2.16 (s)	2.11 (s)	2.13 (s),
	15a			1.96 (s)	1.97 (s)
CH ₂ , α unsat.	4, 11, 20	2.65-2.85	2.65-2.8	2.3-2.7	2.3-2.7
	12				2.65-2.8
O-H	6a, 14a	5.43 (s)	5.43 (s)	-	-
Figure		2.26.c	2.13.d	2.27.c	2.14.d

Table 2.35: ¹H-NMR characteristics of TRI, A, B, C, isolated from the extract of LDPE stabilised with 10% Toc, pass 4 (single screw extruder, 180°C) (see section 2.7.2)

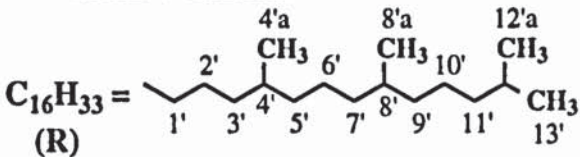
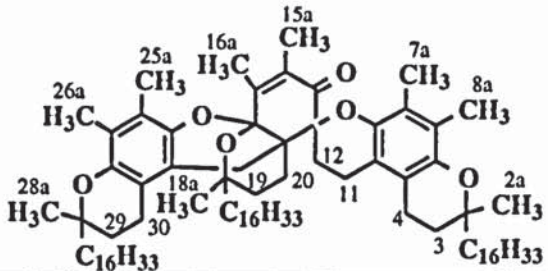
		δ , ppm (multiplicity) (s=singlet)	
			
group	position		
		isolated	synthesised (TRI, B) (see section 2.2.1)
CH ₃ of R	4'a, 8'a, 12'a, 13'	0.8-0.9	0.8-0.9
CH ₃ , sat.	2a, 18a, 28a	1.24 (s)	1.19 (s), 1.21 (s), 1.26 (s)
CH ₂ of R	3', 5', 7', 9'	0.95-1.45	1.0-1.45
	11'	0.95-1.2	1.0-1.2
	6', 10'	1.2-1.45	1.2-1.35
CH ₂ , CH of R	2', 4', 8'		1.35-1.45
CH of R	1', 12'	1.45-1.9	1.45-1.65
CH ₂ , β unsat.	3, 12, 29		1.7-1.9
CH ₃ , unsat.	16a	1.67 (s)	1.67, 1.68
	15a	1.99 (s)	1.97, 1.98
	7a, 8a	2.08 (s), 2.11 (s)	2.09 (s), 2.13 (s)
	25a, 26a	2.17 (s), 2.21 (s)	2.17 (s), 2.23 (s)
CH ₂ , α unsat.	4, 11, 30, 34	2.3-2.9	2.3-2.95
Figure		2.28.c	2.15.f

Table 2.36: ¹H-NMR characteristics of ALD 1 and ALD 2 isolated from the extracts of LDPE stabilised with 0.2% Toc, pass 4 (single screw extruder, 180°C) (see section 2.7.2)

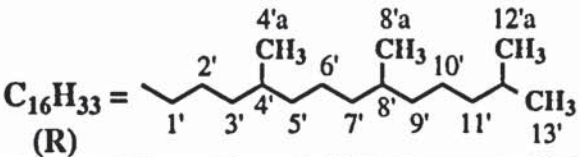
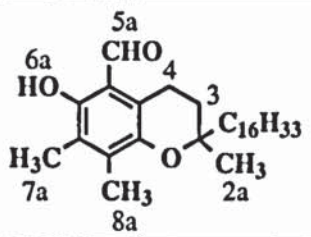
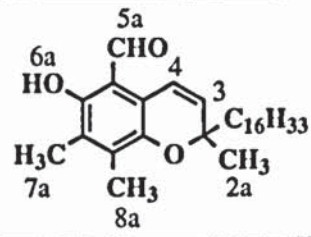
		δ , ppm (multiplicity) (s=singlet, t=triplet, d=doublet, m=multiplet)			
					
group	position				
		ALD 1, isolated	ALD 1, supplied	ALD 2, isolated	ALD 2, isolated (see section 2.7.1)
CH ₃ of R	4'a, 8'a, 12'a, 13'	0.75-0.9	0.7-0.85	0.75-0.95	0.75-0.9
CH ₃ , sat.	2a	1.24 (s)	1.24 (s)	1.25 (s)	1.23 (s)
CH ₂ of R	3', 5', 7', 9'	1.0-1.4	1.0-1.4	1.0-1.4	1.0-1.45
	11'	1.0-1.15	1.0-1.2	1.0-1.2	1.0-1.2
	6', 10'	1.15-1.45	1.15-1.3	1.2-1.4	1.2-1.3
CH ₂ , CH of R	2', 4', 8'		1.3-1.45		1.3-1.45
CH of R	1', 12'	not seen	1.45-1.55	1.4-1.7	1.45-1.6
CH ₂ , β unsat. / α, β unsat.	3	1.75-1.9 (m)	1.75-1.9 (m)	5.75, 5.78 (d)	5.76, 5.79 (d)
CH ₃ , unsat.	7a	2.16 (s)	2.15 (s)	2.18 (s)	2.15 (s), 2.18 (s)
	8a	2.14 (s)	2.39 (s)		
CH ₂ , α unsat. / α, β unsat.	4	2.95-3.05 (t)	2.9-3.1 (t)	6.85, 6.89 (d)	6.85, 6.89 (d)
O-H	6a	12.09 (s)	12.09 (s)	11.88 (s)	11.90 (s)
CHO	5a	10.18	10.17 (s)	10.25 (s)	10.24 (s)
Figure		2.29.c	2.2.d	2.30.d	2.22.d

Table 2.37: GC-MS analysis of SPD, D isolated from the extract of LDPE stabilised with 10% Toc, pass 4 (single screw extruder, 180°C) (see section 2.7.2) (Figure 2.27.d)

Peak mass (g)	possible fragment	possible pathway	name of fragment
856	$C_{58}H_{96}O_4$	molecular ion	M^+ (SPD)
858	$C_{58}H_{98}O_4$	$M^+ + 2H$	M1 (DHD)
631	$C_{42}H_{63}O_4$	$M1 - C_{16}H_{33} - 2H$	M2
428 (100%)	$C_{29}H_{48}O_2$	$M1 - C_{29}H_{49}O_2 - H$	M3 (QM)
218	$C_{14}H_{18}O_2$	$M1 - C_{28}H_{47}O_2 - C_{16}H_{33}$	M4
203	$C_{13}H_{15}O_2$	$M3 - C_{16}H_{33}$	M5
165	$C_{10}H_{13}O_2$	$M5 - C_3H_4 + 2H$	M6

Table 2.38: GC-MS analysis of TRI, A, B, C isolated from the extract of LDPE stabilised with 10% Toc, pass 4 (single screw extruder, 180°C) (see section 2.7.2) (Figure 2.28.d)

Peak mass (g)	possible fragment	possible pathway	name of fragment
856	$C_{58}H_{96}O_4$	molecular ion	M^+ (SPD)
858	$C_{58}H_{98}O_4$	$M^+ - C_{29}H_{46}O_2$ (426g)	M1 (DHD)
631	$C_{42}H_{63}O_4$	$M1 - C_{16}H_{33} - 2H$	M2
430	$C_{29}H_{50}O_2$	$M1 - C_{29}H_{49}O_2 + H$	M3 (Toc)
218	$C_{14}H_{18}O_2$	$M1 - C_{28}H_{47}O_2 - C_{16}H_{33}$	M4
203	$C_{13}H_{15}O_2$	$M3 - C_{16}H_{33} - 2H$	M5
165 (100%)	$C_{10}H_{13}O_2$	$M5 - C_3H_4 + 2H$	M6

Table 2.39: GC-MS analysis of ALD 1 isolated from the extracts of LDPE stabilised with 0.2% Toc, pass 4 (single screw extruder, 180°C) (see section 2.7.2) (Figure 2.29.d)

Peak mass (g)	possible fragment	possible pathway	name of fragment
444 (100%)	$C_{29}H_{48}O_3$	molecular ion	M^+
426	$C_{29}H_{46}O_2$	$M^+ - H_2O$	M1
220	$C_{13}H_{16}O_3$	$M^+ - C_{16}H_{33} + H$	M2
201	$C_{13}H_{13}O_2$	$M1 - C_{16}H_{33}$	M3
192	$C_{11}H_{12}O_3$	$M2 - C_2H_4$	M4
179	$C_{10}H_{11}O_3$	$M4 - CH_2 + H$	M5

Table 2.41: UV analysis of Irg 1076-1, cinnamate of Irg 1076 (C-Irg 1076) and biscinnamate of Irg 1076 (BC-Irg 1076), isolated from the extract of LDPE stabilised with 10% Irg 1076, pass 4 (single screw extruder, 180°C) (see section 2.8.1)

compound	Irg 1076-1	C-Irg 1076 (12)	BC-Irg 1076 (15)	Irg 1076
λ_{\max} , nm (ϵ , l.mol ⁻¹ .cm ⁻¹)	282 (broad)	320 (21230) (broad), 240	308 (35400) (broad), 240	282 (2035)
Figure	2.32.b	2.33.b	2.34.b	2.4.b

Table 2.42: UV analysis of compounds 2-11, 13 and 14 (Irg 1076-2 to -11 and -13 to -14), extracted from LDPE stabilised with 10% Irg 1076, pass 4 (single screw extruder, 180°C) (see section 2.8.1)

compound	2	3	4	5	6	7	8	9	10	11	13	14
λ_{\max} , nm	282	282	282	282	282	282	282	282	282	315 (broad) 238	282, 320 (broad)	320 (broad) 240
Possible structure	unknown									QM	unknown	CBQM
Figure	-									2.35.a	2.35.b	2.35.c

Table 2.43: ¹H-NMR characteristics of C-Irg 1076, isolated from the extract of LDPE stabilised with 10% Irg 1076, pass 4 (single screw extruder, 180°C) (see section 2.8.1)

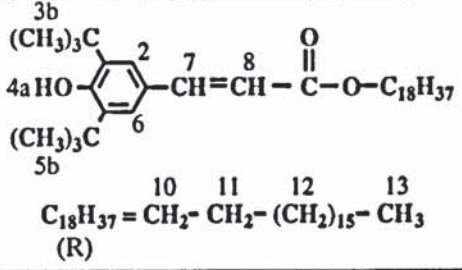
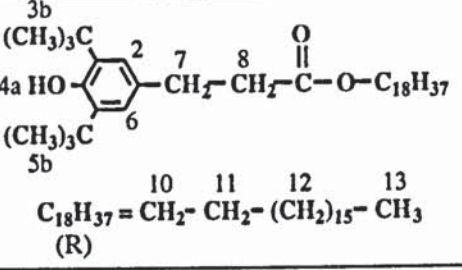
group	position	δ, ppm (multiplicity)	
		C-Irg 1076	Irg 1076
			
CH ₃ of R	13	0.8-0.95 (m)	0.85-0.95 (t)
CH ₂ of R	12	1.15-1.4	1.15-1.4
	11	1.55-1.8	1.6-1.75 (m)
	10	4.12-4.22 (t)	4.05-4.15 (t)
CH ₃ of <i>t</i> -butyl	3b, 5b	1.45 (s)	1.45 (s)
CH ₂ , sat.	7	7.59, 7.61 (d)	2.55-2.65 (t)
	8	6.23, 6.31 (d)	2.85-2.95 (t)
O-H	4a	5.5 (s)	5.1 (s)
C-H, arom.	2, 6	7.37 (s)	7.02 (s)
Figure		2.33.c	2.5.c

Table 2.44: GC-MS analysis of compound 1 (Irg 1076-1), isolated from the extract of LDPE stabilised with 10% Irg 1076, pass 4 (single screw extruder, 180°C) (see section 2.8.1) (figure 2.32.c)

Peak mass (g)	possible fragment	possible pathway	name of fragment
348	C ₂₂ H ₃₆ O ₃	molecular ion	M ⁺
344	C ₂₂ H ₃₂ O ₃	M ⁺ - 4H	M1
287	C ₁₈ H ₂₃ O ₃	M1 - C(CH ₃) ₃	M2
238	C ₁₄ H ₂₂ O ₃	M ⁺ - 2C(CH ₃) ₃ + 2H	M3
149	C ₁₀ H ₁₃ O	M3 - C ₄ H ₉ O ₂	M4
57 (100%)	C ₄ H ₉	<i>t</i> -butyl	M5

Table 2.45: GC-MS analysis of cinnamate of Irg 1076 (C-Irg 1076), isolated from the extract of LDPE stabilised with 10% Irg 1076, pass 4 (single screw extruder, 180°C) (see section 2.8.1) (figure 2.33.d)

Peak mass (g)	possible fragment	possible pathway	name of fragment
528 (100%)	$C_{35}H_{60}O_3$	molecular ion	M^+
529	$C_{35}H_{60}O_3$	molecular ion	$M^+ + 1$
513	$C_{34}H_{57}O_3$	$M^+ - CH_3$	M1
276	$C_{17}H_{24}O_3$	$M^+ - C_{18}H_{37} + H$	M2
259	$C_{16}H_{20}O_3$	$M2 - CH_3 - 2H$	M3
219	$C_{13}H_{15}O_3$	$M3 - C_3H_6 + 2H$	M4
57	C_4H_9	t-butyl	M5

Table 2.46: GC-MS analysis of biscinnamate of Irg 1076 (BC-Irg 1076), isolated from the extract of LDPE stabilised with 10% Irg 1076, pass 4 (single screw extruder, 180°C) (see section 2.8.1) (figure 2.34.c)

Peak mass (g)	possible fragment	possible pathway	name of fragment
1055	$C_{70}H_{118}O_6$	molecular ion	M^+
528	$C_{35}H_{60}O_3$	$M^+ - C_{35}H_{59}O_3 + H$	M1
471	$C_{31}H_{51}O_3$	$M1 - C(CH_3)_3$	M2
219	$C_{13}H_{15}O_3$	$M2 - C_{18}H_{37} + H$	M3
57 (100%)	C_4H_9	t-butyl	M4

Table 2.48: UV analysis of compounds 3 and 6 (Irg 1010-3 and -6), isolated from the extract of LDPE stabilised with 10% Irg 1010, pass 4 (single screw extruder, 180°C) (see section 2.8.2)

compound	Irg 1010-3	Irg 1010-6	Irg 1010
λ_{\max} , nm (ϵ , l.mol ⁻¹ .cm ⁻¹)	282	282	282 (7537)
Figure	2.37.b	2.38.b	2.5.b

Table 2.49: UV analysis of compounds 1, 2, 4, 5 and 7-13 (Irg 1010-1, -2, -4, -5 and -7 to -13), extracted from LDPE stabilised with 10% Irg 1010, pass 4 (single screw extruder, 180°C) (see section 2.8.2)

compound	1	2	4	5	7	8	9	10	11	12	13	14
λ_{\max} , nm	282	282	320 (broad) 282	282	282	282	282	282	282	282	282	312 (broad) 288
Figure	-		2.39.a	-								2.39.b

Table 2.50: $^1\text{H-NMR}$ analysis of compounds 3 and 6 (Irg 1010-3 and 1010-6), isolated from the extract of LDPE stabilised with 10% Irg 1010, pass 4 (single screw extruder, 180°C) (see section 2.8.2)

group	position	δ , ppm (multiplicity)		
		Irg 1010-3 ($n = 3$, $X = \text{H}$)	Irg 1010-6 ($n = 6$, $X = \text{C-CH}_2\text{OH}$)	Irg 1010 ($n = 4$, $X = \text{C}$)
CH_2 , sat.	11	-	-	-
CH_3 , sat.	10	3.7 (s)	4.0 (s)	4.1 (s)
CH_3 of <i>t</i> -butyl	3b, 5b	1.42 (s)	1.42 (s)	1.48 (s)
CH_2 , sat.	7	2.5-2.7 (t)	2.5-2.7 (t)	2.55-2.7 (t)
	8	2.8-2.95 (t)	2.8-2.95 (t)	2.85-2.95 (t)
O-H	4a	5.1 (s)	5.1 (s)	5.1 (s)
	11a	-	3.2 (s)	-
C-H, arom.	2, 6	7.0 (s)	7.0 (s)	7.0 (s)
Figure		2.37.c	2.38.c	2.5.c

Table 2.51: GC-MS analysis of Irg 1010-3, isolated from the extract of LDPE stabilised with 10% Irg 1010, pass 4 (single screw extruder, 180°C) (see section 2.8.2) (figure 2.37.d)

Peak mass (g)	possible fragment	possible pathway	name of fragment
292	$\text{C}_{18}\text{H}_{28}\text{O}_3$	molecular ion	M^+
277	$\text{C}_{17}\text{H}_{25}\text{O}_3$	$\text{M}^+ - \text{CH}_3$	M1
219	$\text{C}_{13}\text{H}_{15}\text{O}_3$	$\text{M1} - \text{C}(\text{CH}_3)_3 - \text{H}$	M2
149	$\text{C}_{10}\text{H}_{13}\text{O}$	$\text{M2} - \text{C}_3\text{H}_3\text{O}_2 + \text{H}$	M3
62 (100%)	$\text{C}_2\text{H}_6\text{O}_2$	$\text{M5} - 2(\text{CH}_3) + 2\text{OH} + \text{H}$	M4
57	C_4H_9	<i>t</i> -butyl	M5

Table 2.52: EI-MS analysis of Irg 1010-6, isolated from the extract of LDPE stabilised with 10% Irg 1010, pass 4 (single screw extruder, 180°C) (see section 2.8.2) (figure 2.38.d)

Peak mass (g)	possible fragment	possible pathway	name of fragment
916	$C_{56}H_{84}O_{10}$	molecular ion	M^+
860	$C_{52}H_{76}O_{10}$	$M^+ - C(CH_3)_3 + H$	M1
803	$C_{48}H_{67}O_{10}$	$M1 - C(CH_3)_3$	M2
748	$C_{44}H_{60}O_{10}$	$M2 - C(CH_3)_3 + 2H$	M3
638	$C_{39}H_{58}O_7$	$M^+ - C_{17}H_{25}O_3 - H$	M4
582	$C_{35}H_{50}O_7$	$M4 - C(CH_3)_3 + H$	M5
259	$C_{17}H_{23}O_2$	$M4 - C_{18}H_{27}O_3 - C - CHO - CH_3 - CH_2O - 2H$	M6
219 (100%)	$C_{15}H_{23}O$	$M6 - C_2HO + H$	M7
57	C_4H_9	t-butyl	M8

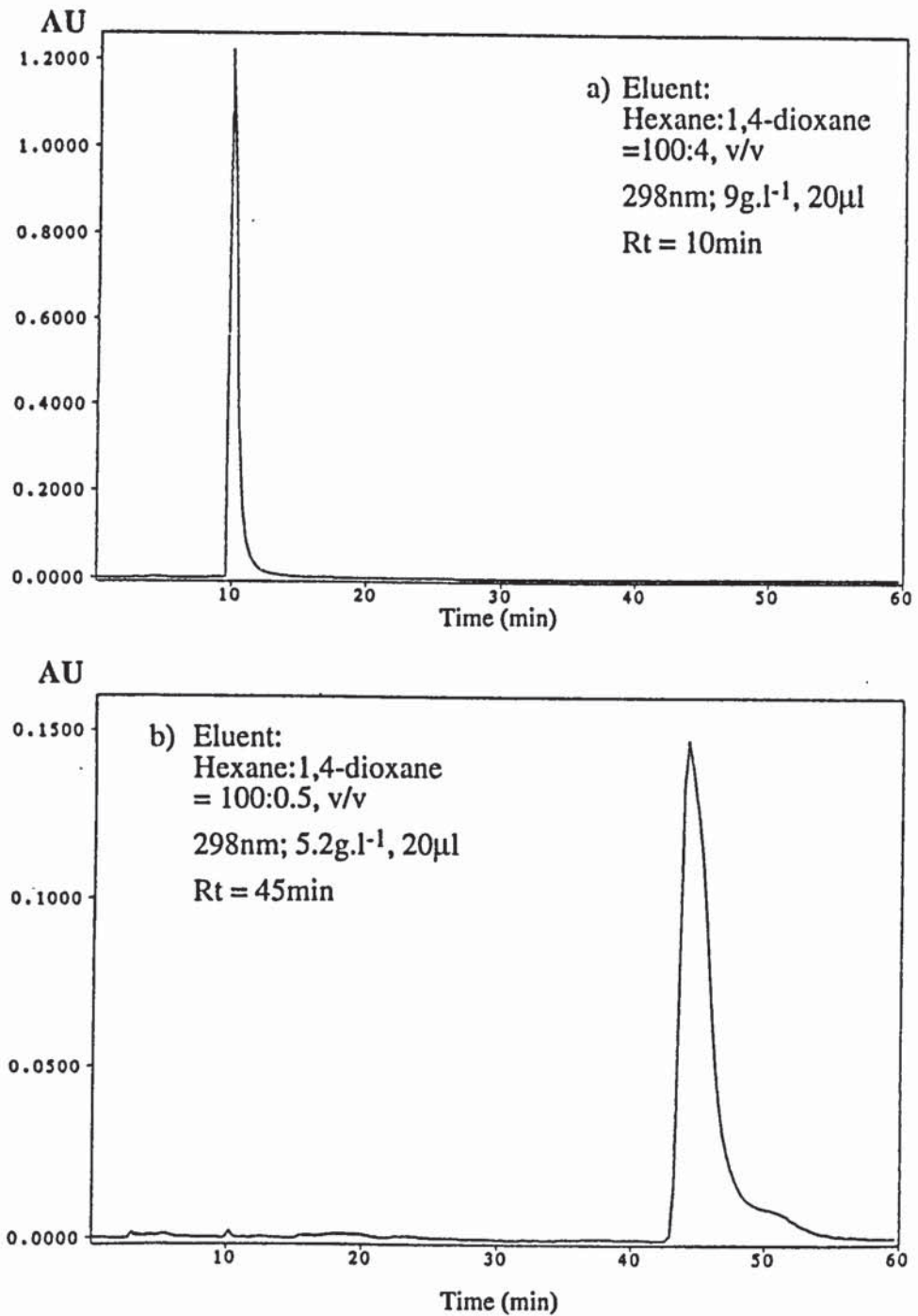
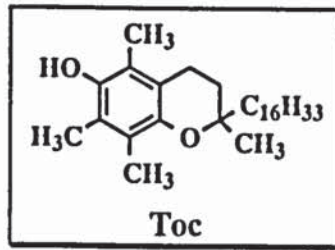


Figure 2.1.a: HPLC chromatograms of Toc (R202) in hexane, at 298nm
 Instruments: Philips PU4100 liquid chromatograph and PU4120 diode
 array detector
 Column: Zorbax SIL (4.6mm x 25cm); Flow rate: 1ml.min⁻¹

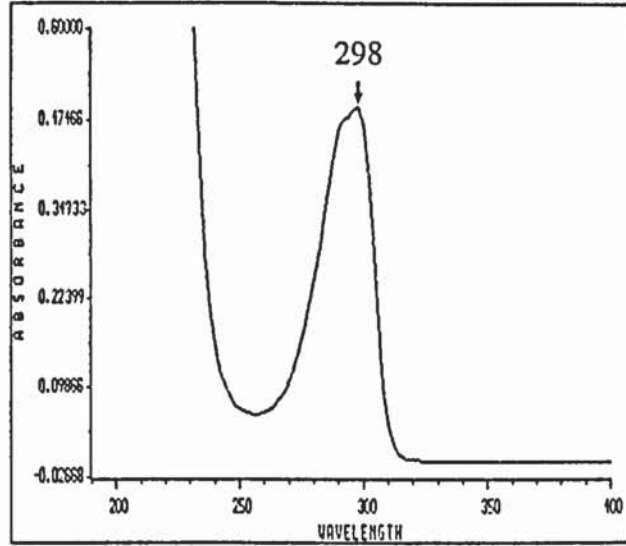
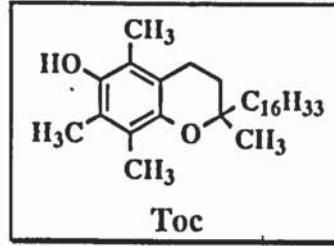


Figure 2.1.b: UV spectrum of Toc (R202) in hexane, 0.6g.l⁻¹ (see table 2.2)

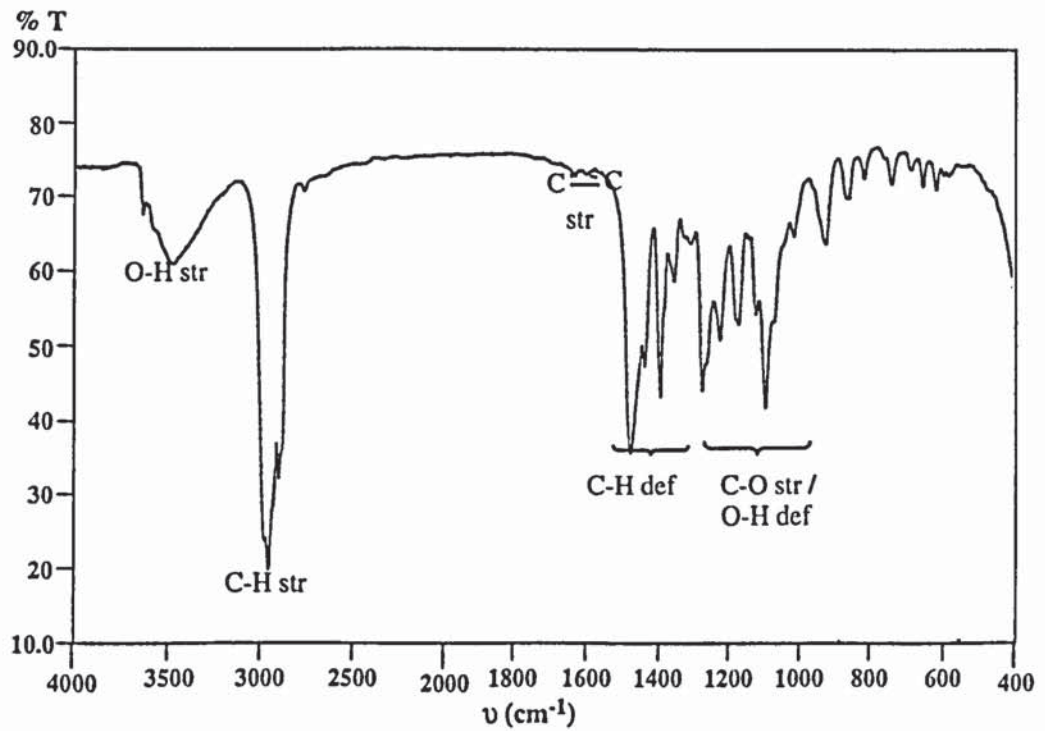
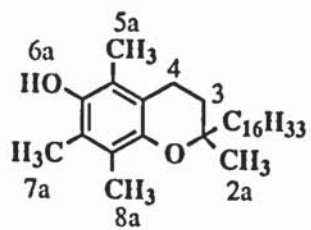


Figure 2.1.c: IR spectrum of Toc (R202), KBr windows (see table 2.2)



Toc

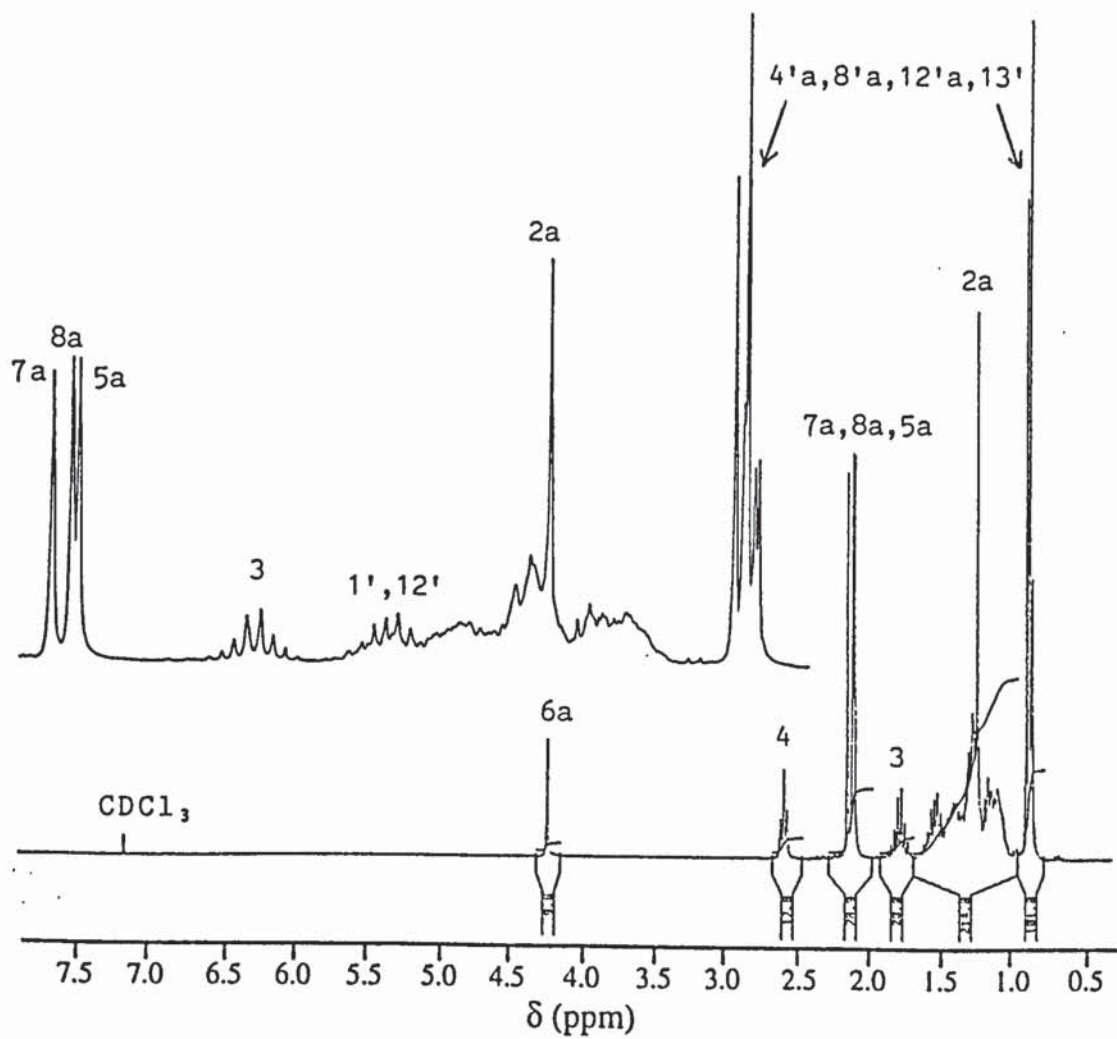
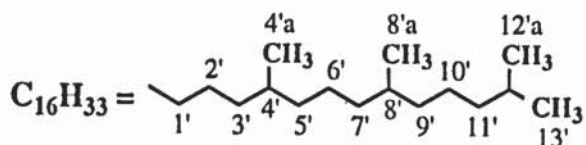


Figure 2.1.d: $^1\text{H-NMR}$ spectrum of Toc (R202) in CDCl_3 , at 300MHz (see table 2.3)

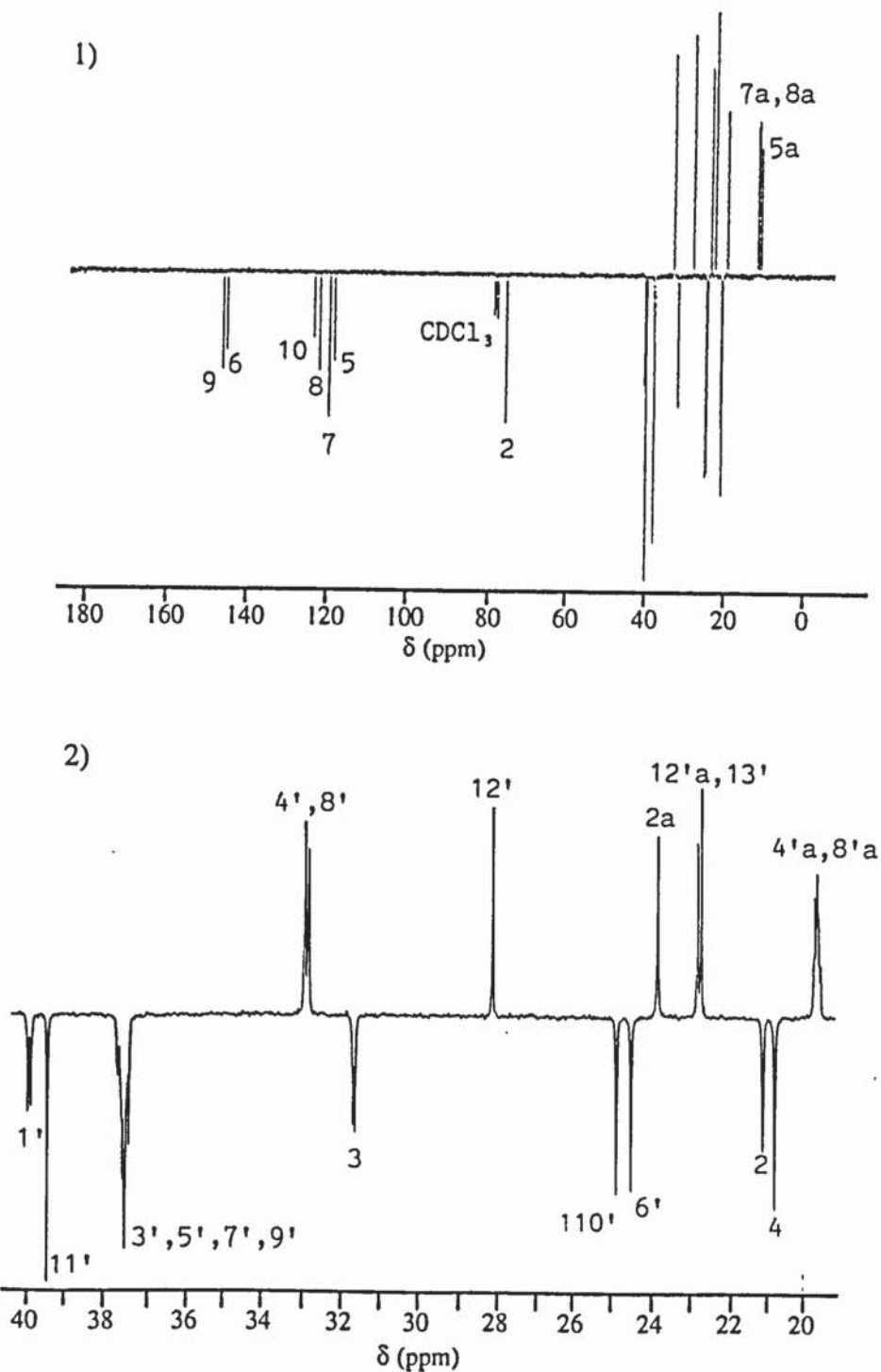
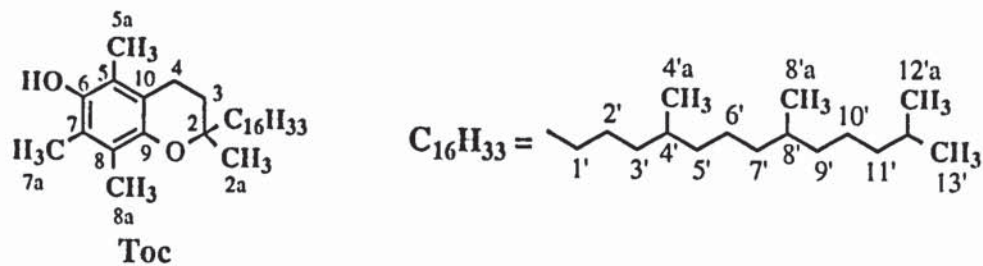
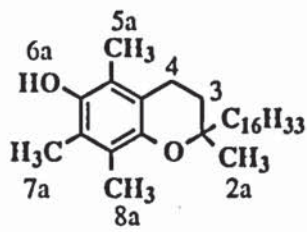


Figure 2.1.e: ^{13}C -NMR spectrum of Toc (R202) in CDCl_3 , at 75 MHz (see table 2.4)
 1) region 0-180ppm 2) expanded region 19-40ppm



Toc

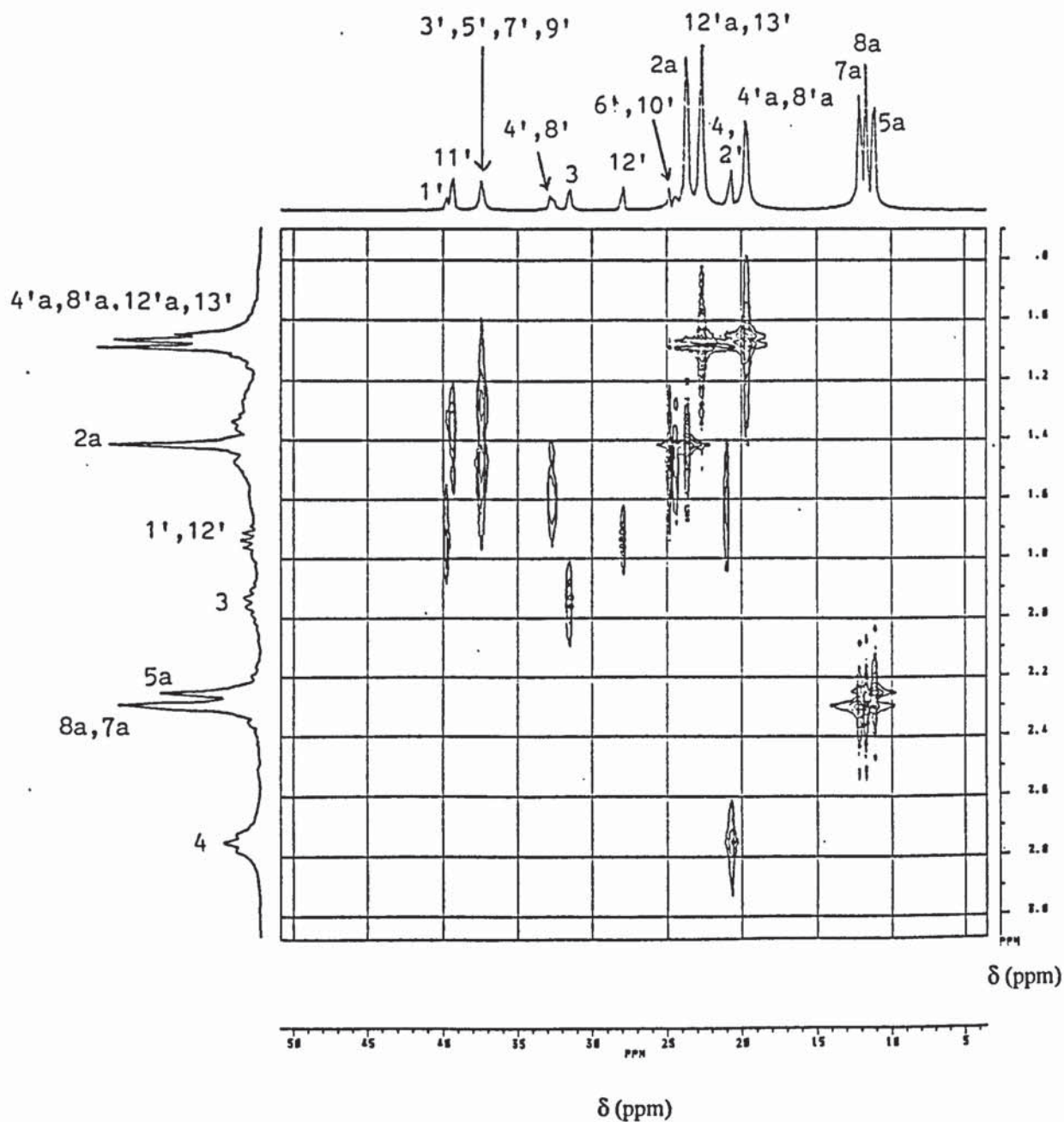
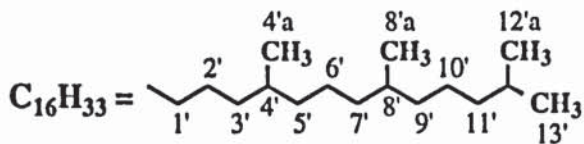


Figure 2.1.f: ^1H , ^{13}C -NMR correlation spectrum of Toc (R202), in CDCl_3

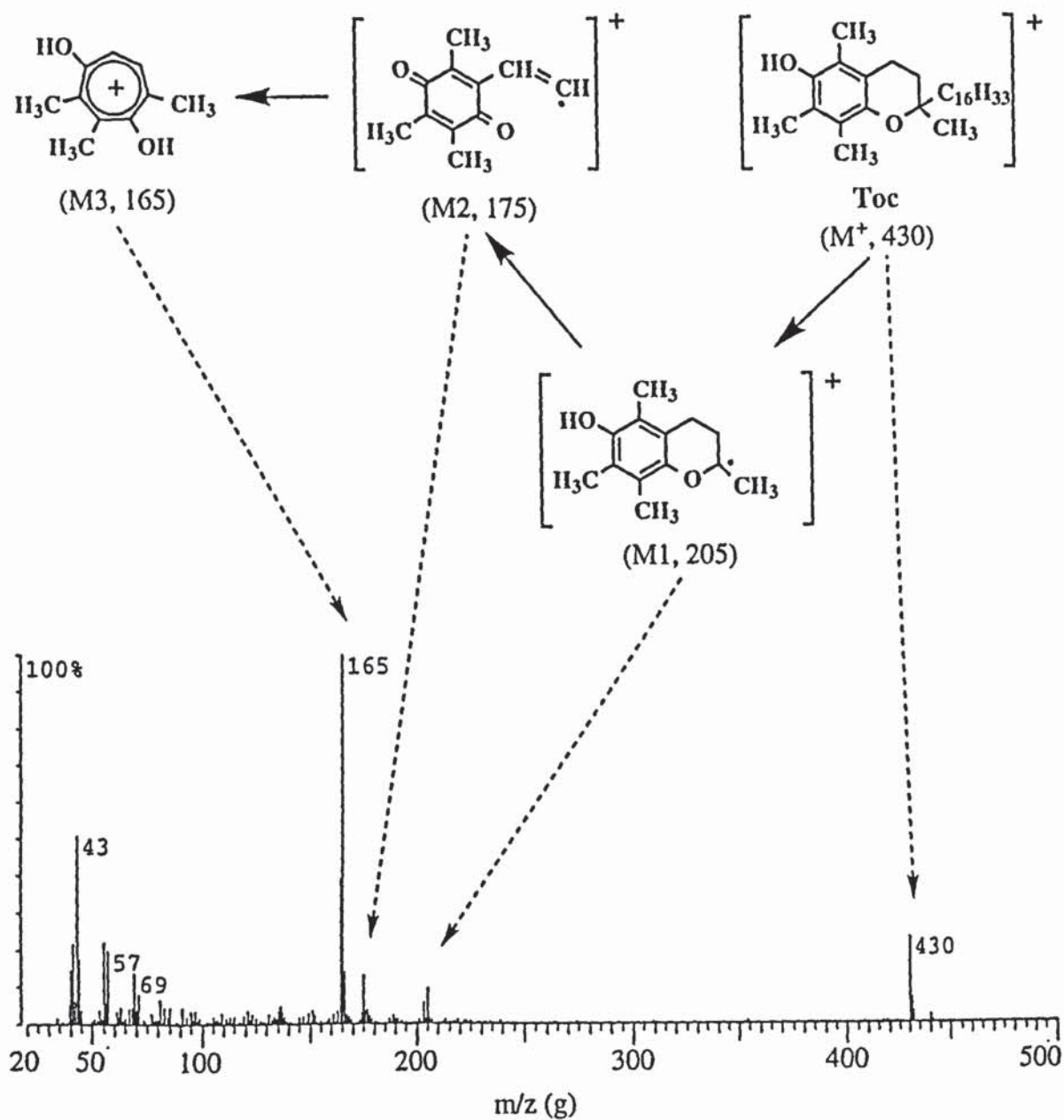


Figure 2.1.g: EI-MS spectrum of Toc (R202) in acetate (see table 2.5)

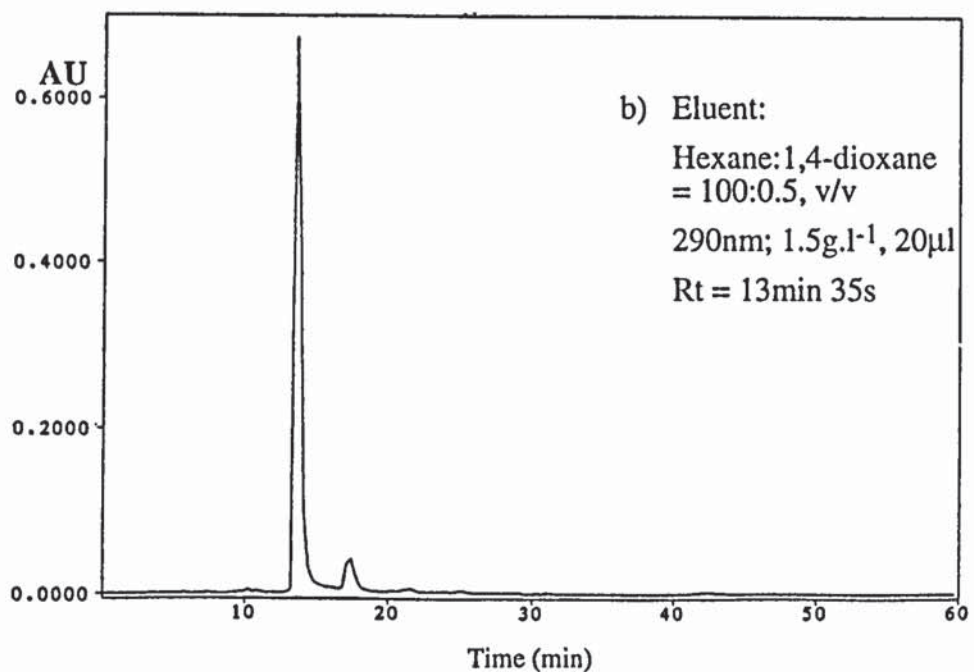
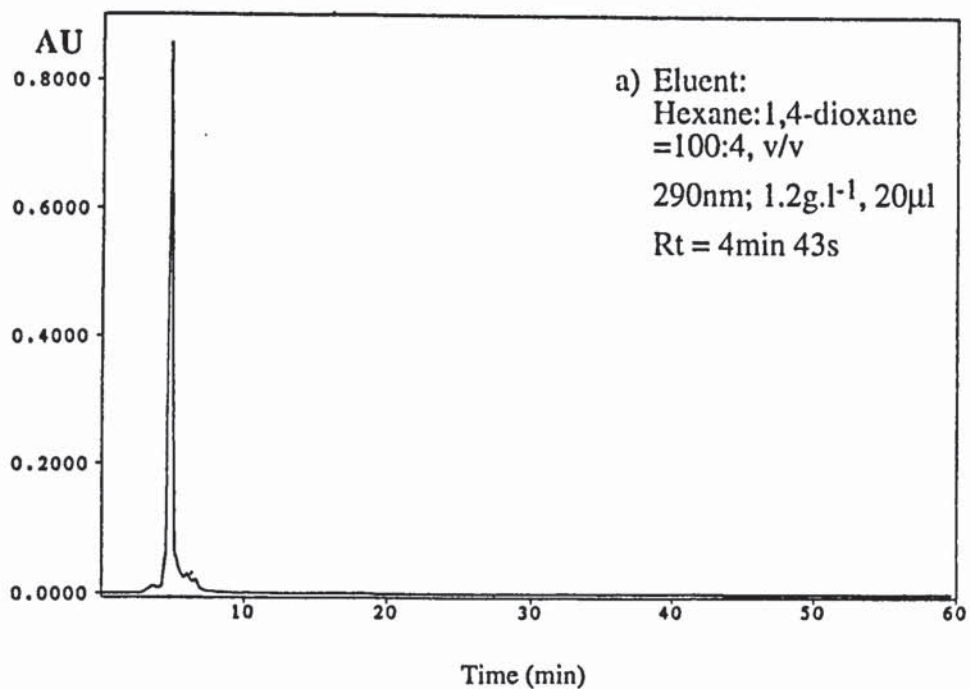
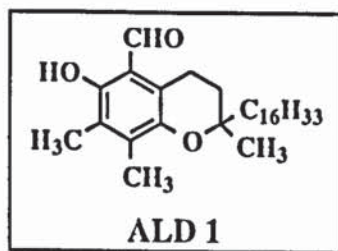


Figure 2.2.a: HPLC chromatograms of supplied ALD 1 in hexane, at 290nm
Instruments: Philips PU4100 liquid chromatograph and PU4120 diode
array detector
Column: Zorbax SIL (4.6mm x 25cm); Flow rate: 1ml.min⁻¹

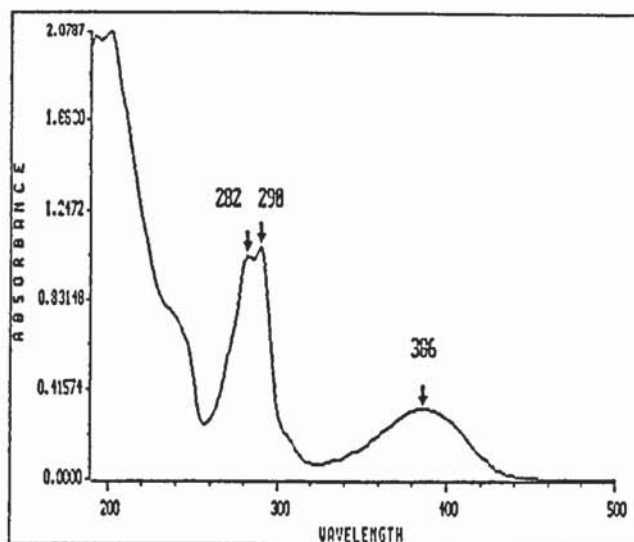
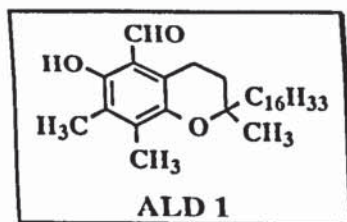


Figure 2.2.b: UV spectrum of supplied ALD 1 in hexane, 0.5g.l^{-1} (see table 2.2)

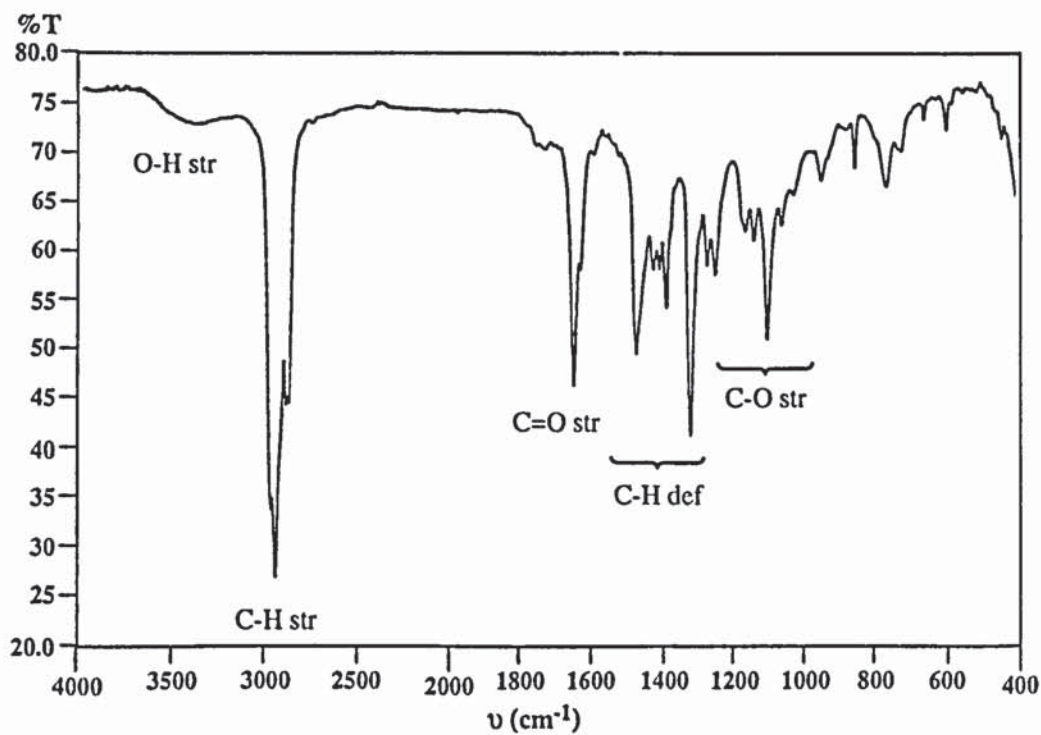
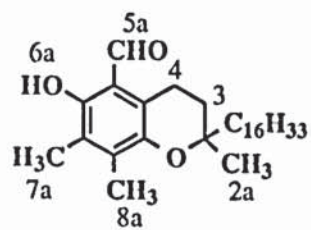


Figure 2.2.c: IR spectrum of supplied ALD 1, KBr windows (see table 2.2)



ALD 1

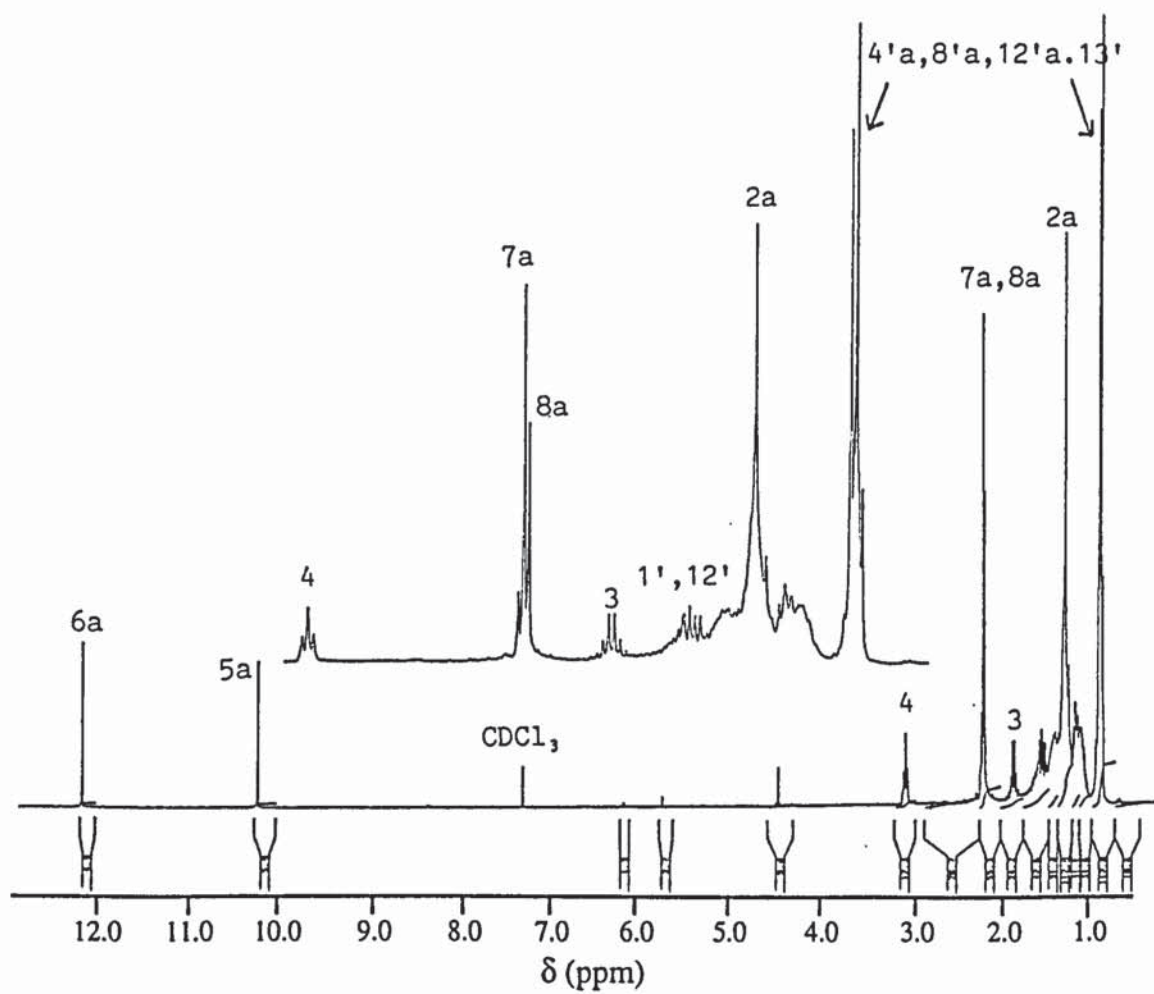
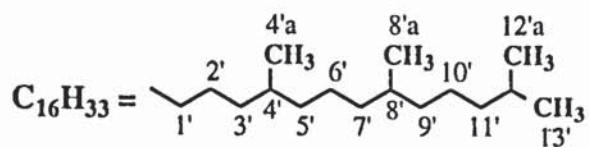
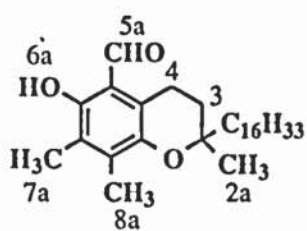


Figure 2.2.d: $^1\text{H-NMR}$ spectrum of supplied ALD 1 in CDCl_3 , at 300MHz (see table 2.3)



ALD 1

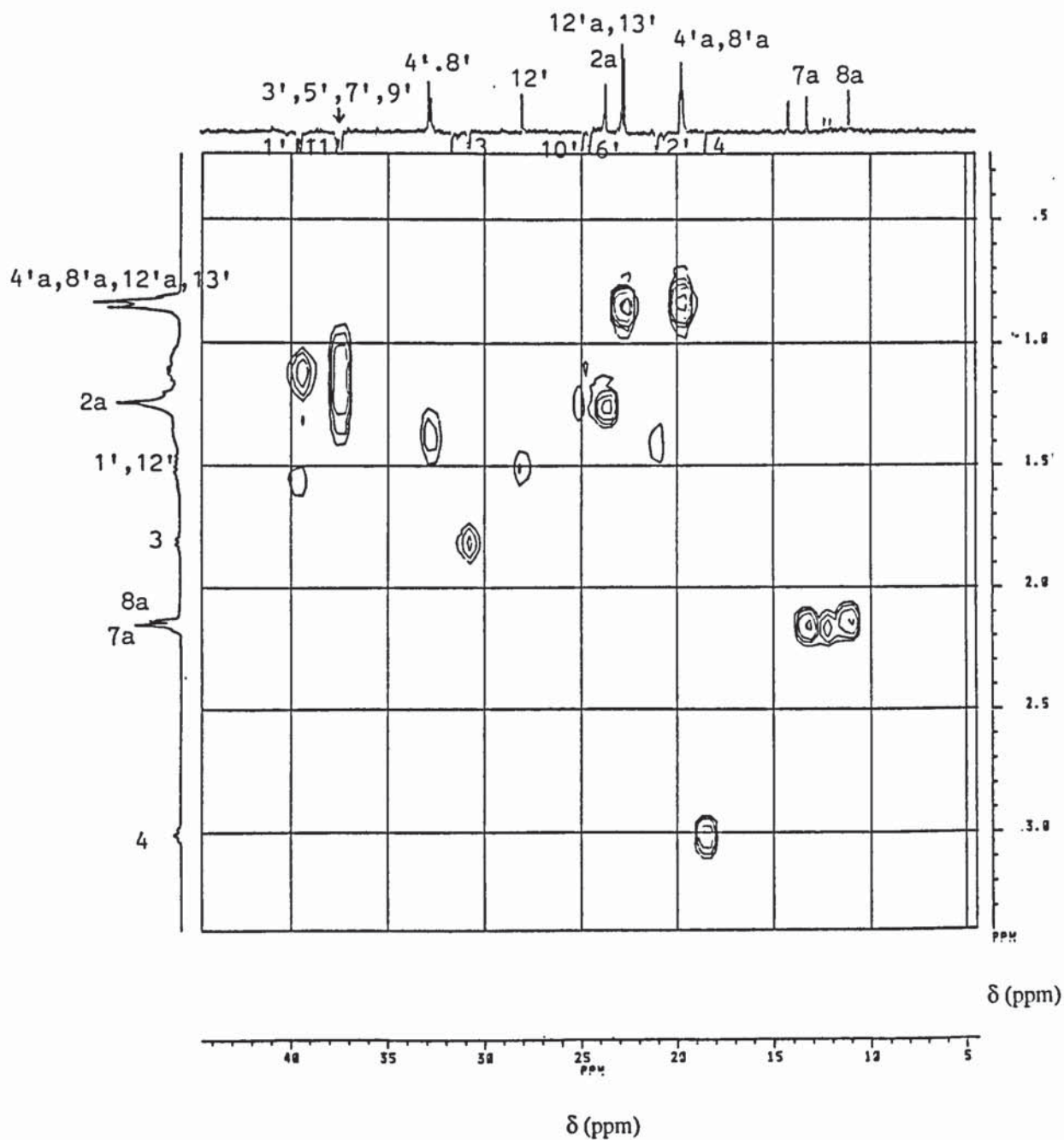
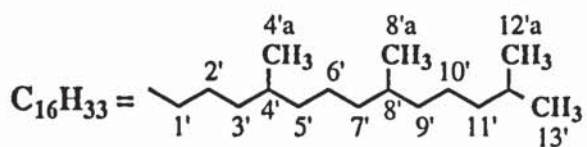


Figure 2.2.f: ^1H , ^{13}C -NMR correlation spectrum of supplied ALD 1 in CDCl_3

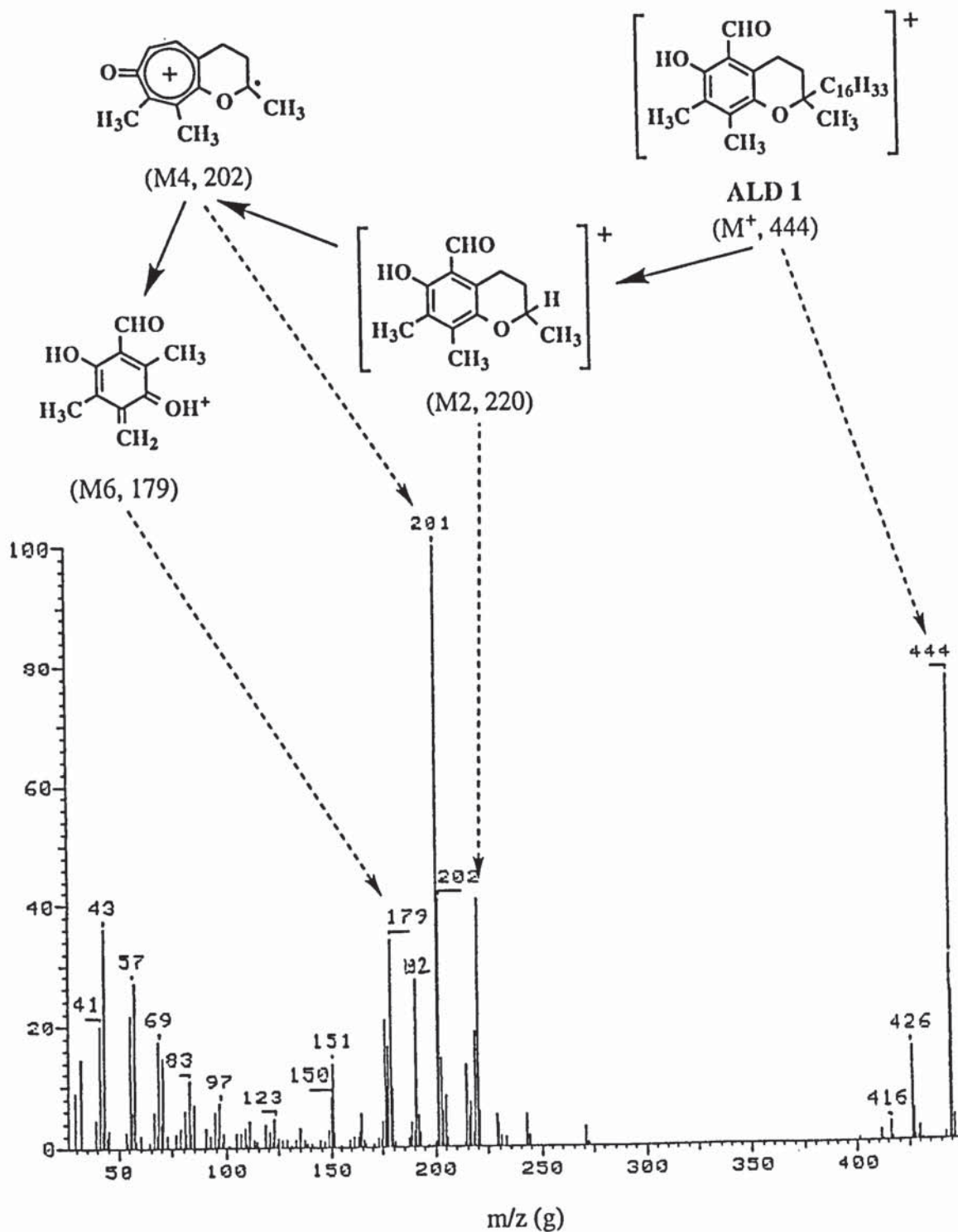


Figure 2.2.g: EI-MS spectrum of supplied ALD 1, in acetate (see table 2.6)

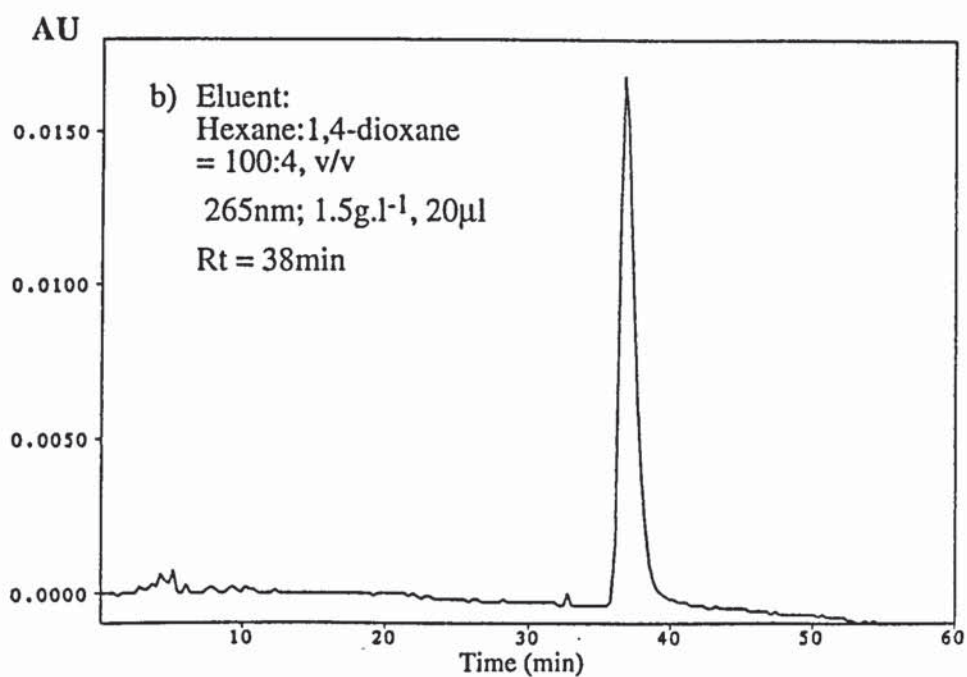
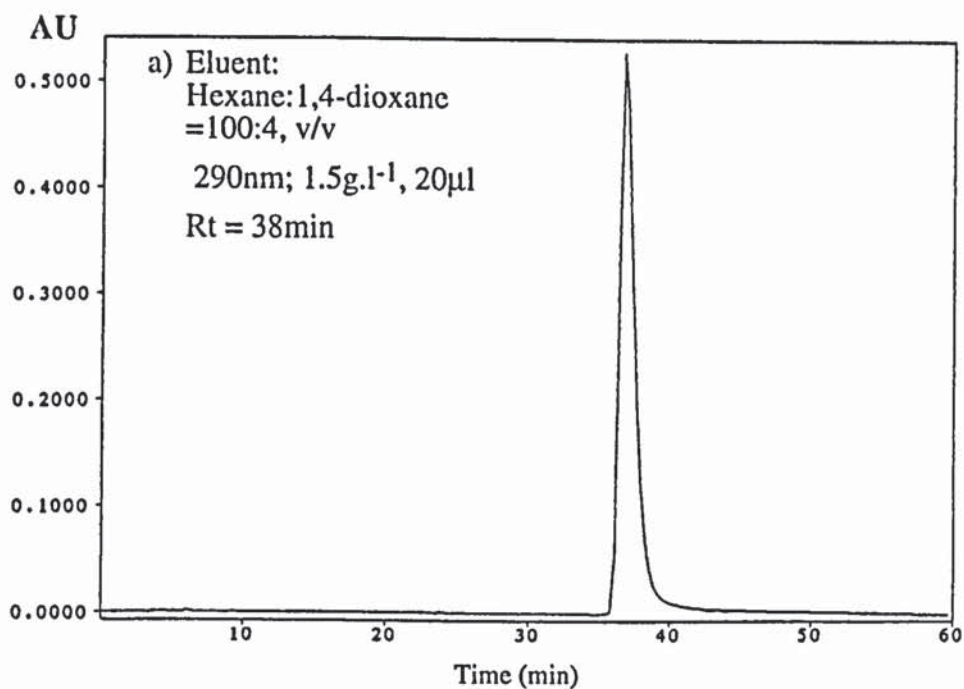
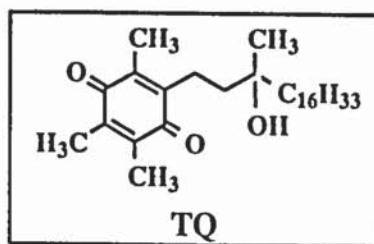


Figure 2.3.a: HPLC chromatograms of TQ in hexane, at 290 and 265nm
 Instruments: Philips PU4100 liquid chromatograph and PU4120 diode array detector
 Column: Zorbax SIL (4.6mm x 25cm); Flow rate: 1ml.min⁻¹

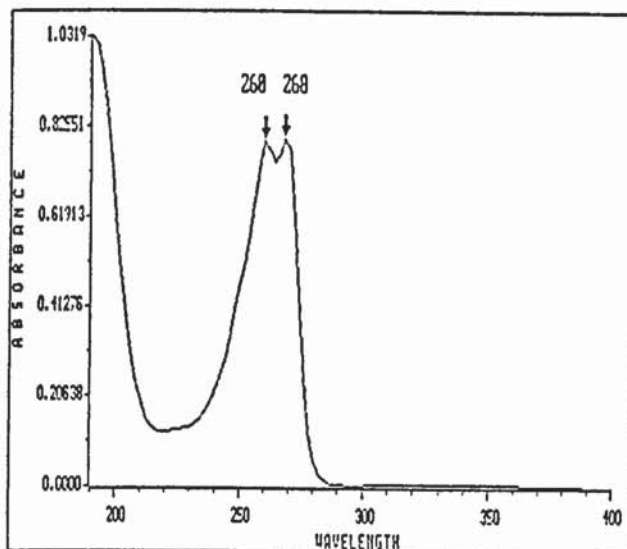
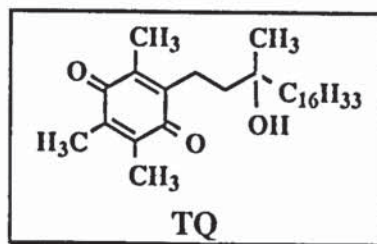


Figure 2.3.b: UV spectrum of TQ in hexane, 0.2g.l⁻¹ (see table 2.2)

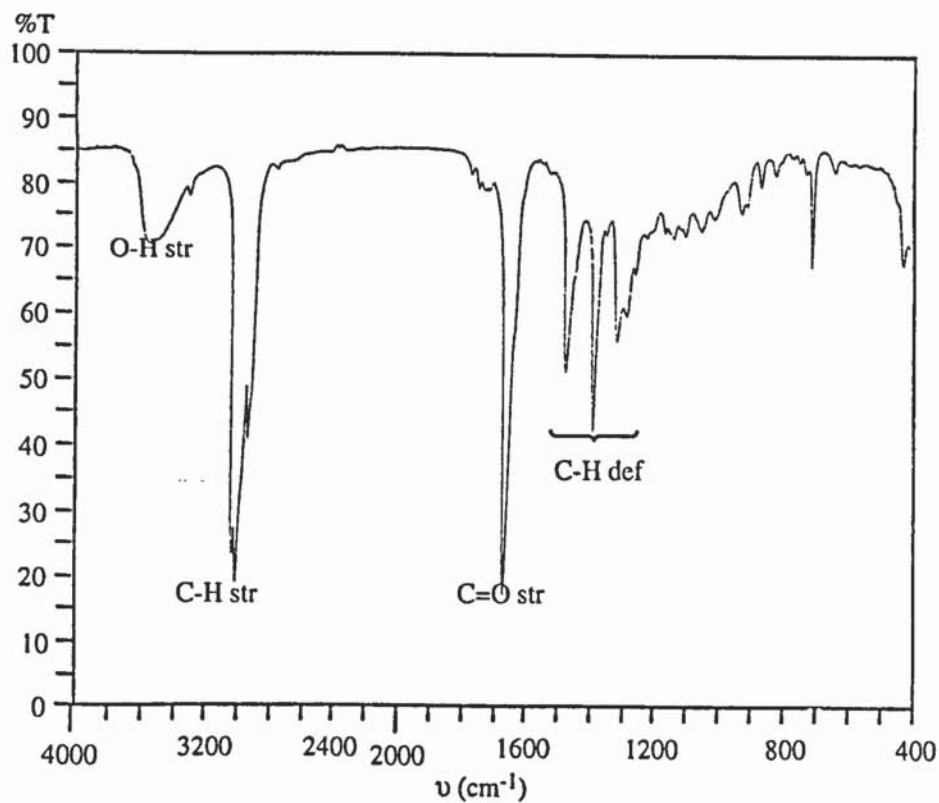


Figure 2.3.c: IR spectrum of TQ, KBr windows (see table 2.2)

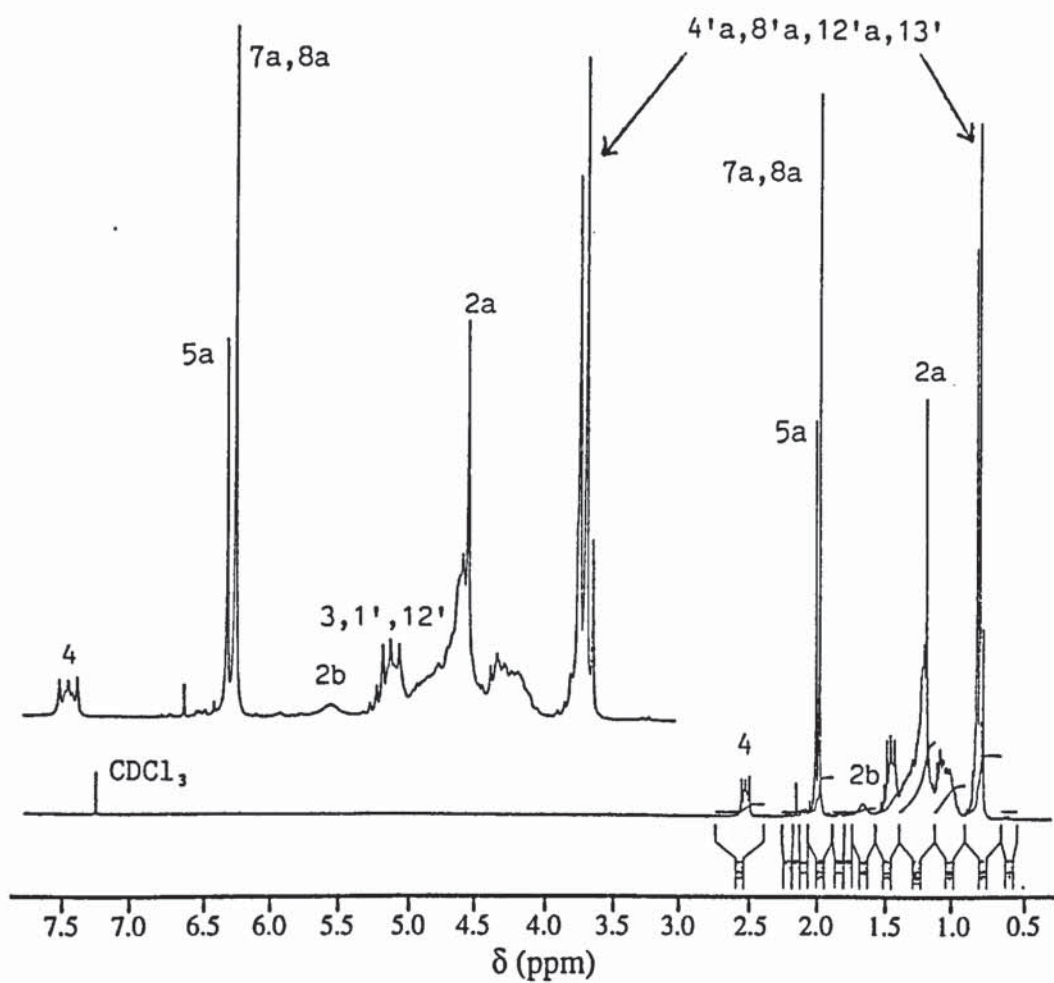
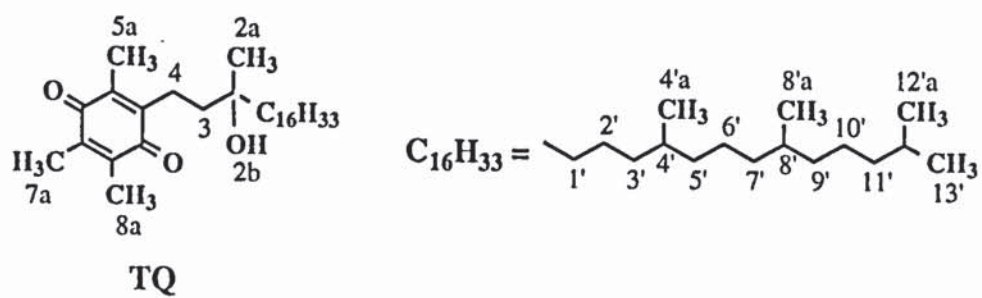


Figure 2.3.d: ^1H -NMR spectrum of TQ (see table 2.3)

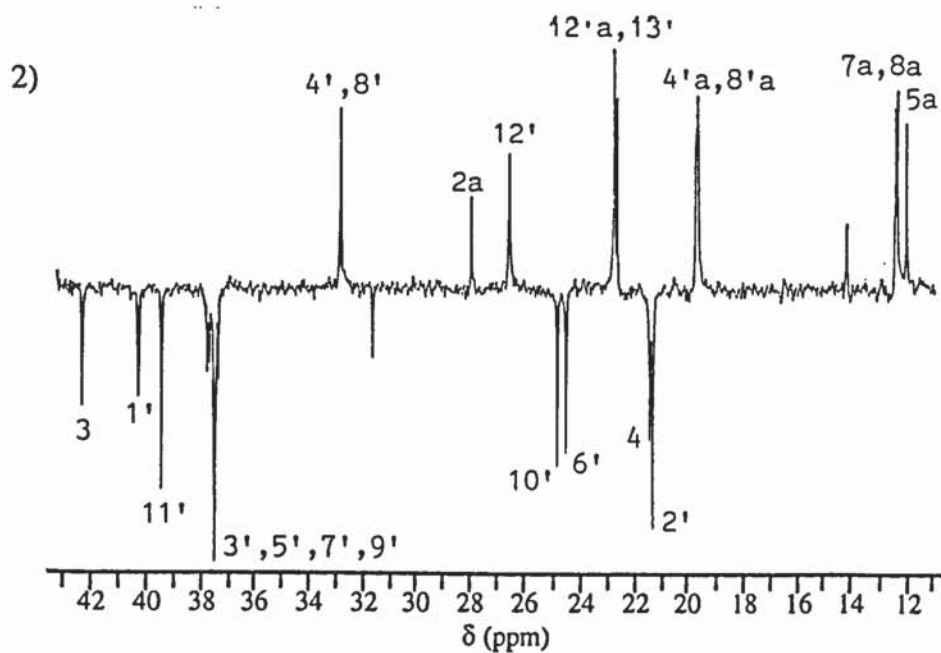
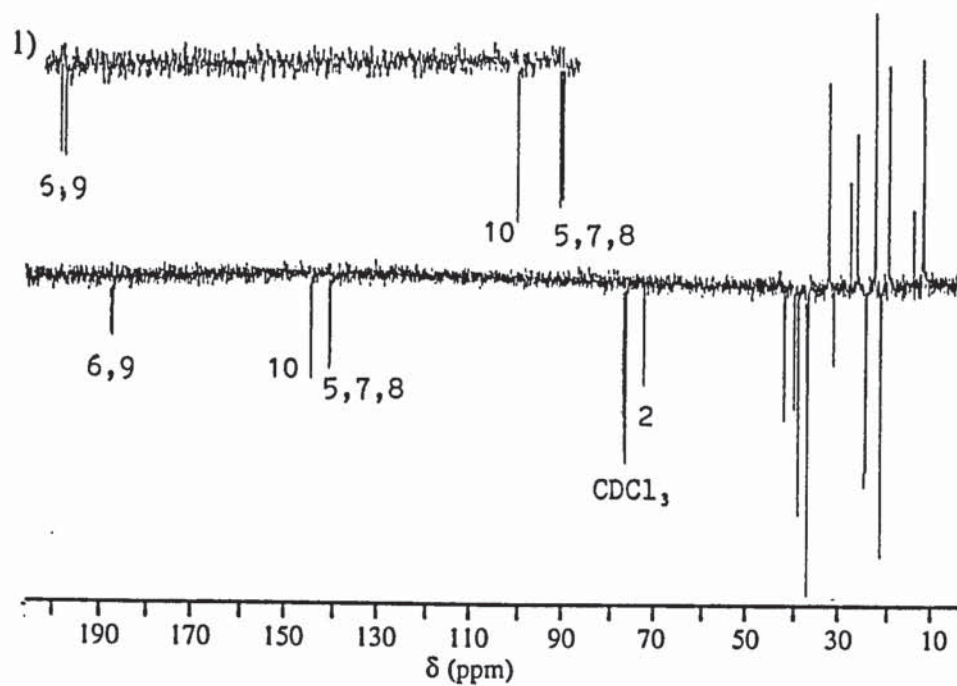
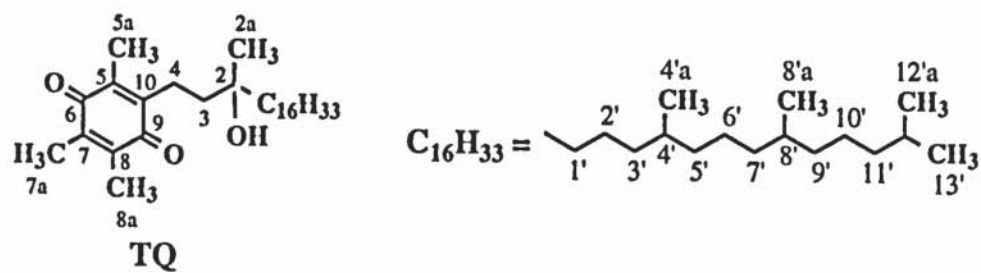
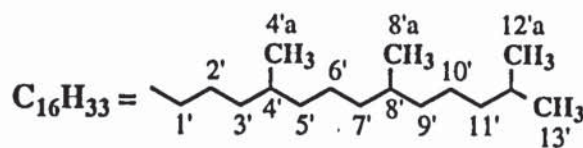
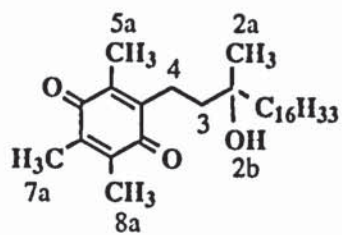


Figure 2.3.e: ^{13}C -NMR spectrum of TQ in CDCl_3 , at 75 MHz (see table 2.4)

1) region 0-210ppm

2) expanded region 11-43ppm



TQ

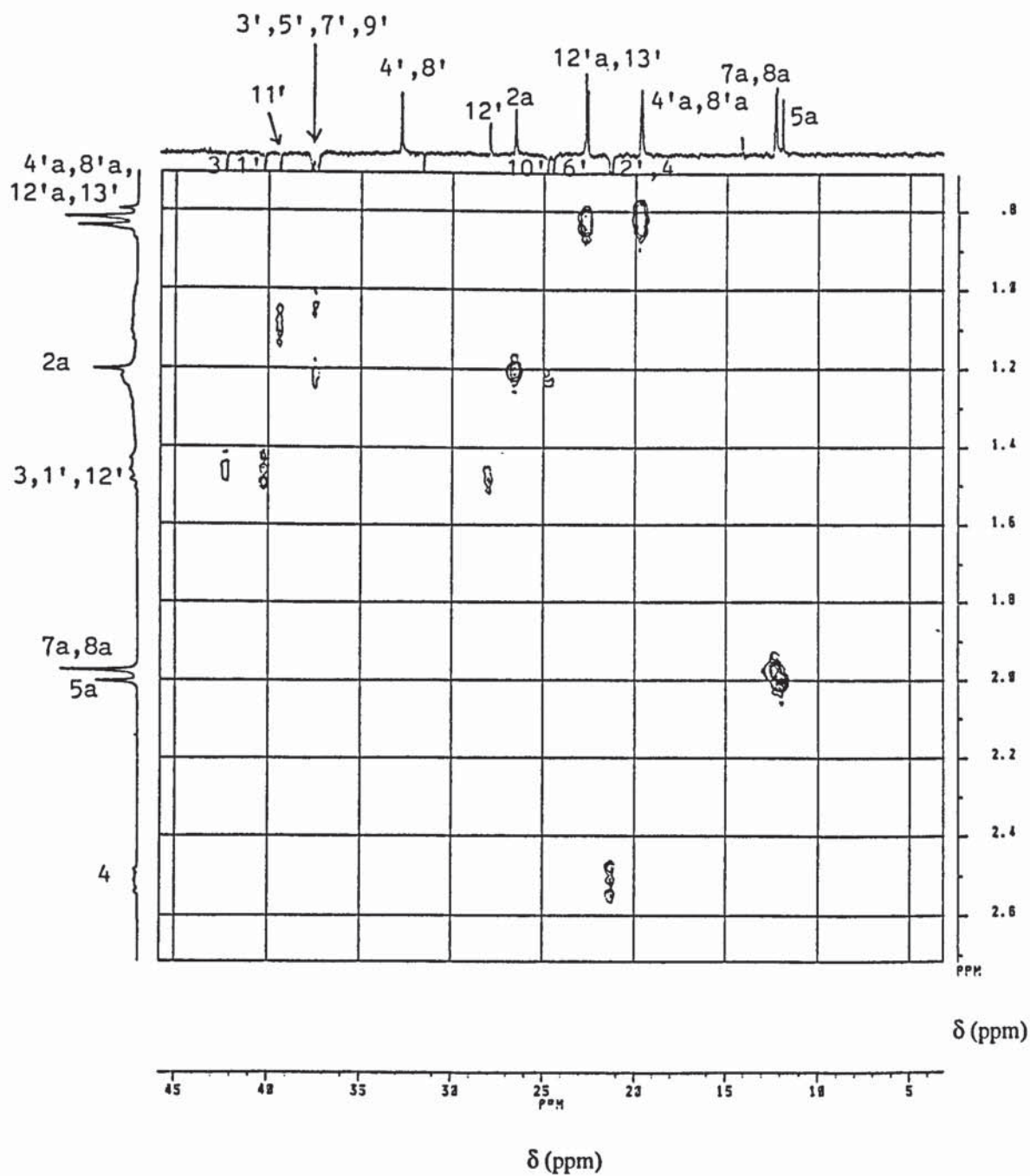


Figure 2.3.f: ¹H, ¹³C-NMR correlation spectrum of TQ, in CDCl₃

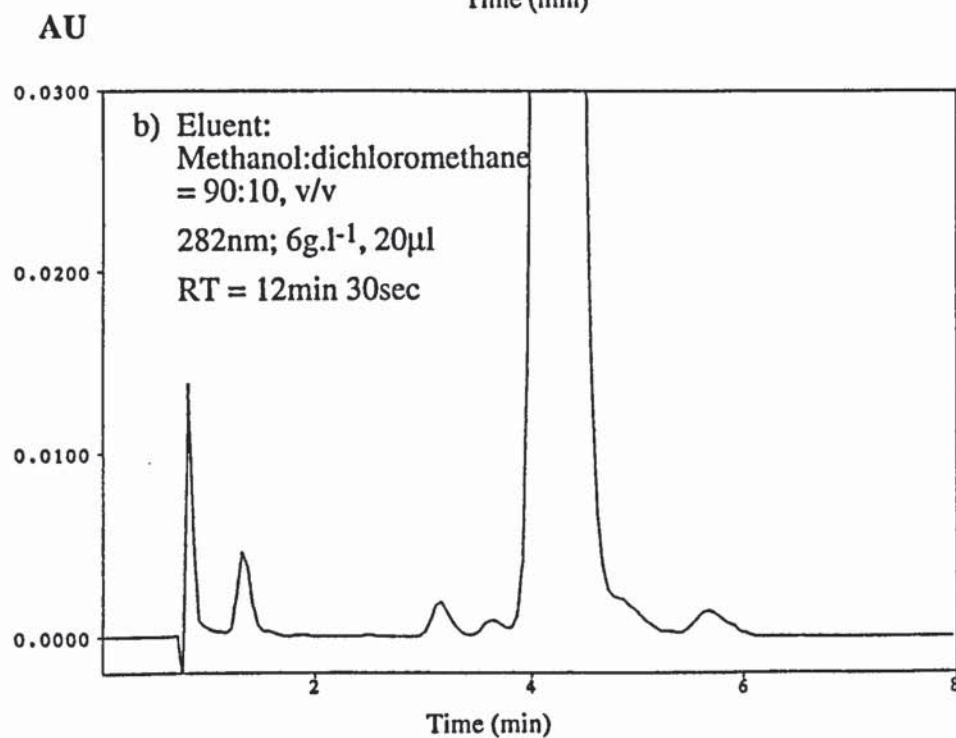
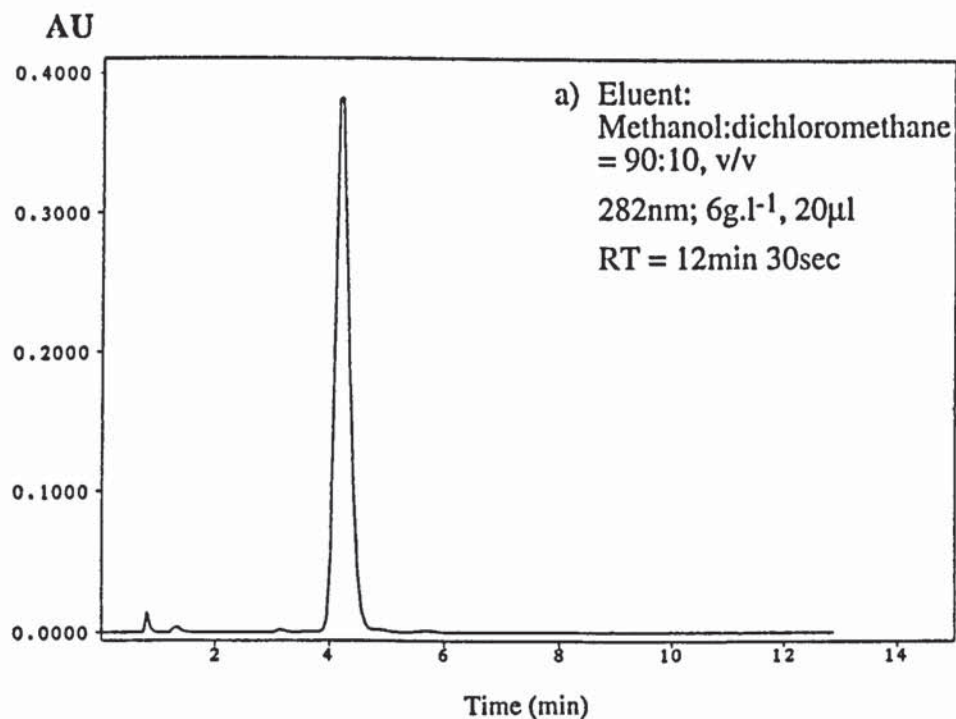
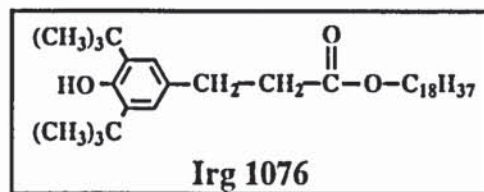


Figure 2.4.a: HPLC chromatograms of Irg 1076 in dichloromethane, at 282nm
Instruments: Philips PU4100 liquid chromatograph and PU4120 diode
array detector
Column: Zorbax ODS (4.6mm x 25cm); Flow rate: 1ml.min⁻¹

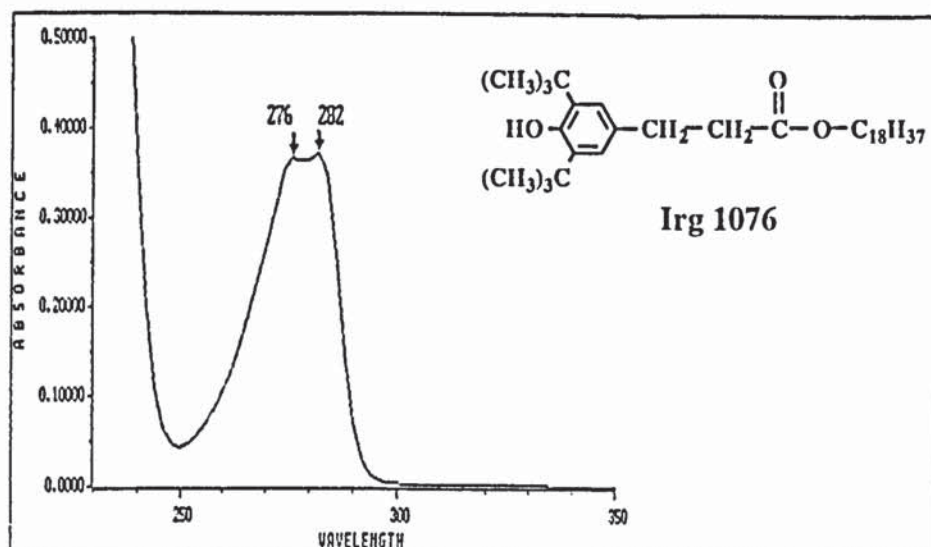


Figure 2.4.b: UV spectrum of Irg 1076 in dichloromethane, $1\text{g}\cdot\text{l}^{-1}$ (see table 2.7)

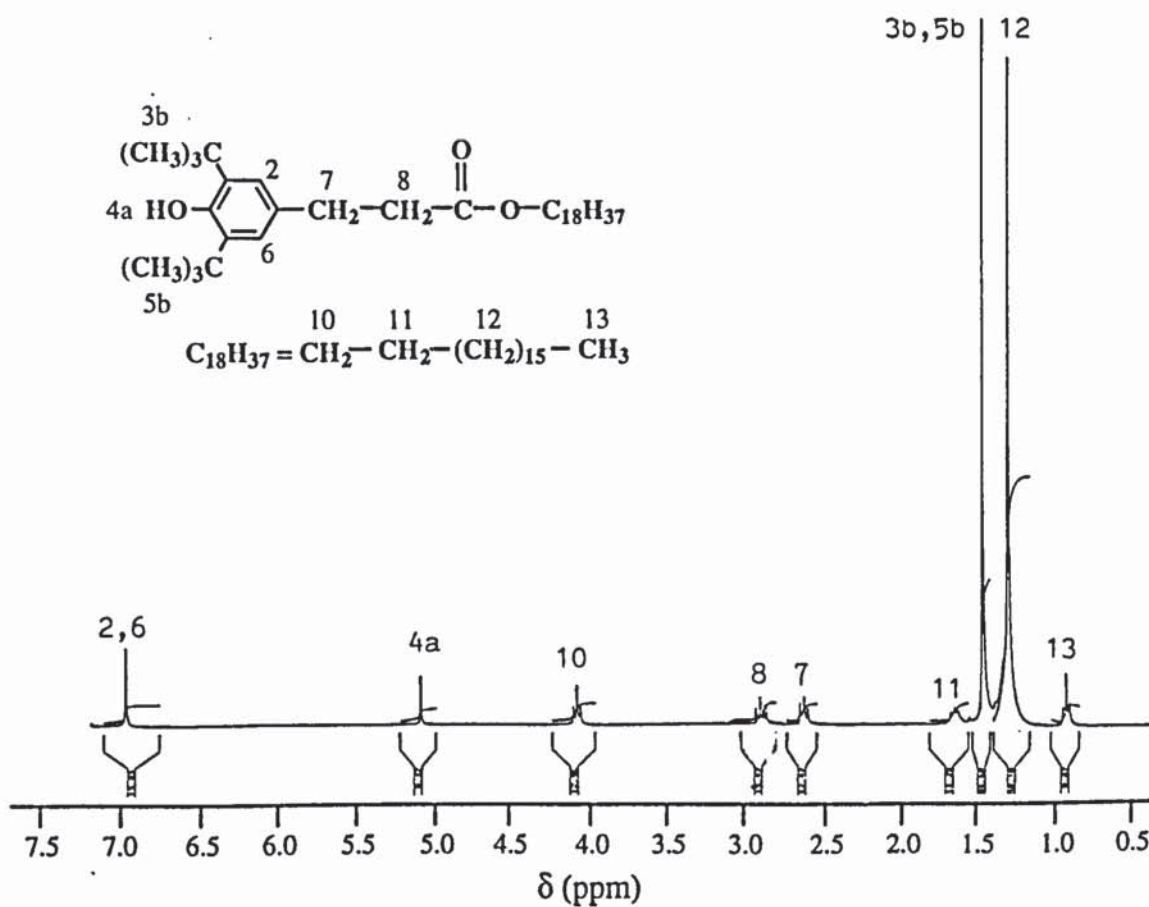


Figure 2.4.c: ^1H -NMR spectrum of Irg 1076 in CDCl_3 , at 300MHz (see table 2.8)

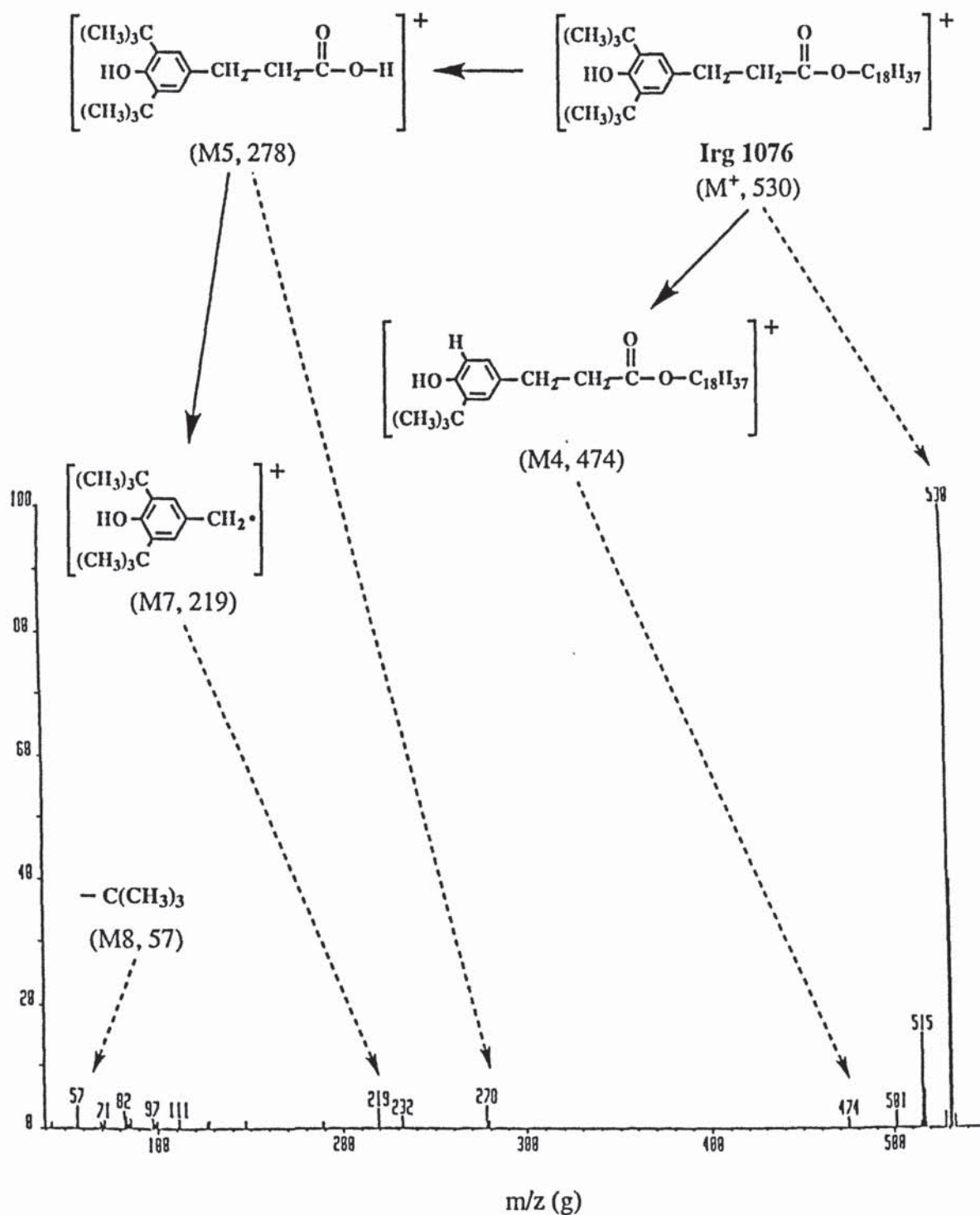


Figure 2.4.d: EI-MS spectrum of Irg 1076 in chloroform (see table 2.9)

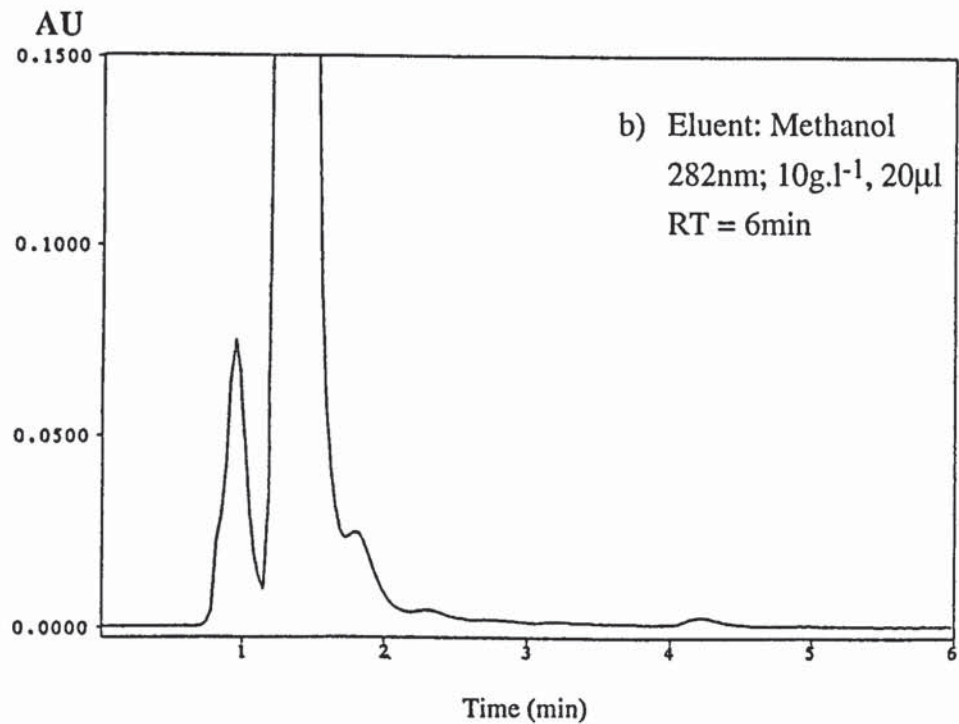
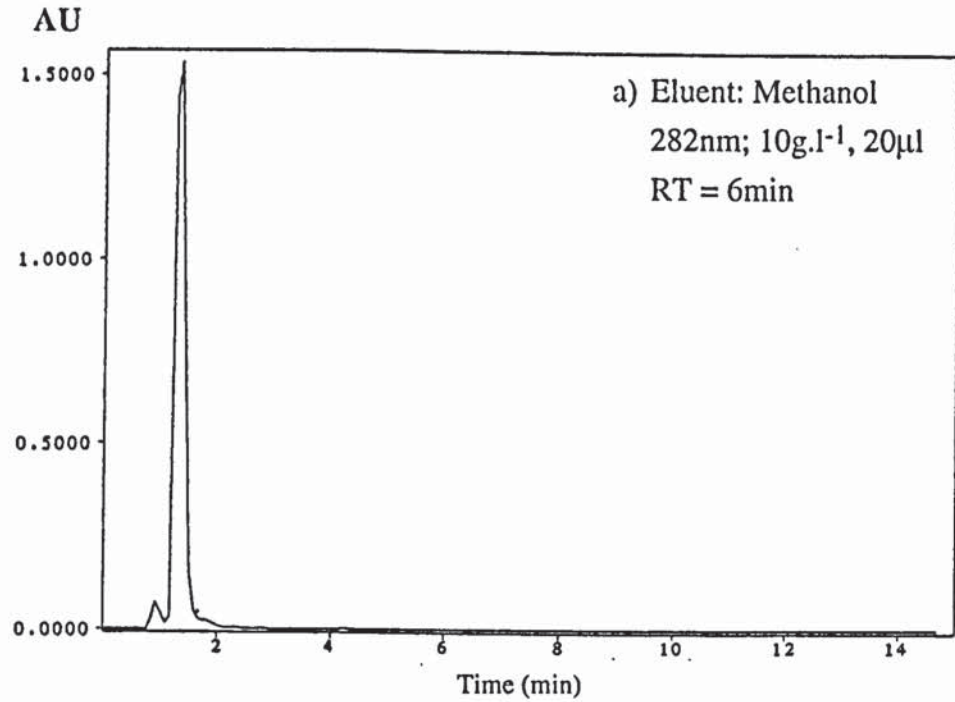
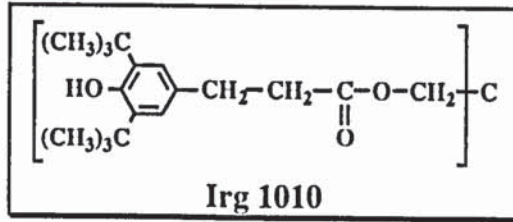


Figure 2.5.a: HPLC chromatograms of Irg 1010 in dichloromethane, at 282nm
Instruments: Philips PU4100 liquid chromatograph and PU4120 diode array detector
Column: Zorbax ODS (4.6mm x 25cm); Flow rate: 1ml.min⁻¹

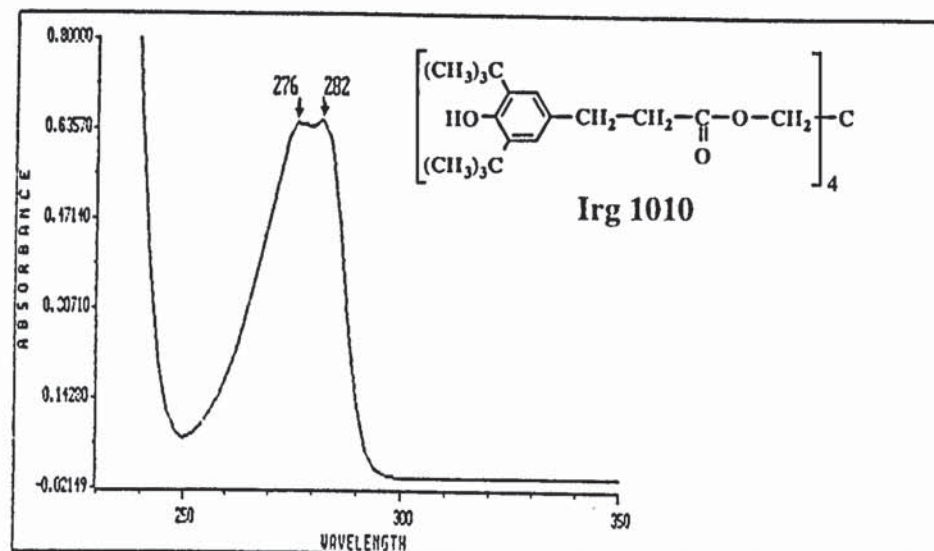


Figure 2.5.b: UV spectrum of Irg 1010 in dichloromethane, 1g.l⁻¹ (see table 2.7)

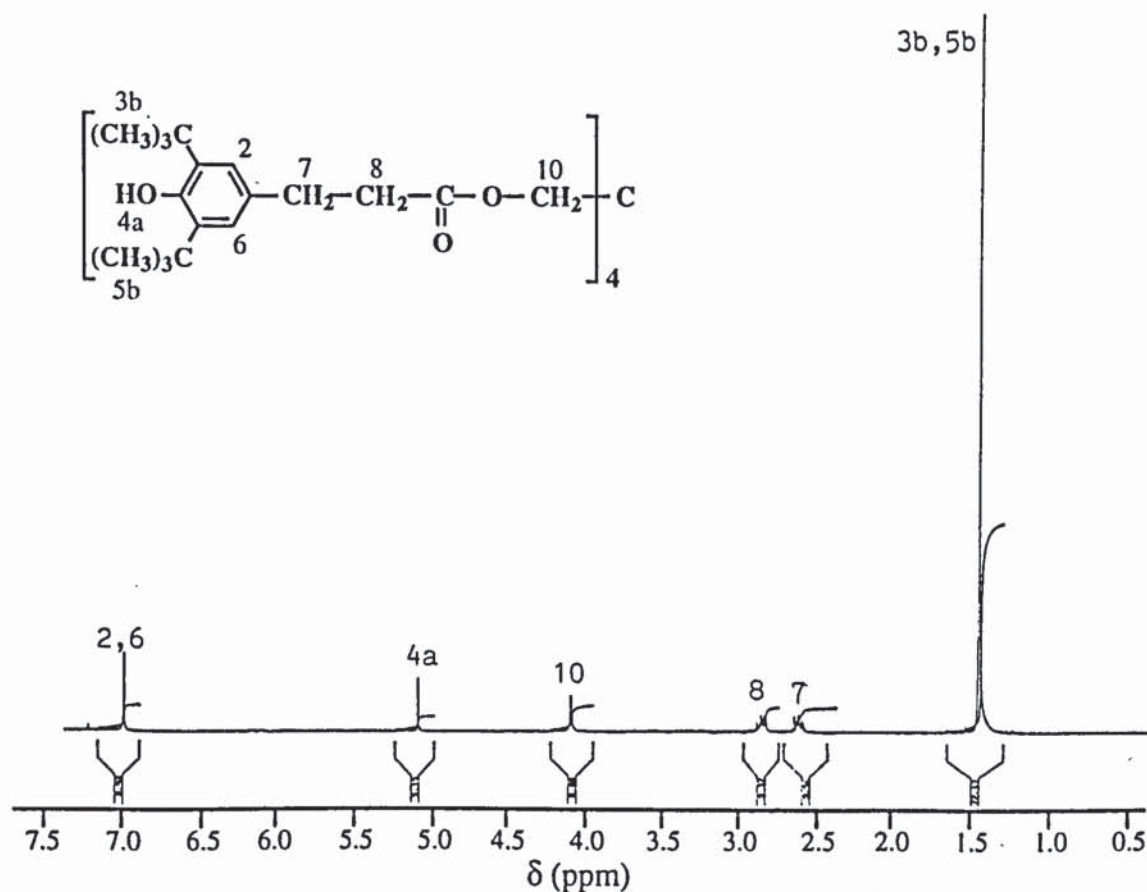


Figure 2.5.c: ¹H-NMR spectrum of Irg 1010 in CDCl₃, at 300MHz (see table 2.8)

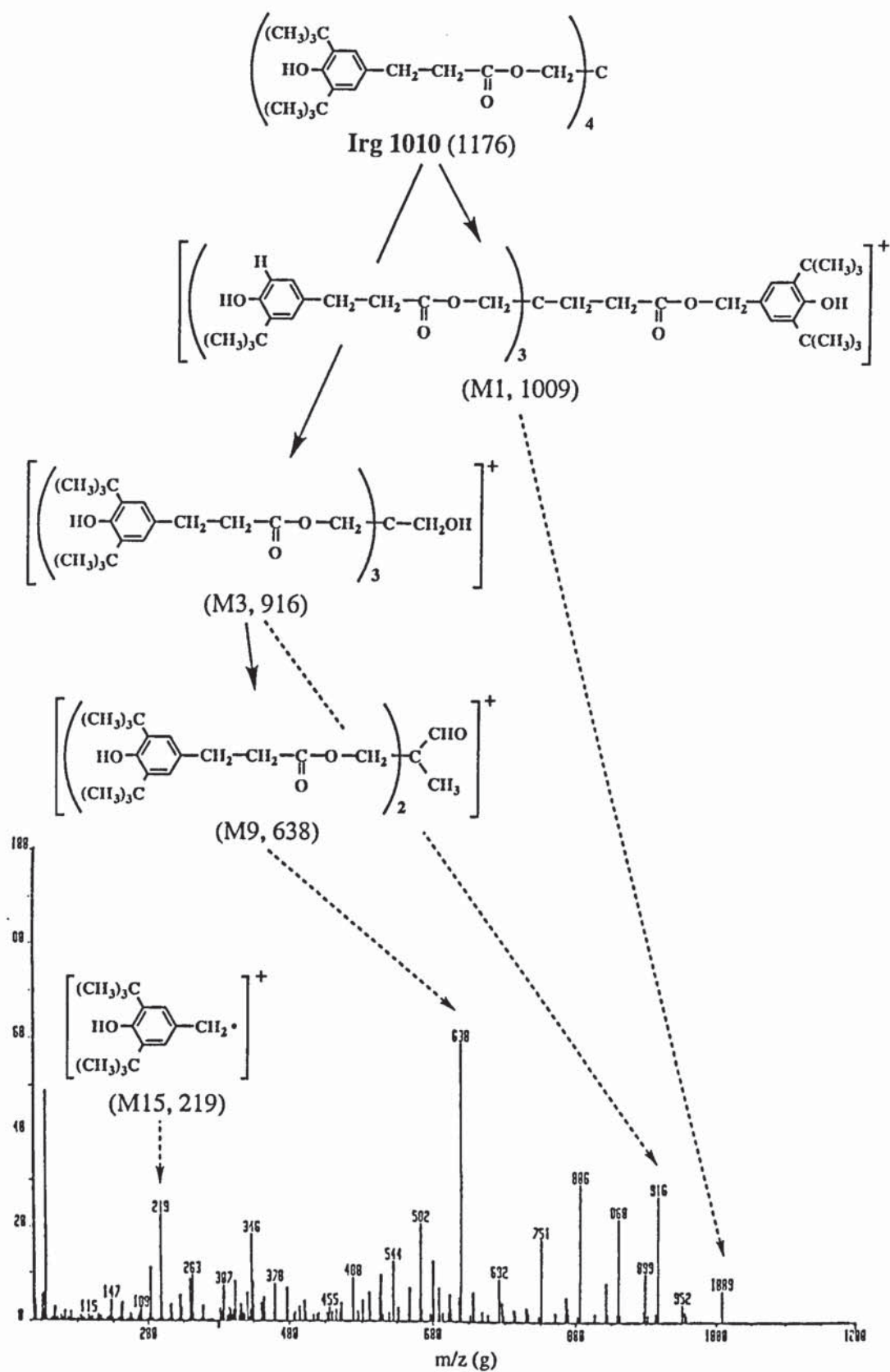


Figure 2.5.d: EI-MS spectrum of Irg 1010 in chloroform (see table 2.10)

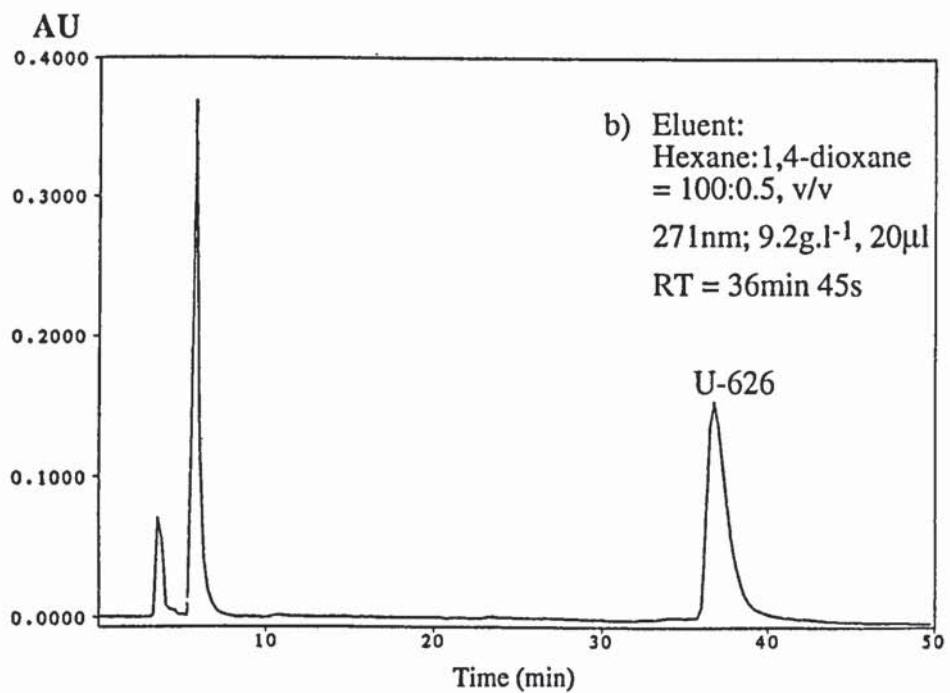
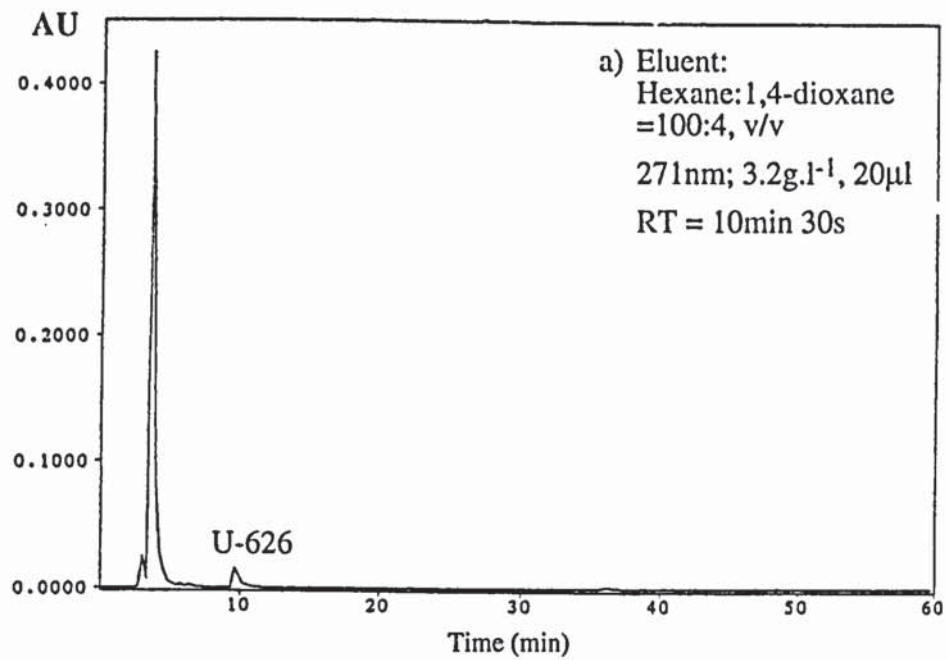
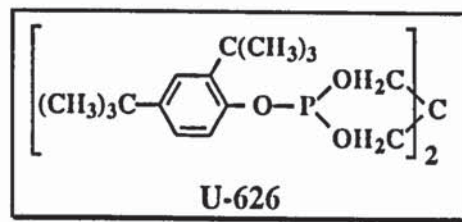


Figure 2.6.a: HPLC chromatograms of U-626 in hexane, at 271nm
Instruments: Philips PU4100 liquid chromatograph and PU4120 diode array detector
Column: Zorbax SIL; Flow rate: 1ml.min⁻¹

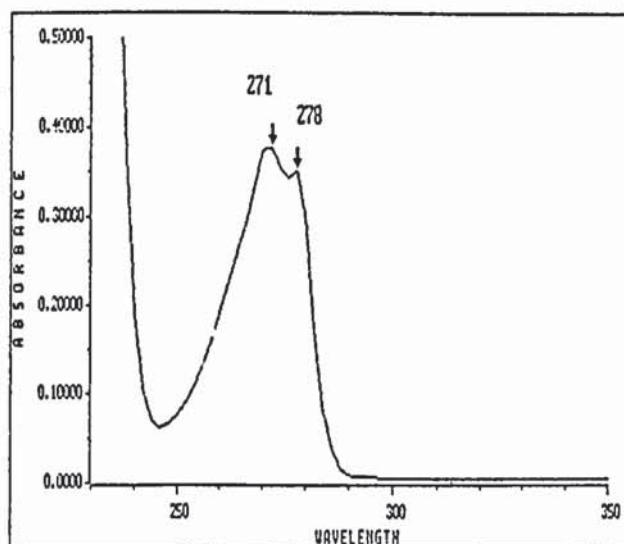
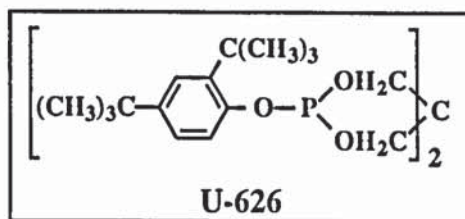


Figure 2.6.b: UV spectrum of U-626 in dichloromethane, 1g.l⁻¹ (see table 2.7)

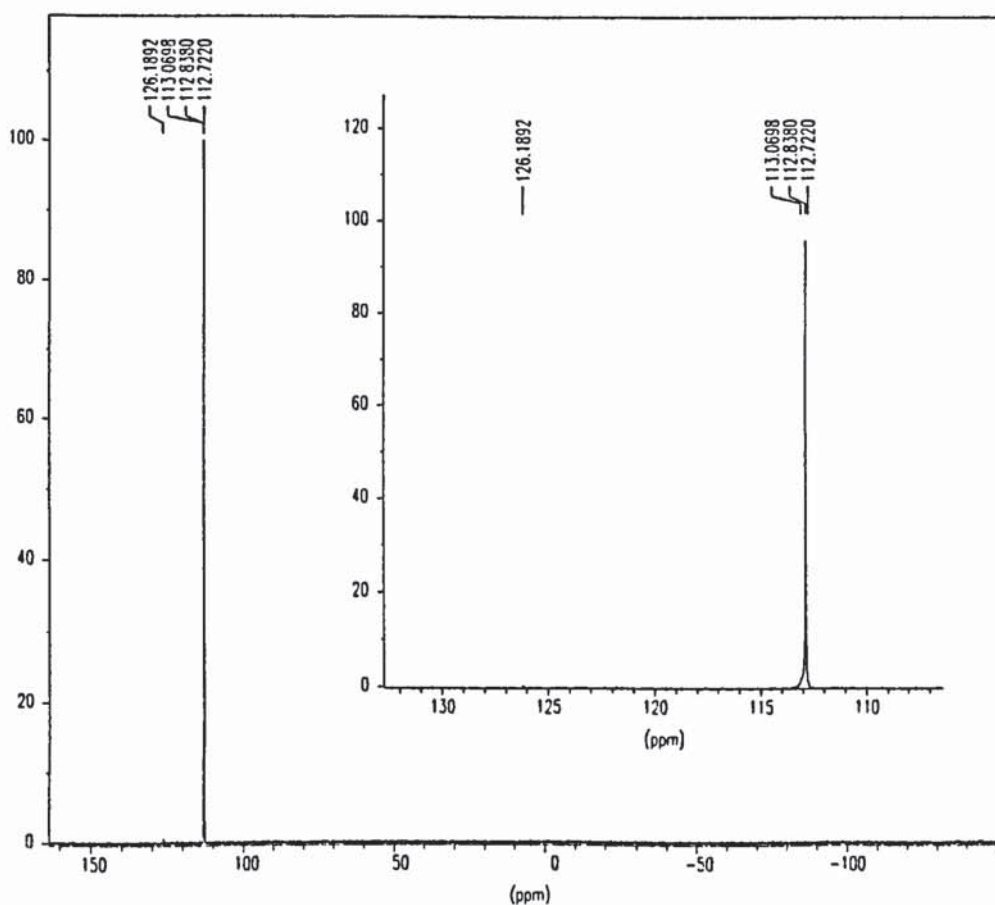


Figure 2.6.c: ³¹P-NMR spectrum of U-626 in CDCl₃, at 120MHz (see table 2.7)

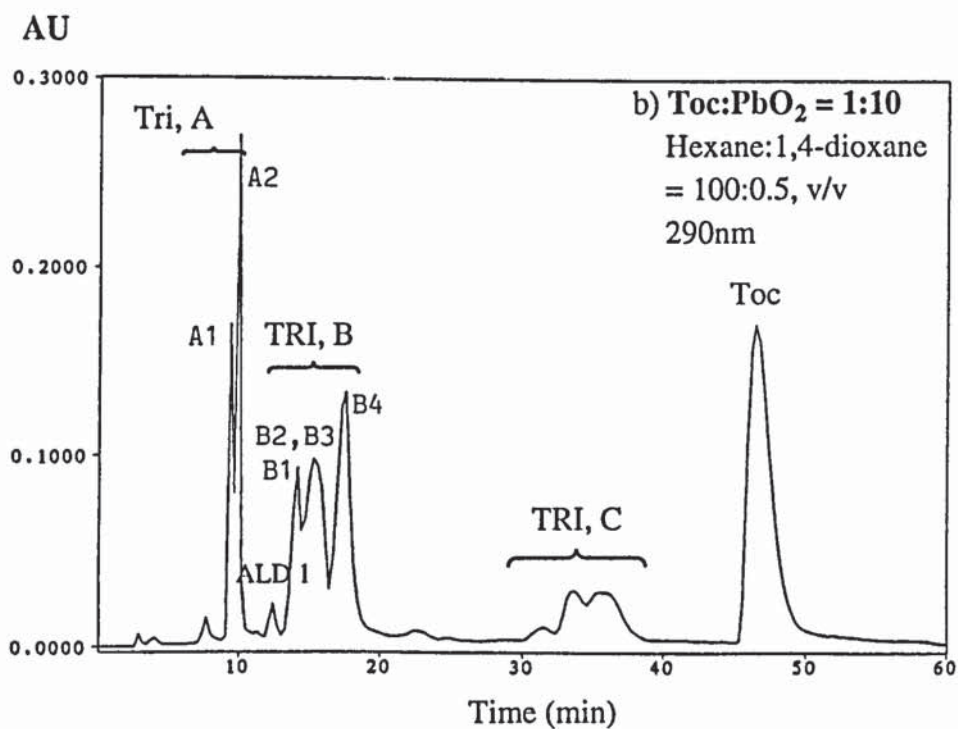
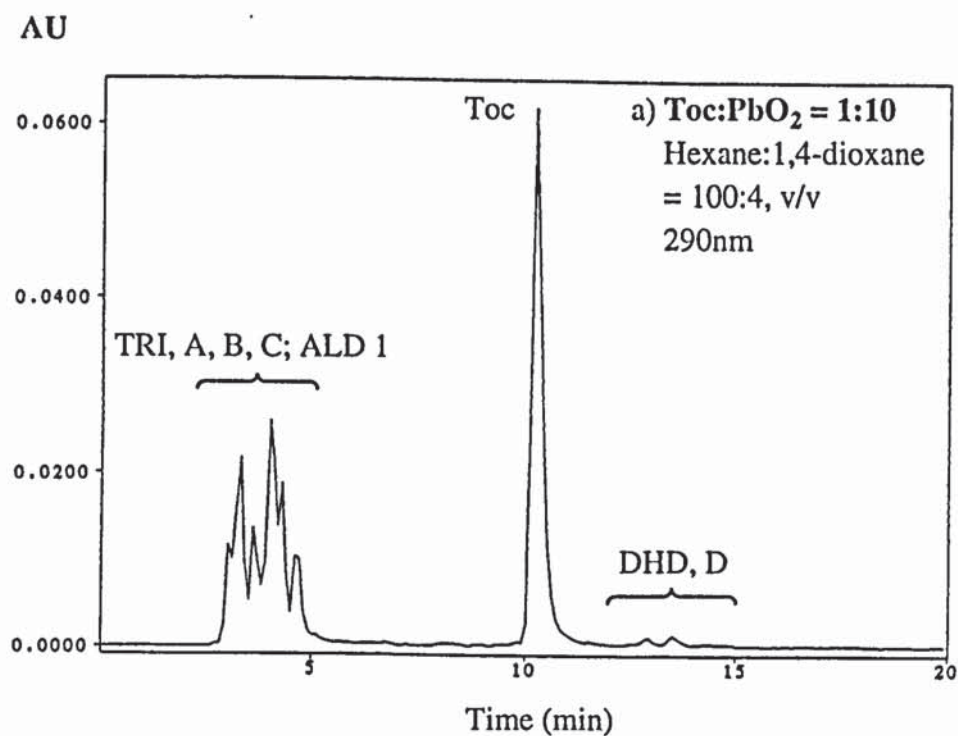


Figure 2.7: HPLC chromatograms of the products of reaction of Toc with PbO₂, ratio 1:10, mol/mol, in Toc:PbO₂, at 290nm (see scheme 2.1)
 Instruments: Philips PU4100 liquid chromatograph and PU4120 diode array detector
 Column: Zorbax SIL (4.6mm x 25cm); Flow rate: 1ml.min⁻¹
 Eluent: hexane:1,4-dioxane = 100:4 (a) and 100:0.5, v/v (b)

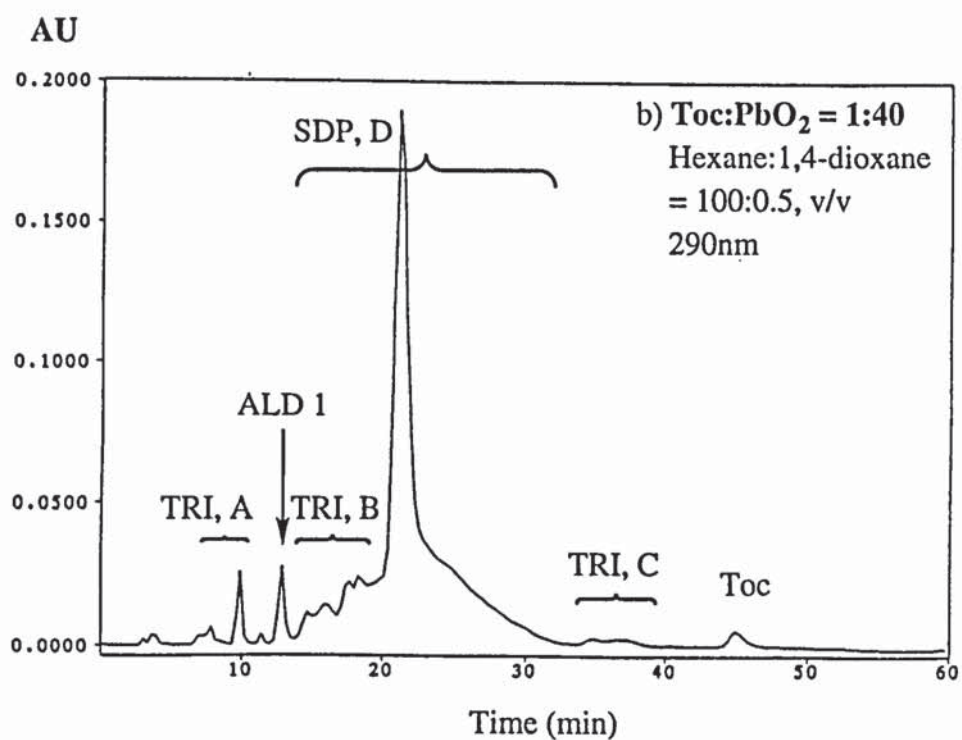
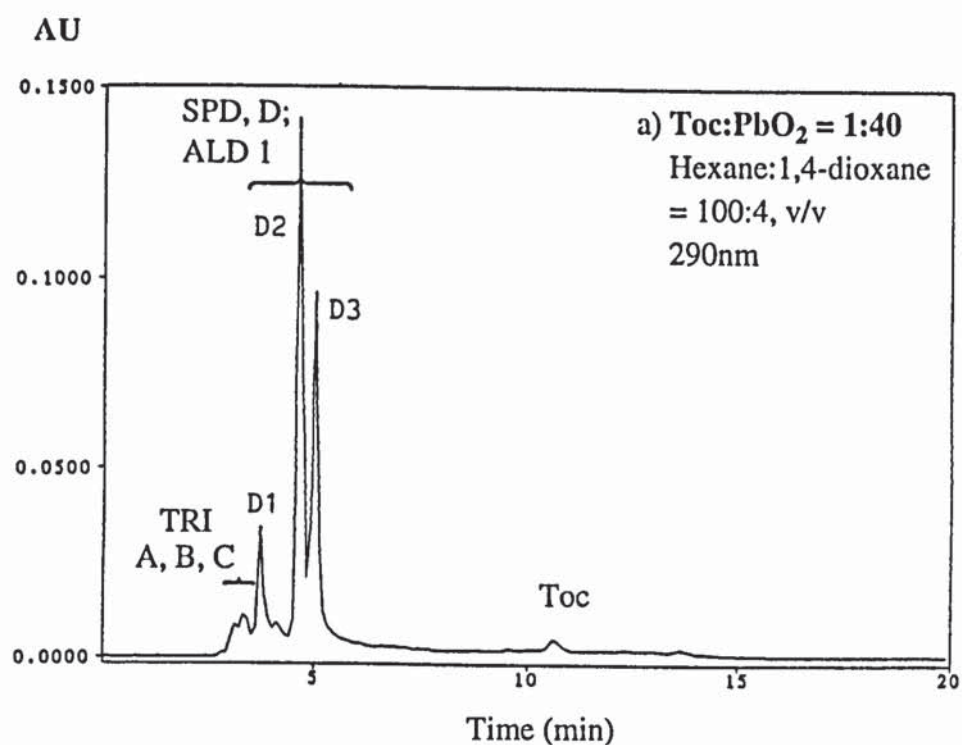


Figure 2.8: HPLC chromatograms of the products of reaction of Toc with PbO₂, ratio 1:40, mol/mol, in Toc:PbO₂, at 290nm (see scheme 2.1)

Instruments: Philips PU4100 liquid chromatograph and PU4120 diode array detector

Column: Zorbax SIL (4.6mm x 25cm); Flow rate: 1ml.min⁻¹

Eluent: hexane:1,4-dioxane = 100:4 (a) and 100:0.5, v/v (b)

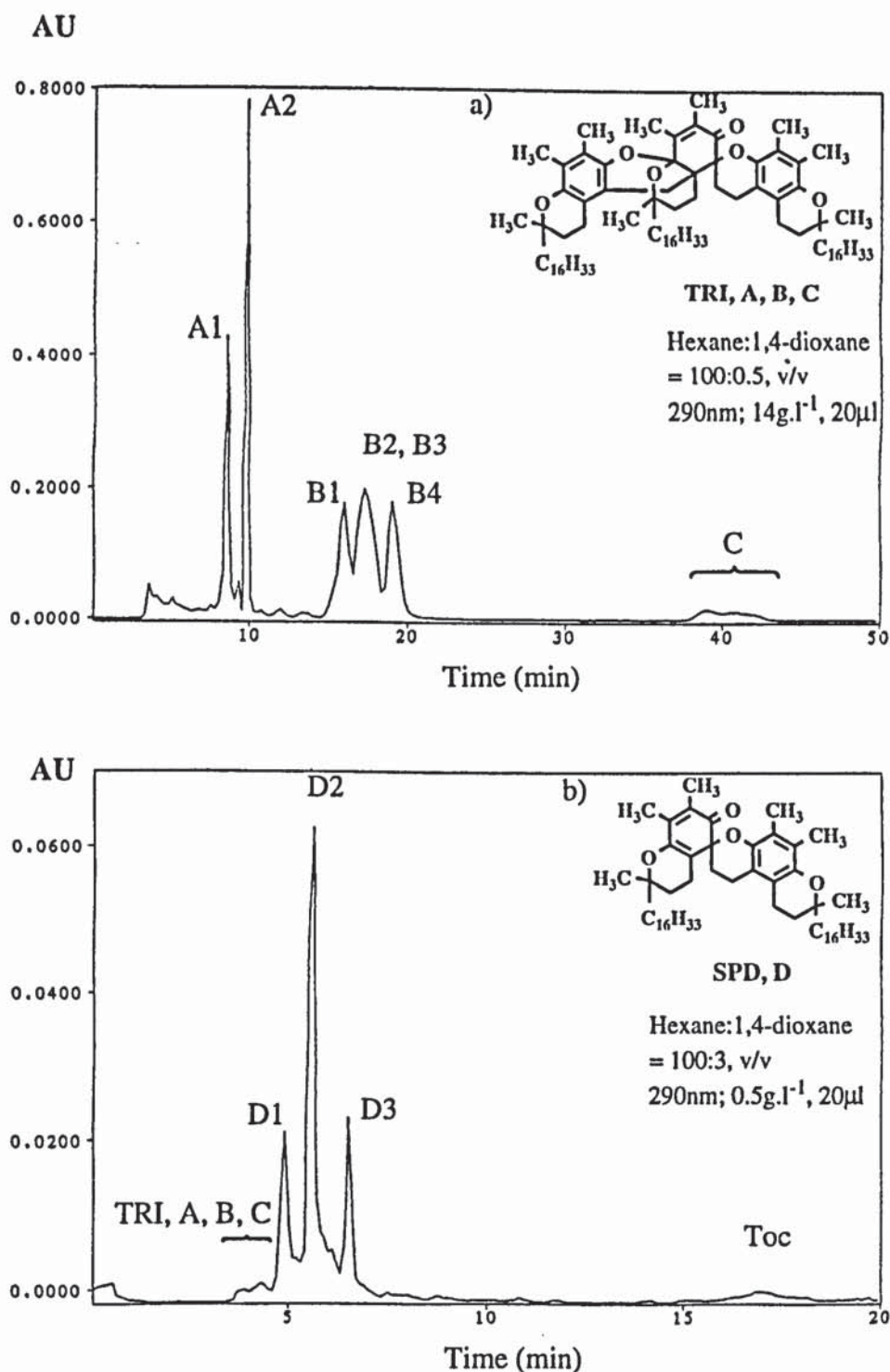


Figure 2.9: HPLC chromatograms of the products isolated by column chromatography of the mixtures of products obtained from the oxidations of Toc with PbO₂, ratios 1:10 (a) and 1:40 (b), mol/mol, in Toc:PbO₂, at 290nm (see scheme 2.1)
 Instruments: Philips PU4100 liquid chromatograph and PU4120 diode array detector
 Column: Zorbax SIL (4.6mm x 25cm); Flow rate: 1ml.min
 Eluent: hexane:1,4-dioxane = 100:0.5 (a) and 100:3, v/v (b)

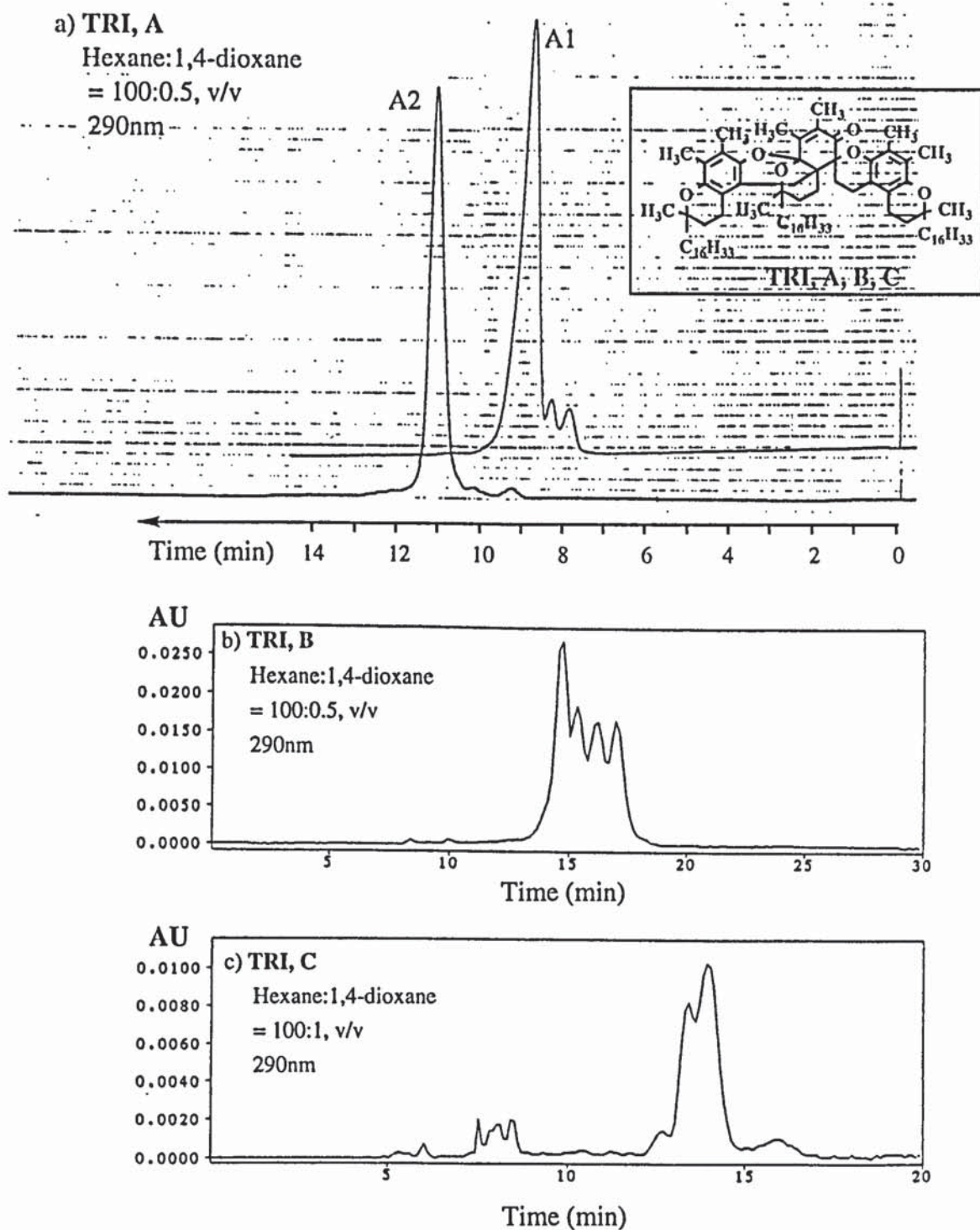


Figure 2.10: HPLC chromatograms of TRI A1, A2, B and C, isolated by semi-preparative HPLC of the mixture of TRI, A, B, C obtained by CC of the products of reaction of Toc with PbO_2 , ratio 1:10 in Toc: PbO_2 (see scheme 2.1)
Instruments: a) Gilson 305 piston pump and variable Dynamax UV-1 variable wavelength absorbance detector; b) and c) Philips PU4100 liquid chromatograph and PU4120 diode array detector
Column: Zorbax SIL (4.6mm x 25cm); Flow rate: $1\text{ml}\cdot\text{min}^{-1}$
Eluent: hexane:1,4-dioxane = 100:0.5 (a, b) and 100:1, v/v (c)

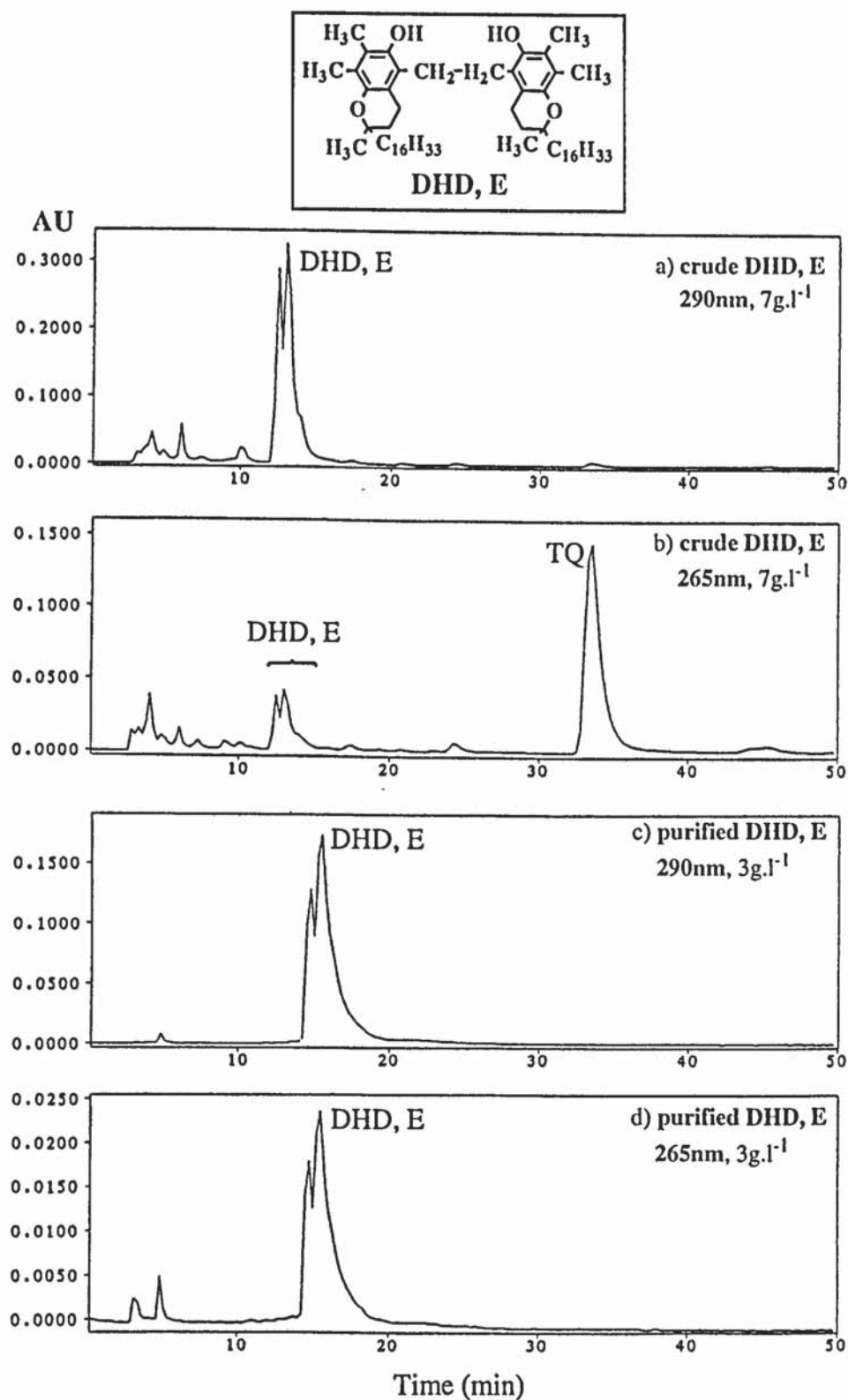


Figure 2.11: HPLC chromatograms of the products of reaction of SPD, D with LiAlH_4 , before and after purification by semi-preparative HPLC of the main DHD, D product (see scheme 2.2)

Instruments: Philips PU4100 liquid chromatograph and PU4120 diode array detector; Column: Zorbax SIL (4.6mm x 25cm); Flow rate: 1ml.min^{-1}
 Eluent: Hexane:1,4-dioxane = 100:4, v/v

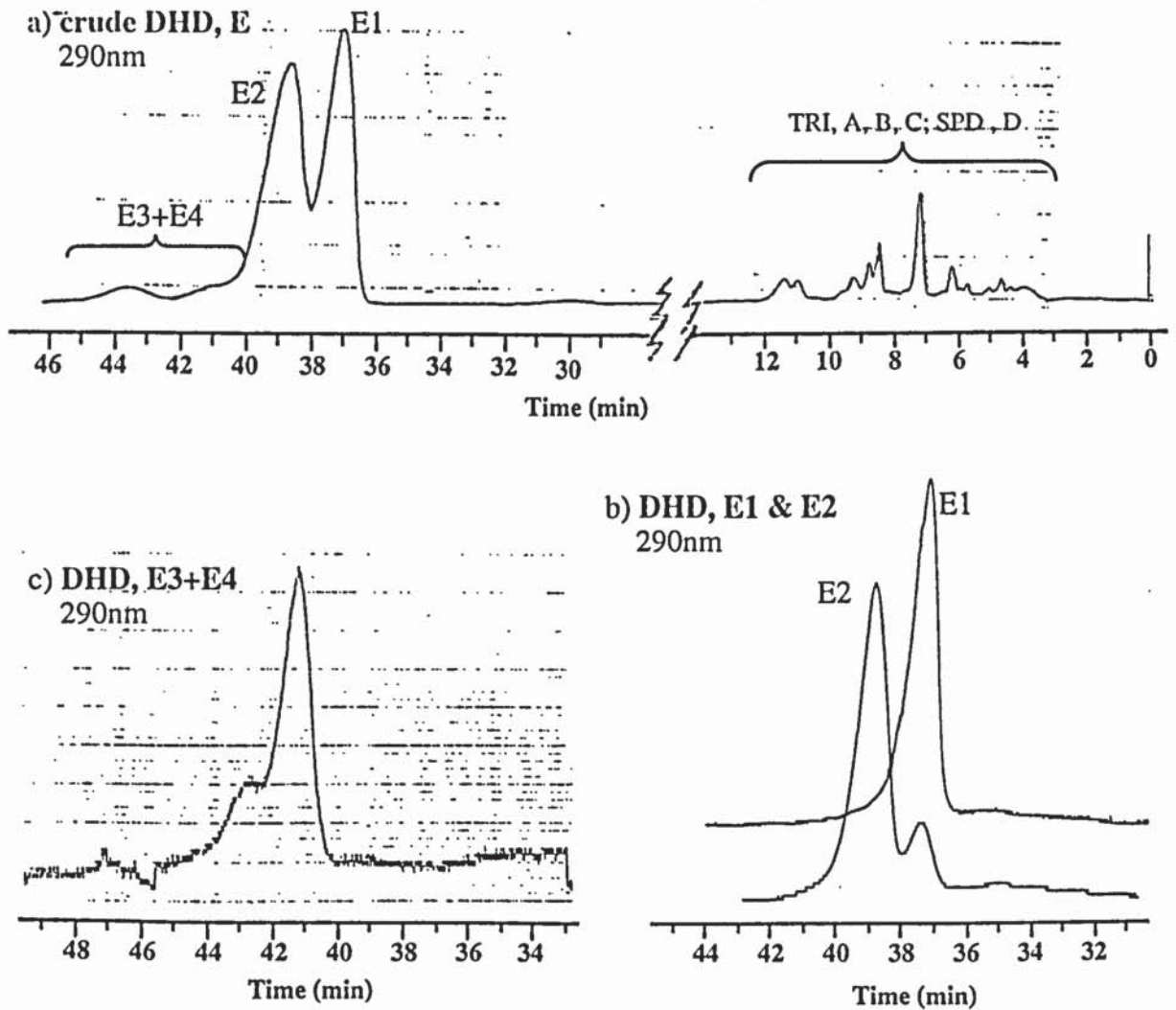
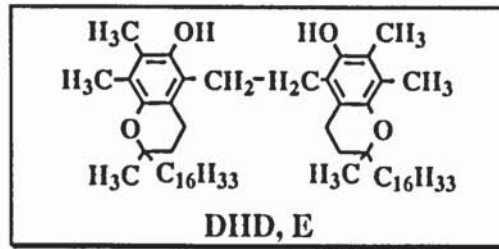


Figure 2.12: Typical HPLC chromatogram of DHD, E in hexane (a) (obtained from the reaction of SPD, D with LiAlH_4 , see scheme 2.2) during the isolation of DHD E1, E2 (b) and E3+E4 (c), at 290nm

Instruments: Gilson 305 piston pump and Dynamax UV-1 variable wavelength absorbance detector

Column: Zorbax SIL (4.6mm x 25cm); Flow rate: $1\text{ml}\cdot\text{min}^{-1}$

Eluent: hexane:1,4-dioxane = 100:2, v/v

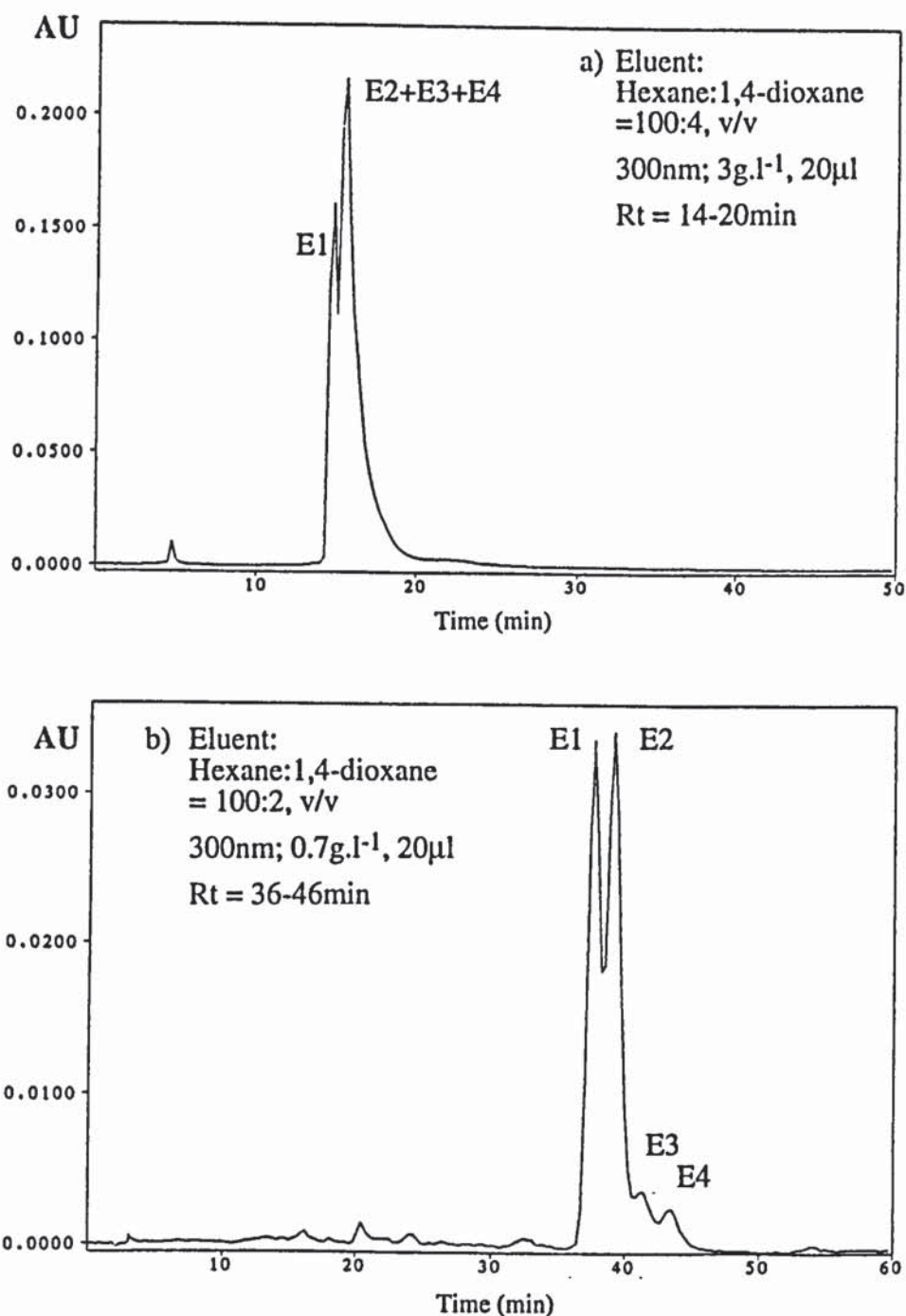
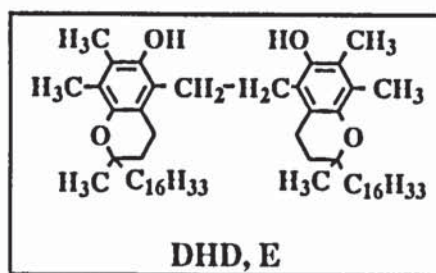


Figure 2.13.a: HPLC chromatograms of synthesised DHD, E in hexane (see scheme 2.2)
Instruments: Philips PU4100 liquid chromatograph and PU4120 diode array detector
Column: Zorbax SIL (4.6mm x 25cm); Flow rate: 1ml.min⁻¹

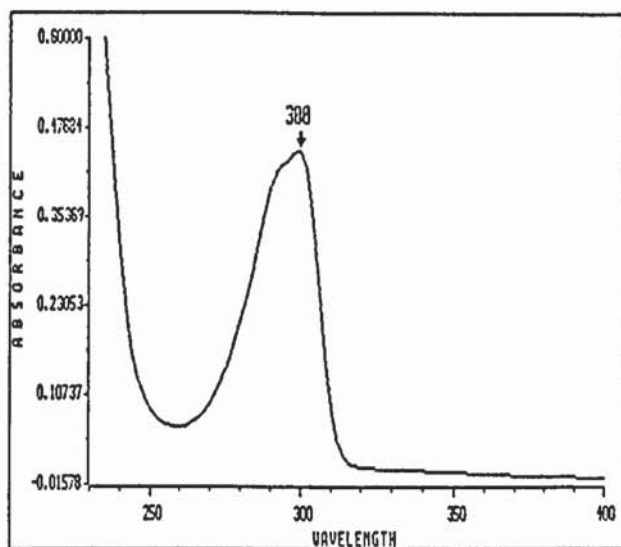
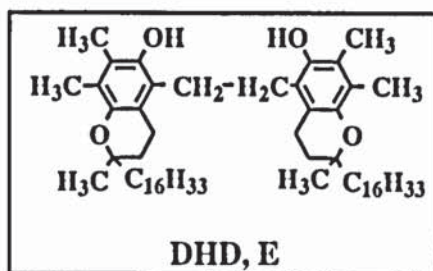


Figure 2.13.b: UV spectrum of synthesised DHD, E in hexane, 0.48g.l^{-1}
(see scheme 2.2 and table 2.16)

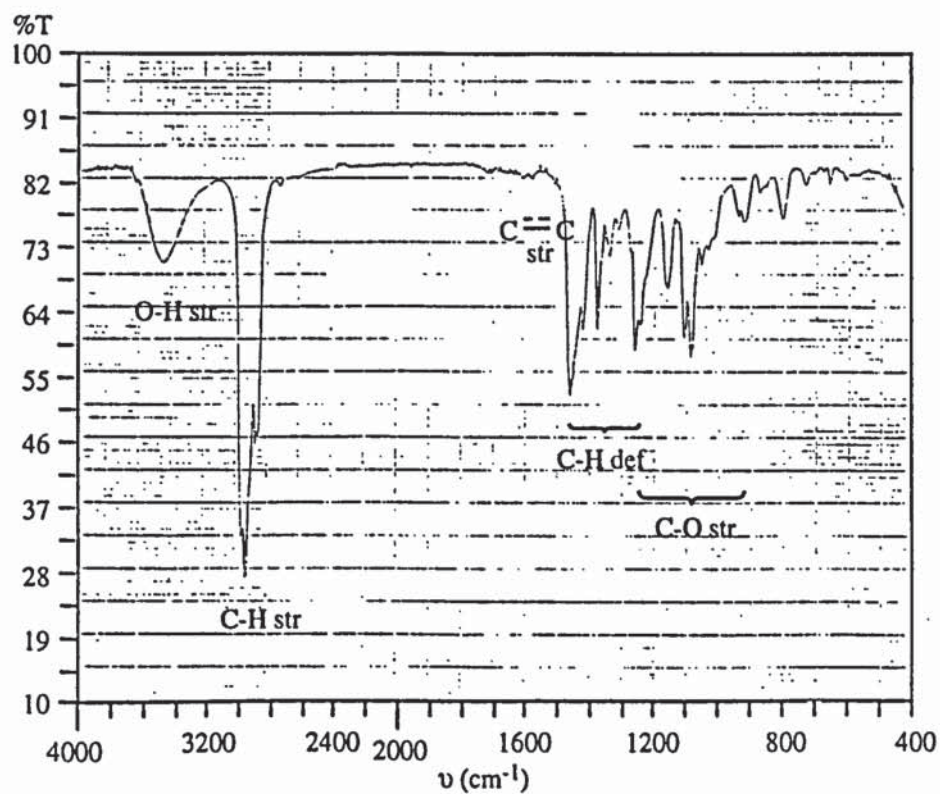
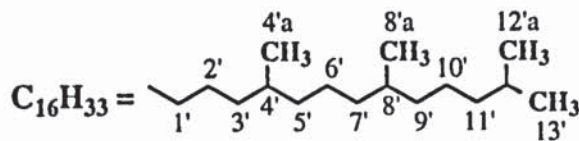
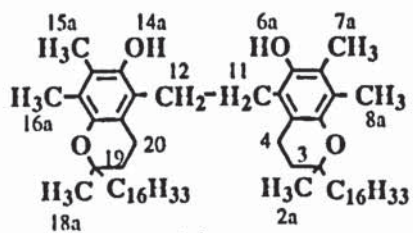


Figure 2.13.c: IR spectrum of synthesised DHD, E, KBr windows
(see scheme 2.2 and table 2.16)



DHD, E1

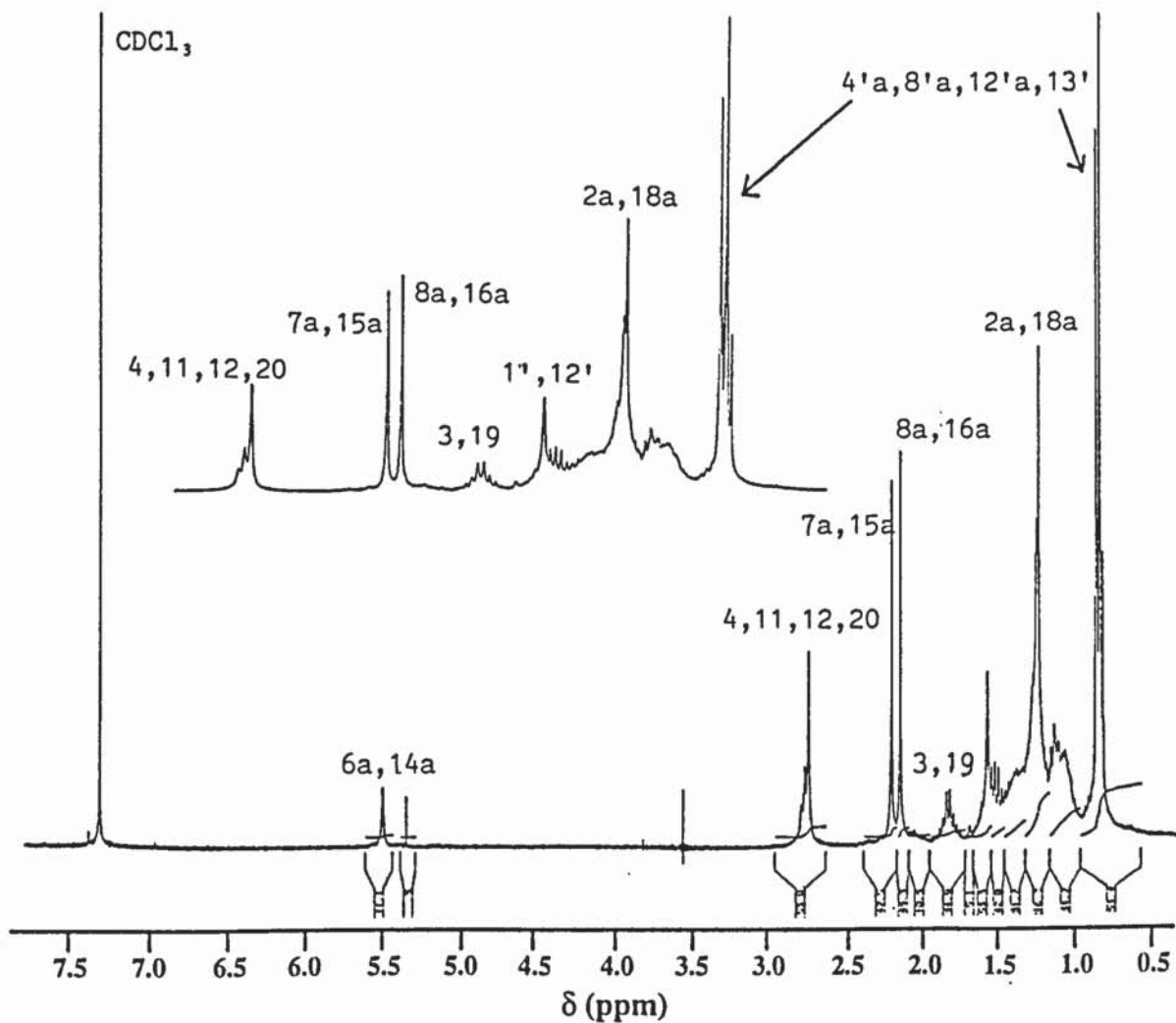
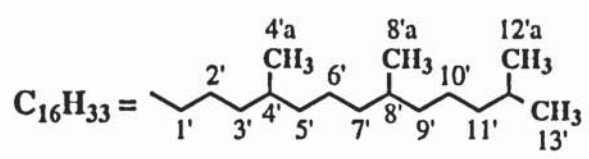
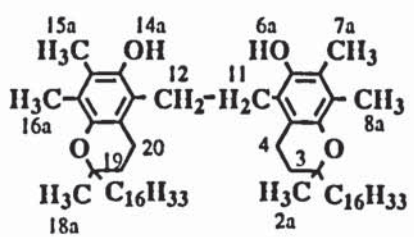


Figure 2.13.d: ^1H -NMR spectrum of DHD, E1, isolated by semi-preparative NP-HPLC from the synthesised DHD, E, in CDCl_3 , at 300MHz (see scheme 2.2 and table 2.17)



DHD, E2

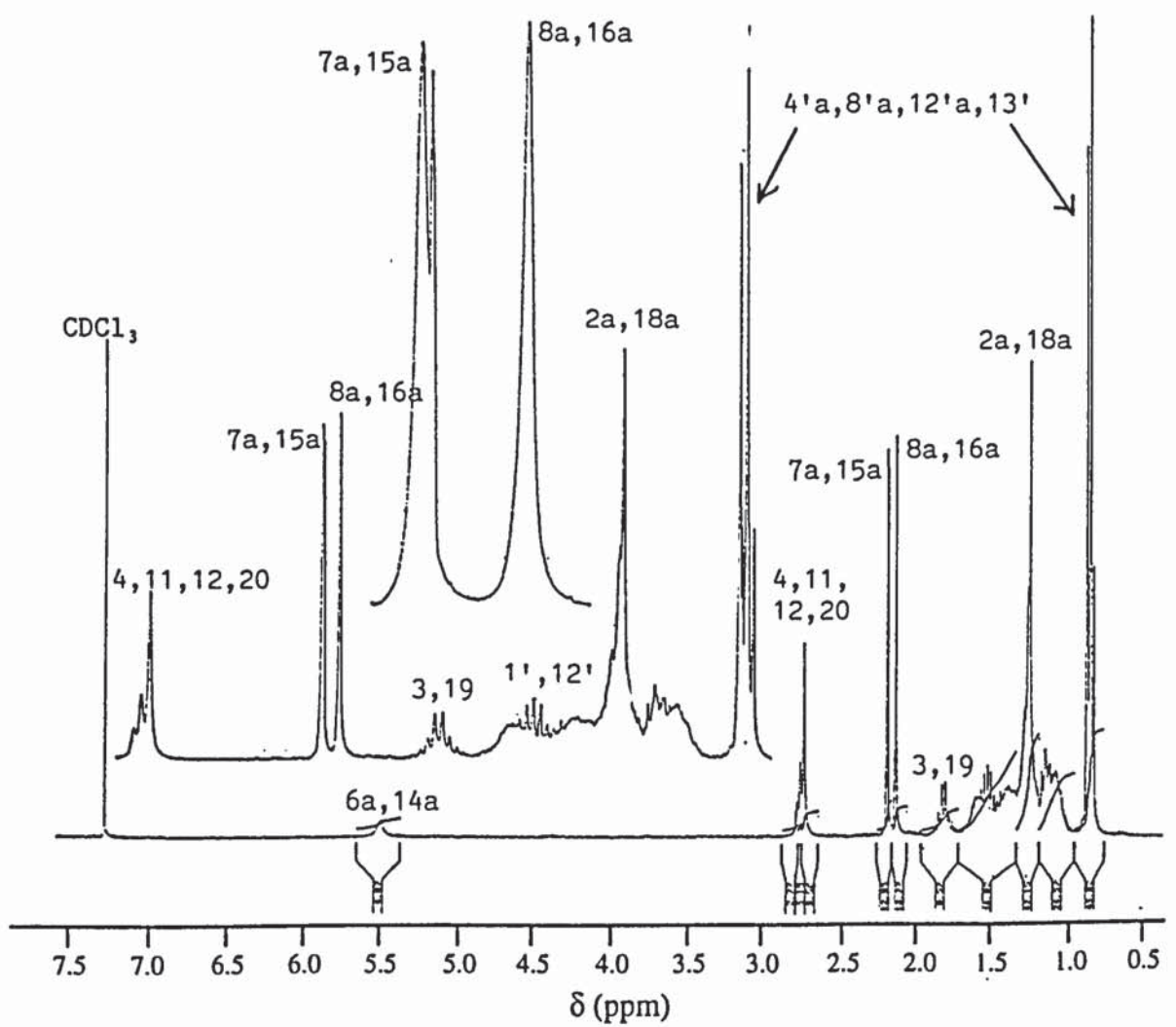


Figure 2.13.e: ¹H-NMR spectrum of DHD, E2, isolated by semi-preparative NP-HPLC from the synthesised DHD, E, in CDCl₃, at 300MHz (see scheme 2.2 and table 2.17)

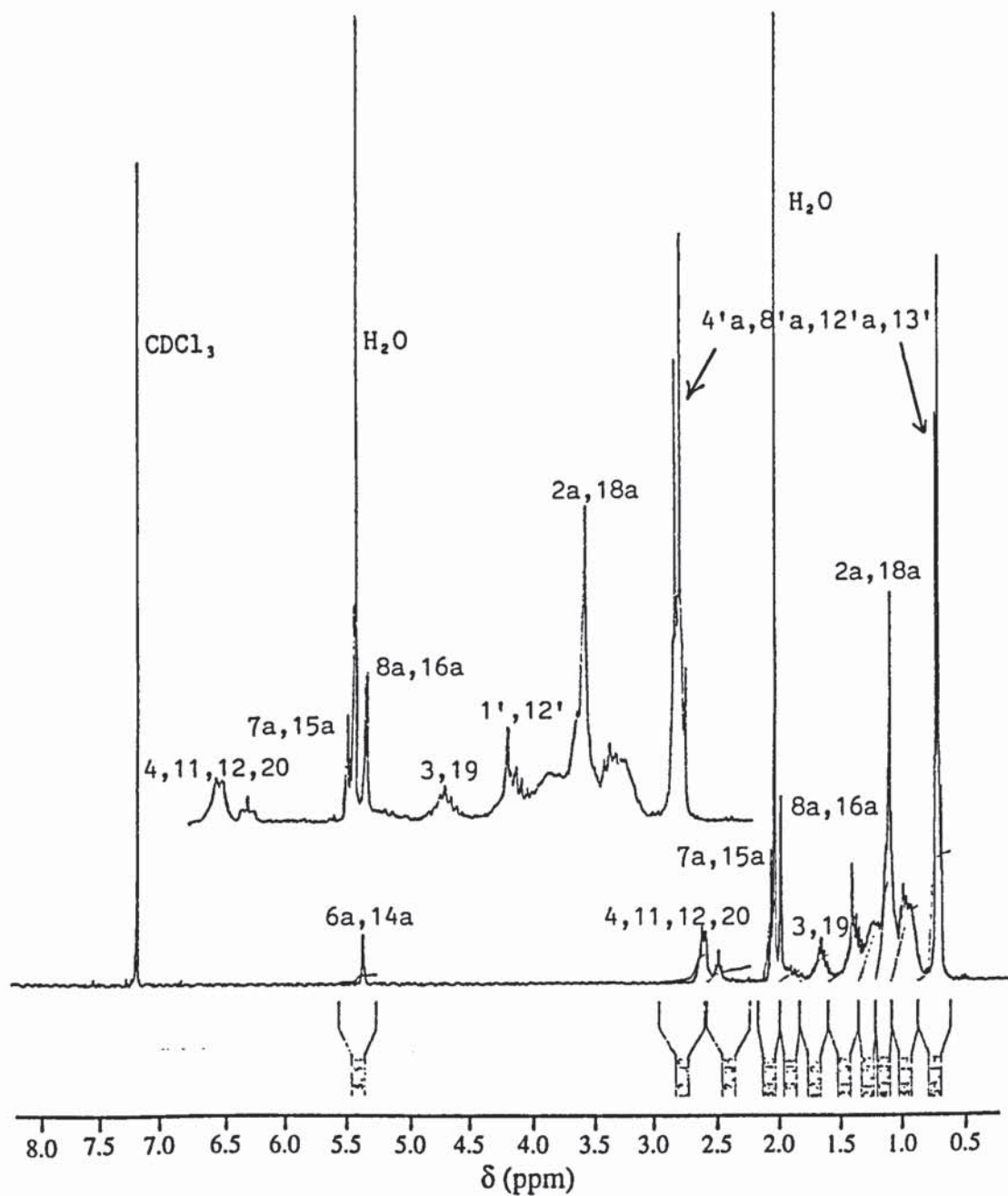
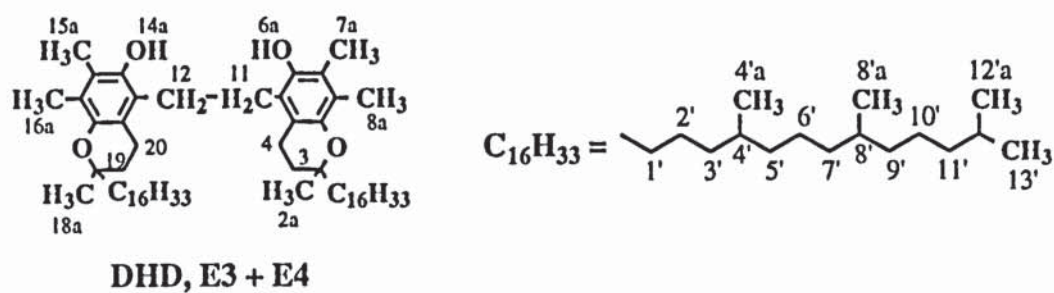


Figure 2.13.f: $^1\text{H-NMR}$ spectrum of DHD, E3 + E4, isolated by semi-preparative NP-HPLC from the synthesised DHD, E, in CDCl_3 , at 300MHz (see scheme 2.2 and table 2.17)

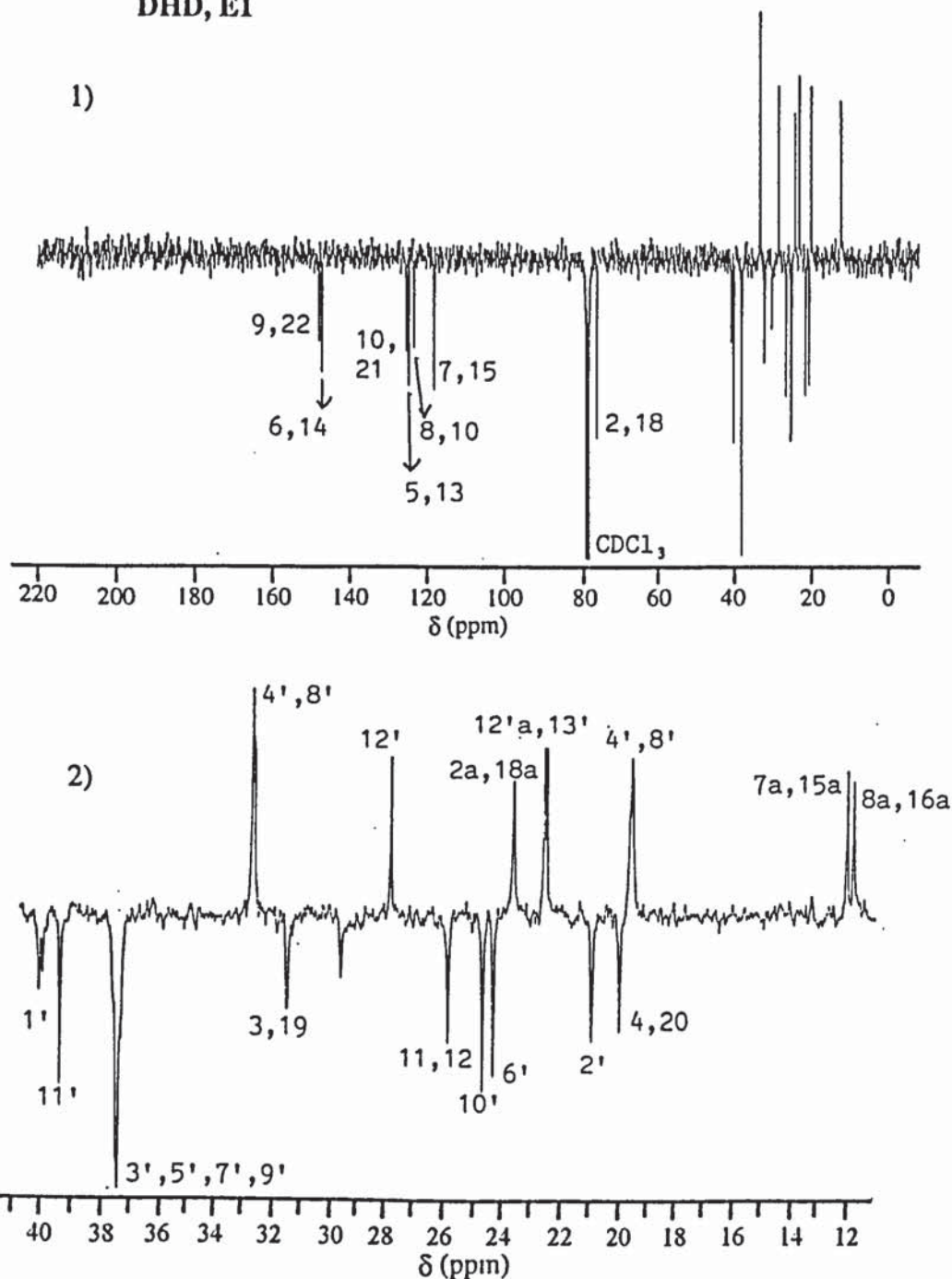
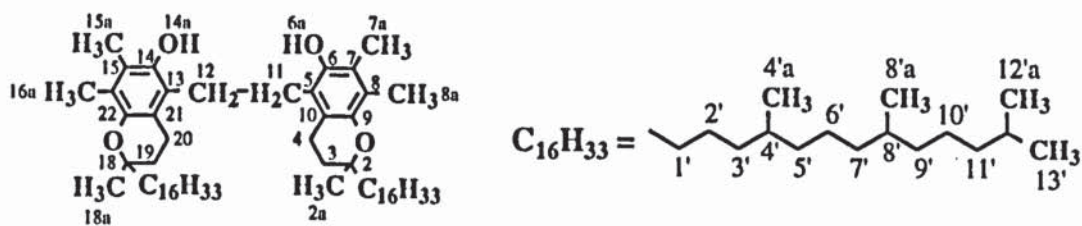


Figure 2.13.g: ^{13}C -NMR spectrum of DHD, E1, isolated by NP-HPLC from the synthesised DHD, E, in CDCl_3 , at 75 MHz (see scheme 2.2 and table 2.19)
 1) region 0-220ppm 2) expanded region 10-41ppm

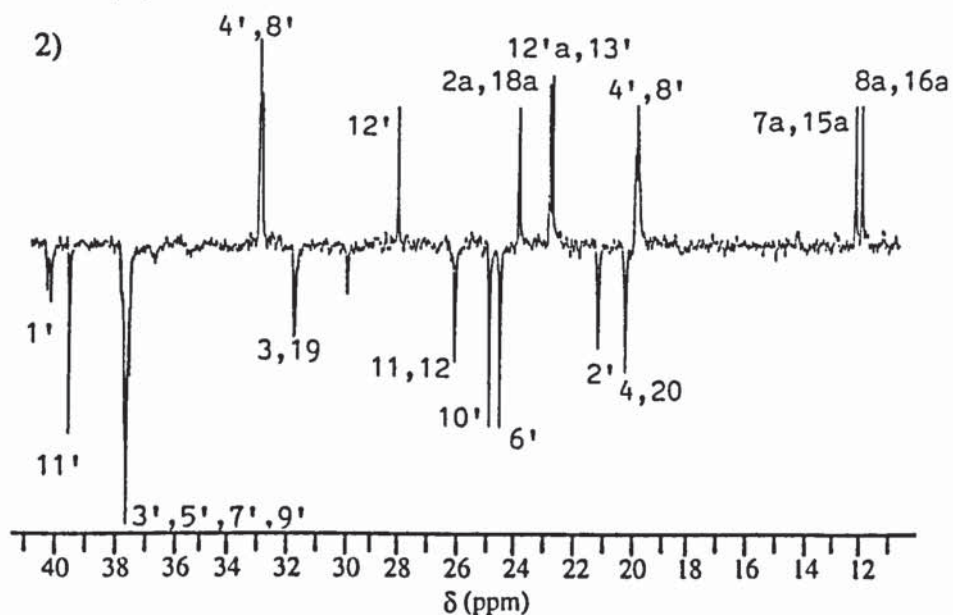
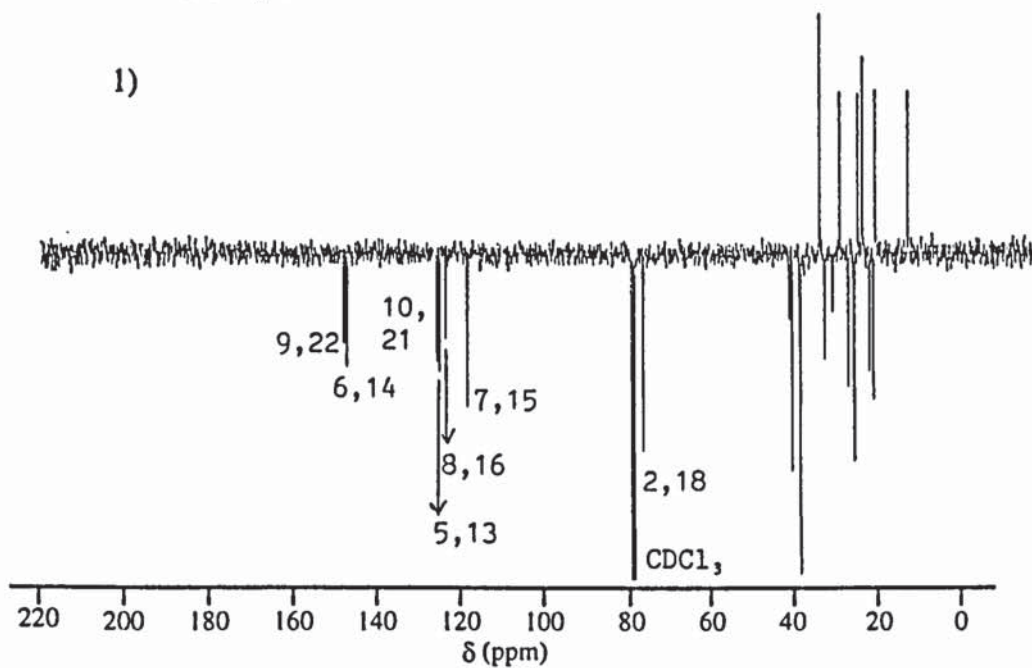
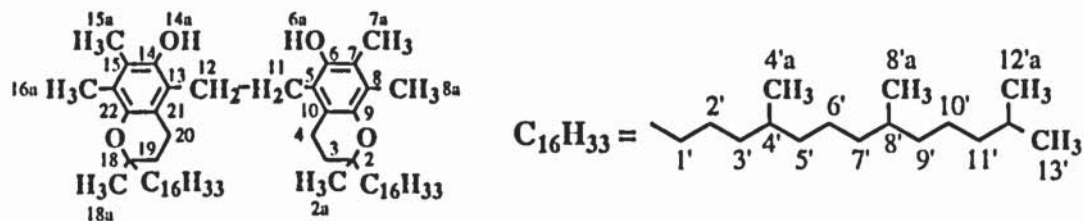


Figure 2.13.h: ^{13}C -NMR spectrum of DHD, E2, isolated by NP-HPLC from the synthesised DHD, E, in CDCl_3 , at 75 MHz (see scheme 2.2 and table 2.19)
 1) region 0-220ppm 2) expanded region 11-41ppm

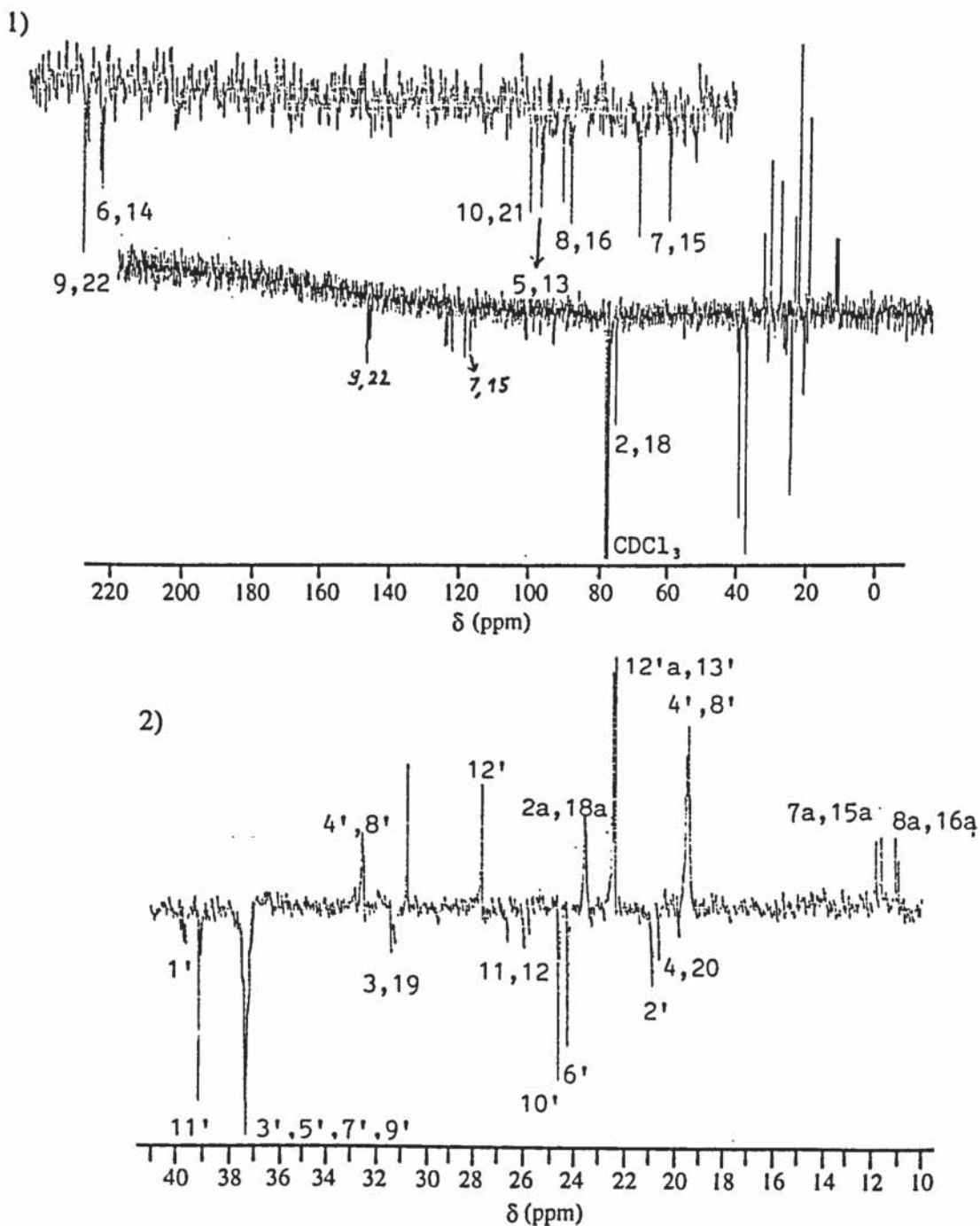
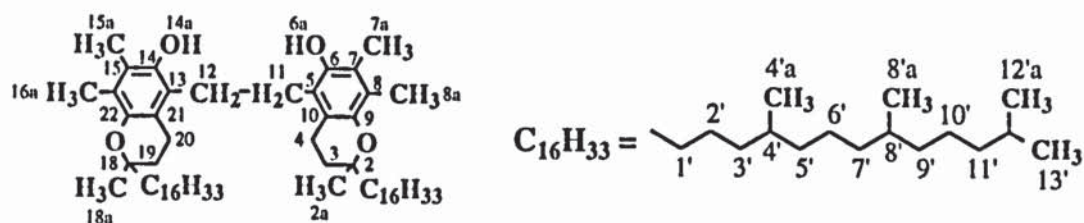


Figure 2.13.i: ^{13}C -NMR spectrum of DHD, E3+E4, isolated by NP-HPLC from the synthesised DHD, E, in CDCl_3 , at 75 MHz (see scheme 2.2 and table 2.19)
 1) region 0-220ppm 2) expanded region 11-41ppm

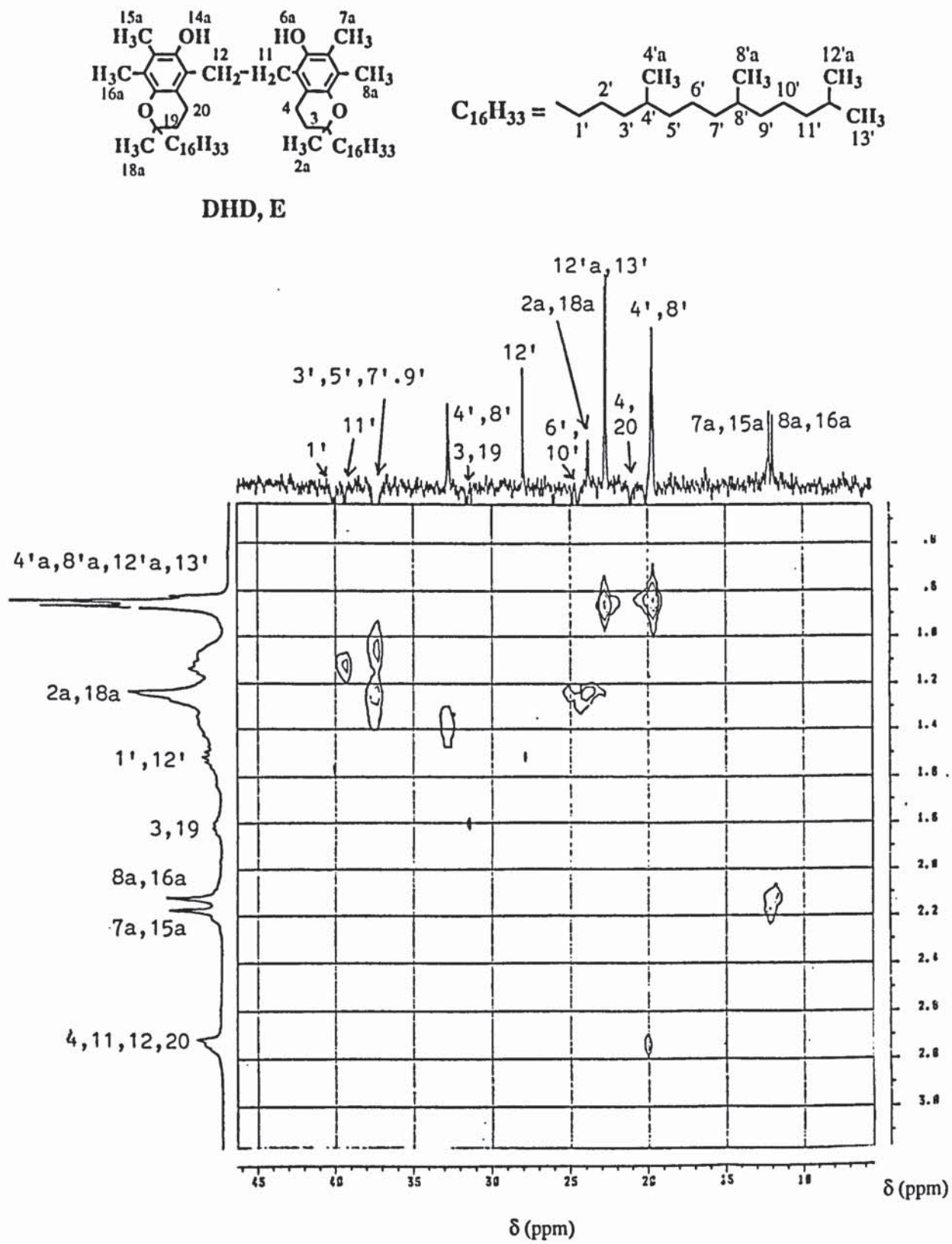


Figure 2.13.j: ¹H, ¹³C-NMR correlation spectrum of synthesised DHD, E, in CDCl₃ (see scheme 2.2)

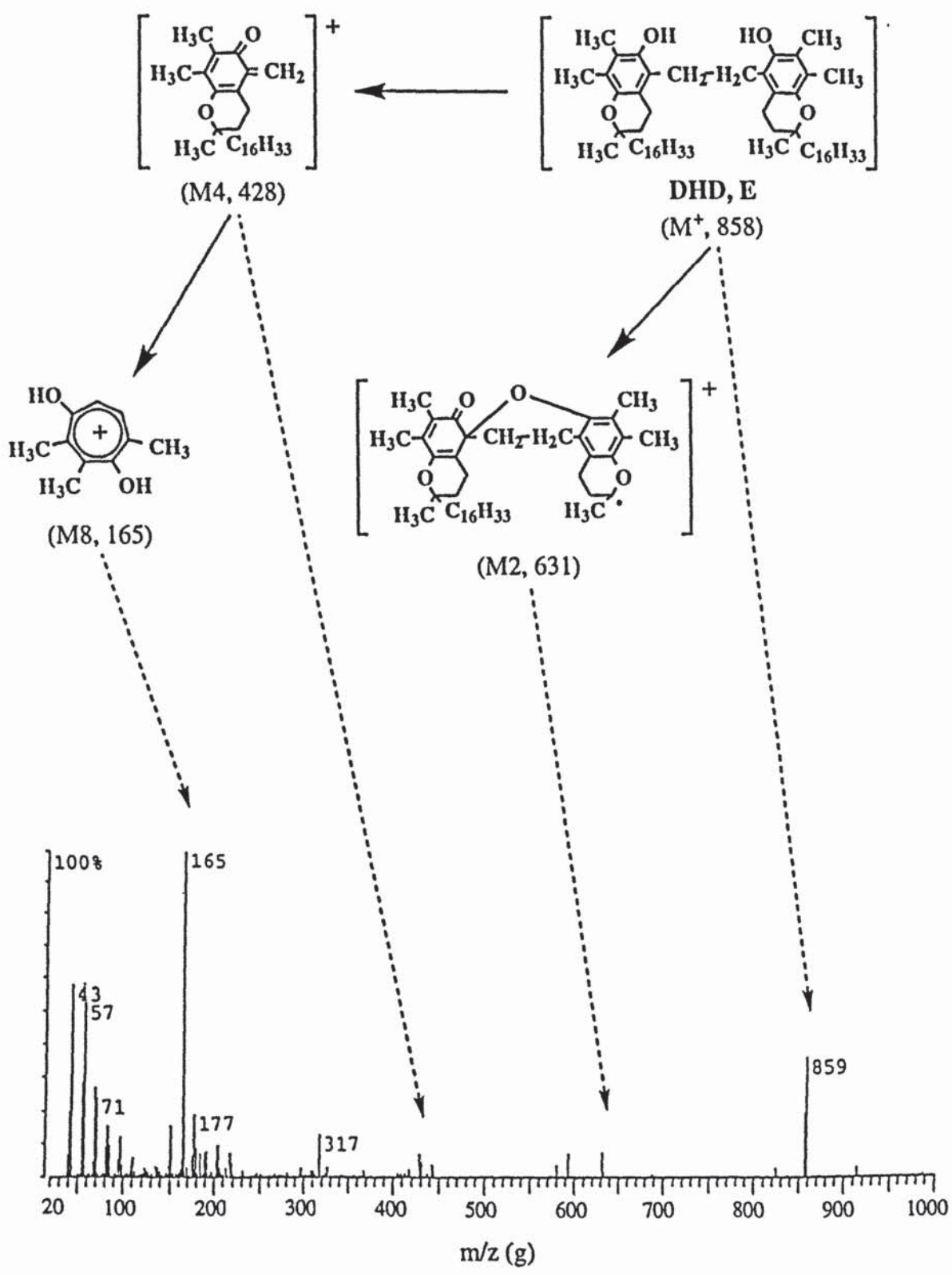


Figure 2.13.k: EI-MS spectrum of synthesised DHD, E in acetate (see scheme 2.2 and table 2.21)

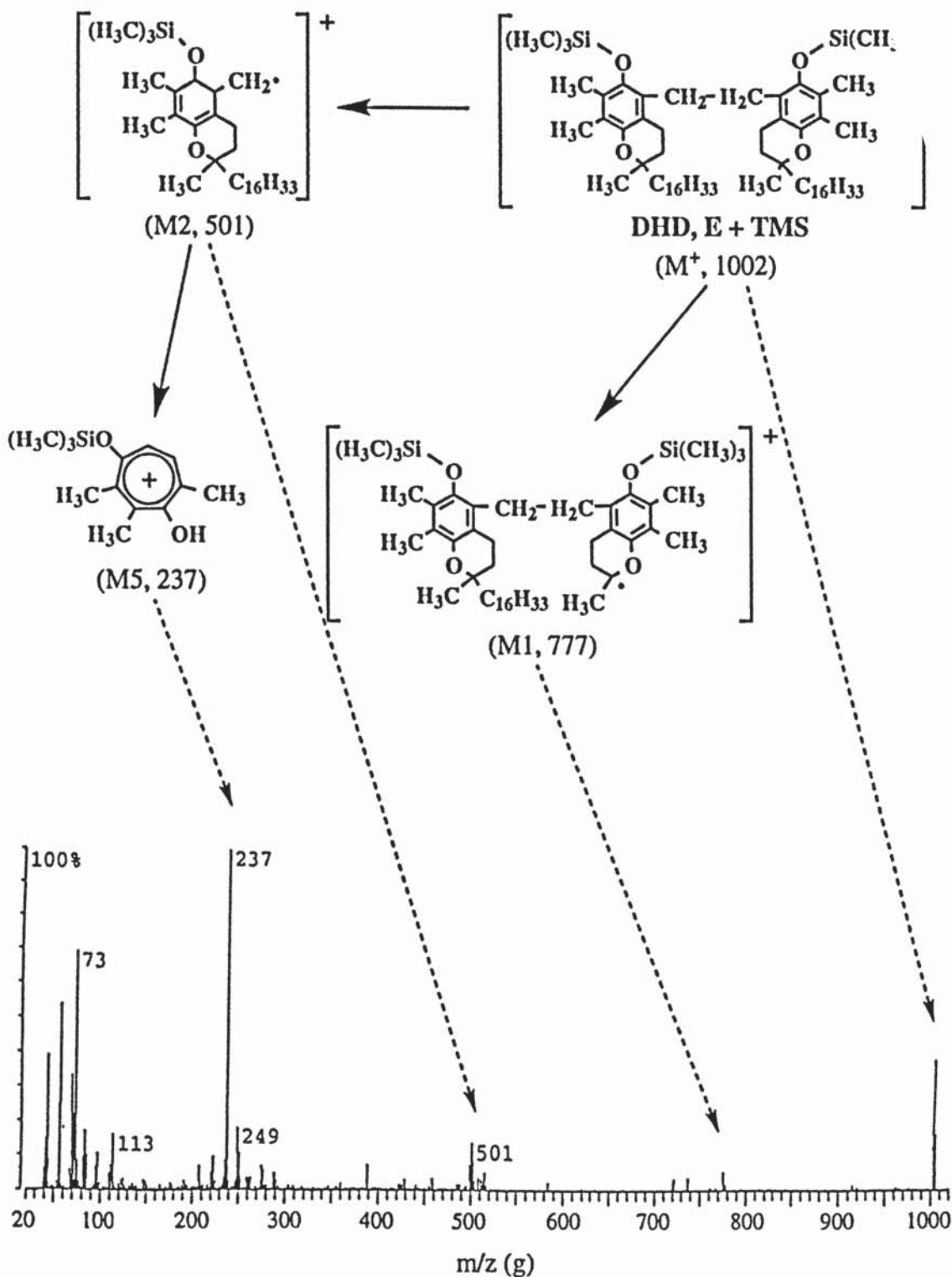


Figure 2.13.1: EI-MS spectrum of synthesised DHD, E in acetate, after silylation with TMS (see scheme 2.2 and table 2.22)

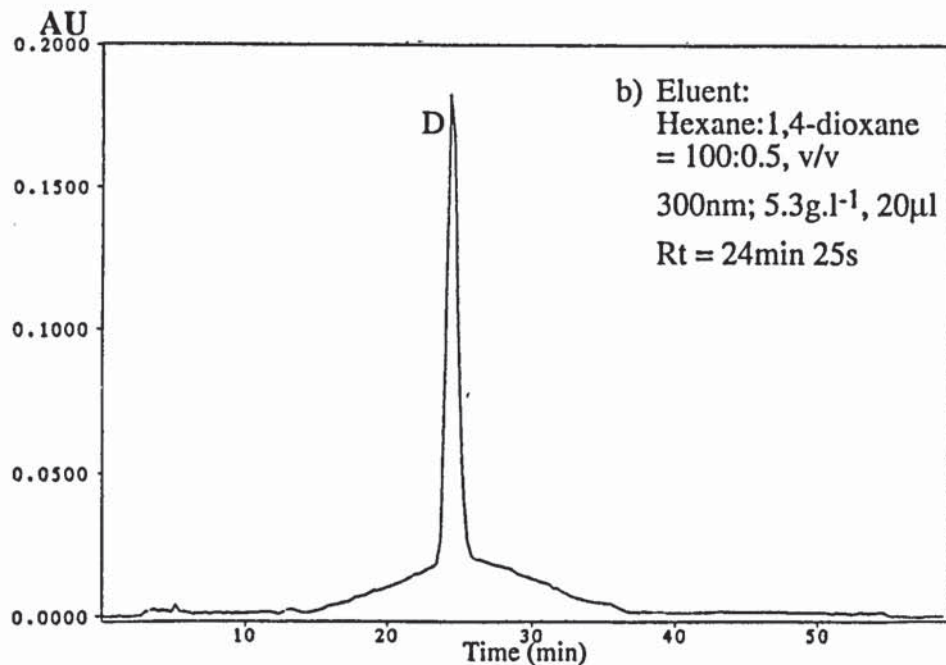
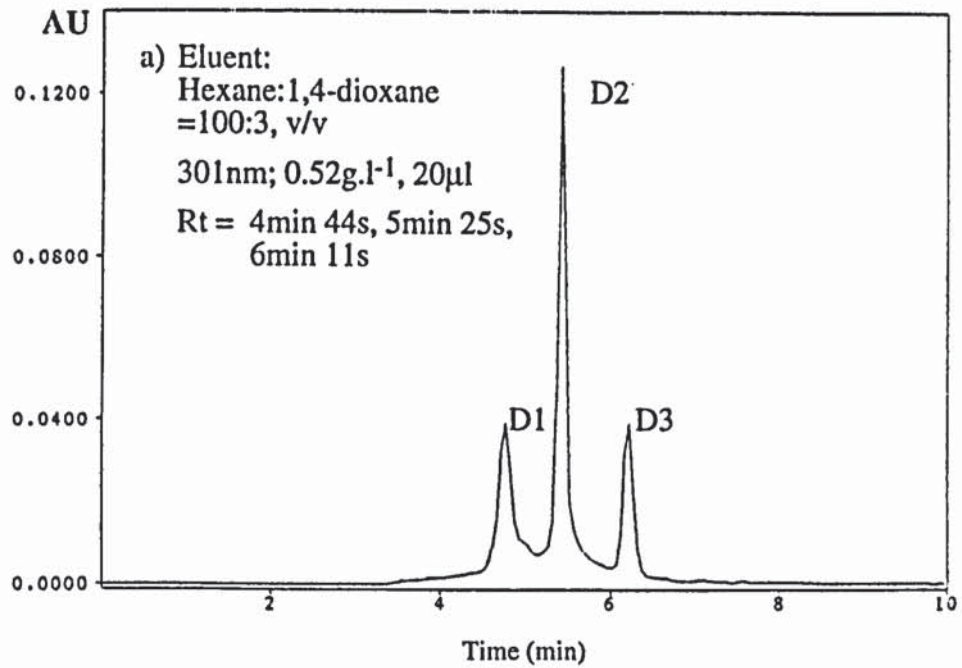
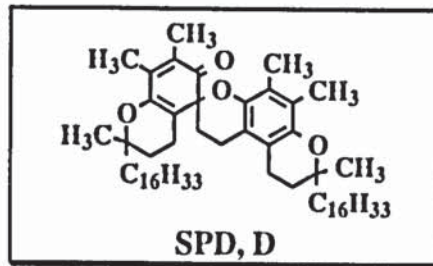


Figure 2.14.a: HPLC chromatograms of synthesised SPD, D, purified by semi-preparative NP-HPLC, in hexane, at 301nm (see scheme 2.1)
Instruments: Philips PU4100 liquid chromatograph and PU4120 diode array detector
Column: Zorbax SIL (4.6mm x 25cm); Flow rate: 1ml.min⁻¹

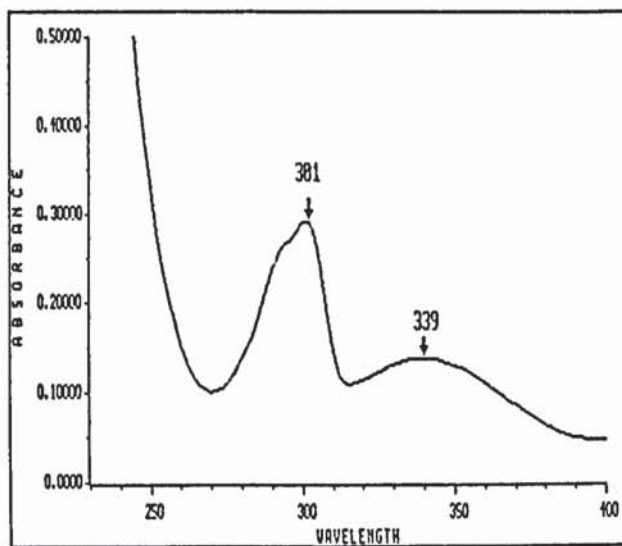
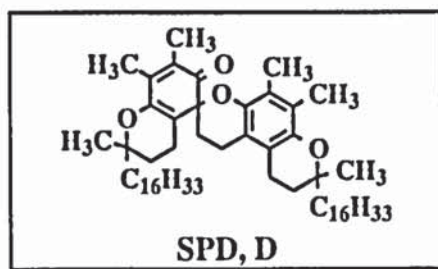


Figure 2.14.b: UV spectrum of synthesised SPD, D in hexane, $0.52\text{g}\cdot\text{l}^{-1}$ (see scheme 2.1 and table 2.16)

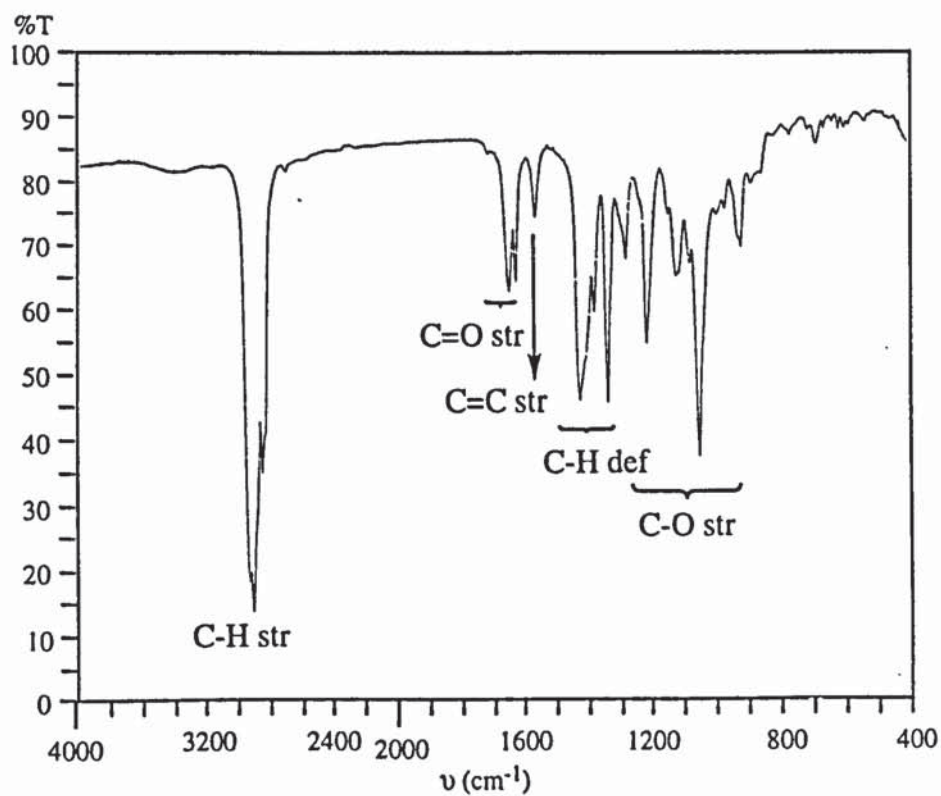
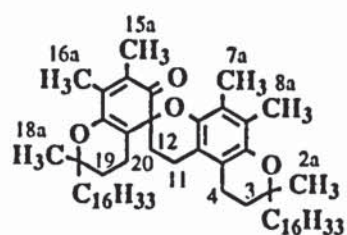


Figure 2.14.c: IR spectrum of synthesised SPD, D, KBr windows (see scheme 2.1 and table 2.16)



SPD, D

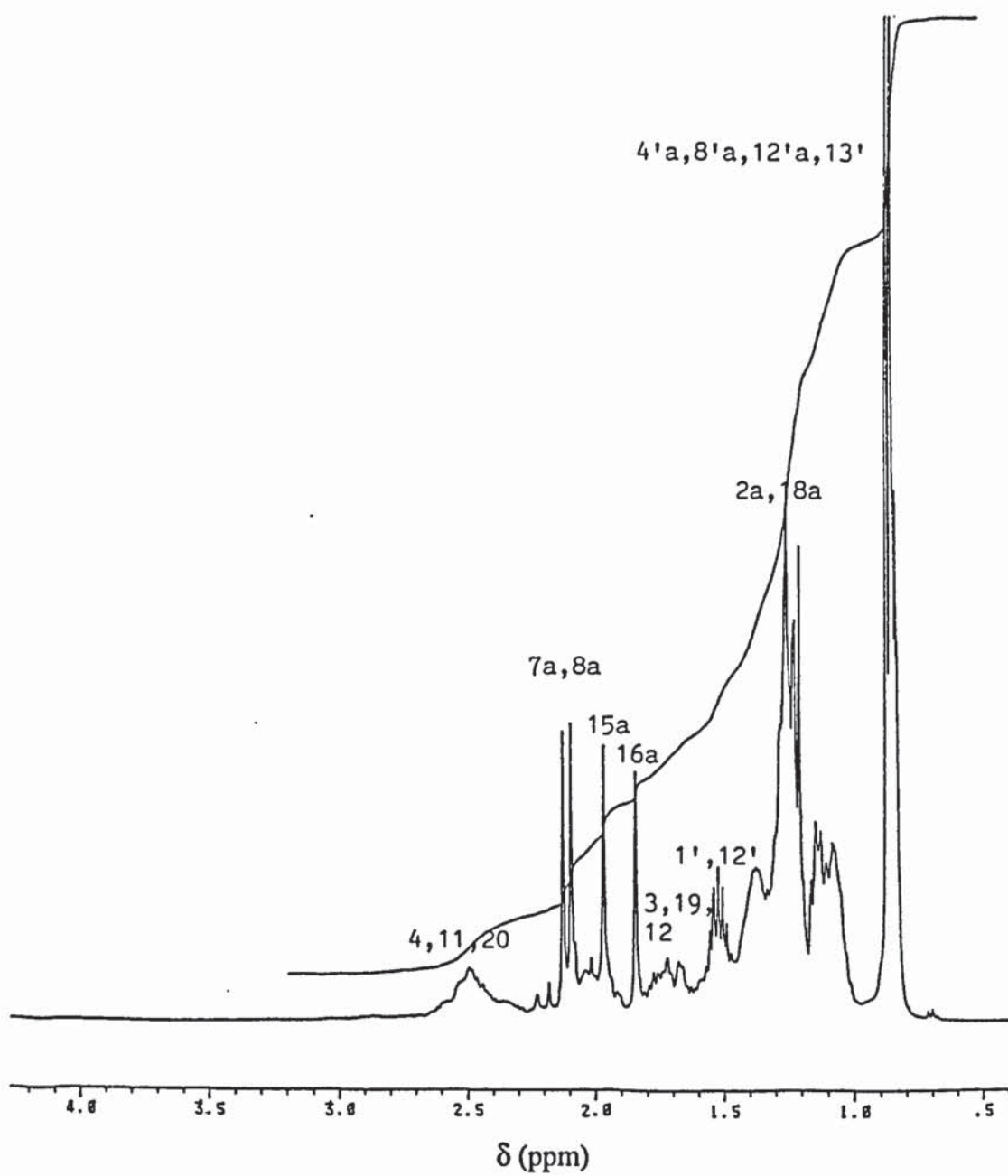
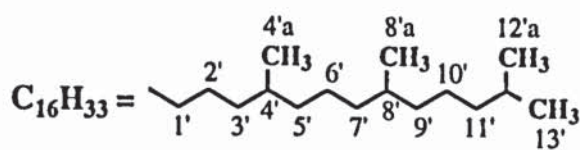


Figure 2.14.d: ¹H-NMR spectrum of synthesised SPD, D, in CDCl₃, at 400MHz (see scheme 2.1 and table 2.17)

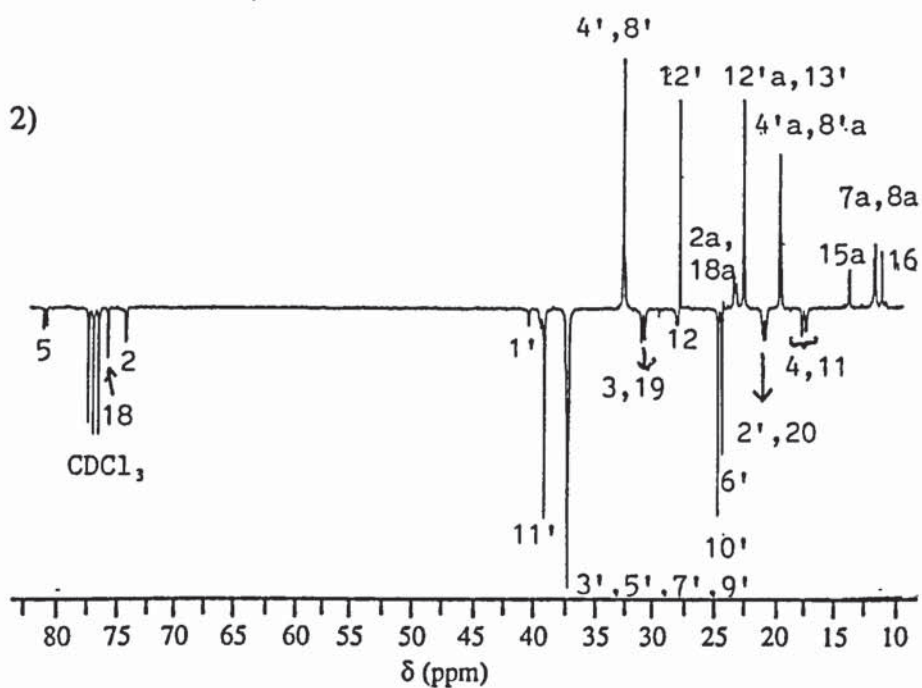
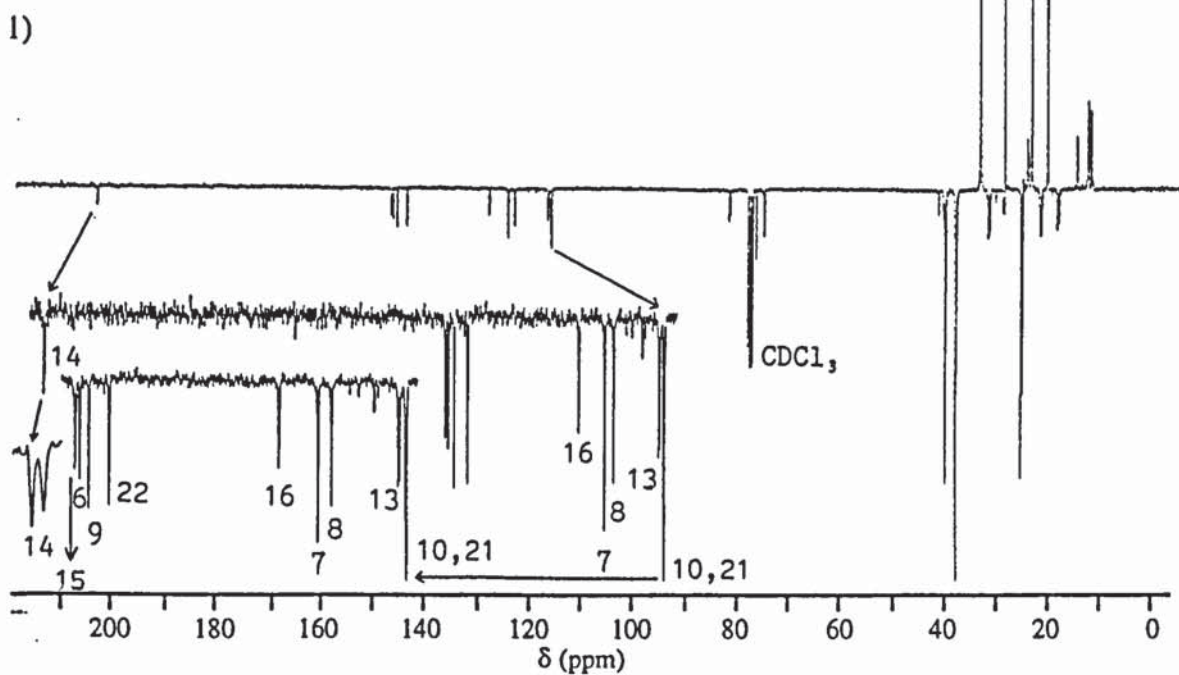
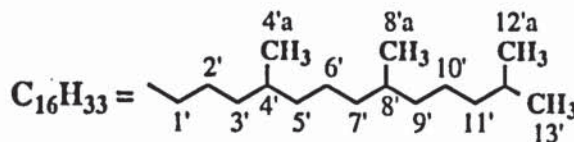
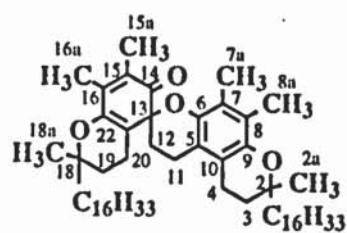
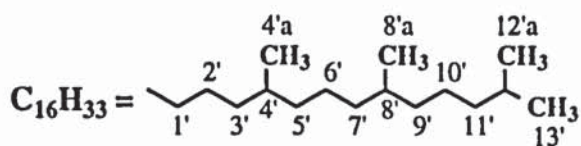
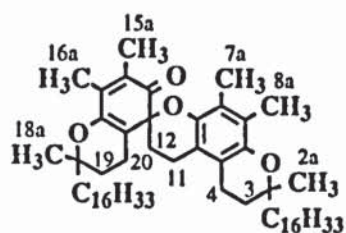


Figure 2.14.g: ^{13}C -NMR spectrum of synthesised SPD, D, in $CDCl_3$, at 75 MHz (see scheme 2.1 and table 2.19)

1) region 0-210ppm

2) expanded region 9-82ppm



SPD, D

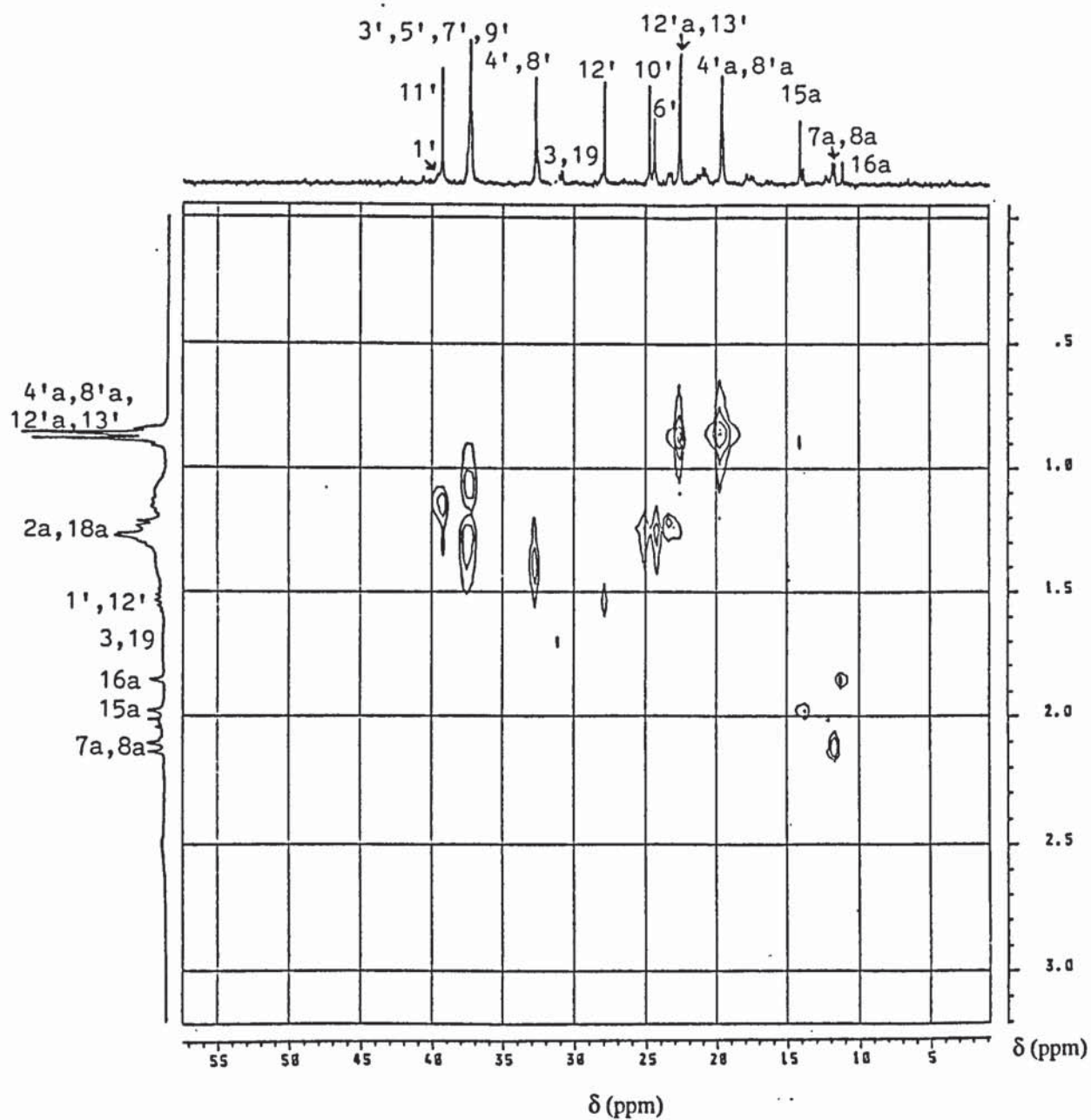


Figure 2.14.f: ¹H, ¹³C-NMR correlation spectrum of synthesised SPD, D, in CDCl₃ (see scheme 2.1)

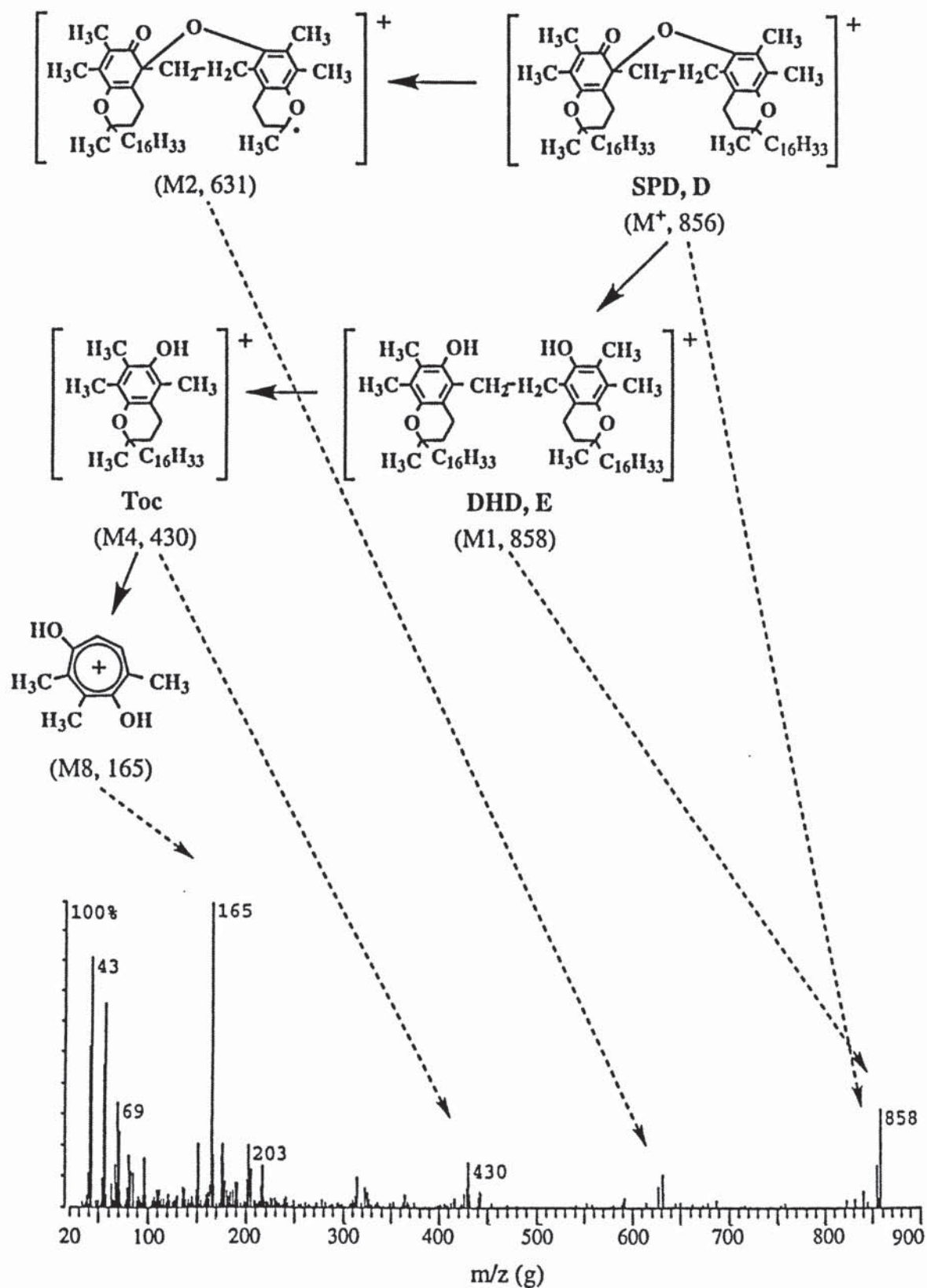


Figure 2.14.g: EI-MS spectrum of synthesised SPD, D in acetate before and after silylation with TMS (see scheme 2.1 and table 2.23)

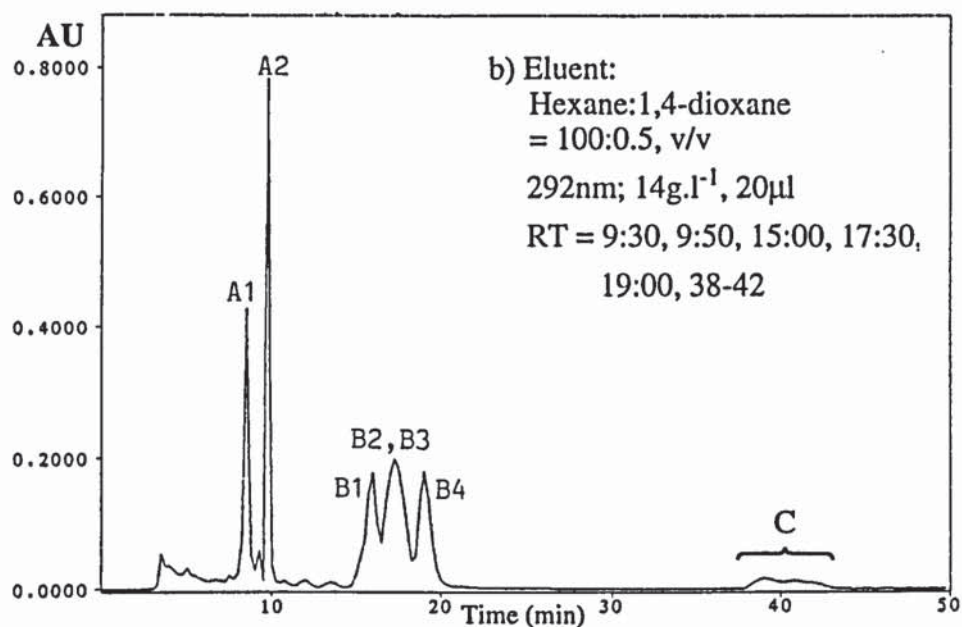
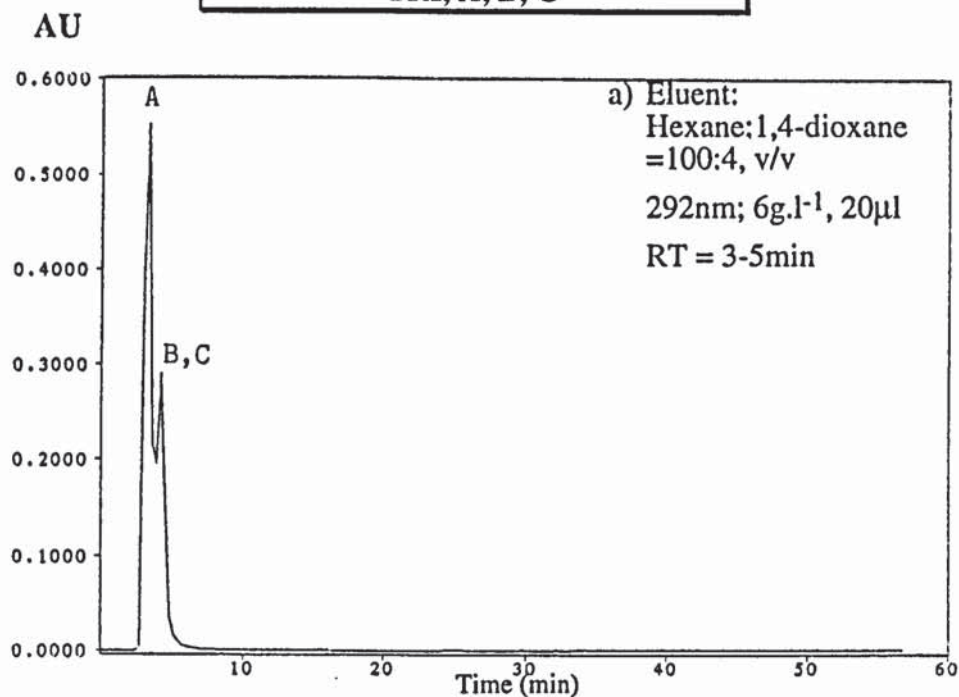
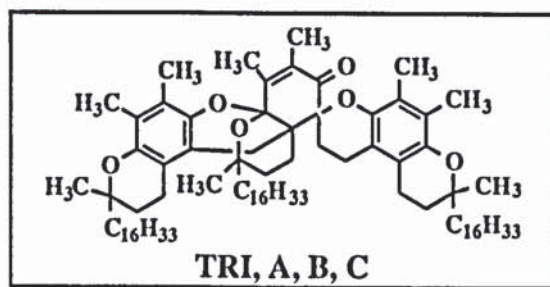


Figure 2.15.a: HPLC chromatograms of TRI, A, B, C (obtained from the oxidation of Toc with PbO₂, ratio 1:10, see scheme 2.1) in hexane, at 292nm
Instruments: Philips PU4100 liquid chromatograph and PU4120 diode array detector
Column: Zorbax SIL (4.6mm x 25cm); Flow rate: 1ml.min⁻¹

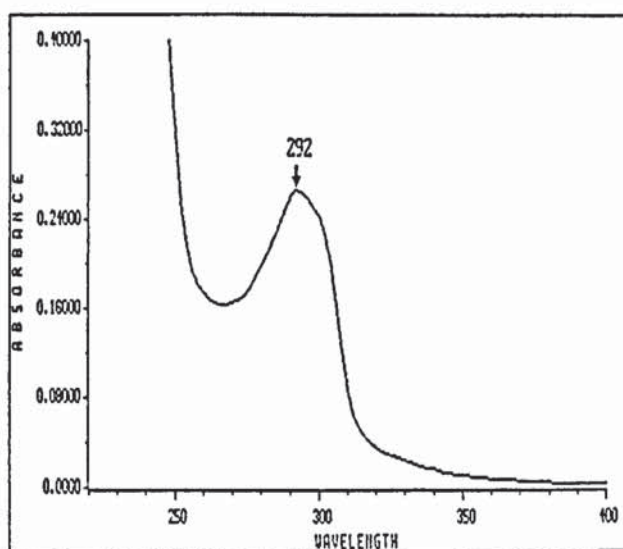
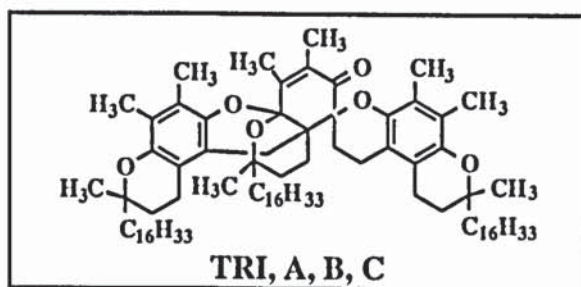


Figure 2.15.b: UV spectrum of synthesised TRI, A, B, C in hexane, 0.5g.l⁻¹ (see scheme 2.1 and table 2.16)

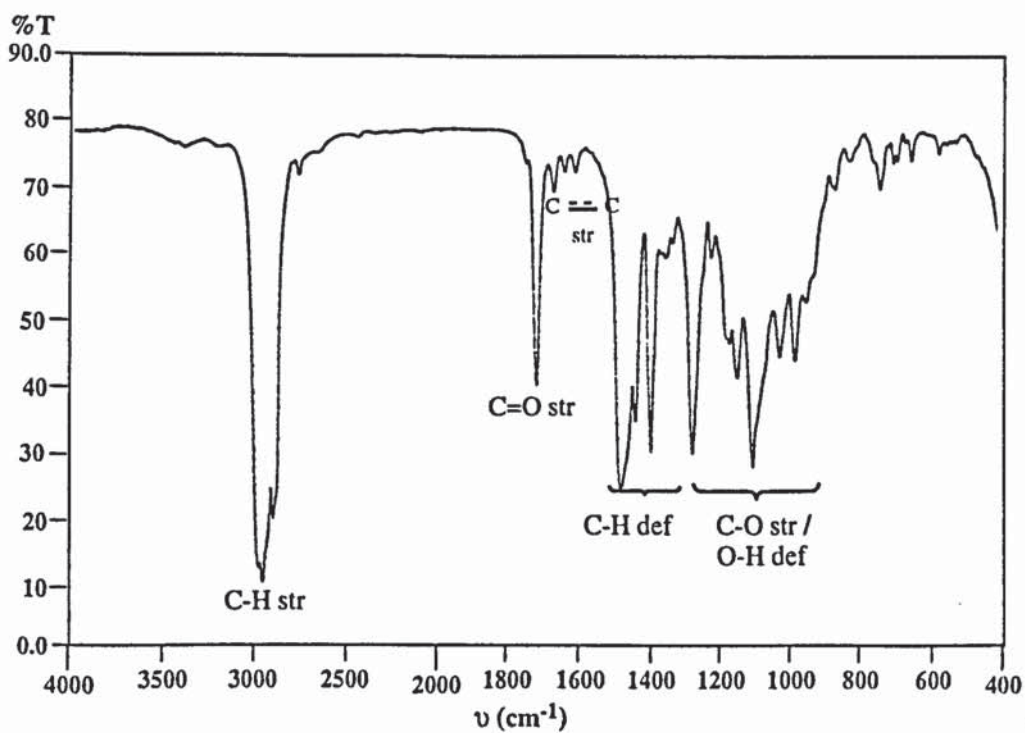


Figure 2.15.c: IR spectrum of synthesised TRI, A, B, C, KBr windows (see scheme 2.1 and table 2.16)

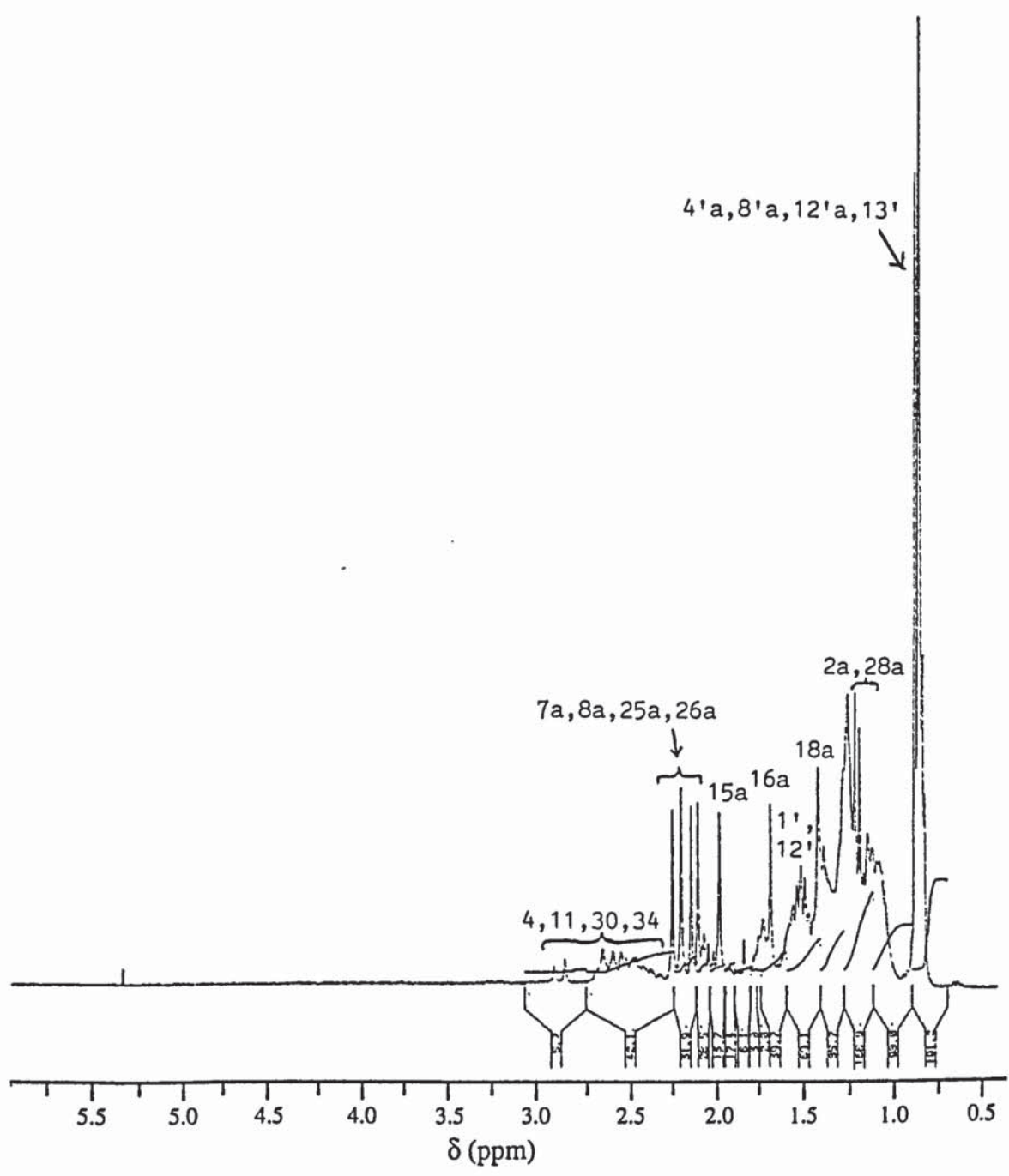
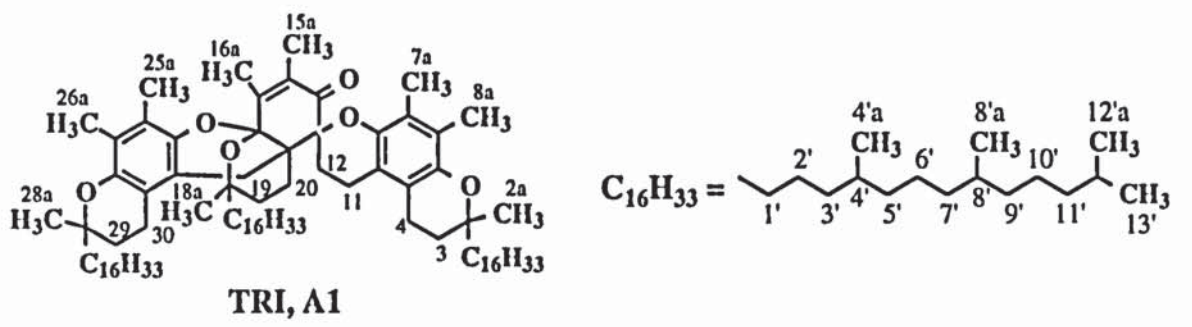


Figure 2.15.d: $^1\text{H-NMR}$ spectrum of TRI, A1, isolated by semi-preparative NP-HPLC from the synthesised TRI, A, B, C, in hexane, at 300MHz (see scheme 2.1 and table 2.18)

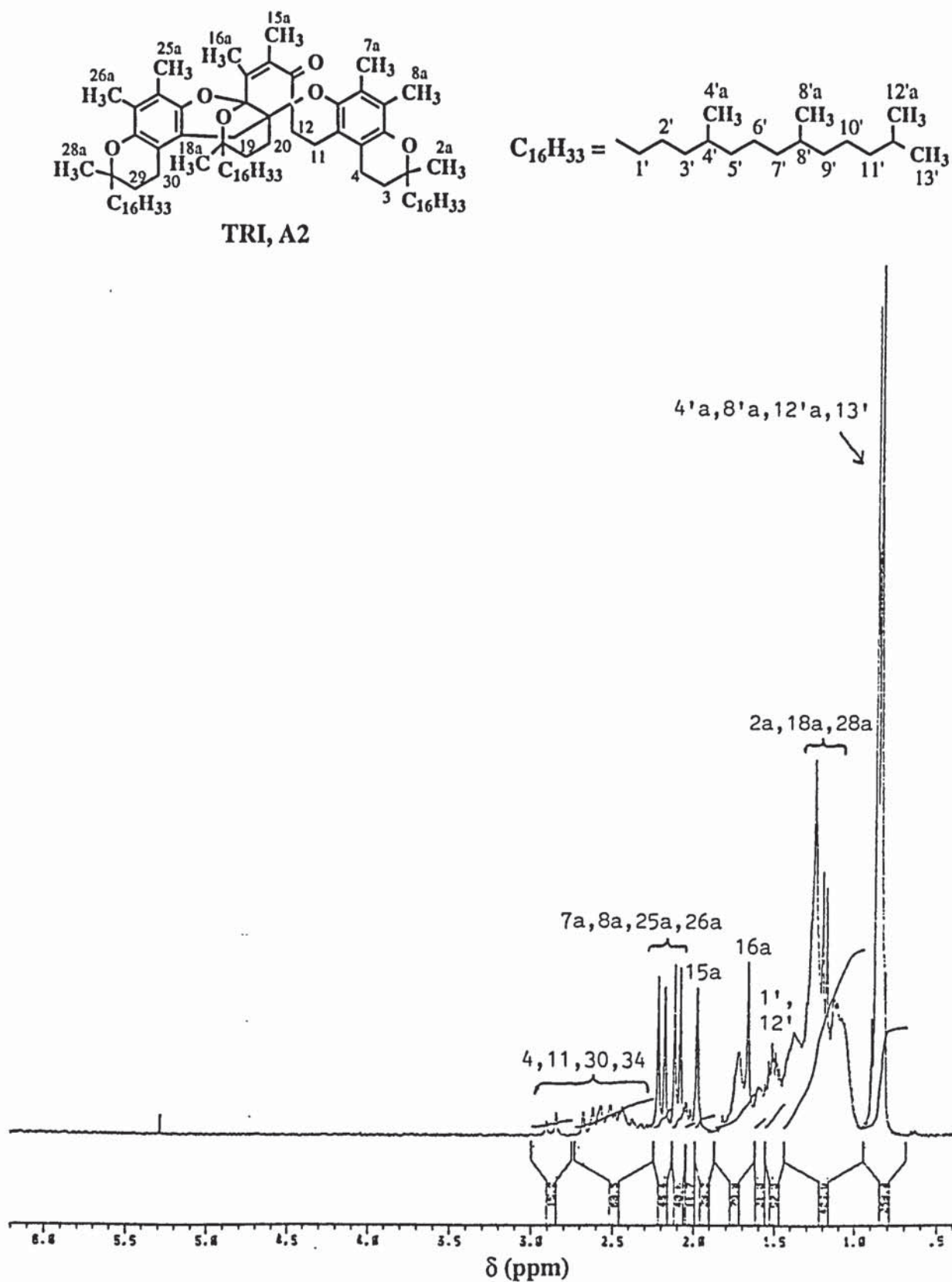


Figure 2.15.e: ¹H-NMR spectrum of TRI, A2, isolated by semi-preparative NP-HPLC from the synthesised TRI, A, B, C, in hexane, at 300MHz (see scheme 2.1 and table 2.18)

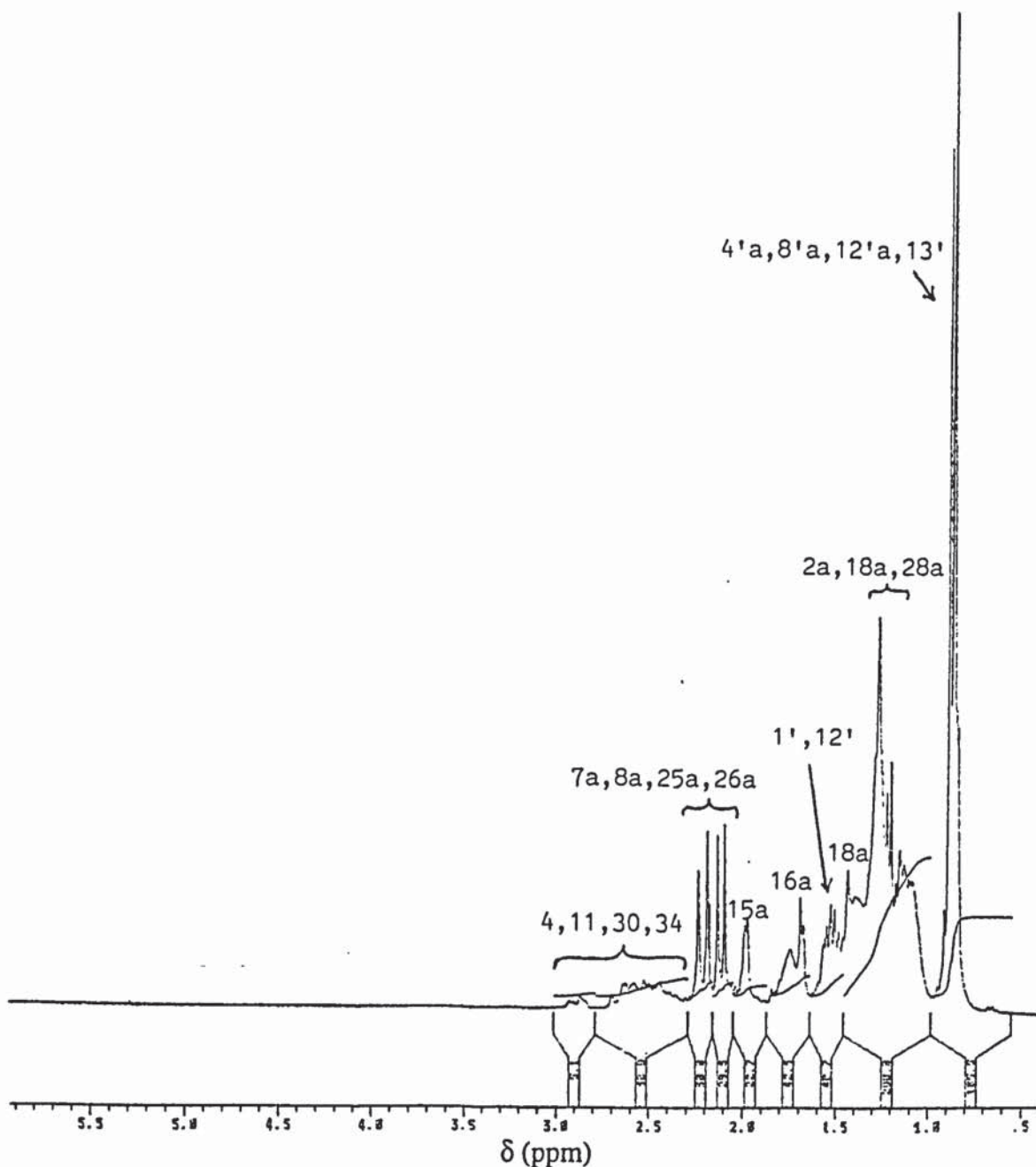
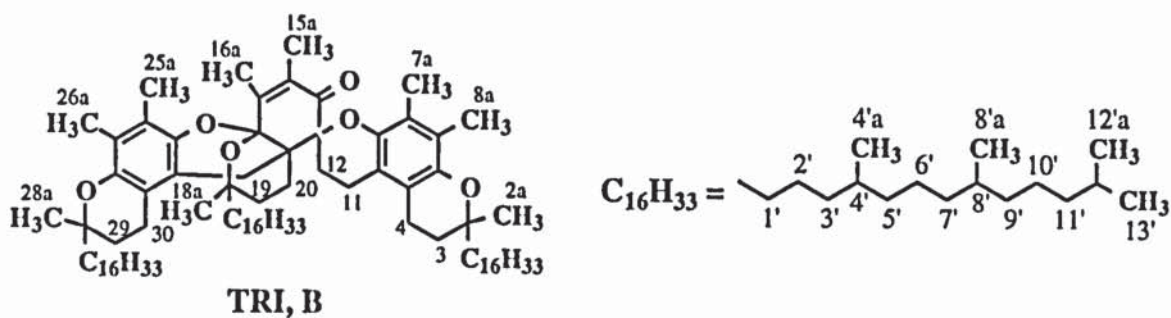


Figure 2.15.f: ¹H-NMR spectrum of TRI, B, isolated by semi-preparative NP-HPLC from the synthesised TRI, A, B, C, in hexane, at 300MHz (see scheme 2.1 and table 2.18)

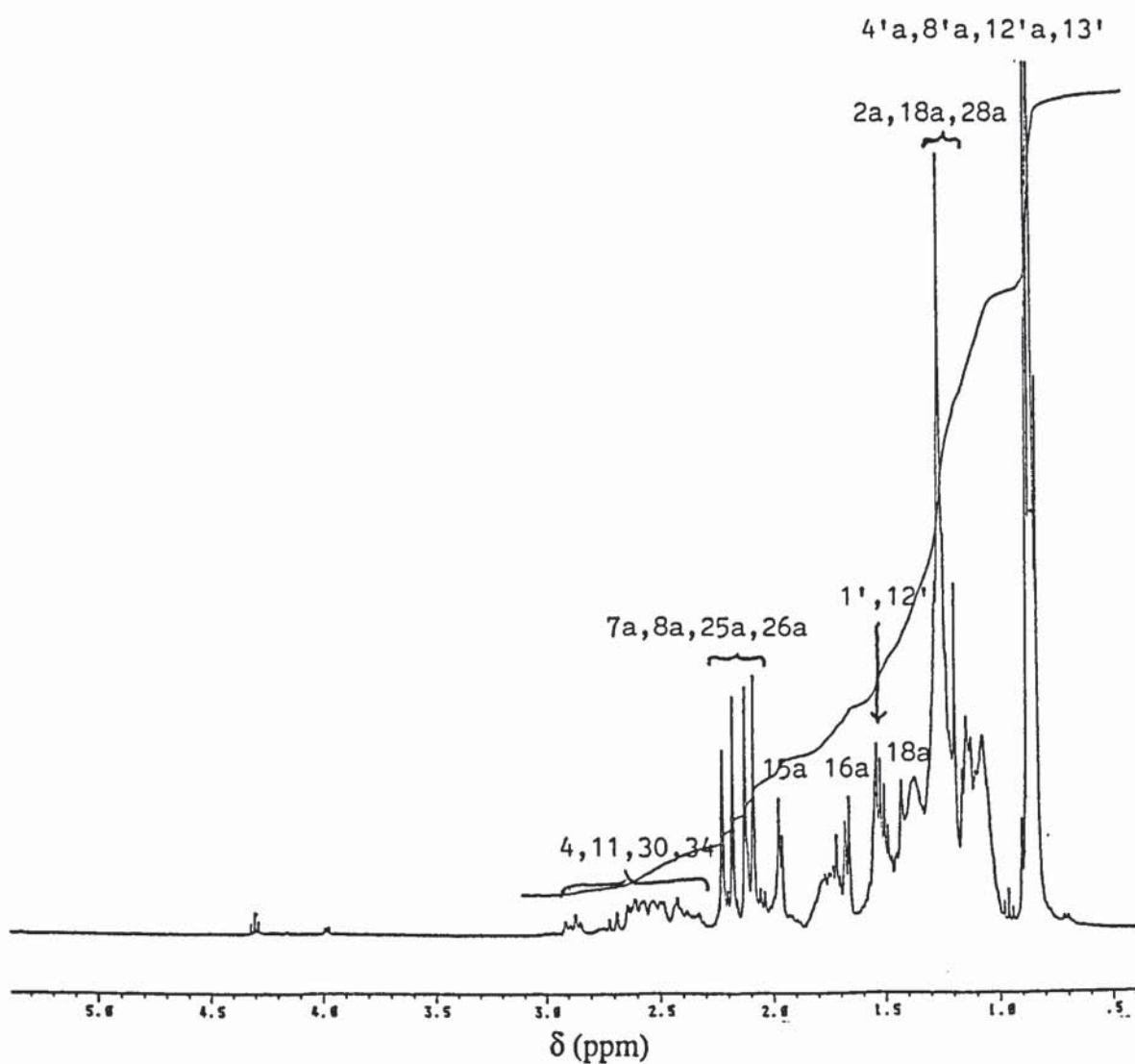
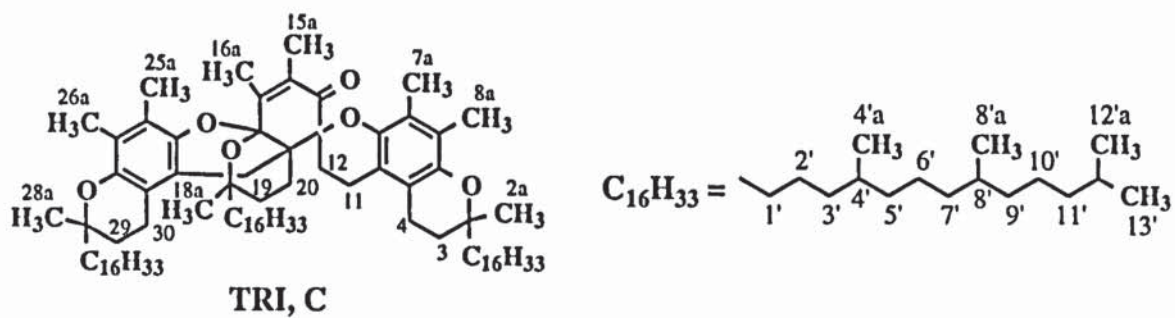


Figure 2.15.g: $^1\text{H-NMR}$ spectrum of TRI, C, isolated by semi-preparative NP-HPLC from the synthesised TRI, A, B, C, in hexane, at 400MHz (see scheme 2.1 and table 2.18)

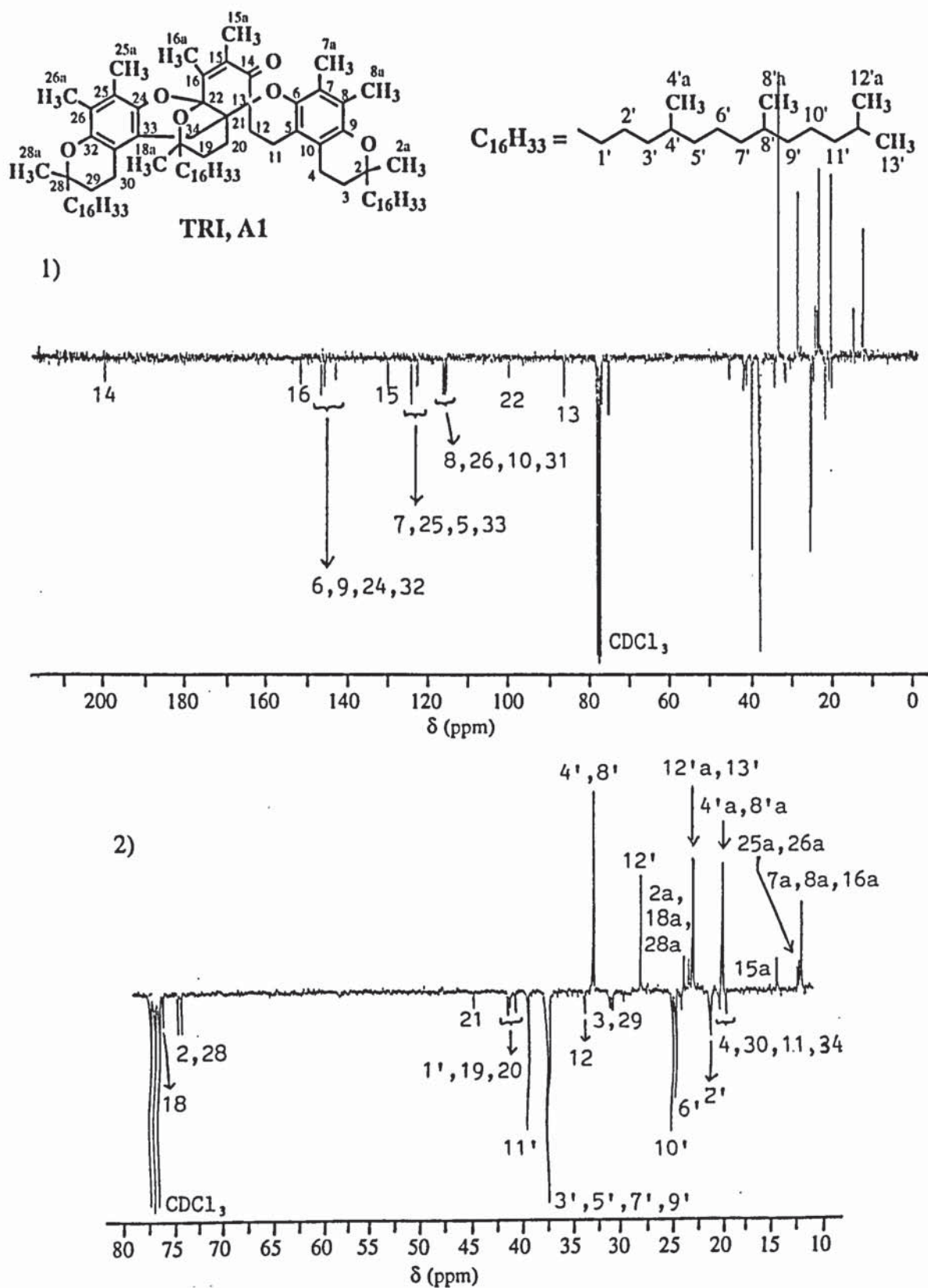
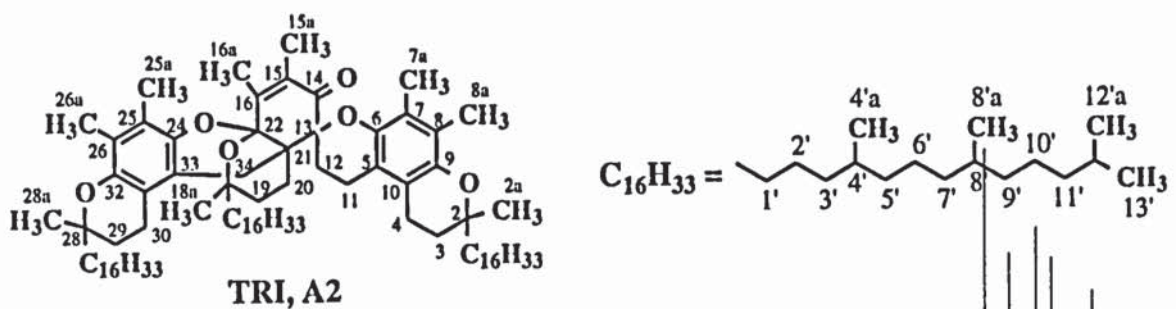
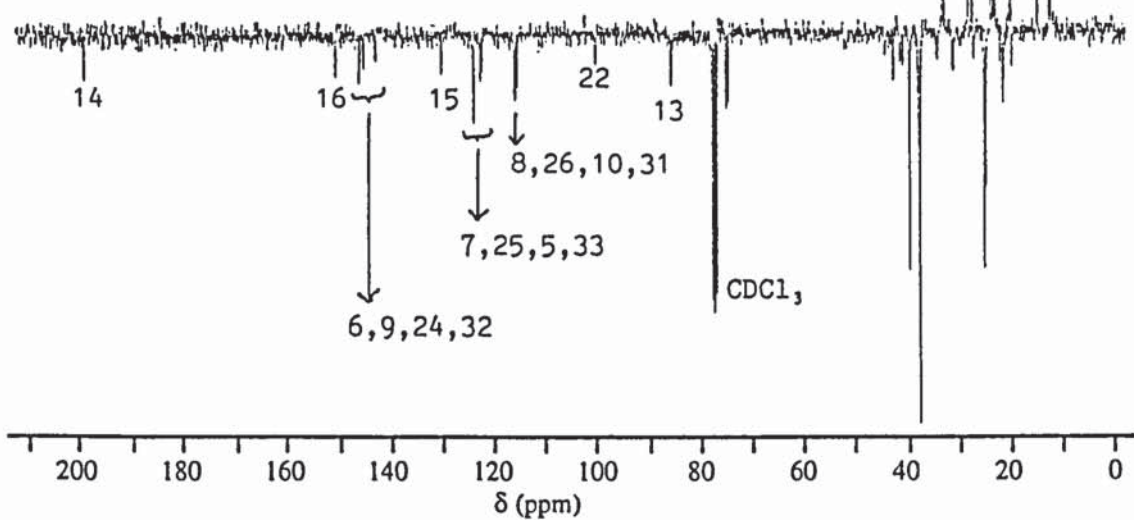


Figure 2.15.h: ^{13}C -NMR spectrum of TRI, A1, isolated by NP-HPLC from the synthesised TRI, A,B,C, in CDCl_3 , at 75 MHz (see scheme 2.1, table 2.20)
 1) region 0-210ppm 2) expanded region 10-80ppm



1)



2)

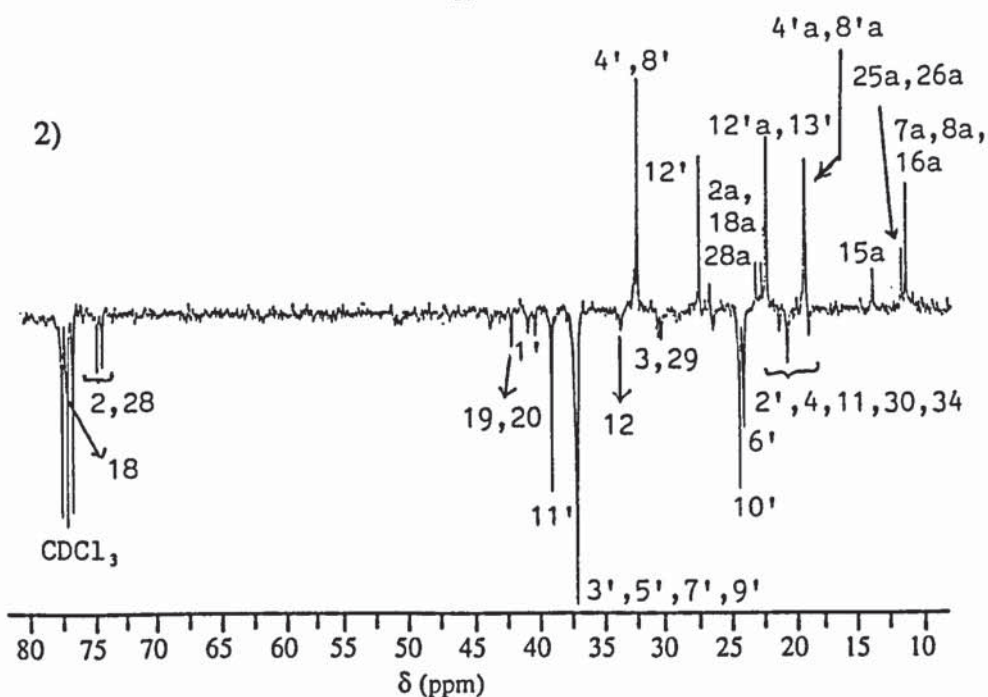


Figure 2.15.i: ^{13}C -NMR spectrum of TRI, A2, isolated by NP-HPLC from the synthesised TRI, A,B,C, in CDCl_3 , at 75 MHz (see scheme 2.1, table 2.20)
 1) region 0-210ppm 2) expanded region 10-80ppm

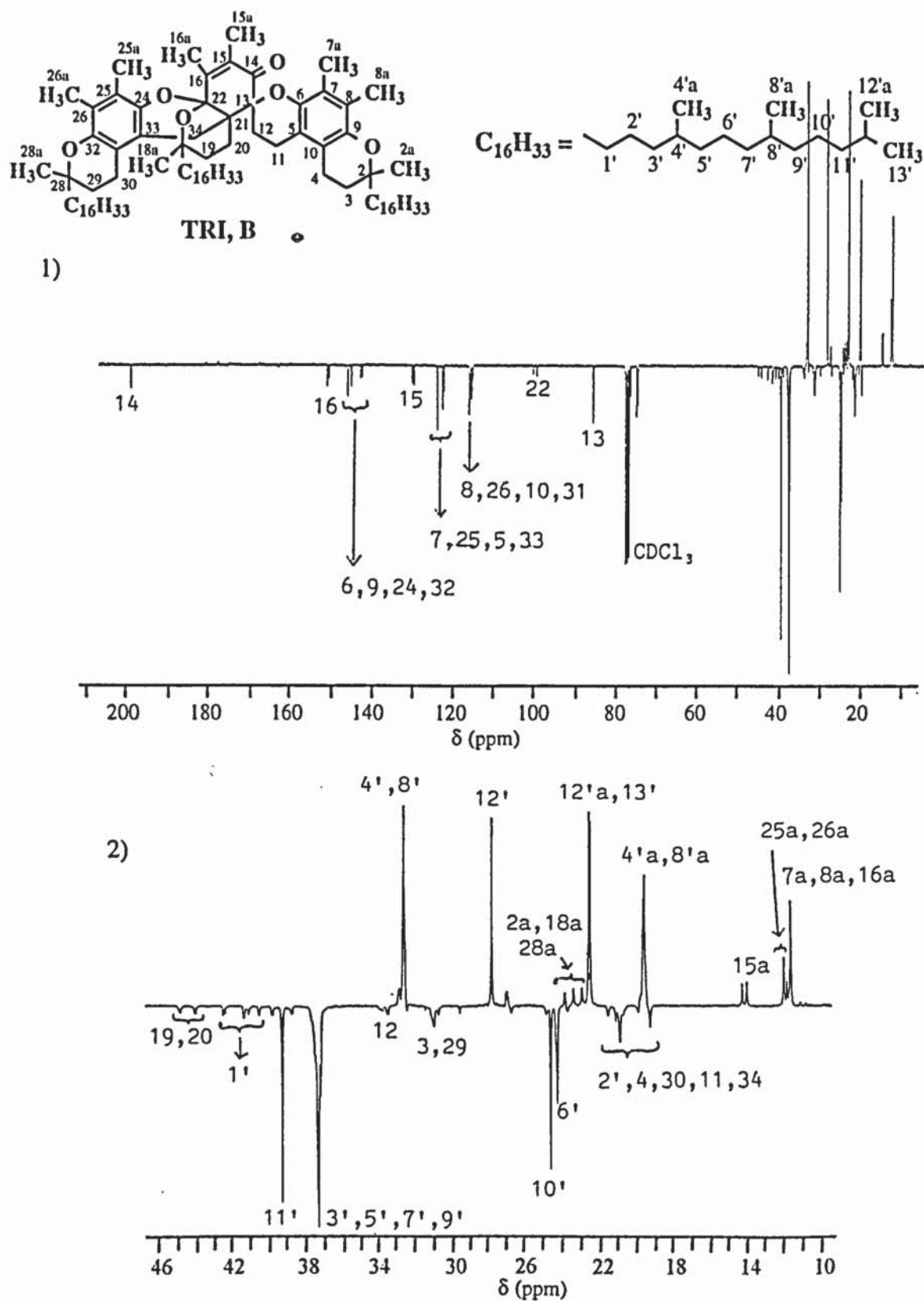


Figure 2.15.j: ^{13}C -NMR spectrum of TRI, B, isolated by NP-HPLC from the synthesised TRI, A,B,C, in CDCl_3 , at 75 MHz (see scheme 2.1, table 2.20)
 1) region 0-210ppm 2) expanded region 10-46ppm

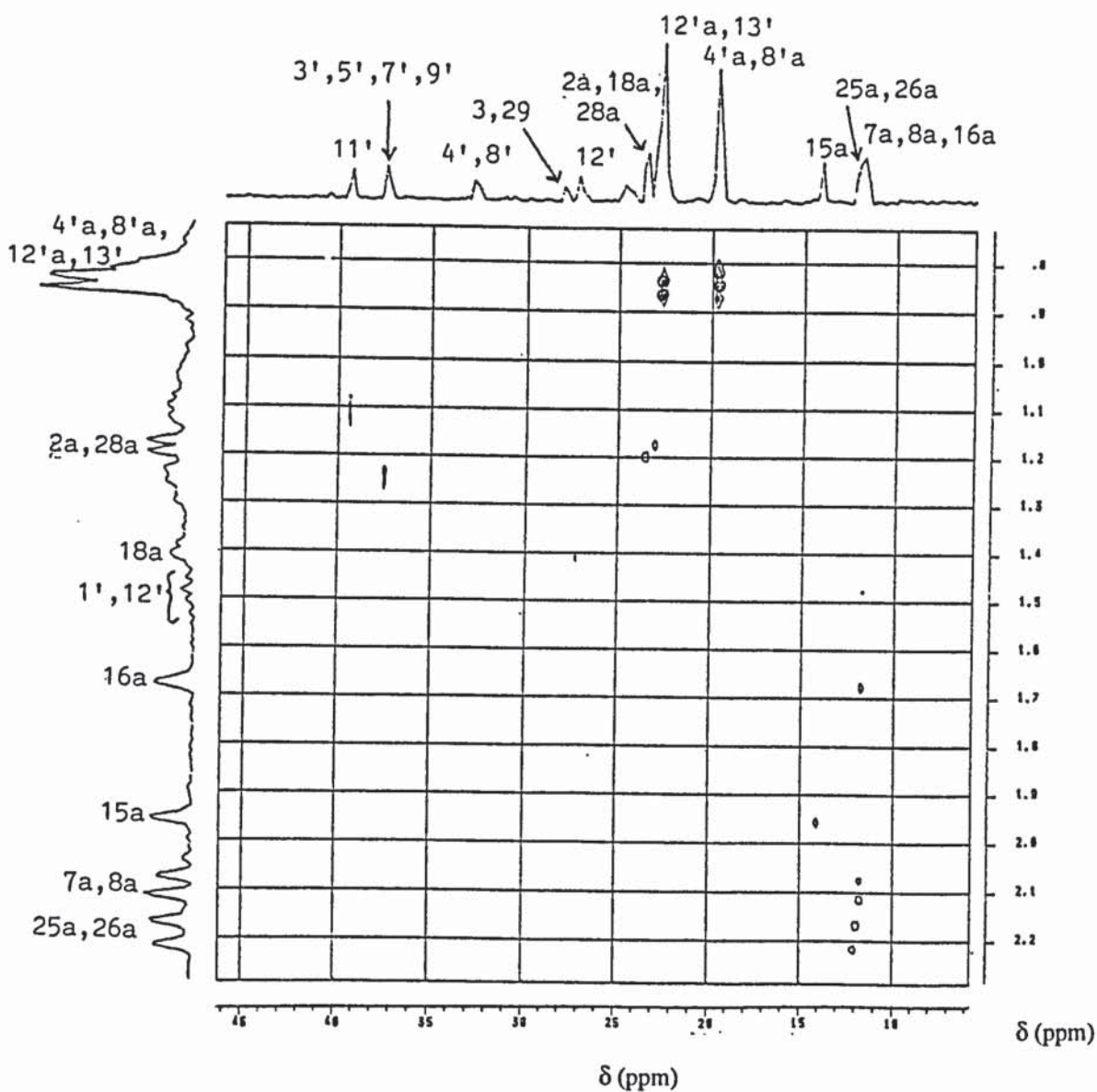
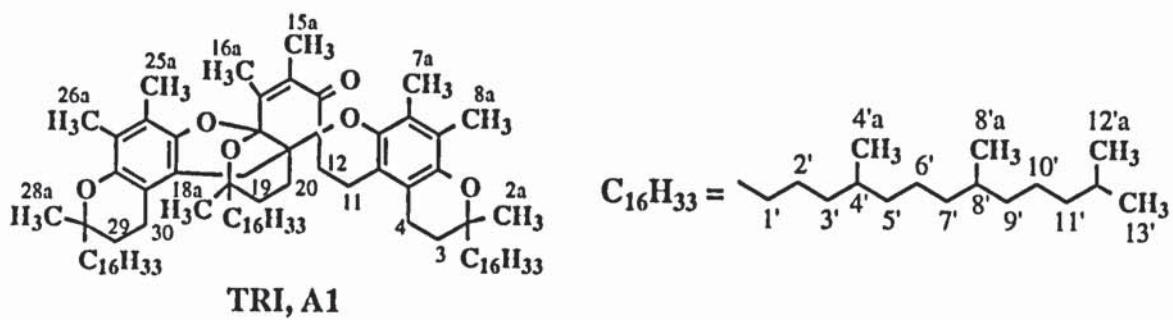


Figure 2.15.k: ^1H , ^{13}C -NMR correlation spectrum of TRI, A1, isolated by NP-HPLC from the synthesised TRI, A, B, C, in CDCl_3 (see scheme 2.1)

a) Eluent:
Hexane:1,4-dioxane = 100:4, v/v
290nm

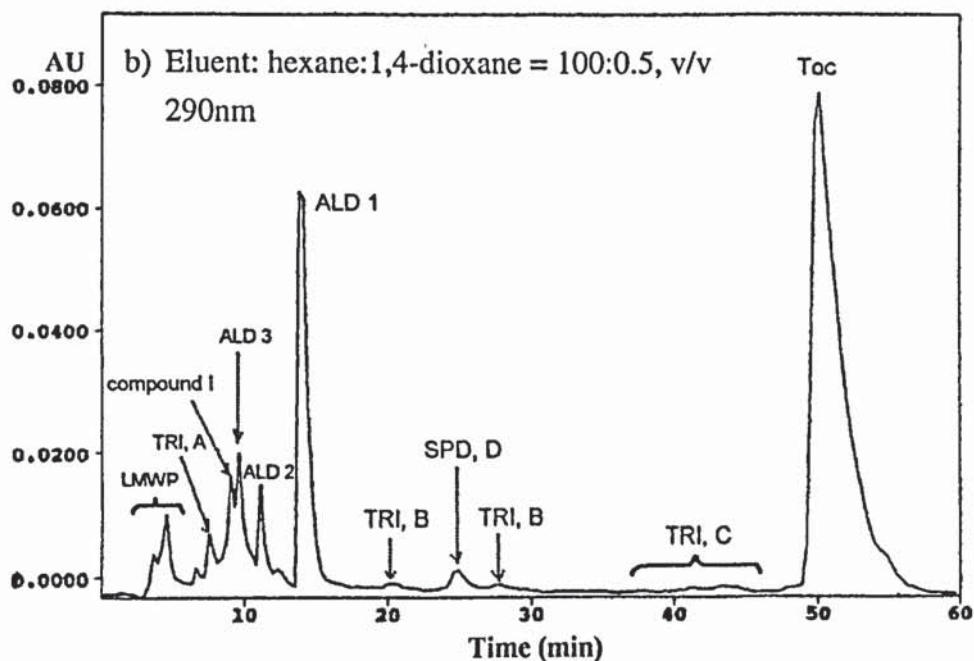
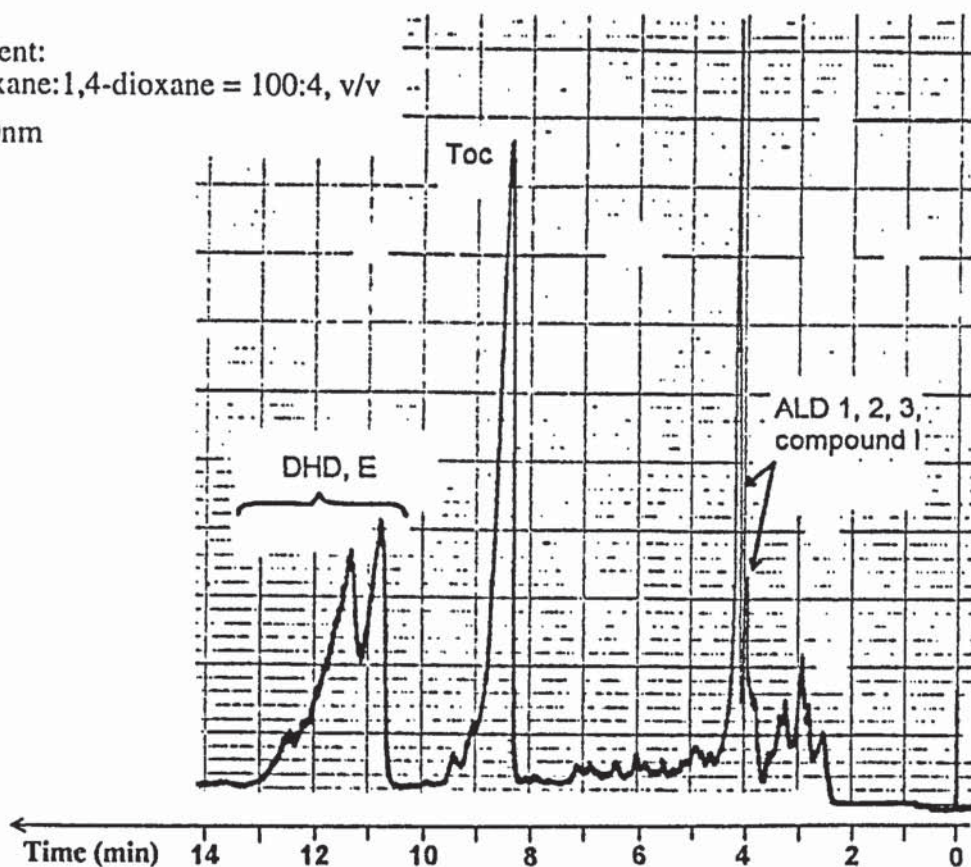
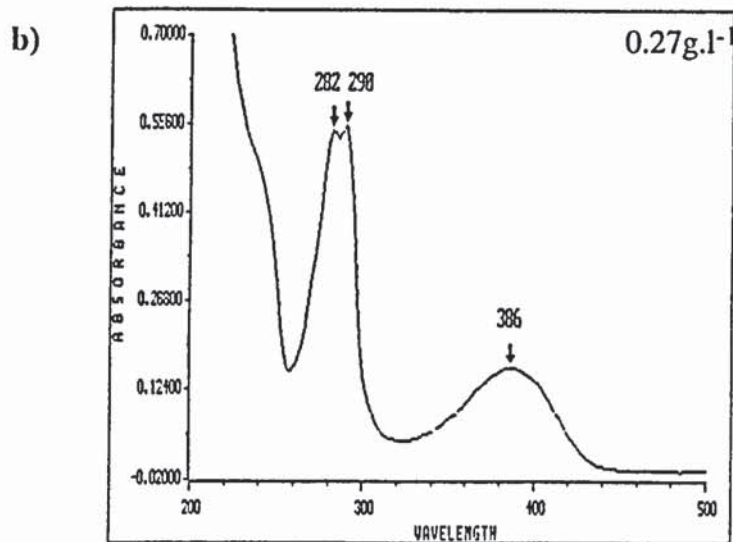
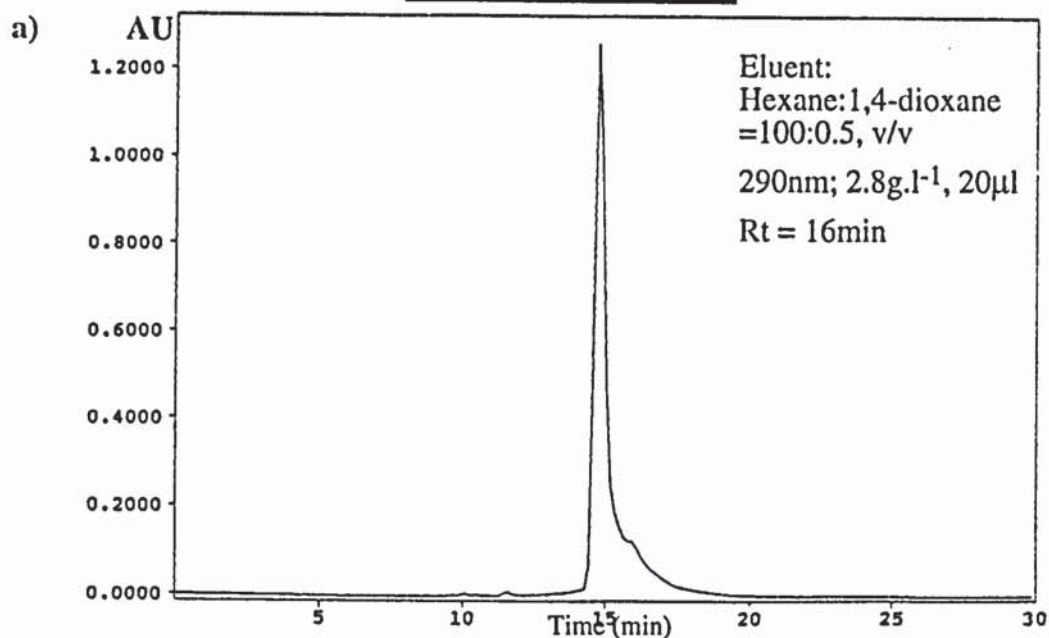
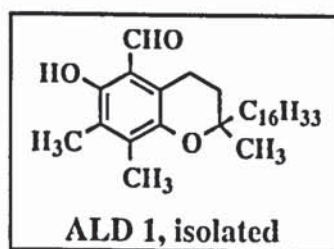
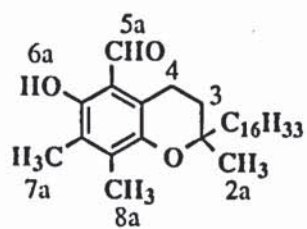


Figure 2.20: HPLC analysis of the extract of PP stabilised with 39% Toc, pass 4 (CPC789 series, single screw extruder, 270°C), in hexane (see section 2.7.1)
Instruments: a) Gilson 305 piston pump and Dynamax UV-1 variable wavelength detector b) Philips PU4100 liquid chromatograph and PU4120 diode array detector; Column: Zorbax SIL (4.6mm x25cm); Flow rate: 1ml.min⁻¹



Figures 2.21: HPLC (a) and UV (b) analysis of ALD 1, isolated from the extract of PP (a-b) stabilised with 39% Toc, pass 4 (CPC789 series, single screw extruder, 270°C), in hexane (see section 2.7.1)

- a) Instruments: Philips PU4100 liquid chromatograph and PU4120 diode array detector; column: Zorbax SIL (4.6mm x25cm); flow rate: 1ml.min⁻¹
- b) Solvent: hexane; 0.27g.l⁻¹ (see table 2.29)



ALD 1, isolated

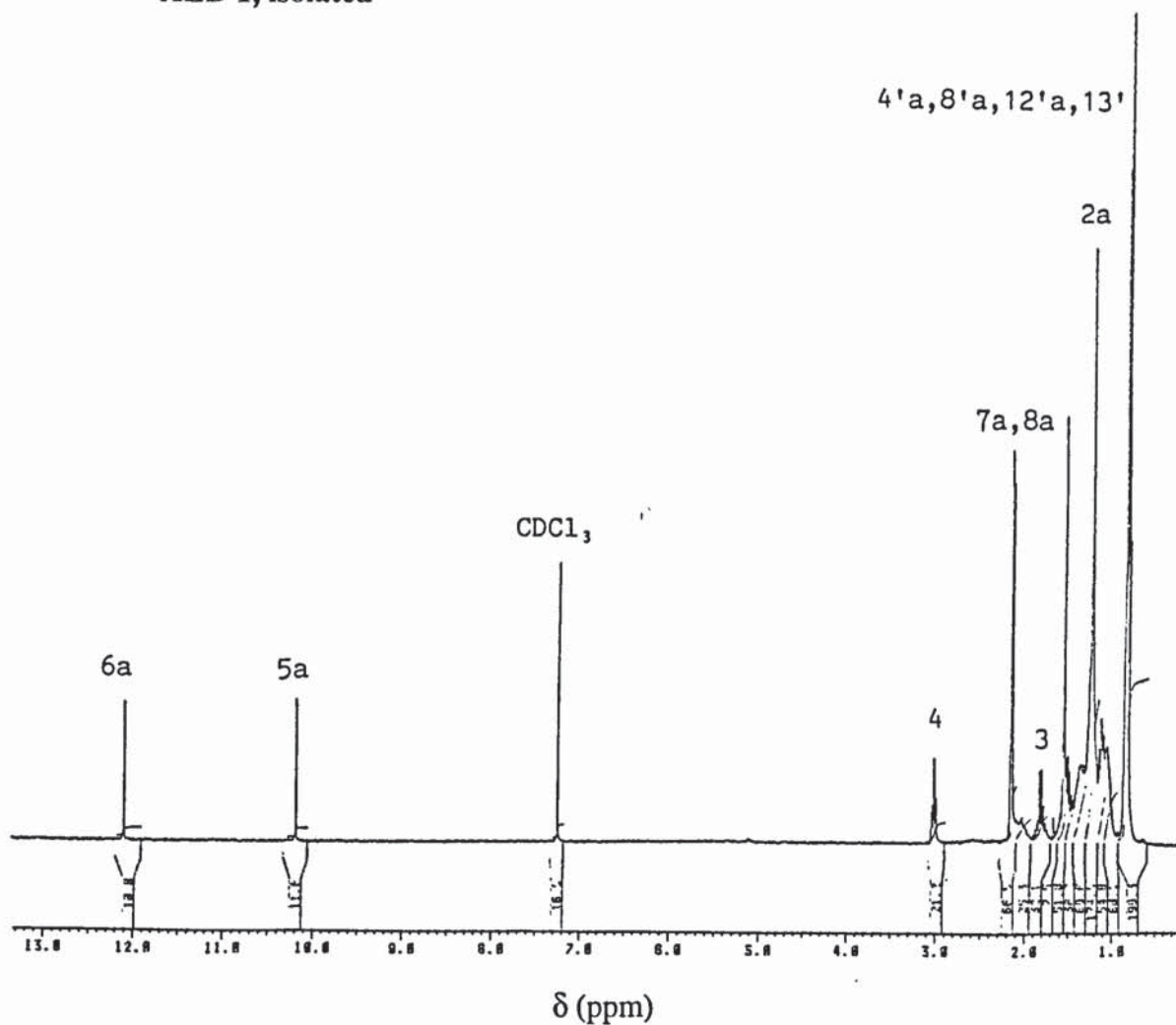
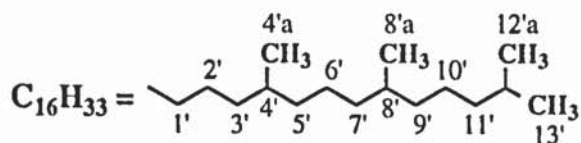


Figure 2.21.c: $^1\text{H-NMR}$ spectrum of ALD 1, isolated from the extract of PP stabilised with 39% Toc, pass 4 (CPC789 series, single screw extruder, 270°C), in CDCl_3 , at 300MHz (see section 2.7.1 and table 2.30)

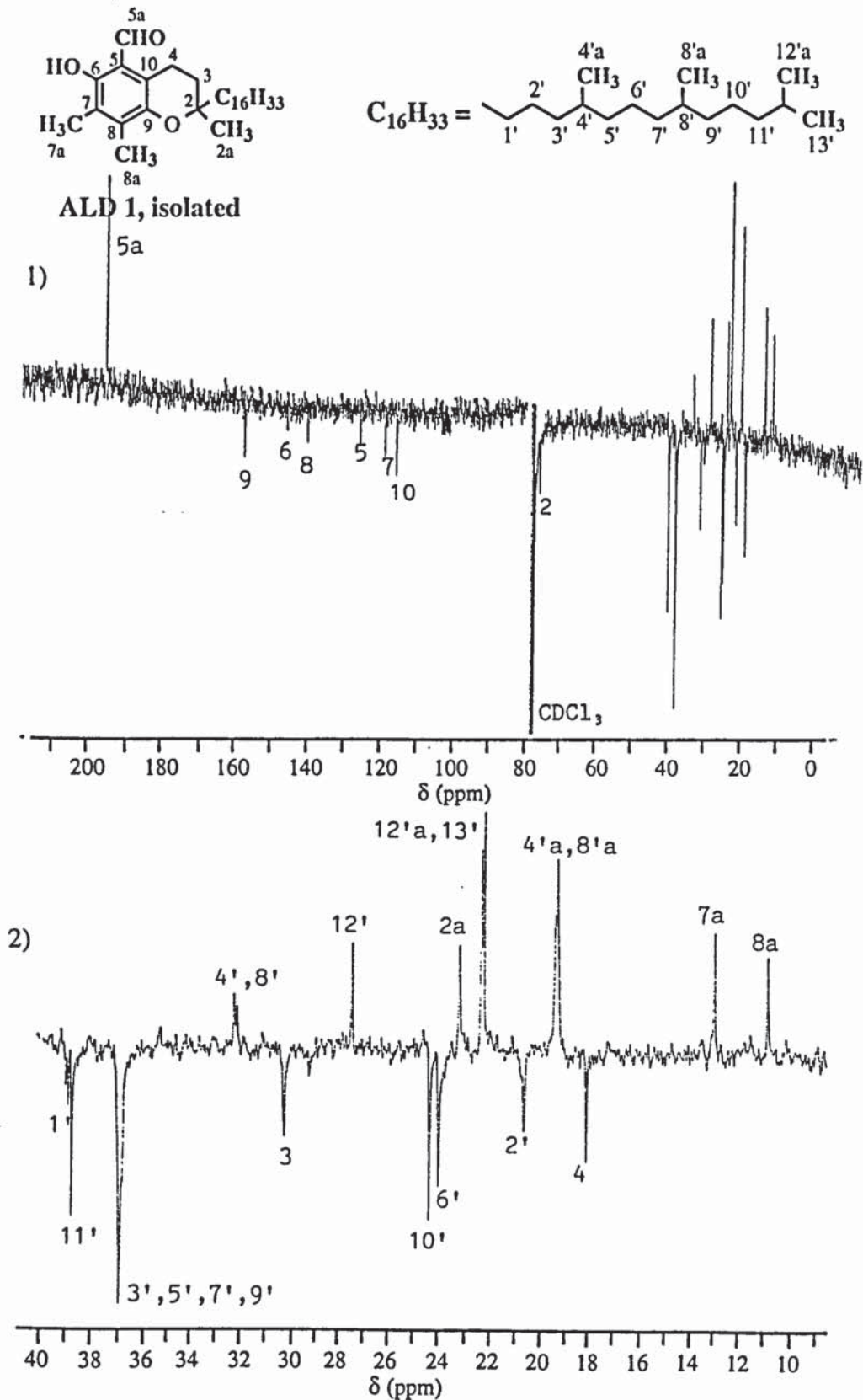
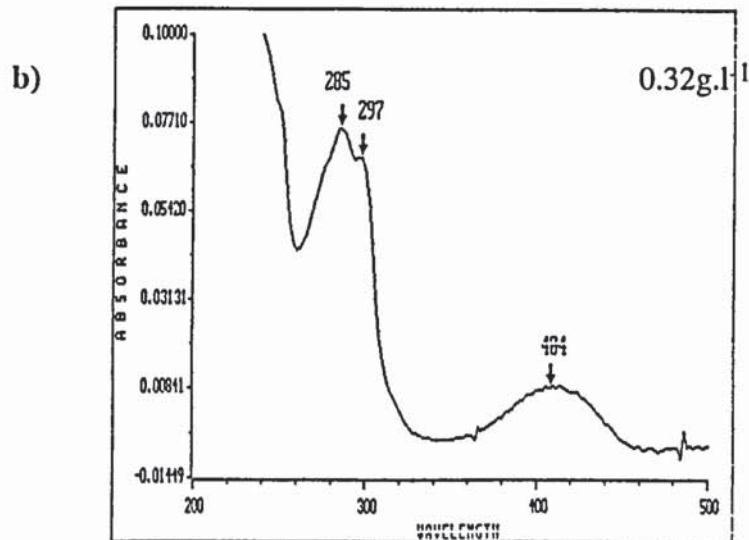
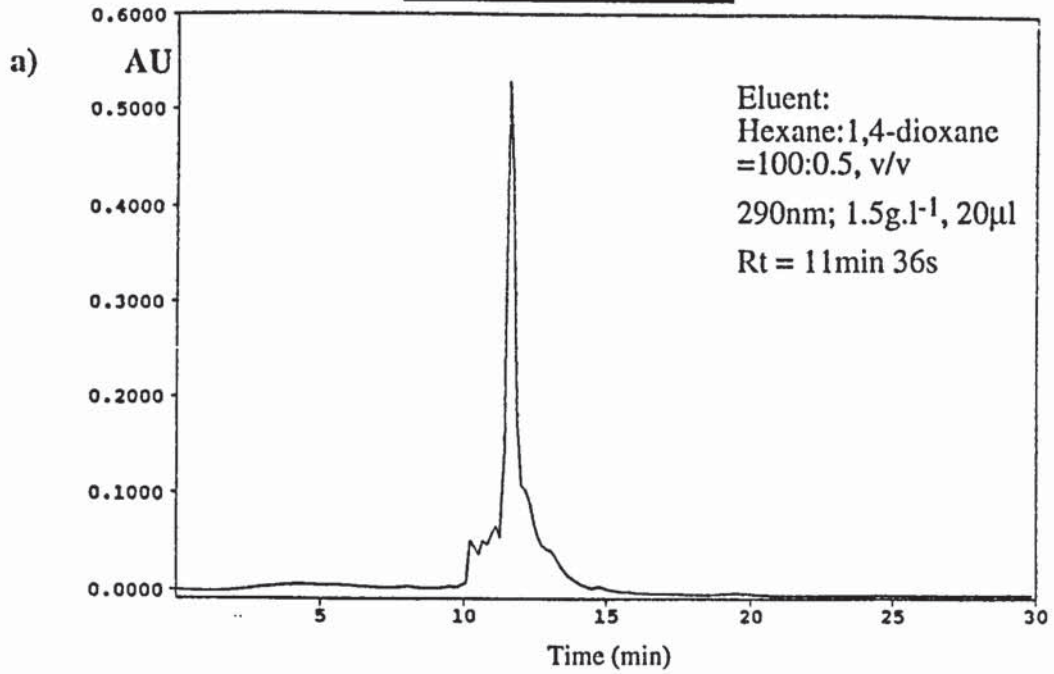
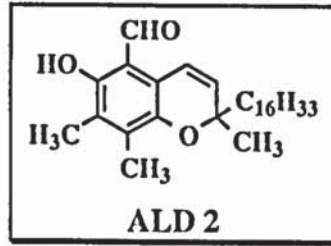


Figure 2.21.d: ¹³C-NMR spectrum of supplied ALD 1, isolated from the extract of PP stabilised with 39% Toc, pass 4 (CPC789 series, single screw extruder, 270°C) in CDCl₃, at 75 MHz (see section 2.7.1 and table 2.31)

1) region 0-210ppm 2) expanded region 9-40ppm

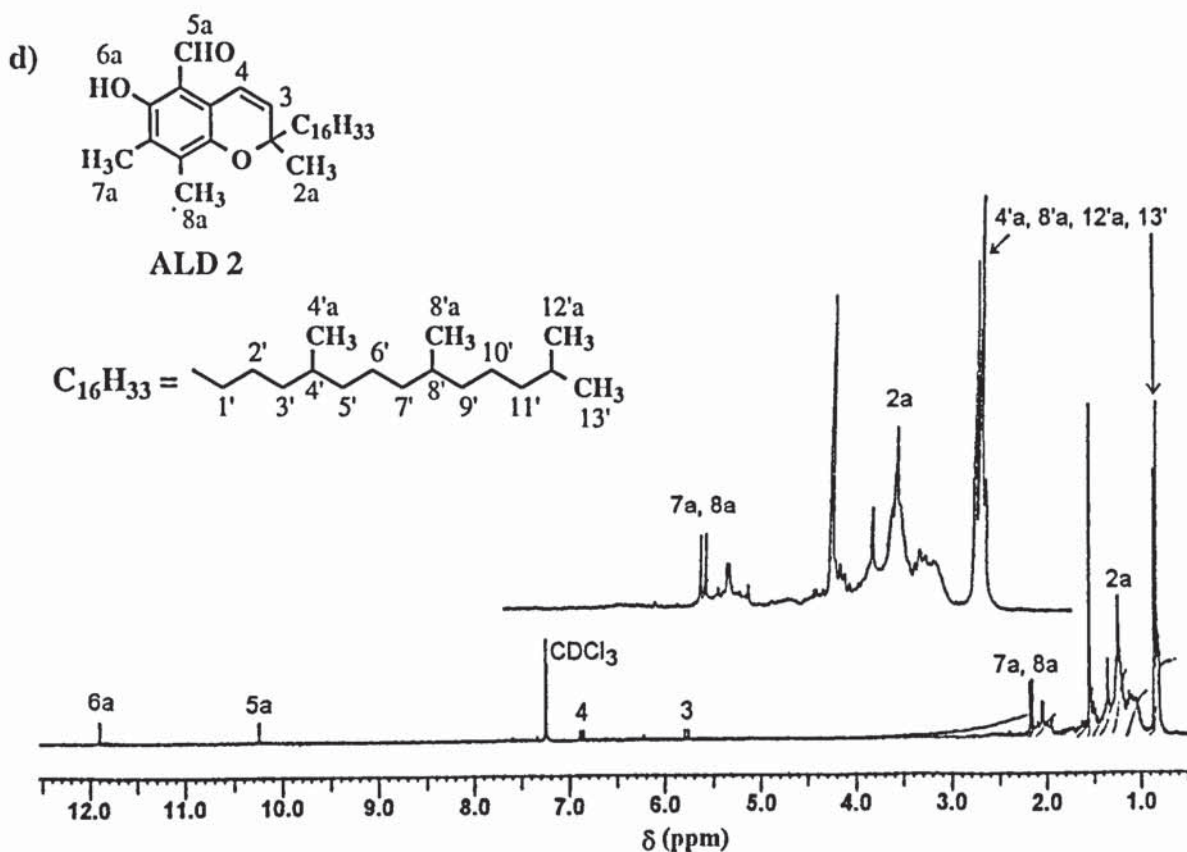
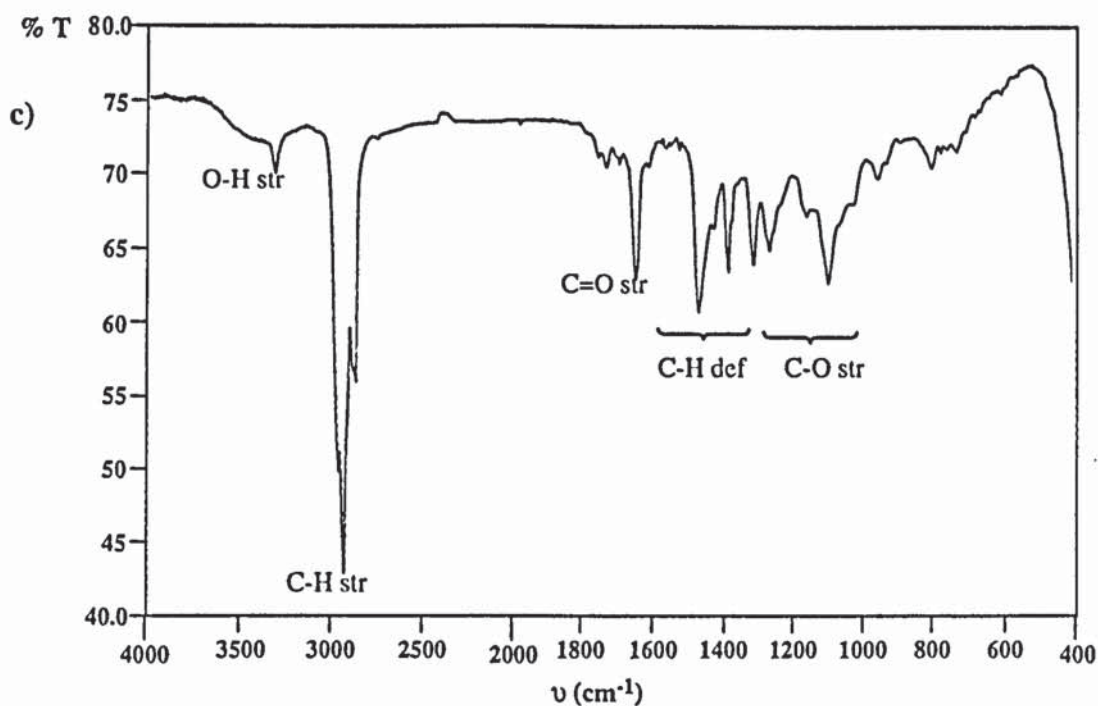


Figures 2.22: HPLC (a) and UV (b) analysis of ALD 2, isolated from the extract of PP

(a-b) stabilised with 39% Toc, pass 4 (CPC789 series, single screw extruder, 270°C), in hexane (see section 2.7.1)

a) Instruments: Philips PU4100 liquid chromatograph and PU4120 diode array detector; column: Zorbax SIL (4.6mm x25cm); flow rate: 1ml.min⁻¹

b) Solvent: hexane; 0.32g.l⁻¹ (see table 2.29)



Figures 2.22: IR (c) (KBr windows) and $^1\text{H-NMR}$ (d) (in CDCl_3 , 300MHz) spectra of (c-d) ALD 2, isolated from the extract of PP stabilised with 39% Toc, pass 4 (CPC series, single screw extruder, 270°C) (see tables 2.29 and 2.30, respectively, and section 2.7.1)

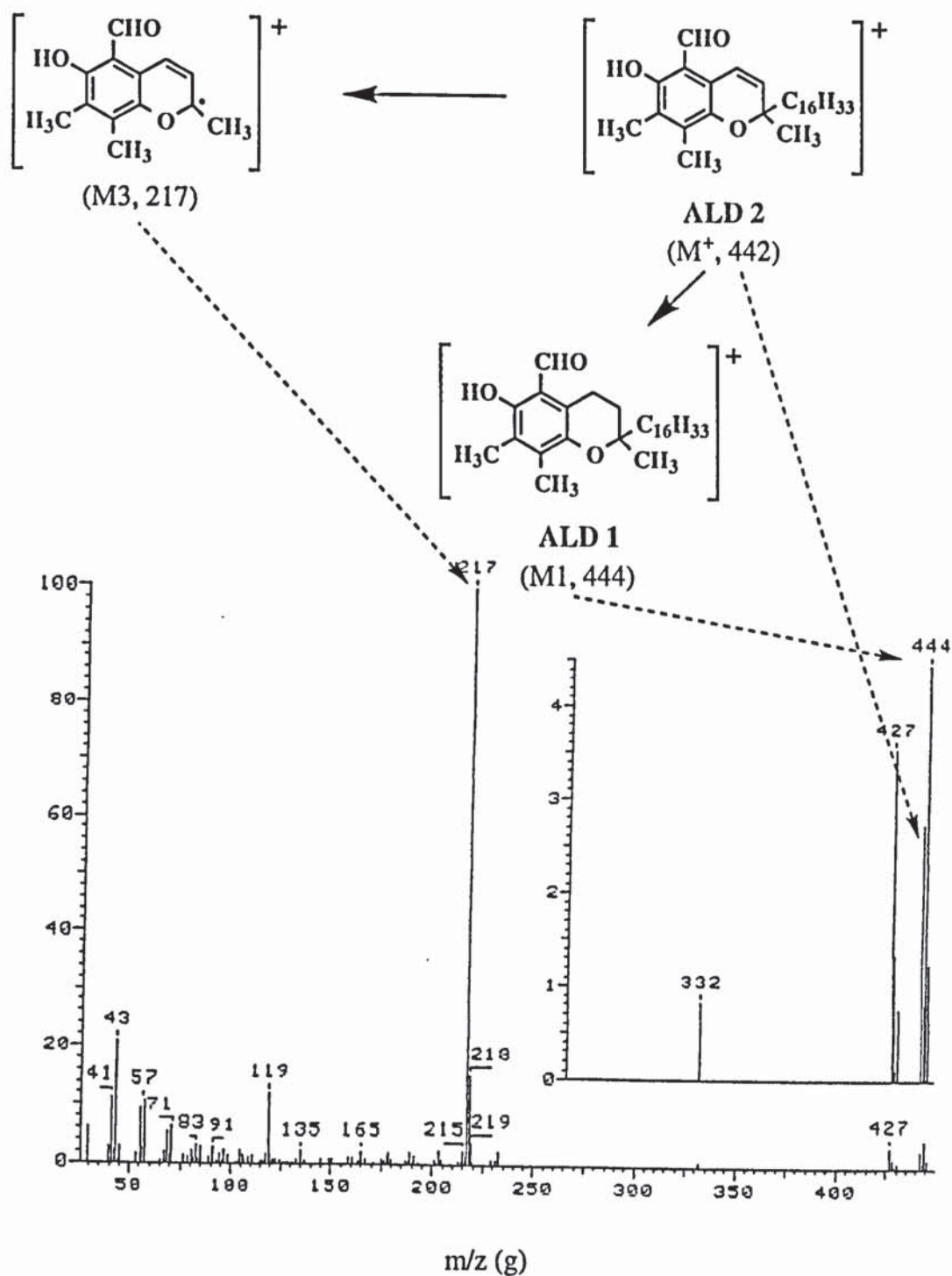
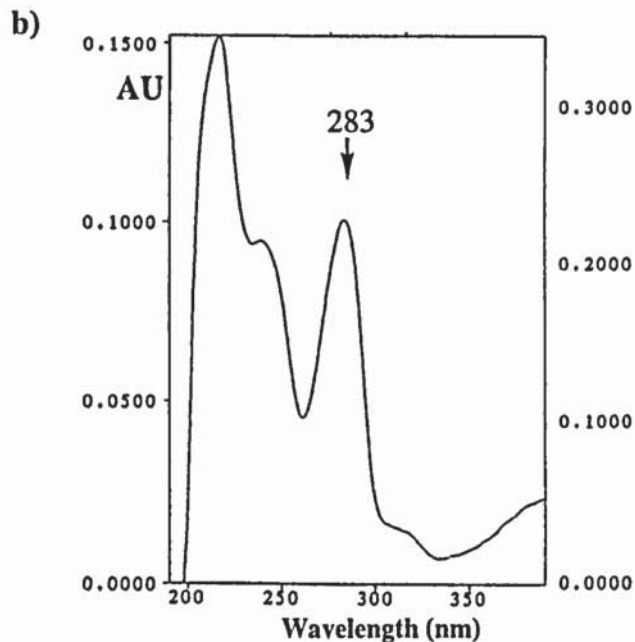
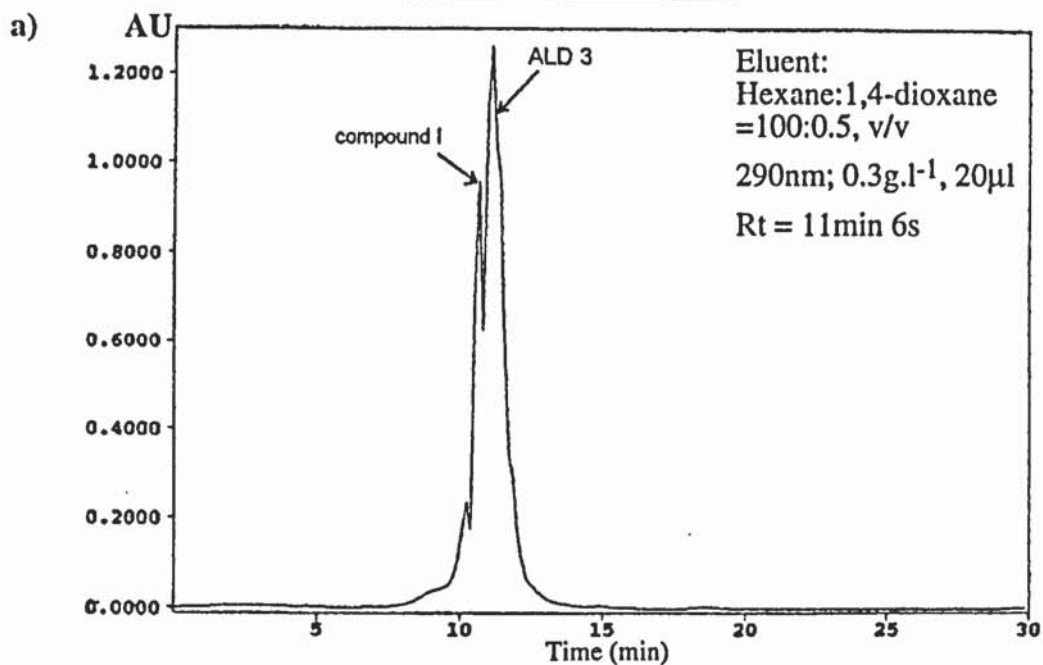
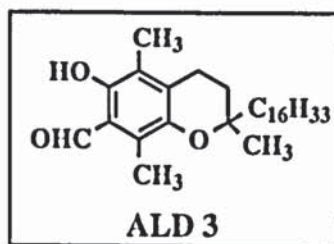


Figure 2.22.e: EI-MS spectrum of ALD 2, isolated from the extract of PP stabilised with 39% Toc, pass 4 (CPC series, single screw extruder, 270°C), in acetate (see section 2.7.1 and table 2.32)



Figures 2.23: HPLC (a) and UV (b) analysis of ALD 3, isolated from the extract of PP

(a-b) stabilised with 39% Toc, pass 4 (CPC789 series, single screw extruder, 270°C), in hexane (see section 2.7.1)

a) Instruments: Philips PU4100 liquid chromatograph and PU4120 diode array detector; column: Zorbax SIL (4.6mm x25cm); flow rate: 1ml.min⁻¹

b) UV spectrum, diode array system (see table 2.29)

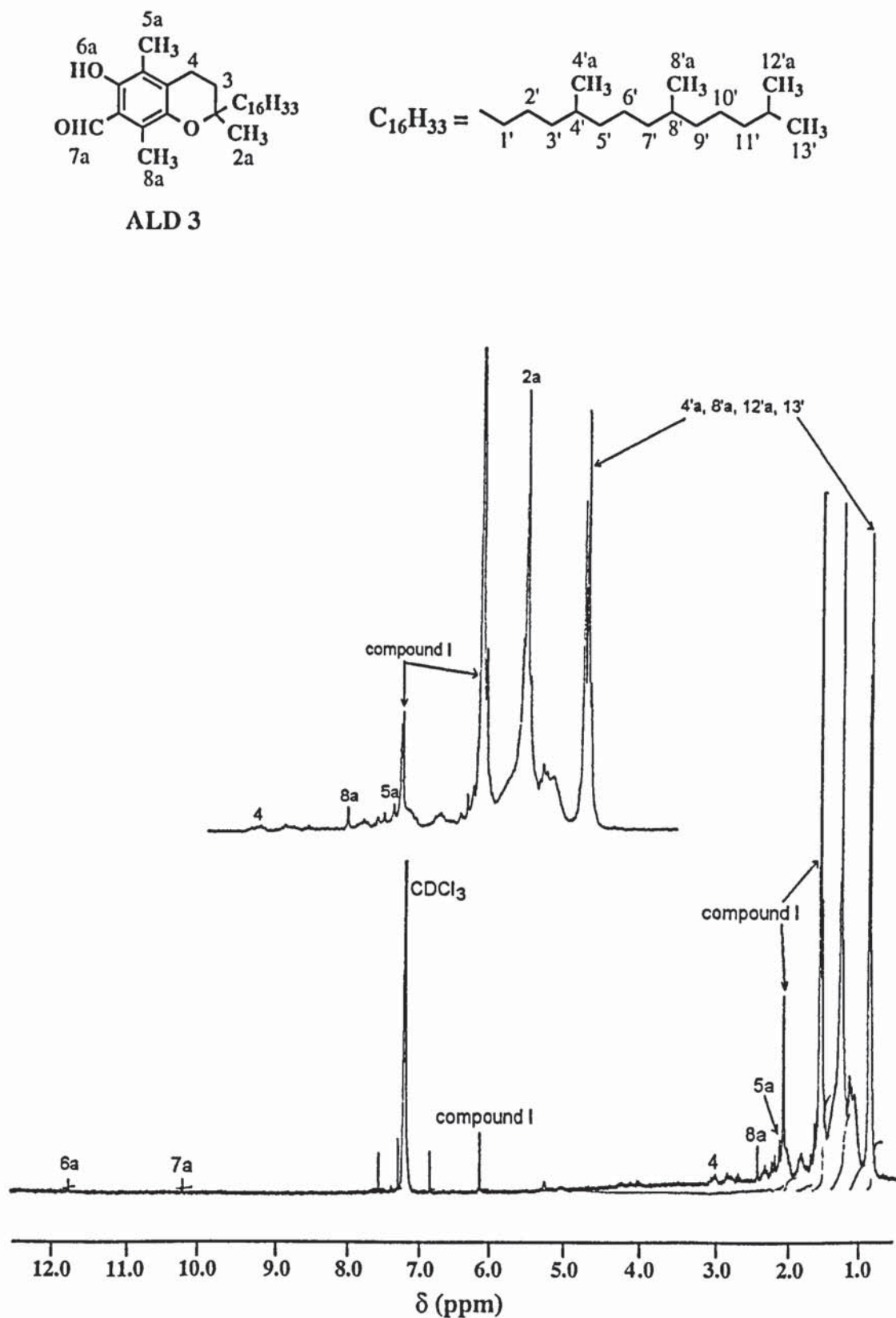
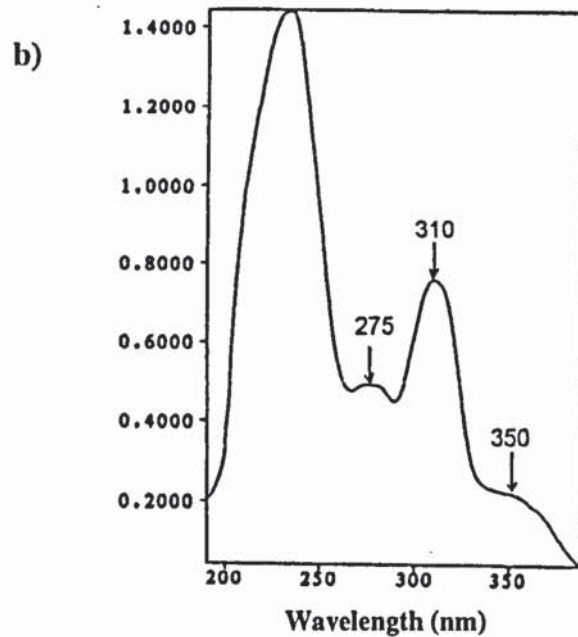
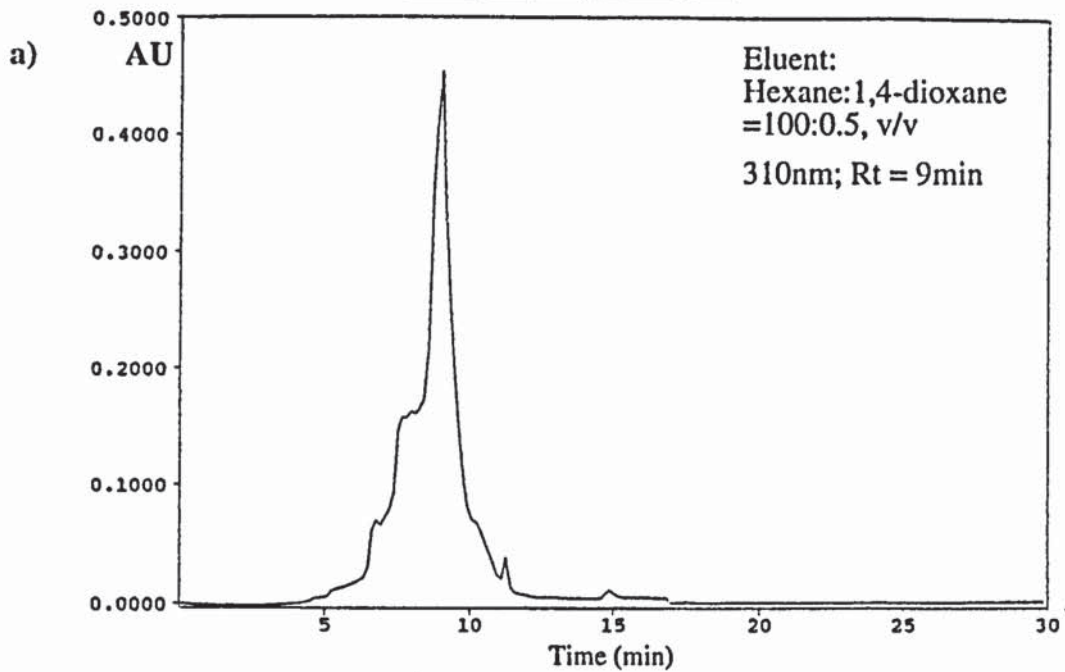
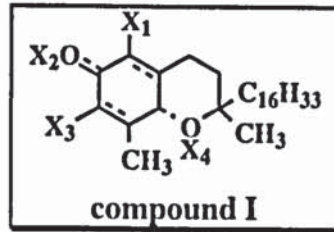


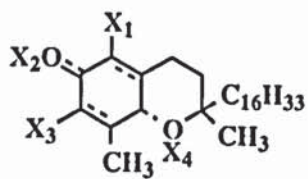
Figure 2.23.c: ¹H-NMR spectrum of ALD 3 (+ presence of compound I), isolated from the extract of PP stabilised with 39% Toc, pass 4 (CPC789 series, single screw extruder, 270°C), in CDCl₃, at 300MHz (see section 2.7.1 and table 2.30)



Figures 2.24: HPLC (a) and UV (b) analysis of compound I, isolated from the extract of (a-b) PP stabilised with 39% Toc, pass 4 (CPC789 series, single screw extruder, 270°C), in hexane (see section 2.7.1)

a) Instruments: Philips PU4100 liquid chromatograph and PU4120 diode array detector; column: Zorbax SIL (4.6mm x25cm); flow rate: 1ml.min⁻¹

b) UV spectrum, diode array system (see table 2.29)



Compound I

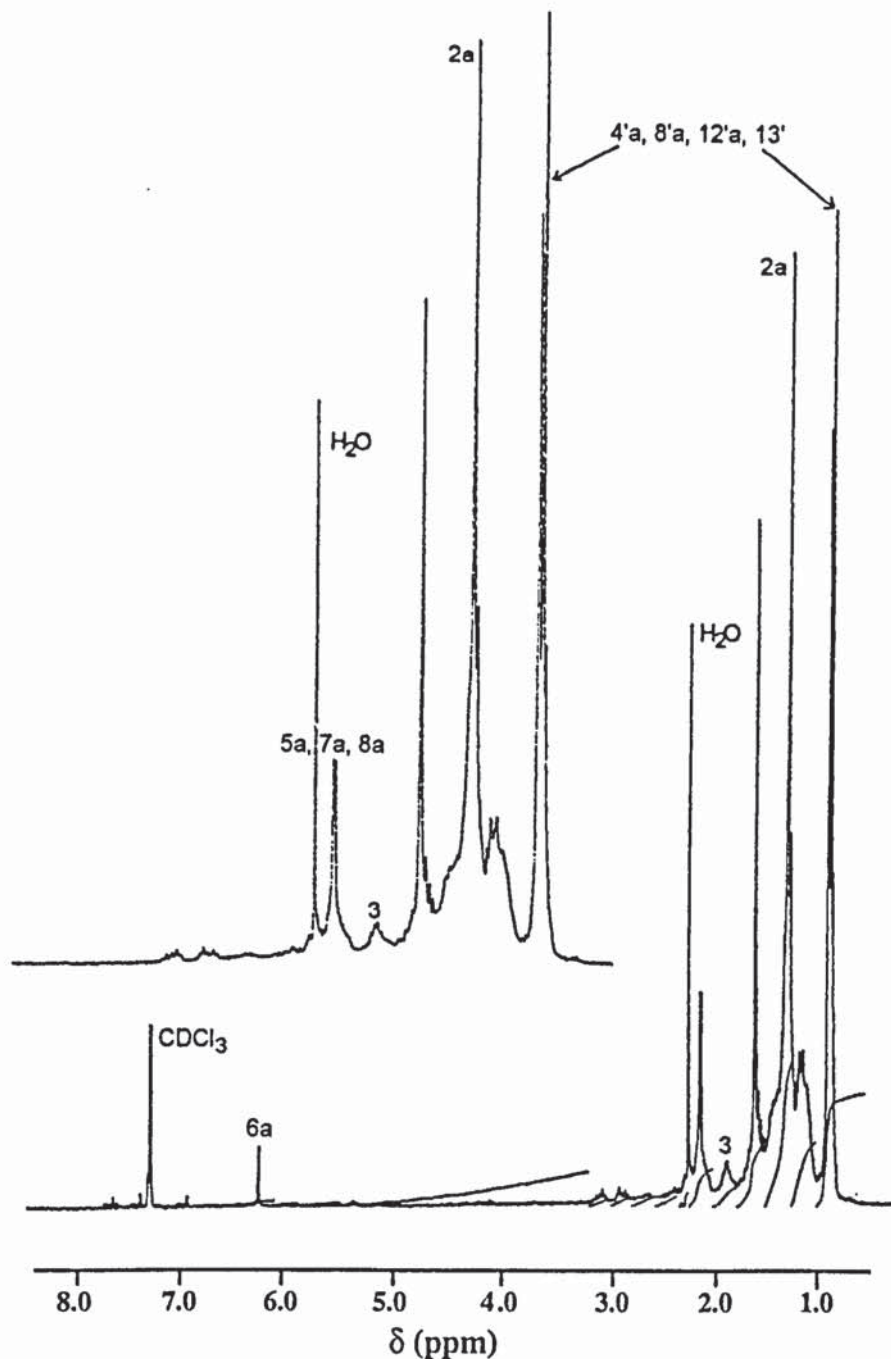
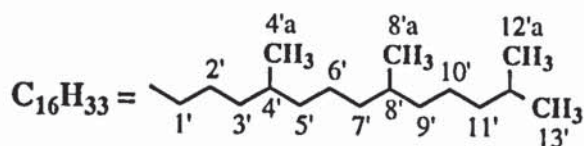


Figure 2.24.c: $^1\text{H-NMR}$ spectrum of compound I, isolated from the extract of PP stabilised with 39% Toc, pass 4 (CPC789 series, single screw extruder, 270°C), in CDCl_3 , at 300MHz (see section 2.7.1 and table 2.30)

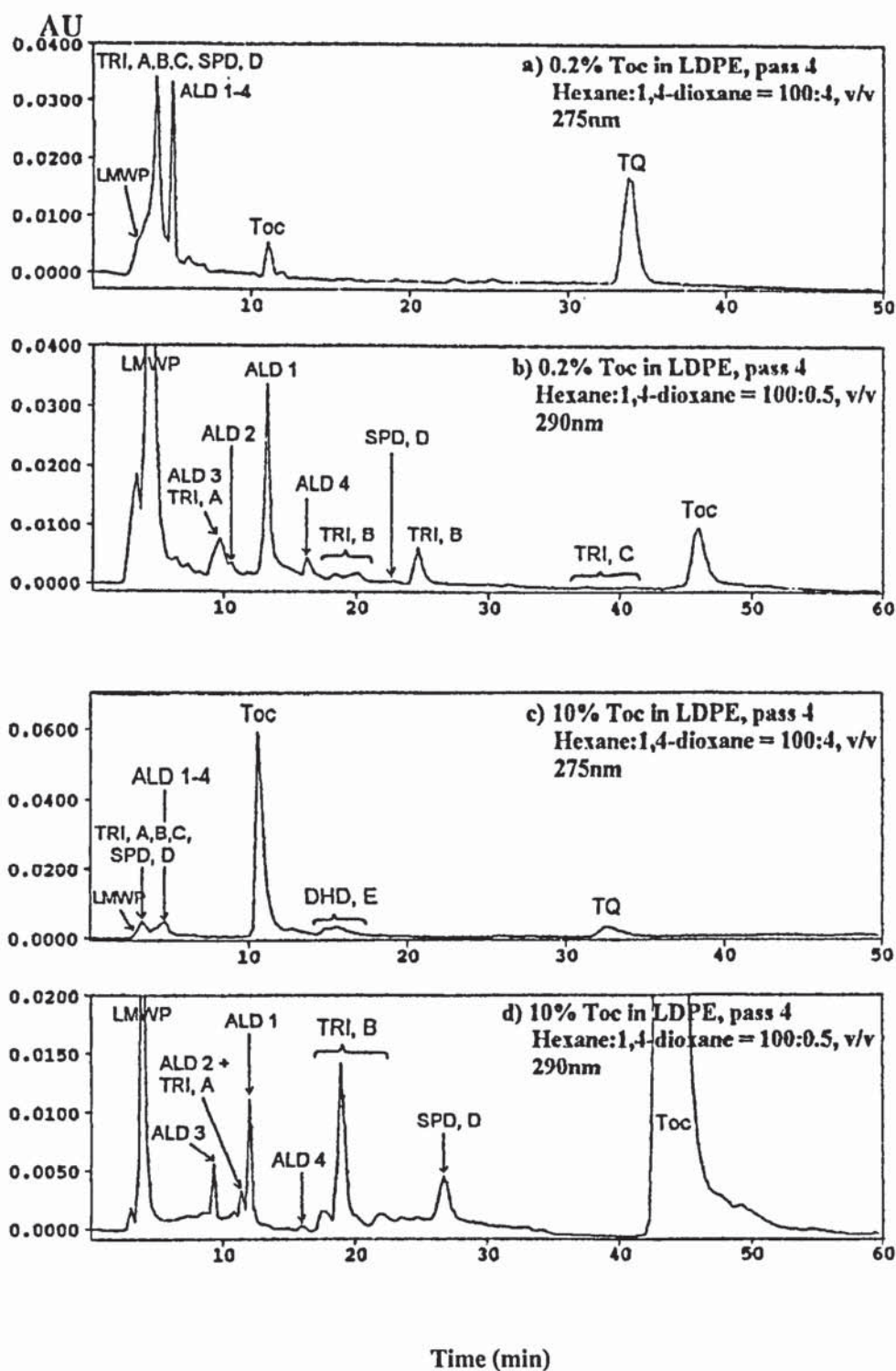
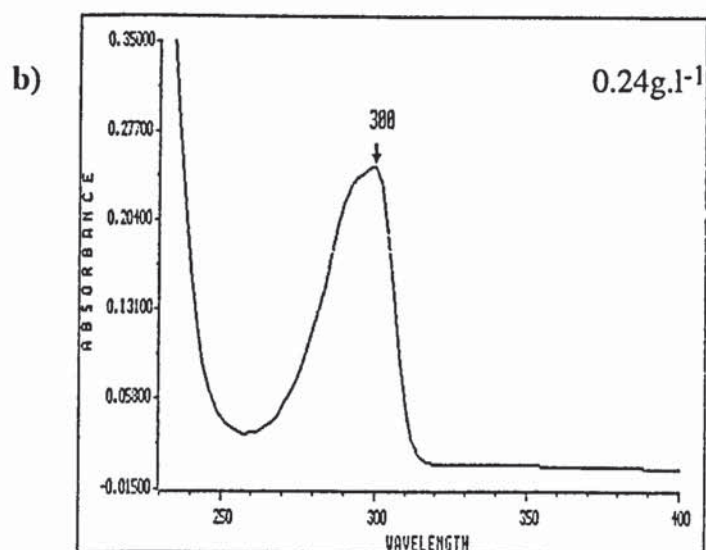
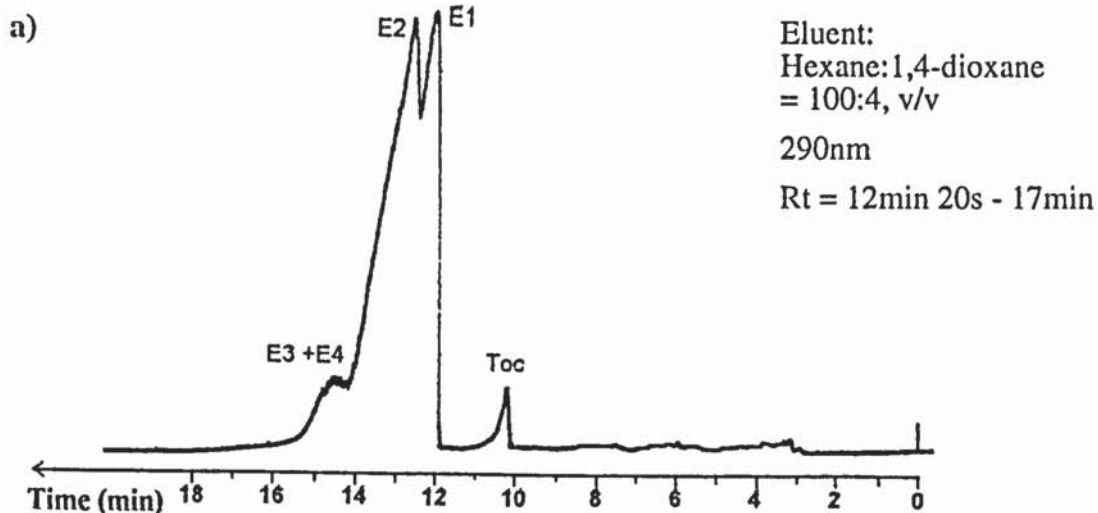
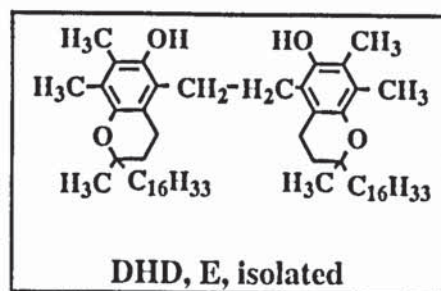


Figure 2.25: HPLC chromatograms of the products extracted from LDPE stabilised with 0.2 (a-b) and 10% (c-d) Toc, passes 4 (single screw extruder, 180°C) (see section 2.8.1)

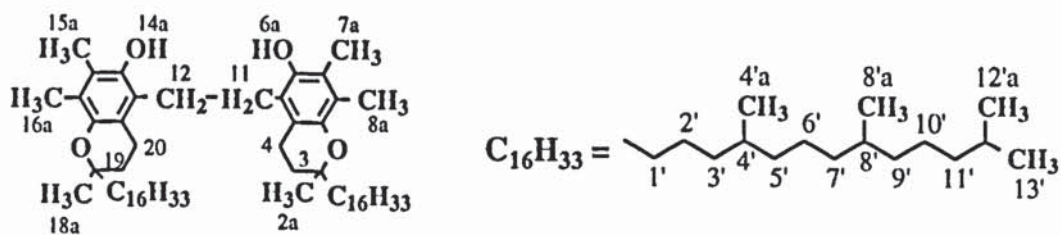
Instrument: Philips PU4100 liquid chromatograph and PU4120 diode array detector; Column: Zorbax SIL (4.6mm x 25cm); Flow rate: 1ml.min⁻¹
 Eluents: hexane:1,4-dioxane = 100:4 (a, c) and 100:0.5 (b, d), v/v



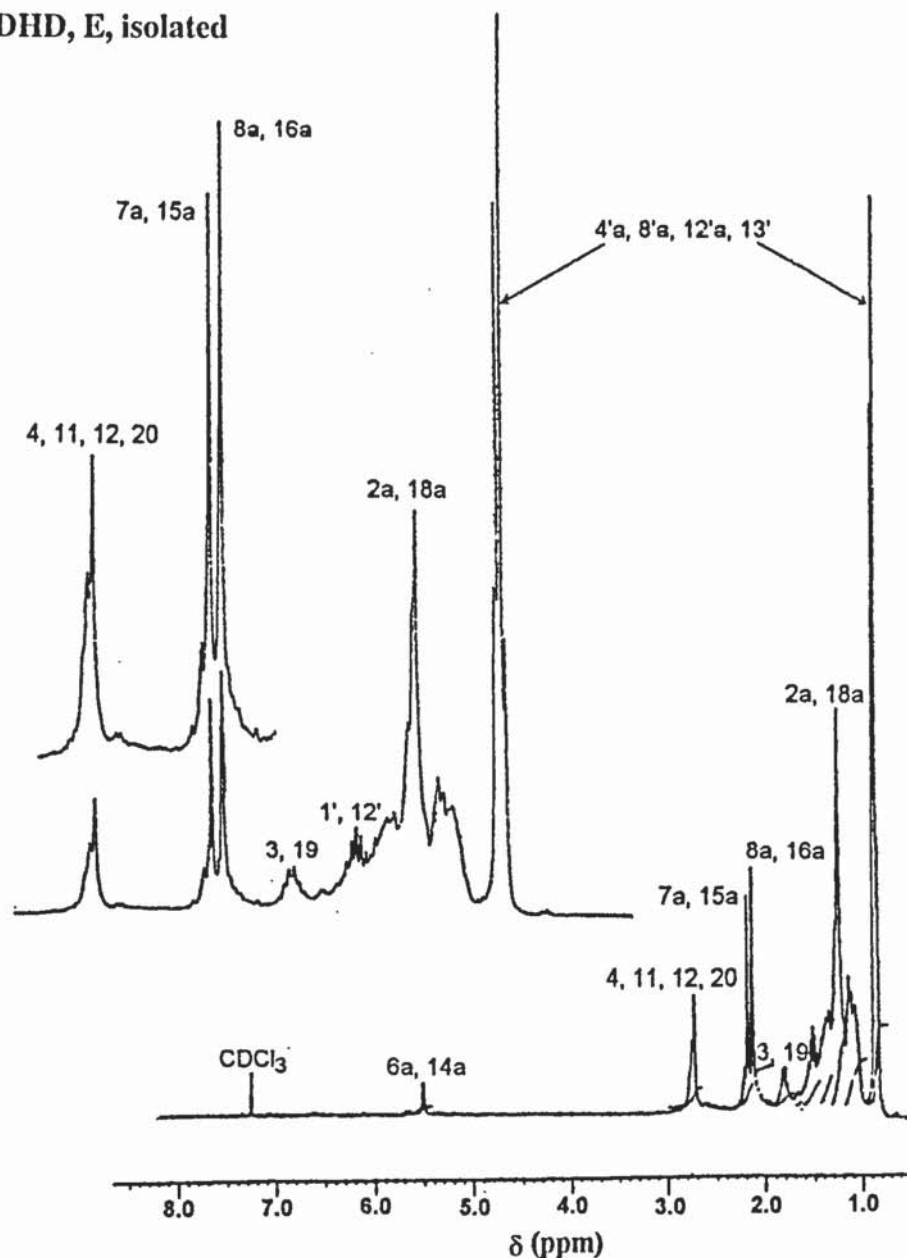
Figures 2.26: HPLC (a) and UV (b) analysis of DHD, E, isolated from the extract of (a-b) LDPE stabilised with 10% Toc, pass 4 (single screw extruder, 180°C), in hexane (see section 2.7.2)

a) Instruments: Gilson 305 piston pump and Dynamax UV-1 variable wavelength detector; column: Zorbax SIL (4.6mm x25cm); flow rate: 1ml.min⁻¹

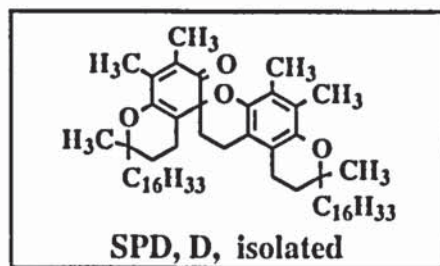
b) Solvent: hexane, 0.24g.l⁻¹ (see table 2.33)



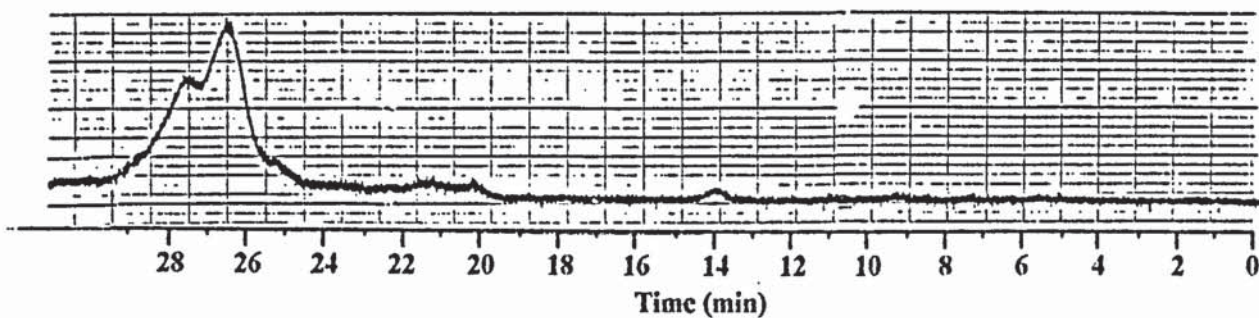
DHD, E, isolated



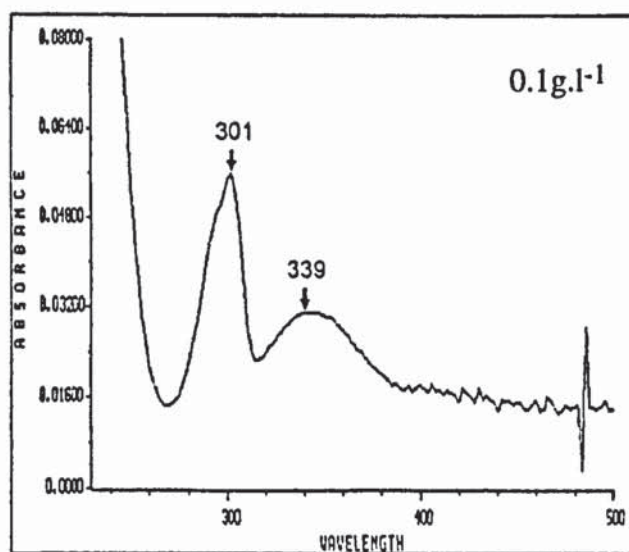
Figures 2.26.c: ^1H -NMR spectrum of DHD, E, isolated from the extract of LDPE stabilised with 10% Toc, pass 4 (single screw extruder, 180°C), in CDCl_3 , at 250MHz (see section 2.7.2 and table 2.34)



- a) Eluent: Hexane:1,4-dioxane
= 100.0.5, v/v
290nm; Rt = 24min

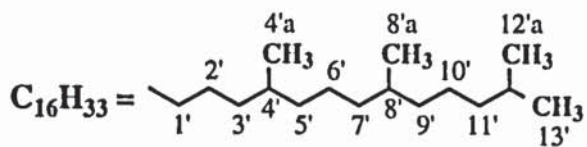
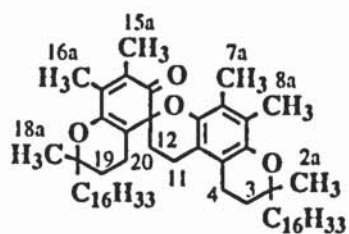


b)

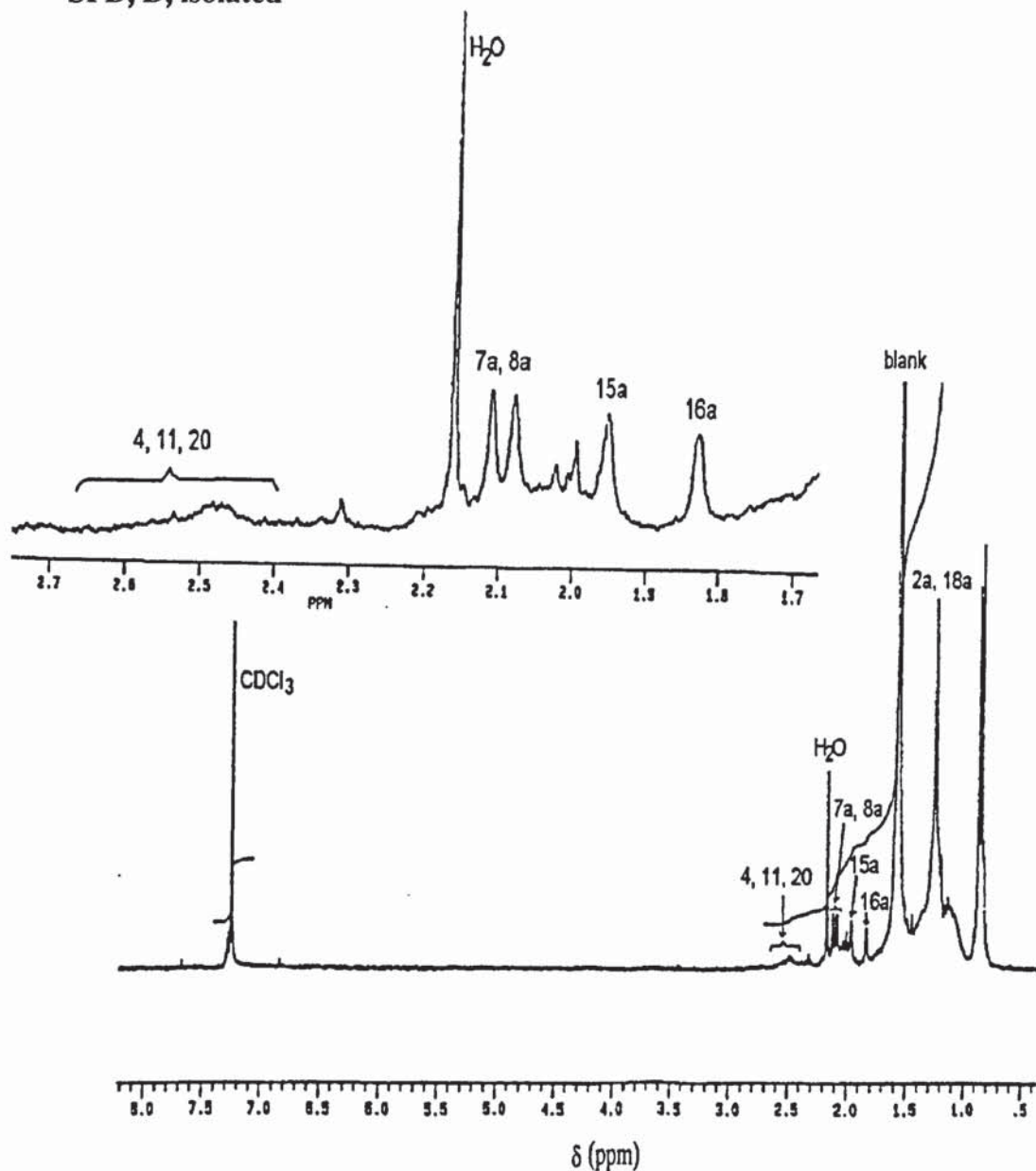


Figures 2.27: HPLC (a) and UV (b) analysis of SPD, D, isolated from the extract of (a-b) LDPE stabilised with 10% Toc, pass 4 (single screw extruder, 180°C), in hexane (see section 2.7.2)

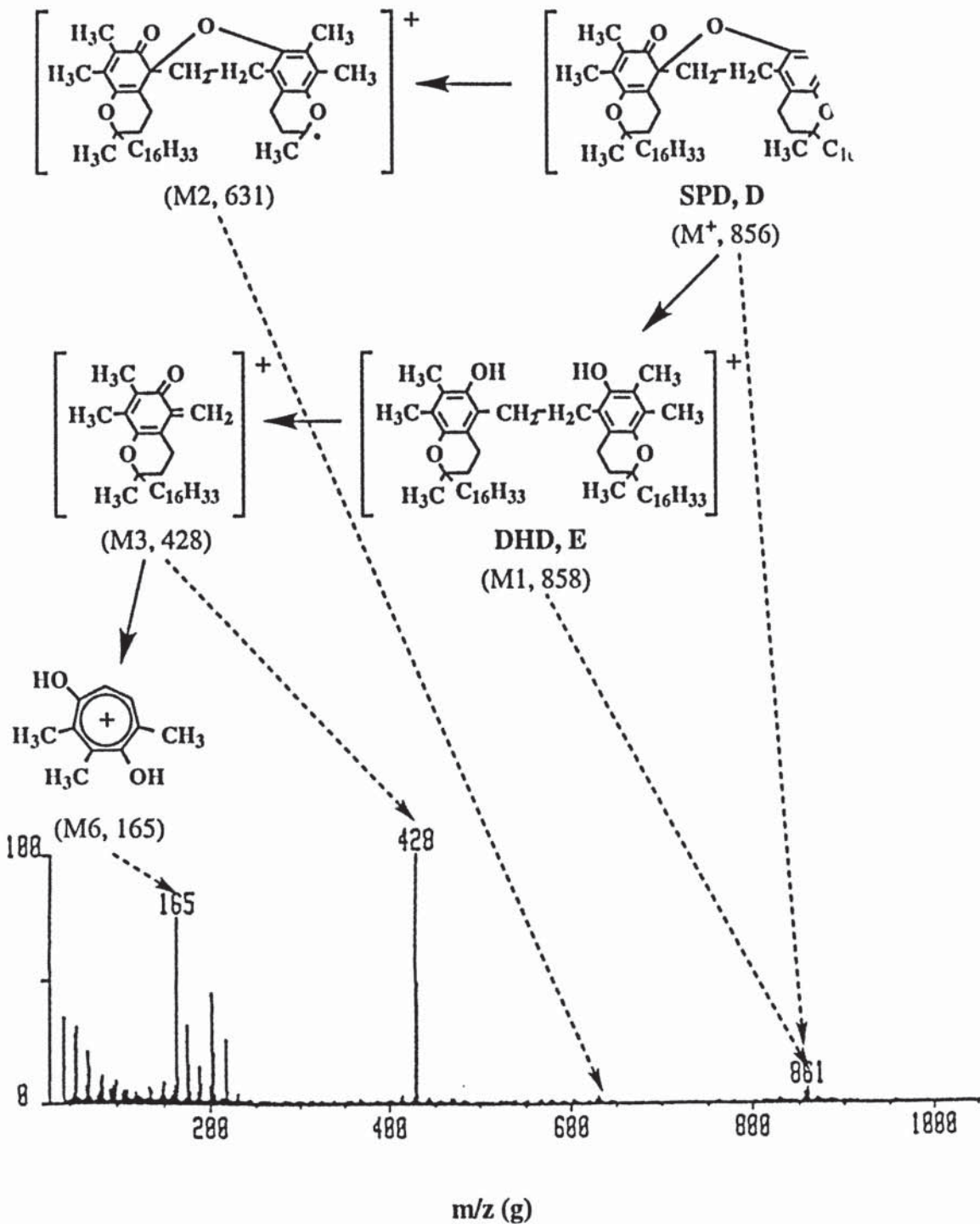
- a) Instruments: Gilson 305 piston pump and Dynamax UV-1 variable wavelength detector; column: Zorbax SIL (4.6mm x25cm); flow rate: 1ml.min⁻¹
b) Solvent: hexane, 0.1g.l⁻¹ (see table 2.33)



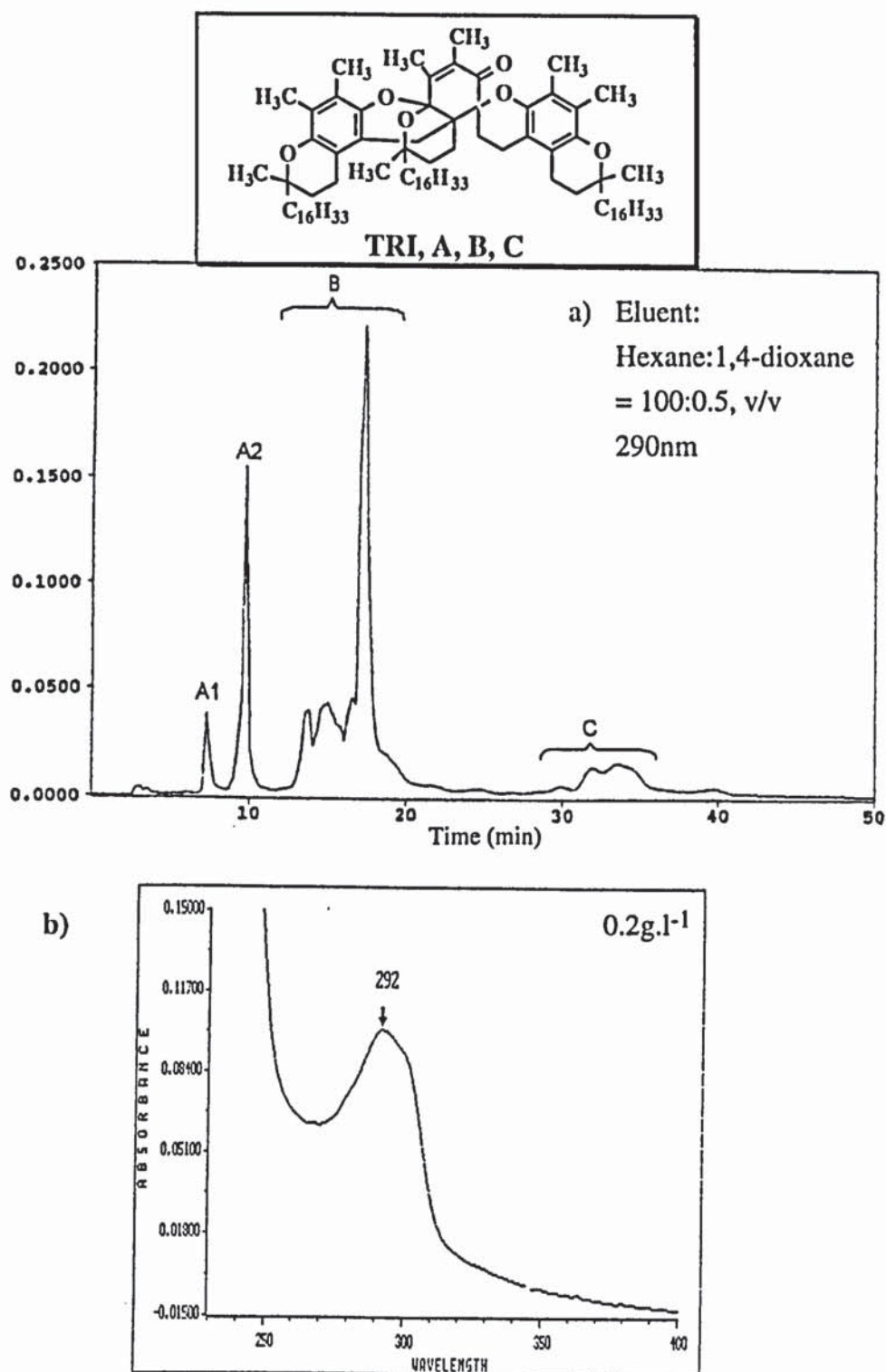
SPD, D, isolated



Figures 2.27.c: $^1\text{H-NMR}$ spectrum of SPD, D, isolated from the extract of LDPE stabilised with 10% Toc, pass 4 (single screw extruder, 180°C), in CDCl_3 , at 250MHz (see section 2.7.2 and table 2.34)

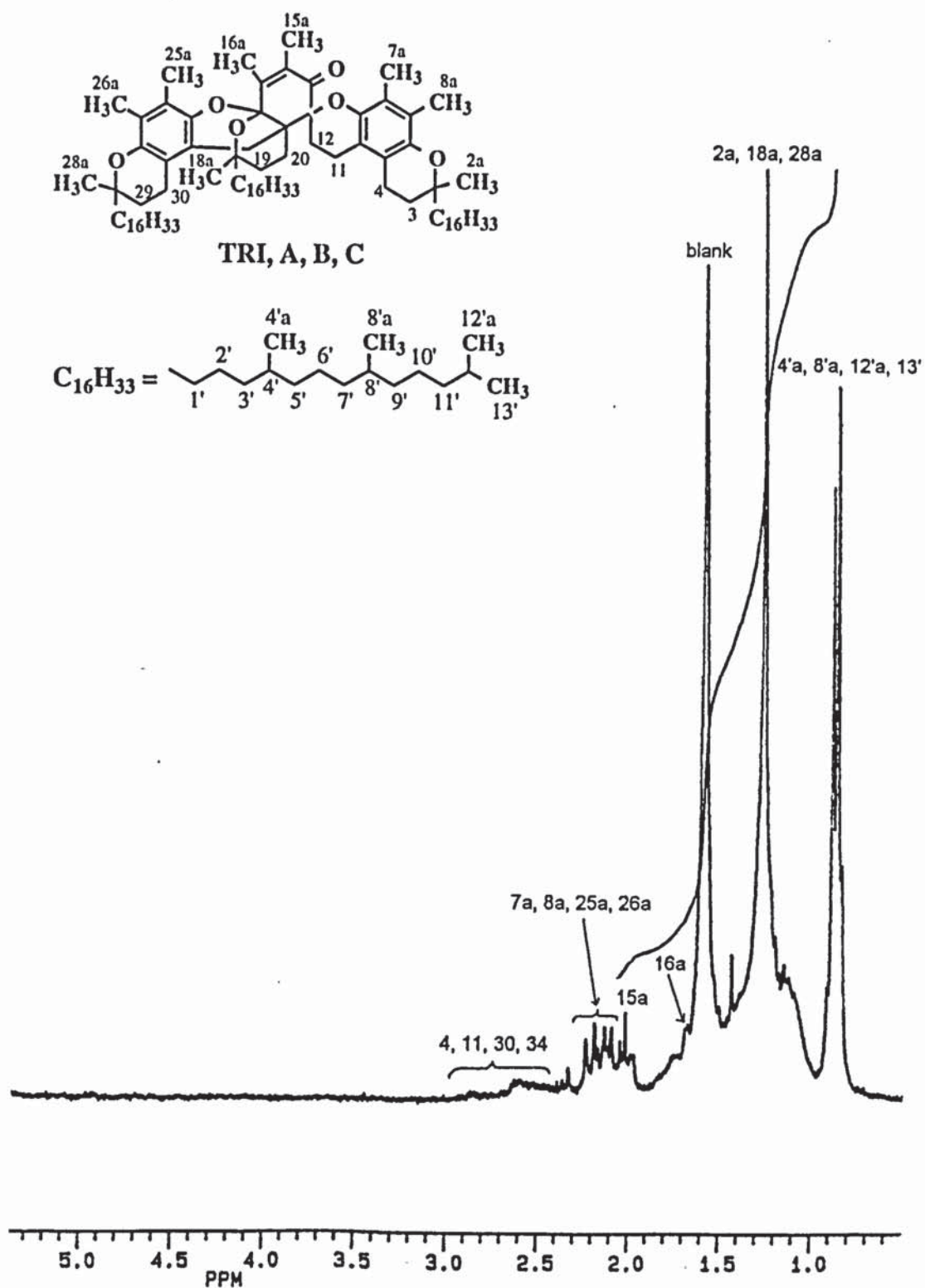


Figures 2.27.d: GC-MS spectrum of SPD, D, isolated from the extract of LDPE stabilised with 10% Toc, pass 4 (single screw extruder, 180°C), in CHCl_3 (see section 2.7.2 and table 2.37)

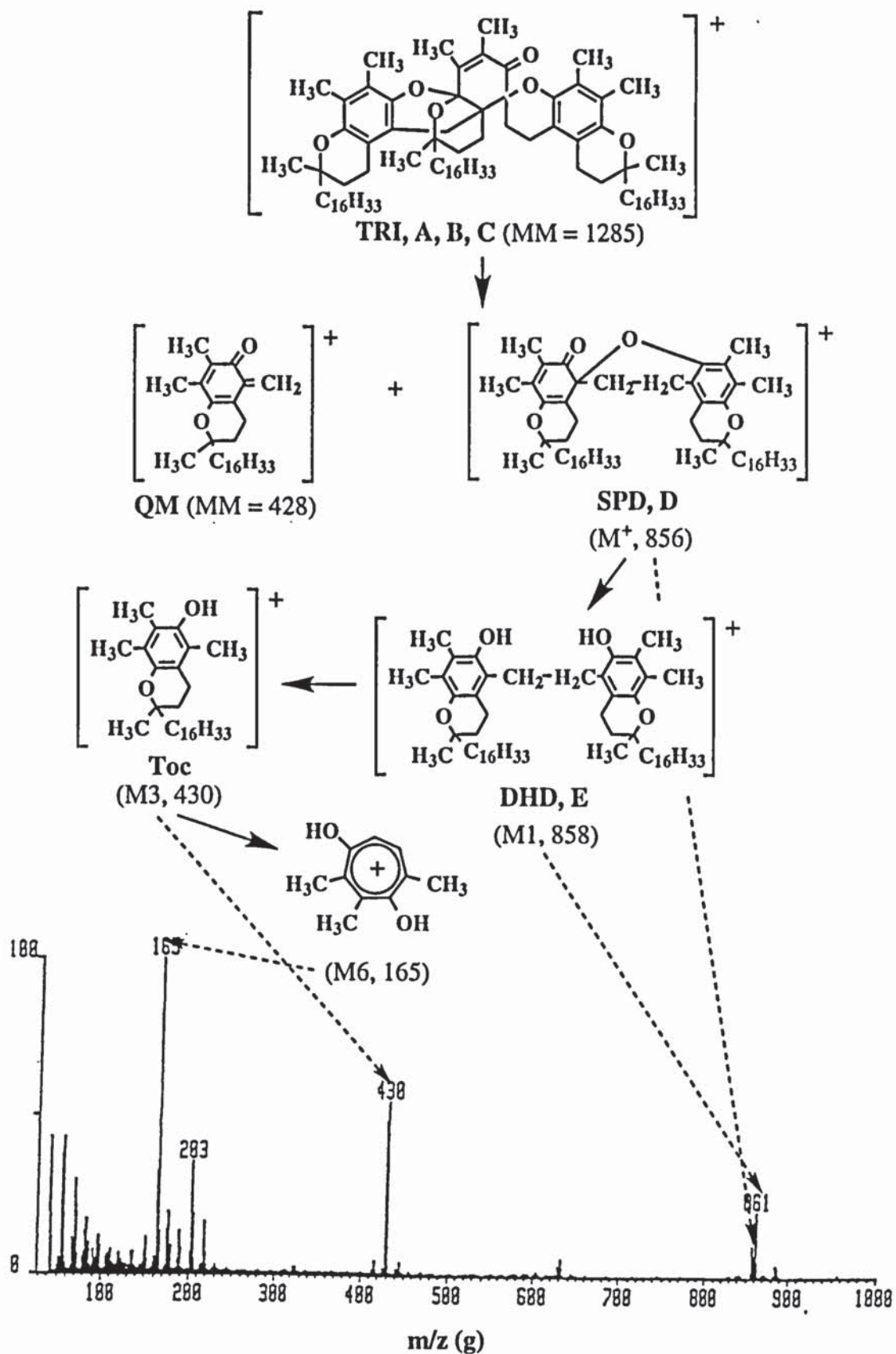


Figures 2.28: HPLC (a) and UV (b) analysis of TRI, A, B, C, isolated from the extract of (a-b) LDPE stabilised with 10% Toc, pass 4 (single screw extruder, 180°C), in hexane (see section 2.7.2)

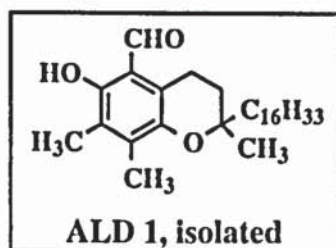
a) Instruments: Gilson 305 piston pump and Dynamax UV-1 variable wavelength detector; column: Zorbax SIL (4.6mm x25cm); flow rate: 1ml.min⁻¹; b) UV spectrum in hexane, 0.2g.l⁻¹ (see table 2.33)



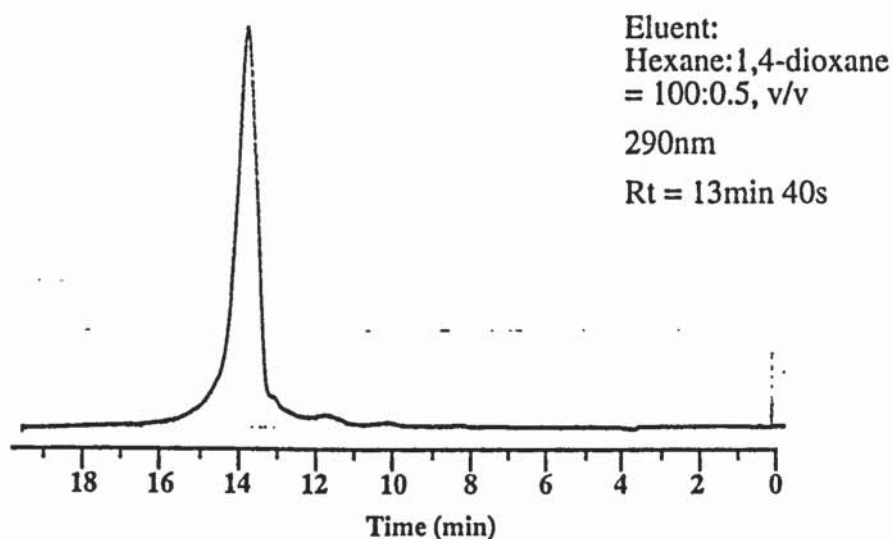
Figures 2.28.c: ¹H-NMR spectrum of TRI, A, B, C, isolated from the extract of LDPE stabilised with 10% Toc, pass 4 (single screw extruder, 180°C), in CDCl₃, at 250MHz (see section 2.7.2 and table 2.35)



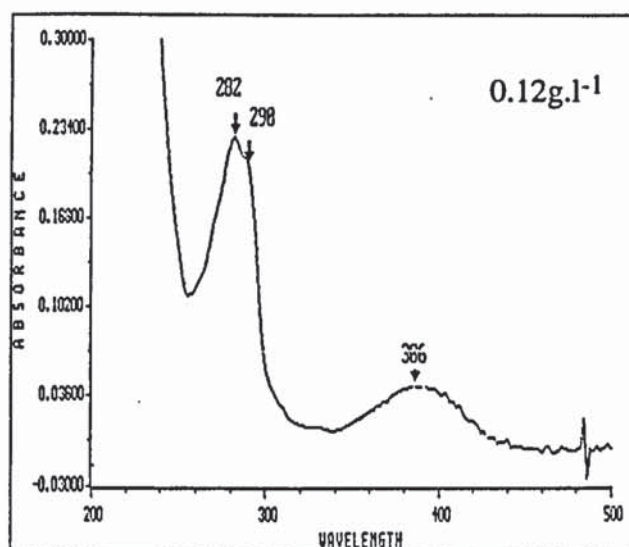
Figures 2.28.d: GC-MS spectrum of TRI, A, B, C, isolated from the extract of LDPE stabilised with 10% Toc, pass 4 (single screw extruder, 180°C), in CHCl₃, (see section 2.7.2 and table 2.38)



a)



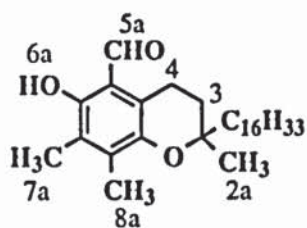
b)



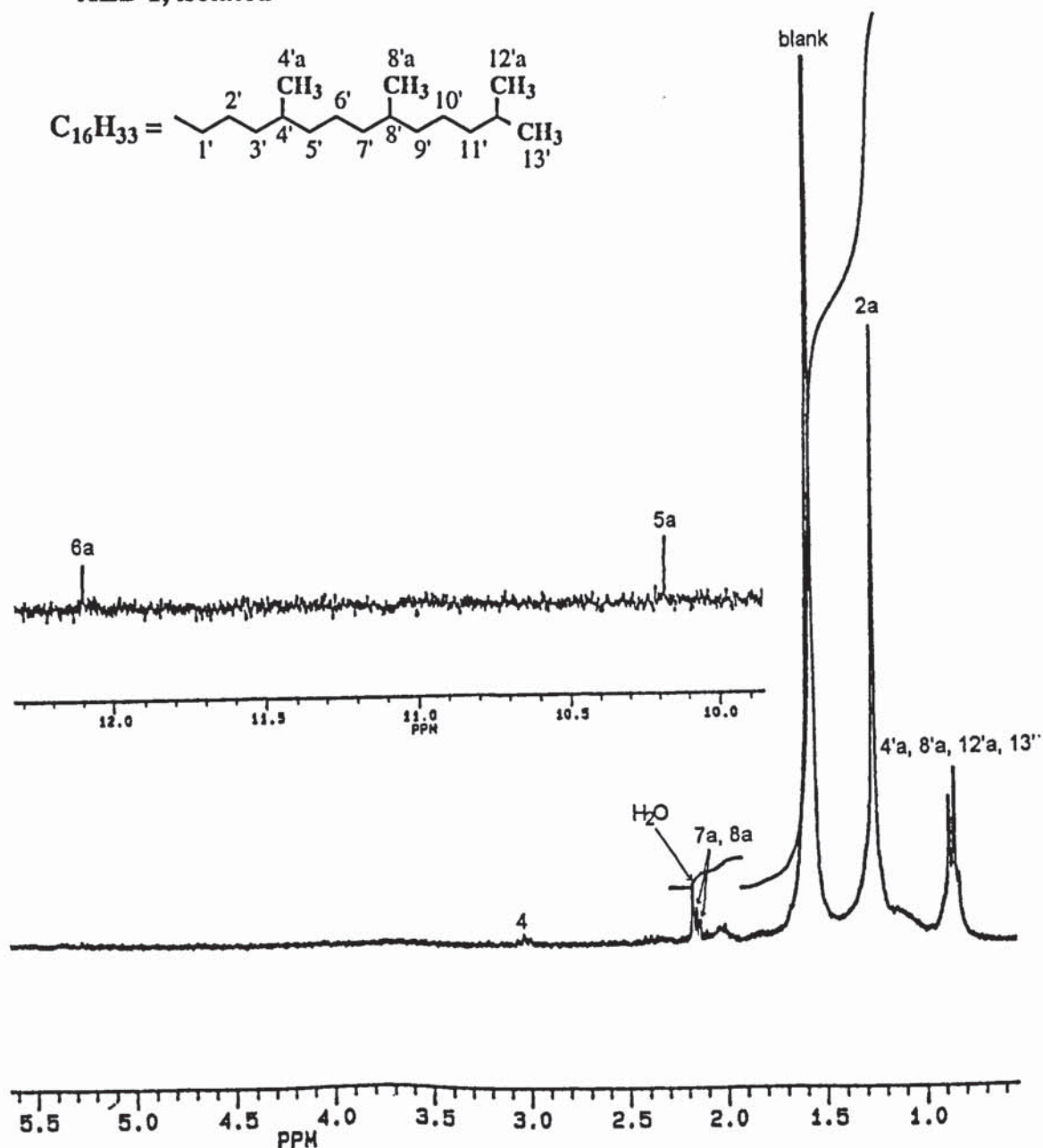
Figures 2.29: HPLC (a) and UV (b) analysis of ALD 1, isolated from the extract of (a-b) LDPE stabilised with 0.2% Toc, pass 4 (single screw extruder, 180°C), in hexane (see section 2.7.2)

a) Instruments: Gilson 305 piston pump and Dynamax UV-1 variable wavelength detector; column: Zorbax SIL (4.6mm x25cm); flow rate: 1ml.min⁻¹

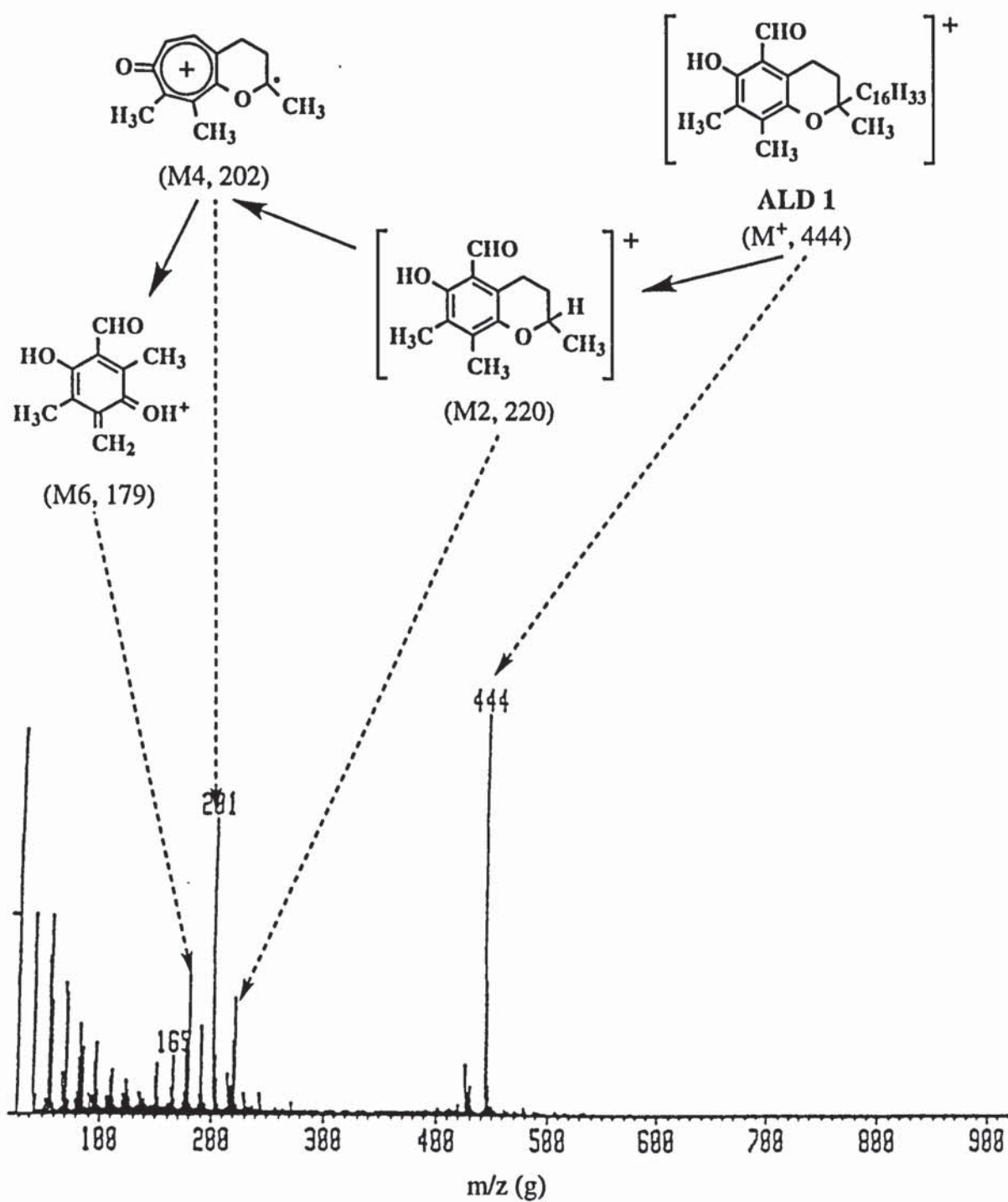
b) Solvent: hexane, 0.12g.l⁻¹ (see table 2.33)



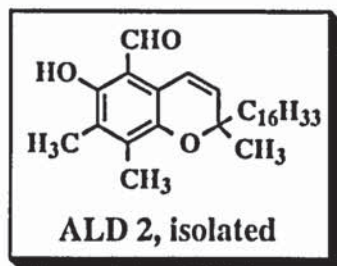
ALD 1, isolated



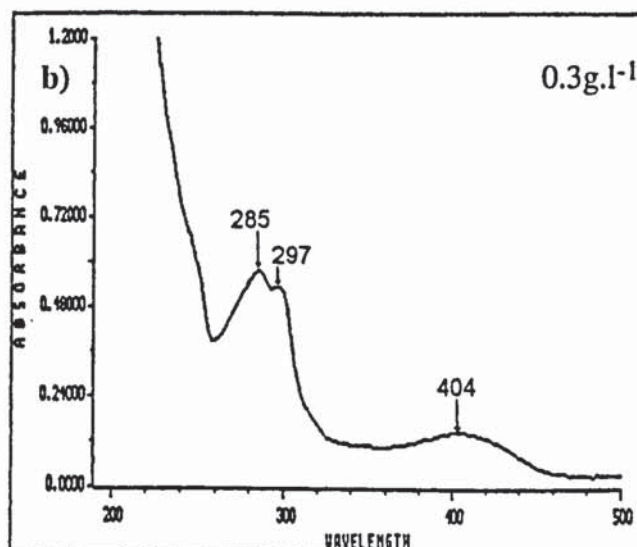
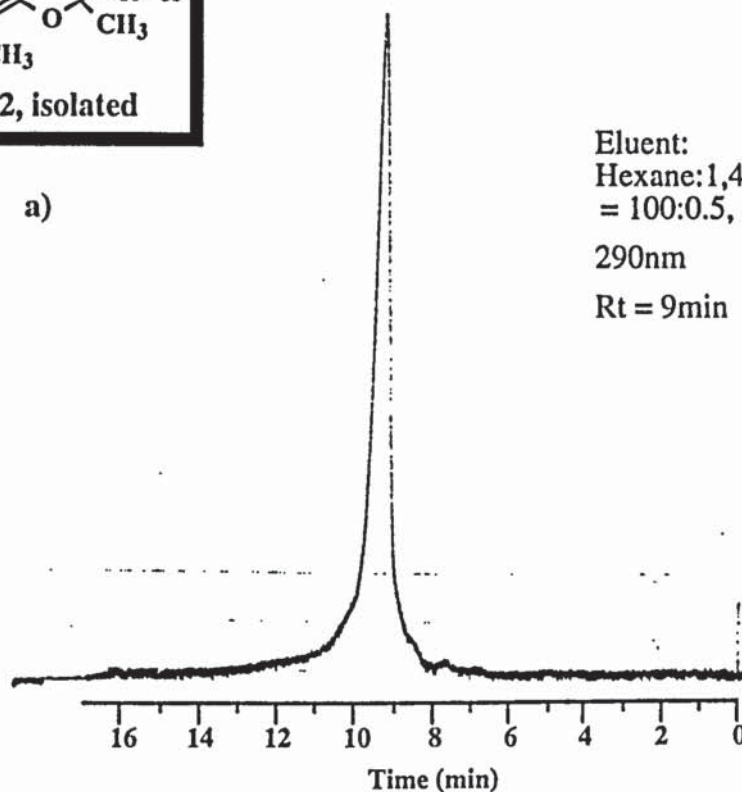
Figures 2.29.c: $^1\text{H-NMR}$ spectrum of ALD 1, isolated from the extract of LDPE stabilised with 0.2% Toc, pass 4 (single screw extruder, 180°C), in CDCl_3 , at 250MHz (see section 2.7.2 and table 2.36)



Figures 2.29.d: GC-MS spectrum of ALD 1, isolated from the extract of LDPE stabilised with 0.2% Toc, pass 4 (single screw extruder, 180°C), in CHCl₃ (see section 2.7.2 and table 2.39)



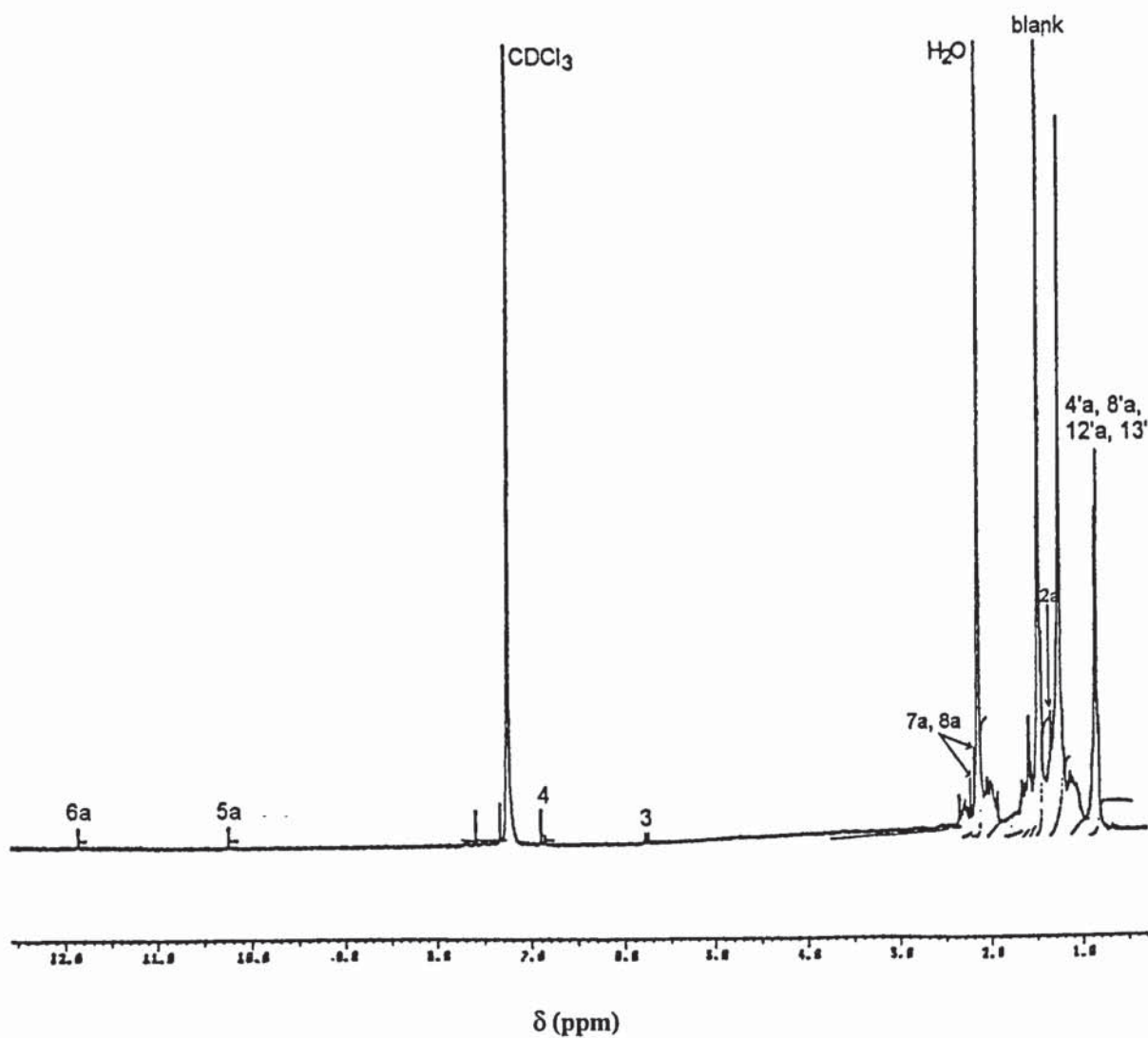
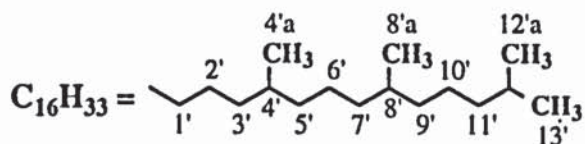
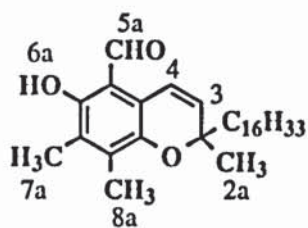
a)



Figures 2.30: HPLC (a) and UV (b) analysis of ALD 2, isolated from the extract of (a-b) LDPE stabilised with 0.2% Toc, pass 4 (single screw extruder, 180°C), in hexane (see section 2.7.2)

a) Instruments: Gilson 305 piston pump and Dynamax UV-1 variable wavelength detector; column: Zorbax SIL (4.6mm x25cm); flow rate: 1ml.min⁻¹

b) Solvent: hexane, 0.3g.l⁻¹ (see table 2.33)



Figures 2.30.c: ¹H-NMR spectrum of ALD 2, isolated from the extract of LDPE stabilised with 0.2% Toc, pass 4 (single screw extruder, 180°C), in CDCl₃, at 250MHz (see section 2.7.2 and table 2.36)

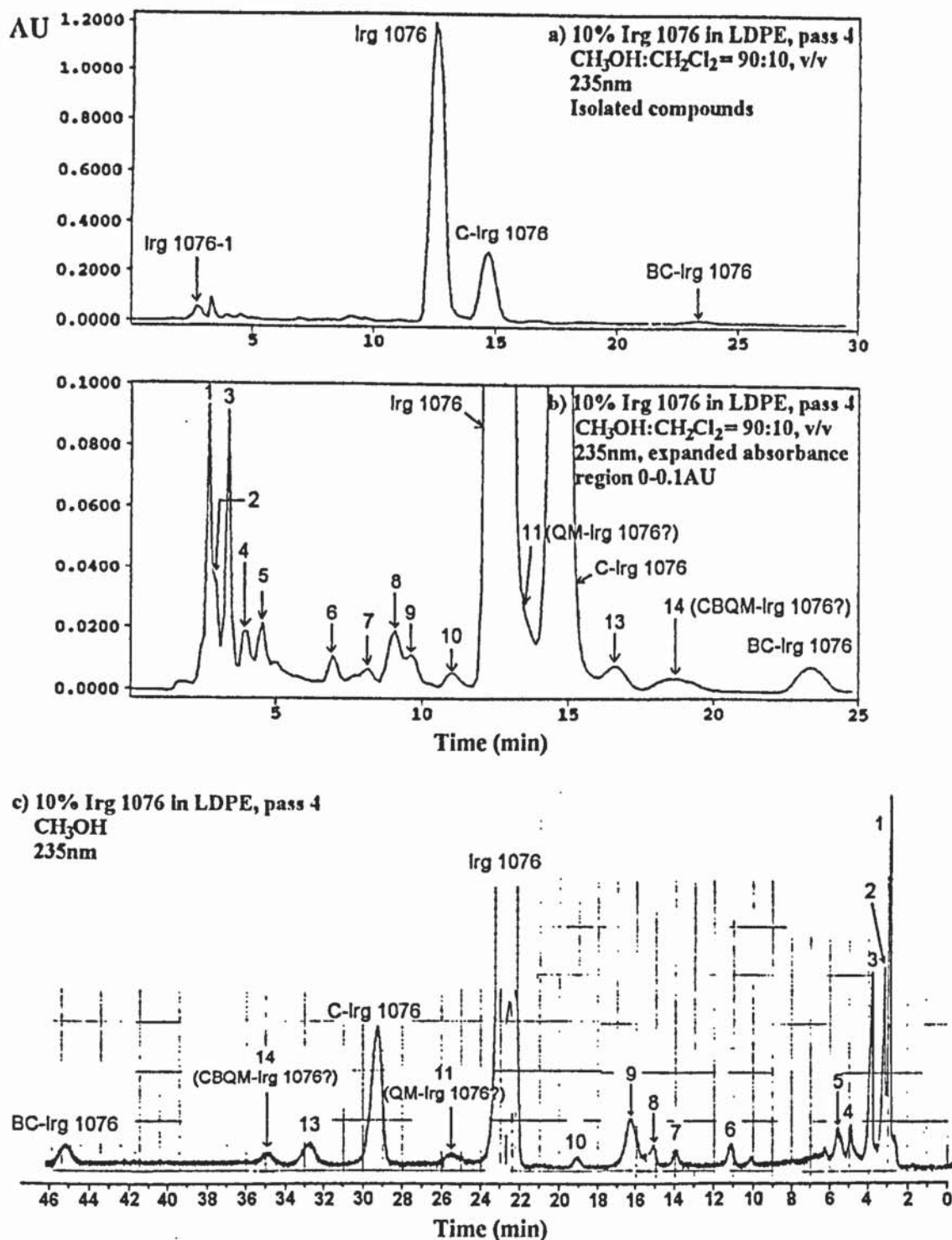


Figure 2.31: HPLC chromatograms of the products extracted from LDPE stabilised with 10% Irg 1076, pass 4 (single screw extruder, 180°C) (see section 2.8.1)
 Instruments: a) and b) Philips PU4100 liquid chromatograph and PU4120 diode array detector, c) Gilson 305 piston pump and variable Dynamax UV-1 variable wavelength absorbance detector; Column: Zorbax ODS (4.6mm x 25cm); Flow rate: 1ml.min⁻¹
 Eluents: $\text{CH}_3\text{OH}:\text{CH}_2\text{Cl}_2 = 90:10, \text{v/v}$, (a and b) and CH_3OH (c)

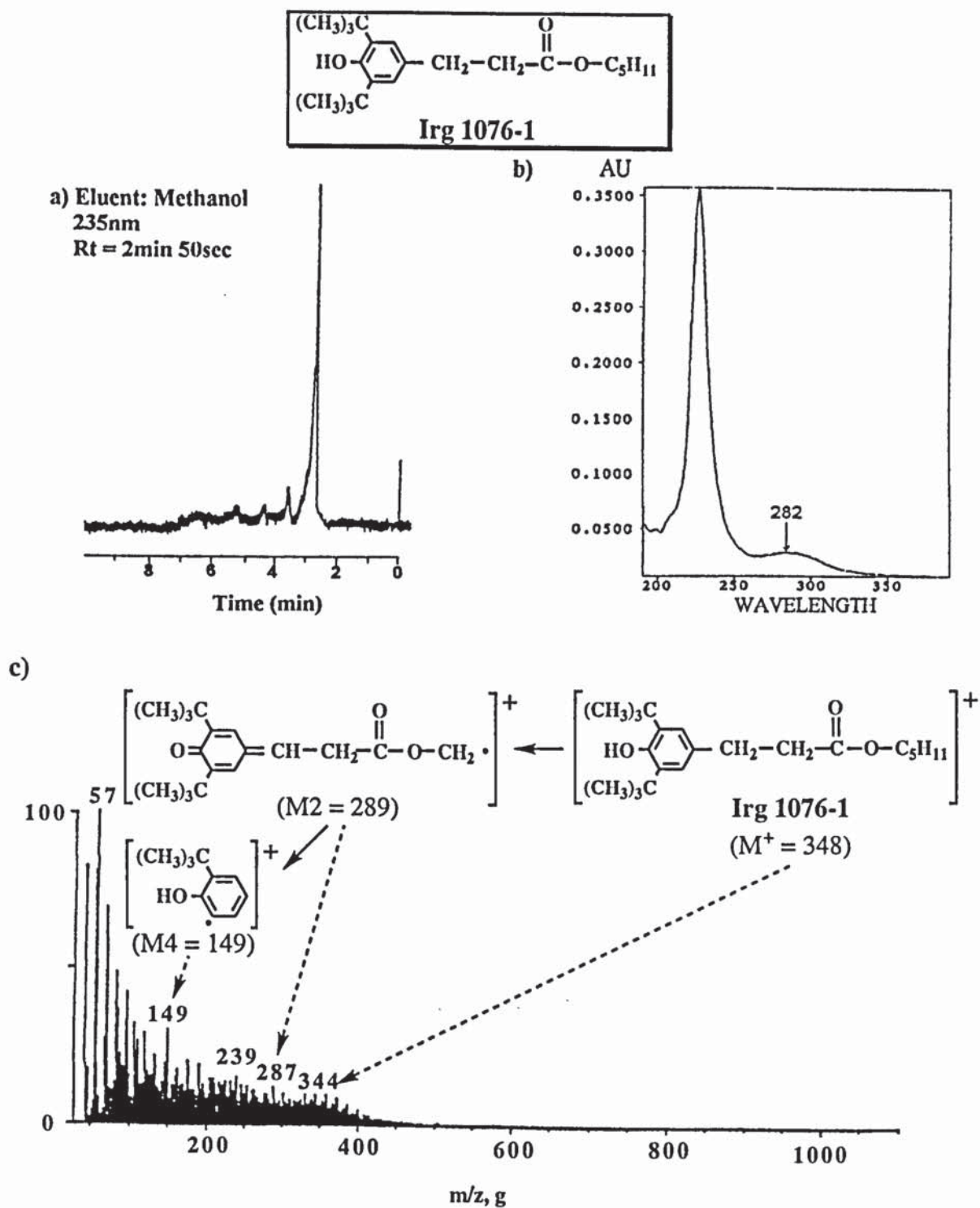


Figure 2.32: HPLC (a), UV (b) and GC-MS analysis (c) of Irg 1076-1 isolated from the extract of LDPE stabilised with 10% Irg 1076, pass 4 (single screw extruder, 180°C) (see section 2.8.1)

- a) Instrument: Gilson 305 piston pump and variable Dynamax UV-1 variable wavelength absorbance detector; Column: Zorbax ODS (4.6mm x 25cm); Flow rate: 1ml.min⁻¹; Eluent: methanol
- b) Solvent: dichloromethane (see table 2.41)
- c) Solvent: chloroform (see table 2.44)

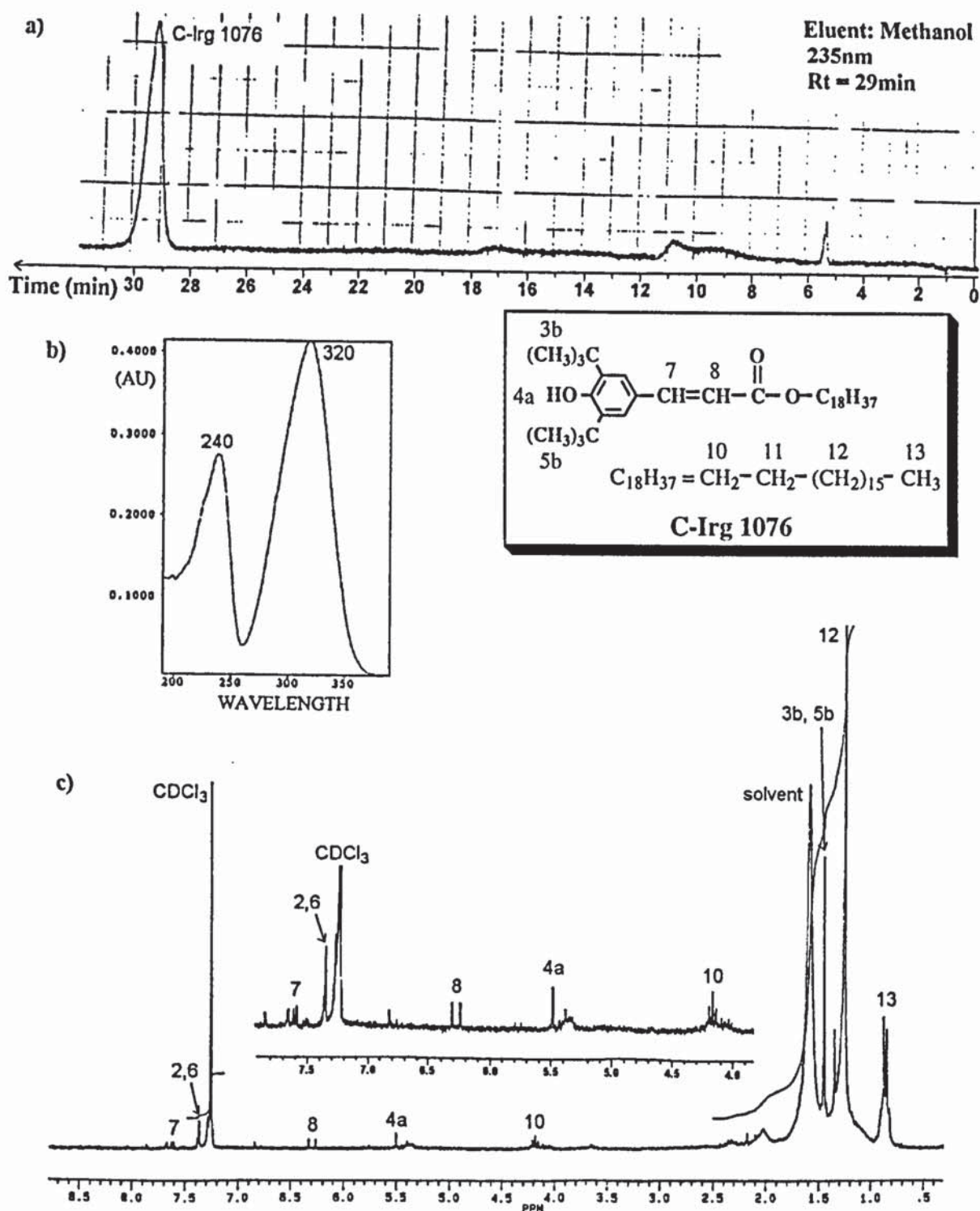


Figure 2.33: HPLC (a), UV (b) and ¹H-NMR analysis (c) of C-Irg 1076 (compound 12)

(a-c) isolated from the extract of LDPE stabilised with 10% Irg 1076, pass 4 (single screw extruder, 180°C) (see section 2.8.1)

a) Instrument: Gilson 305 piston pump and variable Dynamax UV-1 variable wavelength absorbance detector; Column: Zorbax ODS (4.6mm x 25cm); Flow rate: 1ml.min⁻¹; Eluent: methanol

b) Solvent: dichloromethane (see table 2.41)

c) Solvent: deuterated chloroform (see table 2.43)

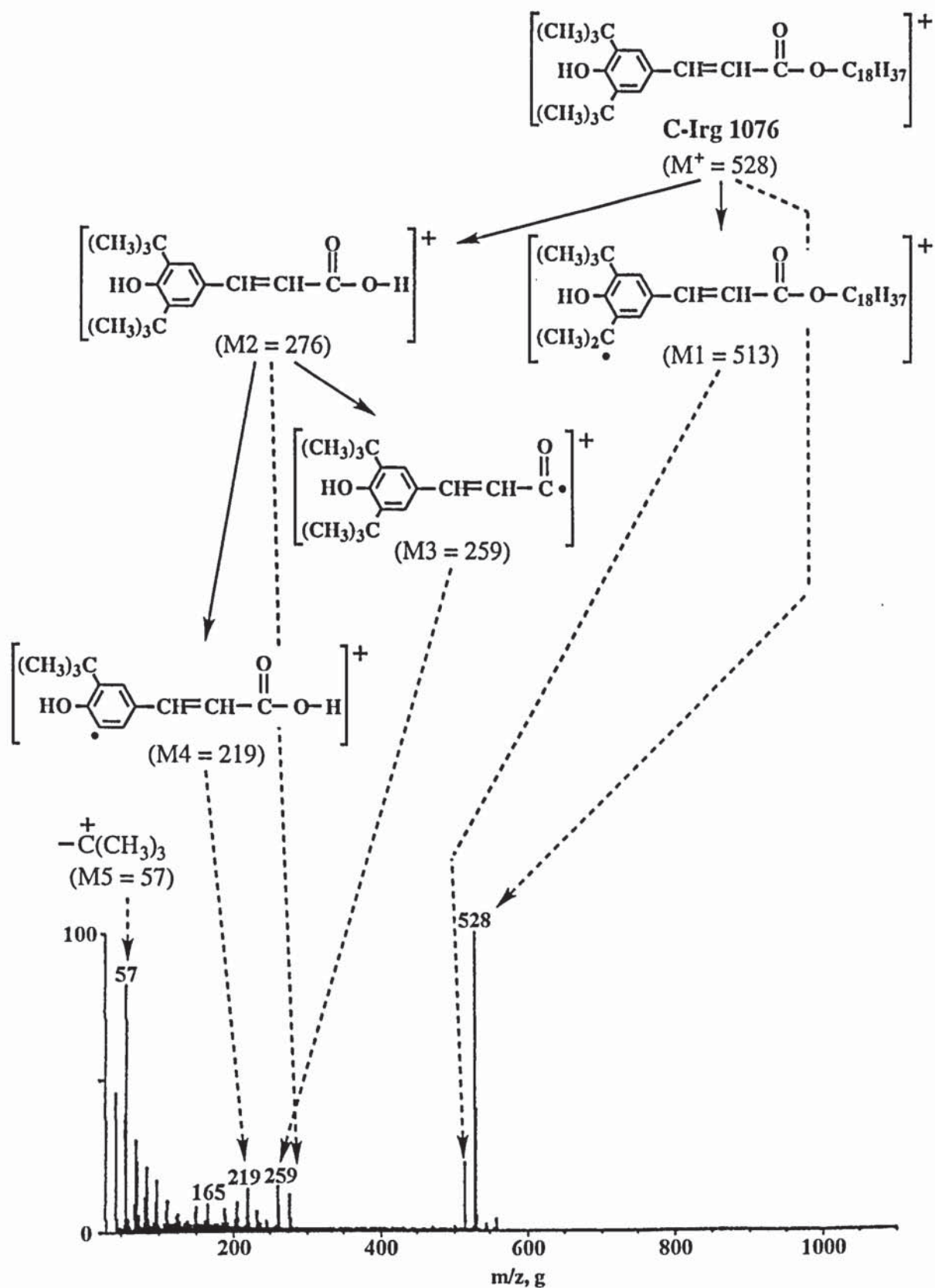


Figure 2.33.d: GC-MS analysis of C-Irg 1076 (compound 12) isolated from the extract of LDPE stabilised with 10% Irg 1076, pass 4 (single screw extruder, 180°C); Solvent: chloroform (see table 2.45 and section 2.8.1)

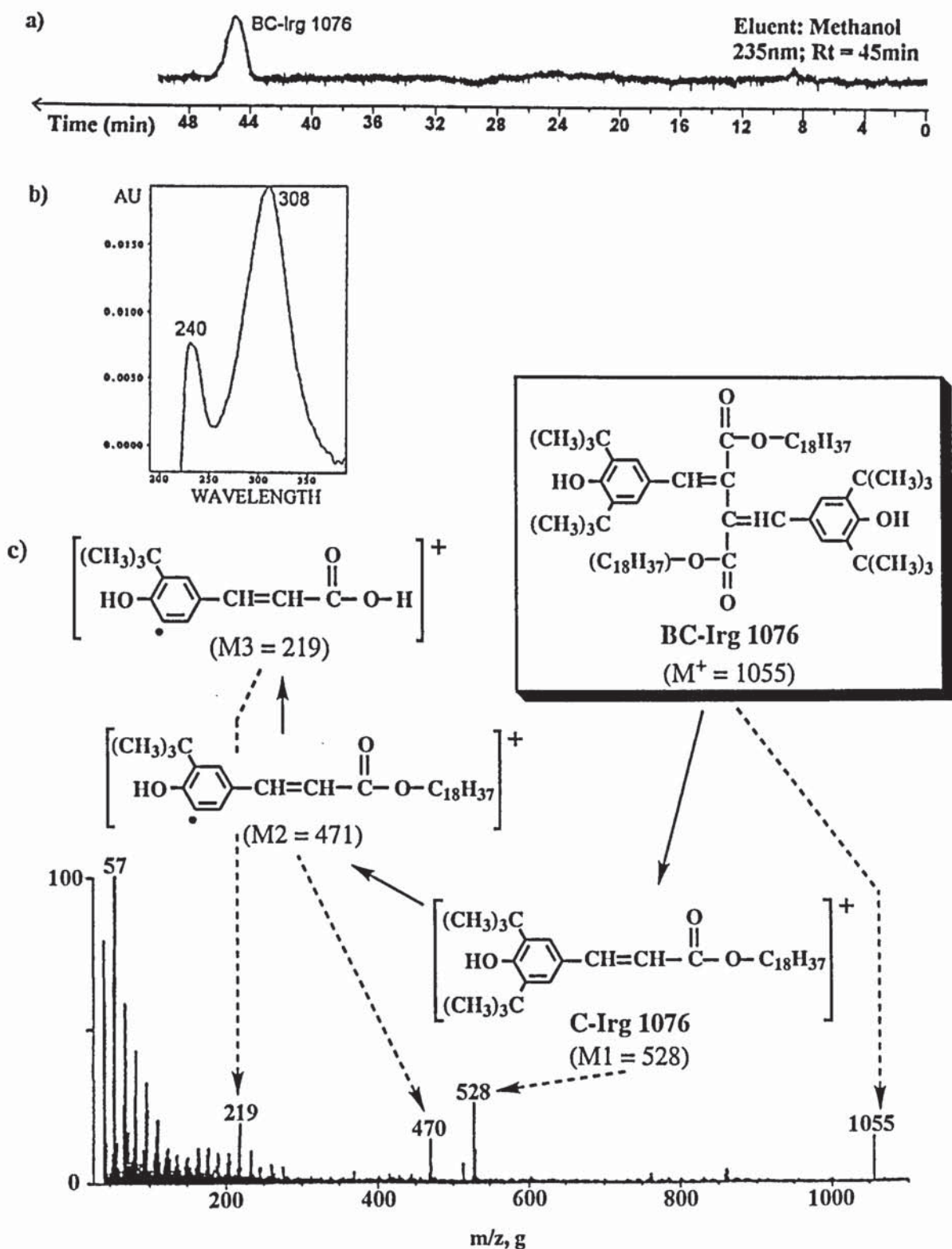


Figure 2.34: HPLC (a), UV (b) and GC-MS analysis (c) of BC-Irg 1076 (compound 15) isolated from the extract of LDPE stabilised with 10% Irg 1076, pass 4 (single screw extruder, 180°C) (see tables 2.41 and 2.46 and section 2.8.1)

a) Instrument: Gilson 305 piston pump and variable Dynamax UV-1 variable wavelength absorbance detector; Column: Zorbax ODS (4.6mm x 25cm); Flow rate: 1ml.min⁻¹; Eluent: methanol

b) Solvent: dichloromethane; c) Solvent: chloroform

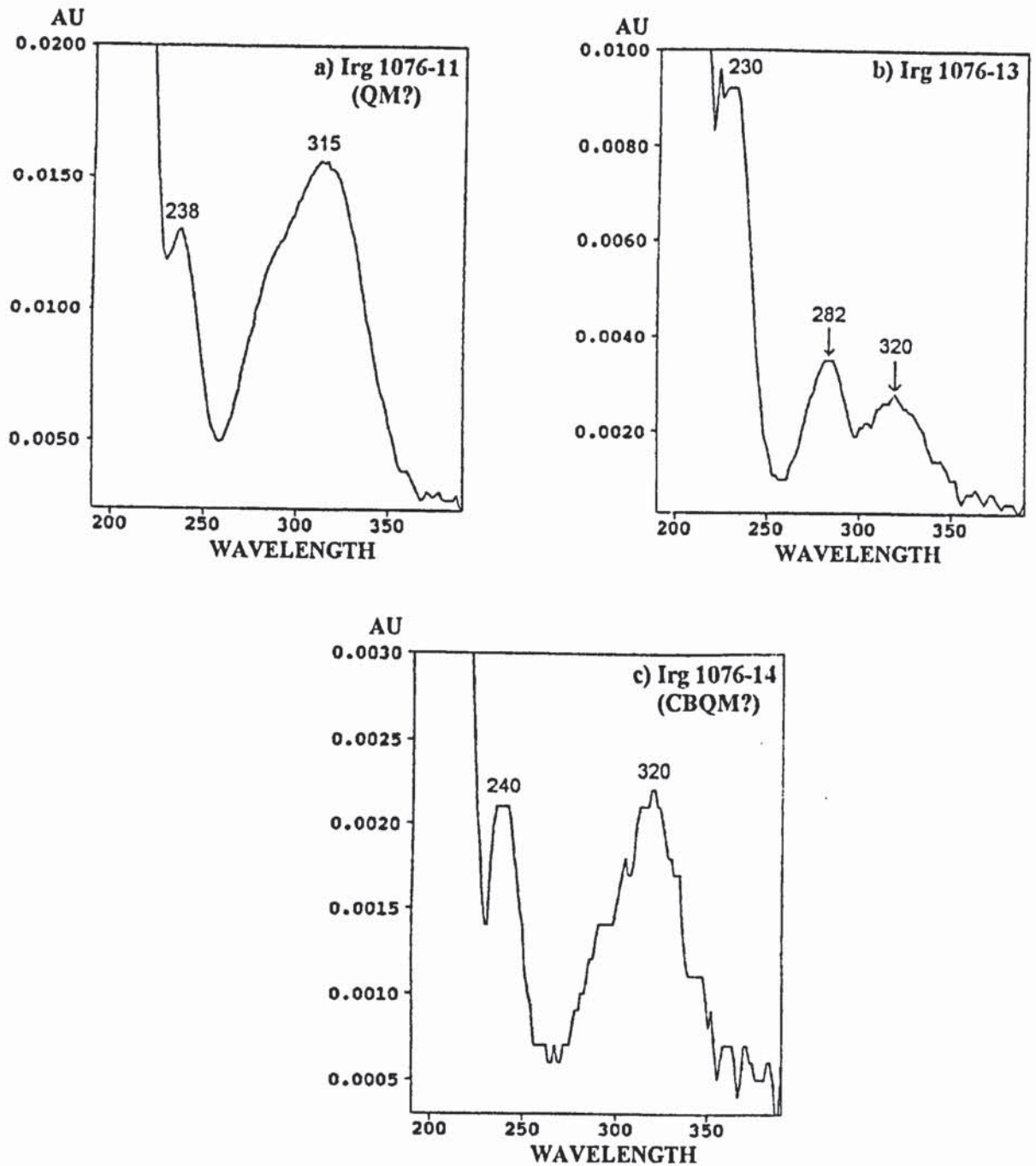


Figure 2.35: Diode array UV analysis of Irg 1076-11, Irg 1076-13 and Irg 1076-14, extracted from LDPE stabilised with 10% Irg 1076, pass 4 (single screw extruder, 180°C), in the solvent system CH₃OH: CH₂Cl₂ = 90:10, v/v Instrument: PU4120 diode array detector (see table 2.42 and section 2.8.1)

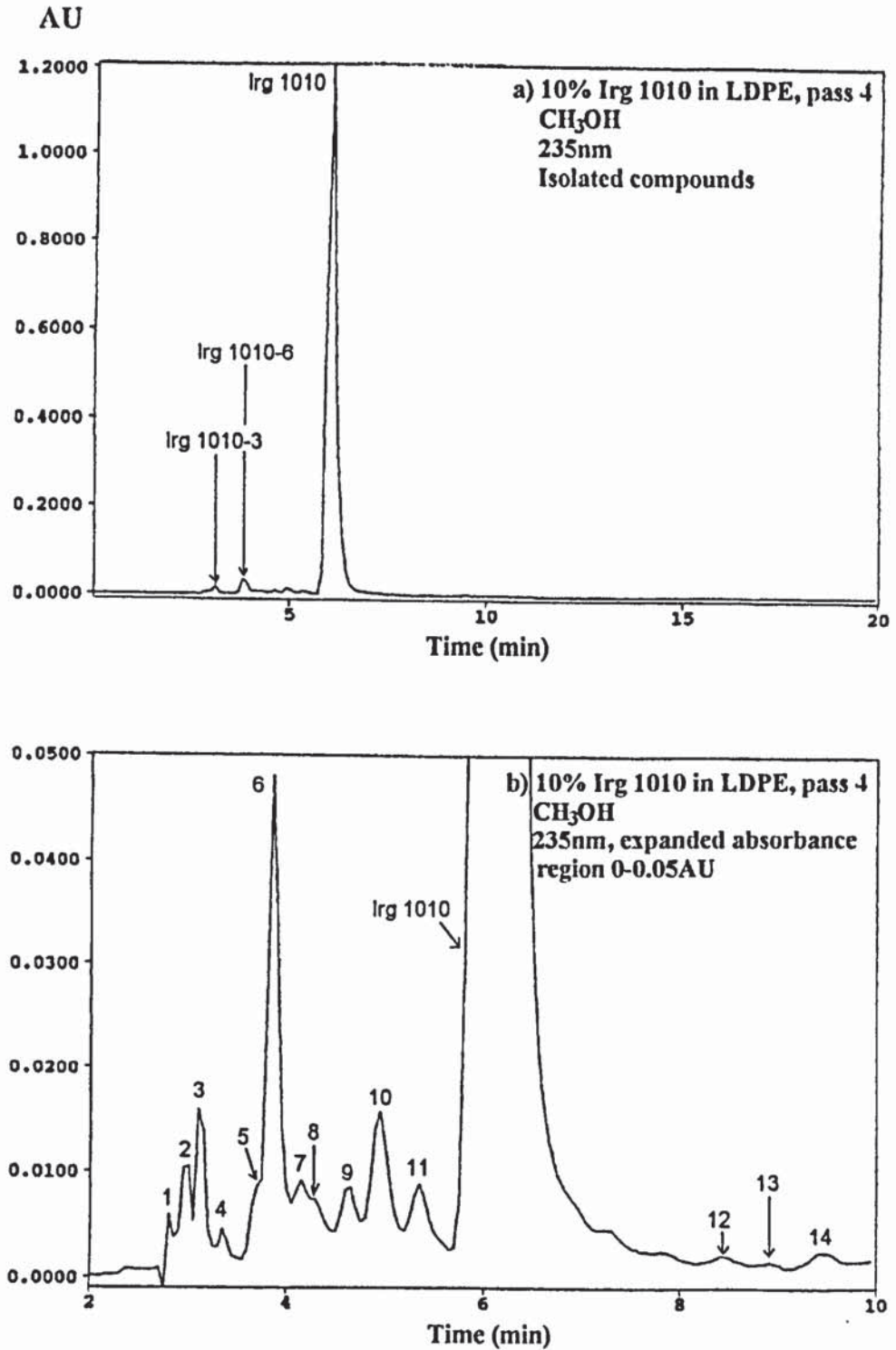


Figure 2.36: HPLC chromatograms of the products extracted from LDPE stabilised with 10% Irg 1010, pass 4 (single screw extruder, 180°C) (see section 2.8.2)
 Instruments: Philips PU4100 liquid chromatograph and PU4120 diode array detector; Column: Zorbax ODS (4.6mm x 25cm); Flow rate: 1ml.min⁻¹
 Eluent: CH₃OH

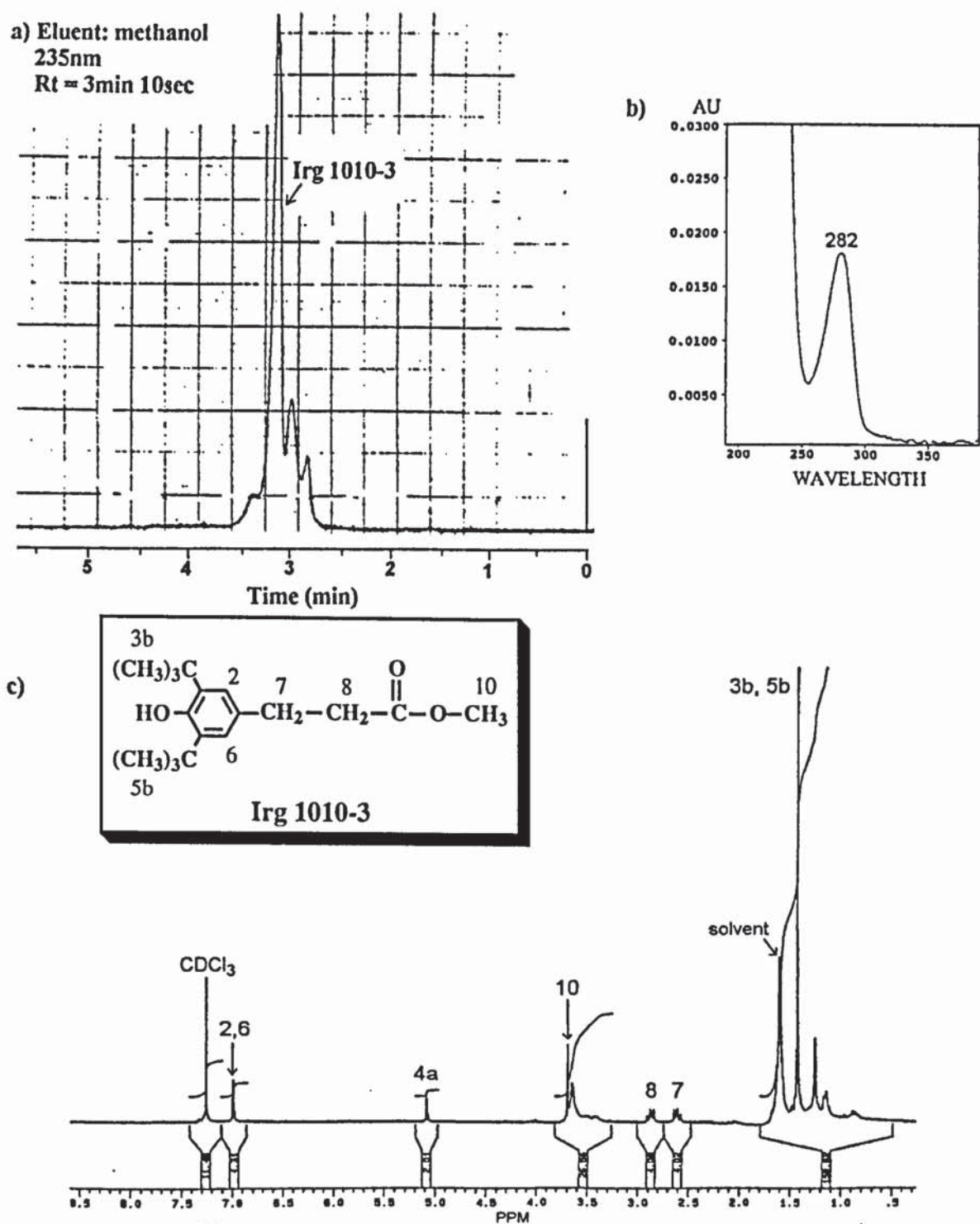


Figure 2.37: HPLC (a), UV (b) and ¹H-NMR analysis (c) of Irg 1010-3 isolated from the (a-c) extract of LDPE stabilised with 10% Irg 1010, pass 4 (single screw extruder, 180°C) (see section 2.8.2)

- a) Instrument: Gilson 305 piston pump and variable Dynamax UV-1 variable wavelength absorbance detector; Column: Zorbax ODS (4.6mm x 25cm); Flow rate: 1ml.min⁻¹; Eluent: methanol
- b) Solvent: dichloromethane (see table 2.48)
- c) Solvent: deuterated chloroform (see table 2.50)

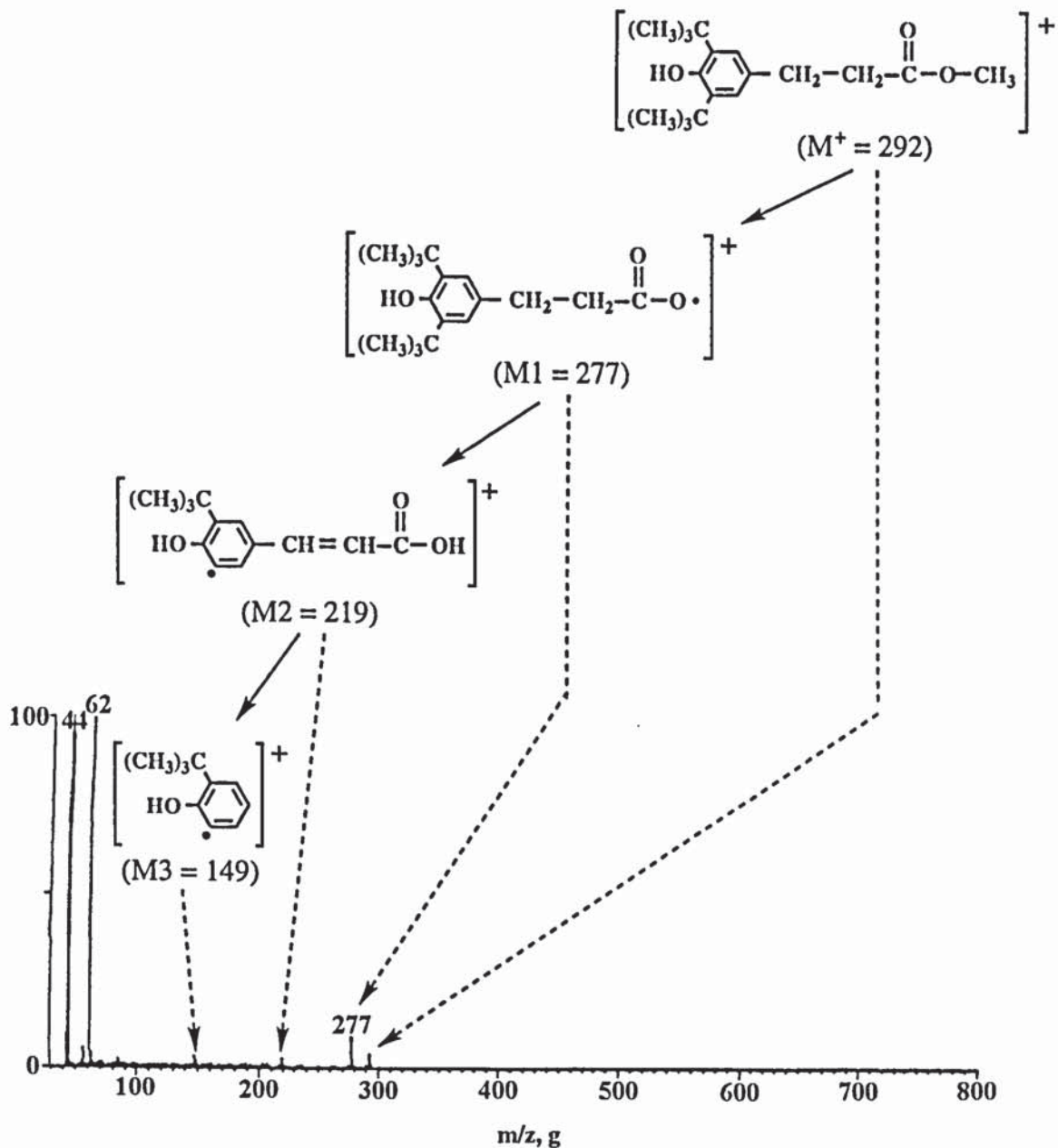


Figure 2.37.d: GC-MS analysis of Irg 1010-3 isolated from the extract of LDPE stabilised with 10% Irg 1010, pass 4 (single screw extruder, 180°C); Solvent: chloroform (see table 2.51 and section 2.8.2)

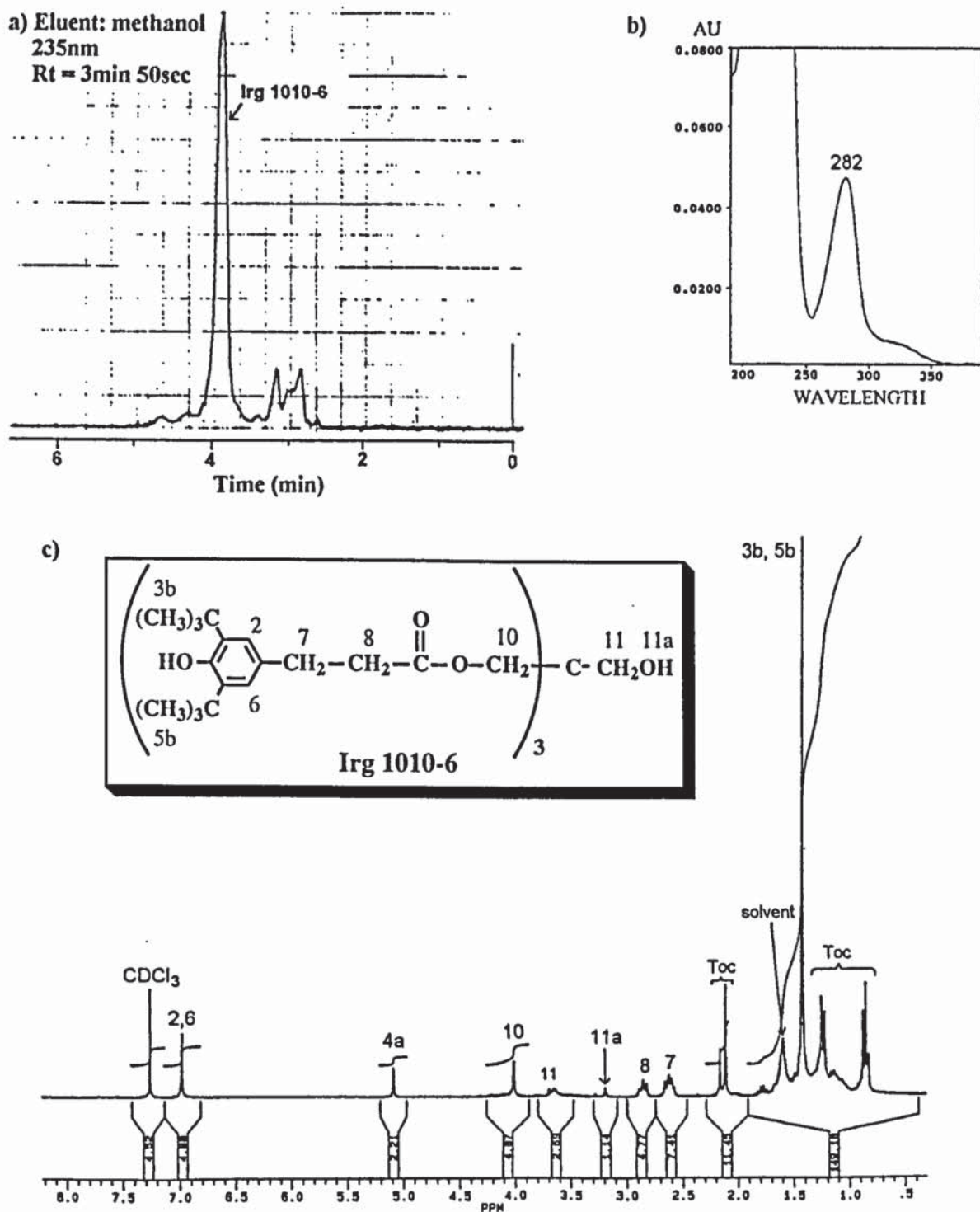


Figure 2.38: HPLC (a), UV (b) and $^1\text{H-NMR}$ analysis (c) of Irg 1010-6 isolated from the (a-c) extract of LDPE stabilised with 10% Irg 1010, pass 4 (single screw extruder, 180°C) (see section 2.8.2)

a) Instrument: Gilson 305 piston pump and variable Dynamax UV-1 variable wavelength absorbance detector; Column: Zorbax ODS (4.6mm x 25cm); Flow rate: $1\text{ml}\cdot\text{min}^{-1}$; Eluent: methanol

b) Solvent: dichloromethane (see table 2.48)

c) Solvent: deuterated chloroform (see table 2.50)

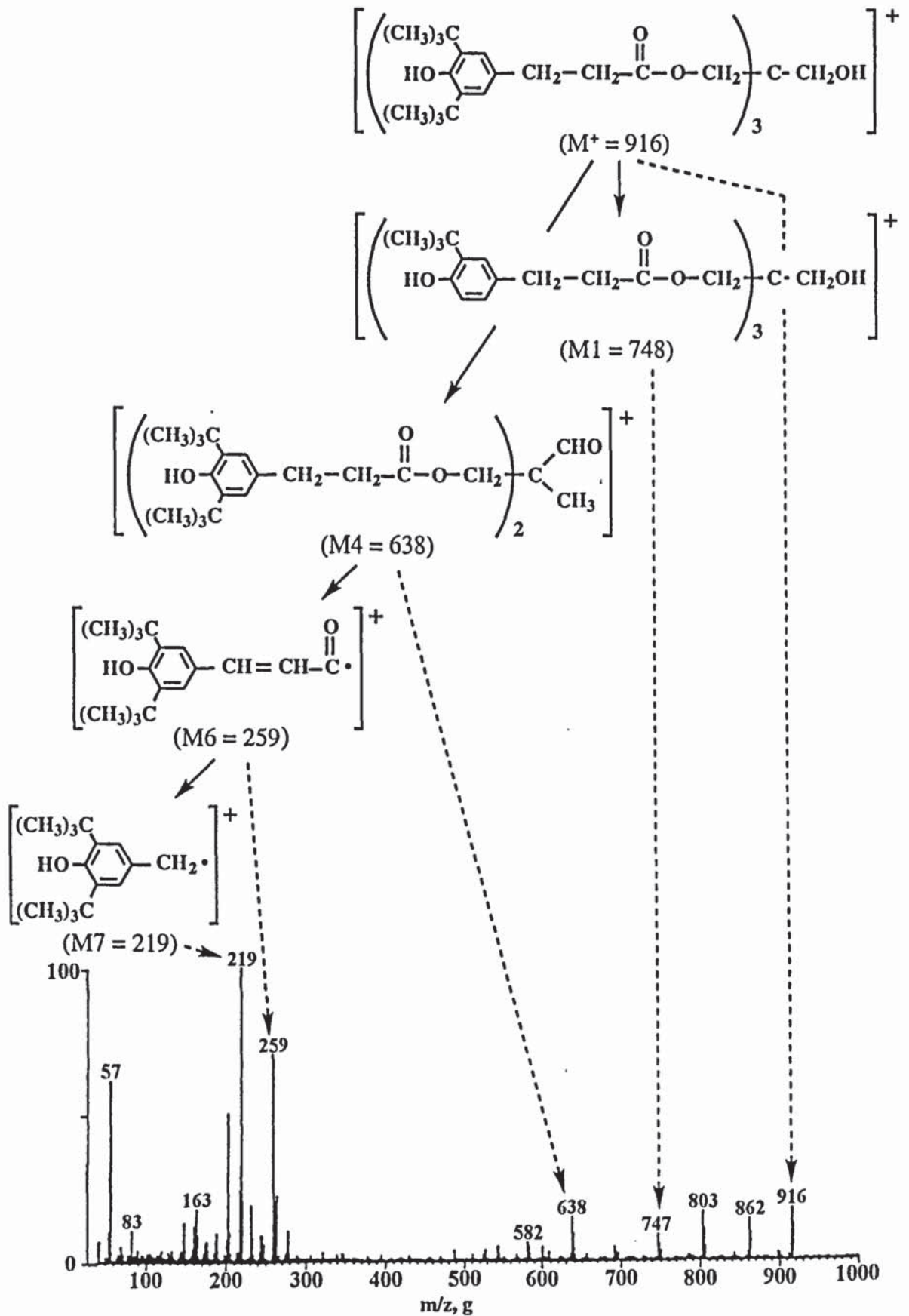


Figure 2.38.d: GC-MS analysis of Irg 1010-6 isolated from the extract of LDPE stabilised with 10% Irg 1010, pass 4 (single screw extruder, 180°C); Solvent: chloroform (see table 2.52 and section 2.8.2)

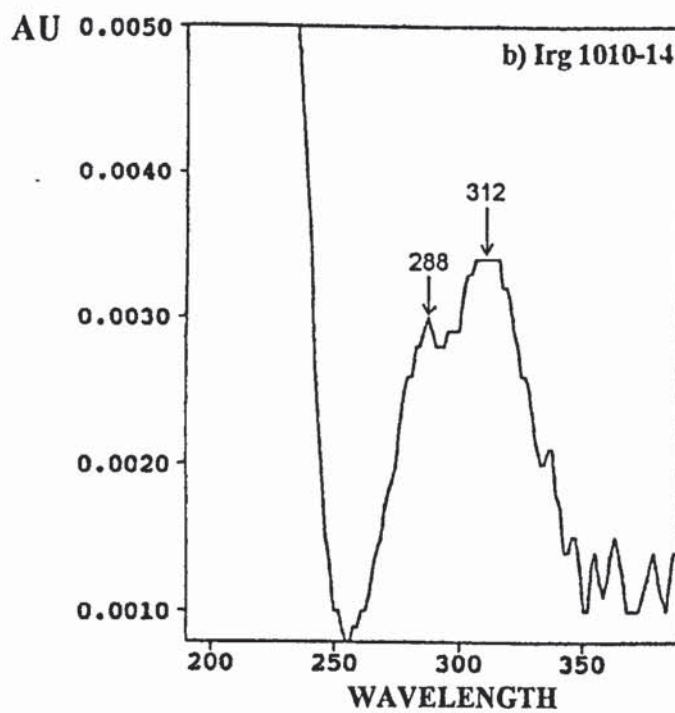
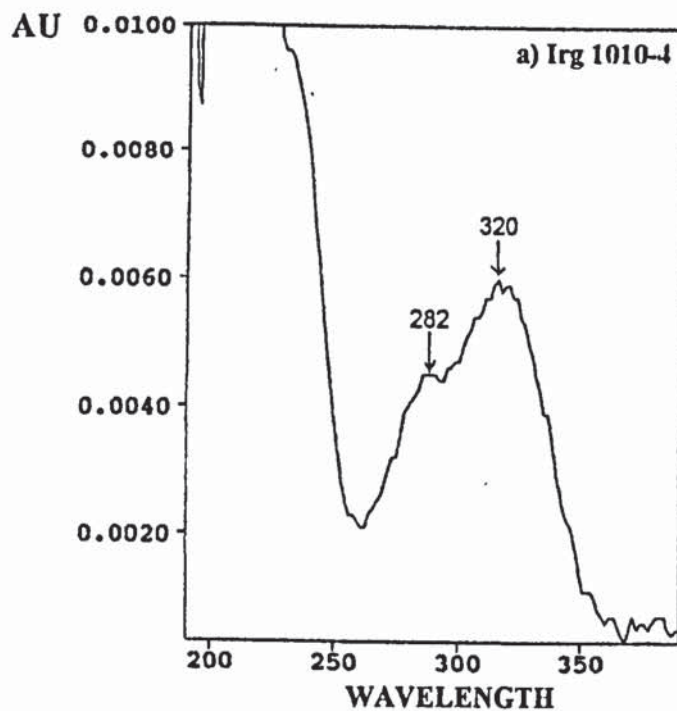


Figure 2.39: Diode array UV analysis of Irg 1010-4 and Irg 1010-14, extracted from LDPE stabilised with 10% Irg 1010, pass 4 (single screw extruder, 180°C); solvent: methanol
Instrument: PU4120 diode array detector (see table 2.49 and section 2.8.2)

CHAPTER THREE

STABILISATION EFFICIENCY OF TOC, TOC DERIVATIVES AND COMMERCIAL HINDERED PHENOLS IN LDPE AND PP AND EFFECT OF HINDERED ARYL PHOSPHITES ON THEIR ANTIOXIDANT ACTION

3.1 OBJECT AND METHODOLOGY

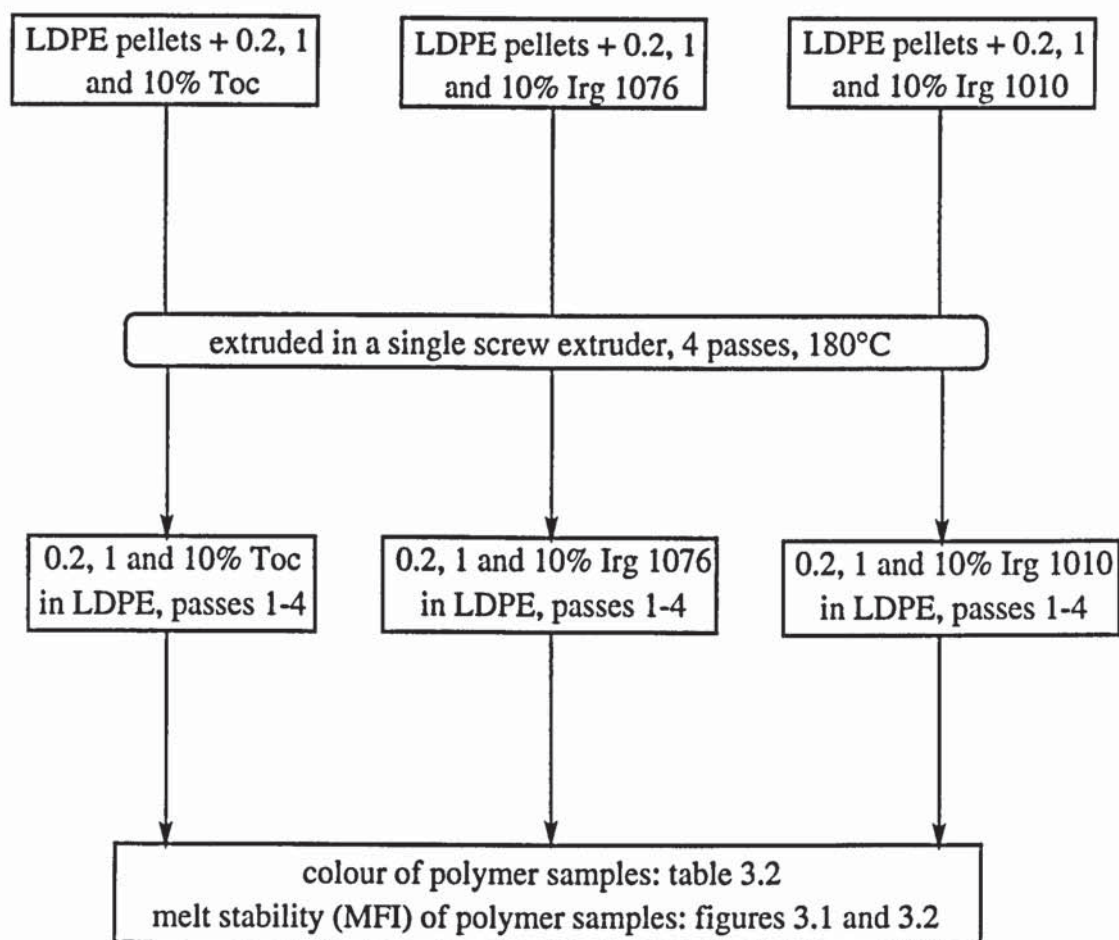
Most polymers require the use of antioxidants in order to inhibit the oxidative degradation reactions which occur at different stages of the polymer lifecycle (see scheme 1.5, p. 46). Antioxidants are normally incorporated in polymers during the high temperature processing operation to impart melt stability (melt stabilisers) and/or to provide protection during service against heat (thermal stabilisers) and UV light (UV stabilisers). However, the overall stabilisation afforded to the polymer depends not only on the initially added antioxidant but, also, on the behaviour of their transformation products which are formed under the normal conditions of processing. Furthermore, a major concern for synthetic antioxidants designed for food packaging plastics, e.g. polyolefins, is mainly associated with the problem of migration of the antioxidants and their transformation products into foodstuffs which represents a major source of contamination for the packaged food, with unknown toxicological consequences. The use of biological antioxidants such as α -tocopherol (Vitamin E is used as a food additive) in packaging plastics is ideally suited for such application as it can be considered as a safe migrant. The object of the work described in this chapter was to compare the stabilising efficiencies of α -tocopherol (Toc) and some of its derivatives (Toc transformation products) in low density polyethylene (LDPE) and polypropylene (PP) with those of some commercially available synthetic hindered phenols and hindered aryl phosphites. Table 3.1 describes all the antioxidants used and schemes 3.1 and 3.2 give an overall view of the methodology employed in the work presented in this chapter.

The LDPE samples, initially containing 0.2%, 1% and 10% of each of the antioxidants Toc, Irganox 1010 (Irg 1010) and Irganox 1076 (Irg 1076), were extruded four times into thin films (0.25mm thick) in a single screw extruder at 180°C (see scheme 3.1). On the other hand, the PP samples, initially containing concentrations of up to 0.2% of each of the antioxidants Toc, Toc derivatives, Irg 1010, Irg 1076 and BHT (used on their own and in combination with phosphites) were processed in an internal mixer at 200°C under different conditions (see scheme 3.2). First, the melt stabilising efficiencies of Toc and its

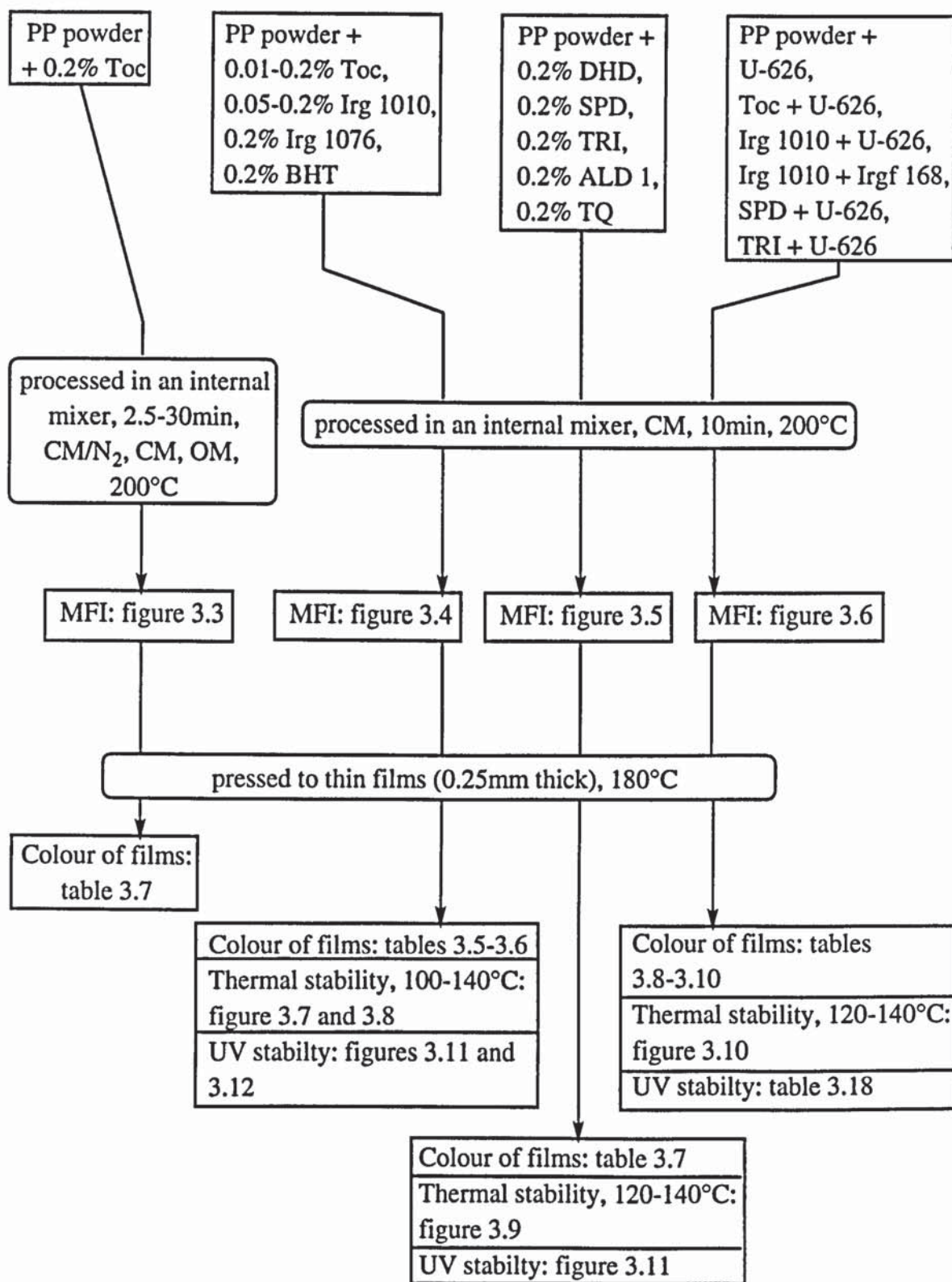
derivatives were compared with those of the commercial melt stabilisers Irg 1010, Irg 1076 and BHT, in some cases in synergistic combination with the aryl phosphites Ultrinox 626 (U-626) and Irgafos 168 (Irgf 168), when processed under different conditions in LDPE and PP. The melt stability of a polymer sample was determined by measuring its melt flow index (MFI) at 190°C and 230°C for LDPE and PP samples, respectively (see chapter two, section 2.4.1). The MFI of each sample was carried out in triplicate to minimise errors. Furthermore, when very low concentrations of the stabiliser were used (i.e. 0.01% to 0.05%), at least two samples were processed, to reduce the overall experimental errors to less than 5% (concentration of 0.01%) and 3% (for all the other samples) (see section 2.4.1). The thermal stabilities of all the PP samples were examined at different temperatures (from 100 to 140°C), showing the beneficial effects of the hindered aryl phosphites U-626 and Irgf 168 on the antioxidant action of hindered phenols and the effect of the temperature. Thermal ageing of a polymer sample was carried out by pressing the PP sample to a thin film (15cm², 0.25mm thick), cutting it to a film strip (5cm x 1cm) and placing it in a circulating air oven (Wallace oven) at the required temperature (see section 2.4.2). The thermal stability of the polymer films was measured as their time to brittle fracture which was taken as an average time of four films for each PP sample, to limit the experimental errors to 10%. Finally, the UV stability of the unstabilised and stabilised PP samples was determined by placing 0.25mm thick PP film strips (5cm x 1cm) in an accelerated sun lamp-black lamp UV ageing cabinet and measuring their time to brittle fracture (see section 2.4.3). Again, four measurements were carried out, so that experimental errors were less than 10%. Although hindered phenols and aryl phosphites are usually poor light stabilisers, they could show limited stabilisation efficiency, depending on the nature of the transformation products formed during UV irradiation. The colour of the processed LDPE and PP samples was recorded throughout this work by visual assessment using a scale of 1 to 5 (1 is colourless and 5 is the most intense colour), as Toc and its transformation products have shown to induce discolouration of the polyolefins. All the figures to the results obtained in this work are displayed at the end of this chapter (p. 311).

Table 3.1: Chemical structures and description of antioxidants used

code name	chemical structure (commercial name)	origin (purity)	MM, g	state / colour (m.p.)
Toc	<p>(α-tocopherol, Ronotec 202)</p>	Hoffmann-La Roche, Switzerland (min. 97%)	430	liquid / orange-brown
Irg 1076	<p>(Irganox 1076)</p>	Ciba-Geigy	530	solid / white (51.6-52.0°C)
Irg 1010	<p>(Irganox 1010)</p>	Ciba-Geigy	1177	solid / white (118-119°C)
BHT	<p>(BHT)</p>	Aldrich	220	solid / white (69.6-70.2°C)
U-626	<p>(Ultrinox 626)</p>	supplied by Hoffmann-La Roche, USA	604	solid / white (177-178°C)
Irgf 168	<p>(Irgafos 168)</p>	Ciba-Geigy	646	solid / white (188-189°C)



Scheme 3.1: Methodology for the determination of the colour and the melt stability of LDPE films (0.25mm thick) stabilised with various concentrations of each of the antioxidants Toc, Irg 1076 and Irg 1010



Scheme 3.2: Methodology for the determination of the colour and the melt, thermal and UV stabilities of PP films (0.25mm thick) stabilised with various concentrations of each of the antioxidants Toc, Irg 1076, Irg 1010 and BHT, Toc derivatives (DHD, SPD, TRI, ALD 1, TQ) and combinations of U-626 with Toc, U-626 with Irg 1010 and Irgf 168 with Irg 1010

3.2 RESULTS

3.2.1 Melt stabilising efficiency of Toc and commercial hindered phenols during multiple extrusions with LDPE

LDPE was extruded four times into thin films (0.25mm thick) in the absence and presence of 0.2%, 1% and 10% of each of the antioxidants Toc, Irg 1010 and Irg 1076 (see section 2.3.1 for procedure and table 3.1 for structures) in a single screw extruder at 180°C and the processed samples were tested, after each extrusion pass, for their melt flow index, MFI (see table 3.2). The change in MFI, Δ MFI, the difference between the first (MFI1) and fourth (MFI4) extrusion pass, was also calculated as the contribution of the antioxidant to the MFI of the polymer varies with its nature and concentration (see table 3.3). Figures 3.1 and 3.2 show the effect of extrusion severity and initial antioxidant concentration on the melt stability of LDPE. Figure 3.1.a reveals that in contrast to the LDPE control (containing no stabiliser), which shows a fast decrease in its MFI (i.e. decrease in melt stability) after the multi-extrusion passes, the Toc-containing samples show a much smaller decrease in their MFI. Although the MFI values of LDPE containing Toc increase with its initial concentration (figure 3.1.a), because of the greater contribution of the antioxidant at higher concentrations to the overall viscosity of the polymer, the change, Δ MFI is much lower for 0.2% Toc than for 1% and 10% (see figure 3.1.b). This suggests that Toc offers higher melt stability to the polymer at lower concentrations. It is also clear that Toc exhibits higher melt stabilising activity than the commercial hindered phenols Irg 1010 and Irg 1076 at all initial concentrations, as shown in figure 3.2. Furthermore, figure 3.2.b suggests that higher concentrations of the commercial stabilisers are required than for Toc, to obtain a better melt stability. The superiority of Toc as a melt stabiliser for polyolefins is even more evident at much lower concentrations (see section 3.2.2.2). However, Toc induced discolouration of LDPE at all its initial concentrations whereas the polymer samples stabilised with commercial hindered phenols remained mostly colourless at concentrations \leq 1% (see table 3.2). Furthermore, in contrast to the LDPE control which remained colourless throughout the four extrusions, the discolouration of all the stabilised

LDPE films increased with extrusion severity. The discolouration of the Toc-containing samples was found to be caused by the formation of oxidation products of Toc, as shown later in chapter four.

Table 3.2: Effect of extrusion severity on the MFI and colour of LDPE extruded in the absence and presence of Toc, Irg 1010 and Irg 1076 (single screw extruder, 180°C) (figures 3.1-3.2)

stabiliser	concentration	extrusion pass	MFI (g/10min)	colour / scale
none (LDPE control)	-	0	0.250	colourless / 1
		1	0.218	
		2	0.192	
		3	0.155	
		4	0.140	
Toc	0.2%	1	0.229	light yellow / 1.5
		2	0.229	light yellow-brown / 2
		3	0.228	light yellow-brown / 2.5
		4	0.224	light yellow-brown / 3
	1%	1	0.256	light yellow / 1.5
		2	0.248	light yellow-brown / 2
		3	0.246	
		4	0.245	
	10%	1	0.406	orange-brown (scale \geq 5, because of blooming)
		2	0.379	
		3	0.376	
		4	0.357	
Irg 1010	0.2%	1	0.217	colourless / 1
		2	0.210	very light yellow-orange / 1.2
		3	0.197	
		4	0.195	light yellow-orange / 1.5
	1%	1	0.251	colourless / 1
		2	0.240	
		3	0.237	
		4	0.233	
	10%	1	0.244	light yellow-orange / 1.5
		2	0.206	light yellow-orange / 2
		3	0.185	
		4	0.158	
Irg 1076	0.2%	1	0.245	colourless / 1
		2	0.239	very light yellow / 1.2
		3	0.234	
		4	0.225	light yellow / 1.5
	1%	1	0.259	colourless / 1
		2	0.254	
		3	0.244	
		4	0.241	
	10%	1	0.249	colourless / 1
		2	0.232	very light yellow / 1.2
		3	0.223	light yellow / 1.5
		4	0.212	light yellow / 2

Table 3.3: Δ MFI (%) $[(\text{MFI4} - \text{MFI1}) \times 100 / \text{MFI1}]$ of LDPE extruded in the absence and presence of Toc, Irg 1010 and Irg1076 (single screw extruder, 180°C) (figures 3.1-3.2)

concentration of stabiliser	Δ MFI (%)		
	Toc	Irg 1010	Irg 1076
0	35.8	35.8	35.8
0.2%	2.2	10.1	8.2
1%	4.3	7.2	6.9
10%	12.1	35.2	14.9

3.2.2 Melt stabilising efficiency of Toc, Toc derivatives and commercial hindered phenols, and effect of hindered aryl phosphites, during processing with PP in an internal mixer

3.2.2.1 Effect of processing severity and oxygen concentration on the melt stabilising efficiency of Toc

The effect of processing severity in an internal mixer on the melt stability of PP containing 0.2% Toc was examined by varying the processing time (see section 2.3.2 for procedure). The samples were processed at 200°C (oil temperature) in a closed mixer (CM) for 2.5, 5, 7.5, 10, 15, 20 and 30min. As a control, PP was processed on its own under the same conditions for 5, 10, 20 and 30min. The effect of oxygen concentration in the mixer on the melt stability was also studied by processing PP with 0.2% Toc in an open mixer (OM), i.e. higher oxygen content in the melt, and in a closed mixer with prior nitrogen flushing (CM/N₂), which corresponds to the condition of minimum amount of oxygen in the melt. The samples were processed for 5, 10, 20 and 30min, at 200°C. The melt stabilities of all the samples were measured and the results are shown in table 3.4. Figure 3.3.a shows the effect of processing severity on the MFI of PP processed in the absence and presence of 0.2% Toc in a CM. In contrast to the PP control which reveals a large increase in MFI (i.e. decrease in melt stability) with increasing processing time, the PP sample containing Toc exhibits excellent melt stability when processed for up to 30min. The increase of oxygen

concentration in the melt (processing in an OM) leads to a slightly higher increase in MFI of the polymer with increasing processing times, compared to the polymer samples processed in a CM/N₂ and a CM (figure 3.3.b). However, like in LDPE, Toc induced discolouration of the polymer, the extent of staining increasing with processing severity (see table 3.4), which is again due to the formation of oxidation products of Toc, as shown in chapter four.

Table 3.4: Effect of processing severity on the MFI and colour of PP processed with 0.2% Toc in an open, closed and closed with prior N₂ flushing mixer (OM, CM and CM/N₂ respectively, 200°C) and of a PP control (CM, 200°C) (figure 3.3)

Processing time (min)	MFI (g/10min)				colour / scale	
	PP control, CM	Toc, OM	Toc, CM/N ₂	Toc, CM	PP + 0.2% Toc, OM, CM/N ₂ and CM	PP control, CM
0	0.19	-	-	-	-	colourless / 1
2.5	-	-	-	0.35	light yellow / 1.5	
5	0.94	0.35	0.35	0.35		
7.5	-	-	-	0.36	light yellow-brown / 2	
10	1.13	0.37	0.35	0.36		
15	-	-	-	0.37	light yellow-brown / 2.5	
20	1.31	0.42	0.37	0.38		
30	1.46	0.46	0.39	0.40	light yellow-brown / 3	

3.2.2.2 Melt stabilising activity of Toc and commercial antioxidants in PP, at low concentrations

PP was processed in the absence and presence of each of the antioxidants Toc, Irg 1010, Irg 1076 and BHT (see table 3.1 for structures) in an internal mixer (CM, 10min, 200°C), at varying initial concentrations of the antioxidants (0.01% to 0.2%) (see section 2.3.2 for procedure). The melt stability, expressed as MFI, and colour of the stabilised polymer samples are displayed in tables 3.5 and 3.6. Figure 3.4 shows the effect of initial Toc and Irg 1010 concentrations in PP on their stabilisation efficiencies and compares the

stabilisation efficiencies of Toc, Irg 1010, Irg 1076 and BHT at a concentration of 0.2%. At high initial concentrations of the stabilisers, e.g. 0.2%, their melt stabilising activities in PP are similar. However, at lower concentrations, the melt stabilising efficiency of Toc is far better than that of the commercial melt stabiliser Irg 1010. Toc shows excellent stabilising activity down to a concentration of 0.05% and is a relatively good melt stabiliser at a concentration of 0.02%. At a concentration of 0.02%, the activity of Toc is approximately equivalent to that exhibited by Irg 1010 at a concentration of 0.2%. It is also clear that, at these low concentrations, the extent of discolouration of the polymer by Toc is far lower than at 0.2% (see table 3.6).

Table 3.5: MFI and colour of PP processed with 0.2% of each of the antioxidants Toc, Irg 1010, Irg 1076 and BHT in an internal mixer (CM, 10min, 200°C) (figure 3.4)

Stabiliser	MFI (g/10min)	colour / scale
Toc	0.36	light yellow-brown / 2
Irg 1010	0.39	colourless / 1
Irg 1076	0.37	
BHT	0.35	

Table 3.6: Effect of concentration on the MFI and colour of PP processed with each of the stabilisers Toc and Irg 1010 in an internal mixer (CM, 10min, 200°C) (figure 3.4)

Stabiliser and concentration	Sample	MFI, g/10min	average MFI, g/10min	colour / scale
PP control	1	1.185	1.19	colourless / 1
0.01% Toc	1	0.536	0.57	very light yellow / 1.2
	2	0.591		
	3	0.573		
0.02% Toc	1	0.403	0.41	very light yellow / 1.2
	2	0.414		
	3	0.409		
0.05% Toc	1	0.372	0.38	very light yellow / 1.2
	2	0.381		
0.1% Toc	1	0.373	0.37	light yellow / 1.5
0.2% Toc	1	0.363	0.36	light yellow-brown / 2
0.05% Irg 1010	1	0.589	0.59	colourless / 1
0.1% Irg 1010	1	0.464	0.46	colourless / 1
0.2% Irg 1010	1	0.393	0.39	colourless / 1

3.2.2.3 Melt stabilising activity of Toc derivatives in PP

PP was processed with 0.2% of a series of Toc derivatives in a closed mixer at 200°C for 10min (see section 2.3.2 for procedure). The derivatives, which are dihydroxydimers (DHD), spirodimers (SPD), trimers (TRI), 5-formyl- γ -Toc (ALD1) and α -tocoquinone (TQ) were isolated from reactions of Toc with lead dioxide and supplied (see table 3.1 for structures and origin). These derivatives were also shown to be formed during processing of Toc with LDPE and PP (e.g. figure 4.28, p. 437 chapter four). Therefore, their presence is expected to affect the melt stability and colour of the polymer system. Table 3.7 shows the MFI and colour of PP stabilised with 0.2% of each of the antioxidants Toc, DHD, SPD, TRI, ALD 1, TQ and Irg 1010. Figure 3.5 compares the melt stabilisation efficiencies of Toc, Toc derivatives and Irg 1010. It is clear that the DHD and SPD exhibit excellent melt

stabilisation activity in PP and the TRI show reasonably good activity. However TQ and ALD 1 lead to lower melt stability than that exhibited by PP containing Irg 1010. TQ and ALD 1 were found to be formed in relatively high concentrations during processing of LDPE and PP with Toc, especially when low concentrations of the stabiliser were used (e.g. figure 4.31, p. 440, chapter four), which explains the lower melt stabilisation activity of Toc at concentrations below 0.02% (see figure 3.4). It is also evident that the SPD, TRI and ALD 1, which are highly coloured oils (see table 3.1), contribute the most to the discolouration of polymer samples stabilised with Toc, themselves producing highly coloured polymers (see table 3.7).

Table 3.7: MFI and colour of PP processed with 0.2% of a series of Toc derivatives and Toc in a closed mixer at 200°C for 10min (figure 3.5)

Stabiliser	MFI (g/10min)	colour / scale
Toc	0.36	light yellow-brown / 2
DHD	0.31	light yellow-brown / 3
SPD	0.36	yellow-brown / 4
TRI	0.38	yellow-brown / 3.5
TQ	0.46	light yellow / 2.5
ALD 1	0.50	yellow / 4
Irg 1010	0.39	colourless / 1

3.2.2.4 Effect of hindered aryl phosphites U- 626 and Irgf 168 on the stabilisation efficiency of antioxidants in PP

U-626, a commercial hindered aryl diphosphite (see table 3.1 for structure), was used to prevent the discolouration of the PP samples processed with Toc at initial concentrations of 0.01-0.2%. Irgf 168 (see table 3.1 for structure) is a commercially used hindered aryl monophosphite and was used in combination with Irg 1010 to produce a widely used commercial melt-stabilising system, for comparison. The melt and colour stabilities of PP processed in the presence of combinations of Toc and U-626 in an internal mixer (CM,

10min, 200°C) were examined, using different concentrations of the stabilisers, and compared with those of a control (PP containing U-626 only), as well as with those of PP containing similar combinations of Irg 1010 with each of the phosphites U-626 and Irgf 168. Tables 3.8 and 3.9 show the different concentrations used for the stabilisers and the melt stability (MFI) as well as the colour they impart to the polymer. Figure 3.6 compares the effect of U-626 on the antioxidant action of Toc at varying concentrations with that of U-626 and Irgf 168 on the antioxidant activity of Irg 1010. Combinations of Toc and U-626 lead to better melt stabilisation of PP at all concentrations examined, than similar combinations of Irg 1010 and U-626. Furthermore, combinations of U-626 with Irg 1010 gave similar melt stabilities to combinations of Irg 168 with Irg 1010. Finally, U-626 prevented the discolouration of the samples containing Toc.

The effect of U-626 on isolated transformation products of Toc (Toc derivatives) was also investigated. PP was processed with 0.4% U-626 in combination with 0.2% of each of the Toc derivatives SPD and TRI (see table 3.1 for structures) in an internal mixer (CM, 10min, 200°C) and the MFI and colour of each processed sample were measured, and compared with those of PP processed in the presence of 0.2% of each of the transformation products only, under the same conditions (see table 3.10). Table 3.10 shows that combinations of the Toc derivatives with U-626 lead to similar melt stabilisation than combinations of Toc with U-626, when the same concentrations of stabilisers were used. Furthermore, the presence of U-626 resulted in reduced discolouration of PP containing Toc derivatives.

Table 3.8: MFI and colour of PP processed with varying concentrations of Toc and U-626 in an internal mixer (CM, 10min, 200°C) (figure 3.6)

concentration (%)		MFI (g/10min)	colour / scale
Toc	U-626		
0.2	-	0.36	light yellow-brown / 2
-	0.4	0.35	colourless / 1
0.2	0.4	0.30	colourless / 1
0.05	-	0.38	very light yellow / 1.2
0.05	0.05	0.31	colourless / 1
0.05	0.1	0.30	colourless / 1
0.05	0.2	0.30	colourless / 1

Table 3.9: MFI and colour of PP processed with varying concentrations of Irg 1010, U-626 and Irgf 168 in an internal mixer (CM, 10min, 200°C) (figure 3.6)

concentration (%)			MFI (g/10min)	colour / scale
Irg 1010	U-626	Irgf 168		
0.05	-	-	0.59	colourless / 1
0.05	0.1	-	0.35	colourless / 1
0.05	-	0.1	0.34	colourless / 1

Table 3.10: MFI and colour of PP processed with 0.4% U-626 in combination with 0.2% of Toc and each of the Toc derivatives SPD and TRI, compared to PP processed with 0.2% of Toc and each of the Toc derivatives on their own (internal mixer, CM, 10min, 200°C)

Stabilising system	MFI (g/10min)	colour / scale
0.2% Toc	0.36	light yellow-brown / 2
0.2% Toc + 0.4% U-626	0.30	colourless / 1
0.2% SPD	0.36	yellow-brown / 4
0.2% SPD + 0.4% U-626	0.31	light yellow / 2.5
0.2% TRI	0.38	yellow-brown / 3.5
0.2% TRI + 0.4% U-626	0.32	light yellow / 2.5

3.2.3 Thermal stabilising activity of Toc, Toc derivatives and commercial hindered phenols, and effect of hindered aryl phosphites, in PP processed in an internal mixer

3.2.3.1 Thermal stabilising activity of Toc and commercial hindered phenols

PP films (0.25mm thick), stabilised with 0.2% of each of the antioxidants Toc, Irg 1010, Irg 1076 and BHT (see table 3.1 for structures) in an internal mixer (CM, 10min, 200°C) were tested for their thermal stability at varying temperatures (100°C to 140°C) in circulating air ovens (see section 2.4.2 for procedure). The results were compared with that of a PP control containing no stabiliser (processed under the same conditions). The embrittlement times for each film are shown in table 3.11. Figure 3.7.a shows the thermal stabilising efficiencies of Toc and the commercial hindered phenols in PP, at 140°C. In contrast to the PP control which shows a very poor thermal stability at 140°C, the presence of Toc and the commercial stabilisers lead to far longer embrittlement times at the same temperature. It is also clear that Toc is a better thermal stabiliser than BHT, because of the higher volatility of the latter. However, Toc shows a lower thermal stabilising activity than Irg 1010 and Irg 1076. Nevertheless, Toc is a far more efficient stabiliser at lower temperatures, as revealed in figure 3.7.b, which compares the thermal stability of PP in the absence and presence of each of the antioxidants Toc and BHT at different temperatures. The better thermal stabilising activity of Toc at lower temperatures is further investigated at lower concentrations of the stabiliser in the next section.

Table 3.11: Effect of temperature on the stability of PP films (0.25mm thick) processed in the absence and presence of 0.2% of each of the antioxidants Toc, Irg 1010, Irg 1076 and BHT (internal mixer, CM, 10min, 200°C) (figure 3.7)

Stabiliser	Embrittlement time (hours)		
	100°C	120°C	140°C
PP control	15	4	1
0.2% BHT	192	16	5
0.2% Toc	> 2000	1043	201
0.2% Irg 1076	-	-	813
0.2% Irg 1010	-	-	> 2000

3.2.3.2 Effect of initial Toc concentration

The effect of the initial concentration of Toc on the thermal stability of PP films (0.25mm thick), stabilised in an internal mixer (CM, 10min, 200°C), was examined at different temperatures (100 to 140°C) (see section 2.4.2 for procedure) and compared with that of PP containing Irg 1010, under the same conditions. The embrittlement times of the stabilised PP films (0.25mm thick) are summarised in table 3.12. Figure 3.8 shows the effects of initial Toc concentration and temperature on the thermal stability of PP. It is clear that at very low Toc concentrations, e.g. 0.01%, the thermal stability of PP is poor at temperatures ranging from 100°C (85h) to 140°C (4h). However, the thermal stability of PP increases rapidly with increasing Toc concentrations, especially at 100°C. Figure 3.8.b emphasises the effect of temperature on the thermal stability of PP containing low Toc concentrations (0.01% to 0.05%). It shows a fast increase in embrittlement times of the latter with decreasing temperatures. The activity of Toc at a concentration of 0.02% and 100°C is approximately equivalent to that exhibited by Irg 1010 at 0.05% and 140°C.

Table 3.12: Effect of temperature on the stability of PP films (0.25mm thick) processed with varying initial concentrations of Toc and 0.05% Irg 1010 (internal mixer, CM, 10min, 200°C) (figure 3.8)

Stabiliser	embrittlement time (h)		
	100°C	120°C	140°C
PP control	15	4	1
0.01% Toc	85	21	4
0.02% Toc	826	148	24
0.05% Toc	> 2000	454	66
0.1% Toc	-	731	129
0.2% Toc	-	1043	201
0.05% Irg 1010	-	> 2500	841

3.2.3.3 Thermal stabilising activities of Toc derivatives

It was shown that Toc derivatives, e.g. DHD, SPD, TRI, ALD 1 and TQ (see table 3.1 for structures), were formed from Toc during processing with both LDPE and PP (e.g. figure 4.31, p. 440, chapter four). These derivatives were therefore also examined for their efficiency as thermal stabilisers (see section 2.4.2 for procedure), as their presence is expected to affect the overall stability of the polymer system. Table 3.13 shows the embrittlement times of PP films (0.25mm thick) stabilised with 0.2% of each of the derivatives and Toc itself in an internal mixer (CM, 10min, 200°C). Figure 3.9 describes the effect of temperature on the thermal stability of PP containing each of the derivatives and Toc itself. It shows that the DHD leads to better thermal stability than Toc and that the SPD seems to be a better thermal stabiliser than Toc at lower temperatures. However, the activities of ALD 1 and TQ at 120-140°C are far lower than those of the other derivatives. Unfortunately, ALD 1 is a major transformation product during processing of Toc with PP, especially at low Toc concentrations (figure 4.31), and is therefore expected to contribute to the lower thermal stabilisation efficiency of Toc at lower concentrations.

Table 3.13: Thermal stability of PP films (0.25mm thick) processed with 0.2% Toc and 0.2% of a series of Toc derivatives in an internal mixer (CM, 10min, 200°C) (figure 3.9)

Toc derivative	embrittlement time (h)	
	120°C	140°C
0.2% DHD	1607	250
0.2% SPD	1252	113
0.2% TRI	719	118
0.2% ALD 1	421	89
0.2% TQ	315	23
0.2% Toc	1043	201

3.2.3.4 Effect of hindered aryl phosphites on the stabilising activity of antioxidants

The effect of the hindered aryl phosphites U-626 and Irg 168 (see table 3.1 for structures) on the antioxidant action, during thermal ageing, of Toc, Toc derivatives and the commercial hindered phenol Irg 1010, in PP, was examined at different concentrations of the stabilisers. Table 3.14 shows the embrittlement times at 120°C and 140°C of the PP films (0.25mm thick) stabilised with combinations of Toc with U-626 and Irg 1010 with U-626 and Irgf 168, and with each of the hindered phenols on their own (internal mixer, CM, 10min, 200°C), for comparison. Figure 3.10.a shows the effect of U-626 on the antioxidant action of Toc, using varying concentrations of the two stabilisers. The thermal stabilisation action of 0.05% Toc in combination with each of the concentrations of 0.1% and 0.2% of U-626 is approximately equivalent to that of 0.2% Toc in PP (without added phosphite). Furthermore, the effect of U-626 is more pronounced at lower concentrations of Toc and U-626. Figure 3.10.b compares the effect of U-626 on the antioxidant action of Toc at 120°C and 140°C with those of U-626 and Irgf 168 on the activity of Irg 1010 at 140°C, in PP. It is clear that U-626 leads to much longer embrittlement times in PP containing Irg 1010, than Irgf 168, and that combinations of Irg 1010 with U-626 and Irgf 168 result in better thermal stabilities than combinations of Toc with U-626 under the

same conditions. However, at lower temperatures (120°C), in the presence of Toc and U-626, PP shows a much higher thermal stability and represents a good thermal stabilising system. It is also clear that U-626 greatly enhances the thermal stabilising activity of the Toc derivatives SPD and TRI (Toc transformation products, formed during processing of PP and LDPE with Toc) (see table 3.15).

Table 3.14: Thermal stability of PP films (0.25mm thick) processed with combinations of Toc with U-626 and Irg 1010 with U-626 and Irgf 168 (internal mixer, CM, 10min, 200°C) (figure 3.10)

stabiliser(s)	embrittlement time (h)	
	120°C	140°C
0.4% U-626	346	38
0.2% Toc	1043	201
0.2% Toc + 0.4% U-626	1428	405
0.05% Toc	454	66
0.05% Toc + 0.05% U-626	-	168
0.05% Toc + 0.1% U-626	1100	228
0.05% Toc + 0.2% U-626	1036	228
0.05% Irg 1010	> 2500	841
0.05% Irg 1010 + 0.1% U-626	> 2500	3032
0.05% Irg 1010 + 0.1% Irgf 168	> 2500	1972

Table 3.15: Thermal stability of PP films (0.25mm thick) processed with combinations of Toc derivatives and U-626 (internal mixer, CM, 10min, 200°C)

Stabiliser(s)	Embrittlement time (h)	
	120°C	140°C
0.2% SPD	1252	113
0.2% SPD + 0.4% U-626	> 1500	643
0.2% TRI	719	118
0.2% TRI + 0.4% U-626	> 1500	664

3.2.4 UV stabilising efficiency of Toc, Toc derivatives and commercial hindered phenols, in PP processed in an internal mixer

3.2.4.1 UV stabilising activity of antioxidants

PP films (0.25mm thick) stabilised with 0.2% of each of the antioxidants Toc, Irg 1010, Irg 1076 and BHT, and the Toc derivatives DHD, SPD, TRI, ALD 1 and TQ (see table 3.1 for structures) in an internal mixer (CM, 10min, 200°C) were tested for their UV stability in an accelerated UV ageing cabinet (see section 2.4.3 for procedure). Table 3.16 shows the embrittlement times of the stabilised films which were compared with that of a PP control (processed under the same conditions). Figure 3.11 shows the embrittlement times of all the stabilised and unstabilised PP films. In contrast to the PP control which shows very poor UV stability, Toc and its derivatives reveal some UV stabilising activity. The commercial hindered phenols show better stabilising action than Toc, but are still poor UV stabilisers, compared to commercial UV stabilisers (e.g. Tinuvin 770, see table 1.8, p. 76)

Table 3.16: UV stability of PP films (0.25mm thick) processed in the absence and presence of 0.2% of each of the antioxidants Toc, Toc derivatives and commercial hindered phenols (internal mixer, CM, 10min, 200°C) (figure 3.11)

stabiliser	embrittlement time (h)
PP control	119
0.2% Toc	201
0.2% DHD	197
0.2% SPD	199
0.2% TRI	187
0.2% TQ	183
0.2% ALD 1	140
0.2% Irg 1010	429
0.2% Irg 1076	424
0.2% BHT	488

3.2.4.2 Effect of initial concentration of Toc and Irg 1010

The UV stabilities of PP films (0.25mm thick) processed with varying concentrations of each of the antioxidants Toc and Irg 1010 (internal mixer, CM, 10min, 200°C) (see table 3.1 for structures) were examined (see section 2.4.3 for procedure). The embrittlement times of the stabilised films are displayed in table 3.17. Figure 3.12 shows the effect of concentration of Toc and Irg 1010 on the embrittlement times of the PP films. The UV stability of the Toc-containing PP films is more or less the same at concentrations above 0.02% of the stabiliser. On the other hand, Irg 1010 shows better UV stabilising activity at higher concentrations (e.g. 0.2%). Like for commercial hindered phenols, The poor UV stabilising efficiency of Toc at very low concentrations is probably caused by its rapid photodecomposition (see scheme 1.6, p. 48).

Table 3.17: UV stability of PP films (0.25mm thick) processed with varying concentrations of each of the antioxidants Toc and Irg 1010 (internal mixer, CM, 10min, 200°C) (figure 3.12)

stabiliser	embrittlement time (h)
0.01% Toc	137
0.02% Toc	185
0.05% Toc	187
0.1% Toc	200
0.2% Toc	201
0.05% Irg 1010	304
0.2% Irg 1010	429

3.2.4.3 Effect of hindered aryl phosphites on the UV stabilising activity of Toc, Toc derivatives and Irg 1010

PP films (0.25mm thick) processed with combinations of Toc with U-626, Toc derivatives with U-626 and Irg 1010 with U-626 and Irgf 168 (internal mixer, CM, 10min, 200°C) (see table 3.1 for structures) were tested for their UV stability which was compared with

that of PP containing each stabiliser on its own. Table 3.18 shows the concentrations of the stabilisers used and the embrittlement times of the PP films. Figure 3.13 shows the effect of the phosphites on the UV stabilising activities of the hindered phenols. The hindered aryl phosphite U-626 possesses some UV stabilising activity when used on its own in PP, and increases the antioxidant action of Toc and Irg 1010. Furthermore, U-626 has a more beneficial effect than Irg 168 on the UV stability of PP containing Irg 1010. However, the UV stabilising action of Toc derivatives is not affected by the presence of U-626. Overall, the presence of U-626 only slightly improves the UV stability of PP containing Toc, considering that the stabilising efficiency of commercial UV stabilisers is far better (e.g., Tinuvin 770, see table 1.8, p. 76)

Table 3.18: UV stability of PP films (0.25mm thick) processed with Toc, Irg 1010 and U-626 and combinations of varying concentrations of U-626 with each of the stabilisers Toc, Toc derivatives and Irg 1010 and of Irg with Irgf 168 (internal mixer, CM, 10min, 200°C) (figure 3.13)

stabiliser(s)	Embrittlement time (h)
0.2% Toc	201
0.4% U-626	181
0.2% Toc + 0.4% U-626	316
0.2% spiroidimers	199
0.2% spiroidimers + 0.4% U-626	199
0.2% trimers	187
0.2% trimers + 0.4% U-626	187
0.05% Toc	187
0.05% Toc + 0.1% U-626	354
0.05% Irg 1010	304
0.05% Irg 1010 + 0.1% U-626	457
0.05% Irg 1010 + 0.1% Irgf 168	398

3.3 DISCUSSION

3.3.1 Melt stabilising efficiency of Toc and commercial hindered phenols during multiple extrusions with LDPE

LDPE films (0.25mm thick) were extruded four times in the absence and presence of 0.2, 1 and 10% Toc, as well as with 0.2, 1 and 10% of each of the commercial hindered phenols Irg 1076 and Irg 1010, in a single screw extruder (180°C) (see table 3.1 for structures). The resulting polymer samples were tested for their melt stability by measuring their melt flow index, MFI. The decrease in MFI of the unstabilised and stabilised LDPE samples with extrusion severity (see figures 3.1 and 3.2) is caused by an increase in the molecular weight of the polymer. During processing, some of the polymer chains undergo homolytic scission which leads to the formation of peroxy radicals by their reaction with oxygen (see reaction 1.2 in scheme 1.1, p. 36). Peroxy radicals lead to the formation of hydroperoxides which are the most important source of initiating radicals (reaction 1.3, scheme 1.1), resulting in cross-linking and/or chain scission (e.g., formation of ketones) of the polymer backbone. It was shown [18-21] that, in LDPE cross-linking reactions are favoured over chain scission reactions under normal processing conditions (i.e. oxygen deficient conditions) (see scheme 1.3, p. 40). Hindered phenols are chain-breaking-donor (CB-D) antioxidants which prevent hydrogen abstraction from the macroalkyl chain by peroxy radicals (reaction 1.26, p. 48), by donating their phenolic hydrogen, leading to stable products.

Toc offers a good melt stabilisation to the polymer, especially at the lower concentration of 0.2%, which is reflected by the much smaller change in MFI between the first and fourth extrusion pass, Δ MFI (figure 3.1). The overall higher values of MFI at higher concentrations of Toc are caused by the greater contribution of the antioxidant to the melt viscosity of the polymer system. It is also clear that Toc exhibits a much higher melt stabilising activity than the commercial hindered phenols Irg 1076 and Irg 1010 (figure 3.2) and that higher concentrations of Irg 1076 and Irg 1010 (e.g. 1%) than Toc (0.2%) lead to a better melt stability of the polymer. The mechanisms of melt stabilisation of Toc,

Irg 1076 and Irg 1010 in LDPE are discussed in sections 4.3.3, 4.3.6 and 4.3.7, respectively.

3.3.2 Melt stabilising efficiency of Toc, Toc derivatives and commercial hindered phenols during processing with PP in an internal mixer

3.3.2.1 Effect of processing severity and oxygen concentration on the melt stabilising activity of Toc

PP was processed in the absence and presence of 0.2% Toc in an internal mixer (200°C) and the effect of processing severity and oxygen concentration in the mixing chamber on the melt stability of the polymer was examined. The formation of macroalkyl radicals in PP during processing leads to chain scission (e.g. formation of ketones) rather than cross-linking reactions like in LDPE (see scheme 1.2, p. 39). Furthermore, PP is more prone to attack by peroxy radicals than LDPE as they abstract tertiary bonded hydrogens in preference to secondary or primary ones [16,17,22]. The extent of degradation of unstabilised PP and PP stabilised with Toc is shown in figure 3.3. The fast increase in MFI, i.e. decrease in melt stability, of unstabilised PP with increasing processing times is caused by its fast degradation, i.e. chain scission of the polymer backbone (figure 3.3.a). The introduction of 0.2% Toc in PP leads to a much smaller increase in MFI with processing severity, indicating that Toc imparts a good melt stability to the polymer. An increase in the oxygen concentration in the melt, i.e. processing in an open mixer (OM) results in an increase in the concentration of peroxy radicals which are responsible for the degradation of the polymer and the loss of antioxidant. Hence, the faster increase in MFI with processing severity of PP stabilised with Toc in an OM, compared to a CM/N₂ (closed mixer with prior nitrogen flushing) and CM, is caused by the formation of higher concentrations of transformation products of Toc (e.g. ALD 1, TRI, see figure 4.28, p. 437), as a consequence of the reaction of Toc with peroxy radicals (see section 4.3.4). The concentration of oxygen in the melt therefore highly affects the melt stability of the polymer.

3.3.2.2 Effect of initial Toc concentration in PP on the melt stability

The melt stability of PP processed with varying concentrations of Toc (0.01-0.2%) in an internal mixer (CM, 10min, 200°C) was determined and compared with that of PP processed with commercial antioxidants under the same conditions (figure 3.4). Like in LDPE, Toc shows far better melt stabilising activity than the commercial antioxidants Irg 1010 and Irg 1076, especially at lower concentrations (e.g. 0.02%). BHT is also a very good melt stabiliser, but its high volatility compared to the other antioxidants lead to poor thermal stability (see section 3.3.4). At a concentration of 0.02%, the melt stabilising efficiency of Toc is equivalent to that exhibited by Irg 1010 at a concentration of 0.2%. The good melt stabilising activity of Toc was also shown in the literature [5,6,8,9] when PP and HDPE were processed with 0.025 and 0.01% Toc, respectively.

3.3.2.3 Melt stabilising activity of Toc derivatives in PP

PP was processed with a series of Toc derivatives in an internal mixer (CM, 10min, 200°C). The derivatives, which are dimers (DHD, SPD), trimers (TRI), an aldehyde (ALD 1) and a quinone (TQ) of Toc (see table 3.1 for structures), were shown to be formed from Toc during processing with LDPE (see figure 4.19, p. 429) and PP (figure 4.31, p. 440). Hence, they are expected to affect the overall stability of the polymer system. It was shown that the melt stabilising efficiency of the derivatives was either better (DHD), similar (SPD, TRI) or lower (ALD 1, TQ) than that of Toc (figure 3.5). This suggests that the formation of dimers and trimers of Toc is beneficial whereas the formation of ALD 1 and TQ is harmful to the melt stability of the polymer. It was shown that the concentrations of TQ and, especially, ALD 1 increases with decreasing initial Toc concentration in PP during processing (figure 4.30.c-d, p. 439), and are very high at the initial concentration of 0.01%. This indicates that the formation of TQ and ALD 1 is responsible for the lower melt stabilising efficiency of Toc at this low concentration (see section 4.3.4.2). The high melt stabilising efficiency of SPD and TRI in PP was shown to be caused by the formation of high concentrations of DHD during processing (see section 4.3.4.3).

3.3.3 Development and prevention of colour during processing of LDPE and PP with antioxidants

The extent of discolouration of the LDPE and PP samples stabilised with Toc, Irg 1076 and Irg 1010 depended on the nature of the antioxidant, its initial concentration and the processing severity. In LDPE stabilised with 0.2, 1 and 10% of each of the antioxidants Toc, Irg 1076 and Irg 1010, the discolouration was highest at initial antioxidant concentrations of 0.2 and 10% and increased with extrusion severity. Furthermore the discolouration was slightly higher in the samples processed with Toc (see table 3.2). Colour development in LDPE and PP can be attributed to the formation of transformation products of the hindered phenols, as a consequence of their antioxidant action (see sections 4.3.3 and 4.3.4). ALD 1, SPD and TRI, which are major transformation products in LDPE stabilised with Toc (figure 4.19, p. 429) were shown to produce highly coloured samples when processed with PP in an internal mixer (see table 3.7) and are most likely to be responsible for the discolouration of the LDPE samples. In LDPE stabilised with Irg 1076 and Irg 1010, the formation of cinnamate (e.g. C-Irg 1076) and quinonoid (e.g. QM-Irg 1076) transformation products (e.g. figure 4.49, p. 450) is likely to cause colour development in the polymer. Similar to the LDPE samples extruded with Toc, in PP stabilised with 0.2% Toc, the discolouration increased with processing severity, which is also caused by the formation of transformation products (e.g. ALD 1, SPD, TRI) (see table 3.4). However, at lower concentrations of Toc (e.g. 0.02%), the discolouration was much lower (table 3.6) and the melt stability was still good. Hence, for the stabilisation of food packaging materials, where a slight discolouration is not a critical factor, Toc seems to be fully acceptable. However, the introduction of commercial hindered aromatic phosphites, U-626 and Irgf 168 (see table 3.1 for structures) prevented totally the discolouration of PP stabilised with Toc and Irg 1010 (tables 3.8 and 3.9) and reduced the discolouration of PP stabilised with Toc transformation products, i.e. SPD and TRI (table 3.10). The mechanism of colour stabilisation with U-626 is discussed in section 4.3.5.

3.3.4 Thermal stabilising efficiency of Toc, Toc derivatives and commercial antioxidants, in PP processed in an internal mixer

3.3.4.1 Comparison of the thermal stabilising activity of Toc with commercial hindered phenols

PP films (0.25mm thick), unstabilised and stabilised with various concentrations of each of the antioxidants Toc, Irg 1076, Irg 1010 and BHT (see table 3.1 for structures) in an internal mixer (CM, 10min, 200°C), were tested for their thermal stability at 100-140°C in circulating air ovens (see figures 3.7 and 3.8). The degradation of PP during thermal ageing is caused by further chain scission of the polymer backbone by peroxy radicals [103] and is largely dependent on the extent of degradation suffered by the polymer during processing and the initial concentration of hydroperoxides (most important source of initiating radicals). Hence, unstabilised PP, which highly degrades during the processing operation (i.e. high MFI values after processing, see figure 3.3.a), shows a very poor thermal stability (embrittlement times of 1h at 140°C and 15h at 100°C) (figure 3.7). Toc offers a good thermal stability to PP (201h at 140°C), but its stabilising activity at 140°C is lower than those of the higher molecular mass (MM) commercial hindered phenols Irg 1076 and Irg 1010 (figure 3.7.a). On the other hand, the stabilising activity of Toc is far better than that of the lower MM hindered phenol BHT. This suggests that the thermal stabilising activity of the antioxidant increases with increasing MM, i.e. decreasing volatility. As a consequence, the thermal stabilising activities of Toc and BHT are higher at lower temperatures, i.e. 120 and 100°C (figure 3.7.b). The physical loss of Toc during thermal ageing at 140°C was shown to take place in PP stabilised with 0.05% Toc (see section 5.5.1)

The thermal stability of PP films stabilised with Toc decreased with increasing initial concentrations of the antioxidant and increased rapidly with decreasing temperature (figure 3.8). At an initial Toc concentration of 0.02%, the thermal stability of PP at 100°C was 5 times higher than at 120°C and 34 times higher than at 140°C. This suggests that at normal temperatures of end-use of the polymer article, which are usually far lower than 100°C

(e.g. food packaching materials), the thermal stabilising activity of Toc is far higher and well acceptable. At lower concentrations of Toc (e.g. 0.01%), Toc is highly oxidised to various transformation products during processing (figure 4.31.a, p. 440). The latter are expected to contribute to the much lower thermal stabilising efficiency of Toc, compared to that observed at higher concentrations (see section 5.5.1.2).

3.3.4.2 Thermal stabilising activity of Toc derivatives

A series of Toc derivatives which are formed from Toc during processing were tested for their thermal stabilising activity in PP films, as their presence is expected to affect the overall stability of the polymer, especially at lower concentrations of Toc (because of higher concentrations of transformation products). The thermal stability of PP films (0.25mm thick) stabilised with 0.2% of each of the Toc derivatives DHD, SPD, TRI, ALD 1 and TQ in an internal mixer (CM, 10min, 200°C) is shown in figure 3.9. The thermal stabilising efficiency of the derivatives is either better (DHD, SPD especially at 120°C), slightly lower (TRI) or much lower (ALD 1, TQ) than that of Toc. In PP stabilised with 0.01% Toc, TRI and ALD 1 are present in very high concentrations after processing (43 and 15.5%, respectively, see figure 4.31.a-b, p. 440), hence they are expected to be largely responsible for the low thermal stability of the polymer. Furthermore, it was shown that Toc is further oxidised during thermal ageing at 140°C of PP stabilised with 0.05% Toc, mainly to TRI and ALD 1 (see figure 5.4, p. 487), which also contributes to the low thermal stability of PP. The mechanism of thermal stabilisation (140°C) of Toc in PP is discussed in section 5.5.1.2)

3.3.5 UV stabilising efficiency of Toc, Toc derivatives and commercial antioxidants, in PP processed in an internal mixer

3.3.5.1 Comparison of the UV stabilising activity of Toc and Toc derivatives with commercial antioxidants

PP films (0.25mm thick), stabilised with 0.2% of each of the antioxidants Toc, Toc derivatives, Irg 1076, Irg 1010 and BHT in an internal mixer (CM, 10min, 200°C), were tested for their thermal stability in an accelerated UV ageing cabinet. Similar to the thermal stability, the UV stability of PP largely depends on the extent of degradation the polymer suffered during processing and on the initial concentration of hydroperoxides [26,28]. The UV stabilising activity of Toc is limited and lower than that of the commercial hindered phenols Irg 1076, Irg 1010 and BHT, which are themselves poor UV stabilisers. The low UV stabilising activity of hindered phenols was attributed [41] to the formation of photosensitising products leading to photodecomposition of the antioxidant (see scheme 1.6, p. 48). The physical loss during UV ageing of Toc from PP stabilised with 1% Toc was determined and was found to be very fast (see section 5.5.2), hence photodecomposition of Toc is also likely to occur. At lower concentrations of Toc (e.g. 0.01%), the UV stabilising activity of Toc is particularly low (figure 3.12), which is probably caused by the initial presence of high concentrations of transformation products of Toc (e.g. TRI, ALD 1, see figure 4.31.a-b, p. 440). ALD 1 was shown to impart lower UV stability to the polymer than other transformation products of Toc (figure 3.13). The mechanism of UV stabilisation of Toc in PP is discussed in section 5.5.2.2.

Compared to commercial UV stabilisers, e.g. Tinuvin 770 (embrittlement time of more than 620h in PP at a concentration of 0.2%, see table 1.8, p. 76), Toc possesses limited UV stabilising activity in PP (201h at 0.2%). However, if efficient outdoor protection of the polymer is required, combinations of phenols with light stabilisers or photo-antioxidants were shown to offer good UV stability to polymers [40].

3.3.6 Effect of hindered aromatic phosphites on the melt, thermal and UV stabilising activity of Toc, in PP processed in an internal mixer

3.3.6.1 Effect of hindered aromatic phosphites on the melt stabilising activity of Toc and Irg 1010

Hindered aromatic phosphites are usually used in combination with hindered phenols to prevent discolouration of the polymer during processing. In section 3.3.5, it was shown that the presence of U-626 prevented the discolouration of PP containing Toc and Irg 1010. In addition to colour prevention, the melt stability of PP stabilised with combinations of U-626 with Toc, U-626 with Irg 1010 and Irgf 168 with Irg 1010 (internal mixer, CM, 10min, 200°C) was much higher than that of PP stabilised with the hindered phenols only (see figure 3.6). Combinations of Toc with U-626 imparted better melt stabilisation to PP than similar combinations of Irg 1010 with U-626 or Irgf 168. The combination of 0.05% Toc + 0.1% U-626 resulted in an excellent melt stabilising system. This suggests that at lower concentrations of Toc (e.g. 0.01-0.02%), the presence of U-626 is also expected to impart a good melt stability to PP. However this observation will have to be further investigated by stabilising PP with the above concentrations of antioxidants (e.g. 0.01% Toc + 0.02% U-626).

PP stabilised with 0.4% U-626 only also lead to a good melt stability, suggesting that U-626 possesses itself some melt stabilisation activity. The melt stabilising activity of hindered aromatic phosphites was mainly attributed [56,59] to their peroxide decomposing and oxygen scavenging abilities (see reactions 1.28 and 1.34, p. 57-58). The better melt stabilising activity of Toc in presence of the phosphite was shown to be caused by the higher retention of Toc, as a consequence of the peroxydolytic antioxidant action of U-626 (see section 4.3.5).

3.3.6.2 Effect of hindered aromatic phosphites on the thermal stabilising activity of Toc and Irg 1010

Similar to the melt stability, the thermal stabilities of PP films (0.25mm thick) stabilised with combinations of Toc with U-626 and Irg 1010 with each of the phosphites U-626 and Irgf 168 (internal mixer, CM, 10min, 200°C) were much higher than those of PP films stabilised with the hindered phenols only (see figure 3.10.a). This is also suggested to be caused by the peroxide decomposing and oxygen scavenging abilities of the phosphites. For example, the thermal stability of PP stabilised with 0.05% Toc + 0.1% U-626 was similar to that of PP stabilised with 0.2% Toc at 120-140°C. When U-626 was used on its own, its thermal stabilising efficiency was quite low (lower than 0.2% Toc in PP) which is probably caused by the formation of alkoxyl and peroxy radicals from the thermal decomposition of hydroperoxides. Hence, the good thermal stability of PP stabilised with combinations of U-626 and Toc can be attributed to the hydroperoxide decomposing and oxygen scavenging ability of the phosphite and the reaction of the hindered phenol with peroxy radicals, leading to stable products. The improved thermal stability of PP stabilised with combinations of each of the Toc derivatives SPD and TRI with U-626, compared to that of PP stabilised with the derivatives only (internal mixer, CM, 10min, 200°C), can also be attributed to the peroxidolytic activity of U-626 (see table 3.15).

3.3.6.3 Effect of hindered aromatic phosphites on the UV stabilising of Toc and Irg 1010

PP films (0.25mm thick) stabilised with combinations of Toc with U-626 and Irg 1010 with each of the phosphites U-626 and Irgf 168 (internal mixer, CM, 10min, 200°C) also showed higher UV stabilities than PP stabilised with the hindered phenols only (figure 3.13). However, U-626 did not have any effect on the UV stability of PP containing the Toc derivatives SPD and TRI, whereas U-626 was shown to improve their melt and thermal stabilising activities in PP. To explain these results it will be necessary to examine the nature of the transformation products formed during UV ageing of PP stabilised with Toc and the Toc derivatives in combination with U-626.

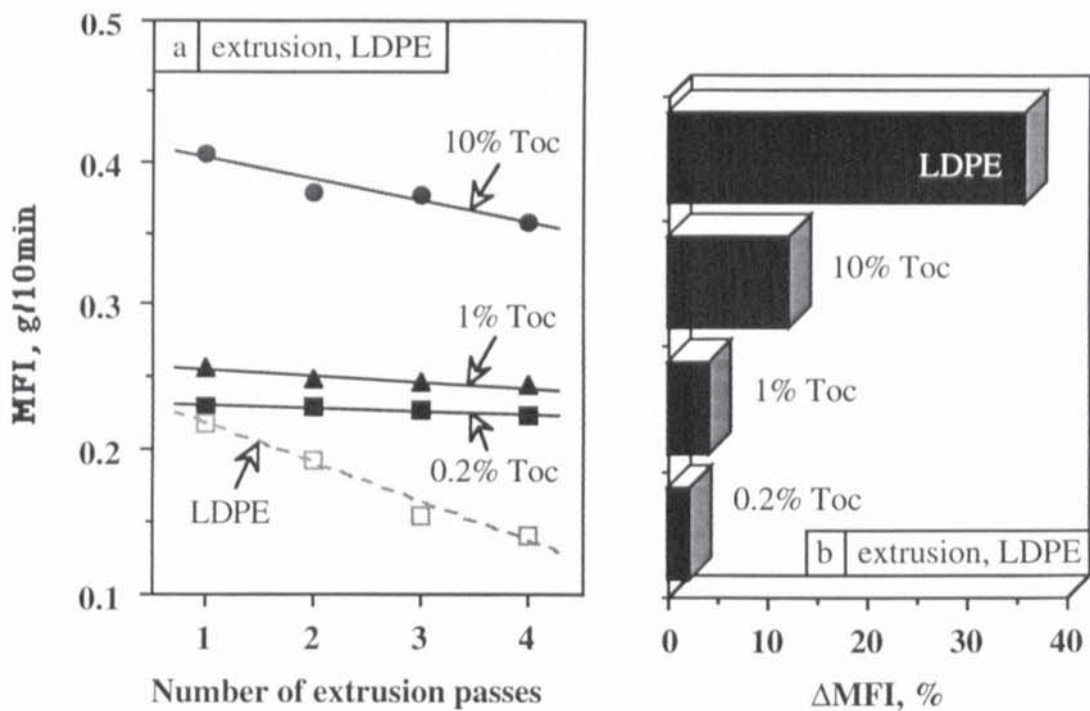


Figure 3.1: Effect of initial Toc concentration in LDPE and extrusion severity on the MFI (a) and Δ MFI (b) of LDPE (single screw extruder, 180°C) (see tables 3.2 and 3.3, p. 286)

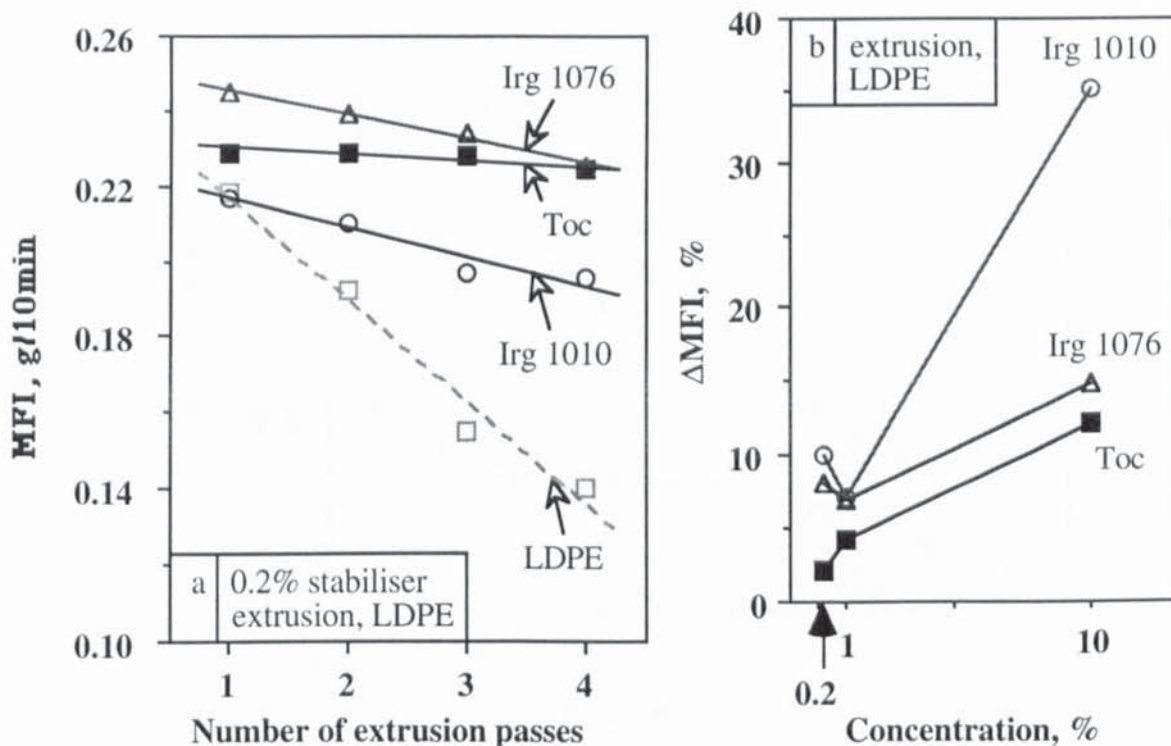


Figure 3.2: Effect of extrusion severity on the MFI (a) and initial antioxidant concentration on the Δ MFI (b) of LDPE extruded in the absence and presence of each of the stabilisers Toc, Irg 1010 and Irg 1076 (single screw extruder, 180°C) (see tables 3.2 and 3.3, p. 286)

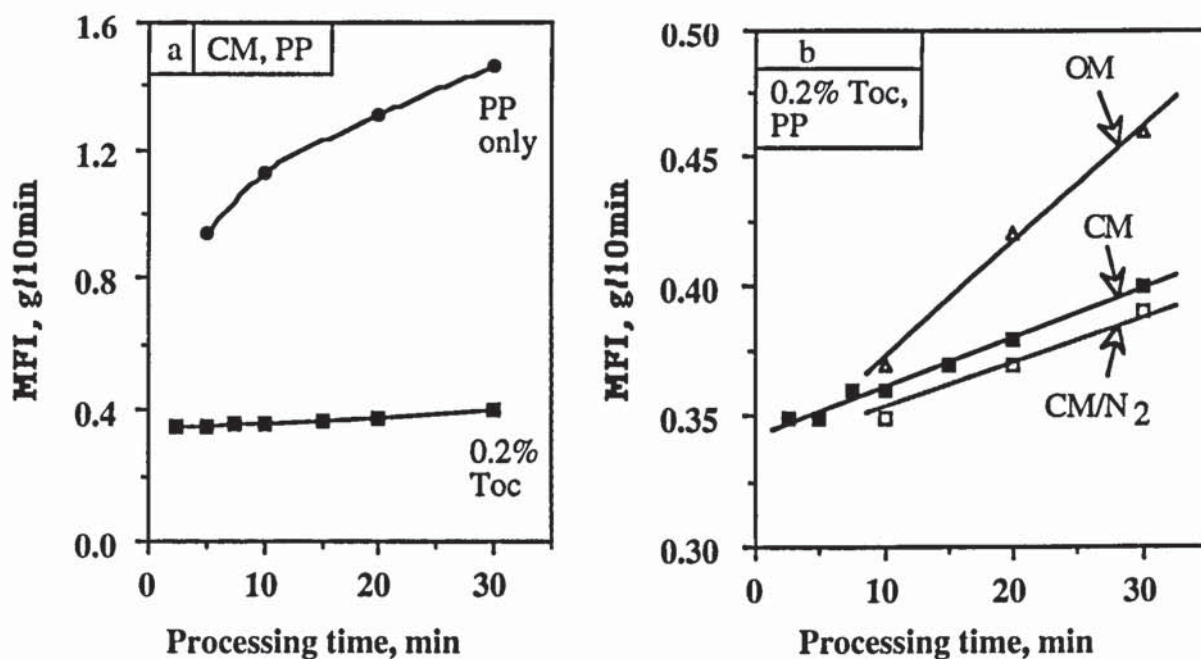


Figure 3.3: Effect of processing severity on the MFI of PP, processed in the absence and presence of 0.2% Toc (CM, 200°C) (a), and effect of oxygen concentration in the internal mixer on the MFI of PP processed with 0.2% Toc (CM/N₂, CM and OM, 200°C) (see table 3.4, p. 288)

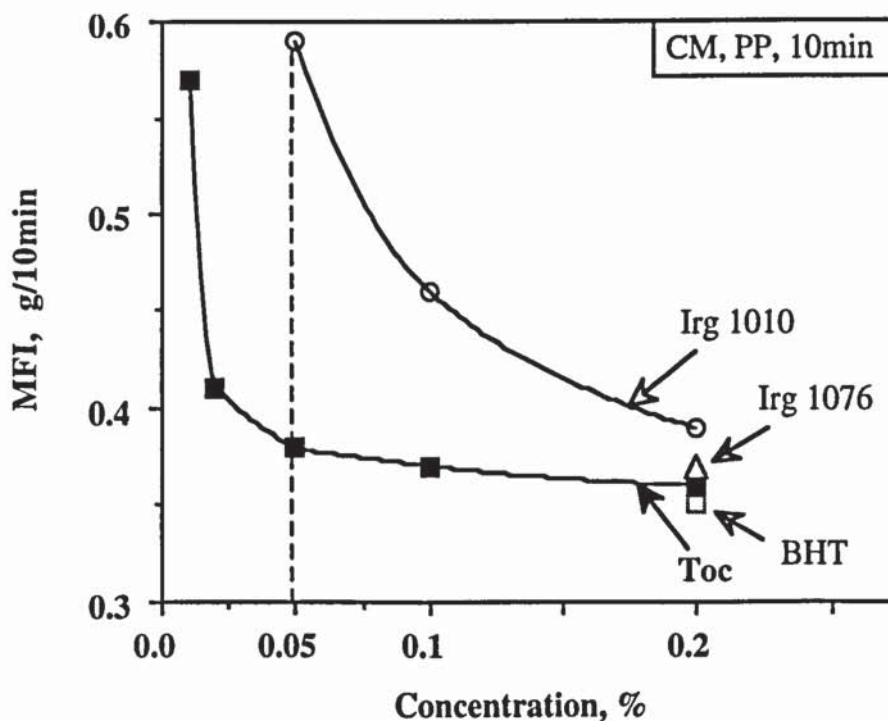


Figure 3.4: Effect of initial antioxidant concentration on the MFI of PP and comparison of the melt stabilising activity of Toc with those of the commercial hindered phenols Irg 1076, Irg 1010 and BHT, in PP (internal mixer, CM, 10min, 200°C) (see tables 3.5 and 3.6, p. 289)

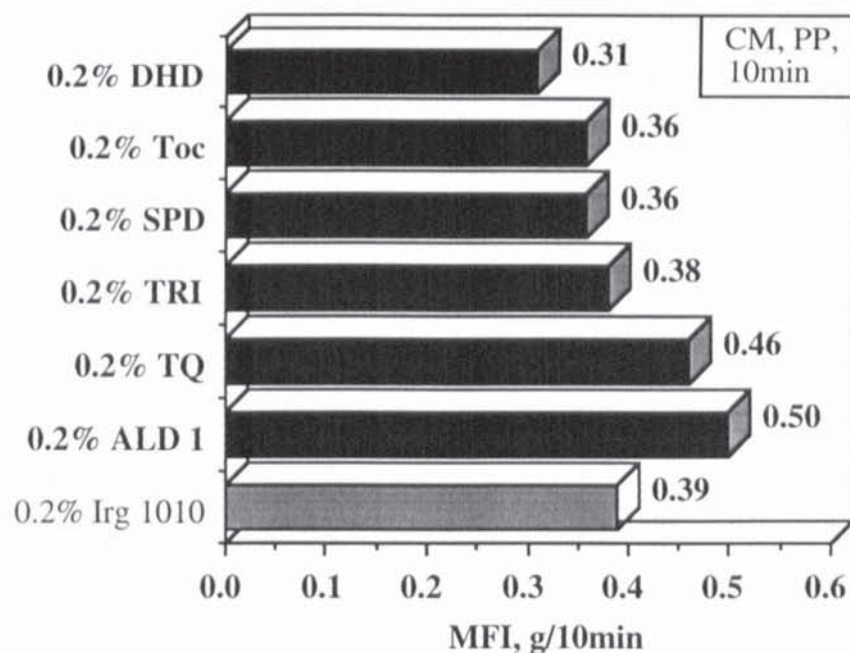


Figure 3.5: MFI of PP processed with 0.2% of each of the stabilisers Toc, Toc derivatives and Irg 1010 in an internal mixer (CM, 10min, 200°C) (see table 3.7, p. 291)

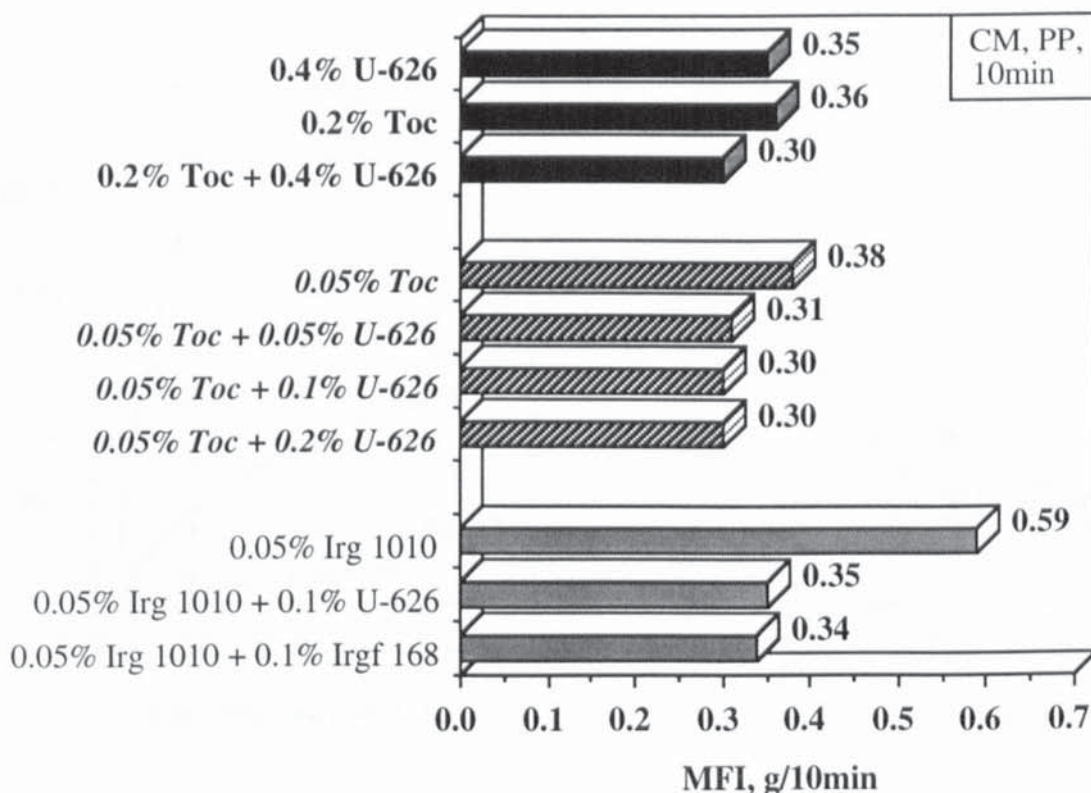


Figure 3.6: Effect of U-626 and Irgf 168 on the melt stabilising activities of Toc and Irg 1010 in PP processed in an internal mixer (CM, 10min, 200°C) (see tables 3.8 and 3.9, p. 293)

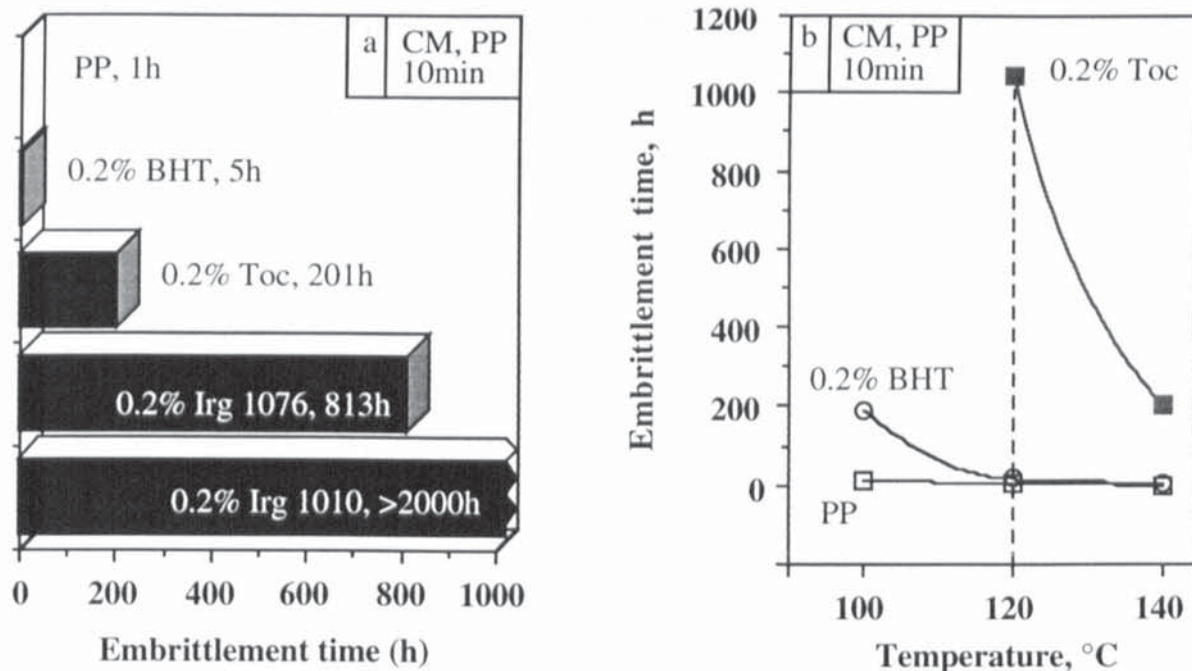


Figure 3.7: Thermal stability of PP films (0.25mm thick) processed in the absence and presence of 0.2% Toc and commercial antioxidants in an internal mixer (CM, 10min, 200°C), at 140°C (a) and 100-140°C (b) (see table 3.11, p. 295)

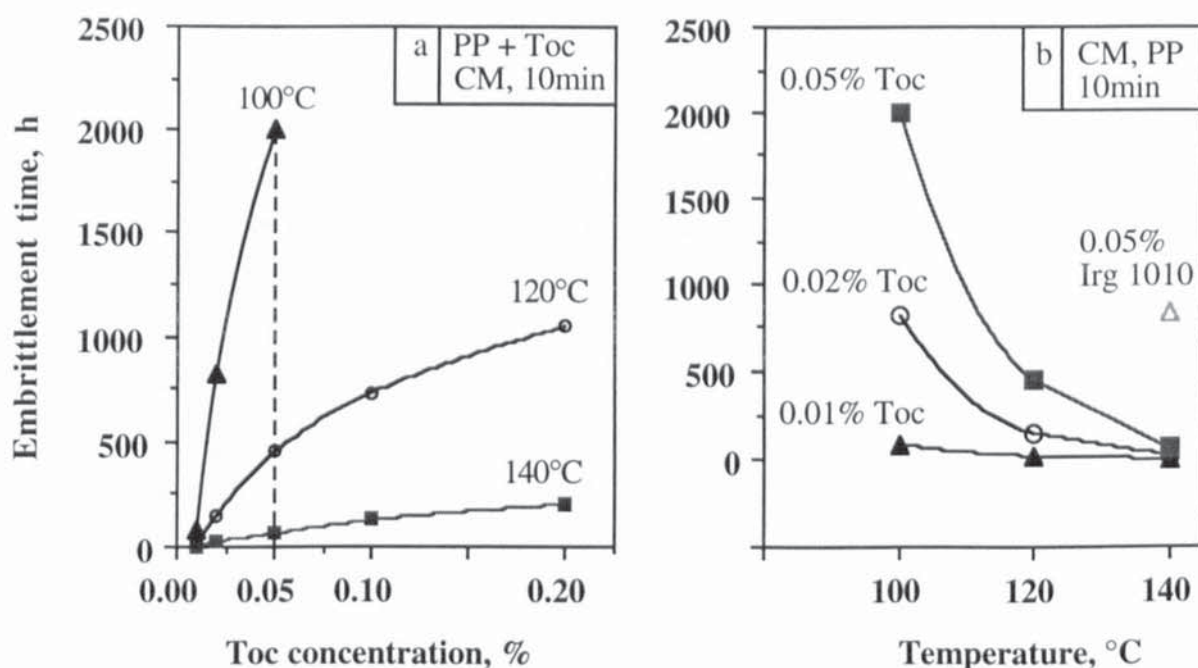


Figure 3.8: Effect of initial Toc concentration (a) and temperature (b) on the thermal stability of PP films (0.25mm thick) processed with Toc in an internal mixer (CM, 10min, 200°C) (see table 3.12, p. 296)

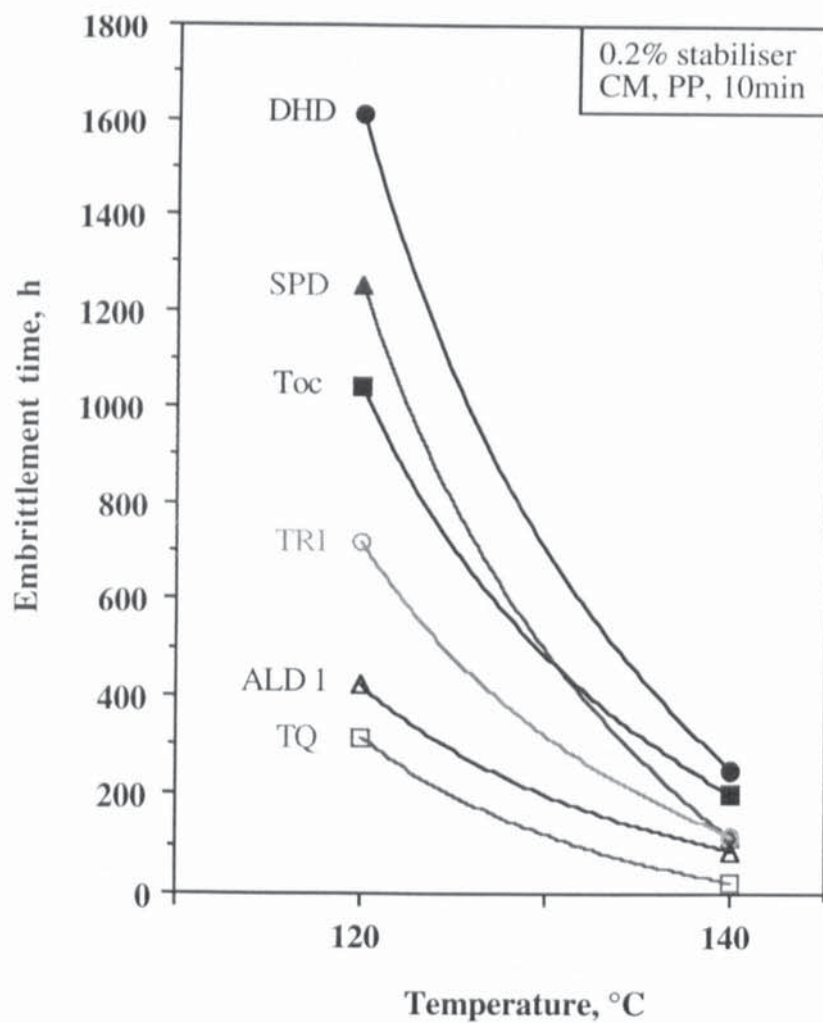


Figure 3.9: Thermal stability of PP films (0.25mm thick) processed with 0.2% Toc and 0.2% of a series of Toc derivatives in an internal mixer (CM, 10min, 200°C) (see table 3.13, p. 297)

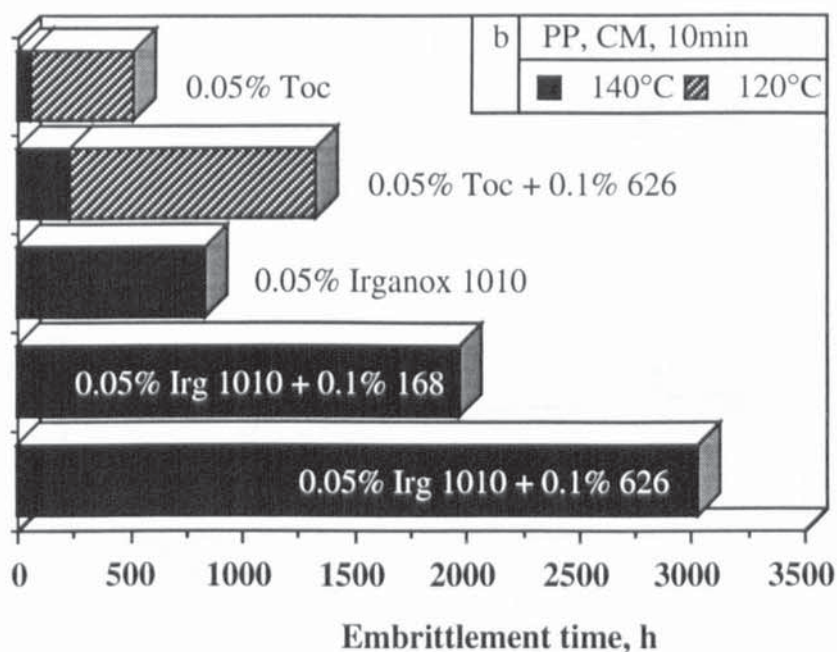
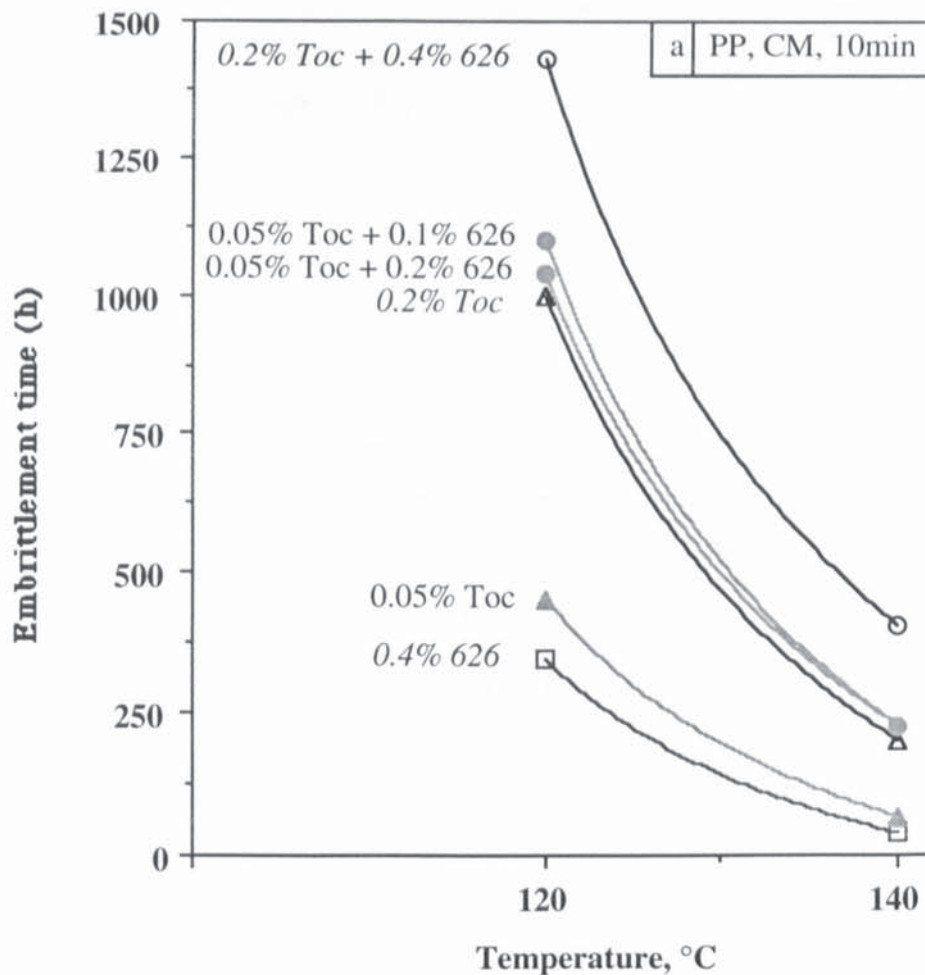


Figure 3.10: Effect of U-626 (626) and Irgf 168 (168) on the thermal stability of PP films (0.25mm thick) processed with Toc (a, b) and Irg 1010 (b) in an internal mixer (CM, 10min, 200°C) (see table 3.14, p. 298)

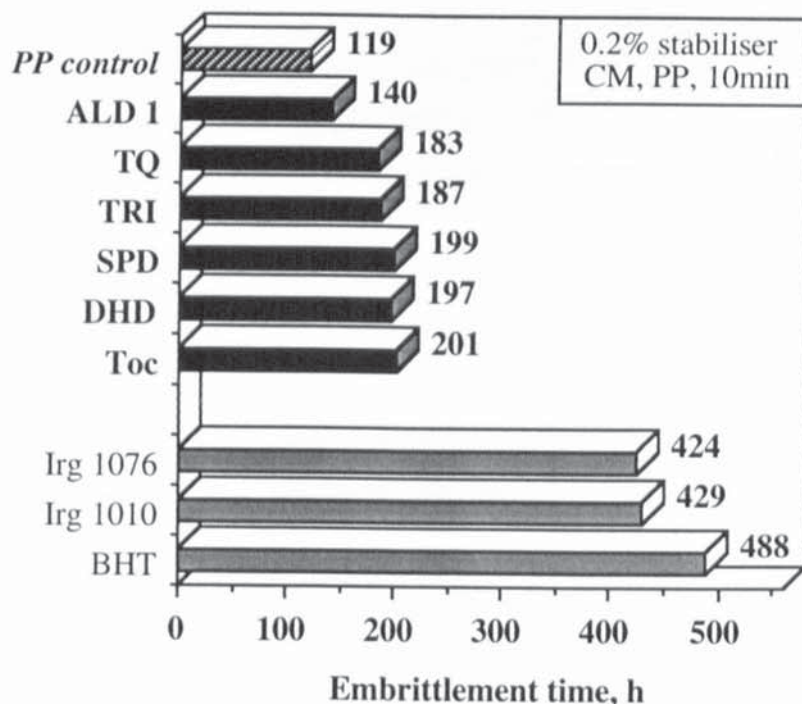


Figure 3.11: UV stability of PP films (0.25mm thick) processed in the absence and presence of 0.2% of each of the antioxidants Toc, Toc derivatives, Irg 1010, Irg 1076 and BHT, in an internal mixer (CM, 10min, 200°C) (see table 3.16, p. 299)

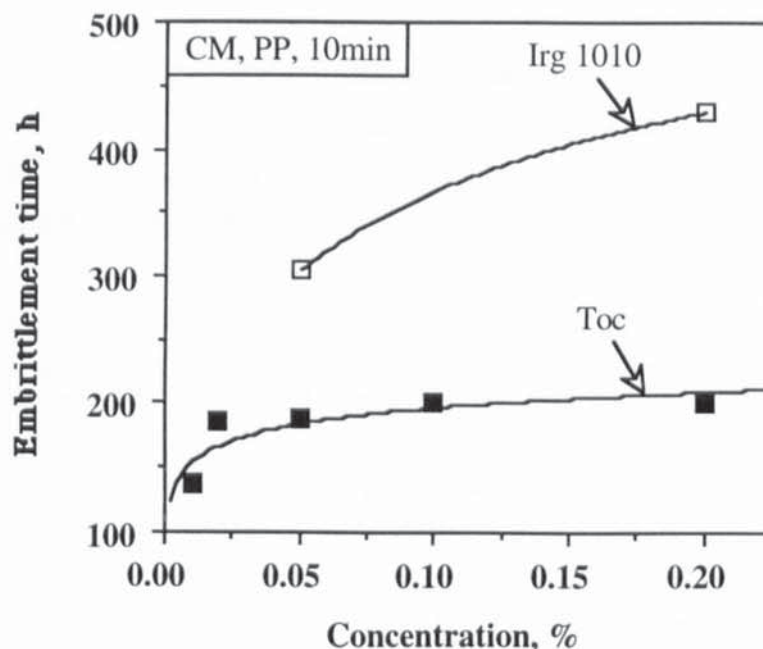


Figure 3.12: Effect of initial antioxidant concentration on the UV stability of PP films (0.25mm thick) stabilised with Toc and Irg 1010 in an internal mixer (CM, 10min, 200°C) (see table 3.17, p. 300)

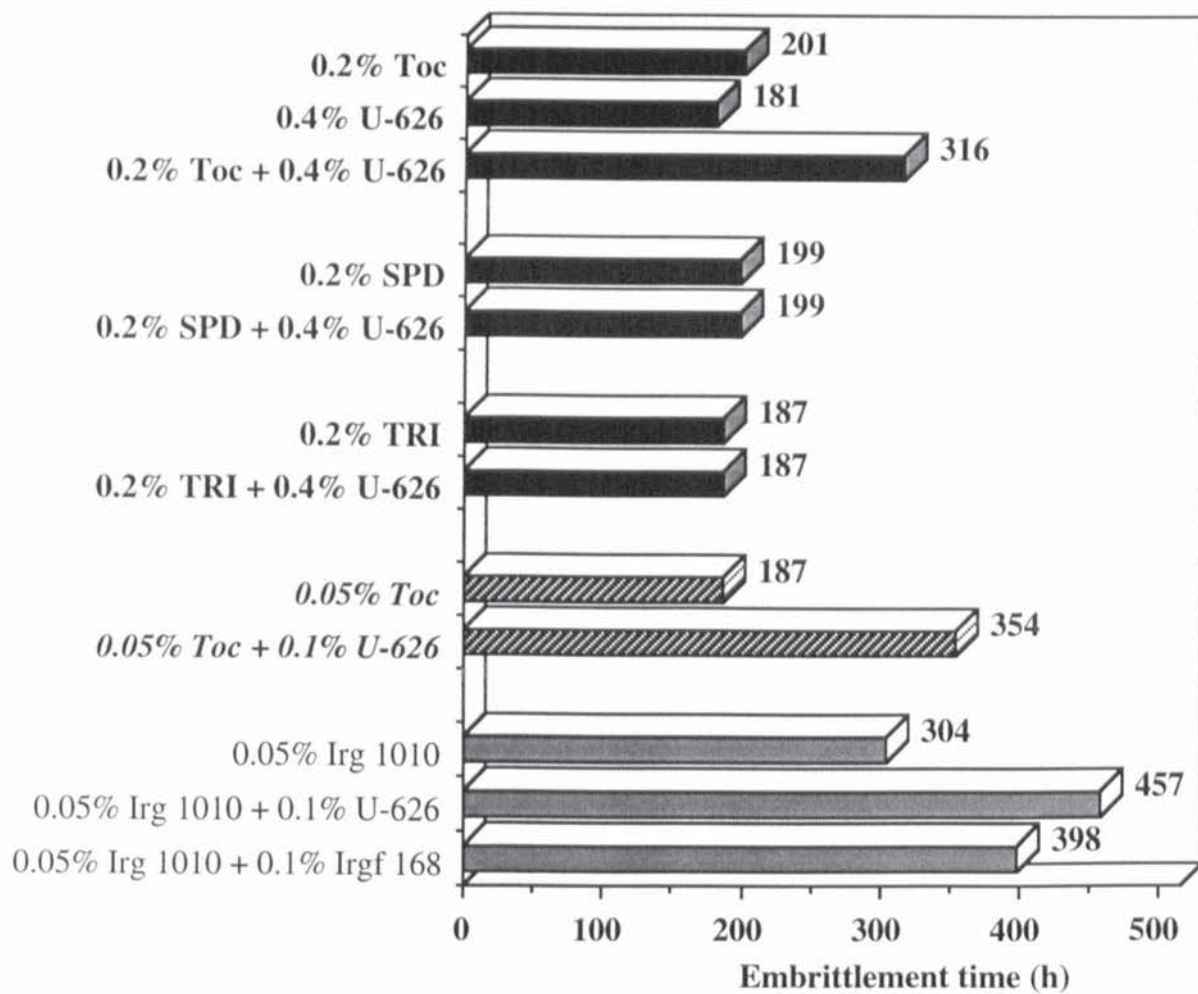


Figure 3.13: Effect of hindered aryl phosphites U-626 and Irgf 168 on the UV stabilising efficiencies of Toc, Toc derivatives and Irg 1010 in PP (internal mixer, CM, 10min, 200°C), at varying concentrations of the stabilisers (see table 3.18, p. 301)

CHAPTER FOUR

NATURE OF TRANSFORMATION PRODUCTS FORMED DURING PROCESSING OF POLYOLEFINS WITH TOC, TOC DERIVATIVES, IRG 1076 AND IRG 1010

»

LIST OF FIGURES - CHAPTER FOUR

Figure	Description	Page
4.1	HPLC chromatogram of compound E at 300nm and UV spectra of compounds E1, E2, E3 and E4	336
4.2	Chemical structure of Toc and suggested configurations of DHD, E1, E2, E3 and E4 (E)	338
4.3	HPLC chromatogram of compound D at 301nm and UV spectra of compounds D1, D2 and D3	339
4.4	Chemical structures and configurations of SPD, D1, D2 and D3	341
4.5	HPLC chromatograms of compounds A1, A2, B and C at 292nm and UV spectra of A1, A2, B1, B2, B3, B4, C1, C2, C3 and C4	342
4.6	¹ H-NMR spectra of TRI, A1, A2, B (B1-B4) and C (C1-C4); region 1.0 to 1.55ppm	345
4.7	Chemical structures and configurations of TRI, A1, A2, B and C	346
4.8	HPLC chromatogram at 290nm and UV spectrum of ALD 1, isolated from the products of reaction of Toc with PbO ₂ , ratio 1:40, mol/mol, in Toc:PbO ₂	347
4.9	Chemical structure of ALD 1, F	348
4.10	Effect of lead dioxide concentration on the nature and concentrations of the products of oxidation of Toc in hexane	351
4.11	HPLC chromatograms and UV spectra of ALD 1, F, ALD 2, G and ALD 3, H	354
4.12	Chemical structures of ALD 1, F, ALD 2, G and ALD 3, H	355
4.13	UV spectra of LDPE films (0.25mm thick) stabilised with 0.2% and 1% Toc, passes 4, before and after extraction with dichloromethane	357
4.14	HPLC analysis of the extracts of unstabilised LDPE, pass 1 and LDPE (a-b) stabilised with 0.2% Toc, pass 4 (LMWP)	423
4.14.c	Diode array UV analysis of the extract of unstabilised LDPE, pass 1	424
4.15	HPLC analysis of the extract of LDPE stabilised with 0.2% Toc, passes 1 (a-d) and 4	425
4.15	HPLC analysis of the extract of LDPE stabilised with 10% Toc, passes 1 (e-h) and 4	426
4.16	Effect of initial Toc concentration in LDPE on the concentrations of Toc and its transformation products after multiple extrusions	427
4.17	Effect of initial Toc concentration in LDPE on the concentration of the transformation products, after the first extrusion pass	428

4.18	Effect of initial Toc concentration in LDPE and extrusion severity on the added concentrations of retained Toc and DHD, E, after multiple extrusions	428
4.19	Effect of initial Toc concentration in LDPE and extrusion severity on the nature and distribution of its transformation products	429
4.20	UV spectra of PP films (0.25mm thick) stabilised with 0.2% Toc (CM/N ₂ and OM, 30min), 0.05% and 0.02% Toc (CM, 10min) and 0.2% SPD, D (CM, 10min), before and after extraction with dichloromethane	367
4.21 (a-d)	HPLC analysis of the extracts of unstabilised PP and PP stabilised with 0.2% Toc (CM, 10min, 200°C) (LMWP)	430
4.21 (e-f)	Diode array UV analysis of the extract of unstabilised PP and FTIR analysis of unstabilised PP film (0.25mm thick) (CM, 10min, 200°C)	431
4.22	HPLC analysis of the extracts of PP processed with 0.2% Toc (CM/N ₂ , 200°C) for 5min and 30min	432
4.23	HPLC analysis of the extracts of PP processed with 0.2% Toc (OM, 200°C) for 5min and 30min	433
4.24	Diode array UV analysis of ALD 4 and ALD 5, extracted from PP stabilised with 0.2% Toc (OM, 10min, 200°C)	434
4.25	Effect of oxygen concentration in the internal mixing chamber and processing severity on the concentration of Toc and its transformation products in PP stabilised with 0.2% Toc (OM, CM and CM/N ₂ , 200°C)	435
4.26	Effect of oxygen concentration in the internal mixing chamber on the concentration of Toc and its transformation products in PP stabilised with 0.2% Toc (OM, CM, CM/N ₂ , 5min, 200°C)	436
4.27	Effect of oxygen concentration on the concentration of ALD 1-5 compared to other products in PP stabilised with 0.2% Toc (CM/N ₂ , CM and OM, 200°C)	436
4.28	Effect of processing severity on the concentration of transformation products of Toc in PP stabilised with 0.2% Toc (OM, CM and CM/N ₂ , 200°C)	437
4.29	HPLC analysis of the extracts of PP stabilised with 0.01% and 0.05% Toc (CM, 10min, 200°C)	438
4.30	Effect of initial Toc concentration in PP on the nature and concentrations of its transformation products (CM, 10min, 200°C)	439
4.31	Effect of initial Toc concentration in PP on the distribution of its oxidation products (CM, 10min, 200°C)	440
4.32	HPLC analysis of the extracts of PP stabilised with 0.2% DHD, E and 0.2% TRI, A, B, C (CM, 10min, 200°C)	441

4.33	Nature of transformation products in PP stabilised with 0.2% of each of the Toc derivatives DHD, E, SPD, D and TRI, A, B, C (CM, 10min, 200°C)	442
4.34	UV spectra of PP films (0.25mm thick) stabilised with 0.4% U-626, 0.05% Toc + 0.1% U-626, 0.2% SPD, D + 0.4% U-626 and 0.2% TRI, A, B, C + 0.4% U-626 (CM, 10min, 200°C), before and after extraction with dichloromethane	378
4.35	³¹ P-NMR spectra of U-626 and the extracts of PP stabilised with 0.4% U-626, 0.4% U-626 + 0.2% Toc, 0.1% U-626 + 0.05% Toc, 0.4% U-626 + 0.2% SPD, D and 0.4% U-626 + 0.2% TRI, A, B, C (CM, 10min, 200°C)	443
4.36 (a-d)	HPLC analysis of the extracts of PP stabilised with 0.4% U-626 and 0.05% Toc + 0.1% U-626 (CM, 10min, 200°C)	444
4.36 (e-h)	HPLC analysis of the extracts of PP stabilised with 0.2% SPD, D + 0.4% U-626 and 0.2% TRI, A, B, C + 0.4% U-626 (CM, 10min, 200°C)	445
4.37	Effect of U-626 in PP containing Toc, SPD, D and TRI, A, B, C on the nature and concentration of their transformation products (CM, 10min, 200°C)	446
4.38	Possible chemical structure of the peak at 344 in the MS spectrum of compound 1, Irg 1076-1	386
4.39	Possible chemical structures of compounds 2-10, Irg 1076-2 to -10	386
4.40	Chemical structure of compound 12, C-Irg 1076	387
4.41	Chemical structure of compound 13, BC-Irg 1076	388
4.42	Possible chemical structures of compounds 11 and 14, QM-Irg 1076 and CBQM-Irg 1076	388
4.43	Chemical structure of compound 3, Irg 1010-3	390
4.44	Chemical structure of compound 6, Irg 1010-6	390
4.45	Possible chemical structures of compounds 1, 2, 5 and 7 to 13, Irg 1010-1, -2, -5 and Irg 1010-7 to -13	391
4.46	Possible chemical structures of compounds 4 and 14, Irg 1010-4 and -14	392
4.47 (a-d)	HPLC analysis of the products extracted from LDPE stabilised with 0.2% Irg 1076, passes 1 and 4	447
4.47 (e-h)	HPLC analysis of the products extracted from LDPE stabilised with 10% Irg 1076, passes 1 and 4	448
4.48	Effect of extrusion severity and initial Irg 1076 concentration on the nature and peak areas (282nm) of the transformation products of Irg 1076 in LDPE and concentrations of C-Irg 1076 and BC-Irg 1076, relative to Irg 1076	449
4.49	Effect of extrusion severity on the peak areas (282nm) and distribution of the transformation products of Irg 1076 in LDPE	450
4.50 (a-d)	HPLC analysis of the products extracted from LDPE stabilised with 0.2% Irg 1010, passes 1 and 4	451

4.50	HPLC analysis of the products extracted from LDPE stabilised with 10%	
(e-h)	Irg 1010, passes 1 and 4	452
4.51	Effect of initial Irg 1010 concentration and extrusion severity on the nature and peak areas (282nm) of its transformation products in LDPE	453
4.52	Effect of extrusion severity on the nature and peak areas (282nm) of the transformation products of Irg 1010 in LDPE	454

4.1 OBJECT AND METHODOLOGY

In chapter three, the melt stabilising efficiencies of α -tocopherol (Toc) and some of its transformation products in PP and LDPE were compared with those of commercial synthetic hindered phenol antioxidants (e.g. Irg 1076 and Irg 1010). The excellent melt stabilising efficiency of Toc was clearly illustrated, especially at very low concentrations (e.g. 0.02%). The use of a hindered aryl phosphite (e.g. U-626) in combination with Toc in PP lead to enhanced melt and colour stabilities of the polymer. Toc derivatives, which were found (in this work) to form during processing of Toc with PP and LDPE, offered either better (DHD), similar (SPD and TRI) or lower (ALD 1 and TQ) melt and thermal stabilities to PP than the parent antioxidant (see table 4.1 for structures). It becomes clear that the overall stability afforded to the polymer depends not only on the initial added antioxidants but, also, on the behaviour of their transformation products. These can either be beneficial (when transformation products are themselves antioxidants) or harmful (when products exert prooxidant effects) to the overall polymer stability. The melt stabilising efficiencies of commercial hindered phenols, e.g. BHT, Irganox 1010 and Irganox 1076, in polyolefins has been shown to be affected by the formation of various oxidative transformation products, including dimers, trimers and quinonoid structures [47,50,51,103]. These products have also been shown to be formed from oxidations of Toc in model reactions [88-92], however no work has been described on the nature of the products formed during the antioxidant action of Toc during melt processing. In the work described in this chapter, the nature and concentration of transformation products formed during processing of Toc, Toc derivatives, Irg 1076 and Irg 1010 in polyolefins are examined, for a better understanding of the melt stabilisation mechanisms of these antioxidants.

First the nature of the oxidation products formed from Toc in model reactions was examined by oxidising Toc with lead dioxide, using different concentrations of the oxidising agent (see section 2.2.1 and scheme 2.1 for procedure). The reactions were carried out in hexane under argon atmosphere, at room temperature, so that products are initially formed via a radical mechanism. The reaction products were separated by NP-

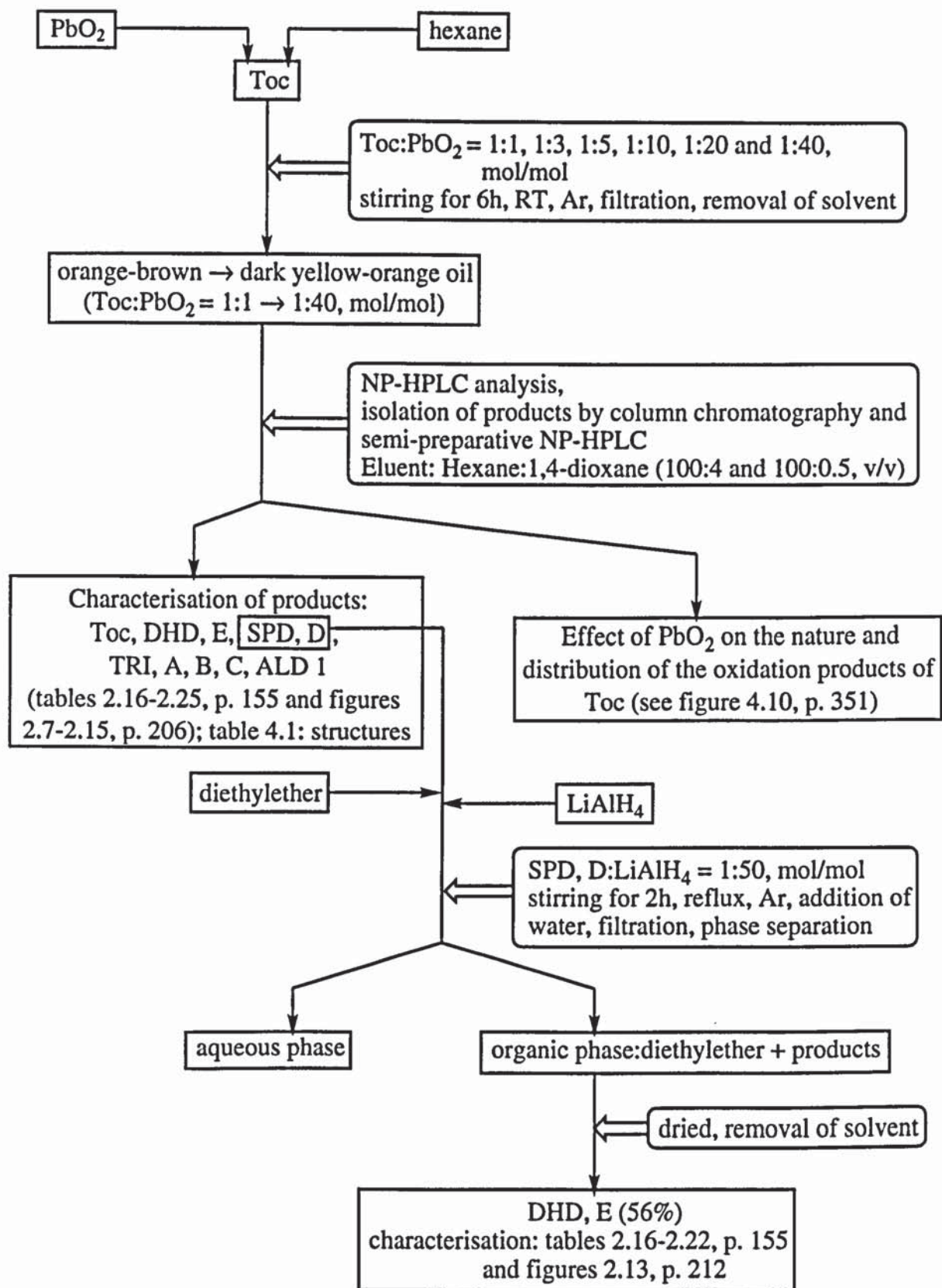
HPLC, isolated by column chromatography or preparative NP-HPLC and characterised using different spectroscopic and spectrometric techniques (see section 2.2.2). Oxidation products of Toc including DHD, SPD, TRI and ALD 1 were isolated and their concentrations were determined from their HPLC peak areas, to study the effect of PbO₂ concentration on the nature and distribution of the products. Scheme 4.1 shows the methodology employed for the isolation, identification and determination of the concentrations of the products and table 4.1 describes all the oxidation products of Toc used and isolated in the work described in this chapter. The above products were compared with transformation products of Toc formed during processing of polymer samples stabilised with high concentrations of the antioxidant, so that high concentrations of products could be extracted. Three aldehydes, ALD 1, ALD 2 and ALD 3 were isolated from PP stabilised with 39% Toc, pass 4 (supplied, CPC789 series, single screw extruder, 270°C) (see section 2.7.1). Furthermore, dimers (DHD and SPD), trimers (TRI) and aldehydes (ALD 1 and ALD 2) of Toc were also isolated from LDPE stabilised with 0.2 and 10% Toc, pass 4 (single screw extruder, 180°C) (see section 2.7.2). All the isolated products were extracted from the polymer with dichloromethane and characterised using spectroscopic and spectrometric techniques. Scheme 4.2 describes the methodology employed for the isolation and characterisation of the products.

To investigate the melt stabilisation mechanism of Toc in polymers, transformation products formed from the antioxidant during multiple extrusion with LDPE (single screw extruder at 180°C) and processing with PP (internal mixer at 200°C, under different conditions) were examined. Furthermore, the mechanisms of stabilisation of products formed from Toc during processing with PP (DHD, SPD, TRI, ALD 1 and TQ) were also studied for a better understanding of the mechanism of melt stabilisation of Toc in polymers. All the products were extracted from the polymer with dichloromethane, analysed by NP-HPLC and UV (diode array system) and identified by comparing their UV characteristics and HPLC retention times with those of supplied products (i.e. ALD 1 and TQ) and the products isolated from the model reactions and polymer extracts. It was found that identical oxidation products, in addition to some new ones (ALD 4 and 5) were

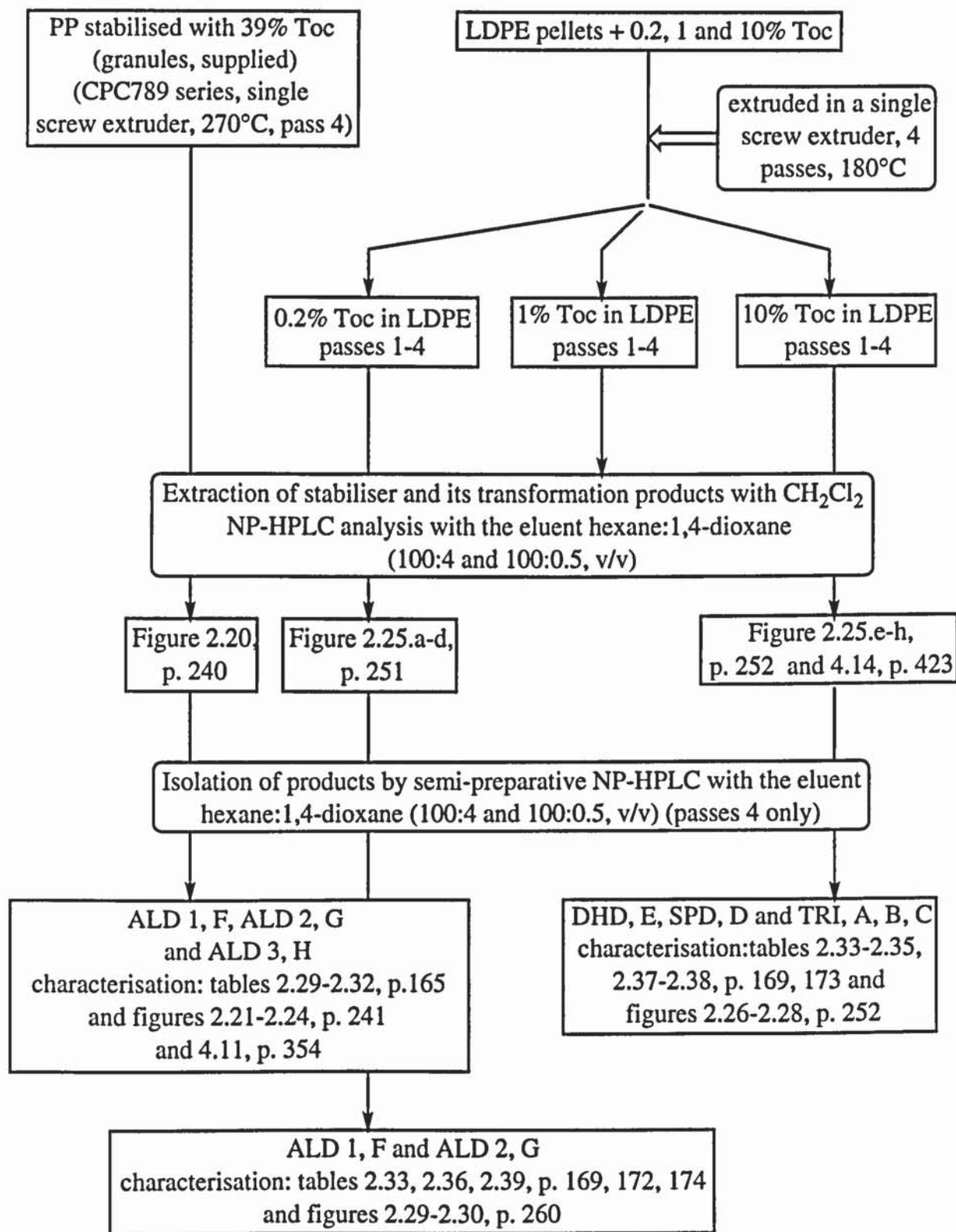
formed in the polymer. The products formed during processing of PP with combinations of Toc and U-626 were also examined to elucidate the reason for the better melt stabilising efficiency of Toc in presence of the phosphite.

Finally, the nature and concentrations of the transformation products formed from Toc during multiple extrusions with LDPE were compared with those formed from Irg 1076 and Irg 1010 during extrusions with LDPE (see section 2.8). The products were extracted from the polymer, isolated by RP-HPLC and characterised using various spectroscopic and spectrometric techniques. Scheme 4.3 describes the methodology employed for the isolation and characterisation of the products and tables 4.2 and 4.3 show the nature of the transformation products of Irg 1076 and Irg 1010, respectively.

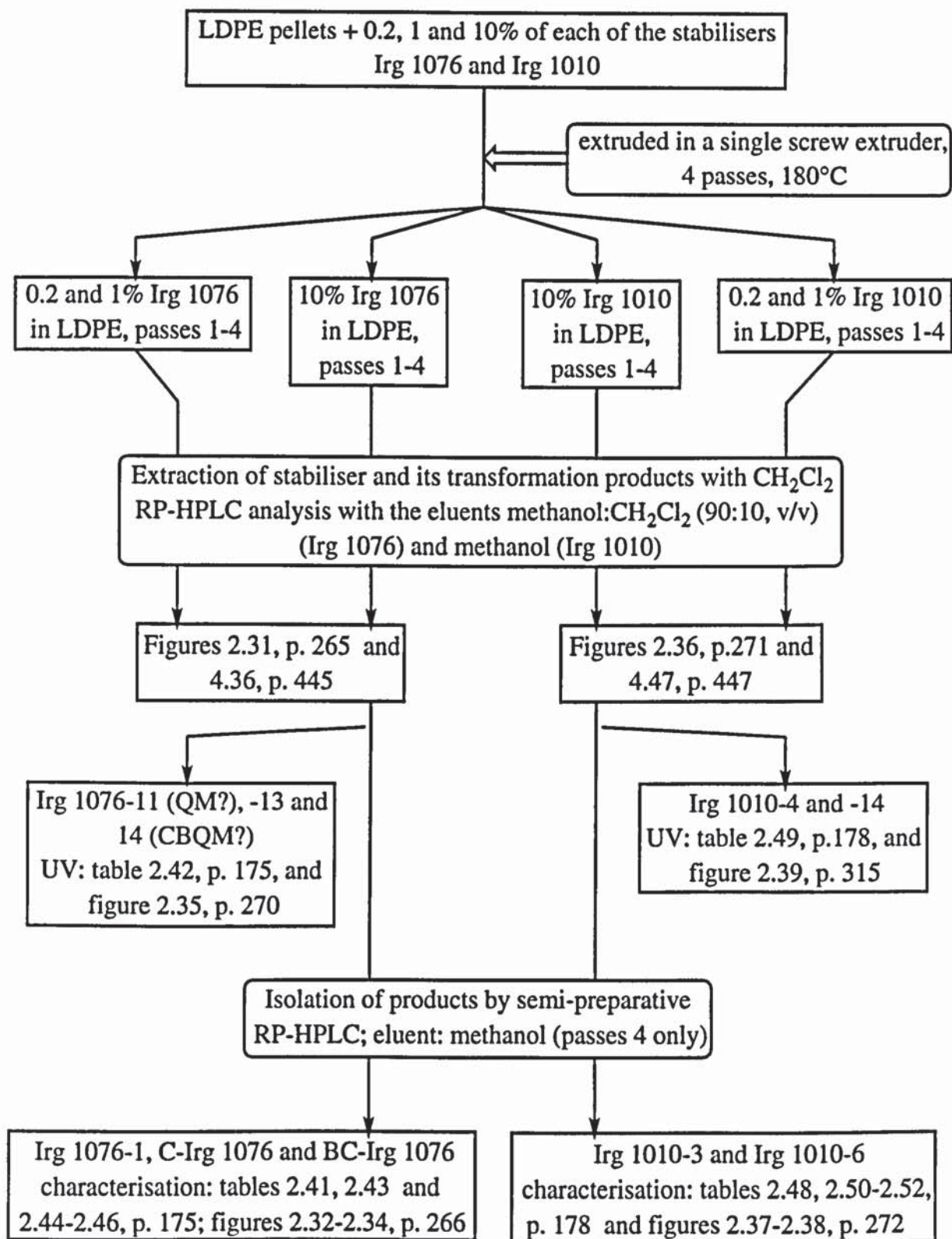
Errors on the concentrations of Toc and Toc derivatives were determined from their HPLC peak areas and extinction coefficients, as described in section 2.11.1. It was found that for concentrations below 10%, between 10-50% and 50-100% (% weight), errors did not exceed 15, 6 and 5%, respectively. In the case of Irg 1076 and Irg 1010 and their transformation products, errors on their HPLC peak areas at 282nm are shown in table 2.65, p. 135. Errors on the concentrations of the Irg 1076 oxidation products C-Irg 1076 and BC-Irg 1076 were found not to exceed 16% (concentrations below 5%) and 10% (concentrations above 5%) (see section 2.11.2).



Scheme 4.1: Methodology for the determination of the nature and concentrations of the products of oxidation of Toc with PbO₂ (see scheme 2.1, p. 86 and scheme 2.2, p. 95)



Scheme 4.2: Methodology for the isolation and identification of transformation products of Toc from PP stabilised with 39% Toc, pass 4 (CPC789 series, single screw extruder, 270°C) and LDPE stabilised with 0.2, 1 and 10% Toc, passes 4 (single screw extruder, 180°C)



Scheme 4.3: Methodology for the isolation and identification of transformation products of Irg 1076 and Irg 1010 from LDPE stabilised with 0.2, 1 and 10% of each of the stabilisers, passes 4 (single screw extruder, 180°C)

Table 4.1: Chemical structures and description of oxidation products of Toc and the hindered aryl phosphite U-626

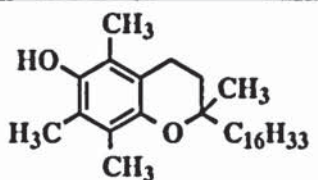
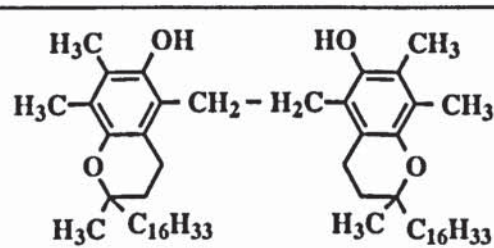
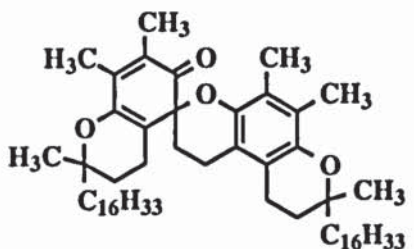
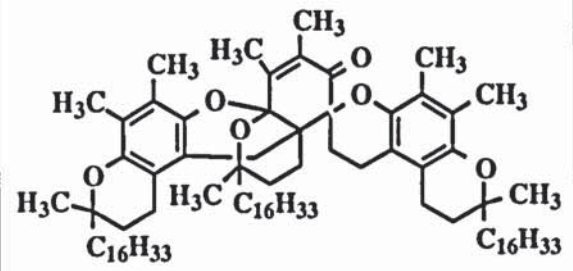
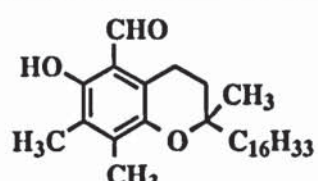
code name	chemical structure and name (MM)	origin (purity)	state / colour	λ (max and 290 and/or 275nm) (E, $l.g^{-1}.cm^{-1}$)
Toc	 <p>α-tocopherol (430g)</p>	Hoffmann-La Roche (Ronotec 202, min. 97%)	liquid / orange-brown	298 (8.6) 290 (8.1) 275 (3.3)
DHD, E (E1, E2, E3, E4)	 <p>dihydroxydimer (858g)</p>	synthesised (98%, section 2.2.3)	liquid / orange-brown	300 (8.9) 290 (7.9) 275 (3.0)
SPD, D (D1, D2, D3)	 <p>spirodimer (856g)</p>	synthesised (99.6% section 2.2.1)	liquid / dark yellow-orange	301 (5.2) 339 (2.5) 290 (4.3)
TRI, A, B, C (A1, A2, B, C)	 <p>trimer (1285g)</p>	synthesised (100%, section 2.2.1)	liquid / pale yellow	292 (5.12) 290 (4.98)
ALD 1, F	 <p>5-formyl-γ-tocopherol (444g)</p>	Hoffmann-La Roche and isolated (section 2.7.1)	liquid / dark yellow-orange	239 290 (20.5) 282 (19.7) 386 (6.4) 275 (15.2)

Table 4.1 continued

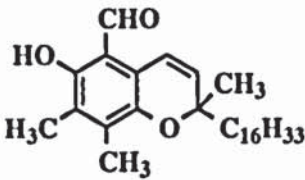
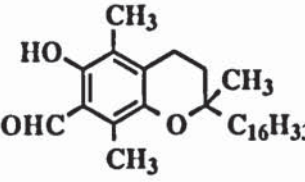
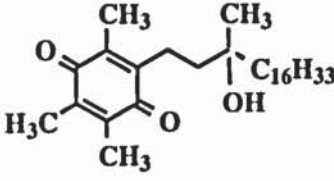
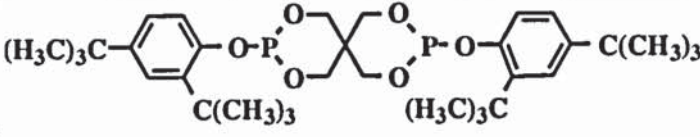
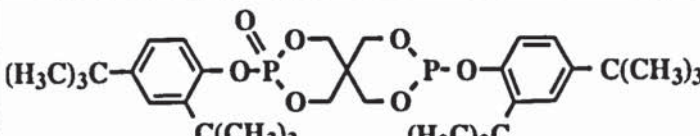
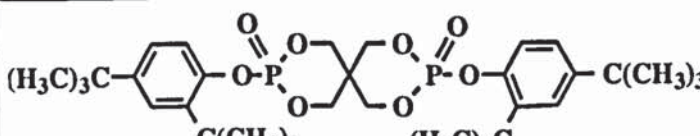
code name	chemical structure and name (MM)	origin	state / colour	λ (max and 290 and/or 275nm) (E, l.g ⁻¹ .cm ⁻¹)
ALD 2, G	 <p>5-formyl-γ-tocopherol-3-en (442g)</p>	Hoffmann-La Roche and isolated (section 2.7.1)	liquid / dark yellow-orange	250 285 (18.6) 297 (16.7) 404 (4.9) 290 (17.7)
ALD 3, H	 <p>7-formyl-β-tocopherol (444g)</p>	isolated (section 2.7.1)	liquid / dark yellow-orange	283 (16.0) 395 (4.3) 290 (15.6)
ALD 4	unknown	-	-	280, 380
ALD 5	unknown	-	-	280, 382
TQ	 <p>α-tocoquinone (446g)</p>	Hoffmann-La Roche	liquid / orange	260 (39.0) 268 (38.4) 275 (11.9)
U-626	 <p>Ultrinox 626 (604g)</p>	Hoffmann-La Roche	solid / white	271 (4.0) 278 (3.7)
U-626, 6	 <p>Ultrinox 626 monophosphate (620g)</p>	extracted (section 4.2.5)		278 350
U-626, 7	 <p>Ultrinox 626 diphosphate (636g)</p>	extracted (section 4.2.5)		278 340

Table 4.2: Chemical structures and description of transformation products of Irg 1076

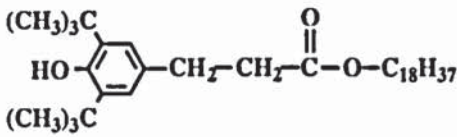
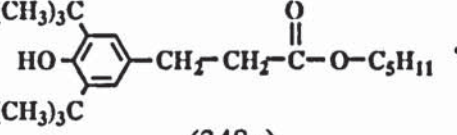
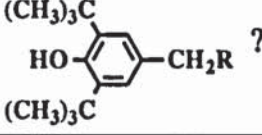
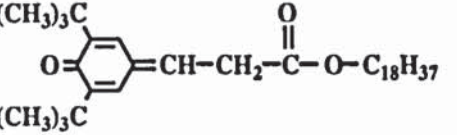
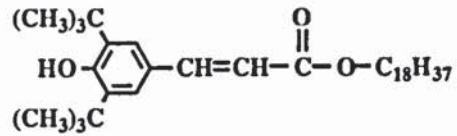
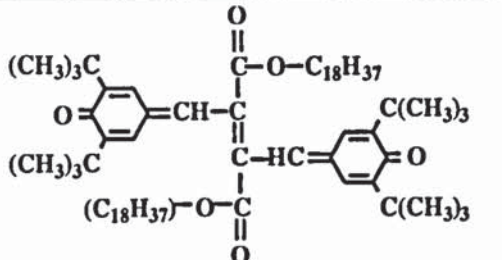
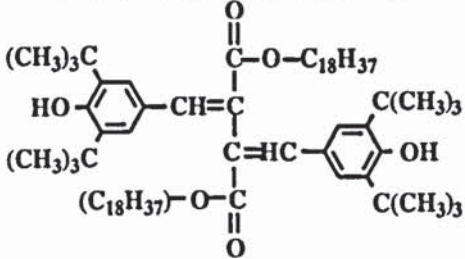
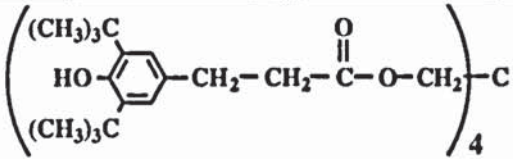
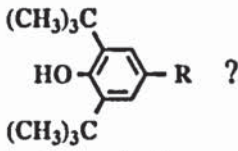
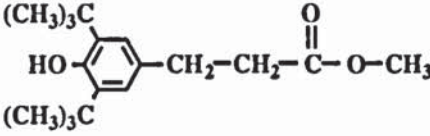
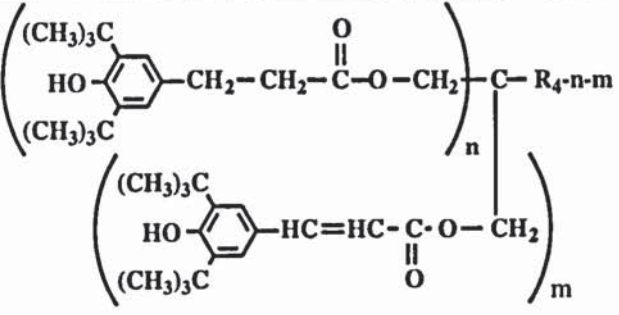
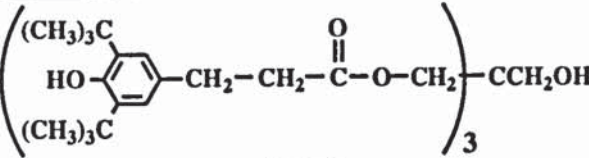
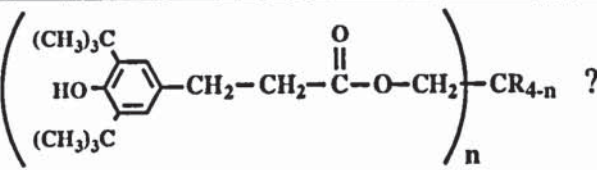
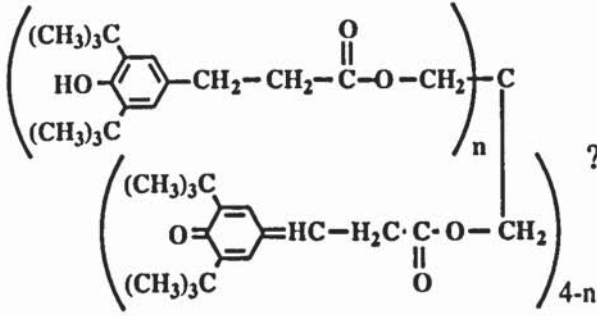
code name	chemical structure and name (MM)	origin	state / colour	λ (max and 282 nm) (E, l.g ⁻¹ .cm ⁻¹)
Irg 1076	 <p>Irganox 1076 (530g)</p>	Ciba-Geigy	solid / white	282 (3.84) 276 (3.80)
Irg 1076-1	 <p>(348g)</p>	isolated (section 2.8.1)	solid / white	282 (broad)
Irg 1076-2-10	 <p>?</p>	extracted (section 2.8.1)		282
QM-Irg 1076 (11)	 <p>quinone methide of Irganox 1076 (528g)</p>	extracted (section 2.8.1)		315 (broad) (26915) [54], 238
C-Irg 1076 (12)	 <p>cinnamate of Irganox 1076 (528g)</p>	isolated (section 2.8.1)	solid / yellow	240 320 (broad) (40.2) 282 (14.6)
Irg 1076-13	contains cinnamate or quinonoid structure	extracted (section 2.8.1)		282, 320 (broad)
CBQM-Irg 1076 (14)	 <p>conjugated bisquinone methide of Irganox 1076 (1053g)</p>	extracted (section 2.8.1)		320 (broad) (33.0) [20], 240
BC-Irg 1076 (15)	 <p>biscinnamate of Irganox 1076 (1055g)</p>	isolated (section 2.8.1)	solid / yellow	308 (33.5) [20], 240

Table 4.3: Chemical structures and description of transformation products of Irg 1010

code name	chemical structure and name (MM)	origin	state / colour	λ_{\max} , nm (E, l.g ⁻¹ .cm ⁻¹)
Irg 1010	 <p>Irganox 1010 (1177g)</p>	Ciba-Geigy	solid / white	282 (6.4) 276 (6.3)
Irg 1010-1, -2		extracted (see section 2.8.2)		282
Irg 1010-3	 <p>(292g)</p>	isolated (section 2.8.2)	solid / white	282
Irg 1010-4		extracted (see section 2.8.2)		320 (broad) 282
Irg 1010-6	 <p>(916g)</p>	isolated (section 2.8.2)	solid / white	282
Irg 1010-5, and -7-11		extracted (see section 2.8.2)		282
Irg 1010-14		extracted (see section 2.8.2)		312 (broad) 288

4.2 RESULTS

4.2.1 Nature of transformation products and mechanism of oxidation of Toc in model systems

4.2.1.1 Isolation and identification of oxidation products of reactions of Toc with lead dioxide

Toc was oxidised with varying concentrations of lead dioxide in hexane (RT, 6h) and the reaction products were isolated for analysis (see section 2.2.1 and scheme 4.1 for methodology). Optimisation of HPLC conditions lead to a good separation of the different oxidation products formed from Toc. Four products, DHD, E, SPD, D, TRI, A, B, C and ALD 1, F (see table 4.1 for structures and table 4.4 for HPLC retention times (Rt)), were separated and isolated from the reaction mixtures containing high concentrations of the latter by NP-HPLC using different ratios of the solvent system hexane:1,4-dioxane (see section 2.10 for procedure), or column chromatography (see section 2.2.2). DHD, E and Toc, which have the highest HPLC Rt were well separated from the other products when the ratio 100:4, v/v, in hexane:1,4-dioxane was used, whereas SPD, D, TRI, A, B, C and ALD 1, F were further separated using the ratio 100:0.5, v/v, resulting in the separation of all their stereoisomers (see figures 2.7 and 2.8, p. 206, for typical HPLC chromatograms). The reduction of SPD, D with LiAlH_4 lead to DHD, E (56%) which was purified by semi-preparative HPLC using the mobile phase hexane:1,4-dioxane (100:4, v/v) (see figure 2.13.a, p. 212, for its HPLC chromatogram and scheme 4.1 for methodology). Table 4.4 shows the HPLC Rt of the different products formed and the solvent ratios in hexane:1,4-dioxane used for the isolation by semi-preparative HPLC of their different stereoisomers. Each of the isolated oxidation product was characterised using various spectroscopic techniques and the results were compared with those obtained for Toc and the supplied Toc derivatives ALD 1 and TQ. The results are shown at the end of chapter two in form of tables (2.16-2.25, p. 155) and figures (2.2, p. 187, and 2.13-215, p. 212) and are explained below.

Table 4.4: HPLC Rt and conditions for isolation of oxidation products of Toc
 (Toc:PbO₂ ratios in mol/mol and solvent ratios in hexane:1,4-dioxane, v/v)
 (figures 2.7 and 2.8, p. 206)

compound		Rt (min:sec)		conditions for preparative HPLC	
		100:4	100:0.5	Toc: PbO ₂	solvent ratio
Toc		10:30	45:00	1:1	100:4
DHD, E	E1	14:00	180		1:10 (figure 2.7)
	E2	15:00			
	E3	15:30			
	E4				
TRI, A, B, C	A1	3:00-5:00	9:30	1:40 (figure 2.8)	100:4, followed by 100:0.5 (A1, A2, B and C isolated separately)
	A2		9:50		
	B1		14:30		
	B2		15:40		
	B3		17:30		
	C1-C4		30-40		
SPD, D	D1	3:35	22:00 (broad)	1:40 (figure 2.8)	100:4, followed by 100:0.5
	D2	4:40			
	D3	4:55			
ALD 1, F		5:10	13:00		100:0.5

Compound E (DHD)

Peaks E1, E2 (major, same peak areas), E3 and E4 (minor, same peak areas) in the HPLC chromatogram of compound E (see figure 2.13.a and 4.1.a), which gave identical UV characteristics (λ_{\max} at 300nm, see figure 4.1.b), were isolated together by semi-preparative HPLC from the products of reaction of SPD, D with LiAlH₄, using the mobile phase hexane:1,4-dioxane (100:4, v/v) (see figure 2.11, p. 210) and subjected to spectral characterisation (see figures 2.13.b, 2.13.c and 2.13.j to 2.13.l, p. 213).

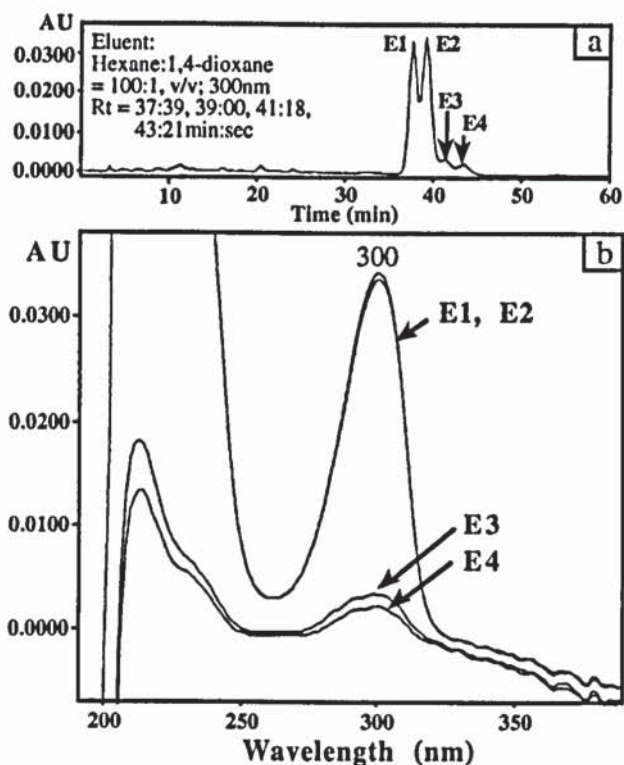


Figure 4.1: HPLC chromatogram of compound E at 300nm (a) and UV spectra of compounds E1, E2, E3 and E4, obtained from the reduction of SPD, D with LiAlH_4 (diode array system) (b); Instrument: Philips PU4100 liquid chromatograph and PU4120 diode array detector; column: Zorbax SIL (4.6mm x 25cm); Flow rate: $1\text{ml}\cdot\text{min}^{-1}$

Compound E was then further separated into compounds E1, E2 and E3+E4 by semi-preparative HPLC using hexane:1,4-dioxane (100:2, v/v) (see figure 2.12, p. 211) and the latter were themselves characterised by ^1H -NMR and ^{13}C -NMR (see figures 2.13.d to 2.13.i). Table 4.5 compares the UV, IR, ^1H -NMR, ^{13}C -NMR and MS main characteristics of Toc and compound E. The FTIR spectrum of compound E (figure 2.13.c) is similar to that of Toc (figure 2.1.c, p. 182), both showing the presence of a hydroxyl group. The ^1H and ^{13}C -NMR spectra of compounds E1, E2 and E3+E4 are very similar, only showing very small variations in the chemical shifts, specially between E1 and E2, (see tables 2.17 and 2.19), suggesting that they are all stereoisomers. The ^1H -NMR spectrum of compound E1 is almost identical to that of Toc except that in the former there are two aromatic methyl group peaks (at 2.11 and 2.16 ppm) instead of the three observed for Toc (hydrogens 5a, 8a and 7a at 2.16, 2.17 and 2.20 ppm, respectively, see figure 4.2 for

positions), see table 4.5. If compound E is symmetrical, each of the two aromatic methyl peaks corresponds to two identical methyl groups (hydrogens 7a+15a and 8a+16a, see figure 4.2 for positions) and the hydroxy peak at 5.43ppm also corresponds to two identical groups. A similar behaviour was observed in ^{13}C -NMR, showing two aromatic methyl groups for compound E and three for Toc (see table 4.5 and figures 2.1.e, p. 184, and 2.13.g-2.13.i). The above results suggest that E1, E2, E3 and E4 are stereoisomers with a symmetrical dimeric structure of Toc, i.e. the dihydroxydimer of Toc (DHD), which was confirmed by EI-MS analysis (figure 2.13.k), showing the molecular ion peak M^+ at 859 (MM of Toc = 430). The EI-MS spectrum of silylated compound E (figure 2.13.l) confirmed the presence of two hydroxy groups, with the molecular ion peak at 1009 (mass of DHD - 2H + 2(mass of TMS)).

The ^{13}C -NMR spectra of E1 and E2 have identical chemical shifts, apart from very small variations of the shifts at positions 3, 19 (31.53ppm for E1 and 31.55ppm for E2) and 2a, 18a (23.78ppm for E1 and 23.77ppm for E2), as shown in table 2.19. Compounds E3+E4 show small variations in the chemical shifts for almost all the positions compared to E1 and E2. This suggests different configurations at chiral centres 2 and 18 for compounds E1, E2, E3 and E4 (see figure 4.2).

The above information and information from the literature [81-84,95] reveal that compounds E1, E2, E3 and E4 are stereoisomers of the same compound, the dihydroxydimer of Toc (see figure 4.1 for structure). However, the literature only stated the existence of one HPLC peak for the DHD of Toc [83,104,105].

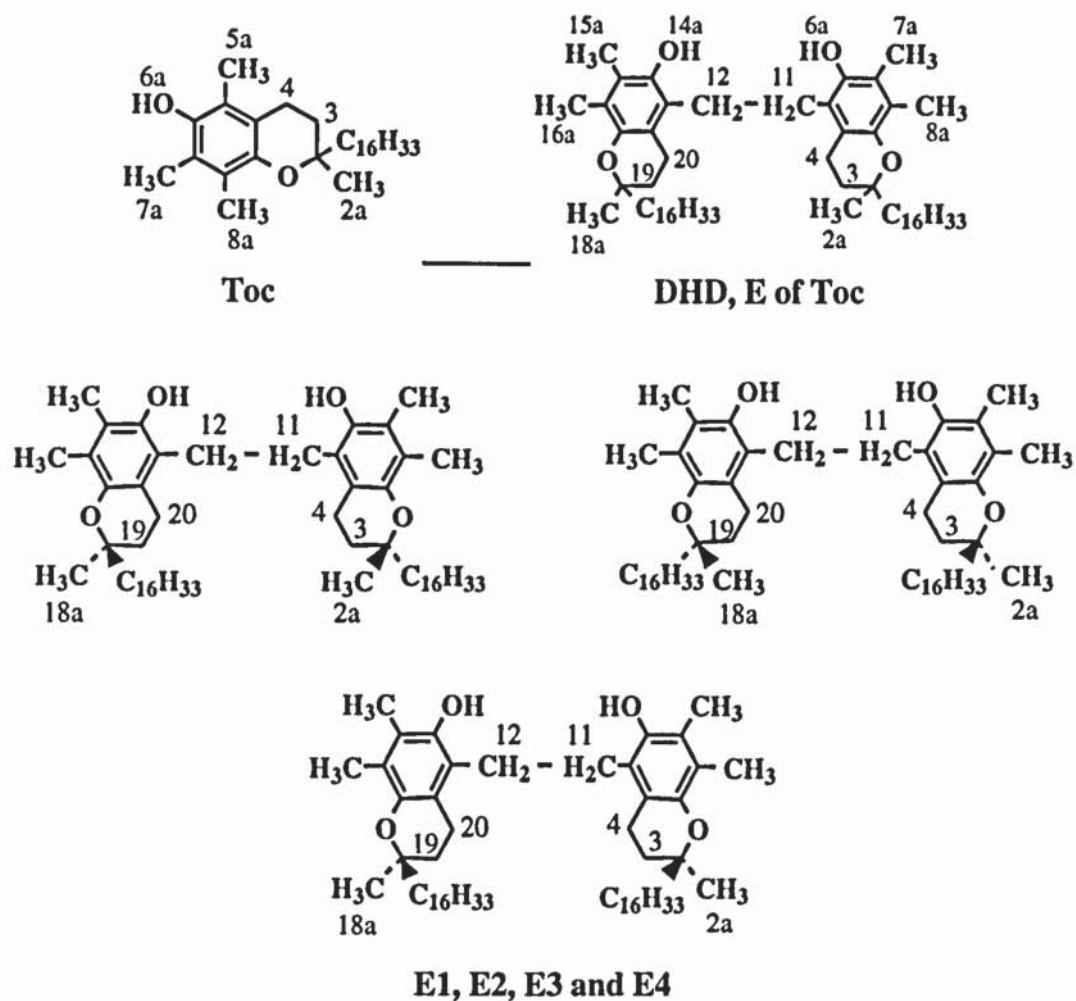


Figure 4.2: Chemical structure of Toc and suggested configurations of DHD, E1, E2, E3 and E4 (E)

Compound E, obtained from the oxidations of Toc with PbO₂ as a minor product, had identical HPLC and UV characteristics and the same HPLC Rt as DHD, E characterised and identified above. To check the identity of the former, compound E was isolated from the products obtained when the ratio 1:1 in Toc:PbO₂ was used (yield of 10%), by semi-preparative HPLC using the mobile phase hexane:1,4-dioxane (100:4, v/v), and was characterised by ¹H-NMR (see table 2.25, p. 164). Its ¹H-NMR characteristics were identical to those of the synthesised DHD, E, confirming that compound E obtained in the oxidations of Toc with PbO₂ is also the dihydroxydimer of Toc.

Compound D (SPD)

Compound D, which was obtained as a major product (81%) in the oxidation of Toc with PbO₂, ratio 1:40, mol/mol, in Toc:PbO₂ (see scheme 4.1 and figure 2.8, p. 207), was purified by column chromatography (bright yellow band), analysed by HPLC using the mobile phase hexane:1,4-dioxane (100:3, v/v) (see figures 4.3.a and 2.9.b) and subjected to spectral characterisation (figures 2.14.b to 2.14.g, p. 224). Table 4.5 compares its main spectral characteristics with those of Toc and DHD, E. The three well separated HPLC peaks D1, D2 and D3 (figure 4.3.a) showed the same UV characteristics (figure 4.3.b), but compared to Toc (λ_{max} at 298nm), compound D shows a new long wavelength absorption at 339nm, suggesting a possible presence of a conjugated carbonyl group.

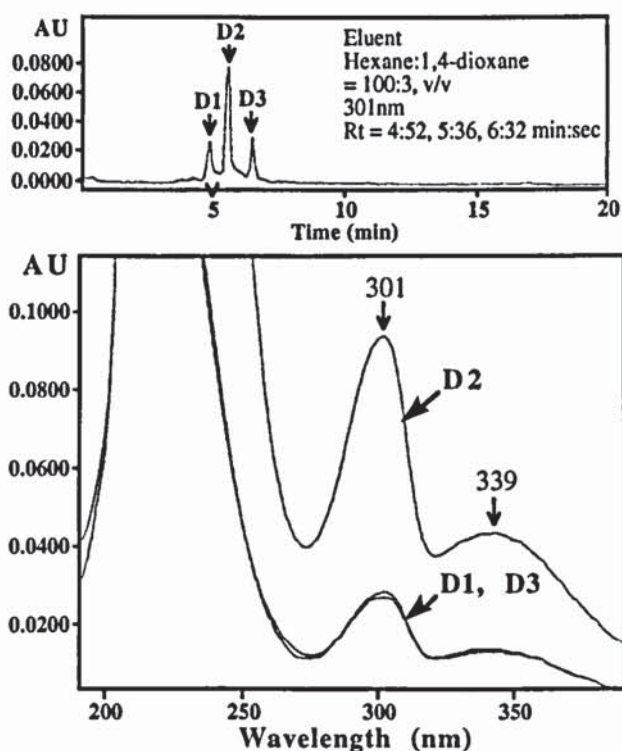


Figure 4.3: HPLC chromatogram of compound D at 301nm (a) and UV spectra of compounds D1, D2 and D3 obtained from the oxidation of Toc with PbO₂ (ratio 1:40, mol/mol, in Toc:PbO₂) (diode array system) (b); Instruments:Philips PU4100 liquid chromatograph and PU4120 diode array detector; column: Zorbax SIL (4.6mm x 25cm); Flow rate: 1ml.min⁻¹

The presence of a conjugated carbonyl was confirmed by FTIR analysis of compound D which reveals a new absorption for conjugated carbonyl (1677cm⁻¹), as well as

unsaturation (1657, 1598 cm^{-1}), in addition to the absence of an OH absorption (see figure 2.14.c) which is observed in the parent Toc and DHD, E (figure 2.1.c, p. 182, and 2.13.c) respectively), see table 4.5. The ^1H -NMR spectrum of compound D (figure 2.14.d) shows two aromatic methyl groups (at 2.09 and 2.13ppm, hydrogens 7a and 8a, see figure 4.4 for positions) and two conjugated methyl groups (hydrogens 16a and 15a at 1.84 and 1.97ppm, respectively), and so does the ^{13}C -NMR spectrum (see figure 2.14.e), according to the ^1H , ^{13}C -NMR correlation spectrum (figure 2.14.f), see table 4.5. The ^{13}C -NMR spectrum of compound D also shows a high chemical shift at 202ppm which corresponds to a conjugated carbonyl.

Furthermore, the ^{13}C -NMR spectrum of compound D shows doubling of the resonances of the carbon at position 13 (115.57, 115.77ppm), which is a chiral centre if compound D is the spirodimer of Toc (see figure 4.4 for structure), and of carbons 14 and 15, at (202.35, 202.49) and (145.79, 145.88) ppm, respectively. This indicates the presence of two groups of stereoisomers, i.e. the R and S configurations of SPD, D at position 13 (see figure 4.4). This is in accordance with the HPLC chromatogram of compound D, showing the two peaks D1 and D3 with identical peak areas which are resolved (R and S forms), and the larger peak D2 with a peak area about twice as large as D1 and D3 which must be a racemic mixture of R and S forms (see figure 4.3.a). If the chiral centres at positions 2, 13 and 18 only are considered (there are also two chiral centres in each phytyl chain), in each group of R and S stereoisomers (at position 13), there can be four different stereoisomers, hence a total of eight possible structures which are four pairs of diastereomeric enantiomers. The possible pairs of enantiomers of SPD, D for positions 2, 13 and 18, respectively, are the following:

RRR,	SSS
RRS,	SSR
SRR,	RSS
SRS,	RSR
(R forms,	S forms)

However, the above pairs of structures can only be real enantiomers if the chiral centres in the two phytyl chains are of opposite configuration for each structure in a pair. So far, the two R and S forms of the spirodimer of Toc have only been separated on an optically active HPLC column [106], however the model compound (phytyl chain replaced by a methyl group) was used. Otherwise, when other HPLC columns were used, only one peak was observed for the spirodimer [83,98,105-107]. The structure of compound D was confirmed by EI-MS analysis (see figure 2.14.g), showing the molecular ion peak M^+ at 856 (MM of Toc = 430) and the silylation of compound D was unsuccessful, indicating the absence of hydroxy groups. The above spectral characteristics and information from the literature [83,94,100,106] reveal that D1, D2 and D3 are stereoisomers of the spirodimer of Toc.

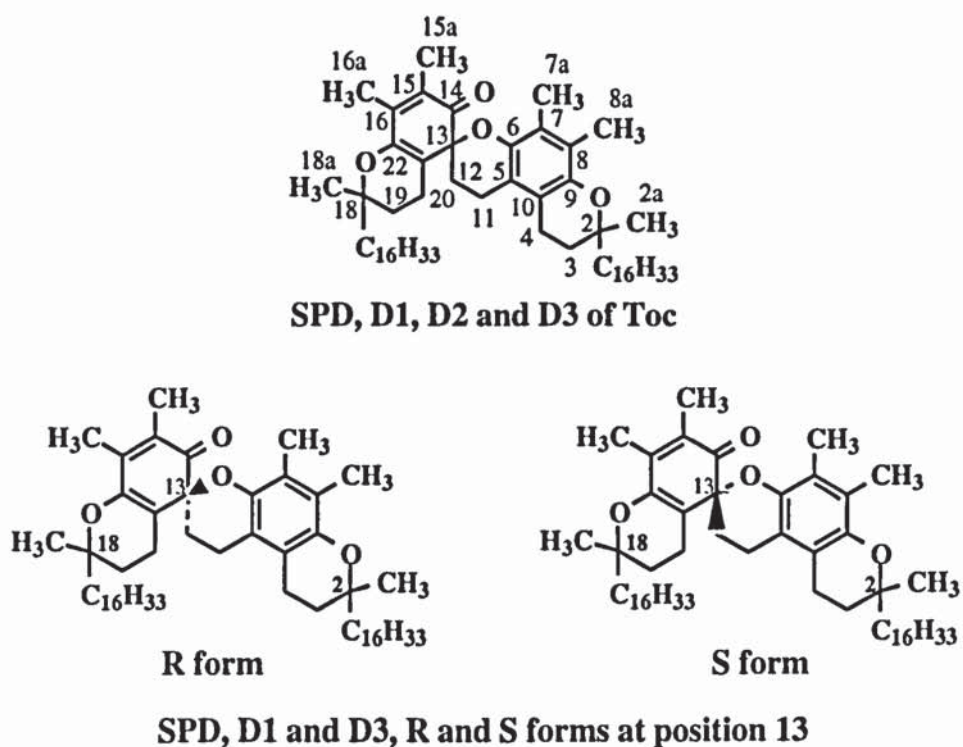


Figure 4.4: Chemical structures and configurations of SPD, D1, D2 and D3

Compounds A, B, C

Compounds A1, A2 (A), B1-B4 (B) and C1-C4 (C), which were obtained as major products (65%) in the oxidation of Toc with PbO₂, ratio 1:10, mol/mol, in Toc:PbO₂, (see scheme 4.1) were analysed by HPLC (see figure 2.7, p. 206, and 4.5.a) and were found to possess identical UV characteristics (λ_{\max} at 292nm, see figure 4.5.b, d, f). Compounds A, B, C were then further separated into compounds A1, A2, B and C (figure 2.10, p. 209) and characterised separately by ¹H-NMR and ¹³C-NMR (figures 2.15.d-2.15.j, p. 231) and were shown to have very similar spectral characteristics, suggesting stereoisomeric structures.

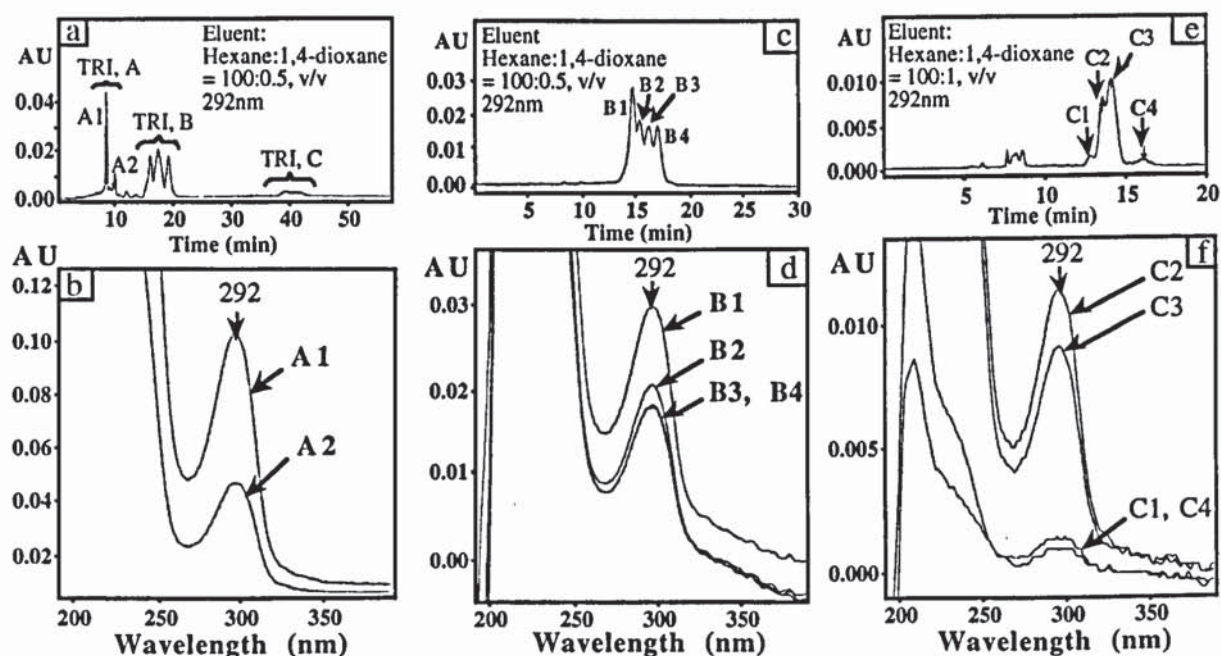


Figure 4.5: HPLC chromatograms of compounds A1, A2 (a), B (c) and C (e) at 292nm and UV spectra of A1, A2 (b), B1, B2, B3, B4 (d), C1, C2, C3 and C4 (f), obtained from the oxidation of Toc with PbO₂ (ratio 1:10, mol/mol, in Toc:PbO₂) (diode array system); Instruments: Philips PU4100 liquid chromatograph and PU4120 diode array detector; column: Zorbax SIL (4.6mm x 25cm); Flow rate: 1ml.min⁻¹

The ¹H-NMR spectra of A1, A2, B and C (figures 2.15.d-2.15.g) all showed four aromatic methyl groups (at 2.07, 2.11, 2.16 and 2.21ppm for A1, see table 4.5) and two conjugated methyl groups (at 1.67 and 1.99ppm for A1), suggesting trimeric structures.

Table 4.5 compares the main spectral characteristics of TRI, A, B, C with those of SPD, D, DHD, E and Toc. The IR spectrum of the mixture of compounds A, B, C reveals that, unlike Toc and DHD, E, the OH group absorption is absent (this is also the case with SPD, D), but like SPD, D, the spectrum of compounds, A, B, C shows an unsaturated carbonyl absorption which is shifted to a higher frequency (1693 compared to 1677cm⁻¹ for SPD, D), as shown in table 4.5. This suggests a lower degree of conjugation in compounds A, B, C compared to SPD, D. In the ¹H-NMR spectra of compounds A1, A2, B and C, two of the four aromatic methyl groups have similar chemical shifts (hydrogens 25a and 26a at 2.16 and 2.21ppm for A1, see figure 4.7) to the two aromatic methyls of Toc and the other two (hydrogens 7a and 8a at 2.11 and 2.07ppm for A1) have chemical shifts close to the aromatic methyl groups of SPD, D, as shown in table 4.5. Compounds A1, A2, B and C also show two methyl groups which are attached to a conjugated carbonyl system (enone). The hydrogens of the methyl group α to the carbonyl (position 15a) have a similar chemical shift (1.99ppm for A1) to the α -methyl of SPD, D (1.97ppm). However, the β -methyl group (position 16a) in compounds A, B, C shows a chemical shift lower than that of the corresponding methyl group of SPD, D (1.67ppm for A1 compared to 1.84ppm for SPD, D). The ¹³C-NMR spectra of compounds A1, A2 and B (figures 2.15.h-2.15.j) only show two or three aromatic peaks, which is due to identical or very similar chemical shifts for methyls at positions 7a, 8a, 25a and 26a, as revealed by the ¹³C, ¹H-NMR correlation spectrum of compound A1 (figure 2.15.k). Furthermore, like for SPD, D, the spectra of the trimers show a conjugated methyl group at position 15a (14.07ppm for A1), and a conjugated carbonyl group at a slightly lower chemical shift (199ppm) than that of SPD, D (202ppm), see table 4.5.

Unlike compounds A1 and A2, compounds B1-B4 (B, four HPLC peaks) and C1-C4 (C, at least four HPLC peaks) show doubling of the resonances in their ¹H-NMR spectra at positions 15a and 16a (conjugated methyl groups) (see table 2.18, p. 157), indicating that the latter are themselves mixtures of stereoisomers. This is confirmed by the doubling of the resonances in the ¹³C-NMR spectrum of compound B at positions 15a (conjugated methyl), 2, 18, 28, 21 (chiral centres), 14 (carbonyl), 15 and 16 (conjugated carbons) and

the tripling of the resonances at position 22 (chiral centre) (see table 2.20, p.160). Furthermore, the small variations in the chemical shifts in the ^{13}C -NMR spectra of compounds A1, A2 and B at positions 15a (conjugated methyl), 14 (carbonyl), 15, 16 (conjugated carbons), 12, 19 and 20 (methylene groups) are due to the presence of chiral centres at positions 13, 21, 22, 2, 18 and 28, the latter showing themselves small changes in their chemical shift. The above results suggest that A1, A2, B1, B2, B3, B4, C1, C2, C3 and C4 are stereoisomers.

The trimeric structure of compounds A, B, C (see figure 4.7) was confirmed by FAB-MS (figure 2.15.l), showing the molecular ion peak at 1285 (3x(MM of Toc) - 6H). According to the literature two trimers were formed from the oxidation of Toc with alkaline ferricyanide [84] and were separated by TLC on silica gel and were found to have similar UV and IR characteristics. Two stereoisomers of the trimer of RRR- α -tocopherol have also been separated by HPLC [81,108] and characterised, the latter differing in the configuration at chiral centres 21 and 22, e.g. structures I and III (see figure 4.7 for positions and structures). However, no comment was made about the configuration at chiral centre 13, which can be R or S, revealing that more stereoisomers can exist (see figure 4.7). Furthermore different configurations at chiral centres 2, 28 and specially 18, e.g. structures I and V (which all have the R configuration in natural vitamin E) can also cause changes in the R_t times of the HPLC spectra. Indeed, the ^1H -NMR spectra of RRR-TRI showed [81] that when the third chroman moiety is *trans* to the 18a methyl group (1.22ppm), e.g. structures V and VI, the latter is placed in a shielding environment above the plane of the enone system and when the third chroman is *cis* to the 18a methyl group (1.44ppm), e.g. structures III and IV, deshielding of 18a is observed. In this work, the ^1H -NMR spectrum of TRI A1 (figure 2.15.d) showed that the latter has a *cis* structure (methyl 18a at 1.4 ppm), whereas the ^1H -NMR spectrum of TRI A2 (figure 2.15.e) shows a *trans* structure (methyl 18a at 1.25ppm), as shown in figure 4.6. On the other hand, TRI B and C, which are both mixtures of stereoisomers, contain both *trans* and *cis* structures (figures 2.15.f and 2.15.g). Figure 4.6 compares the ^1H -NMR chemical shifts of methyl groups 2a, 18a and 28a for TRI A1, A2, B and C. As a consequence, 8 main structures can be

expected for TRI, A, B, C (see figure 4.7). However, variations in the configurations at chiral centres 2 and 28 give rise to three more possible structures for each main structure, i.e. a total of 32 stereoisomers (excluding the structures caused by changes in the configurations in the chiral centres in the phytyl chain). Literature information [81,82] confirmed the trimeric structure of compounds A, B, C.

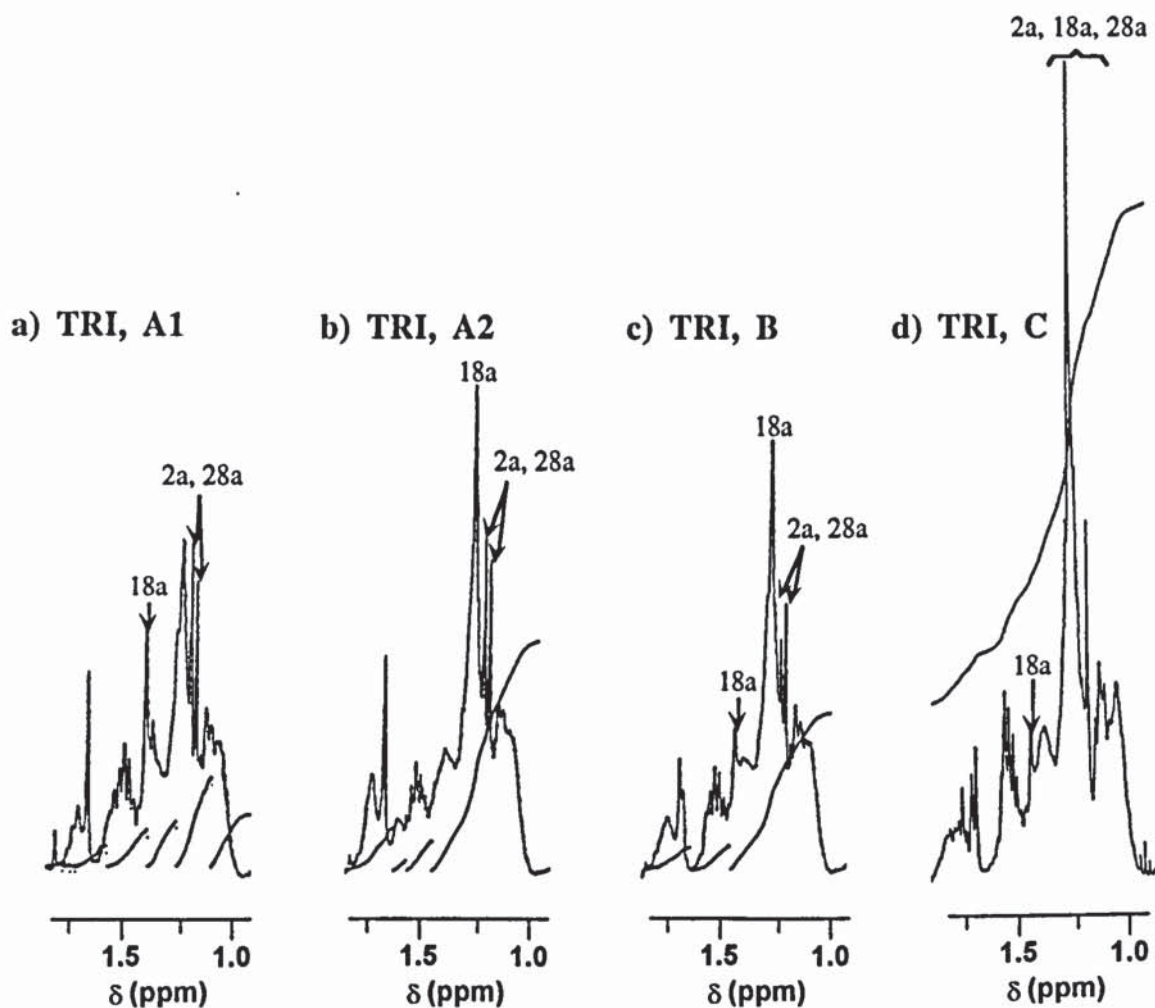
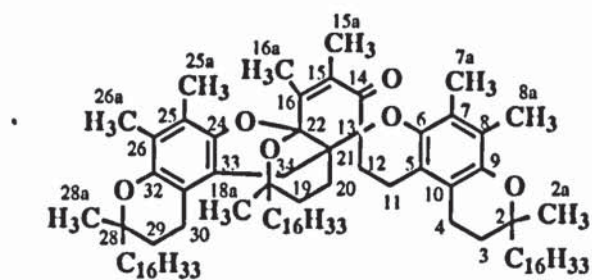
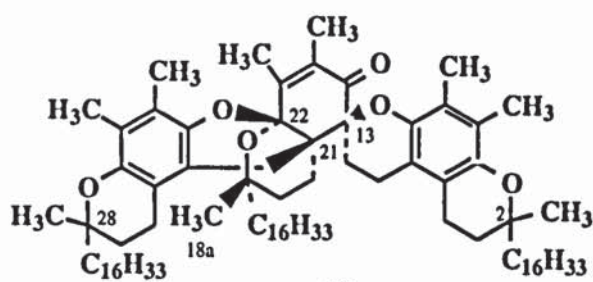


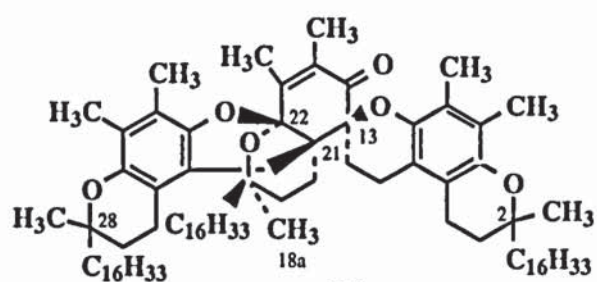
Figure 4.6: ^1H -NMR spectra of TRI, A1, A2, B (B1-B4) and C (C1-C4) in CDCl_3 , at 300 (a-c) and 400MHz (d); region 1.0 to 1.55ppm (see figures 2.15.d to 2.15.g, p. 231)



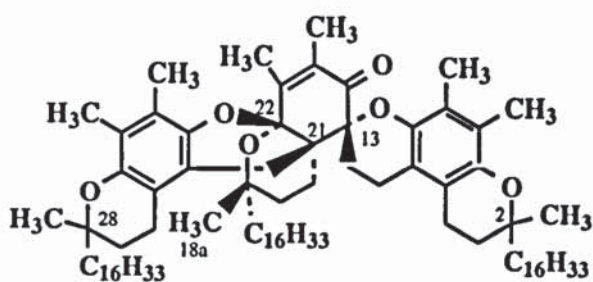
TRI, A, B, C



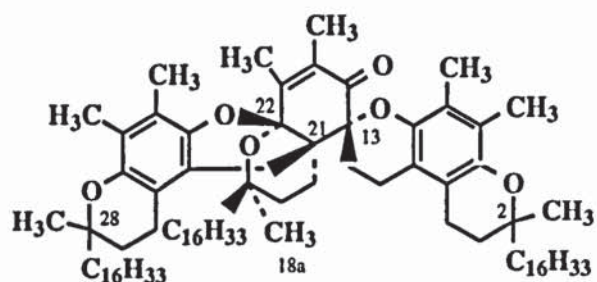
(I)



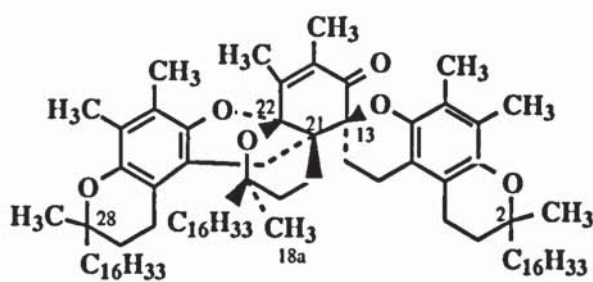
(V)



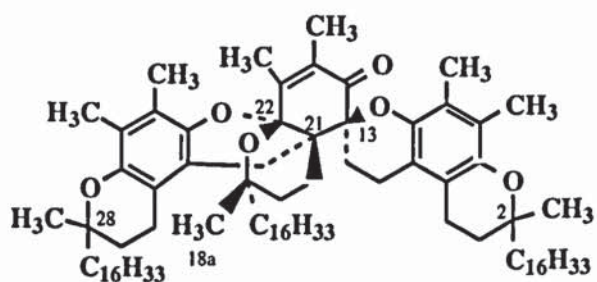
(II)



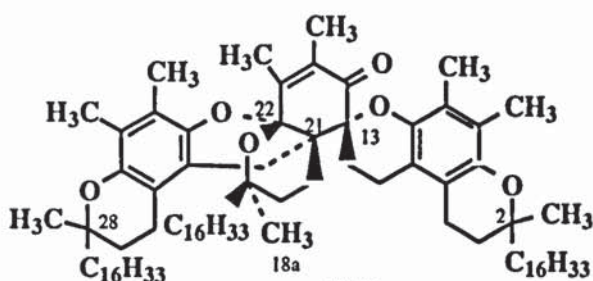
(VI)



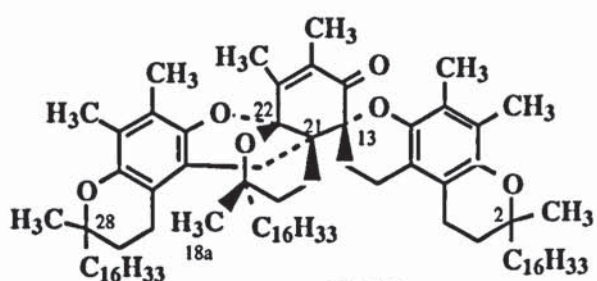
(III)



(VII)



(IV)



(VIII)

TRI, A1, B, C, *cis* structures

TRI A2, B, C, *trans* structures

Figure 4.7: Chemical structures and configurations of TRI, A1, A2, B and C

Compound F (ALD 1)

Compound F was formed as a minor product in the oxidations of Toc with PbO₂ and was isolated from the products obtained when the ratio 1:40, mol/mol, in Toc:PbO₂ was used (yield of 0.7%) (see figure 2.8, p. 207). Compound F was isolated by semi-preparative HPLC using the mobile phase hexane:1,4-dioxane, ratio 100:4, v/v, to exclude Toc and DHD, E, followed by the ratio 100:0.5, v/v to separate compound F from TRI, A, B, C and SPD, D (see figure 4.8.a), and was characterised by HPLC and UV (see figures 4.8.b below). The HPLC Rt, UV and ¹H-NMR characteristics of compound F were identical with those of the supplied Toc derivative 5-formyl- γ -tocopherol (ALD 1, see figure 4.9 for structure) (see table 2.25, p. 164).

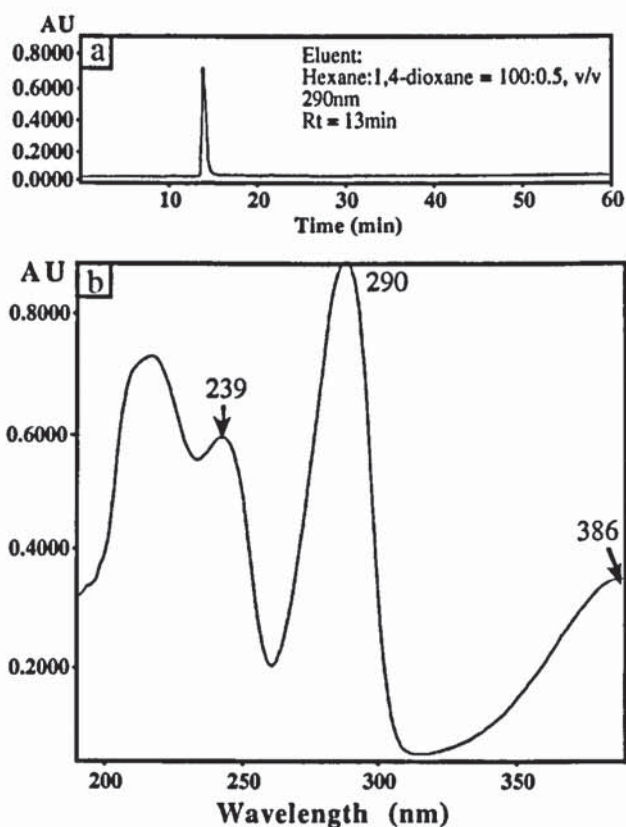


Figure 4.8: HPLC chromatogram at 290nm (a) and UV spectrum (diode array system) (b) of ALD 1, isolated from the products of reaction of Toc with PbO₂, ratio 1:40, mol/mol, in Toc:PbO₂; Instruments: Philips PU4100 liquid chromatograph and PU4120 diode array detector; column: Zorbax SIL (4.6mm x 25cm); Flow rate: 1ml.min⁻¹

The supplied ALD 1 was fully characterised (figures 2.2.b-2.2.g, p. 188) as detailed below. Table 4.5 compares its main spectral characteristics with those of Toc. The UV spectrum of ALD 1 (figure 2.2.b) shows a longer wavelength absorption (at 386nm) compared to Toc ($\lambda_{\text{max}} = 298\text{nm}$), which is caused by the aryl aldehyde group. The IR spectrum of ALD 1 (figure 2.2.c) reveals the presence of a weak OH absorption (3374cm^{-1}) and an aldehydic carbonyl absorption (1636cm^{-1}). Comparison of the $^1\text{H-NMR}$ spectrum of ALD 1 (figure 2.2.d) with that of Toc (figure 2.1.d, p. 183) reveals that a new signal due to an aldehydic proton (at 10.17ppm) appears in the former, and the phenolic OH signal, which has a chemical shift of 4.3ppm in Toc, is shifted downfield to 12.09ppm in ALD 1, due to strong hydrogen bonding [102], as shown in figure 4.9. Furthermore, instead of the three characteristic aromatic methyl groups (hydrogens 5a, 7a and 8a) of Toc, ALD 1 only shows two methyl signals (hydrogens 7a and 8a) (see table 4.5 and figure 4.9), confirming the oxidation of one methyl group to an aldehyde group. Similar behaviour can be observed in the $^{13}\text{C-NMR}$ spectrum of ALD 1 (figure 2.2.e) which also reveals only two methyl groups and, furthermore, the presence of a carbonyl group at 194ppm, as shown in table 4.5. The EI-MS spectrum of ALD 1 clearly showed a molecular ion peak at 444, which is the molar mass of 5-formyl- γ -Toc (see figure 4.9 for structure). Literature information [90,93,109] was also in accordance with the structure of 5-formyl- γ -Toc for compound F.

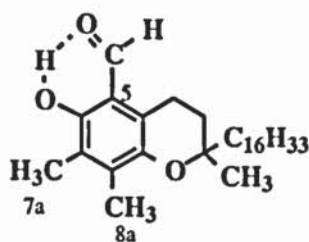


Figure 4.9: Chemical structure of ALD 1, F

Table 4.5: Comparison of the spectral characteristics of Toc and its products of oxidation with PbO₂, DHD, E, SPD, D, TRI, A, B, C and ALD 1, F

		Toc	DHD, E1	SPD, D	TRI, A1	ALD 1, F (supplied)
λ_{\max} , nm		298	300	301, 339	292	239, 290, 282, 386
ν , cm ⁻¹	O-H str	3457	3445	-	-	3374 (weak)
	C=O str	-	-	1677	1693	1636
¹ H: δ , ppm	CH ₃ arom. (positions)	2.16, 2.17, 2.20 (5a,8a,7a)	2.11, 2.16 (8a,16a,7a,15a)	2.09, 2.13 (7a,8a)	2.07, 2.11, 2.16, 2.21 (8a,26a,7a,25a)	2.14, 2.15 (7a, 8a)
	CH ₃ conj. (positions)	-	-	1.84, 1.97 (16a,15a)	1.67, 1.99 (16a,15a)	-
	OH	4.30	5.43	-	-	12.09
	CHO	-	-	-	-	10.17
¹³ C: δ , ppm	CH ₃ arom. (positions)	11.23, 11.75, 12.16 (5a,8a,7a)	11.90, 12.12 (8a,16a,7a,15a)	11.64, 11.79 (7a,8a)	11.71(2), 11.90, 12.07 (8a,26a,7a,25a)	11.01, 13.18 (8a, 7a)
	CH ₃ conj. (positions)	-	-	11.82, 13.82 (16a,15a)	11.71, 14.07 (16a,15a)	-
	C=O	-	-	202.35, 202.49	198.75	193.98
MS: M ⁺ , m/z		430	859, 1003 (after silylation)	856 (before and after silylation)	1285	444
Structures		p. 338	p. 338	p. 341	p. 346	p. 348
Figures (page)		2.1.b-2.1.g (182)	2.13.b-2.13.l (213) and 4.1	2.14.b-2.14.g (224) and 4.3	2.15.b-2.15.l (230) 4.5 and 4.6	2.2.b-2.2.g (188) and 4.8

4.2.1.2 Effect of PbO₂ concentration on the nature of the oxidation products

After the identification and characterisation of the products of oxidation of Toc with PbO₂ in hexane, the concentrations of the latter were calculated from their HPLC peak areas and their extinction coefficients at 290nm, at which wavelength all products absorb strongly (see section 2.11.1 for procedure). Table 4.6 shows the extinction coefficients at 290nm of Toc and its oxidation products, including DHD, E, SPD, D, TRI, A, B, C and ALD 1, F, and table 4.7 gives their concentrations for each PbO₂ initial concentration used. Figure 4.10 below reveals the effect of initial PbO₂ concentration on the nature and concentrations of the different products formed. It shows that up to a concentration of 10mol of PbO₂ / mol of Toc, TRI, A, B, C and DHD, E are formed as the major products and ALD 1 as a minor product, whereas SPD, D is absent. Furthermore, the sharp decrease in Toc and DHD concentrations with an increase in PbO₂ concentration, is accompanied by a fast increase in the concentration of the TRI. On the other hand, at higher concentrations of PbO₂ (> 10mol / mol of Toc), the formation of SPD is favoured, its concentration increasing rapidly with the PbO₂ concentration to reach a high yield (81%), and at the same time, the amount of TRI decreases and ALD 1 remains a minor product. The above results suggest that the formation of TRI is favoured at lower PbO₂ concentrations, whereas SPD is preferably formed at high concentrations of the oxidising agent. The formation of ALD 1 is probably a side reaction as it is formed at very low levels.

Table 4.6: Extinction coefficients of Toc and its products of oxidation with PbO₂ at 290nm

product	Toc	DHD, E	SPD, D	TRI, A, B, C	ALD 1, F
E at 290nm, l.g ⁻¹ .cm ⁻¹	8.1	7.9	4.3	4.98	20.5

Table 4.7: Concentrations of the products of the oxidations of Toc with PbO₂ in hexane

ratio in Toc:PbO ₂ , mol/mol	concentration, % weight				
	Toc	DHD, E	SPD, D	TRI, A, B, C	ALD 1, F
1:1	76	10	0	14	0.04
1:3	75	2.8	0	23	0.1
1:5	65	2.0	0	33	0.4
1:10	33	1.7	0	65	0.3
1:20	1.1	0.3	64	34	0.6
1:40	0.9	1.3	81	16	0.7

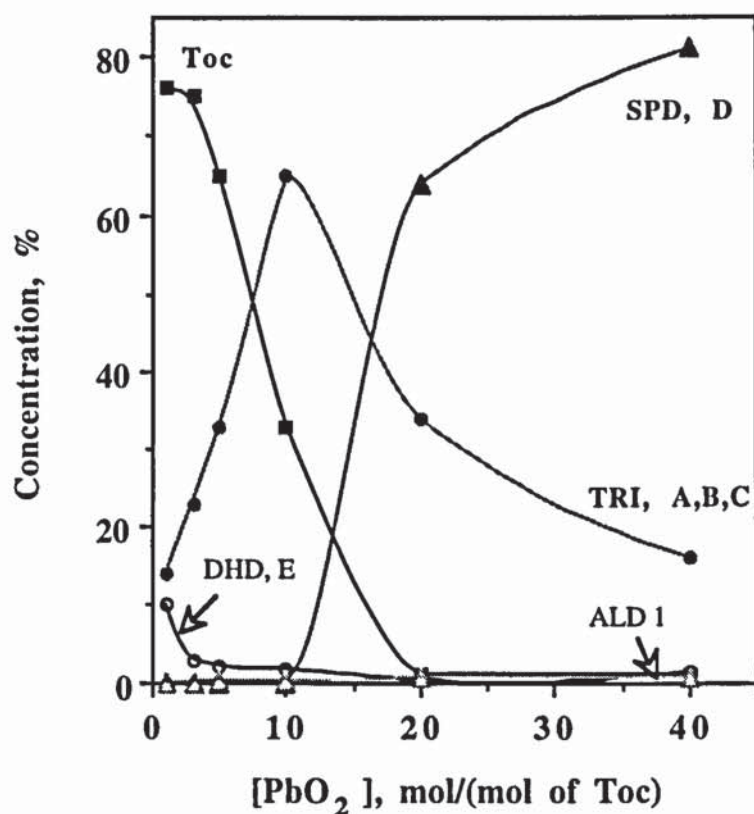


Figure 4.10: Effect of lead dioxide concentration on the nature and concentrations of the oxidation products of Toc in hexane

4.2.2 Isolation and characterisation of transformation products of Toc from PP stabilised with 39% Toc

PP granules (type Accurel) stabilised with 39% Toc and extruded four times (CPC789 series, single screw extruder, 270°C, see section 2.3.1) were subjected to Soxhlet extraction with dichloromethane (see section 2.6 for procedure) in order to isolate high concentrations of transformation products of Toc (see scheme 4.2 for methodology). The resulting extract was analysed by NP-HPLC using the mobile phase hexane:1,4-dioxane, ratios 100:4 and 100:0.5, v/v (see figure 2.20, p. 240). The UV characteristics of the transformation products, obtained by diode array scanning, and their HPLC R_t were similar to those of previously identified and supplied oxidation products of Toc, suggesting the presence of low concentrations of TRI, A, B, C and SPD, D and high concentrations of DHD, D and ALD 1, F, as well as some new products which were formed in relatively high concentrations. Two of the new products, compounds G and H, had close HPLC R_t and similar UV characteristics to those of ALD 1 (see table 4.8 and figure 4.11), both showing a long wavelength absorption at about 400nm in addition to the maximum absorptions at about 280 and 290nm for G and H, respectively. This suggests that both compounds have an aldehydic structure. ALD 1, F, compounds G and H and another new compound I were isolated from the polymer extract by semi-preparative NP-HPLC using the solvent system hexane:1,4-dioxane (100:0.5, v/v) (see figure 2.20.b). The isolated compounds were then characterised using various spectroscopic and spectrometric techniques and the results are shown at the end of chapter two in form of tables (2.29-2.32, p. 165) and figures (2.21-2.24, p. 241) and were interpreted as follows.

ALD 1, F:

The HPLC chromatogram of ALD 1, F showed a very pure sample of the product (figure 2.21.a, p. 241 and 4.11.a) and its UV, $^1\text{H-NMR}$ and $^{13}\text{C-NMR}$ characteristics (figures 2.21.b-d, p. 241) were identical with those of the supplied sample of ALD 1, 5-formyl- γ -tocopherol confirming its structure (see figures 2.2, p. 187 for the supplied sample). Figure 4.12 below shows its structure.

Compound G (ALD 2):

G was obtained as a relatively pure compound (see figure 2.22.a, p. 244, and 4.11.c). Table 4.8 compares its main spectral characteristics with those of ALD 1, F and figures 2.22, p. 244, show its spectral characteristics. The UV spectra of both compounds show a long wavelength absorption at 386 and 404nm for ALD 1 (figure 2.2.b and 4.11.b) and G (figure 2.22.b and 4.11.d), respectively, and the IR spectra both reveal the presence of a carbonyl absorption at 1636cm^{-1} for ALD 1 (figure 2.2.c) and 1638cm^{-1} for compound G (figure 2.22.c), in addition to a weak OH absorption. The above results suggest that compound G is aldehydic. The $^1\text{H-NMR}$ spectra of ALD 1 (figure 2.2.d) and compound G (figure 2.22.d) also show some similarities, both revealing the presence of an aldehydic proton (at 10.24ppm for G), a phenolic OH signal subjected to hydrogen bonding (at 11.90ppm for G), and two aromatic methyl groups, suggesting a monomeric structure. However, unlike ALD 1, the $^1\text{H-NMR}$ spectrum of compound G shows the presence of two doublets at (5.76-5.79)ppm and (6.85, 6.89)ppm, and the absence of the characteristic multiplet and triplet seen for positions 3 (1.7-1.9ppm) and 4 (3.0-3.1ppm), respectively, in the spectra of Toc (figure 2.1.d, p. 183) and ALD 1 (figure 2.21.c, p. 242), indicating an unsaturation in the 3,4-carbon bond, i.e. the structure of 5-formyl- γ -tocopherol-3en, ALD 2 (see figure 4.12 below). The structure of compound G was confirmed by EI-MS analysis (figure 2.22.e) which showed a molecular ion peak at 442 (MM of ALD 1 - 2H). Information from the literature [102] confirmed the structure of 5-formyl- γ -tocopherol for compound G.

Compound H (ALD 3):

The isolated compound H was contaminated with the unknown compound I (see figure 2.23.a, p. 247 and 4.11.e) but the latter was itself isolated and characterised (see below), allowing the identification of the spectral $^1\text{H-NMR}$ data corresponding to compound H (figures 2.23.c, p. 248). Table 4.8 compares the characteristic spectral data of compound H with that of ALD 1 and ALD 2. Like for ALD 1 and ALD 2, the UV spectrum of compound H (figure 2.23.b and 4.11.f), obtained by diode array scanning, showed a long

wavelength absorption (at about 390nm), in addition to the shorter wavelength (at 283nm), suggesting an aldehydic structure. This was confirmed by the $^1\text{H-NMR}$ spectrum of compound H (figure 2.23.c), revealing the presence of the characteristic aldehydic proton (at 10.27ppm) and a hydrogen bonded OH signal (at 11.81ppm). Furthermore, like ALD 1, there is no sign of unsaturation in the heterocyclic ring. As concerns the aromatic methyl protons, compound H has two signals at 2.10 and 2.39ppm, compared two 2.14 and 2.15ppm for ALD 1, indicating that the aldehyde group is at position 5 of the chroman structure, compared to position 7 for ALD 1. The above results and information from the literature [102] suggest that compound H is 7-formyl- β -tocopherol, ALD 3 (see figure 4.12 below for structure).

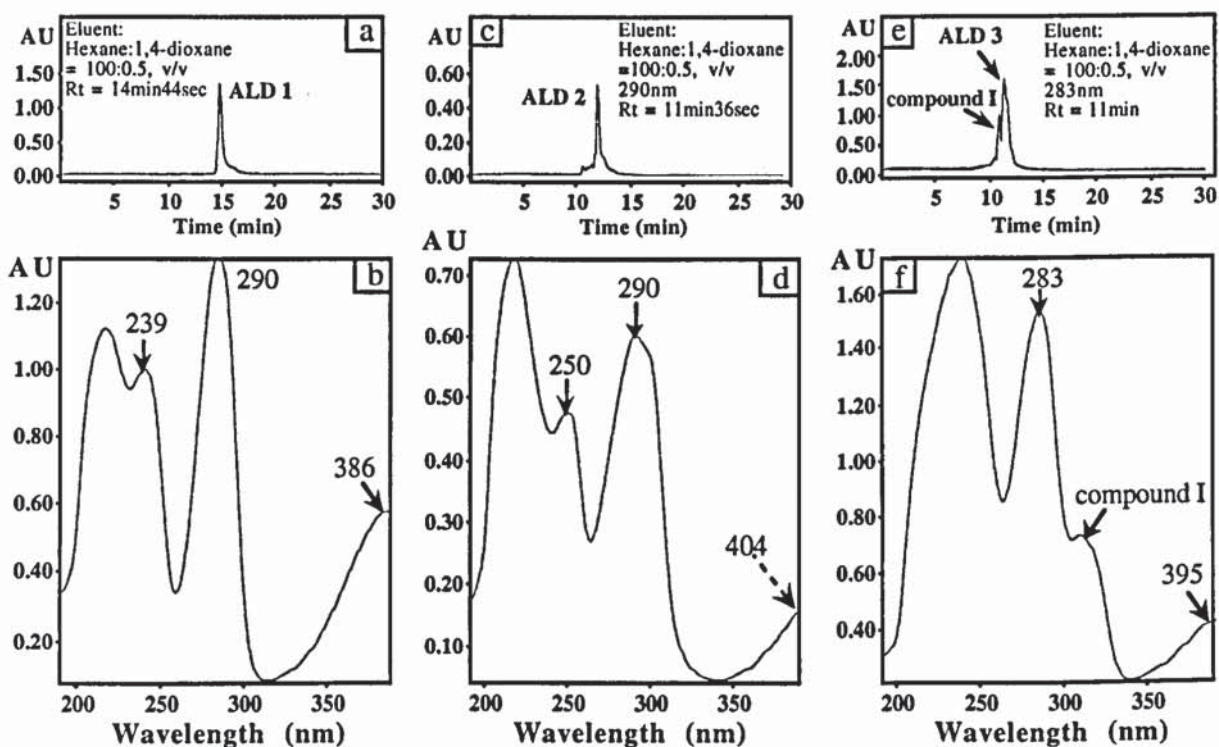


Figure 4.11: HPLC chromatograms and UV spectra (diode array system) of ALD 1, F (a, b), ALD 2, G (c, d) at 290nm and ALD 3, H (e, f) at 283nm; Instruments: Philips PU4100 liquid chromatograph and PU4120 diode array detector; column: Zorbax SIL (4.6mm x 25cm); Flow rate: $1\text{ml}\cdot\text{min}^{-1}$

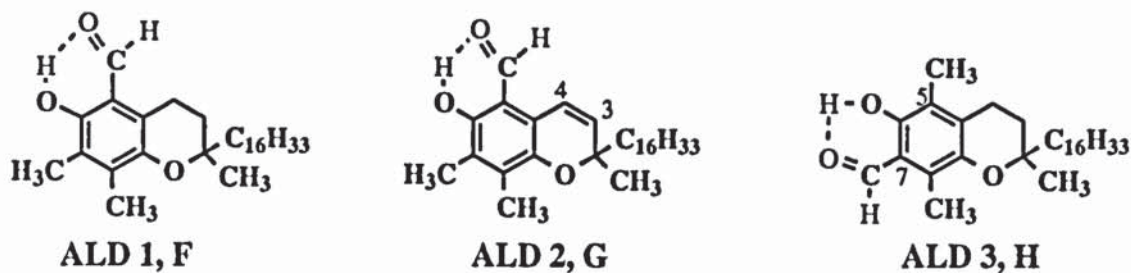


Figure 4.12: Chemical structures of ALD 1, F, ALD 2, G and ALD 3, H

Compound I:

The structure of isolated compound I (HPLC Rt = 11min) could not be determined as it was obtained in very small amounts and its purity was uncertain according to its HPLC chromatogram (figure 2.24.a, p. 249). The diode-array UV spectrum (figure 2.24.b, p. 249) showed maximum absorptions at 310 and 350nm, suggesting a conjugated system. The $^1\text{H-NMR}$ spectrum of compound I (figure 2.24.c) revealed a singlet at 6.22ppm which could correspond to an OH group, and two methyl group signals attached to a conjugated system (possibly aromatic) at 2.11 and 2.12ppm. The latter signals could be observed in the $^1\text{H-NMR}$ spectrum of ALD 3 (figure 2.23.c, p. 248), revealing that the latter is polluted by compound I.

Table 4.8: Comparison of the spectral characteristics of ALD 1, F, ALD 2, G and ALD 3, H, isolated from the extract of PP stabilised with 39% Toc (CPC789 series, pass 4, single screw extruder, 270°C)

		ALD 1, F	ALD 2, G	ALD 3, H
HPLC Rt, min:sec (hexane: 1,4-dioxane ratio in v/v)		5:10 (100:4) 14 (100:0.5)	5:00 (100:4) 11 (100:0.5)	4:50 (100:4) 10 (100:0.5)
λ_{\max}, nm		239, 290, 282, 386	250, 285, 297, 404	283, 395
ν, cm⁻¹	O-H str	3375, weak	3400, weak	-
	C=O str	1636	1638	
¹H: δ, ppm	CH ₃ aromatic (positions)	2.14, 2.15 (7a, 8a)	2.15, 2.18 (7a, 8a)	2.10, 2.39 (5a, 8a)
	CH ₂ , CH on heterocyclic ring (positions)	1.7-1.9, multiplet (3) 2.95-3.1, triplet (4)	5.76,5.79, doublet (3) 6.85,6.89, doublet (4)	1.7-1.9, multiplet (3) 2.95-3.1, triplet (4)
	OH	12.09	11.90	11.81
	CHO	10.16 (5a)	10.24 (5a)	10.27 (7a)
MS: M⁺, m/z		-	442	-
Figures (page)		2.21.b-2.21.c (241) and 4.11.a, b	2.22.b-2.22.e (244) and 4.11.c, d	2.23.b-2.23.c (247) and 4.11.e, f

4.2.3 Nature of transformation products and mechanism of melt stabilisation of Toc in LDPE, during multiple extrusions

4.2.3.1 Extraction efficiency

LDPE was extruded four times into thin films (0.25mm) in the absence and presence of 0.2, 1 and 10% Toc in a single screw extruder at 180°C (see section 2.3.1 for procedure), and the products were extracted with dichloromethane for analysis (see section 2.6 for procedure). The extraction efficiency was determined by comparing the UV spectra of the polymer films before and after extraction and from the UV absorbances of the extracts at 290nm (see section 2.6.2). As an example, figure 4.13 below shows the change in UV

spectra of LDPE stabilised with 0.2% and 1% Toc, passes 4, before and after extraction. Similar results were found for LDPE stabilised with 10% Toc and for all the extrusion passes, suggesting that the extraction efficiency is high. Table 4.9 shows the results of UV analysis of the extracts, the final % weight of products recovered, m'_{AO} , being calculated using equation 2.8, p. 108. The results confirm the high extent of recovery of Toc and its transformation products, particularly at lower concentrations of the parent antioxidant (0.2 and 1%), indicating minimum loss of the antioxidant during processing. The more pronounced "loss" of Toc and its products from LDPE containing a high initial concentration of Toc (10%) is probably due to its loss during processing, as blooming is likely to occur at this high concentration. The error on the amount of products recovered from the polymer samples, m'_{AO} , was calculated using equation 2.17, p. 111, and was found not to exceed 15%.

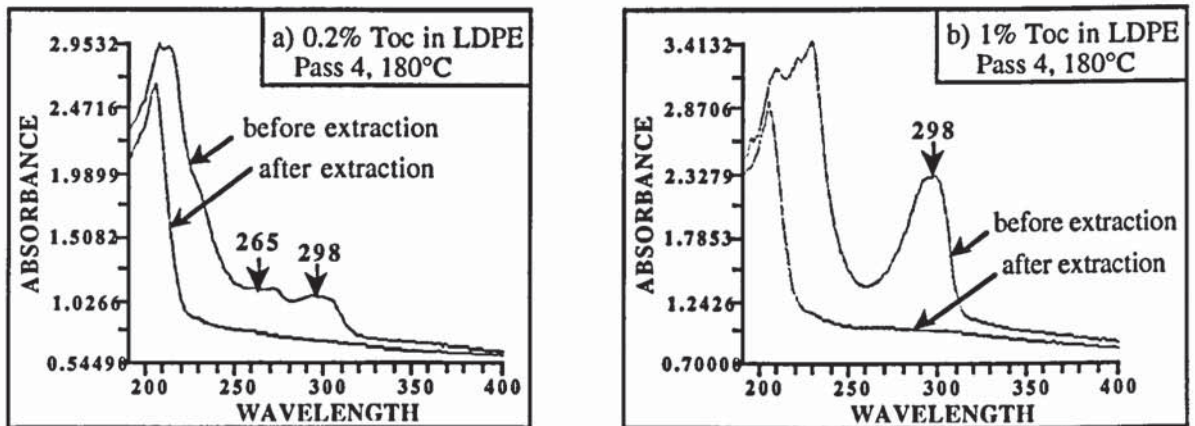


Figure 4.13: UV spectra of LDPE films (0.25mm thick) stabilised with 0.2% (a) and 1% Toc (b), passes 4 (single screw extruder, 180°C), before and after 8 hours extraction with dichloromethane

Table 4.9: Total concentration of Toc and its transformation products recovered from LDPE films (0.25mm thick) stabilised with 0.2, 1 and 10% Toc (single screw extruder, 180°C), measured by UV analysis of the extracts at 290nm

[Toc], %	pass	absorbance, 290nm	\bar{E} , $\text{l.g}^{-1}.\text{cm}^{-1}$	c_{TQ} , % weight	v, ml	m_i , g	m'_{AO} , % weight	Yield of total products, %
0.2	1	0.95816	8.35	3.4	2	1.5293	0.16	80
	2	1.0415	9.78	11.7	2	1.5670	0.15	75
	3	0.67258	11.15	27.6	2	1.0700	0.14	70
	4	0.47030	13.63	22.9	2	0.6196	0.14	70
1	1	1.0382	8.06	2.3	6	0.8995	0.88	88
	2	1.4738	8.00	2.0	6	1.4127	0.80	80
	3	0.65715	8.38	2.3	6	0.6189	0.78	78
	4	0.69421	8.31	3.4	6	0.6593	0.79	79
10	1	0.8947	7.99	2.5	15	0.2523	6.82	68
	2	0.8006	7.96	2.4	15	0.2423	6.38	64
	3	0.7981	8.00	2.7	15	0.2512	6.12	61
	4	0.6058	8.07	2.5	15	0.1868	6.18	62

Where,

\bar{E} = extinction coefficient of the extract ($\text{l.g}^{-1}.\text{cm}^{-1}$)

c_{TQ} = concentration of TQ in the extract (% weight)

v = volume of solvent (l)

m_i = weight of polymer films before extraction (%)

m'_{AO} = weight of extract in the polymer (%)

4.2.3.2 Identification and extent of extraction of LMWP

LMWP products, present in the extracts of LPDE stabilised with Toc were identified by comparing their HPLC Rt and UV characteristics with those of the products extracted from LDPE extruded without any stabilisers (see figures 4.14.a-c, p. 423 and table 4.11). It was found that 4 products with low Rt (2:50-4 min:sec when hexane:1,4-dioxane = 100:0.5, v/v, was used as the mobile phase) and maximum absorbances at 210, 243 and 251nm (see figure 4.14.c) were present in the extracts of unstabilised LDPE and LDPE stabilised with

Toc, indicating that they were LMWP products. The extent of extraction of LMWP was determined by comparing the weight of unstabilised and stabilised LDPE films, passes 1 to 4, before and after extraction with dichloromethane, using equation 2.18, p. 111. Table 4.10 shows the extent of extraction of LMWP, m_{LMWP} , in unstabilised LDPE and LDPE stabilised with 0.2 and 1% Toc.

Table 4.10: Extent of extraction of LMWP from unstabilised LDPE and LDPE stabilised with 0.2% Toc (single screw extruder, 180°C)

Pass	m_{LMWP} , %		
	unstabilised LDPE	LDPE + 0.2% Toc	LDPE + 1% Toc
1	1.2	1.1	0.98
2	1.1	1.0	0.89
3	1.0	0.90	0.95
4	1.0	1.1	1.0

4.2.3.3 Isolation and identification of transformation products of Toc

The extracts of LDPE stabilised with 0.2, 1 and 10% Toc were analysed by NP-HPLC with the mobile phase hexane:1,4-dioxane (100:4 and 100:0.5, v/v) leading to a good separation of all the products and stereoisomers (see figures 4.15, p. 425, for typical chromatograms). The UV spectra, obtained by diode array scanning, and the HPLC R_t of the different products formed were compared with those of synthesised, isolated and supplied oxidation products of Toc (see table 4.1 for structures and origin and table 4.11 for HPLC and UV data). The results revealed that some products extracted from LDPE had similar characteristics. Table 4.11 shows the nature of the products formed, their HPLC R_t and UV characteristics. In addition to Toc transformation products, LMWP products were also present in the extracts and were identified as described previously (section 4.2.3.2). To confirm the nature of Toc transformation products, the products from LDPE stabilised with 0.2% and 10% Toc, passes 4, were extracted from the polymer with dichloromethane (see section 2.6 for procedure), isolated by semi-preparative NP-HPLC using the mobile phase

hexane:1,4-dioxane (100:4 and 100:0.5, v/v), characterised using various spectroscopic and spectrometric techniques and identified as explained below (see scheme 4.2 for methodology).

Table 4.11: HPLC Rt of transformation products of Toc and LMWP extracted from LDPE stabilised with 0.2, 1 and 10% Toc (single screw extruder, 180°C) (solvent ratios in hexane:1,4-dioxane, v/v) (figures 4.15, p. 425)

compound		Rt, min:sec		λ_{\max} , nm
		100:4	100:0.5	
LMWP (peak name)		2:50	2:50 (1), 3:10 (2), 3:40 (3), 4:00 (4)	243 (1), 210 (2), 251 (3), 243 (4) (broad)
TRI	A (A1, A2)	3:00-5:00	9:30, 9:50	292
	B (B1-B4)		15-24	
	C (C1-C4)	5:40	30-40	
ALD	1, F	5:10	13:00	290, 282, 386
	2, G	5:00	10:30	285, 297, 404
	3, H	4:50	9:30	283, >390
	4, J	5:10	17:00	280, 380
SPD	D (D1, D2, D3)	3:30-5:00	22-27	301, 339
Toc		11:00	45:00	298
DHD	E (E1-E4)	13-17	180	300
TQ		32:00	-	262, 268

Compound E (DHD):

Compound E was isolated from the extract of LDPE stabilised with 10% Toc, pass 4, as it was a major transformation product of Toc in the latter (Yield of 11%) (see figure 4.15.f). It was isolated by semi-preparative HPLC using the solvent system hexane:1,4-dioxane = 100:4, v/v (figure 2.26.a, p. 252) and characterised (figures 2.26.b-c, p. 252). Tables 2.33 and 2.34, p. 169, compare the spectral characteristics of compound E with those of DHD, E. The HPLC chromatogram of compound E showed 3 peaks, E1, E2 and E3+E4 with maximum UV absorbances at 300nm (see figure 2.26.b), which is in accordance with the

structure of DHD, E (see table 4.1 for structure). This was confirmed by the $^1\text{H-NMR}$ spectrum of compound E (figure 2.26.c) which showed two aromatic methyl signals for positions 7a, 15a (at 2.17ppm) and 8a, 16a (at 2.12ppm) and the OH signal at 5.43ppm (see table 2.34).

Compound D (SPD):

Compound D, present in a relatively high concentration (2%) in the extract of LDPE stabilised with 10% Toc, pass 4, (see figure 4.15.h) was isolated from the latter by semi-preparative HPLC using the solvent hexane:1,4-dioxane = 100:0.5, v/v (figure 2.27.a, p. 254) and characterised (figures 2.27.b-d, p. 254). Its spectral characteristics were compared with those of SPD, D (see tables 2.33 and 2.34, p. 169). The UV spectrum (figure 2.27.b) (λ_{max} at 301 and 339nm) and $^1\text{H-NMR}$ characteristics (figure 2.27.c) corresponded to those of SPD, D, obtained from the oxidation of Toc with PbO_2 (see figures 2.14.b and 2.14.d, p. 224 and table 4.1 for structure). The dimeric structure of compound D was confirmed by EI-MS analysis (figure 2.27.d) which showed a molecular ion peak at 856.

Compounds A, B, C (TRI):

Compounds A, B, C were major transformation products in the extract of LDPE stabilised with 10% Toc, pass 4 (8%, see figure 4.15.h) and showed similar HPLC and UV characteristics (λ_{max} at 292nm, see figure 2.28.b, p. 257) to those of TRI, A, B, C (see table 2.33, p. 169). Hence compounds A, B, C were collected together from the latter extract by semi-preparative HPLC with the solvent system hexane:1,4-dioxane = 100:0.5, v/v (figure 2.28.a, p. 257) and characterised (figures 2.28.b-d, p. 257) The $^1\text{H-NMR}$ spectrum (figure 2.28.c and table 2.35, p. 171) showed the characteristic four trimeric aromatic methyl groups for positions 7a, 8a, 25a and 26a (at 2.08, 2.11, 2.17 and 2.21ppm) and the two conjugated methyl groups for positions 15a and 16a (at 1.67 and 1.99ppm), confirming their trimeric structures (see figure 4.7 and table 4.1 for structures). The EI-MS spectrum of compounds A, B, C (figure 2.28.d) showed a molecular ion peak at 858 which corresponds to DHD, E. This was shown [81] to be due to the initial fragmentation of the

high molecular weight trimer to the spirodimer ($m/z = 857$) and a quinone methide (QM, $m/z = 428$), followed by an immediate addition of two hydrogens to give the DHD. The initial fragmentation could be prevented by using FAB-MS which gave a molecular ion peak at 1285 for TRI, A, B, C obtained from the oxidation of Toc with PbO_2 (see figure 2.15.1, p. 239).

Compound F (ALD 1):

Compound F, a major oxidation product of Toc in the extract of LDPE stabilised with 0.2% Toc, pass 4 (yield of 13%, see figure 4.15.d), was isolated from the latter by semi-preparative HPLC, using the solvent system hexane:1,4-dioxane = 100:0.5, v/v (see figure 2.29.a, p. 260), and was characterised by UV, 1H -NMR and EI-MS (see tables 2.33, 2.36 and 2.39, p. 169, respectively and figures 2.29.b-d, p. 260). The UV spectrum (figure 2.29.b) showed maximum absorbances at 290, 282 and 386nm, which are characteristic of the structure of ALD 1 (see table 4.1). Furthermore, like ALD 1, the 1H -NMR spectrum of compound F (figure 2.29.c) revealed the presence of two aromatic methyl groups (at 2.14 and 2.16ppm), the hydrogen bonded hydroxyl signal (at 12.09ppm) and the aldehydic proton (at 10.18ppm). Finally, the structure of ALD 1 for compound G was confirmed by EI-MS (figure 2.29.d) which showed a molecular ion peak at 444.

Compound G (ALD 2):

Compound G which was also obtained in a relatively high concentration in the extract of LDPE stabilised with 0.2% Toc, pass 4 (yield of 2%, see figure 4.15.d), was isolated from the latter by semi-preparative HPLC, using the solvent system hexane:1,4-dioxane = 100:0.5, v/v (see figure 2.30.a, p. 263), and was characterised by UV and 1H -NMR (see tables 2.33 and 2.36, p. 169, respectively and figures 2.30.b-c, p. 263). The UV spectrum (figure 2.30.b) was characteristic of that of ALD 2 (see table 4.1 for structure), showing λ_{max} at 285, 297 and 404nm. The structure of ALD 2 for compound G was confirmed by 1H -NMR analysis (figure 2.30.c) which revealed the two characteristic doublets for

positions 3 and 4 (at 5.76 and 6.87ppm, respectively), the hydroxyl signal at 11.88ppm and the aldehydic proton at 10.25ppm.

4.2.3.4 Effect of extrusion severity and Toc initial concentration on the nature of the transformation products

The nature of the products in the extracts of LDPE stabilised with 0.2, 1 and 10% Toc, passes 1 to 4 (see figures 4.15, p. 425, for typical chromatograms), was determined by comparing their HPLC Rt and diode array UV characteristics with those of the products isolated from the extracts of LDPE stabilised with 0.2 and 10% Toc (passes 4) and known products (Toc, TQ, ALD 3) (see table 4.11). ALD 4 was a new product, present in low concentrations in all the extracts ($\leq 3\%$), which was not isolated but its UV characteristics (λ_{\max} at 280 and 380nm, see figure 4.24.a, p. 434) suggested that it was aldehydic and was allocated an extinction coefficient of $18 \text{ l.g}^{-1}.\text{cm}^{-1}$ for the determination of the concentrations. The concentrations of the products in each extract were determined from their HPLC peak areas and their extinction coefficients at 290 and 275nm (see section 2.11.1 for procedure) and are shown in table 4.12.

Figures 4.16 to 4.19, p. 427, describe the effect of initially added Toc concentration in LDPE and extrusion severity on the nature and concentrations of the transformation products of Toc. The polymer samples containing high initial concentrations of Toc (1 and 10%) retain high levels ($\geq 80\%$) of the parent antioxidant, even after four extrusion passes (see figure 4.16.a), whereas at the lower initial concentration of 0.2% Toc, severe processing leads to a pronounced "loss" of Toc. Single and multiple extrusions of LDPE containing Toc was found to be accompanied by chemical transformations. UV analysis of the extracted products has shown that the physical loss of the antioxidant during processing was minimum at lower concentrations of the latter (0.2 and 1%) and 20-30% at the higher concentration of 10% (see table 4.9, p. 358). HPLC analysis of the extracts revealed that eight major transformation products of Toc were formed in LDPE containing Toc (see table 4.12). The initial concentration of Toc (added to the polymer before

processing) was shown to have a dramatic effect on the relative distribution of its transformation products. Figure 4.17 shows the effect of Toc concentration and the distribution of the products after the first extrusion pass. TRI, A, B, C are formed in high concentrations and are major products at concentrations of 0.2 and 10% Toc. The formation of DHD, E is favoured at higher concentrations of Toc, whereas the concentrations of SPD, D, ALD 1-4 and TQ are higher at lower Toc concentrations. Re-extrusions of LDPE also affect the distribution of the transformation products, as shown in figure 4.19. In general, the concentrations of ALD 1-4 and TQ increase with extrusion severity (figures 4.16.e, f). The increase of the aldehyde concentration is mainly caused by ALD 1, which is a major aldehyde in all the samples (figures 4.19.b, d, f). The concentration of DHD, which is a major transformation product at higher concentrations of Toc (figure 4.16.b and 4.19.a, c, e), also increases with extrusion severity. On the other hand, the concentration of TRI, A, B, C increases with extrusion severity at lower concentration of the parent antioxidant (0.2 and 1%) and decreases at the higher concentration (10%) (figure 4.16.d and 4.19.a, c, e), whereas the concentration of SPD, D remains low at all initial Toc concentrations. Figure 4.18 reveals the effect of initial Toc concentration and extrusion severity on the added concentrations of retained Toc and DHD, E, as the latter has been shown to be itself an excellent melt stabiliser and a good thermal stabiliser (see figures 3.5, p. 313, and 3.9, p. 315, respectively)

Table 4.12: Concentration of products extracted from LDPE stabilised with 0.2, 1 and 10% Toc (single screw extruder, 180°C) (figures 4.16-4.19, p. 427)

[Toc]	pass	concentration, % weight								
		Toc	DHD, E	SPD, D	TRI, A, B, C	ALD 1, F	ALD 2, G	ALD 3, H	ALD 4, J	TQ
0.2%	1	79.4	0.7	3.4	11.1	1.0	0	0	1.0	3.4
	2	52.2	0	3.8	24.1	3.9	0.8	2.0	1.5	11.7
	3	34.0	1.0	1.2	24.8	5.9	1.0	2.8	1.8	27.6
	4	15.6	1.1	0.6	37.6	13.2	2.2	4.0	3.0	22.9
1%	1	90.8	3.0	0.8	2.9	0.05	0	0	0.1	2.3
	2	85.5	3.2	1.3	7.1	0.3	0	0.2	0.4	2.0
	3	83.5	4.3	1.2	6.8	0.6	0	0.5	0.8	2.3
	4	80.0	4.7	2.6	7.5	0.6	0.1	0.6	0.5	3.4
10%	1	79.2	6.5	1.8	9.5	0.3	0.02	0.06	0.02	2.5
	2	77.4	9.4	1.6	8.9	0.2	0.01	0.04	0.02	2.4
	3	74.5	11.1	1.9	9.3	0.4	0.02	0.1	0.05	2.7
	4	75.7	10.7	2.1	8.2	0.5	0.03	0.2	0.03	2.5

4.2.4 Nature of transformation products of Toc and derivatives during processing with PP in an internal mixer

4.2.4.1 Extraction efficiency

PP was processed in the absence and presence of various concentrations of Toc (0.01-0.2%) and 0.2% of each of the Toc derivatives DHD, E, SPD, D, TRI, A, B, C, ALD 1 and TQ (see table 4.1 for structures and origin) in an internal mixer at 200°C, under different conditions (OM, CM and CM/N₂, with different processing times) and the resulting polymer samples were pressed to thin films (0.25mm) (see sections 2.3.2 and 2.3.3 for procedure). The polymer films were then subjected to Soxhlet extraction with dichloromethane (see section 2.6 for procedure) to recover the antioxidants and their products. The extraction efficiency was determined by comparing the UV spectra of the films before and after extraction and from the UV absorbances of the extracts at 290nm (see section 2.6.2). For example, figure 4.20 shows the change in UV spectra of PP films stabilised with 0.2% Toc (OM and CM/N₂, 30min), 0.05 and 0.02% Toc (CM, 10min), and 0.2% SPD, D (CM, 10min), before and after extraction with dichloromethane. Similar results were obtained for the other PP films stabilised with Toc and its derivatives, indicating that the extraction efficiency is high. Tables 4.13, 4.14 and 4.15 show the results of UV analysis of the extracts of PP stabilised with 0.2% Toc (CM/N₂, CM and OM), 0.01-0.2% Toc (CM, 10min) and 0.2% of each of the Toc derivatives (CM, 10min), respectively, leading to the concentration in % weight, m'_{AO} , of total products recovered, using equation 2.8, p. 108. The yield of recovered products is high, even after long processing times (e.g. 30min) and low antioxidant concentrations (e.g. 0.01%), indicating minimum loss of antioxidants during processing. Errors on the concentrations, m'_{AO} , were calculated using equation 2.17, p. 111, and were found to be below 14%.

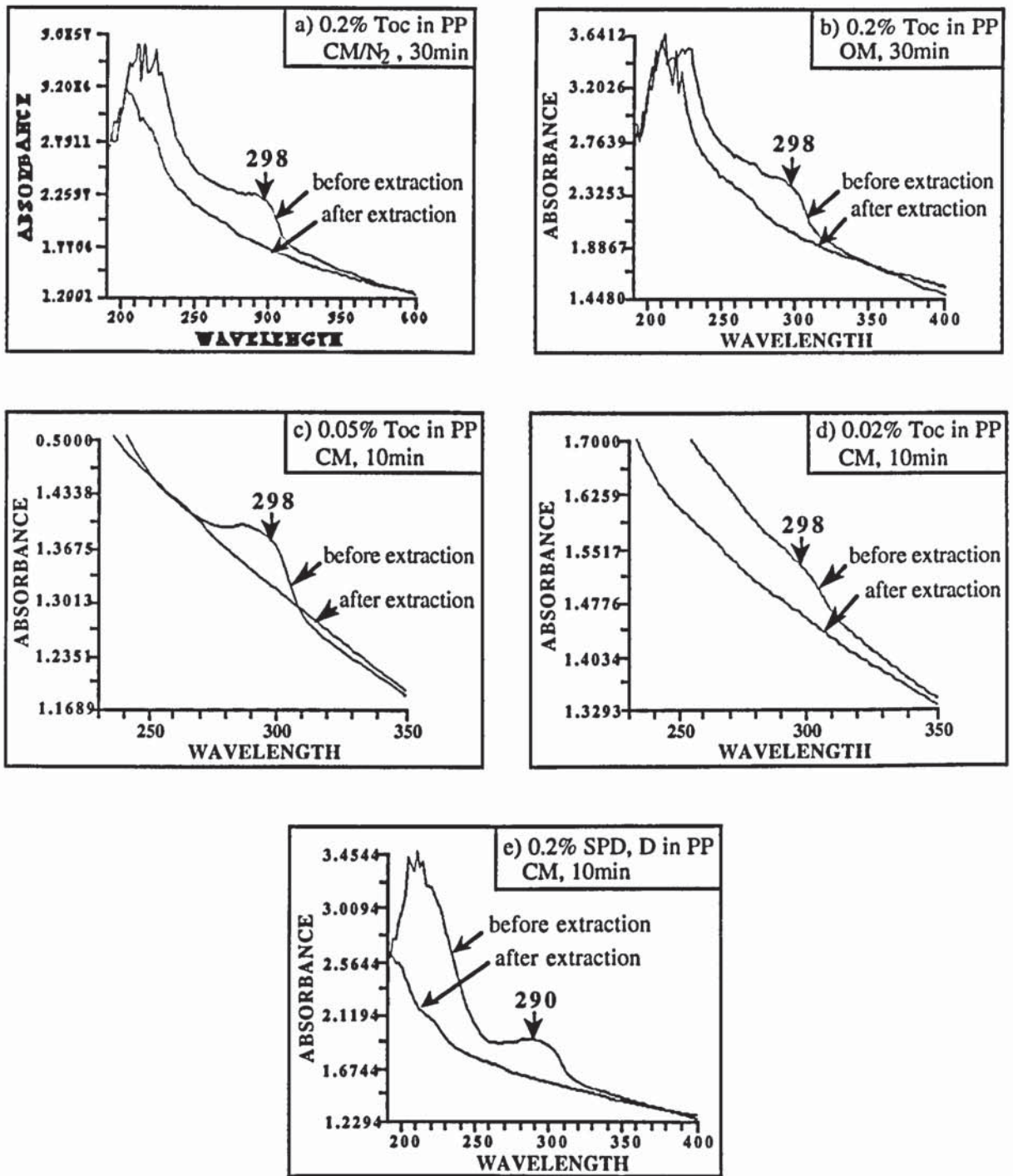


Figure 4.20: UV spectra of PP films (0.25mm thick) stabilised with 0.2% Toc (CM/N₂ and OM, 30min) (a, b), 0.05% and 0.02% Toc (CM, 10min) (c, d) and 0.2% SPD, D (CM, 10min) (e) in an internal mixer at 200°C, before and after 8 hours extraction with dichloromethane

Table 4.13: Total concentration of Toc and its transformation products recovered from PP films (0.25mm thick) stabilised with 0.2% Toc (internal mixer, 200°C), measured by UV analysis of the extracts at 290nm

[O ₂]	processing time, min	absorbance 290nm	\bar{E} , l.g ⁻¹ .cm ⁻¹	ϵ_{TQ} , % weight	v, ml	m _i , g	m'AO, % weight	Yield of total products, %
CM/N ₂	5	0.68922	8.3	1.0	6	2.8475	0.18	90
	10	0.70050	8.6	1.0	4	1.9471	0.17	85
	20	0.53134	8.9	1.2	6	2.3135	0.16	80
	30	0.49515	9.3	1.6	4	1.3461	0.16	80
CM	5	1.1101	8.2	1.2	2	1.5628	0.18	90
	10	0.82983	8.4	1.0	2	1.3103	0.15	75
	20	0.57610	8.9	1.7	4	1.5605	0.17	85
	30	0.37035	9.2	2.1	6	1.4783	0.17	85
OM	5	0.37729	8.7	0.3	4	1.0634	8.7	80
	10	0.53639	9.0	0.9	6	2.3714	9.0	75
	20	0.58453	9.6	1.4	4	1.5266	9.6	80
	30	0.53587	10.1	1.4	4	1.3042	10.1	85

Table 4.14: Total concentration of Toc and its transformation products recovered from PP films (0.25mm thick) stabilised with 0.2-0.01% Toc (internal mixer, CM, 10min, 200°C), measured by UV analysis of the extracts at 290nm

[Toc]	sample	absorbance 290nm	\bar{E} , l.g ⁻¹ .cm ⁻¹	ϵ_{TQ} , % weight	v, ml	m _i , g	m'AO, % weight	Yield of total products, %
0.2%	1	0.82983	8.4	1.0	2	1.3103	0.15	75
0.1%	1	0.64563	8.8	1.3	2	1.7287	0.086	86
0.05%	1	0.69212	8.8	1.1	2	3.8326	0.041	82
	2	0.62051	9.0	1.4	2	2.9885	0.047	94
0.02%	1	0.36552	9.3	2.5	2	4.1727	0.019	95
	2	0.42499	9.8	2.7	2	4.3878	0.020	100
	3	0.34660	9.8	2.7	2	3.6339	0.020	100
0.01%	1+2	0.23859	13.2	8.6	2	5.5622	0.0071	71
	3	0.36224	12.4	6.1	1	3.7843	0.0082	82
	4	0.44255	13.6	4.4	1	3.7730	0.0090	90

Table 4.15: Total concentration of Toc derivatives and their transformation products recovered from PP films (0.25mm thick) stabilised with 0.2% Toc derivatives in an internal mixer (CM, 10min, 200°C), measured by UV analysis of the extracts at 290 (DHD, SPD and TRI) or 268nm (TQ)

Toc derivative	absorbance, 290 or 268nm	\bar{E} , l.g ⁻¹ .cm ⁻¹ at 290 or 268nm	c _{TQ} , % weight	v, ml	m _i , g	m'AO, % weight	Yield of total products, %
DHD, E	0.75134	9.5	2.1	3	1.1841	0.20	100
SPD, D	0.64075	11.7	2.6	4	1.2105	0.19	95
TRI, A, B, C	0.32317 (s2)	10.9	1.6	6	1.0325	0.18	90
ALD 1	0.77339	20.5	0	6	1.1719	0.19	95
TQ	0.93022	38.4 (268)	0	6	0.9285	0.16	80

Where,

\bar{E} = extinction coefficient of the extract (l.g⁻¹.cm⁻¹)

c_{TQ} = concentration of TQ in the extract (% weight)

v = volume of solvent (l)

m_i = weight of polymer films before extraction (%)

m'AO = weight of extract in the polymer (%)

4.2.4.2 Identification and extent of extraction of LMWP

LMWP products, which were extracted from PP in addition to the antioxidants and their transformation products, were identified by comparing their HPLC Rt and UV characteristics with those of the products extracted from unstabilised PP, processed under the same conditions (see figures 4.21.a-d, p. 430, and table 4.16). 5 major LMWP products with low HPLC Rt (2:50-6:10, when the mobile phase hexane:1,4-dioxane = 100:0.5, v/v, was used) and maximum absorbances at 250, 232, 275, 281 and 245nm (see figure 4.21.e, p. 431) were found. The IR spectrum of unstabilised PP film (0.25mm thick), processed in an internal mixer (CM, 10min, 200°C) (see figure 4.21.f), shows the presence of carbonyl groups (1600-1750cm⁻¹, e.g. ketone, aldehyde, acid), which are likely to be responsible for the UV absorbances of the LMWP products extracted [19]. The extent of extraction of LMWP was determined by comparing the weight of unstabilised and stabilised PP films

(0.25mm thick) before and after extraction with dichloromethane using equation 2.18 (p. 111). Table 4.17 shows the extent of extraction of LMWP, m_{LMWP} , in different polymer samples. It was found that the average m_{LMWP} was $(0.5 \pm 0.1)\%$ for all PP samples, unstabilised and stabilised with Toc.

Table 4.16: HPLC Rt and UV characteristics of LMWP products extracted from unstabilised PP and PP stabilised with Toc in an internal mixer (CM, 10min, 200°C) (solvent systems are in v/v) (see figure 4.21.a-f, p. 430)

HPLC Rt, min:sec		λ_{max} , nm	peak name
hexane:1,4-dioxane = 100:4	hexane:1,4-dioxane = 100:0.5		
3:00	3:20	250	1
3:30	3:40	232	2
	3:55	232, 275	3
3:50	4:30	281	4
4:50	6:10	245	5

Table 4.17: Extent of extraction of LMWP from unstabilised PP and PP stabilised with 0.2% Toc (CM/N₂ and OM) and 0.01-0.05% Toc (CM, 10min) in an internal mixer at 200°C

processing time, min	m_{LMWP} , %				
	PP, CM	PP + 0.2% Toc, CM/N ₂	PP + 0.2% Toc, OM	PP + 0.05% Toc, CM	PP + 0.01% Toc, CM
10	0.41	0.46	0.41	0.52	0.48
20	0.49	0.45	0.51		
30	0.54	0.55	0.51		

4.2.4.3 Effect of O₂ concentration and processing severity on the nature of products in PP stabilised with 0.2% Toc

The extracts of PP stabilised with 0.2% Toc (in CM/N₂, CM and OM, at 200°C) were analysed by NP-HPLC using the mobile phase hexane:1,4-dioxane (100:4 and 100:0.5, v/v), leading to a good separation of all the products and their stereoisomers (see figures

4.22 and 4.23, p. 432, for typical chromatograms). The products were identified by comparing their HPLC Rt and UV characteristics (obtained by diode array scanning) with those of previously isolated and supplied oxidation products of Toc (see table 4.18 for HPLC and UV data and table 4.1 for structures). ALD 5 is a new product, mainly present in the extract of PP stabilised with 0.2% Toc under OM condition (see figure 4.23.d). Its UV characteristics (281 and 372nm, see figure 4.24.b) suggested that it was aldehydic and was allocated an extinction coefficient of $18 \text{ l.g}^{-1}.\text{cm}^{-1}$. The concentrations of the products in each extract were calculated (see section 2.11 for procedure) and table 4.19 reveals the results. Figures 4.25 to 4.28, p. 435, show the effect of oxygen concentration in the internal mixing chamber and processing severity on the nature and concentrations of the transformation products of Toc in PP stabilised with 0.2% Toc.

Figure 4.25.a shows clearly that all the polymer samples (processed in OM, CM and CM/N₂) retain high levels of the parent antioxidant, even after 30min processing (> 82%). However, the polymer samples processed in an OM show a more pronounced loss of Toc after 30min processing. UV analysis of the extracts of the polymer samples showed that loss of the antioxidant during processing was minimum (see table 4.13), indicating that chemical transformations of Toc are responsible for its loss. HPLC analysis of the extracts revealed the presence of nine major transformation products (see table 4.18). Their distribution is dramatically affected by the amount of oxygen present in the mixing chamber. The samples processed in an OM show much higher concentrations of ALD 1-5 which are the major products (figure 4.25.e, 4.27 and 4.28.e), whereas in the samples processed in a CM and CM/N₂, TRI, A, B, C are the major products (figure 4.25.d and 4.28.a, c). Like in the LDPE samples stabilised with 0.2% Toc in an extruder (180°C), the concentrations of ALD 1-5 and TRI, A, B, C, which are the major products in both cases, increase with processing severity, whereas the concentration of SPD decreases (see figures 4.19.a, p. 429, and 4.28.a, 4.28.c and 4.28.e). This is accompanied by a general increase in DHD concentration with processing severity in the LDPE samples and in the PP samples processed in a CM and CM/N₂ (figures 4.19.a and 4.28.a and 4.28.c). Furthermore, like in

the LDPE sample stabilised with 0.2% Toc, ALD 1 is the major aldehyde present (figures 4.19.b and 4.28.b, d, f).

Table 4.18: HPLC Rt and UV characteristics of transformation products of Toc and LMWP extracted from PP stabilised with 0.2% Toc (internal mixer, CM/N₂, CM and OM, 200°C) (solvent ratios in hexane:1,4-dioxane, v/v) (figures 4.22-4.23, p. 432)

compound		Rt, min:sec		λ_{\max} , nm
		100:4	100:0.5	
LMWP		3:00, 3:30, 3:50, 4:50	3:20, 3:40, 3:55, 4:30, 6:10	250, 232, (232, 275), 281, 245
TRI	A (A1, A2)	3:00-5:00	9:30, 9:50	292
	B (B1-B4)		15-24	
	C (C1-C4)	5:40	30-40	
ALD	1, F	5:10	13:00	239, 290, 282, 386
	2, G	5:00	10:30	250, 285, 297, 404
	3, H	4:50	9:30	283, >390
	4, J	5:10	17:00	281, 379
	5, K		23:00	281, 372
SPD	D (D1, D2, D3)	3:30-5:00	22-27	301, 339
Toc		11:00	45:00	298
DHD	E (E1-E4)	13-17	180	300
TQ		32:00	-	262, 268

Table 4.19: Concentration of products extracted from PP stabilised with 0.2% Toc (internal mixer, 200°C) (figures 4.25-4.28, p. 435)

[O ₂]	processing time, min	concentration, % weight									
		Toc	DHD, E	SPD, D	TRI, A, B, C	ALD 1, F	ALD 2, G	ALD 3, H	ALD 4, J	ALD 5, K	TQ
CM/N ₂	5	92.0	1.8	1.6	2.4	0.6	0.1	0.3	0.2	0	1.0
	10	90.8	2.2	0.2	3.5	1.4	0.4	0.3	0.2	0	1.0
	20	87.9	2.2	0	5.1	2.1	0.7	0.4	0.2	0.2	1.2
	30	85.0	1.9	0	5.9	2.7	0.9	1.1	0.2	0.7	1.6
CM	2.5	91.3	1.0	0.6	5.4	0.2	0.07	0	0.2	0	1.1
	5	91.0	2.0	0.7	4.4	0.5	0.09	0.05	0.1	0	1.2
	7.5	90.5	2.0	1.0	4.5	0.6	0.2	0.06	0.2	0	1.0
	10	90.0	2.3	1.1	4.6	0.7	0.2	0.04	0.2	0	1.0
	15	88.2	2.8	0.6	5.5	0.9	0.3	0.2	0.3	0	1.4
	20	86.0	3.1	0.4	5.5	2.0	0.7	0.6	0.1	0	1.7
	30	85.0	2.9	0	5.2	2.8	0.9	0.7	0.2	0.3	2.1
OM	5	89.3	4.5	0	3.2	1.6	0.5	0.4	0.1	0.03	0.3
	10	88.9	4.0	0	2.5	1.9	0.6	0.6	0.3	0.3	0.9
	20	85.4	2.4	0	4.1	2.7	1.0	1.1	0.7	1.3	1.4
	30	82.9	2.3	0	4.4	3.9	1.1	1.6	1.0	1.4	1.4

4.2.4.4 Effect of initial Toc concentration on the nature of its transformation products

The products extracted from PP stabilised with 0.01 to 0.2% Toc (CM, 10min, 200°C) were analysed by NP-HPLC using the mobile phase hexane:1,4-dioxane (100:4 and 100:0.5, v/v) (see figure 4.29, p. 438, for typical chromatograms) and were identified by comparing their HPLC Rt and diode array UV characteristics with those of known oxidation products of Toc and PP (see table 4.18). Samples containing 0.01, 0.02 and 0.05% Toc were processed 4, 3 and 2 times, respectively, to reduce experimental errors. The concentrations of the products were then calculated (see section 2.11.1 for procedure) and the results are displayed in table 4.20. Figures 4.30 and 4.31, p. 349, show the effect of initial Toc concentration on the nature and concentrations of the transformation products.

Figure 4.30.a shows that the extent of oxidation of Toc increases with its decreasing initial concentration in PP, and is particularly high at the initial concentration of 0.01% (only 27% Toc retained). However at higher initial Toc concentrations (0.02-0.2%), over 75% Toc remains unchanged. The UV analysis of the extracts has shown that loss of the antioxidant during processing is minimal at all concentrations used (see table 4.14), indicating that chemical transformations account for its loss. Figures 4.30.b-d reveal that TRI, A, B, C are the major transformation products at all Toc concentrations used, followed by ALD 1-4 (0.01-0.1% Toc) or DHD, E (0.2% Toc). The concentrations of TRI, A, B, C and ALD 1-4 increase rapidly with decreasing initial Toc concentration, especially between 0.01 and 0.02% Toc (figure 4.30.c). TQ and SPD are minor products at all concentrations and DHD, E is favoured at higher concentrations of Toc (0.2%) (figure 4.30.d). This was also the case in LDPE stabilised with 0.2 to 10% Toc (see figures 4.16.b and 4.17, p. 427). Furthermore, TRI, A, B, C were also the major transformation products in LDPE stabilised with 0.2% Toc (see figure 4.19.a, p. 429). Figures 4.31 show the effect of initial Toc concentration on the distribution of its transformation products. It is clear that the concentrations of ALD 1-4 increase more rapidly than those of the other transformation products, and ALD 1 is the major aldehyde at all initial Toc concentrations.

Table 4.20: Concentration of products extracted from PP stabilised with 0.01 to 0.2% Toc in an internal mixer (CM, 10min, 200°C) (figures 4.30-31, p. 439)

[Toc], %	sample	concentration, % weight								
		Toc	DHD,E	SPD, D	TRI, A, B, C	ALD 1, F	ALD 2, G	ALD 3, H	ALD 4, J	TQ
0.01	1+2	33.0	0	3.3	32.7	16.6	2.5	2.6	0.8	8.6
	3	30.3	0	2.4	43.0	14.0	2.0	1.6	0.6	6.1
	4	16.2	0	0	52.2	16.2	7.7	2.9	0.4	4.4
	mean	26.5	0	1.9	42.6	15.6	4.0	2.4	0.6	6.4
0.02	1	78.4	0	0.9	12.9	3.5	0.5	0.8	0.4	2.5
	2	75.0	0	1.2	13.7	5.2	0.7	1.1	0.4	2.7
	3	73.3	0	2.6	14.0	5.2	0.9	1.2	0.2	2.7
	mean	75.6	0	1.6	13.5	4.6	0.7	1.0	0.4	2.7
0.05	1	87.7	0	0.5	7.3	2.3	0.4	0.6	0.1	1.1
	2	89.6	0	0.4	4.6	2.7	0.4	0.7	0.2	1.4
	mean	88.7	0	0.5	5.9	2.5	0.4	0.7	0.2	1.2
0.1		90.7	0	0.6	5.3	1.3	0.2	0.4	0.2	1.3
0.2		90.0	2.3	1.1	4.6	0.7	0.2	0.04	0.1	1.0

4.2.4.5 Nature of transformation products in PP stabilised with Toc derivatives

PP was processed with synthesised and supplied Toc derivatives including DHD, E, SPD, D, TRI, A, B, C, ALD 1 and TQ (see table 4.1 for structures and origin) in an internal mixer (CM, 10min, 200°C), for a better understanding of the stabilisation mechanism of Toc in polyolefins, as these products were formed during processing of LDPE and PP with Toc (see figures 4.15-4.31, p. 426). The extracted products were analysed by NP-HPLC using the mobile phase hexane:1,4-dioxane (100:4 and 100:0.5, v/v) (see figures 4.32, p. 441, for chromatograms) and identified by comparing their HPLC Rt and diode array UV characteristics with known oxidation products of Toc (see table 4.18). The concentrations of the products were then determined (see section 2.11.1 for procedure) and the results are displayed in table 4.21. ALD 1, F and TQ did not undergo any chemical transformations during processing with PP. Figure 4.33, p. 442, shows the nature of the products formed

during processing of PP with 0.2% DHD, E, SPD, D and TRI, A, B, C. DHD, E was relatively highly retained (73%) during processing with PP and its major transformation products are, in decreasing concentration, SPD, D, TRI, A, B, C and ALD 1 (figure 4.33.a). On the other hand, in PP stabilised with SPD, D, the latter was highly transformed (only 11% retained), mainly into TRI, A, B, C and DHD, E (figure 4.33.b). Furthermore, ALD 1 was formed in relatively high concentration (13%) and a smaller concentration of Toc was also present. When TRI, A, B, C were used as stabilisers, the latter were half transformed, mainly into DHD, E and ALD 1 (figure 4.33.c). Smaller concentrations of SPD, D and Toc were also present. The above results suggest that the dimers and trimers of Toc can be reversibly reduced and re-oxidised during processing.

Table 4.21: Concentration of products extracted from PP stabilised with 0.2% of each of the Toc derivatives in an internal mixer (CM, 10min, 200°C) (figure 4.33, p. 442)

Toc derivative	concentration, % weight							
	Toc	DHD, E	SPD, D	TRI, A, B, C	ALD 1, F	ALD 2, G	ALD 4, J	TQ
DHD, E	1.1	73.3	10.0	7.2	4.5	1.3	0.5	2.1
SPD, D	6.9	28.8	10.9	35.4	12.8	2.3	0.4	2.6
TRI, A, B, C	6.7	23.4	7.1	48.8	10.9	1.2	0.3	1.6
ALD 1, F	unchanged							
TQ	unchanged							

4.2.5 Effect of hindered aryl phosphite U-626 on the nature of transformation products of Toc and derivatives during processing with PP in an internal mixer

4.2.5.1 Extent of extraction of Toc, Toc derivatives, U-626 and their transformation products from PP

PP was processed in the presence of various concentrations of Toc, Toc derivatives and the hindered aryl phosphite U-626 in an internal mixer (CM, 10min, 200°C) and the resulting polymer samples were pressed to thin films (0.25mm) (see sections 2.3.2 and 2.3.3 for procedure). The polymer films were then subjected to Soxhlet extraction (see section 2.6 for procedure) and the extraction efficiency was determined by analysing the films by UV spectroscopy before and after extraction (see section 2.6.2). Figure 4.34 shows the UV spectra of PP stabilised with 0.4% U-626, 0.05% Toc + 0.1% U-626, 0.2% SPD, D + 0.4% U-626 and 0.2% TRI, A, B, C + 0.4% U-626 before and after extraction with dichloromethane. Although U-626 decomposes during NP-HPLC analysis into two main products (see figure 2.6.a, p. 204), ³¹P-NMR analysis of the extracts has shown that U-626 is highly retained during processing with PP (see figure 4.35, p. 443). Hence, an average extinction coefficient of the extracts containing U-626 and Toc or Toc derivatives could not be determined from the HPLC peak areas of the products, preventing the determination of the extent of recovery of the products from the polymer films by UV spectroscopy. However, the extent of recovery of U-626 from PP stabilised only with the latter could be calculated using equation 2.8 (p. 108) as U-626 did hardly undergo any transformations when used on its own (see figure 4.35.b and table 4.22). It was found that the extent of recovery was high. Furthermore, it was shown that the extent of recovery of Toc and Toc derivatives is also high in PP (see tables 4.13 to 4.15, p. 368).

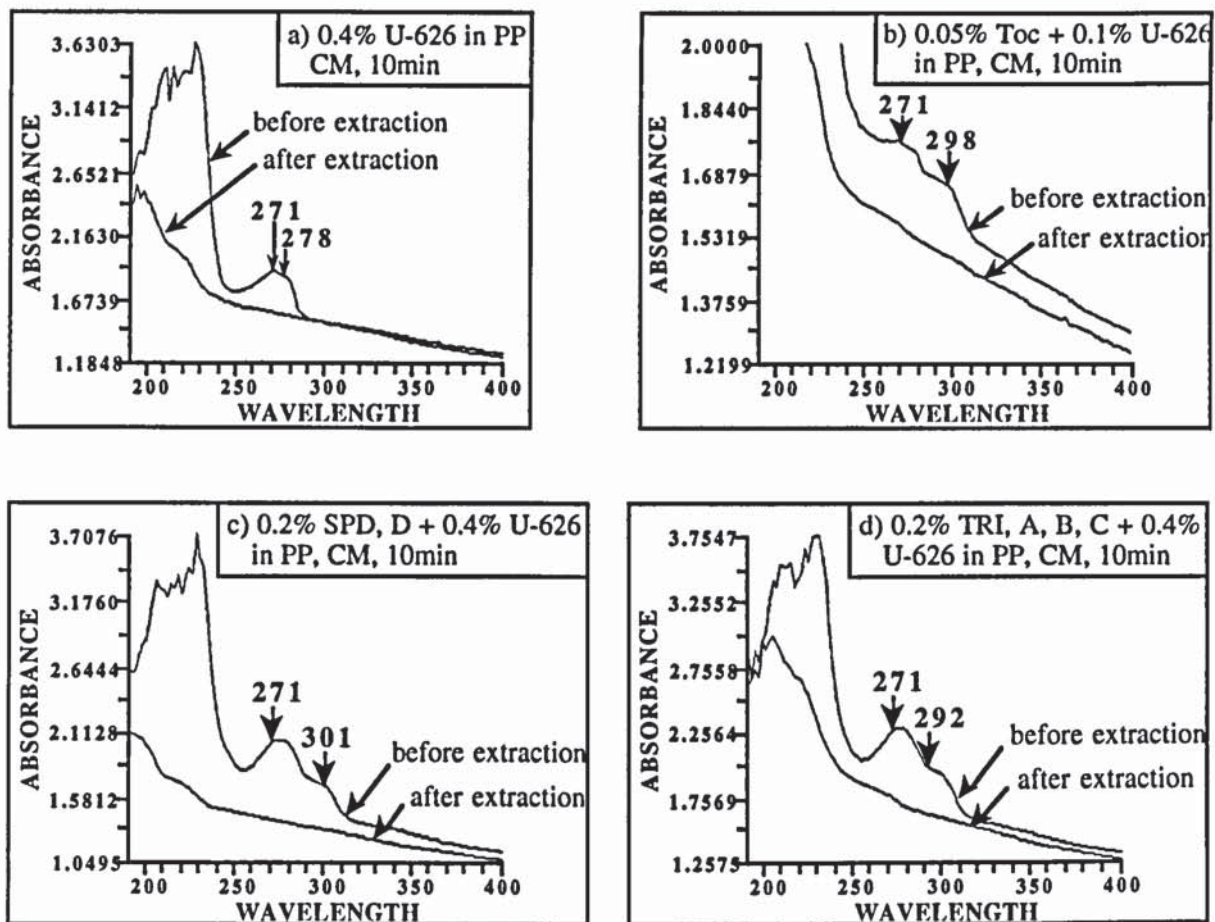


Figure 4.34: UV spectra of PP films (0.25mm thick) stabilised with 0.4% U-626 (a), 0.05% Toc + 0.1% U-626 (b), 0.2% SPD, D + 0.4% U-626 (c) and 0.2% TRI, A, B, C + 0.4% U-626 (d) (internal mixer, CM, 10min, 200°C), before and after 8 hours extraction with dichloromethane

Table 4.22: Extent of recovery of U-626 from PP stabilised with 0.4% U-626 in an internal mixer (CM, 10min, 200°C), by UV analysis of the extract at 271nm

Absorbance, 271nm	\bar{E} , l.g ⁻¹ .cm ⁻¹	v, ml	m _i , g	m'AO, %	Yield, %
0.50430	4.0	4	1.5823	0.32	80

Where,

\bar{E} = extinction coefficient of the extract (l.g⁻¹.cm⁻¹)

v = volume of solvent (l)

m_i = weight of polymer films before extraction (%)

m'AO = weight of extract in the polymer (%)

4.2.5.2 Nature of transformation products of U-626

The products extracted from PP stabilised with Toc, Toc derivatives and U-626 (CM, 10min, 200°C), were analysed by NP-HPLC using the mobile phase hexane:1,4-dioxane (100:4 and 100:0.5, v/v) (see figures 4.36, p. 444, for typical chromatograms), leading to a good separation of all the antioxidants (U-626, Toc and Toc derivatives) and their products. The transformation products of U-626 were identified by comparing their HPLC Rt and UV characteristics with those of the products extracted from PP stabilised with U-626 only (see table 4.23). As mentioned previously, U-626 decomposes during HPLC analysis (see figure 4.36.a-b), but ^{31}P -NMR analysis has shown that only a small amount of U-626 is transformed during processing with PP stabilised with the latter and Toc or Toc derivatives (see figure 4.35). Hence, HPLC peaks of the extracts corresponded to both decomposition products of U-626 formed during HPLC analysis (peaks 1 to 5) and transformation products (peaks 6 and 7). Table 4.24 shows the HPLC peak areas at 280nm of U-626 and its products in the polymer extracts, when the solvent system hexane:1,4-dioxane (100:4 and 100:0.5, v/v) was used. Table 4.25 reveals the relative signal intensities in ^{31}P -NMR of U-626 and its transformation products.

Table 4.23: HPLC Rt and UV characteristics of LMWP and U-626 decomposition and transformation products extracted from PP stabilised with Toc, Toc derivatives and U-626 in an internal mixer (CM, 10min, 200°C) (solvent systems are in hexane:1,4-dioxane, v/v) (figures 4.36, p. 444)

compound	Rt, min:sec		λ_{\max} , nm	peak name
	100:4	100:0.5		
LMWP	2:44, 4:36	3:20, 3:40, 4:30	250, 232, 281	1, 2, 4
U-626 decomposition products	3:10	3:30	272	1
	4:20	4:20	272	2
	3:50	5:40	273	3
	5:20	10:20	248, 290 (broad)	4
	7:10	13:18	240, 290 (broad)	5
U-626	10:20	36:40	282	-
U-626 transformation products	12:30	-	281, 350	6
	14:00	-	284, 335	7

Table 4.24: HPLC peak areas of U-626 and its decomposition (U-626, 1-5) and transformation products (U-626, 6-7) extracted from PP stabilised with Toc, Toc derivatives and U-626 in an internal mixer (CM, 10min, 200°C) (solvent system: hexane:1,4-dioxane = 100:4, v/v)

stabiliser	peak areas at 280nm, %					
	U-626, 1-3	U-626, 4	U-626, 5	U-626	U-626, 6	U-626, 7
0.4% U-626	94.8	2.7	0	2.5	0	0
0.2% Toc + 0.4% U-626	86.0	11.4	1.5	1.1	0	0
0.05% Toc + 0.1% U-626	71.9	21.7	3.1	0.8	2.6	0
0.2% SPD, D + 0.4% U-626	20.2	1.8	0	69.0	5.1	4.0
0.2% TRI, A,B,C + 0.4% U-626	31.9	1.6	0	61.1	3.4	2.0

Table 4.25: Relative signal intensities and chemical shifts in ^{31}P -NMR of U-626 and its transformation products (U-626, 6-7) extracted from PP stabilised with Toc, Toc derivatives and U-626 in an internal mixer (CM, 10min, 200°C), in CDCl_3 (figure 4.35, p. 443)

stabiliser	relative signal intensities (%)		
	U-626 (diphosphite)	U-626 monophosphate (HPLC peak 6)	U-626 diphosphate (HPLC peak 7)
0.4% U-626	100.0	9.3	0
0.2% Toc + 0.4% U-626	100.0	5.6, 5.1	0
0.05% Toc + 0.1% U-626	100.0	13.3, 10.2	0
0.2% SPD, D + 0.4% U-626	100.0	14.6, 14.4	3.0
0.2% TRI, A,B,C + 0.4% U-626	100.0	18.2, 16.7	5.5
δ , ppm	112.8	112.3, -16.7	-17.1

According to the HPLC spectra of the extracts of PP stabilised with U-626 and Toc or Toc derivatives, two oxidation products of U-626 (peaks 6 and 7) were formed. The latter have slightly higher R_t than U-626 when the solvent system hexane:1,4-dioxane (100:4, v/v) was used (see table 4.23), suggesting a higher polarity than U-626. The diode array UV spectra of peaks 6 and 7 each showed, in addition to a maximum absorbance at about 282nm (U-626 shows a maximum absorbance at 282nm), a longer wavelength absorption at 350 and 340nm, respectively. The latter are in accordance with the corresponding mono- and diphosphate structures of U-626, for peaks 6 and 7, respectively. This was confirmed by literature information [58,59] which revealed similar ^{31}P -NMR chemical shifts for the mono- and diphosphates of phosphites with the same or comparable structures.

The ^{31}P -NMR spectra and HPLC chromatograms of the extracts (figures 4.35 and 4.36, respectively) show that the concentration of the phosphates is highest in the extracts of PP stabilised with U-626 and the Toc derivatives SPD, D and TRI, A, B, C, but remains low in all the extracts, according to the HPLC peak areas at 280nm and ^{31}P -NMR signal intensities (see tables 4.24 and 4.25, respectively). The concentrations are lowest and similar in the extracts of PP stabilised with 0.4% U-626 and 0.2% Toc + 0.4% U-626. Furthermore, the diphosphate of U-626 is only present in the extracts of PP stabilised with combinations of U-626 and the Toc derivatives.

4.2.5.3 Nature of transformation products of Toc and Toc derivatives

The transformation products of Toc and Toc derivatives were identified by comparing their HPLC Rt and UV characteristics with those of known oxidation products of Toc (see table 4.18 p. 372). The concentrations of the products were then calculated from their HPLC peak areas (see section 2.11.1 for procedure) and the results are displayed in table 4.26.

Figure 4.37, p. 446, shows the effect of added U-626 in PP containing each of the antioxidants Toc, SPD, D and TRI, A, B, C on the nature and distribution of their transformation products after processing (CM, 10min, 200°C). Figure 4.37.a reveals that in the presence of the phosphite, Toc is highly retained at both initial concentrations (0.2 and 0.05%) and the loss of Toc is lower than in the absence of the phosphite. The presence of the phosphite also affects the nature and distribution of the transformation products of Toc (figures 4.37.b-c). In PP stabilised with 0.2% Toc and 0.2% Toc + 0.4% U-626 (figure 4.37.b), TRI, A, B, C are the major products in each case (apart from TQ). However, unlike in the absence of U-626, DHD, E and SPD, D are not formed in PP containing U-626 and Toc. At the lower initial concentration of Toc (0.05%), the same transformation products are formed, regardless of the presence of the phosphite (figure 4.37.c). However, in the presence of the phosphite, the concentration of ALD 1-4 was far lower than in its absence, but TRI, A, B, C remained the major products. The nature and concentration of the products formed during processing of PP with 0.2% SPD, D and 0.2% TRI, A, B, C, in

the absence and presence of U-626 are very similar (figures 4.37.d-e), with exception of the concentrations of DHD, which are about 10% higher in the samples containing U-626.

Table 4.26: Concentration of Toc and Toc derivatives and their transformation products extracted from PP stabilised with Toc and Toc derivatives and U-626 in an internal mixer (CM, 10min, 200°C) (figure 4.37, p. 446)

stabiliser	concentration, % weight						
	Toc	DHD, E	SPD, D	TRI, A,B,C	ALD 1, F	ALD 2, G	TQ
0.2% Toc + 0.4% U-626	97.0	0	0	0.8	0.2	0	2.1
0.05% Toc + 0.1% U-626	92.5	0	0.9	3.9	0.5	0	2.2
0.2% SPD, D + 0.4% U-626	0	38.7	2.1	31.9	18.4	3.1	5.8
0.2% TRI, A,B,C + 0.4% U-626	8.7	32.4	0	38.5	16.4	1.9	2.2

4.2.6 Isolation and characterisation of transformation products of Irg 1076 and Irg 1010 from polymer extracts

4.2.6.1 Isolation of transformation products of Irg 1076 and Irg 1010

LDPE was extruded four times into thin films (0.25mm) with each of the antioxidants Irg 1076 and Irg 1010 using three different concentrations (0.2, 1 and 10%) in a single screw extruder at 180°C (see section 2.3.1 for procedure and scheme 3.1, p. 282). The LDPE films stabilised with 10% Irg 1076 and 10% Irg 1010, extruded four times, were Soxhlet extracted with dichloromethane (see section 2.6). The resulting extracts were analysed by RP-HPLC at 235nm using the mobile phases CH₃OH:CH₂Cl₂ = 90:10, v/v, and CH₃OH for Irg 1076 and Irg 1010, respectively (see figures 2.31, 2.36, p. 265 and 271, for chromatograms). At least 15 different transformation products of Irg 1076 and 14 oxidation products of Irg 1010 were separated. Tables 4.27 and 4.28 show the HPLC Rt and diode array UV characteristics of the different products formed. Some of the main

transformation products, Irg 1076 products 1, 12 and 15 and Irg 1010 products 3 and 6 (see tables 4.2 and 4.3 for structures) were isolated by semi-preparative RP-HPLC at 235nm using methanol as the mobile phase.

Table 4.27: HPLC Rt and UV characteristics of the products extracted from LDPE stabilised with 10% Irg 1076, pass 4 (single screw extruder, 180°C) (solvents systems are in CH₃OH:CH₂Cl₂ = 90:10, v/v and CH₃OH) (figures 2.31, p. 265, and 4.47, p. 447)

HPLC peak name	Rt, min:sec		λ_{\max} , nm
	CH ₃ OH:CH ₂ Cl ₂	CH ₃ OH	
1 (isolated)	2:40	2:50	282 (broad)
2	2:55	3:10	282
3	3:20	4:00	282
4	3:55	5:00	282
5	4:30	5:40	282
6	7:00	11:10	282
7	7:30	14:00	282
8	8:40	15:10	282
9	9:36	16:20	282
10	11:00	19:00	282
Irg 1076	12:30	23:00	282
11, QM-Irg 1076 (?)	13:15	25:30	315 (broad), 238
12, C-Irg 1076 (isolated)	14:40	29:10	320 (broad), 240
13	16:40	32:50	282, 320 (broad)
14, CBQM-Irg 1076 (?)	19:30	35:00	320 (broad), 240
15, BC-Irg 1076 (isolated)	23:30	45:00	308 (broad), 240

Table 4.28: HPLC Rt and UV characteristics of the products extracted from LDPE stabilised with 10% Irg 1010, pass 4 (single screw extruder, 180°C) (figures 2.36, p. 271, and 4.50, p. 451)

HPLC peak name	Rt, min:sec	λ_{\max} , nm
1	2:40	282
2	3:00	282
3 (isolated)	3:10	282
4	3:20	320 (broad), 282
5	3:40	282
6 (isolated)	3:50	282
7	4:10	282
8	4:15	282
9	4:40	282
10	5:00	282
11	5:20	282
Irg 1010	6:00	282
12	8:30	282
13	9:00	282
14	9:30	312 (broad), 288

4.2.6.2 Characterisation of transformation products of Irg 1076

Isolated compounds 1, 12 and 15 were characterised by UV and MS and compound 12 was also characterised by $^1\text{H-NMR}$ and all the compounds extracted were identified as described below. Figure 2.31, p. 265, shows the HPLC chromatogram of the mixture of all the products extracted.

Compound 1 (Irg 1076-1)

The HPLC chromatogram of isolated compound 1 showed a sharp peak with the shortest Rt (see figures 2.31 and 2.32.a, p. 266). Table 4.29 compares its UV and MS characteristics with those of Irg 1076. The UV spectrum (figure 2.32.b) shows a maximum absorbance at 282nm which is broader (260-340nm) than that of Irg 1076. In the MS

spectrum of compound 1 (figure 2.32.c) the molecular ion peak could not be identified, showing a series of small peaks below 400. The peak at 344 could correspond to a structure similar to that shown in figure 4.38. However the structure of compound 1 remains uncertain.

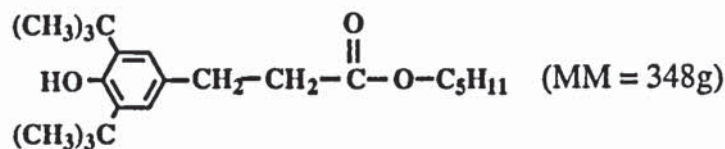


Figure 4.38: Possible chemical structure of the peak at 344 in the MS spectrum of compound 1, Irg 1076-1

Compounds 2-10 (Irg 1076-2 to Irg 1076-10)

Compounds 2 to 10 show similar diode array UV characteristics to Irg 1076 (λ_{max} at 282nm) (see table 4.27) indicating the presence of intact phenolic groups, without further conjugation. The above observation and the fact that these compounds have lower R_t than Irg 1076 (see figure 2.31) suggest that they are 2,6-di-*tert*-butyl phenol derivatives, with the chain in the 4-position increasing in size with increasing R_t (see figure 4.39 below). In the literature it has been shown [51] that cleavage of *tert*-butyl groups was also occurring during processing of Irg 1076 with PE.

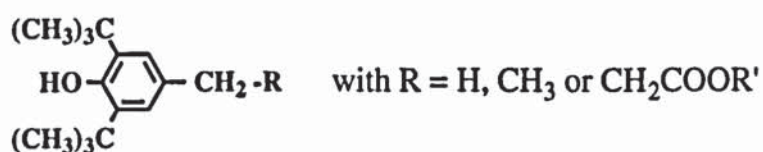


Figure 4.39: Possible chemical structures of compounds 2-10, Irg 1076-2 to Irg 1076-10

Compound 12 (C-Irg 1076)

The isolated compound 12 is the major transformation product of Irg 1076 according to its HPLC peak area (see figure 2.31 and 2.33.a, p. 267). Table 4.29 compares its UV and main $^1\text{H-NMR}$ and MS characteristics (see figures 2.33.b-d, p. 267) with those of Irg 1076. The UV spectrum of compound 12 (figure 2.33.b) shows a maximum absorbance at 320nm which is broad (Irg 1076 absorbs at 282nm), indicating the presence of a conjugated

system. The $^1\text{H-NMR}$ spectrum of compound 12 (figure 2.33.c) shows two doublets at 7.6 and 6.3ppm and the absence of the characteristic triplets at 2.6 and 2.9ppm for methylenes at positions 7 and 8 (see figure 4.40 below for positions). The above observations and the presence of the hydroxyl group (5.5ppm) suggest that compound 12 is the cinnamate of Irg 1076 (see figure 4.40 for structure). This was confirmed by GC-MS analysis (figure 2.33.d) which revealed a molecular ion peak at 528 (MM of Irg 1076 - 2H). Literature information [45,48] also confirmed the structure of cinnamate of Irg 1076 (C-Irg 1076) for compound 12.

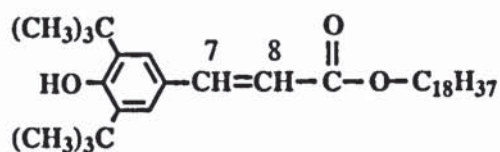


Figure 4.40: Chemical structure of compound 12, C-Irg 1076

Compound 15 (BC-Irg 1076)

Isolated compound 15 had the highest HPLC Rt (see figures 2.31 and 2.34.a, p. 269) and was present in a small amount. Table 4.29 compares its UV and MS characteristics (figures 2.34.b-d, p. 269) with those of Irg 1076 and the cinnamate of Irg 1076, C-Irg 1076. The UV spectrum (figure 2.34.b) of compound 15 (figure 2.34.b) is very similar to that of C-Irg 1076 (figure 2.33.b, p. 267), revealing a broad maximum absorption at 308nm, compared to 320nm for C-Irg 1076. Hence, like for C-Irg-1076, this indicates the presence of a conjugated system. The MS spectrum of compound 15 (figure 2.34.c) shows a molecular ion peak at 1055, indicating a dimeric structure of Irg 1076, i.e. the biscinnamate of Irg 1076 (BC-Irg 1076) (see figure 4.41 below for structure). This was confirmed by literature information [20,48].

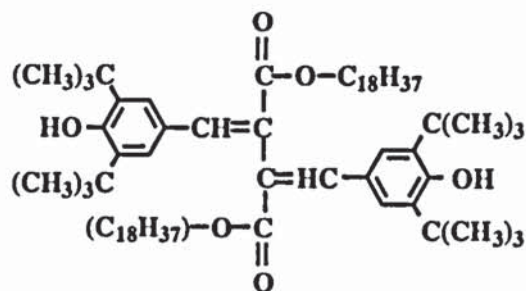


Figure 4.41: Chemical structure of compound 13, BC-Irg 1076

Compounds 11, 13 and 14 (QM-Irg 1076 (?), Irg 1076-13 and CBQM-Irg1076 (?))

Compounds 11, 13 and 14 had higher R_t than Irg 1076 (see figure 2.31) and all showed a long wavelength absorption above 300nm (see figure 2.35, p. 270). According to the literature [54] (see table 1.2, p. 54), compound 11, which has maximum wavelengths at 238 and 315 (broad) nm, could be the quinone methide of Irg 1076 (QM-Irg 1076) (see figure 4.42 below for structure). The UV spectrum of compound 13 shows maximum absorbances at 282 and 320nm (broad), and compound 14 has a maximum wavelength at 320nm (broad), also indicating conjugated systems. It is likely that compound 14 is the conjugated bisquinone methide of Irg 1076 (CBQM-Irg 1076) (see figure 4.42 below for structure). Indeed, in the literature it was shown [20] that CBQM-Irg 1076 has a maximum wavelength at 322nm in the UV region. However, the structures of compounds 11, 13 and 14 remain uncertain.

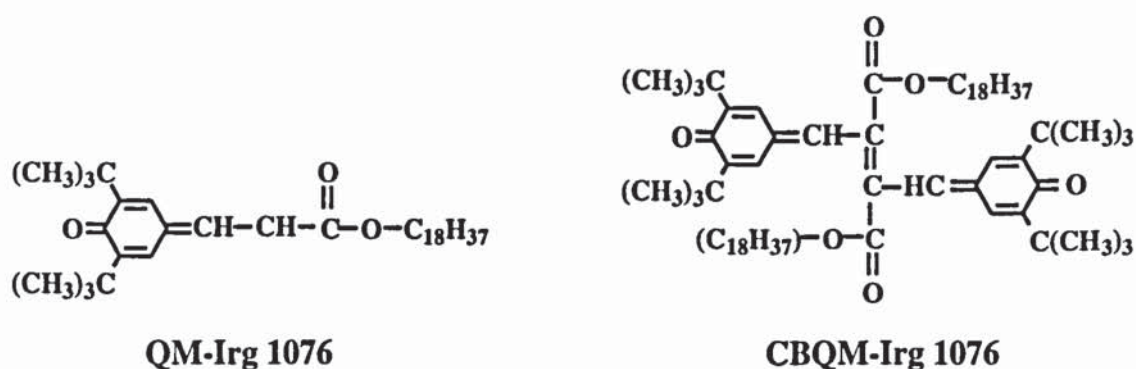


Figure 4.42: Possible chemical structures of compounds 11 and 14, QM-Irg 1076 and CBQM-Irg 1076

Table 4.29: Comparison of the main spectral characteristics of Irg 1076-1, C-Irg 1076 and BC-Irg 1076, isolated from the extract of LDPE stabilised with 10% Irg 1076, pass 4 (single screw extruder, 180°C), with those of Irg 1076

λ_{\max} , nm		Irg 1076-1	BC-Irg 1076	C-Irg 1076	Irg 1076
		282 (weak, broad)	308 (broad), 240	320 (broad), 240	282
$^1\text{H-NMR}$: δ , ppm	CH ₂ sat., CH unsat. (7, 8)	-	-	7.59, 7.61 (d) 6.23, 6.31 (d)	2.55-2.65 (t) 2.85-2.95 (t)
	OH (4a)			5.5 (s)	5.1 (s)
	CH, arom. (2, 6)			7.37 (s)	7.02 (s)
MS: M⁺, m/z		≥ 344	1055	528	530
Structure		p. 386 and 332	p. 388 and 332	p. 387 and 332	p. 332
Figures (page)		2.32.b-2.32.c (266)	2.34.b-2.34.c (269)	2.33.b-2.33.d (267)	2.4.b-2.4.d (150)

4.2.6.3 Characterisation of transformation products of Irg 1010

Isolated compounds 3 and 6 were characterised by UV, $^1\text{H-NMR}$ and MS all the compounds extracted were identified as described below. Figure 2.36, p. 271, shows the HPLC chromatogram of the mixture of all the products extracted.

Compound 3 (Irg 1010-3):

Isolated compound 3, which had a relatively short HPLC Rt compared to most of the other transformation products (see figures 2.36 and 2.37.a, p. 271), was characterised by UV, $^1\text{H-NMR}$ and MS (figures 2.37.b-d, p. 272). Its UV spectrum (figure 2.37.b) showed a maximum absorbance at 282nm, indicating that the phenolic group is present and that there is no further conjugation. Table 4.30 compares the main spectral characteristics of compound 3 with those of Irg 1010. The $^1\text{H-NMR}$ spectrum of compound 3 (figure 2.37.c) reveals the presence of a new singlet at 3.7ppm (methyl group) and the absence of the

characteristic methylene group signal at 4.1ppm (position 10, see figure 4.43 below) in the spectrum of Irg 1010. This suggests that compound 3 has a single sub-unit structure of Irg 1010 as shown in figure 4.43. The MS spectrum (figure 2.37.d) showed a molecular ion peak at 292 which corresponds to methyl-3-(3,5-di-*t*-butyl-4-hydroxyphenyl)-propionate (Irg 1010-3). In the literature [47] it was shown that the latter was formed during processing of Irg 1010 with PE and PP by MS analysis.

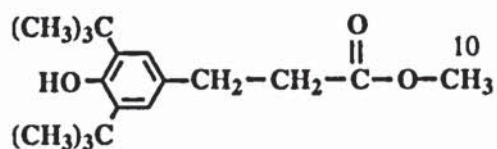


Figure 4.43: Chemical structure of compound 3, Irg 1010-3

Compound 6 (Irg 1010-6)

Isolated compound 6 was the major transformation product of Irg 1010 according to its HPLC peak area (see figure 2.36) and was also characterised by UV, ¹H-NMR and MS (figure 2.38.b-d, p. 274). Its UV spectrum was similar to those of compound 3 and Irg 1010, i.e. λ_{max} at 282nm (see figure 2.38.b). The ¹H-NMR spectrum of compound 6 (figure 2.38.c) showed an additional singlet at 3.2ppm compared to that of Irg 1076 (see table 4.30) which is likely to be caused by a hydroxyl group. The GC-MS spectrum (figure 2.38.d) revealed a molecular ion peak at 916 which is compatible with the structure shown in figure 4.44 below, i.e. a compound containing three Irg 1010 type sub-units, the fourth sub-unit being replaced by a methyl alcohol (Irg 1010-6). This was confirmed by literature information [49] which showed a very similar MS spectrum for an electron-beam generated transformation product of Irg 1010 in PP.

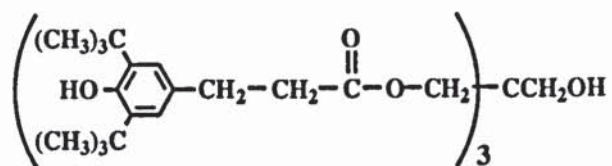
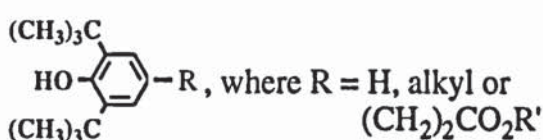


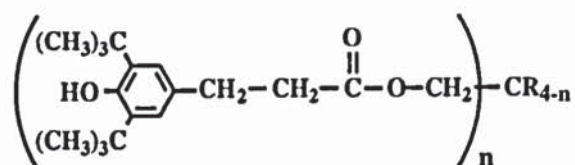
Figure 4.44: Chemical structure of compound 6, Irg 1010-6

Compounds 1, 2, 5 and 7-13 (Irg 1010-1, -2, -5 and Irg 1010-7 to -13)

Compounds 1, 2, 5 and 7 to 11 were analysed by diode array UV spectroscopy (see table 4.28) and all showed maximum wavelengths at 282nm, suggesting intact phenolic groups without any further conjugation. Because of their shorter HPLC Rt (see figure 2.36), compounds 1 and 2 are likely to contain only one Irg 1010 type sub-unit, like compound 3, or to be derivatives of 2,6-di-*t*-butyl-phenol (see figure 4.45 for possible structures). Compound 5 is likely to contain between one and three ($1 \leq n \leq 3$) Irg 1010 sub-units and compounds 7 to 13 probably contain at least three Irg 1010 sub-unit ($3 \leq n \leq 4$) (see figure 4.45). Some of the structures could also correspond to simple loss of *tert*-butyl groups.



Irg 1010-1 and -2

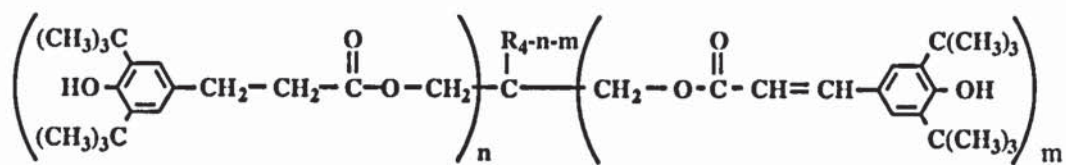


Irg 1010-5 ($1 \leq n \leq 3$) and Irg 1010-7 to -13 ($3 \leq n \leq 4$)

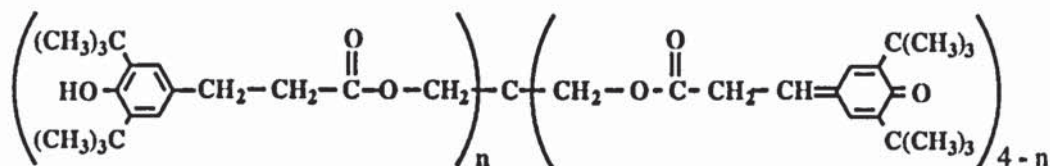
Figure 4.45: Possible chemical structures of compounds 1, 2, 5 and 7 to 13, Irg 1010-1, -2, -5 and Irg 1010-7 to -13

Compounds 4 and 14 (Irg 1010-4 and Irg 1010-14)

Compounds 4 and 14 showed, in addition to maximum wavelengths at 282 and 288nm, respectively, maximum wavelengths above 300nm (see figure 2.39, p. 276) which are characteristic of cinnamate or quinonoid structures (see table 1.2, p. 54). Compound 4 which had λ_{max} at 320nm and a shorter Rt than Irg 1010 (see figure 2.36), is likely to contain 1-4 Irg 1010 sub-units with at least one of them being oxidised to a cinnamate (see figure 4.46 for possible structure). On the other hand, compound 14, which had a higher Rt than Irg 1010 (figure 2.36) and λ_{max} at 312nm, is suggested to have all 4 Irg 1010 sub-units with at least one of them being oxidised to a quinonoid (see figure 4.46).



Irg 1010-4



Irg 1010-14

Figure 4.46: Possible chemical structures of compounds 4 and 14, Irg 1010-4 and -14

Table 4.30: Comparison of the main spectral characteristics of Irg 1010-3 and Irg 1010-6, isolated from the extract of LDPE stabilised with 10% Irg 1010, pass 4 (single screw extruder, 180°C), with those of Irg 1010

		Irg 1010-3	Irg 1010-6	Irg 1010
λ_{max} , nm		282	282	282
$^1\text{H-NMR}$: δ , ppm	CH ₃ , CH ₂ , sat. (10)	3.7 (s)	4.0 (s)	4.1 (s)
	CH ₂ sat. (7, 8)	2.5-2.7 (t)	2.5-2.7 (t)	2.5-2.7 (t)
		2.8-2.95 (t)	2.8-2.97 (t)	2.8-2.95 (t)
	OH (4a, 11a)	5.1 (s)	5.1 (s, 4a), 3.2 (s, 11a)	5.1 (s)
	CH, arom. (2, 6)	7.0 (s)	7.0 (s)	7.0 (s)
MS: M ⁺ , m/z		292	916	1176
Structure		p. 390 and 333	p. 390 and 333	p. 333
Figures (page)		2.37.b-2.37.d (272)	2.38.b-2.38.d (274)	2.5.b-2.5.d (202)

4.2.7 Effect of extrusion severity on the nature of the transformation products of Irg 1076 in LDPE

The products extracted from LDPE films stabilised with 0.2, 1 and 10% Irg 1076 in a single screw extruder (4 passes, 180°C) were analysed by RP-HPLC (see section 2.6 for procedure) using the mobile phase CH₃OH:CH₂Cl₂ (90:10, v/v), at 282nm (see figures

4.47, p. 448, for typical chromatograms). At least 15 different transformation products of Irg 1076 were separated. The products were identified by comparing their HPLC Rt and diode array UV characteristics with those of the oxidation products of Irg 1076 extracted from LDPE stabilised with 10% Irg 1076, pass 4 (see table 4.27 for HPLC and UV data and table 4.2 for structures). The major transformation product in all the extracts was the cinnamate of Irg 1076 (C-Irg 1076) according to its HPLC peak area at 282nm (see table 4.31). Smaller quantities of the biscinnamate of Irg 1076 (BC-Irg 1076) were also present. C-Irg 1076 and BC-Irg 1076 were both isolated and characterised (see tables 2.41, 2.43, 2.45, 2.46, p. 175, and figures 2.33-2.34, p. 267). Two other transformation products, compounds 11 and 14 (see figure 4.47) were suggested to be the quinone methide (QM) and conjugated bisquinone methide (CBQM) of Irg 1076, respectively, according to their UV spectra (figure 2.35) but their structures remain uncertain. The other products (Irg 1076-1 to -10) had very similar UV characteristics to Irg 1076 (λ_{max} at 282nm), suggesting that they contain intact phenolic groups and no further conjugation. As many of the minor products could not be identified, it was not possible to determine the exact concentrations of the products in the extracts. However, their HPLC peak areas were determined at 282nm (see table 4.31) and the concentrations of isolated C-Irg 1076 and BC-Irg 1076 relative to Irg 1076 were calculated from their extinction coefficients (table 4.32).

Figures 4.48 and 4.49, p. 449, show the effect of initial concentration of the antioxidant and extrusion severity on the HPLC peak areas at 282nm of Irg 1076 and its transformation products, and the concentrations of C-, and BC-Irg 1076 relative to Irg 1076. The polymer samples containing high initial concentrations of Irg 1076 (1 and 10%) retain higher levels of the parent antioxidants than the samples containing the lower initial concentration of 0.2% (figure 4.48.a). A similar effect was observed in LDPE stabilised with Toc (see figure 4.16.a, p. 427). Furthermore, at the lower initial concentration of 0.2% Irg 1076, severe processing seems to lead to a more pronounced "loss" of the antioxidant than at the higher concentrations. Single and multiple extrusions of LDPE containing Irg 1076 lead to chemical transformations of the antioxidant. The formation of C-Irg 1076 (major transformation product) seems to be favoured at a lower initial concentration of Irg

1076 (0.2%) and at a very high concentration of the antioxidant (10%) (see figure 4.48.b). BC-Irg 1076 showed a similar behaviour (figure 4.48.c), but the concentrations of the latter were much smaller than those of C-Irg 1076. Figures 4.48.e-g reveal the concentrations of C-Irg 1076 and BC-Irg 1076, relative to Irg 1076. It is clear that the concentrations of C- and BC-Irg 1076 are much smaller than their HPLC peak areas because of their high extinction coefficients compared to Irg 1076 (see table 4.2, p. 332). Similarly, Irg 1076-11 (possibly QM-Irg 1076), -13 and -14 (possibly CBQM-Irg 1076), which were found to contain cinnamate or quinonoid structures, are expected to have higher extinction coefficients than Irg 1076. On the other hand, Irg 1076-1 to 10, which showed similar UV characteristics to Irg 1076 (λ_{\max} at 282nm) are expected to have similar extinction coefficients to Irg 1076. Irg 1076-11 was only present in the extract of LDPE stabilised with 0.2% (see figure 4.49.a). Irg 1076-1, which was also isolated, was present in small amounts in all the extracts and its peak area was not affected by extrusion severity.

Table 4.31: HPLC peak areas at 282nm of the products extracted from LDPE stabilised with Irg 1076 (single screw extruder, 180°C) (figures 4.48-4.49, p. 449)

[Irg 1076]	pass	peak areas, 282nm, %							
		Irg 1076	1	2-10	11	13	14	C-Irg 1076	BC-Irg 1076
0.2%	1	87.3	1.1	4.7	1.4	0.3	0	5.2	0
	2	67.6	1.2	11.9	4.2	0.3	0	14.8	0
	3	57.9	1.3	11.6	3.8	0.6	0.6	23.1	1.1
	4	51.4	1.3	11.5	3.8	0.4	0.4	29.1	2.2
1%	1	94.4	0.7	1.6	0	0.4	0	3.0	0
	2	89.8	0.6	2.1	0	0.5	0	7.0	0
	3	84.6	1.3	3.2	0	0.4	0	10.4	0
	4	82.2	0.9	3.5	0	0.5	0.03	12.8	0.04
10%	1	90.9	0.8	5.5	0	0.4	0	2.5	0
	2	80.9	1.0	6.6	0	0.5	0.1	10.0	0.7
	3	72.7	1.1	5.7	0	0.6	0.3	18.2	1.5
	4	70.1	1.1	4.8	0	0.5	0.4	21.1	2.0

Table 4.32: Relative concentrations of Irg 1076, C-Irg 1076 and BC-Irg 1076 (total 100%) extracted from LDPE stabilised with Irg 1076 (single screw extruder, 180°C) (figure 4.48.e-g, p. 449)

[Irg 1076]	pass	concentration, % weight		
		Irg 1076	C-Irg 1076	BC-Irg 1076
0.2%	1	98.5	1.5	0
	2	94.6	5.4	0
	3	90.2	9.4	0.5
	4	86.3	12.7	1.0
1%	1	99.2	0.8	0
	2	98.0	2.0	0
	3	96.9	3.1	0
	4	96.1	3.9	0.01
10%	1	99.3	0.7	0
	2	96.7	3.1	0.2
	3	93.4	6.1	0.5
	4	92.1	7.2	0.7

4.2.8 Effect of extrusion severity on the nature of the transformation products of Irg 1010 in LDPE

The products extracted from LDPE films stabilised with 0.2, 1 and 10% Irg 1010 in a single screw extruder (4 passes, 180°C) were analysed by RP-HPLC (see section 2.6 for procedure) using methanol as the mobile phase, at 282nm (see figure 4.50, p. 451, for typical chromatograms). At least 14 different transformation products of Irg 1010 were separated. The products were identified by comparing their HPLC Rt and diode array UV characteristics with those of the oxidation products of Irg 1010 isolated from the extract of LDPE stabilised with 10% Irg 1010, pass 4 (see table 4.28 for HPLC and UV data and table 4.3 for structures). The main transformation product in all the extracts was tris-[methylene-(3, 5-di-*t*-butyl-4-hydroxy-phenyl)propionate]-hydroxymethylmethane, Irg 1010-6, according to its HPLC peak area at 282nm (see table 4.33). Methyl-3-(3',5'-di-*t*-butyl-4'-hydroxyphenyl)propionate, Irg 1010-3, was also present in high concentrations in

all the extracts, compared to other products. Irg 1010-3 and Irg 1010-6 were both isolated and characterised (see tables 2.48 and 2.50-2.52, p. 178, and figures 2.37-2.38, p. 272). Two other transformation products, compounds 4 and 14 were suggested to contain cinnamate and quinonoid structures, respectively, but their structures remain uncertain. The other products had very similar UV characteristics to Irg 1010 (λ_{\max} at 282nm), suggesting that they contain intact phenolic groups without further conjugation. The HPLC peak areas of the products were determined at 282nm (see table 4.33). Concentrations could not be determined as the amount of products isolated was too low and many of the minor products could not be identified.

Figures 4.51 and 4.52, p. 453, show the effect of initial concentration of Irg 1010 and extrusion severity on the HPLC peak areas at 282nm of Irg 1010 and its transformation products. Like in LDPE stabilised with Irg 1076 under the same conditions, the polymer samples containing the higher initial concentrations of Irg 1010 (1 and 10%) retain higher levels of the antioxidant (figure 4.51.a) and, at the lower concentration of 0.2%, a more pronounced loss of Irg 1010 is observed after multiple extrusions. The loss of antioxidant is caused by chemical transformations. The formation of Irg 1010-6 and Irg 1010-3 (major transformation products) is favoured at lower initial concentrations and their peak areas increase with extrusion severity (fig 4.51.b-c and 4.52). The total peak area of Irg 1010-1, -2, -5 and -7 to -13 is also higher at the lower concentration of the antioxidant and increases with extrusion severity at all concentrations (figures 4.51.d and 4.52). Irg 1010-4 and -14 are initially (after the first extrusion pass) minor products in all the extracts (figures 4.51.e-f and 4.52) and their peak areas remain more or less constant after multiple extrusions, except the peak area of Irg 1010-14 in LDPE stabilised with 1% Irg 1010 which shows an increase with extrusion severity (figure 4.52.b).

Table 4.33: HPLC peak areas at 282nm of the products extracted from LDPE stabilised with Irg 1010 (single screw extruder, 180°C) (figures 4.51-4.52, p. 453)

[Irg 1010]	pass	peak areas, 282nm, %					
		Irg 1010	1, 2, 5, 7-13	4	14	Irg 1010-3	Irg 1010-6
0.2%	1	94.2	3.0	0	0.4	0.5	1.9
	2	89.5	6.7	0	0.2	0.8	2.7
	3	83.5	9.8	0.6	0.3	1.8	4.0
	4	79.2	12.0	0.7	0.4	2.3	5.4
1%	1	96.5	0.9	0.06	0	0.5	1.8
	2	95.6	1.7	0.08	0.2	0.5	1.9
	3	94.9	2.3	0	0.5	0.3	2.0
	4	94.2	2.8	0	0.6	0.3	2.1
10%	1	95.4	1.7	0.2	0.3	0.6	1.9
	2	92.6	3.8	0.08	0.8	0.7	2.0
	3	92.7	4.4	0.2	0.2	0.6	2.0
	4	92.0	5.0	0.2	0.2	0.5	2.0

4.3 DISCUSSION

4.3.1 Mechanism of oxidation of Toc with lead dioxide in hexane

4.3.1.1 Isolation and identification of oxidation products

The nature of the products formed from the oxidation of Toc with PbO₂ in hexane was investigated thoroughly and figures 2.2, p. 187, and 2.13 to 2.15, p. 212 show that these are of dimeric, trimeric and aldehydic structures. Dimers, trimers and aldehydes have also been isolated and characterised in the literature [88-100] as products of oxidation of Toc with peroxy radicals (e.g. generated from methyl linoleate) and alkaline potassium ferricyanide, mainly in unpolar solvents. However, in the literature there is no reference to any separation of the different stereoisomeric structures that exist for the dimers and trimers of Toc, which were extensively investigated and separated by NP-HPLC in this work (section 4.2.1).

The dihydroxydimer of Toc, DHD, D, which was formed as a minor product in the oxidations with PbO₂ and synthesised by reducing SPD, D with LiAlH₄ (yield of 56%), showed 4 peaks E1, E2, E3 and E4 in its HPLC chromatogram which were extensively characterised (figures 2.13.a, p. 212, and 4.1.a, p. 336) and were found to be stereoisomers. The different stereoisomeric structures are suggested to be caused by the presence of the chiral centres at positions 2 and 18 (supporting the phytyl chain) (see figure 4.2, p. 338). Different positions of the two phenolic hydroxyls in structures E1, E2, E3 and E4, caused by the rotation of the ethyl bond (positions 11 and 12), could also cause changes in their HPLC Rt.

The spirodimer of Toc, SPD, D, obtained as a major product (81%) when high concentrations of the oxidising agent were used (Toc:PbO₂ = 1:40, mol/mol), showed 3 HPLC peaks (see figures 2.9.b, p.208, and 4.3.a, p. 339), which were characterised (figures 2.14, p. 223) and shown to correspond to a mixture of stereoisomers. Doubling of the resonances in their ¹³C-NMR spectrum at chiral centre 13 and positions 14 (carbonyl) and

15 (carbon α to the carbonyl) (see table 2.19, p. 158) and the identical peak areas for D1 and D3 (figure 4.3.a) suggest that D1 and D3 correspond to the R and S configurations at position 13 and, that D2 is a racemic mixture (see figure 4.4, p. 341 for structures). The partial resolution of the racemic modification is probably caused by the larger difference in polarity between some of the R and S configurations, caused by different configurations of the chiral centres at positions 2 and 18 (supporting the phytyl chain), hence being more or less retained on the column. So far only the R and S configurations of Toc model have been separated on an optically active column [106]. It has been shown [100] that the spirodimer from synthetic all-rac- α -tocopherol (Toc) shows no optical rotation, suggesting equal amounts of all possible stereoisomers, whereas the spirodimer from RRR- α -tocopherol has a relatively high specific rotation $[\alpha]^{25D} = 31.5^\circ$. This is because the R and S forms of RRR- α -tocopherol are not enantiomers, as the chiral centres at positions 2 and 18 remain unchanged (R configuration).

The trimers of Toc, TRI, A, B, C, obtained in high concentrations when a ratio of 1:10, mol/mol, in Toc:PbO₂ was used (65%), showed at least 10 HPLC peaks (see figure 2.9.a, p. 208 and 4.5 p. 342) and these were also found to be stereoisomers (see figures 2.15, p. 229 for spectral characterisations). Their ¹H- and ¹³C-NMR chemical shifts (tables 2.18 and 2.20, p. 157 and 160) suggest that they mainly differ in the configurations at chiral centres 13, 18, 21 and 22, giving rise to 8 main structures, as shown in figure 4.7, p. 346. Different configurations at chiral centres 2 and 28 could cause changes in their HPLC Rt. According to their ¹H-NMR spectra (figure 4.6, p. 345) TRI A1 and some of the trimers B and C were found to have a *cis* structure for methyl 18a and the third chroman moiety (structures I to IV in figure 4.7), whereas TRI, A2 and the other TRI, B and C were shown to have a *trans* structure (structures V to VIII). For natural α -tocopherol, RRR-Toc, only 4 structures would be expected (III to VI), as the chiral centres at positions 2, 18, 28 and the ones in the phytyl chain all have the R configuration. However, only two trimers of RRR-Toc were mentioned in the literature [81] and separated by HPLC. The latter were shown to differ at positions 21 and 22, but no comment was made about the configuration at position 13, which can be R or S.

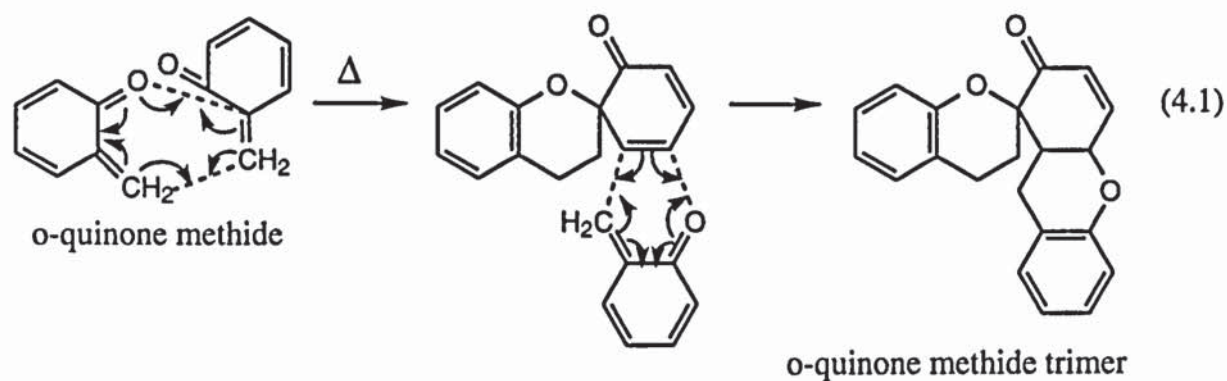
The aldehyde, 5-formyl- γ -Toc, ALD 1, obtained as a minor product in the oxidations of Toc with PbO₂, was characterised (table 2.25, p. 164) and its characteristics were compared with those of the supplied sample of ALD 1 (figures 2.2, p. 187). Its low HPLC Rt compared to Toc is caused by hydrogen bonding between the phenolic hydrogen and the aldehyde group, as shown in figure 4.9, p. 348.

4.3.1.2 Mechanism of oxidation

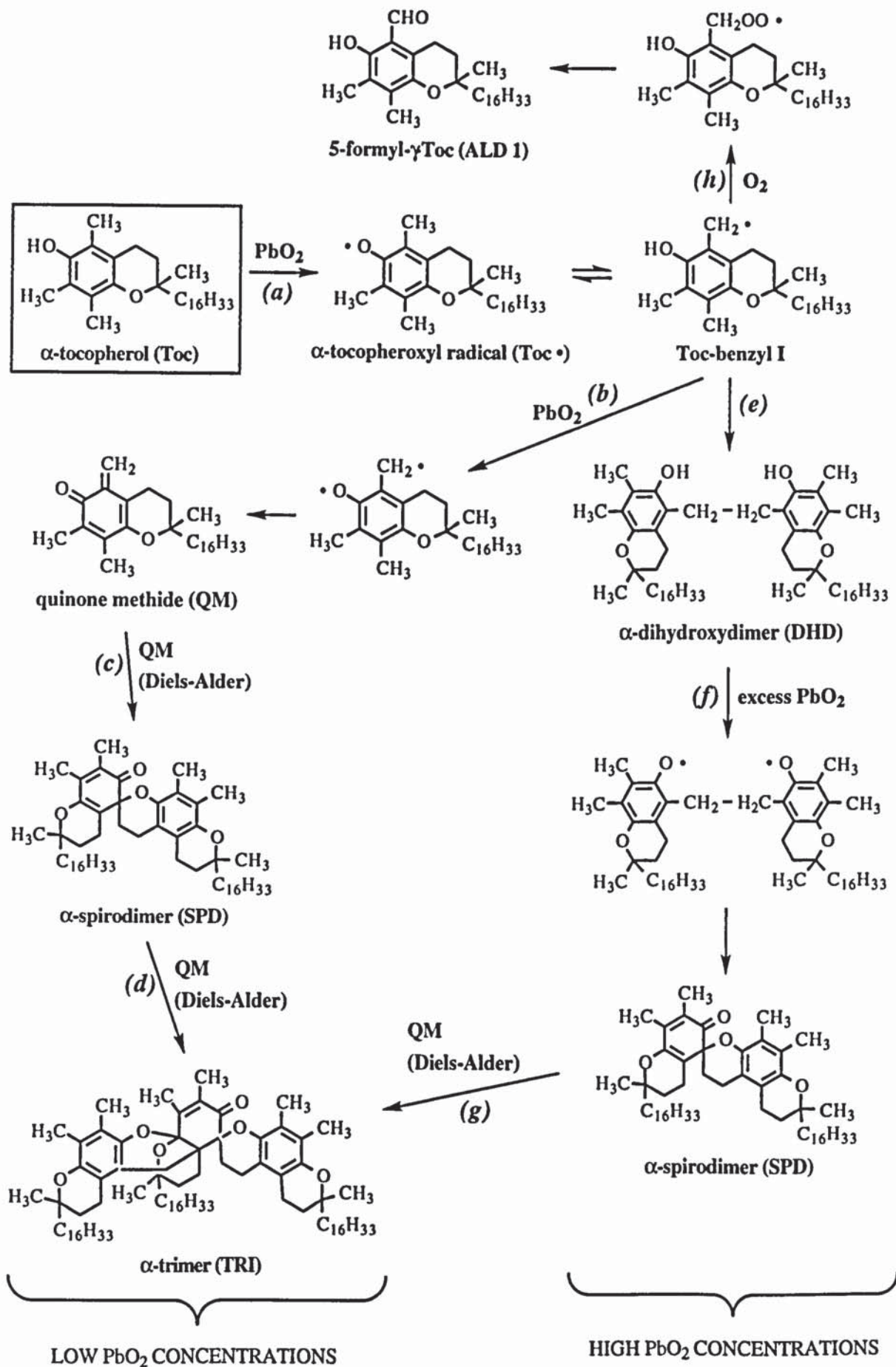
After the identification of the products of reaction of Toc with PbO₂ in hexane, the mechanism of oxidation of Toc was investigated by studying the effect of oxidising agent concentration on the nature and concentration of the different products formed (see figure 4.10, p. 351). Figure 4.10 shows that the extent of oxidation of Toc increases with increasing PbO₂ concentrations and that the nature and distribution of the products change with the amount of PbO₂ added. The formation of DHD, D and TRI, A, B, C is favoured at lower PbO₂ concentrations, whereas SPD, D is preferably formed at high concentrations of the oxidising agent. The formation of ALD 1 is minor for all the concentrations used and therefore probably a side reaction. In the light of the different oxidation products formed from Toc, a mechanism of oxidation is proposed in scheme 4.4. ESR measurements have shown that the formation of the α -tocopheroxyl radical (Toc•), i.e. phenolic hydrogen abstraction (reaction a, scheme 4.4), is the first step in the oxidations of Toc with PbO₂ in toluene [86,87]. The latter isomerises to the corresponding benzyl radical, Toc-benzyl I which can then react further to form a quinone methide (QM) (reaction b) or the DHD (reaction e). The formation of SPD and TRI was suggested to be via the QM (reactions c and d, respectively) or via DHD (reaction f) or both pathways simultaneously [84,85], as also shown in scheme 1.9, p. 57 in chapter one.

At low PbO₂ concentrations, the concentration of initial Toc• produced is expected to be low, which explains the limited formation of DHD, the latter being formed by coupling of two Toc• (reaction e). Instead the Toc• produced is more likely to react again with PbO₂ to form a biradical (reaction b), leading to the quinone methide of Toc (QM). The QM can

then react with another QM to form SPD via a Diels-Alder reaction (reaction c) and the latter can react again with QM to yield TRI (reaction d). The study of the chemistry of simple o-quinone methides has shown that trimerisation is one of their most facile reactions [110]. Trimerisation was shown to be the result of two successive Diels-Alder reactions, as shown in reaction 4.1.



The trimer of Toc can be formed in a similar way, hence explaining the high concentration of the latter at lower PbO₂ concentrations. As the concentration of lead dioxide increases, the concentration of Toc• also increases, hence the latter are more likely to encounter to form DHD via radical coupling, instead of reacting again with PbO₂ to form the QM. If the concentration of PbO₂ is high enough, the DHD can be oxidised to the SPD by giving away its two phenolic hydrogens (reaction f). The SPD itself can only be oxidised to the TRI (reaction g) if QM is formed. However, the latter is favoured at lower concentrations of the oxidising agent, which explains a decrease in the formation of TRI and an increase in the formation of the SPD, when the concentration of PbO₂ is high enough.



Scheme 4.4: Mechanism of oxidation of Toc with PbO_2 in hexane

4.3.2 Isolation and characterisation of transformation products of Toc from polymer extracts

Transformation products of Toc have been isolated from polymer samples processed with high concentrations of the antioxidant, so that high amounts of transformation products could be isolated. NP-HPLC analysis (figure 2.20, p. 240) of the extract of the supplied PP granules stabilised with 39% Toc and extruded four times (CPC789 series, single screw extruder, 270°C) showed the presence of high concentrations of ALD 1 (also formed during oxidation of Toc with PbO₂), ALD 2 and ALD 3 (see figure 4.12, p. 355 for structures). These aldehydes were isolated and fully characterised (figures 2.21-2.23, p. 241) and their structures were confirmed by literature information [90,93,95,109]. An unknown compound I was also isolated but the amount obtained was too small for a full characterisation. Its UV spectrum showed maximum wavelengths at 275, 310 and 350nm (figure 2.24.b, p. 249).

In addition to other products, ALD 1, 2 and 3 were also shown to be present in the extracts of LDPE processed with various concentrations of Toc (0.2, 1 and 10%) in a single screw extruder (180°C) (see figures 4.15, p. 426). Transformation products of Toc present in the extract of LDPE stabilised with 0.2% (ALD 1 and ALD 2) and 10% Toc (DHD, E, SPD, D and TRI, A, B, C), passes 4, were isolated and fully characterised (figures 2.26-2.30, p. 252) and their spectral characteristics were found to be identical with those of previously isolated dimers, trimers and aldehydes of Toc.

4.3.3 Mechanism of melt stabilisation of Toc during multiple extrusions with LDPE

The nature of the transformation products formed from Toc during multiple extrusions with LDPE in a single screw extruder (180°C) were identified by comparing their HPLC Rt and UV characteristics with those of previously isolated and characterised oxidation products of Toc. Figure 4.15, p. 425, shows that these are of dimeric (DHD, E and SPD, D), trimeric (TRI, A, B, C), aldehydic (ALD 1-4) and quinonoid (α -tocoquinone, TQ)

structures. The formation of these transformation products was found to be responsible for the loss of antioxidant during extrusions. In the light of their distribution as a function of initial Toc concentration in LDPE (see figures 4.16 to 4.19, p. 427) a mechanism for the antioxidant action of Toc as a melt stabiliser is proposed in scheme 4.5.

At the lower initial concentration of Toc (0.2%) the ratio of peroxy radicals to Toc is higher than at Toc concentrations of 1 and 10%. This leads to a higher extent of oxidation of Toc at lower concentrations, especially after multiple extrusions, as shown in figure 4.16.a. As an effective chain-breaking donor (CB-D) antioxidant (see section 1.4), Toc reacts with peroxy radicals ($\text{ROO} \bullet$) to give the tocopheroxyl radical ($\text{Toc} \bullet$) (reaction a) which isomerises to the corresponding benzyl radical Toc-benzyl I (reaction b). The latter can then react again with $\text{ROO} \bullet$ to give QM (reaction c) or couple with another Toc-benzyl I to form the DHD (reaction f). The formation of QM can lead to SPD, followed by TRI via two consecutive Diels-Alder type reactions (reactions d and e). After the first extrusion pass, the extent of loss of Toc is similar at all initial Toc concentrations (figure 4.16.a) and is accompanied by the formation of TRI in high concentrations (figure 4.17). The latter are the major transformation products at initial Toc concentrations of 0.2 and 10%. On the other hand, the formation of DHD is favoured at higher concentrations of Toc. Because of the higher ratio of $\text{ROO} \bullet$ to Toc-benzyl I at lower initial concentrations of the parent antioxidant (0.2%), the formation of QM (reaction c) is expected to be mainly responsible for the high concentration of TRI (reactions d and e). Furthermore, under the above conditions, the DHD is expected to react further with peroxy radicals by giving away its two phenolic hydrogens to form the SPD (reactions g and h) which leads to the formation of TRI by reaction with QM (reaction e). This explains the initial high concentrations of TRI and SPD compared to other products after the first extrusion pass in LDPE stabilised with 0.2% Toc and, the higher concentration of DHD present in LDPE stabilised 1 and 10% Toc (figure 4.17). In the latter case DHD is more likely to form because of the higher ratio of $\text{Toc} \bullet$ to $\text{ROO} \bullet$, hence it is less likely to react further with peroxy radicals. A similar effect was observed during the oxidation of Toc with PbO_2 ,

where the concentration of DHD decreased with increasing PbO₂ concentrations (figure 4.10, p. 341).

The high ratio of ROO • to Toc and its transformation products at the lower initial concentration of Toc (0.2%) leads to a fast increase in the concentration of TRI and decrease in SPD concentration with extrusion severity (figures 4.16.c, d and 4.19.a). The latter can oxidise to TRI (reaction e) in the presence of QM. The DHD is a minor product under the above conditions and shows a low increase in its concentration with extrusion severity (figure 4.16.b and 4.19.a). On the other hand, at higher concentrations of Toc, the increase of the concentration of DHD (major products after the first extrusion pass) with extrusion severity is more pronounced, especially at a concentration of 10% Toc (figures 4.16.b and 4.19.c, e). Furthermore the concentration of SPD increases with extrusion severity, suggesting low levels of QM under these conditions (figure 4.16.c).

At the higher Toc concentrations the contribution of ALD 1-4 to the total products is very small whereas the aldehydes are present in relatively high concentrations at the lower concentration of 0.2% Toc (figures 4.16.e and 4.19.a, c, e). Furthermore the increase in ALD concentration with extrusion severity is much faster at lower concentrations of Toc. This is caused by the higher ratio of oxygen to Toc • at lower concentrations of the antioxidant., as ALD 1, 2 and 3 are formed via further oxidation of the benzyl radicals I and II with oxygen (reactions j, k and m, respectively). Toc benzyl II does not lead to the formation of dimers and trimers which is probably caused by steric hindrance from the *meta* aromatic methyl group. ALD 1 is a major aldehyde at all concentrations of Toc (figures 4.19.b, d, f). The formation of TQ is also favoured at lower initial levels of Toc (figures 4.16.f and 4.19.a, c, e) which is caused by the higher ratio of peroxy radicals to Toc. TQ has been suggested [111] to be formed via the Toc radical III by the attack of peroxy radicals (reaction p), followed by hydrolysis (reaction q) which causes the opening of the chroman ring.

ALD 1 and TQ were shown to impart lower melt stability, i.e. lower MFI, to PP than Toc, whereas DHD, SPD and TRI showed better or similar melt stabilising activity compared to

Toc (figure 3.5, p. 313). However, although the concentrations of ALD and TQ are higher at lower concentrations of Toc, the melt stabilising activity of Toc in LDPE was found to be higher at the lower initial concentration of 0.2% (figure 3.1, p. 265). This suggests that only low levels of Toc are required for a good melt stabilisation activity in LDPE. However, processing of PP with 0.2% of each of the products ALD 1 and SPD resulted in severe discolouration of the polymer samples (table 3.7, 291). Hence, ALD 1 and SPD are probably also responsible for the discolouration of LDPE (see table 3.2, p. 286).

4.3.4 Mechanism of melt stabilisation of Toc during processing with PP in an internal mixer

4.3.4.1 Effect of processing severity and oxygen concentration on the nature of the transformation products

The effect of processing severity in an internal mixer on the nature of the products formed from Toc in PP was examined by varying the processing time, and the oxygen concentration in the mixing chamber was changed by processing the samples in a closed mixer with prior nitrogen flushing (CM/N₂), closed mixer (CM) or open mixer (OM). The products were identified by comparing their HPLC Rt and UV characteristics with those of known oxidation products of Toc. Figures 4.22 and 4.23, p. 432, show that these are of dimeric (DHD, E, SPD, D), trimeric (TRI, A, B, C), aldehydic (ALD 1-5) and quinonoid (TQ) structures, like in LDPE. The formation of these products was also found to cause the loss of Toc. Figures 4.25 to 4.28, p. 435, show that the nature and concentration of the products depend on the processing conditions. The extent of oxidation of Toc increases with increasing oxygen concentrations and processing severity (figure 4.25.a). However the concentration of unchanged antioxidant remains high ($\geq 82\%$) in all cases, even after 30min processing.

The distribution of the transformation products of Toc is highly affected by the amount of O₂ in the mixer. Initially, after 5min processing TRI are formed in high concentrations in all cases and are the major products in the samples processed under restricted O₂ access

(CM/N₂ and CM) (figure 4.26.a-b). On the other hand, the formation of DHD and ALD 1-5 is favoured in the presence of high concentrations of O₂. Oxygen reacts with alkyl radicals to form peroxy radicals (ROO •), leading to a higher concentration of Toc • (reaction a in scheme 4.5) in an OM. The latter can isomerise to Toc-benzyl I and II (reactions b and l). Toc-benzyl I can lead to the formation of DHD (reaction f) or react with O₂ to yield ALD 1 and 2 (reactions j and k), and Toc-benzyl II can react with O₂ to form ALD 3 (reaction m). This explains the initial high concentrations of DHD and ALD 1-5 in an OM. Alternatively, Toc-benzyl I can be further oxidised to QM (reaction c) leading to the formation of TRI via SPD (reactions d and e). QM is more likely to form at lower ROO • concentrations as less Toc-benzyl I are available to form DHD, justifying the initial higher concentrations of TRI compared to other products under CM/N₂ and CM conditions.

Under restricted O₂ access (CM/N₂), an increase in TRI concentration with processing severity is accompanied by a decrease in SPD concentration (figure 4.28.a) confirming that the latter is oxidised to TRI via QM (reaction e). In a CM, at very low processing times (2.5-5min), a decrease in TRI concentration is accompanied by an increase in SPD concentration (figure 4.28.c), suggesting that the TRI can be reduced back to SPD (reaction e'). However, after 5min processing, as it is the case with a CM/N₂, an increase in TRI and decrease in SPD concentrations with increasing processing time is observed. Furthermore, under both CM/N₂ and CM conditions, the concentration of DHD remains more or less constant or increases with processing severity. On the other hand, the higher concentrations of peroxy radicals in an OM lead to a decrease in the DHD concentration (figure 4.28.e) which is caused by its oxidation to TRI via SPD (reactions g, h and e). A similar effect was observed during the oxidation of Toc with PbO₂ (figure 4.10, p. 351). An increase in PbO₂ concentration (equivalent to an increase in ROO •) lead to a decrease in DHD concentration which was accompanied by an increase in SPD concentration when the concentration of PbO₂ was high enough. However, because of the lower concentration of QM at high PbO₂ concentration the latter did not oxidise to TRI.

The major difference between the products formed in a CM/N₂, CM or OM is the much higher concentration of ALD 1-5 (mainly ALD 1, 2 and 3, see figures 4.28.b, d, f) in an OM (figures 4.25.e and 4.27). The latter become the major products after 10min processing (figure 4.28.e) and are mainly responsible for the higher loss of Toc under these conditions (figure 4.27). Although their overall concentration remains low ($\geq 10\%$), they are most certainly responsible for the decrease in melt stability, i.e. increase in MFI, of the polymer (see figure 3.3.b, p. 312) with processing severity (ALD 1 has lower melt stabilisation activity than Toc, see figure 3.5, p. 313). In LDPE stabilised with 0.2% Toc, it was found that the high concentration of ALD 1-4 after multiple extrusions (over 20% after the fourth pass, see figure 4.19.a, p. 429) did not lead to large changes in the MFI of the polymer. This suggests that lower concentrations of Toc are necessary in LDPE compared to PP for a good melt stabilisation. This is probably caused by the much faster degradation of PP compared to LDPE under normal processing conditions as the former is more prone to attack by peroxy radicals [16,17,22].

The major difference between the products in extruded LDPE and processed PP, both stabilised with 0.2% Toc, was the extent of oxidation of Toc with processing severity (much higher in LDPE, see figures 4.16.a and 4.24.a) and the higher ratios of TQ compared to other products in LDPE, especially after multiple extrusions (figures 4.19.a and 4.27.a, c, e), suggesting the formation of higher concentrations of peroxy radicals during extrusions. When leaving the extruder, the hot polymer is exposed to air which can lead to further degradation. On the other hand, after processing in an internal mixer the polymer samples are quickly quenched in cold water to avoid further thermal oxidation. However, although lower concentrations of products are obtained in PP, their distribution under CM/N₂ and CM conditions is similar to that obtained in LDPE (apart from TQ), indicating similar stabilisation mechanisms (see figures 4.19.a and 4.28.a, c). Like in LDPE, discolouration of the polymer samples increases with processing severity (see table 3.4, p. 341). This is mainly caused by the increase in ALD 1 concentration as the latter was found to lead to high discolouration in PP (see table 3.7, p. 291).

4.3.4.2 Effect of initial Toc concentration on the nature of the transformation products

The products formed in PP stabilised with various concentrations of Toc (0.01-0.2%) in an internal mixer (CM, 10min, 200°C) were identified and were also found to be of dimeric (DHD, E and SPD, D), trimeric (TRI, A, B, C), aldehydic (ALD 1-4) and quinonoid (TQ) structures (see figure 4.29, p. 438). The formation of these products was found to account for the loss of Toc. The initial Toc concentration in PP was found to have a dramatic effect on the concentration of unchanged antioxidant and the distribution of the transformation products (figures 4.30 and 4.31, p. 392). Toc was highly retained at concentrations of 0.02% and above ($\geq 75\%$), whereas at the lower concentration of 0.01% only 27% Toc was retained (figure 4.30.a). This is caused by the higher ratio of ROO • to Toc at lower antioxidant concentrations, leading to a higher extent of oxidation of the antioxidant. TRI are the major transformation products at all initial concentrations (figures 4.30.b and 4.31.a, c, e, g, i). Like in LDPE stabilised with 0.2, 1 and 10% Toc (figure 4.17, p. 428), the DHD is favoured at higher concentrations of Toc (reactions **b** and **f** in scheme 4.5) because of the higher Toc • to ROO • ratios and ALD 1-4 are preferably formed at lower Toc concentrations (reactions **b**, **i**, **j**, **k** and **l**, **m**, **n**) as the ratio of O₂ to Toc • is higher. ALD 1 was the major aldehyde in all cases (figures 4.31.b, d, f, h and j). Like in PP stabilised with 0.2% Toc in an OM (CM, 200°C) (figures 4.28.e-f, p. 437), ALD 1 is present in high concentrations (16%) in PP stabilised with 0.01% Toc (figures 4.31.a-b) and is responsible for the sharp decrease in melt stability (i.e. increase in MFI) of the polymer (figure 3.4, p. 312).

4.3.4.3 Antioxidant activity of Toc derivatives

The products formed in PP stabilised with 0.2% of each of the Toc derivatives DHD, SPD and TRI in an internal mixer (CM, 10min, 200°C) were identified to examine their antioxidant activity and for a better understanding of the melt stabilisation mechanism of Toc in polyolefins. Figures 4.32 and 4.33, p. 441, show the nature and concentration of the products formed. It is clear that DHD, which is a better melt stabiliser than Toc (figure 3.5,

p. 313) is highly retained during processing with PP (figure 4.33.a). Transformation products mainly include SPD, TRI and ALD 1 and smaller concentrations of Toc. The SPD is formed via the reaction of ROO • with DHD (reactions g and h in scheme 4.5). The formation of TRI from SPD requires the presence of QM (reaction e). This suggests that SPD can be reduced back to QM during processing (reaction d'). This was confirmed by the formation of high concentrations of TRI in PP stabilised with SPD (figure 4.33.b). The high concentration of DHD formed in PP stabilised with SPD indicates that SPD can be reduced back to DHD with alkyl radicals, leading to unsaturation in the polymer (reaction g'). The formation of ALD 1 and 2 from each Toc derivatives requires the initial presence of Toc-benzyl I (reactions i, j and k) which can be formed from QM and Toc (reaction c'). Toc itself is suggested to be formed from the reduction of QM with DHD (reaction r). The TRI can also be reduced back to SPD, as shown in figure 2.33.c. ALD 1 and TQ did not undergo any transformations during processing with PP.

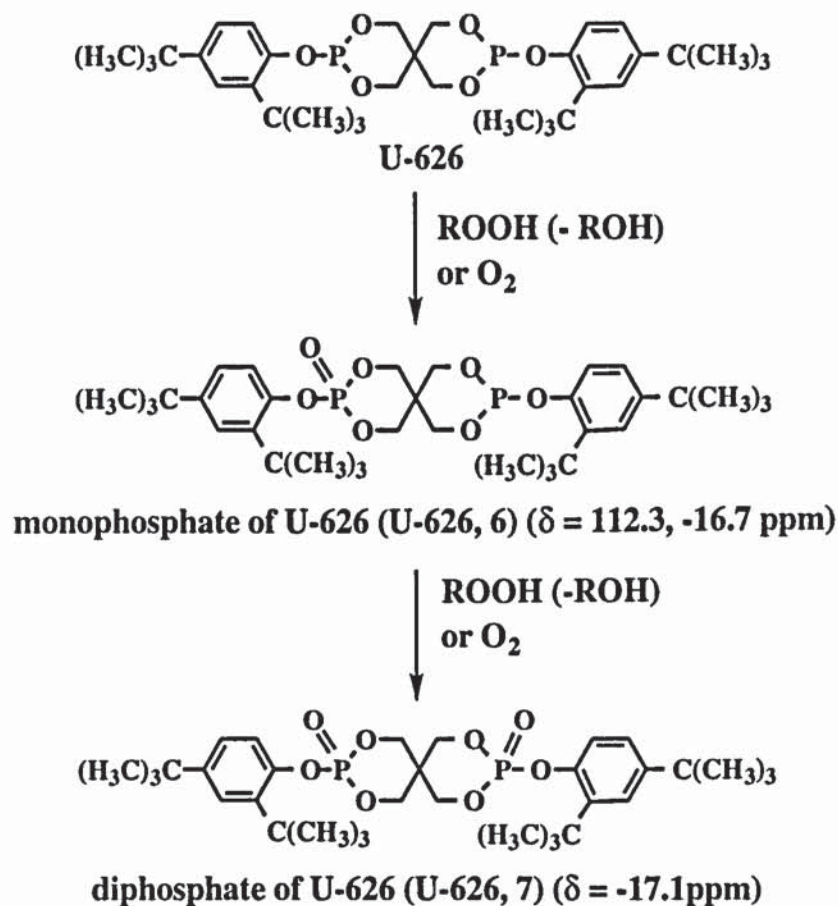
The similar melt stabilisation activity of SPD and TRI compared to Toc (figure 3.5, p. 313) can be explained as a function of DHD concentration formed during processing, as the latter is a better melt stabiliser than Toc.

4.3.5 Effect of hindered aryl phosphite U-626 on the antioxidant activity of Toc during processing with PP in an internal mixer

Organic phosphites like U-626 are used in combination with hindered phenols to prevent discolouration of the polymer caused by transformation products of the phenol (e.g. quinonoid structures, see section 1.3.3). Transformation products of Toc (e.g. ALD 1, SPD) have also shown to be responsible for the discolouration of PP (see table 3.7, p. 291). It was reported [8] that the optimum ratio of Toc to U-626 in the melt stabilisation of HDPE and PP was 1:4 and 1:2, respectively. In this work, it was shown that combinations of 0.2% Toc + 0.4% U-626 and 0.05% Toc + 0.1% U-626 in PP improved the melt and colour stability of the polymer (figure 3.6, p. 313).

The nature of the products formed from Toc and U-626 in PP stabilised with the above combinations as well as U-626 only and with combinations of U-626 and each of the Toc derivatives SPD and TRI in an internal mixer (CM, 10min, 200°C) were examined. ³¹P-NMR analysis of the polymer extracts has shown (figure 4.35, p. 443) that transformation products of U-626 include the mono and diphosphate of U-626, according to their chemical shifts ((112.3, -16.7)ppm and -17.1ppm, respectively) [58,59] The latter are mainly formed as a consequence of the antioxidant action of U-626 as a peroxidolytic (PD-S) antioxidant, i.e. hydroperoxide decomposition (see section 1.3.3) (see scheme 1.5, p. 46) and/or from the reaction of U-626 with O₂ [56,59], as shown in scheme 4.6. The antioxidant activity of U-626 was found to be highest (presence of both mono and diphosphate of U-626) in PP stabilised with combinations of U-626 and each of the Toc derivatives SPD and TRI (figures 4.35.e-f, p. 443, and table 4.25, p. 381) which is probably caused by the lower antioxidant activity of the latter compared to Toc in PP. In PP stabilised with mixtures of Toc and U-626 and U-626 on its own, only the monophosphate (112.3, -16.7ppm) was formed (figures 4.35.c-d and table 4.25) and its concentration was higher when used at lower concentrations (0.1%), which is most certainly caused by the higher ratios of O₂ and ROO• to U-626. During HPLC analysis, U-626 decomposed to products with lower Rt (figures 4.36, p. 444). However, the mono

and diphosphate of U-626 (U-626, 6 and 7, respectively, see figures 4.36.c, e, g) were stable and their UV characteristics and peak areas could be determined at 280nm (table 4.24). The peak areas were more or less in accordance with the ^{31}P -NMR peak intensities (table 4.25).



Scheme 4.6: Mechanism of melt stabilisation of U-626 in PP

The presence of U-626 in PP stabilised with Toc lead to higher retentions of Toc compared to PP stabilised with Toc only (figure 4.37.a) which is caused by the PD-S antioxidant activity and O_2 scavenging ability of U-626. Like in PP stabilised with Toc only, transformation products of Toc in the presence of U-626 are of dimeric (SPD, D), trimeric (TRI, A, B, C), aldehydic (ALD 1, 2 and 4) and quinonoid (TQ) structures, with TRI being present in high concentrations (figures 4.36.c-d and 4.37.b-c), suggesting that the melt stabilisation mechanism of Toc in combination with U-626 is similar to that of Toc when used on its own (see scheme 4.5). In PP stabilised with mixtures of U-626 and each of the Toc derivatives SPD and TRI (figures 4.36.e-h and 4.37.d-e), the presence of the phosphite

lead to slightly higher concentrations of DHD which is also an effective melt stabiliser (figures 3.5, p. 313).

Unlike in PP stabilised with commercial antioxidants (e.g. BHT) [50] there is no interaction between Toc transformation products and the phosphite leading to colourless products (see reactions 1.35, 1.36 and 1.37, p. 59). The formation of lower concentrations of transformation products in PP stabilised with combinations of Toc and U-626, compared to PP stabilised with Toc only, are responsible for the improved colour stability and, at least in part, the improved melt stability of the polymer. But PP stabilised with mixtures of U-626 with each SPD and TRI only showed a slight improvement of the colour stability because the products responsible for discolouration are still present in relatively high concentrations.

4.3.6 Mechanism of melt stabilisation of Irg 1076 during multiple extrusions with LDPE

4.3.6.1 Isolation and characterisation of transformation products of Irg 1076

Two major transformation products of Irg 1076 have been isolated from LDPE stabilised with 10% Irg 1076, pass 4 (single screw extruder, 180°C) and characterised (see figure 4.47.g-h, p. 448, for HPLC chromatograms and figures 2.33 and 2.34, p. 267, for characterisation). They were found to be the cinnamate of Irg 1076, C-Irg 1076, and the biscinnamate of Irg 1076, BC-Irg 1076 (see figures 4.40 and 4.41, p. 387 and 388, respectively, and scheme 4.7 for structures) and their structures were confirmed by literature information [20,45,48]. The transformation products with lower HPLC Rt than Irg 1076 (Irg 1076-1 to -10) showed similar UV characteristics to Irg 1076 (see table 4.27, p. 384) suggesting intact phenolic groups without further conjugation, i.e. derivatives of 2,6-di-*t*-butylphenol (see figures 4.38 and 4.39, p. 386). Three other compounds, Irg 1076-11, -13 and -14, revealed UV characteristics which correspond to cinnamate or quinonoid structures ($\lambda_{\text{max}} > 300\text{nm}$, figure 2.35, p. 270). According to their HPLC Rt and UV characteristics [20] it was suggested that compounds 11 and 14 could be the quinone

methide, QM-Irg 1076, and the conjugated bisquinone methide, CBQM-Irg 1076, of Irg 1076, respectively (see figures 4.42, p. 388). However, their structures remained uncertain. Cinnamate and quinonoid structures of Irg 1076 were also found to be formed during the oxidation of Irg 1076 with $K_3Fe(CN)_6$ [45,46,20] and during processing of Irg 1076 with PP in a Brabender plastograph for 2h at 200°C [51], as well as during thermal ageing at 180°C of HDPE containing Irg 1076 [50]. Based on the isolated products, a mechanism of oxidation of propionate-type phenolic antioxidants was proposed [4,50] (see scheme 1.7, p. 50).

4.3.6.2 Effect of initial Irg 1076 concentration and extrusion severity on the nature of the transformation products

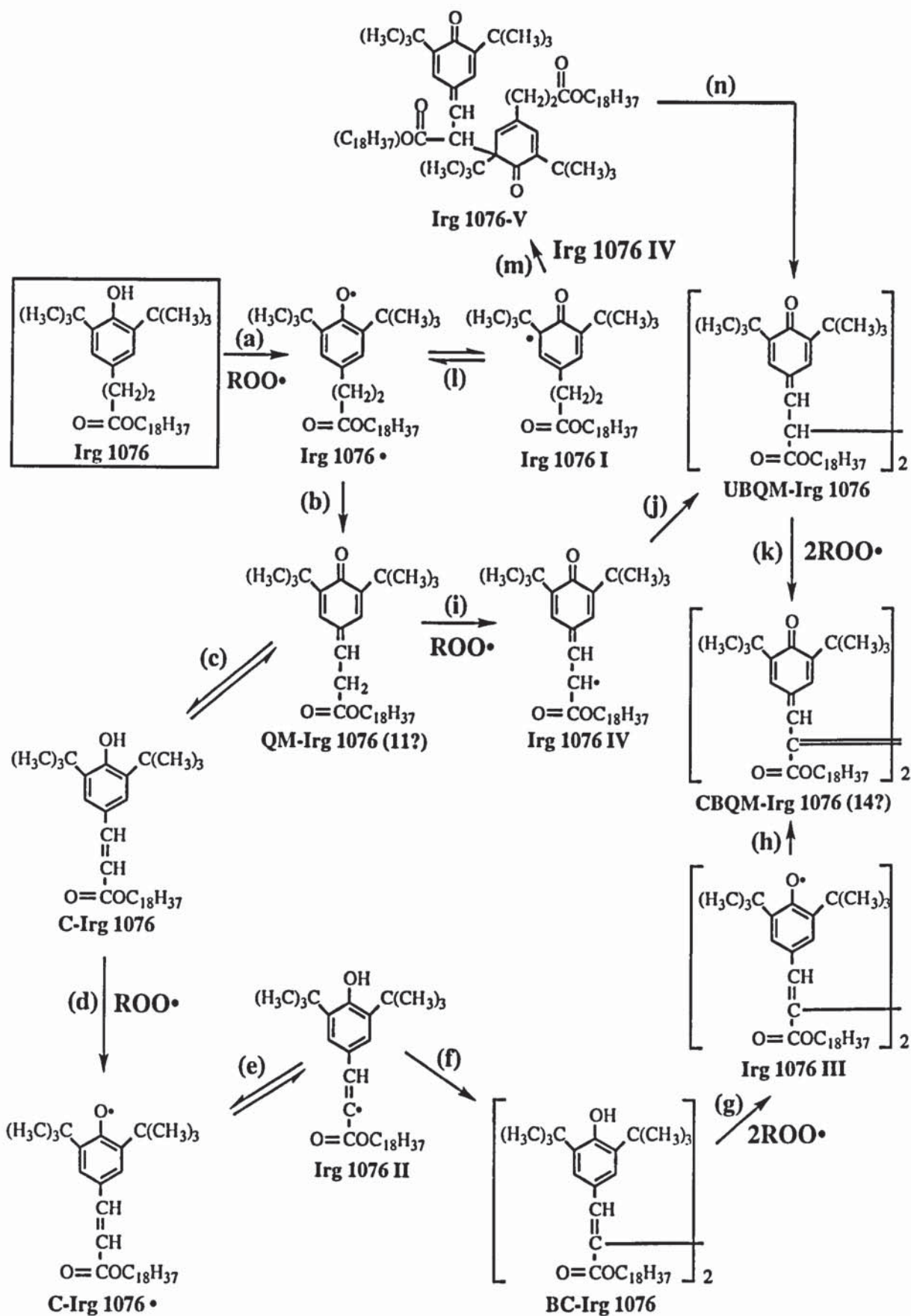
The nature of the products formed from Irg 1076 during multiple extrusions in LDPE in a single screw extruder (180°C) (see figures 4.47, p. 447, for HPLC chromatograms) were identified by comparing their HPLC Rt and UV characteristics (see table 4.27, p. 384) with those of the products isolated and extracted from LDPE stabilised with 10% Irg 1076, pass 4. Although their concentrations could not be determined because of the number of unidentified products, peak areas for Irg 1076 and its products could be calculated at 282nm (figures 4.48 and 4.49, p. 449). Furthermore, the concentrations of two major transformation products, C-Irg 1076 and BC-Irg 1076, relative to Irg 1076 could be determined (figure 4.48.e-g). Like in LDPE stabilised with Toc (figure 4.16.a, p. 427), at the lower initial concentration of Irg 1076 (0.2%), the higher ratio of $ROO \cdot$ to the antioxidant leads to a higher extent of oxidation of Irg 1076, especially after multiple extrusions (figure 4.48.a). Consequently, the peak areas of all the transformation products of Irg 1076 are higher at the lower concentration (figure 4.48.b-d).

Based on the nature of the transformation products of Irg 1076 formed and suggested to be formed, a mechanism of melt stabilisation of Irg 1076 in LDPE is proposed in scheme 4.7. Irg 1076, which is a well known commercial antioxidant, acts as CB-D antioxidant (see section 1.3.2) to give the corresponding phenoxyl radical, Irg 1076 \cdot (see reaction a in

scheme 4.7). The latter leads to the formation of QM-Irg 1076 (reaction b) which can isomerise to the more stable C-Irg 1076 (reaction c). Figure 4.49 shows that C-Irg 1076 is a major transformation product at all initial antioxidant concentrations and its peak area at 282nm increases with extrusion severity. The latter can also act as a chain-breaking antioxidant to form C-Irg 1076 • (reaction d) which isomerises to the corresponding benzyl radical, Irg 1076 II (reaction e) resulting in the formation of BC-Irg 1076 (reaction f). The concentration of the latter, which is only formed in very small amounts in all the extracts (figures 4.48.c and 4.48.e-g), increases with extrusion severity which is caused by the increase of ROO •. The BC-Irg 1076 itself can also act as a chain-breaking antioxidant by giving away its two phenolic hydrogens to form Irg 1076 III (reaction g) which gives the CBQM-Irg 1076 (reaction h). Alternatively, the latter can be formed from the oxidation of UCBM-Irg 1076 (reaction k). UBQM-Irg 1076 itself can be formed from the quinone methide radical Irg 1076 IV (reaction j) obtained from further oxidation of QM-Irg 1076 (reaction i). Dimer Irg 1076 V was also shown [45] to be an intermediate in the formation of UBQM-Irg 1076 during the oxidation of Irg 1076 with K₃Fe(CN)₆. Irg 1076 V is formed via radical coupling of Irg 1076 I (isomer of Irg 1076 •, reaction l) and Irg 1076 IV (reaction m). It was suggested that Irg 1076-11 and Irg 1076-14 could be the QM- and CBQM-Irg 1076, respectively, according to their UV characteristics (see table 4.27, p. 384). Irg 1076-11 can only be observed at the lower initial concentration of the antioxidant (0.2%) (figure 4.49.a) suggesting that it is less stable than C-Irg 1076. Irg 1076-14, on the other hand, is present in small amounts in all the polymer extracts and its peak area increases with extrusion severity (figure 4.49). Irg 1076 transformation products 2-10, which were suggested to be derivatives of 2,6-di-*t*-butyl-phenol, show large total peak areas in all the extracts (figure 4.48.d and 4.49), and are likely to act themselves as chain-breaking antioxidants.

Although Irg 1076 is more highly retained than Toc in LDPE, especially after multiple extrusions and lower concentrations (figures 4.16.a, p. 427, and 4.48.a), the latter is a better melt stabiliser than Irg 1076 (figure 3.2, p. 311), indicating that lower concentrations of Toc compared to Irg 1076 are required for a good melt stabilisation in LDPE. Irg 1076

was found to have the best melt stabilisation efficiency at the initial concentration of 1% (figure 3.2.b) which is probably caused by its lower extent of oxidation under these conditions (figure 4.48.a). The discolouration of the polymer samples (table 3.2, p. 286), especially after multiple extrusions, is suggested to be caused mainly by the formation of C-Irg 1076 (yellow solid) which is a major transformation product. Quinonoid (e.g. CBQM-, UBQM-Irg 1076) and cinnamate structures of Irg 1076 (e.g. BC-Irg 1076) have shown ^[20] to induce discolouration of PP and PE.



Scheme 4.7: Suggested mechanism of melt stabilisation of Irg 1076 in LDPE

4.3.7 Mechanism of melt stabilisation of Irg 1010 during multiple extrusions with LDPE

4.3.7.1 Isolation and characterisation of transformation products of Irg 1010

Two major transformation products of Irg 1010, Irg 1010-6 and Irg 1010-3 (see figures 4.43 and 4.44, p. 390, respectively, and scheme 4.8 for structures), have been isolated from LDPE stabilised with 10% Irg 1010, pass 4 (single screw extruder, 180°C) and characterised (see figure 4.50.g-h, p. 452, for HPLC chromatograms and figures 2.37 and 2.38, p. 272, for characterisation). Their structures were confirmed by literature information [47,49]. Irg 1010-3 was also shown [47] to be formed during processing of Irg 1010 with PE and PP by MS analysis. Irg 1010 transformation products 1, 2, 5 and 7-13 showed similar UV characteristics to Irg 1010 (see table 4.28, p. 385) and were suggested to contain 1 (Irg 1010-1, -2), between 1 and 3 (Irg 1010-5) and at least 3 (Irg 1010-7 to -13) Irg 1010 sub-units without further conjugation (see figure 4.45, p. 391, for structures). Two other compounds, Irg 1076-4 and -14, revealed maximum wavelengths above 300nm (figure 2.39, p. 276) and were suggested to contain cinnamate and quinonoid structures, respectively (see figure 4.46, p. 392, for structures).

4.3.7.2 Effect of initial Irg 1010 concentration and extrusion severity on the nature of the transformation products

The nature of the products formed from Irg 1010 during multiple extrusions in LDPE in a single screw extruder (180°C) (see figures 4.50, p. 451, for HPLC chromatograms) were identified by comparing their HPLC Rt and UV characteristics (see table 4.28, p. 385) with those of the products isolated and extracted from LDPE stabilised with 10% Irg 1010, pass 4. The concentrations could not be determined because of the number of unidentified products. However, peak areas for Irg 1010 and its products could be calculated at 282nm (figures 4.51 and 4.52, p. 453). Like in LDPE stabilised with Toc and Irg 1076 (figures 4.16.a, p. 427, and 4.48.a, p. 449, respectively), the extent of oxidation of Irg 1010 is highest at the lower initial concentration of Irg 1010 (0.2%), especially after multiple

extrusions (figure 4.51.a) which is caused by the higher ratio of ROO • to the antioxidant. This leads to larger peak areas of the transformation products of Irg 1010 at the lower concentration (figure 4.51.b-f).

A mechanism of melt stabilisation of Irg 1010 in LDPE is proposed in scheme 4.8, according to the nature of the transformation products of Irg 1010 formed and suggested to be formed. Irg 1010 is a widely used commercial CB-D antioxidant. Because Irg 1010 contains 4 phenolic groups (compared to 1 in Irg 1076) it can react 4 times with peroxy radicals by donating its phenolic hydrogens to give Irg 1010 • ($1 \leq n \leq 4$) (reaction a in scheme 4.8). Irg 1010 • leads to the formation of QM-Irg 1010 (possibly Irg 1010-14) which contains between 1 and 4 oxidised Irg 1010 sub-units (reaction b) and the latter can isomerise to the corresponding C-Irg 1010 (reaction c). Irg 1010-14 and Irg 1010-4 (contains cinnamate structures) were present in relatively small amounts in all the extracts (figure 4.51.e-f and 4.52). Irg 1010-4 is suggested to be formed from C-Irg 1010 and, possibly, cleavage of some of the Irg 1010 sub-units (reactions c and d). The major reactions seem to be thermal cleavage of Irg 1010 sub-units (reactions d-g). Irg 1010-3 and Irg 1010-6, which are major transformation products in all the extracts, contain one and three Irg 1010 sub-units, respectively, and are suggested to be formed via reactions f and g, respectively. Irg 1010-1, -2, -5 and -7 to -13 which contain phenolic groups without further conjugation are also suggested to be formed from the cleavage of Irg 1010 sub-units and/or loss of *tert*-butyl groups (e.g. Irg 1010 I, II). Most of the transformation products of Irg 1010 are expected to be themselves CB-D antioxidants as they contain phenolic groups.

Irg 1010 is more highly retained than Irg 1076 and Toc (figures 4.16.a, p. 427, 4.48.a, p. 449, and 4.51.a). However, like Irg 1076, Irg 1010 has a lower melt stabilisation activity than Toc (figure 3.2, p. 311) and the melt stabilisation efficiencies of Irg 1010 and Irg 1076 are similar at the lower concentrations of 0.2 and 1% (figure 3.2.b). Furthermore, like Irg 1076, Irg 1010 was found to impart the best melt stability at its initial concentration of 1%, which could be due to its higher retention under these conditions (figure 4.51.a). The discolouration of the polymer samples stabilised with Irg 1010 also increases with

extrusion severity and is suggested to be caused by the formation of quinonoid and cinnamate structures (e.g. Irg 1010-4 and -14).

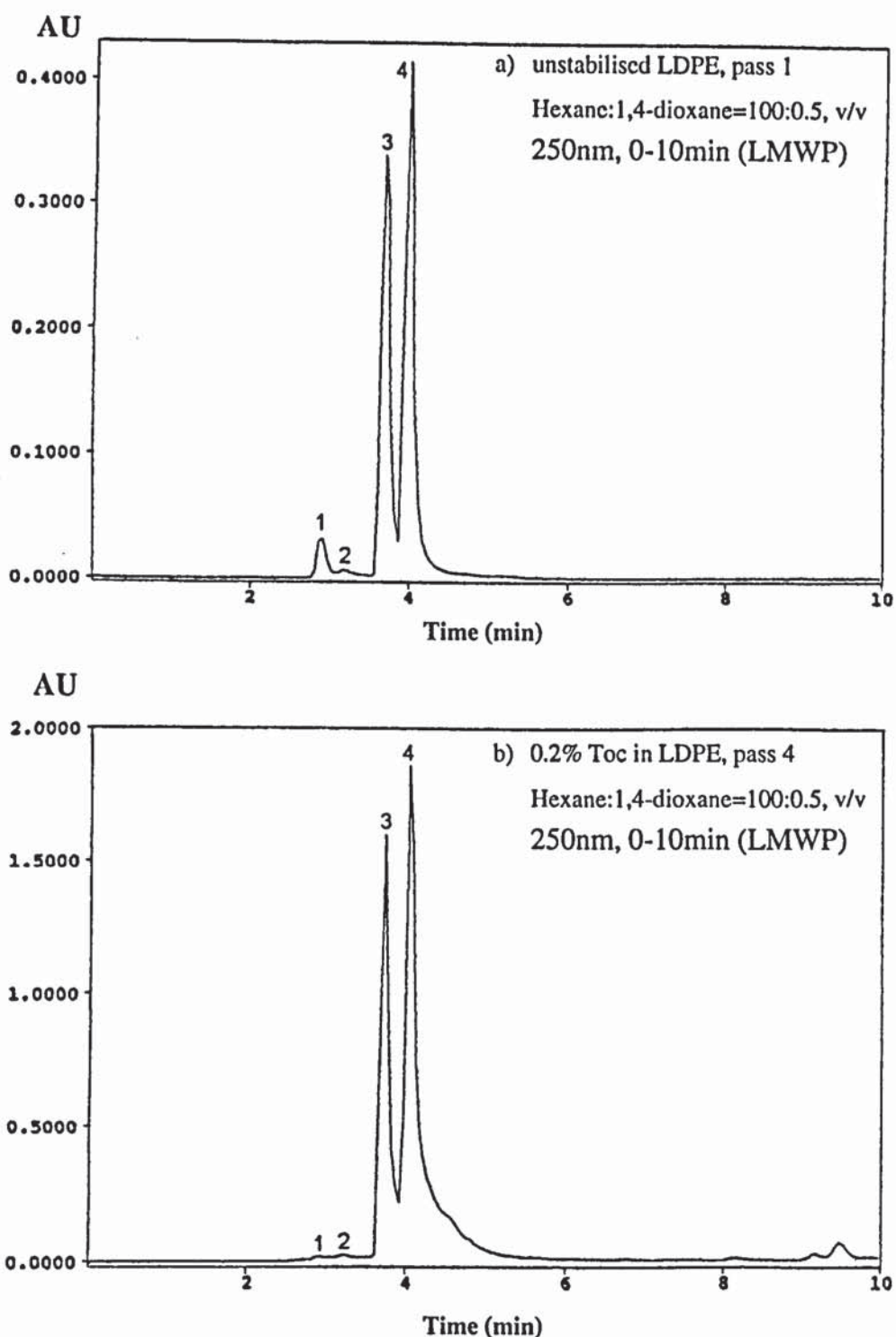


Figure 4.14: HPLC analysis of the extracts of unstabilised LDPE, pass 1 (a) and LDPE (a-b) stabilised with 0.2% Toc, pass 4 (b) (single screw extruder, 180°C), in hexane at 250nm, expanded region 0-10min (LMWP) (see section 4.2.3.2, p. 358)

Instrument: Philips PU4100 liquid chromatograph and PU4120 diode array detector; Column: Zorbax SIL (4.6mm x 25cm); Flow rate: 1ml.min⁻¹
Eluent: hexane:1,4-dioxane = 100:0.5, v/v

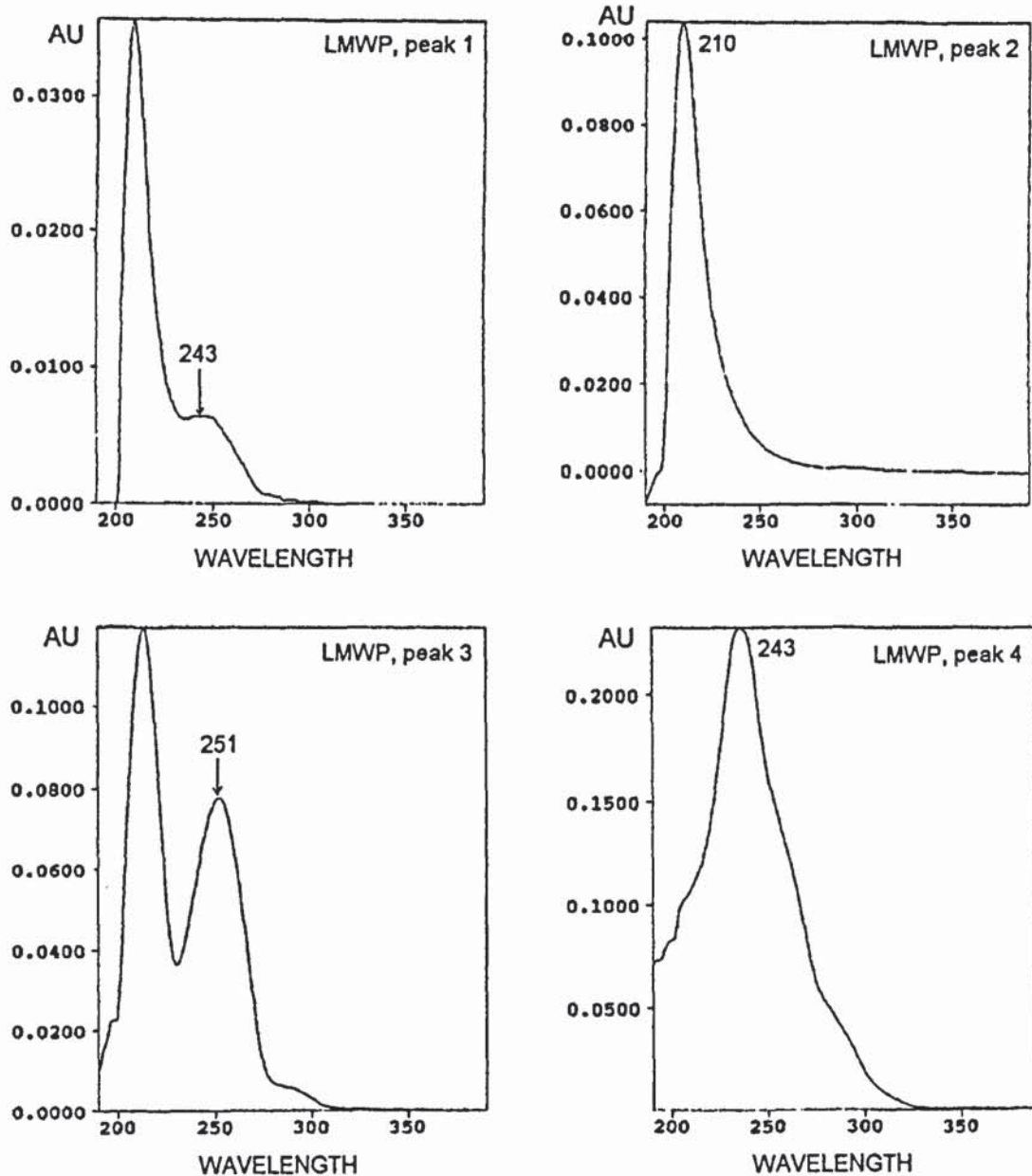


Figure 4.14.c: Diode array UV analysis of the extract of unstabilised LDPE, pass 1 (single screw extruder, 180°C), in hexane
 (see section 4.2.3.2, p. 358 and table 4.11, p. 360)
 Instrument: PU4120 diode array detector

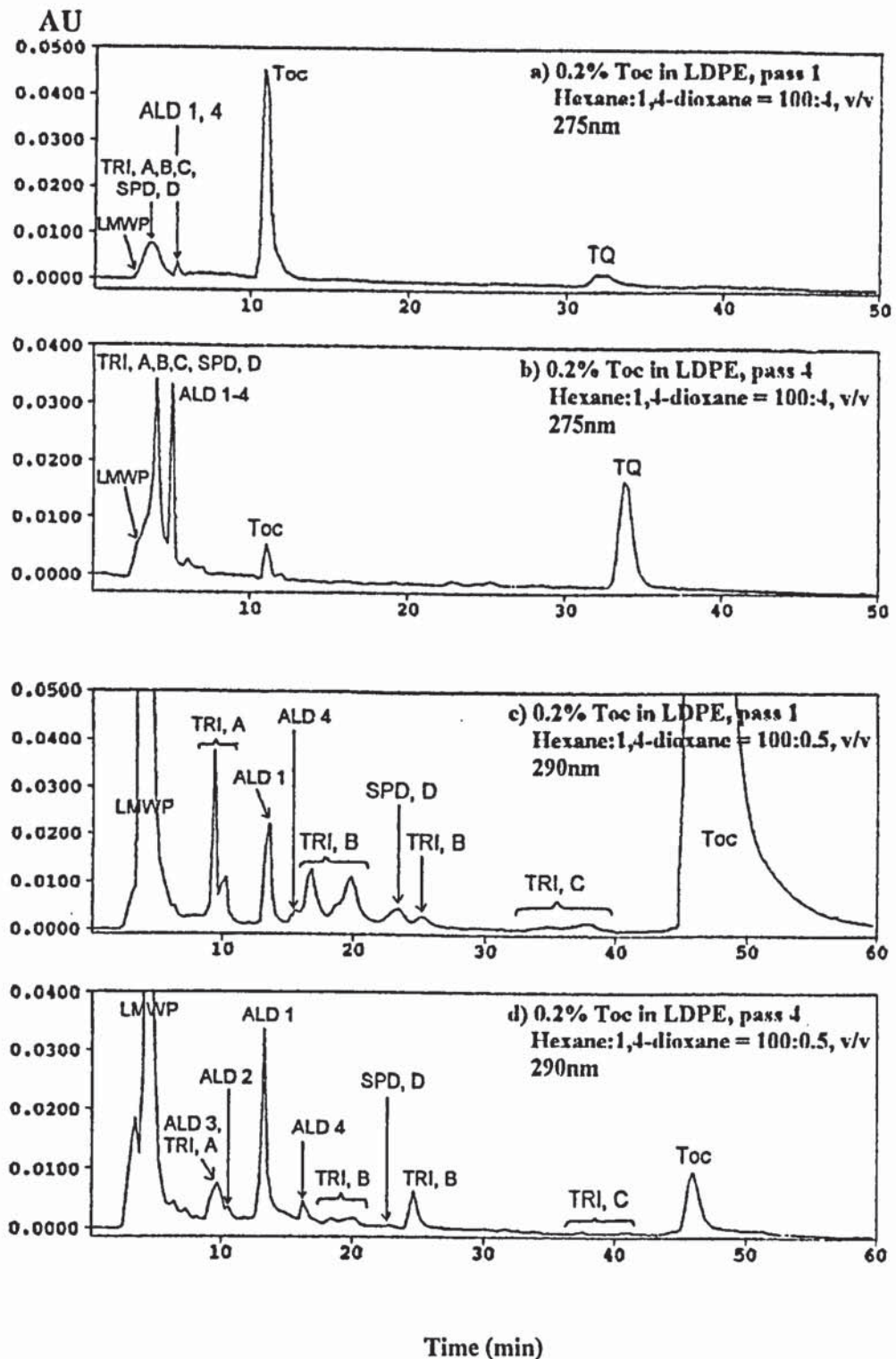


Figure 4.15: HPLC analysis of the extract of LDPE stabilised with 0.2% Toc, passes 1 (a, (a-d) c) and 4 (b, d) (single screw extruder, 180°C), in hexane (see section 4.2.3.4, p. 364, and table 4.11, p. 360)
 Instrument: Philips PU4100 liquid chromatograph and PU4120 diode array detector; Column: Zorbax SIL (4.6mm x 25cm); Flow rate: 1ml.min⁻¹
 Eluents: hexane:1,4-dioxane = 100:4 (a, b) and 100:0.5, v/v (b, d)

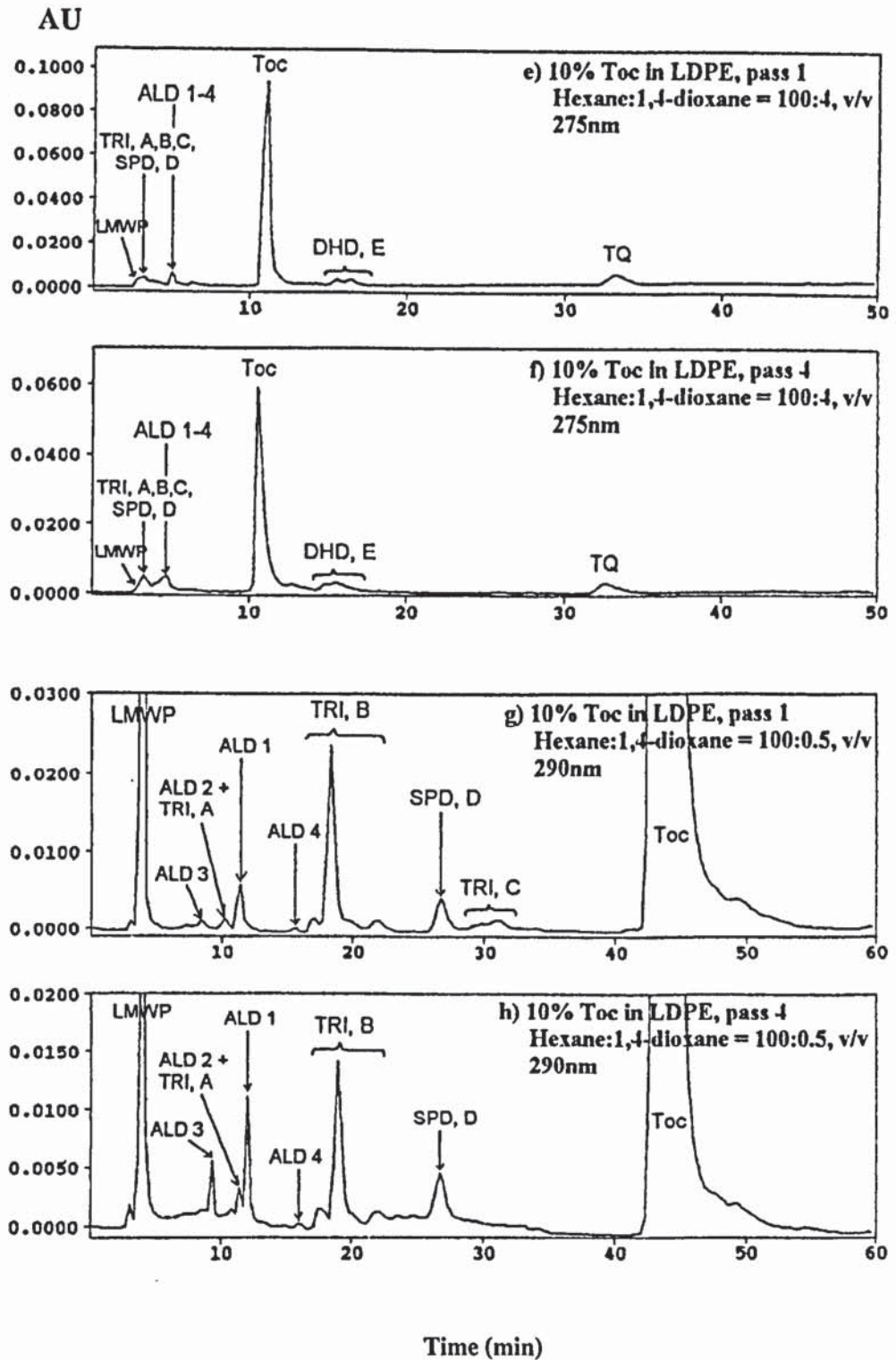


Figure 4.15: HPLC analysis of the extract of LDPE stabilised with 10% Toc, passes 1 (e, (e-h) g) and 4 (f, h) (single screw extruder, 180°C), in hexane (see section 4.2.3.4, p. 364, and table 4.11, p. 360)
 Instrument: Philips PU4100 liquid chromatograph and PU4120 diode array detector; Column: Zorbax SIL (4.6mm x 25cm); Flow rate: 1ml.min⁻¹
 Eluents: hexane:1,4-dioxane = 100:4 (e, f) and 100:0.5, v/v (g, h)

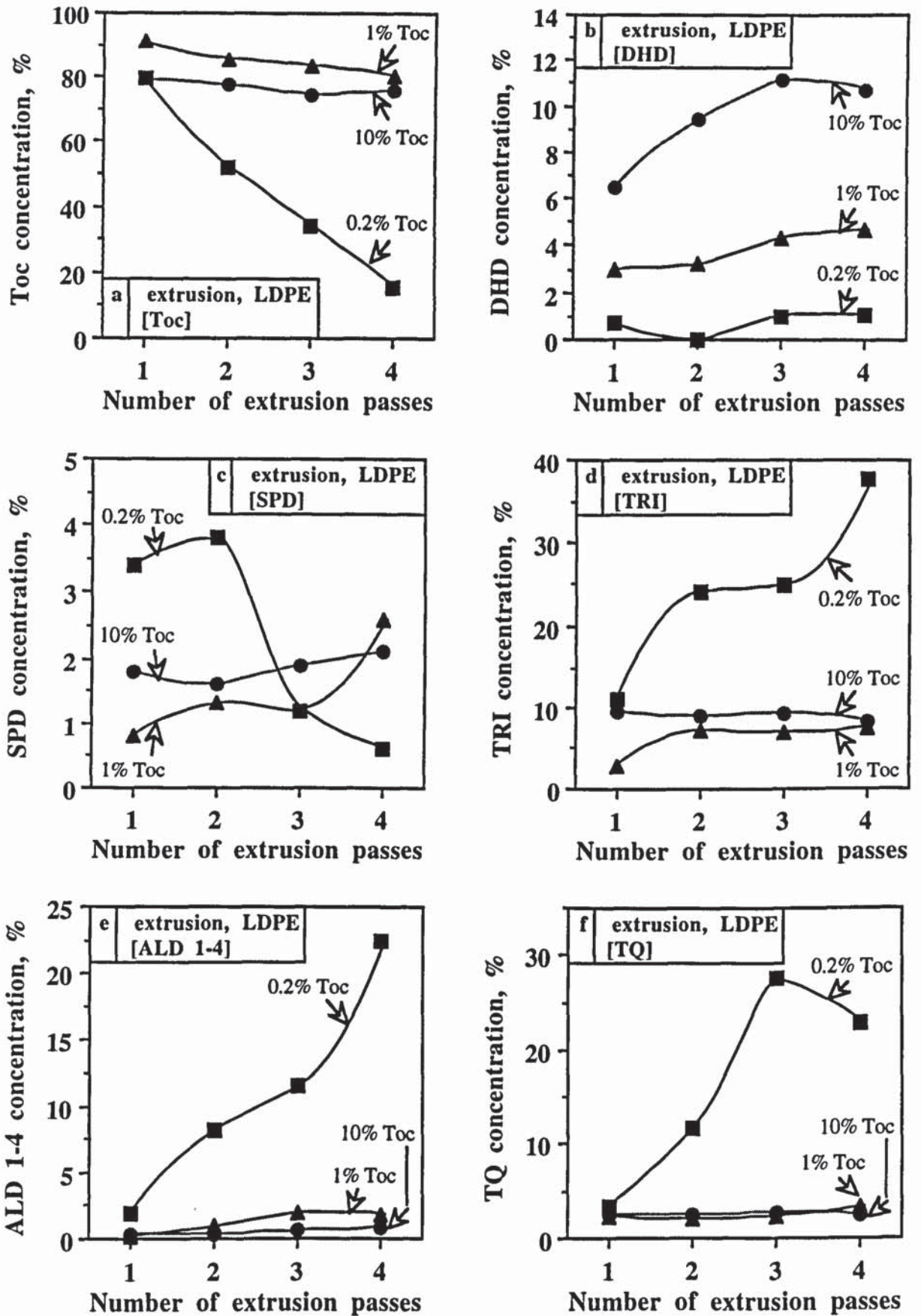


Figure 4.16: Effect of initial Toc concentration in LDPE on the concentrations of Toc and its transformation products after multiple extrusions (single screw extruder, 180°C) (see table 4.12, p. 365)

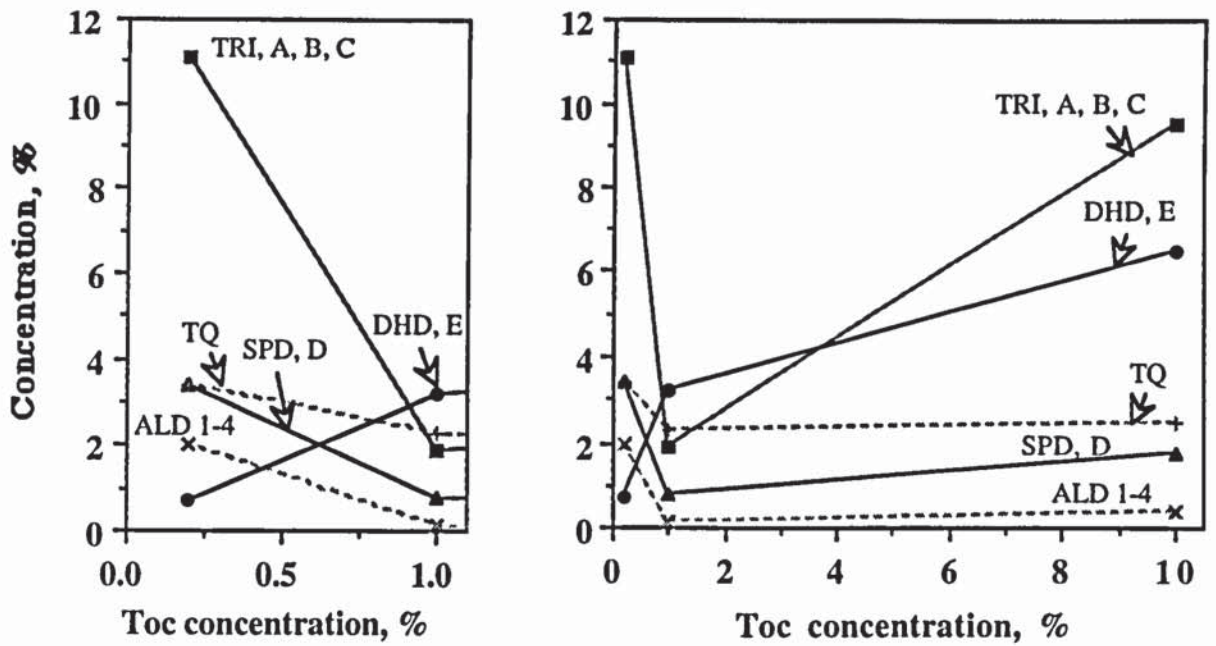


Figure 4.17: Effect of initial Toc concentration in LDPE on the concentration of its transformation products, after the first extrusion pass (single screw extruder, 180°C) (see table 4.12, p. 365)

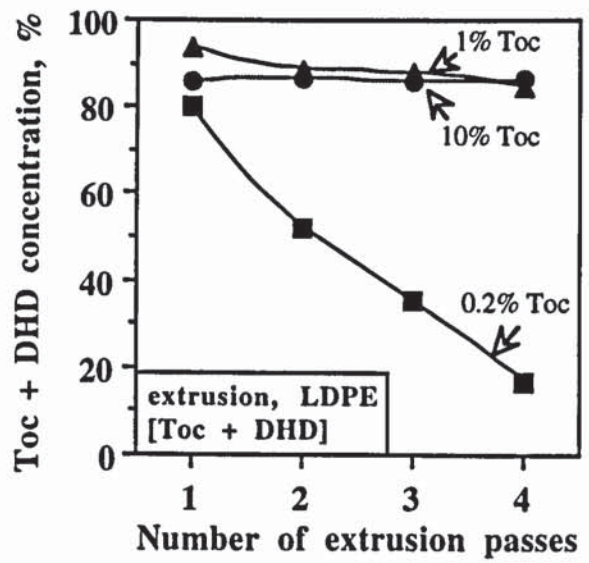


Figure 4.18: Effect of initial Toc concentration in LDPE and extrusion severity on the added concentrations of retained Toc and DHD, E, after multiple extrusions (single screw extruder, 180°C) (see table 4.12, p. 365)

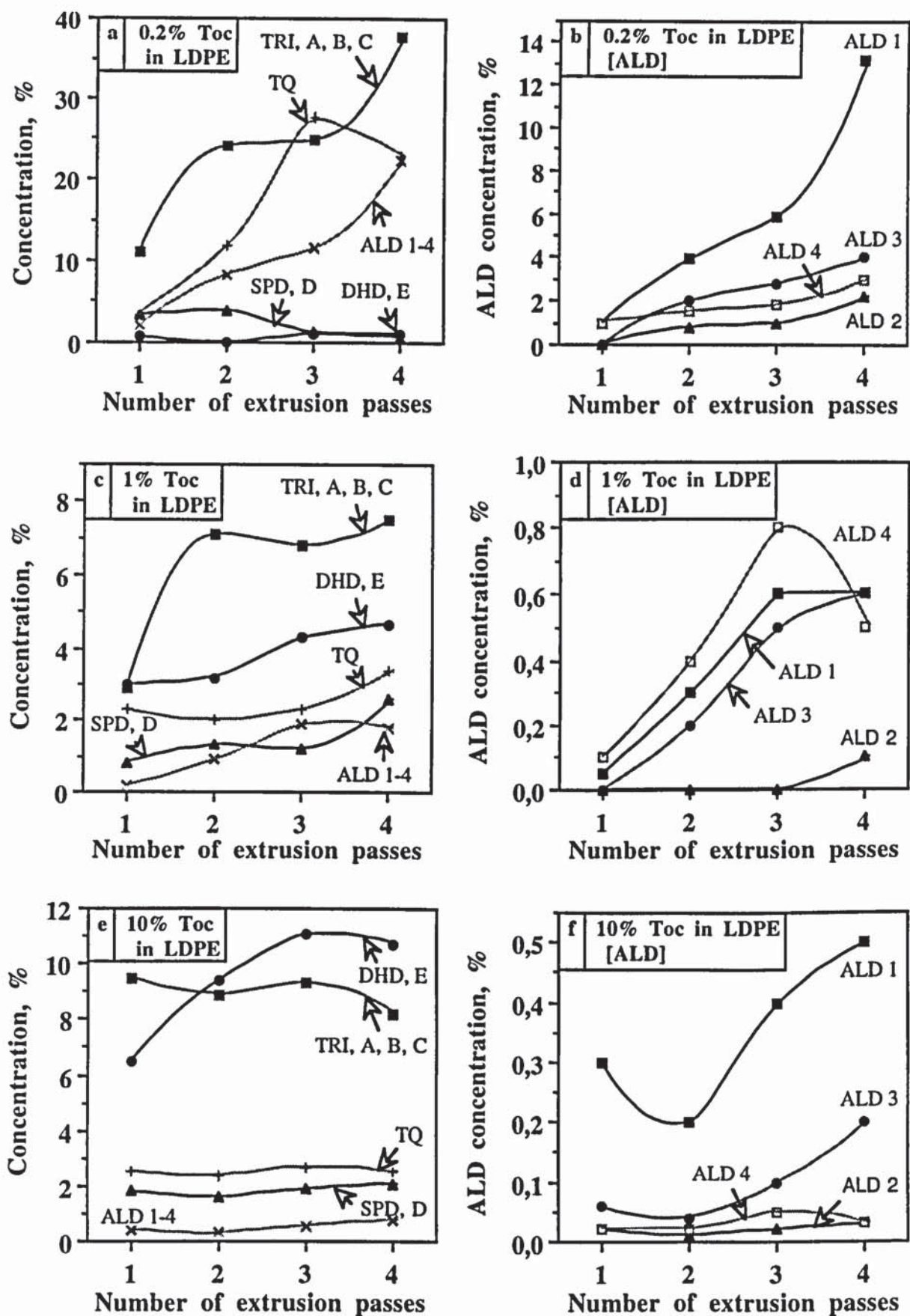


Figure 4.19: Effect of initial Toc concentration in LDPE and extrusion severity on the nature and distribution of its transformation products (single screw extruder, 180°C) (see table 4.12, p. 365)

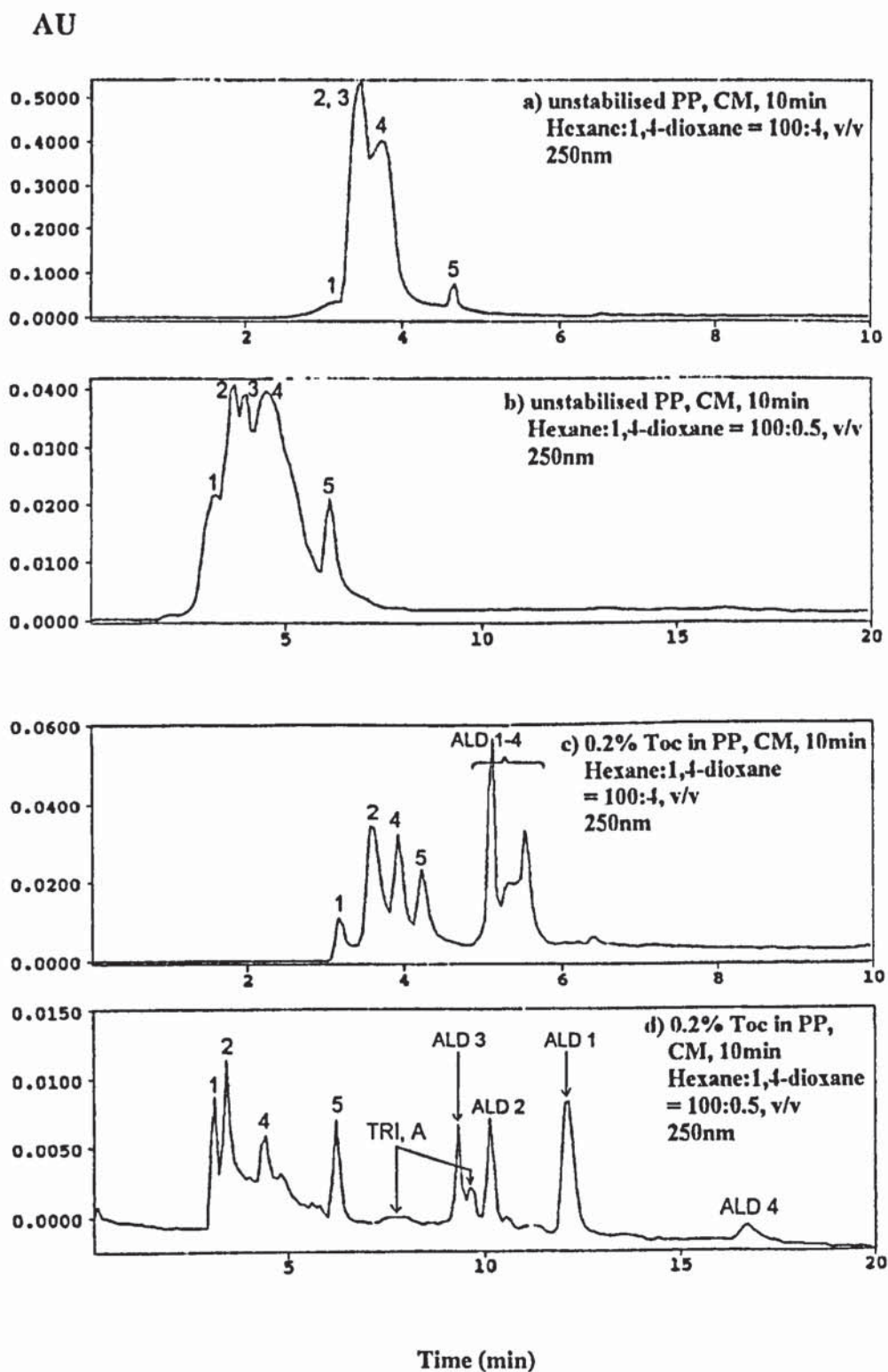


Figure 4.21: HPLC analysis of the extracts of unstabilised PP (a, b) and PP stabilised with (a-d) 0.2%Toc (c, d) in an internal mixer (CM, 10min, 200°C), in hexane, expanded regions 0-10min (a, c) and 0-20min (b, d) (LMWP) (see table 4.16, p. 370)

Instrument: Philips PU4100 liquid chromatograph and PU4120 diode array detector; Column: Zorbax SIL (4.6mm x 25cm); Flow rate: 1ml.min⁻¹
Eluents: hexane:1,4-dioxane = 100:4 (a, c) and 100:0.5, v/v (b, d)

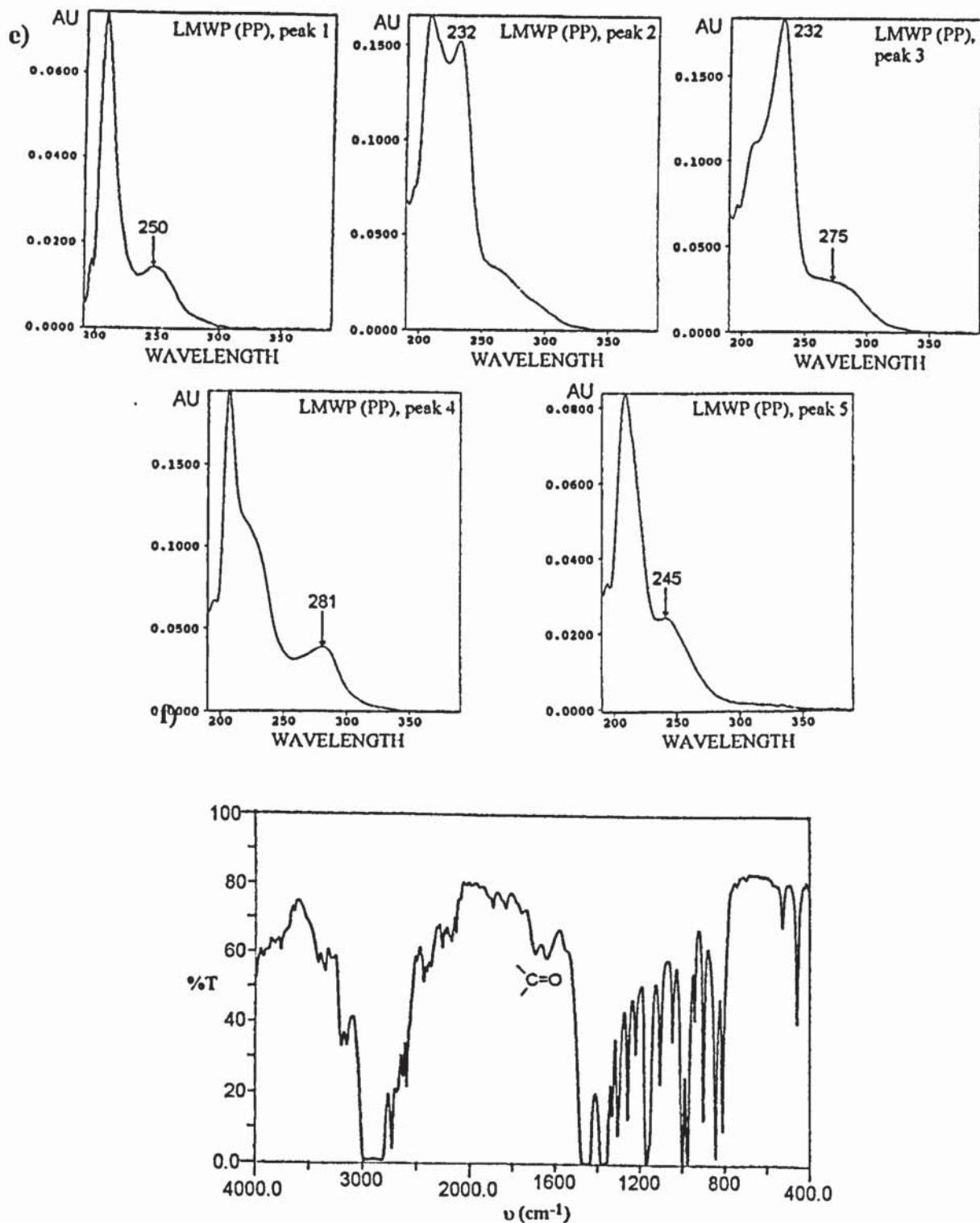


Figure 4.21: Diode array UV analysis (e) of the extract of unstabilised PP, in hexane and (e-f) FTIR analysis (f) of unstabilised PP film (0.25mm thick) (internal mixer, CM, 10min, 200°C) (see section 4.2.4.2, p. 369, and table 4.16, p. 370) Instruments: PU4120 diode array detector and Perkin Elmer

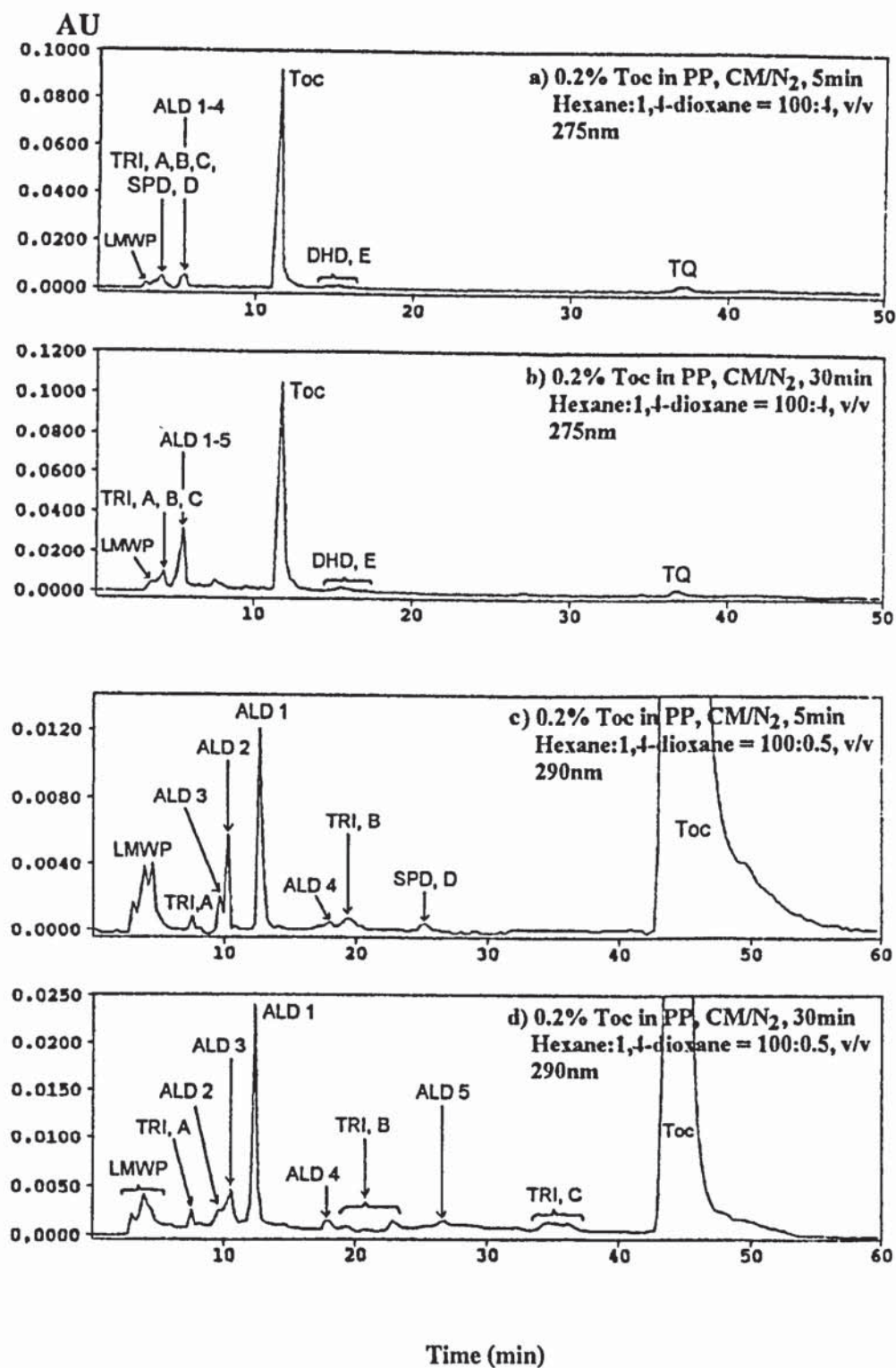


Figure 4.22: HPLC analysis of the extracts of PP stabilised with 0.2%Toc in an internal mixer (CM/N₂, 200°C) for 5min (a, c) and 30min (b, d), in hexane (see section 4.2.4.3, p. 371, and table 4.18, p. 372)

Instrument: Philips PU4100 liquid chromatograph and PU4120 diode array detector; Column: Zorbax SIL (4.6mm x 25cm); Flow rate: 1ml.min⁻¹
 Eluents: hexane:1,4-dioxane = 100:4 (a, b) and 100:0.5, v/v (c, d)

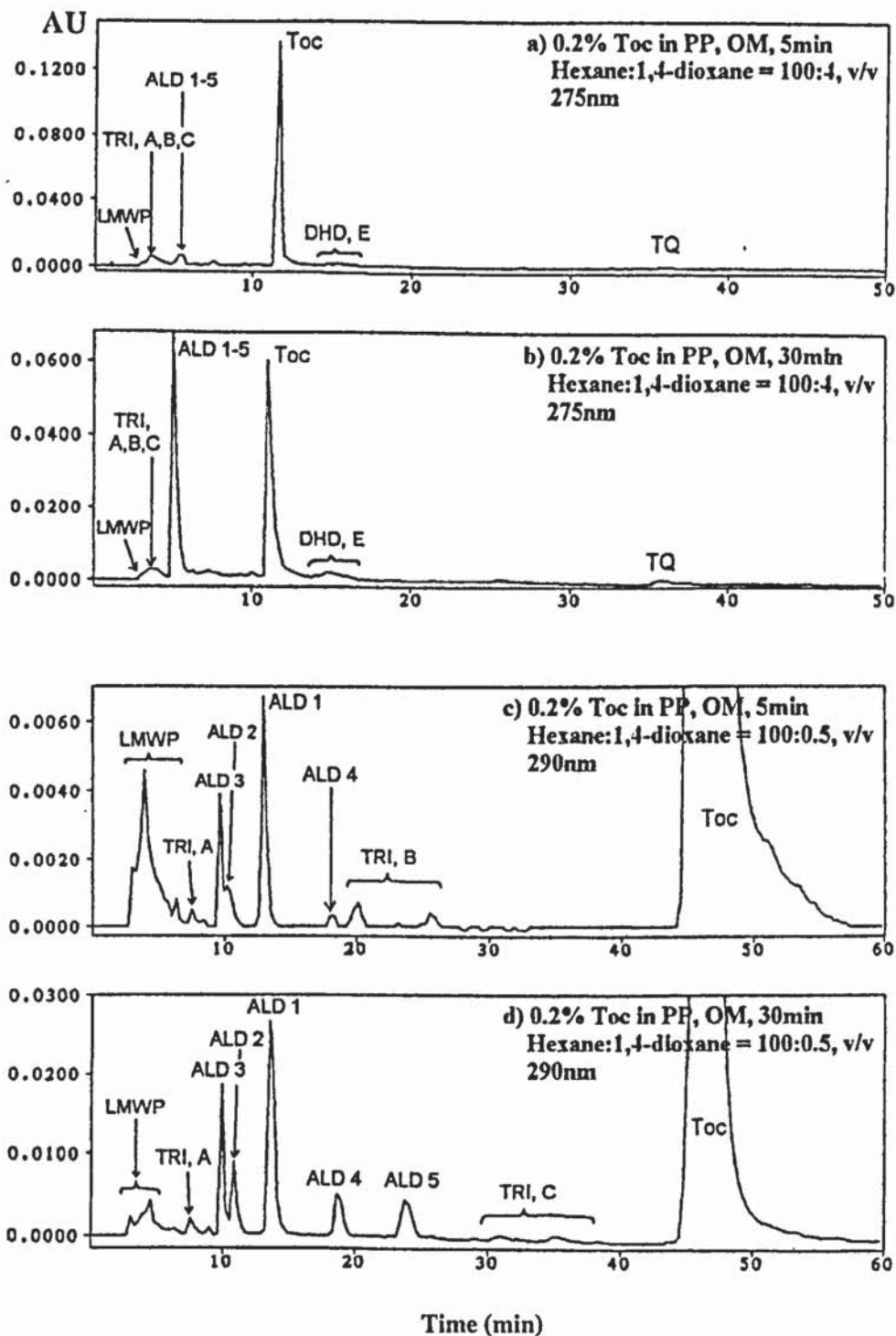
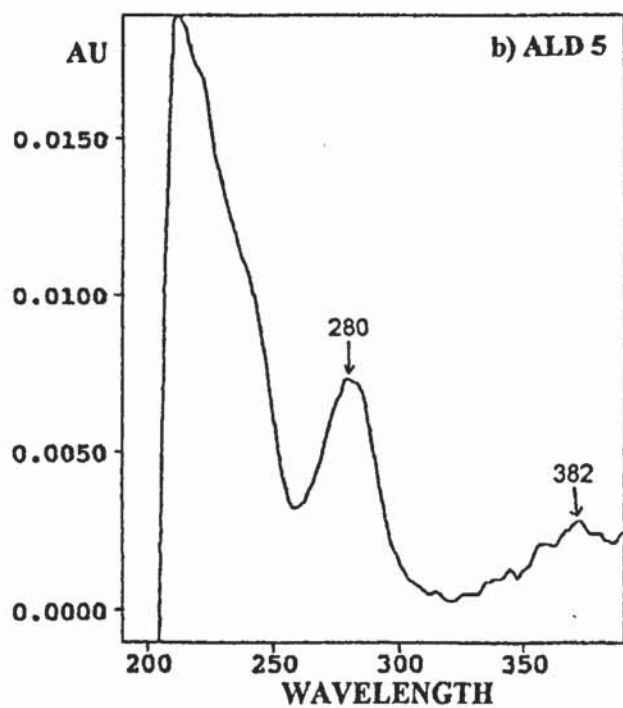
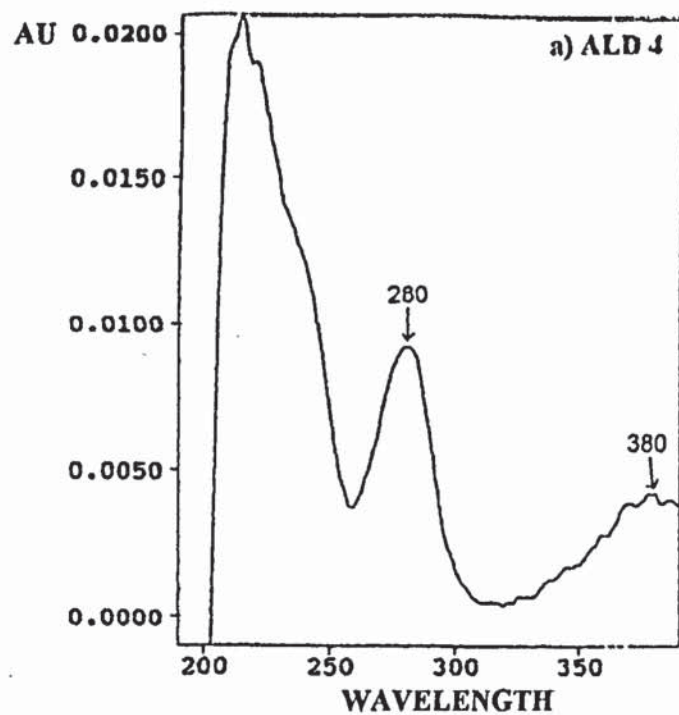


Figure 4.23: HPLC analysis of the extracts of PP stabilised with 0.2%Toc in an internal mixer (OM, 200°C) for 5min (a, c) and 30min (b, d), in hexane (see section 4.2.4.3, p. 371, and table 4.18, p. 372)

Instrument: Philips PU4100 liquid chromatograph and PU4120 diode array detector; Column: Zorbax SIL (4.6mm x 25cm); Flow rate: 1ml.min⁻¹
 Eluents: hexane:1,4-dioxane = 100:4 (a, b) and 100:0.5, v/v (c, d)



4.24: Diode array UV analysis of ALD 4 and ALD 5, extracted from PP stabilised with 0.2% Toc (OM, 10min, 200°C) (see section 4.2.4.3, p. 371)

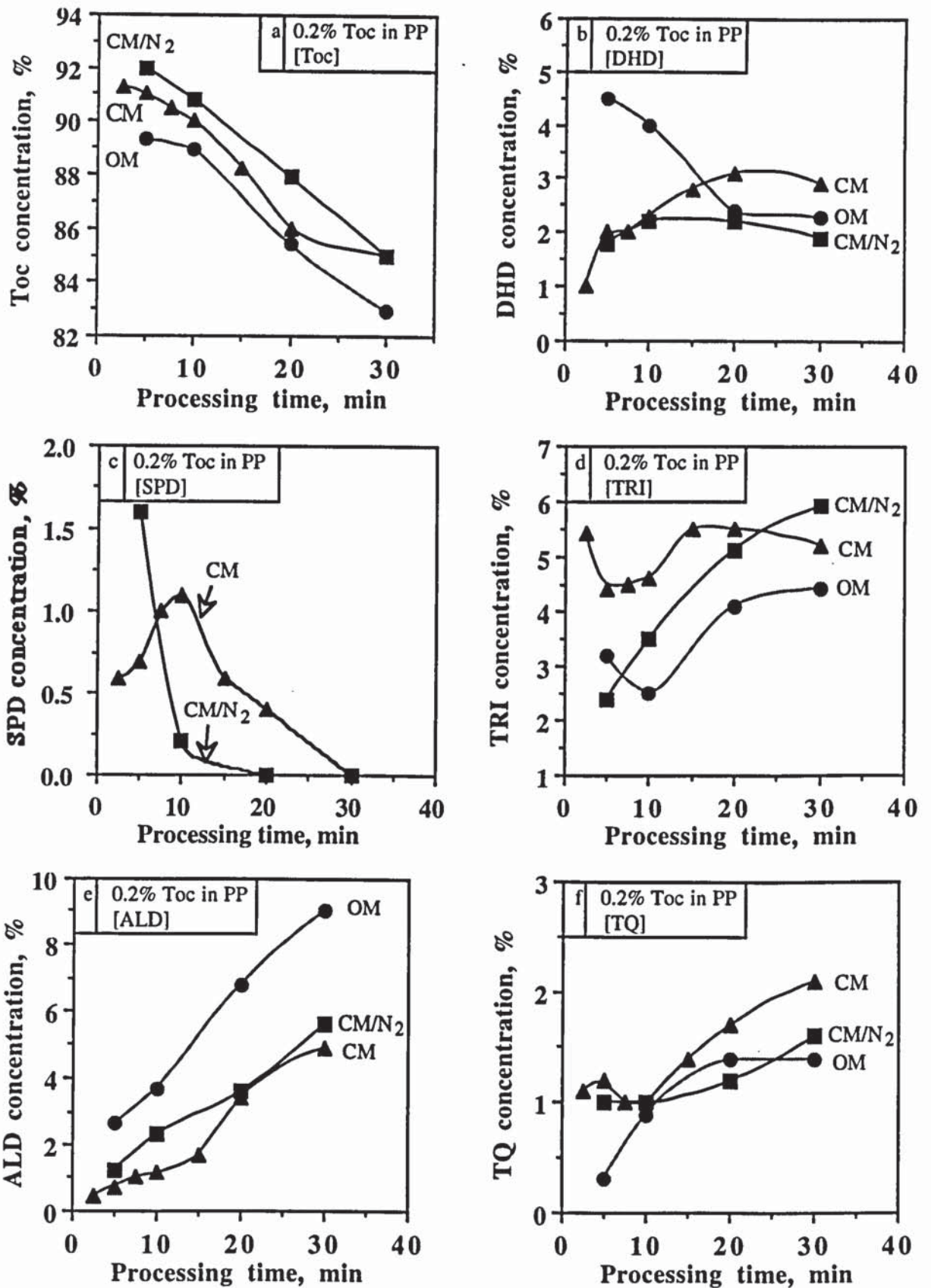


Figure 4.25: Effect of oxygen concentration in the internal mixing chamber on the concentration of Toc and its transformation products in PP stabilised with 0.2% Toc in an internal mixer (OM, CM and CM/N₂, 200°C) (see table 4.19, p. 373)

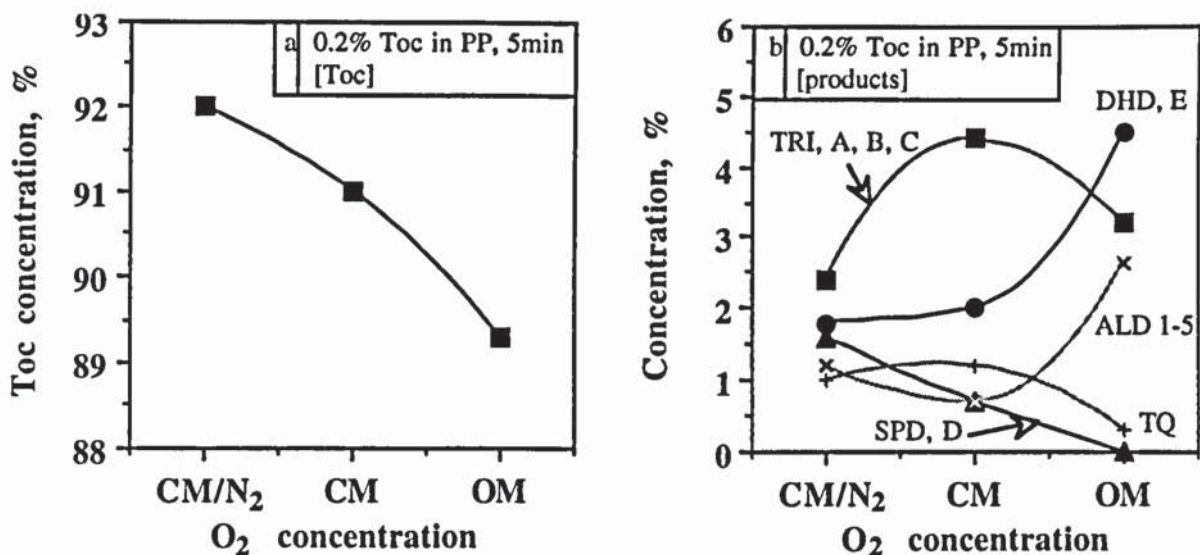


Figure 4.26: Effect of oxygen concentration in the internal mixing chamber on the concentration of Toc and its transformation products in PP stabilised with 0.2% Toc (OM, CM and CM/N₂, 5min, 200°C) (see table 4.19, p. 373)

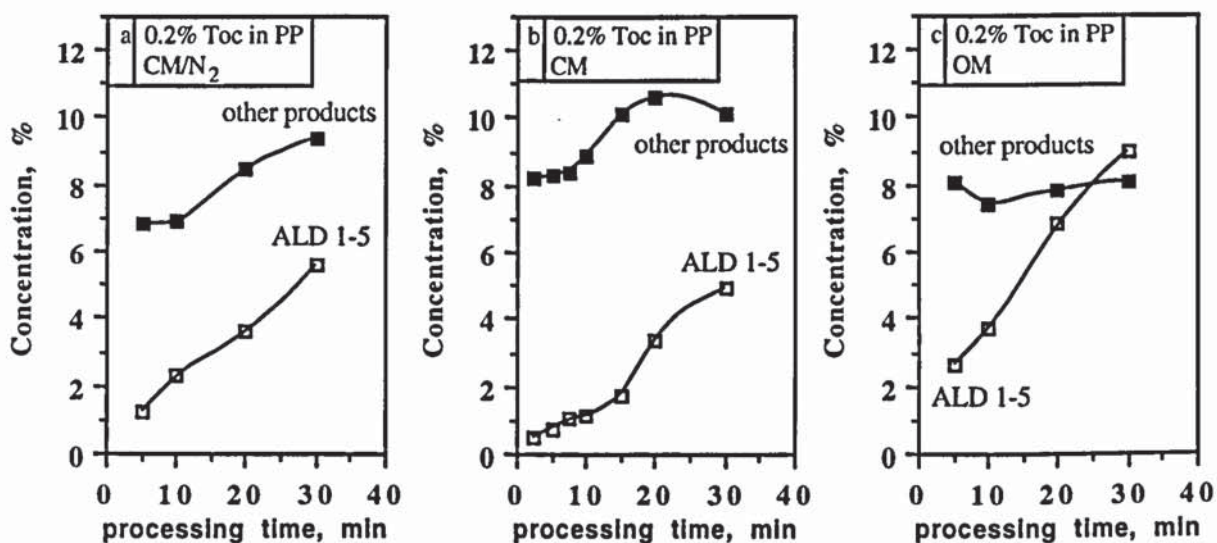


Figure 4.27: Effect of oxygen concentration on the concentration of ALD 1-5 compared to other products in PP stabilised with 0.2% Toc in an internal mixer (CM/N₂, CM and OM, 200°C) (see table 4.19, p. 373)

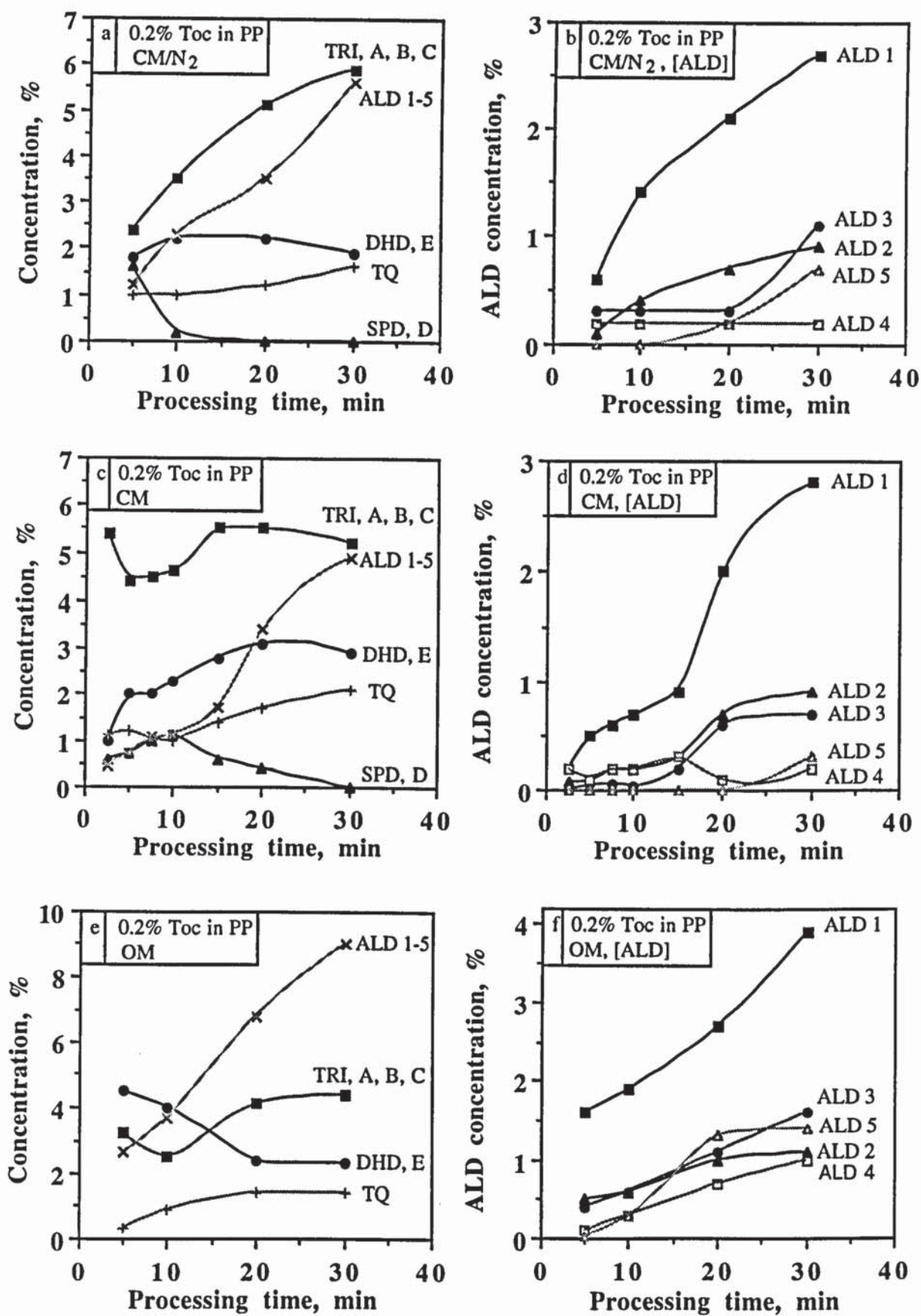


Figure 4.28: Effect of processing severity on the concentration of transformation products of Toc in PP stabilised with 0.2% Toc in an internal mixer (OM, CM and CM/N₂, 200°C) (see table 4.19, p. 373)

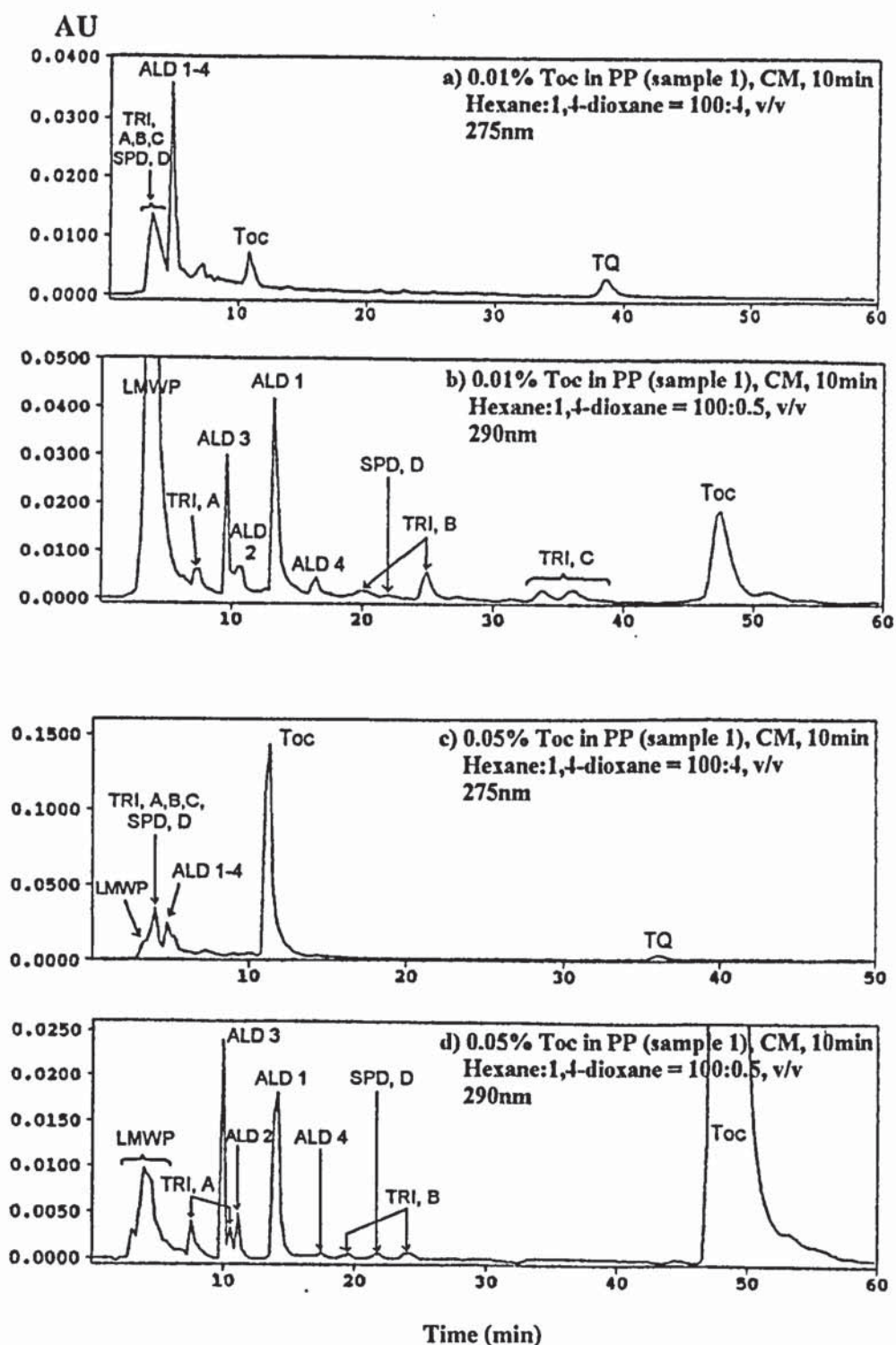


Figure 4.29: HPLC analysis of the extracts of PP stabilised with 0.01% (a, b) and 0.05% Toc (c, d) in an internal mixer (CM, 10min, 200°C), in hexane (see section 4.2.4.4, p. 373)

Instrument: Philips PU4100 liquid chromatograph and PU4120 diode array detector; Column: Zorbax SIL (4.6mm x 25cm); Flow rate: 1ml.min⁻¹
Eluents: hexane:1,4-dioxane = 100:4 (a, c) and 100:0.5, v/v (b, d)

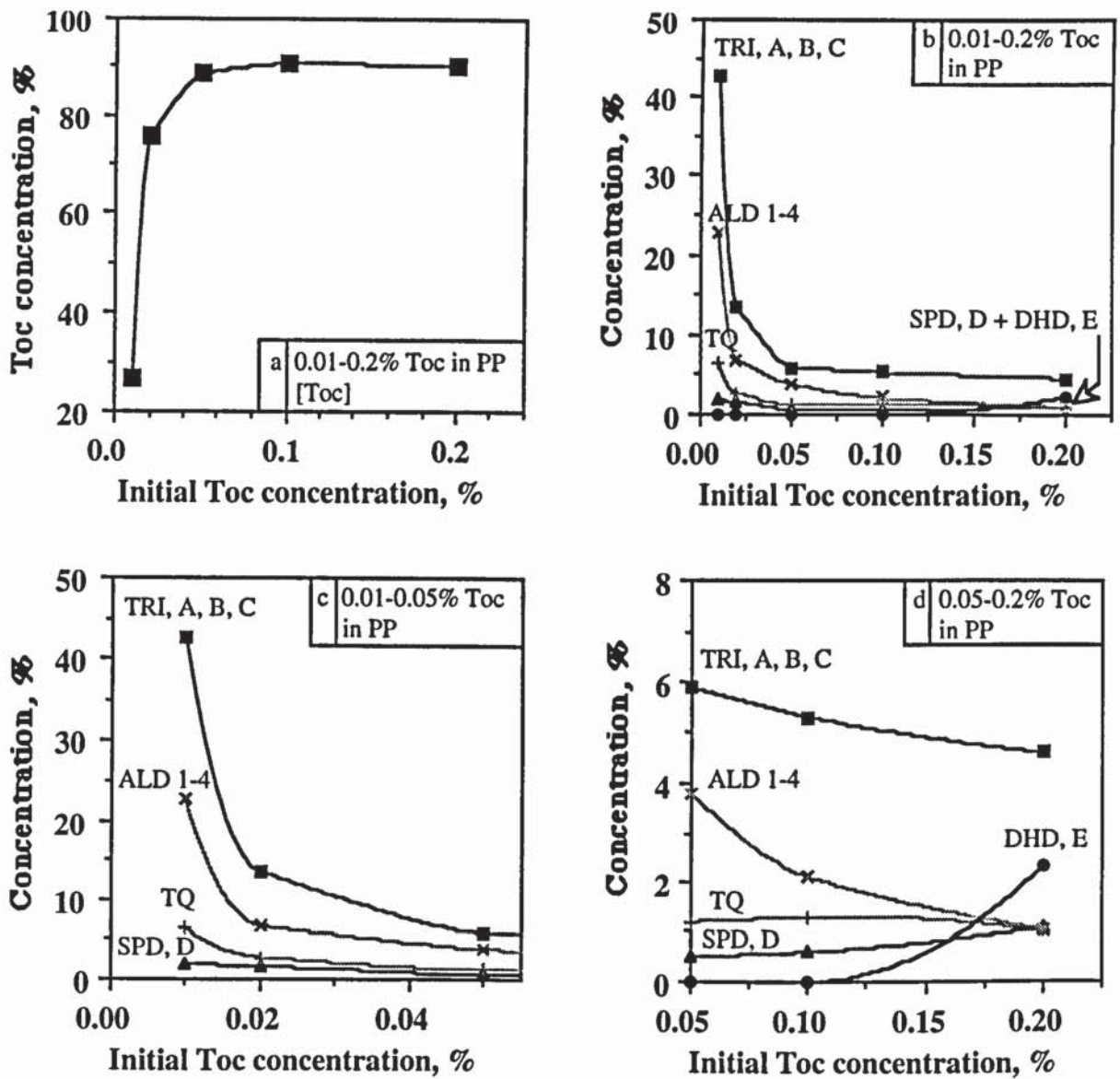


Figure 4.30: Effect of initial Toc concentration in PP on the nature and concentration of its transformation products (internal mixer, CM, 10min, 200°C)
 (see table 4.20, p. 375)

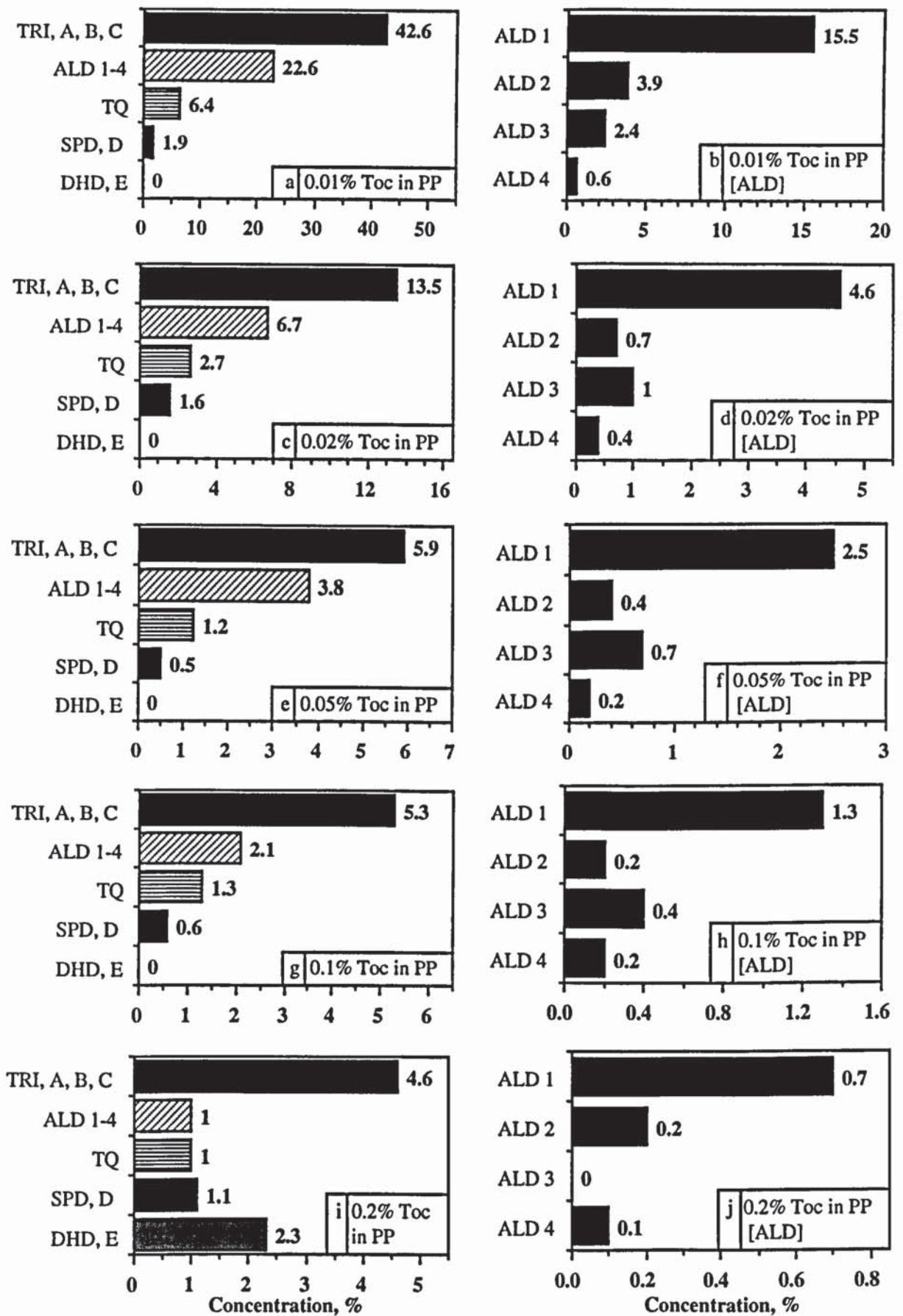


Figure 4.31: Effect of initial Toc concentration in PP on the distribution of its oxidation products (internal mixer, CM, 10min, 200°C) (see table 4.20, p. 375)

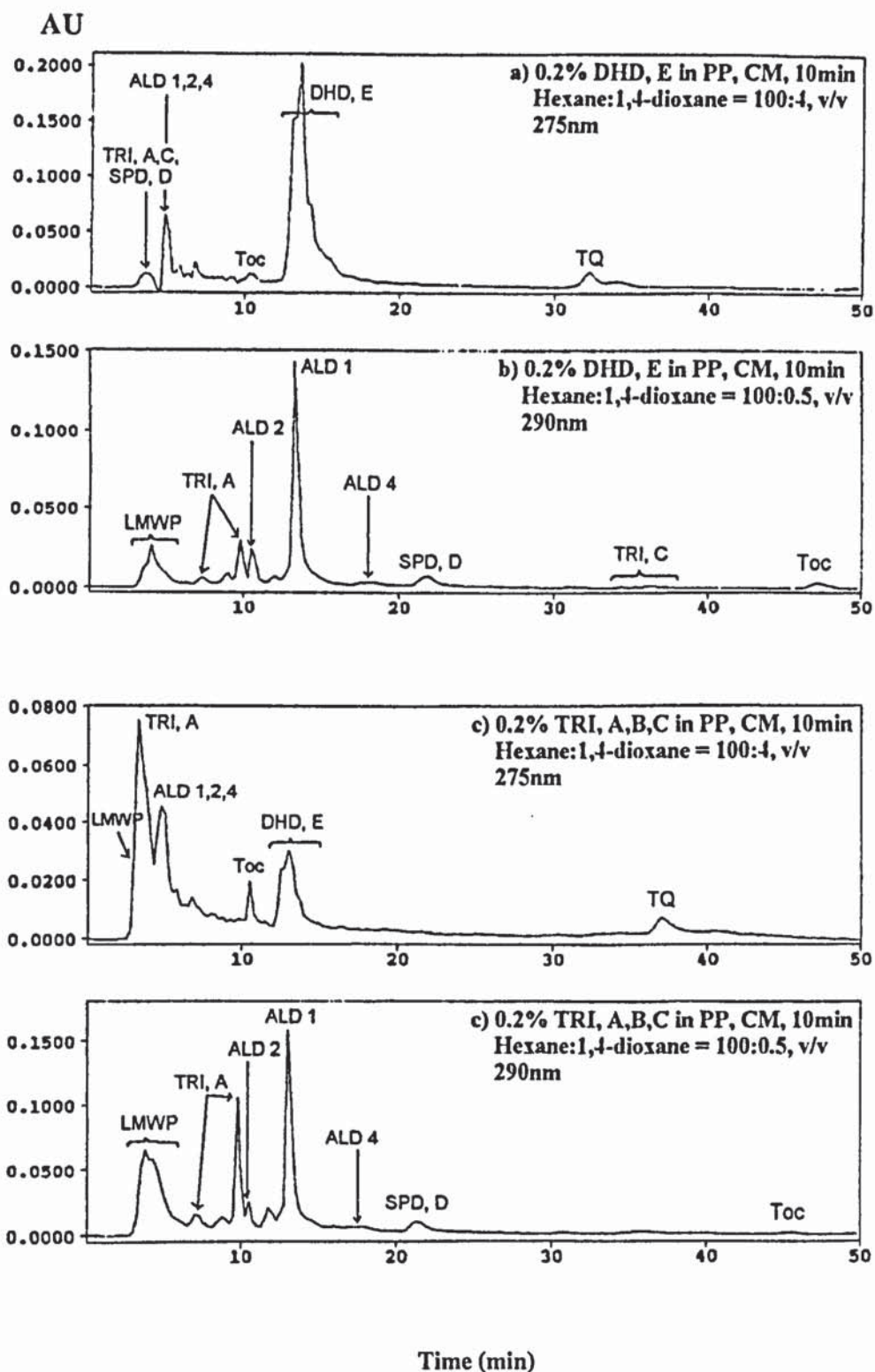


Figure 4.32: HPLC analysis of the extracts of PP stabilised with 0.2% DHD, E (a, b) and 0.2% TRI, A, B, C (c, d) in an internal mixer (CM, 10min, 200°C), in hexane (see section 4.2.4.5, p. 375)

Instrument: Philips PU4100 liquid chromatograph and PU4120 diode array detector; Column: Zorbax SIL (4.6mm x 25cm); Flow rate: 1ml.min⁻¹
 Eluents: hexane:1,4-dioxane = 100:4 (a, c) and 100:0.5, v/v (b, d)

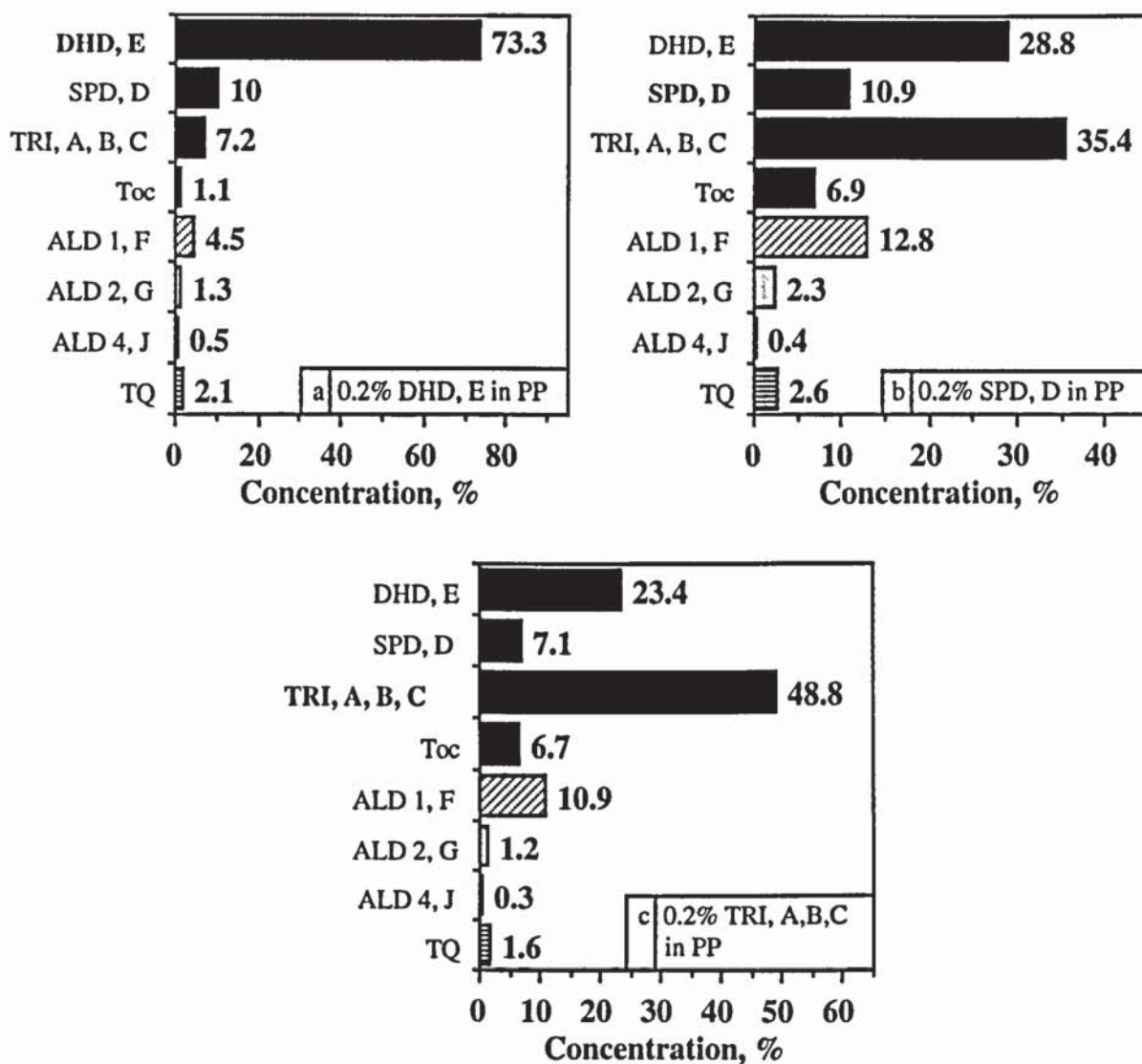


Figure 4.33: Nature of transformation products in PP stabilised with 0.2% of each of the Toc derivatives DHD, E, SPD, D and TRI, A, B, C in an internal mixer (CM, 10min, 200°C) (see table 4.21, p. 376)

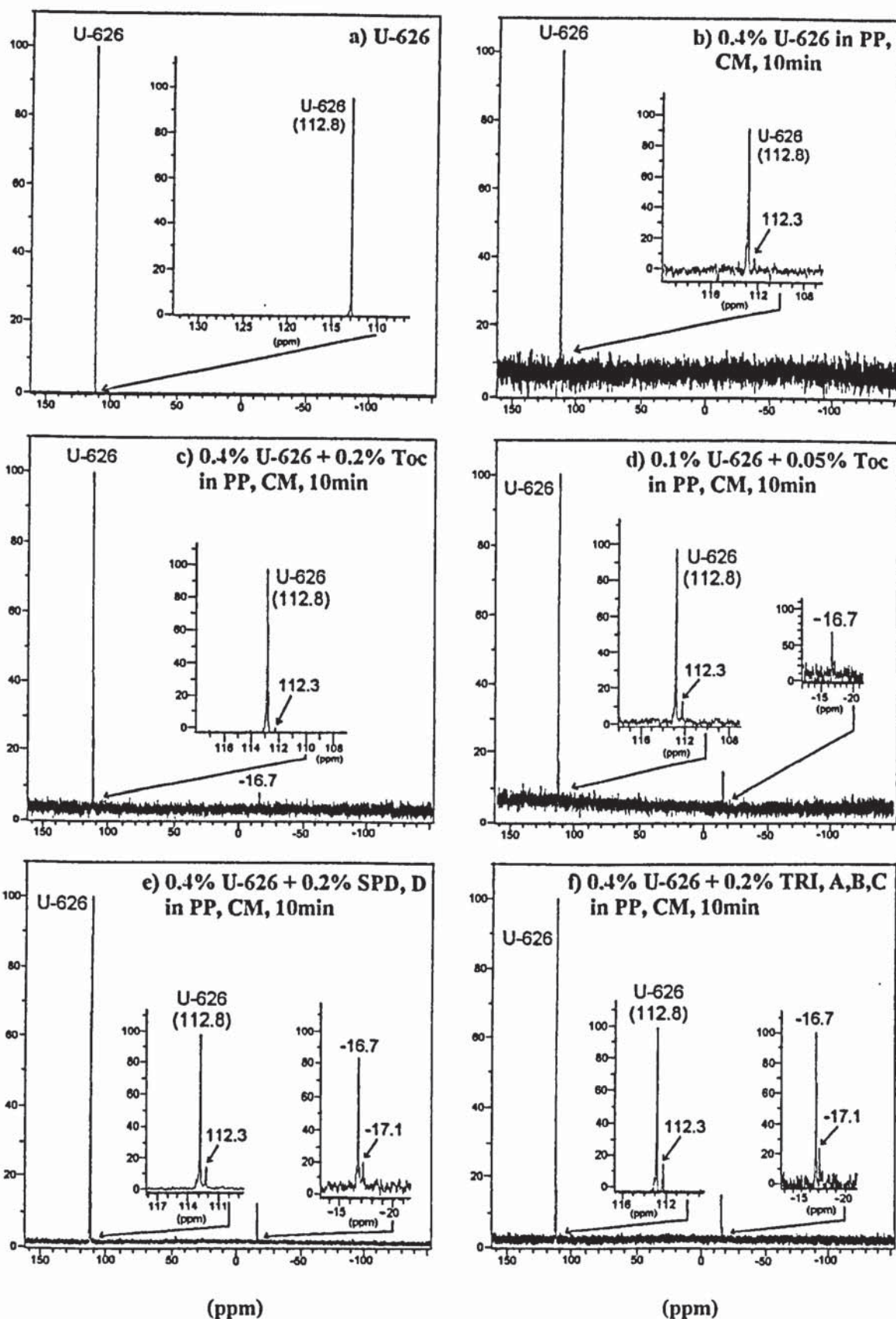


Figure 4.35: ^{31}P -NMR spectra of U-626 (a) and the extracts of PP stabilised with 0.4% U-626, 0.4% U-626 + 0.2% Toc, 0.1% U-626 + 0.05% Toc, 0.4% U-626 + 0.2% SPD, D and 0.4% U-626 + 0.2% TRI, A, B, C (b-f) in an internal mixer (CM, 10min, 200°C), in CDCl_3 at 120MHz (see table 4.25, p. 381)

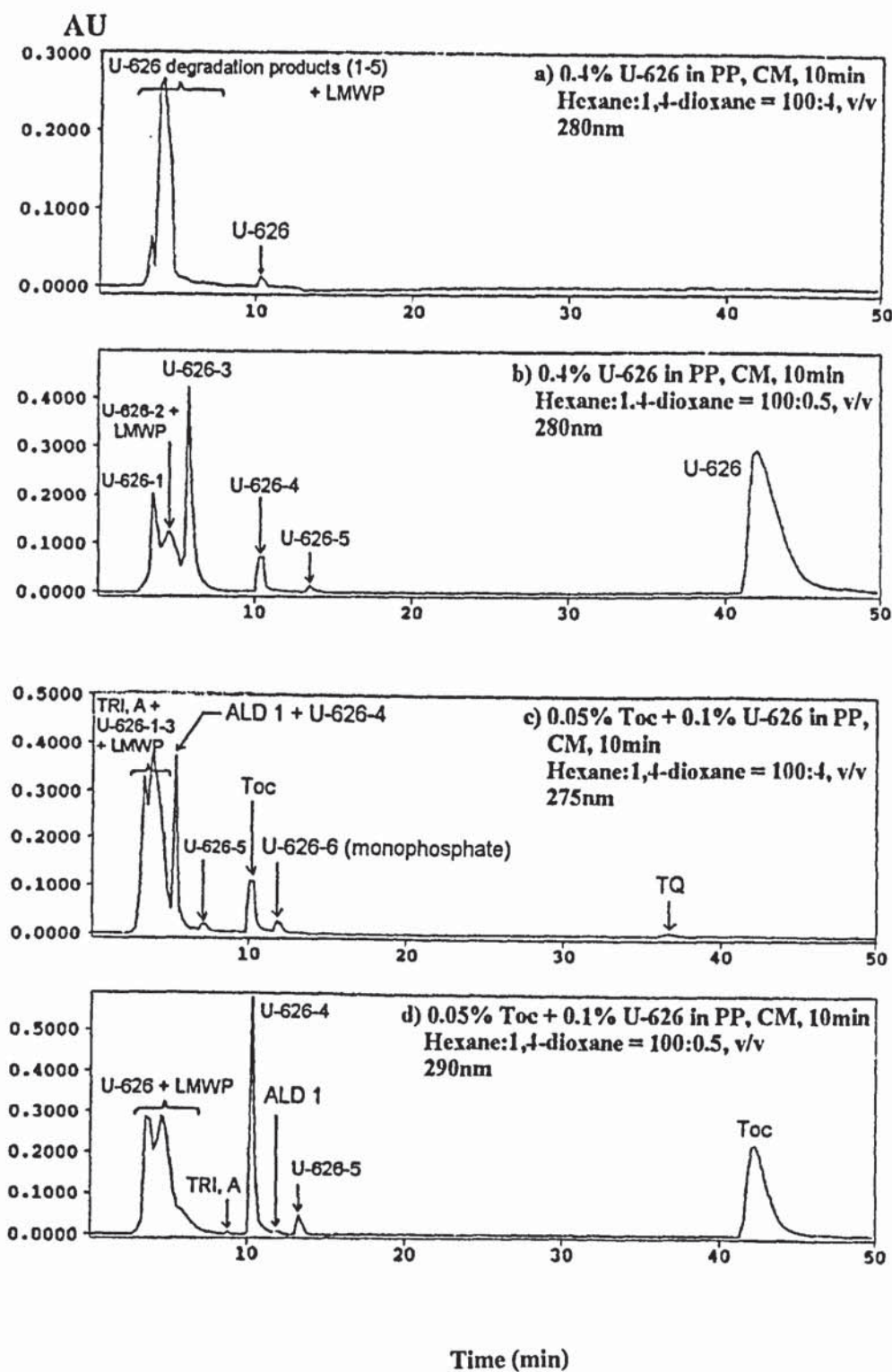


Figure 4.36: HPLC analysis of the extracts of PP stabilised with 0.4% U-626 (a, b) and (a-d) 0.05% Toc + 0.1% U-626 (c, d) in an internal mixer (CM, 10min, 200°C), in hexane (see section 4.2.5, p. 377)

Instrument: Philips PU4100 liquid chromatograph and PU4120 diode array detector; Column: Zorbax SIL (4.6mm x 25cm); Flow rate: 1ml.min⁻¹
 Eluents: hexane:1,4-dioxane = 100:4 (a, c) and 100:0.5, v/v (b, d)

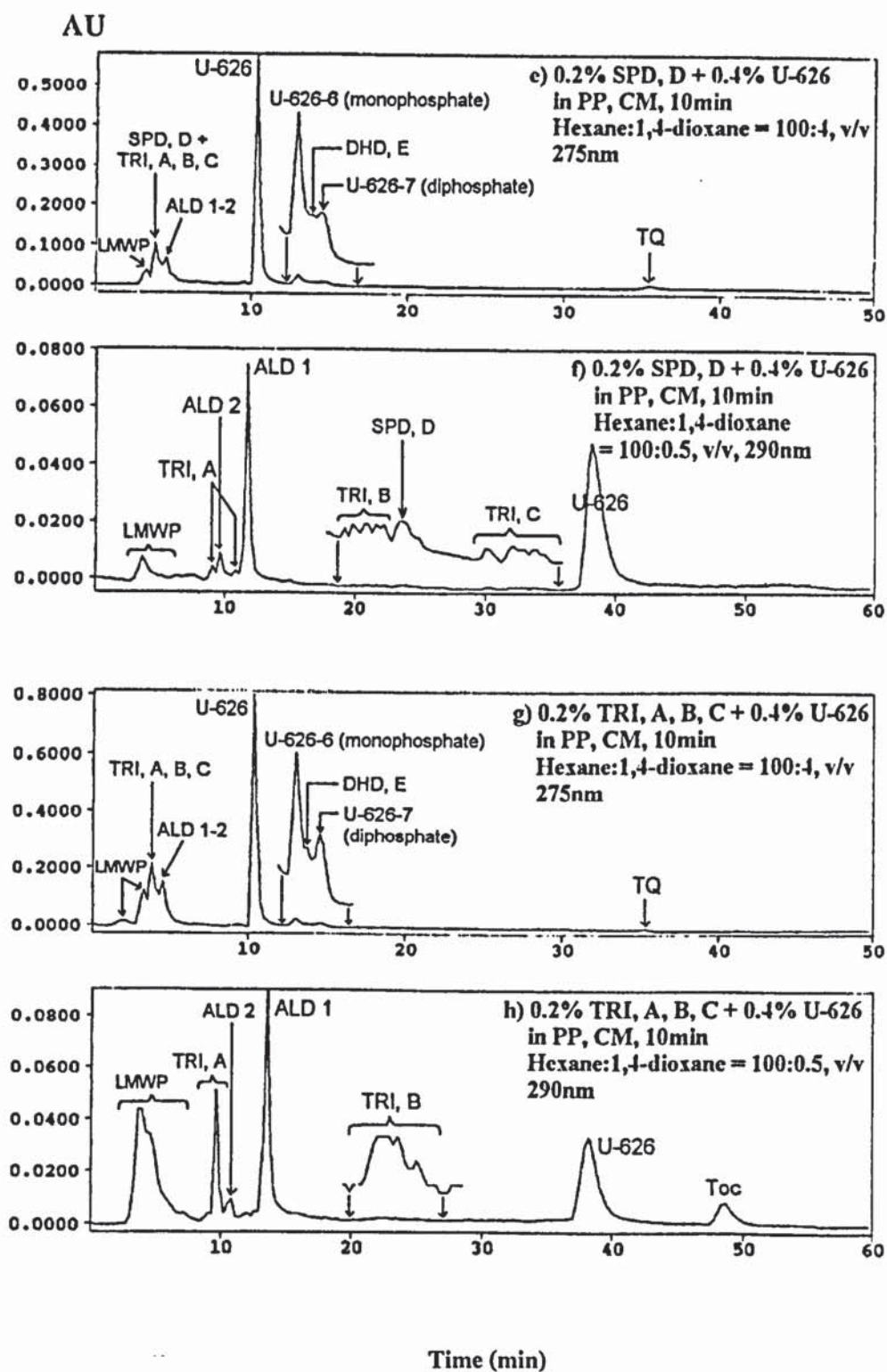


Figure 4.36: HPLC analysis of the extracts of PP stabilised with 0.2 % SPD, D + 0.4% U-626 (e, f) and 0.2% TRI, A, B, C + 0.4% U-626 (g, h) in an internal mixer (CM, 10min, 200°C), in hexane (see section 4.2.5, p. 377)
 Instrument: Philips PU4100 liquid chromatograph and PU4120 diode array detector; Column: Zorbax SIL (4.6mm x 25cm); Flow rate: 1ml.min⁻¹
 Eluents: hexane:1,4-dioxane = 100:4 (a, c) and 100:0.5, v/v (b, d)

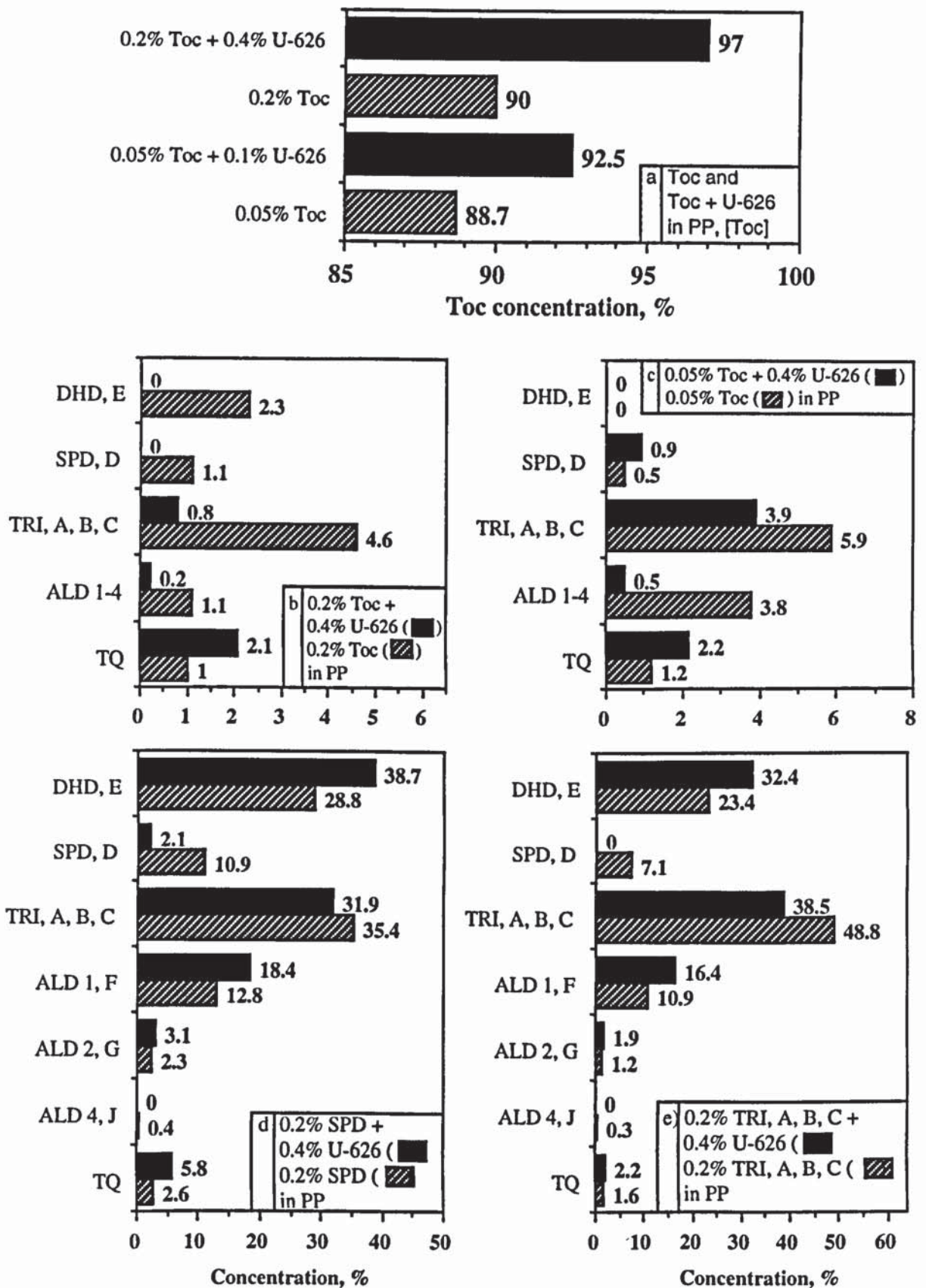


Figure 4.37: Effect of U-626 in PP containing Toc (a-c), SPD, D (d) and TRI, A, B, C (e) on the nature and concentration of their transformation products after processing in an internal mixer (CM, 10min, 200°C) (see tables 4.20, p. 375, 4.21, p. 376, and 4.26, p. 383)

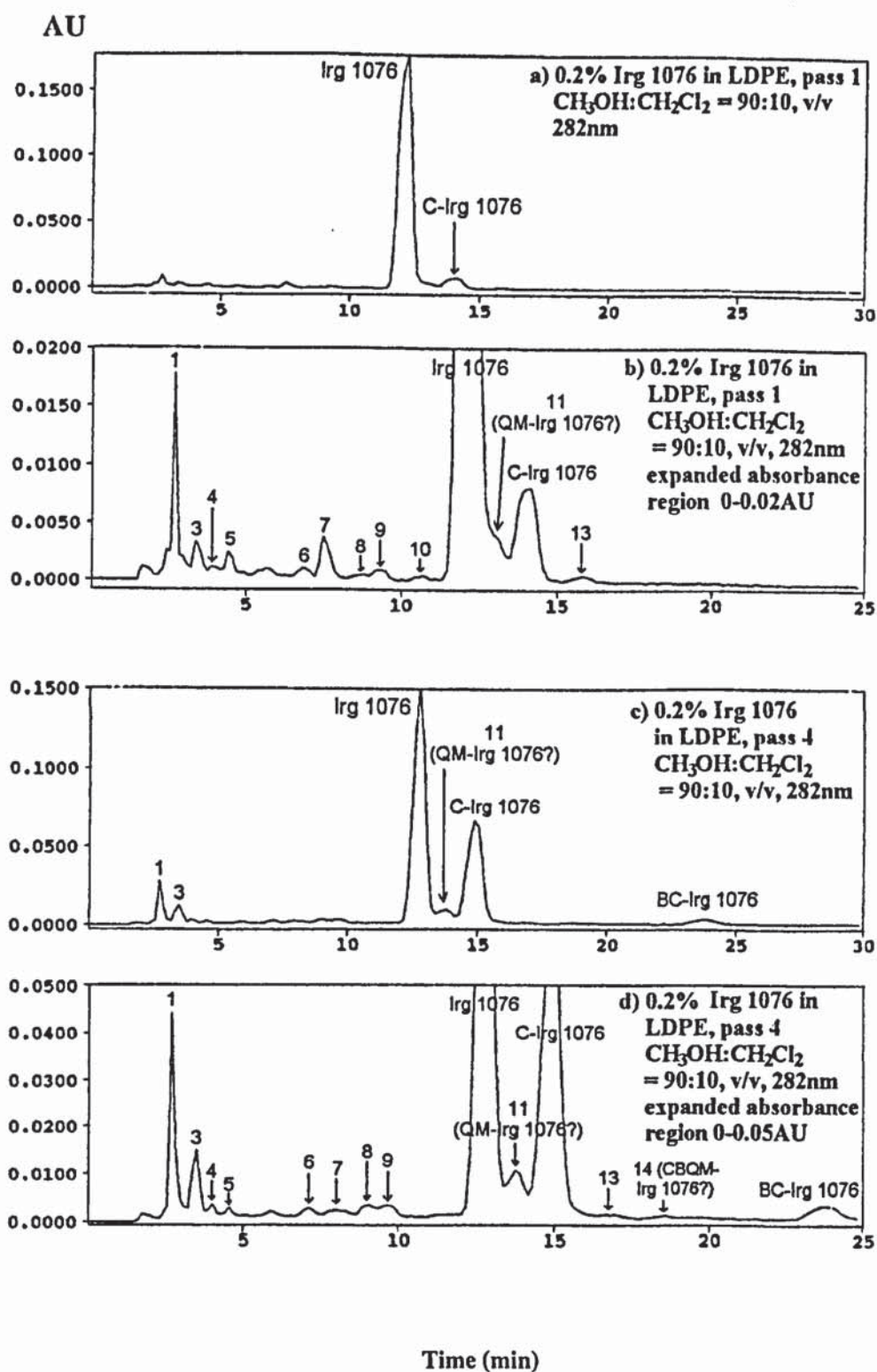


Figure 4.47: HPLC chromatograms of the products extracted from LDPE stabilised with (a-d) 0.2% Irg 1076, passes 1 (a, b) and 4 (c, d) (single screw extruder, 180°C) (see section 4.2.7, p. 392, and table 4.27, p. 384)

Instruments: Philips PU4100 liquid chromatograph and PU4120 diode array detector; Column: Zorbax ODS (4.6mm x 25cm); Flow rate: $1\text{ml}\cdot\text{min}^{-1}$
 Eluent: $\text{CH}_3\text{OH}:\text{CH}_2\text{Cl}_2 = 90:10, \text{v/v}$

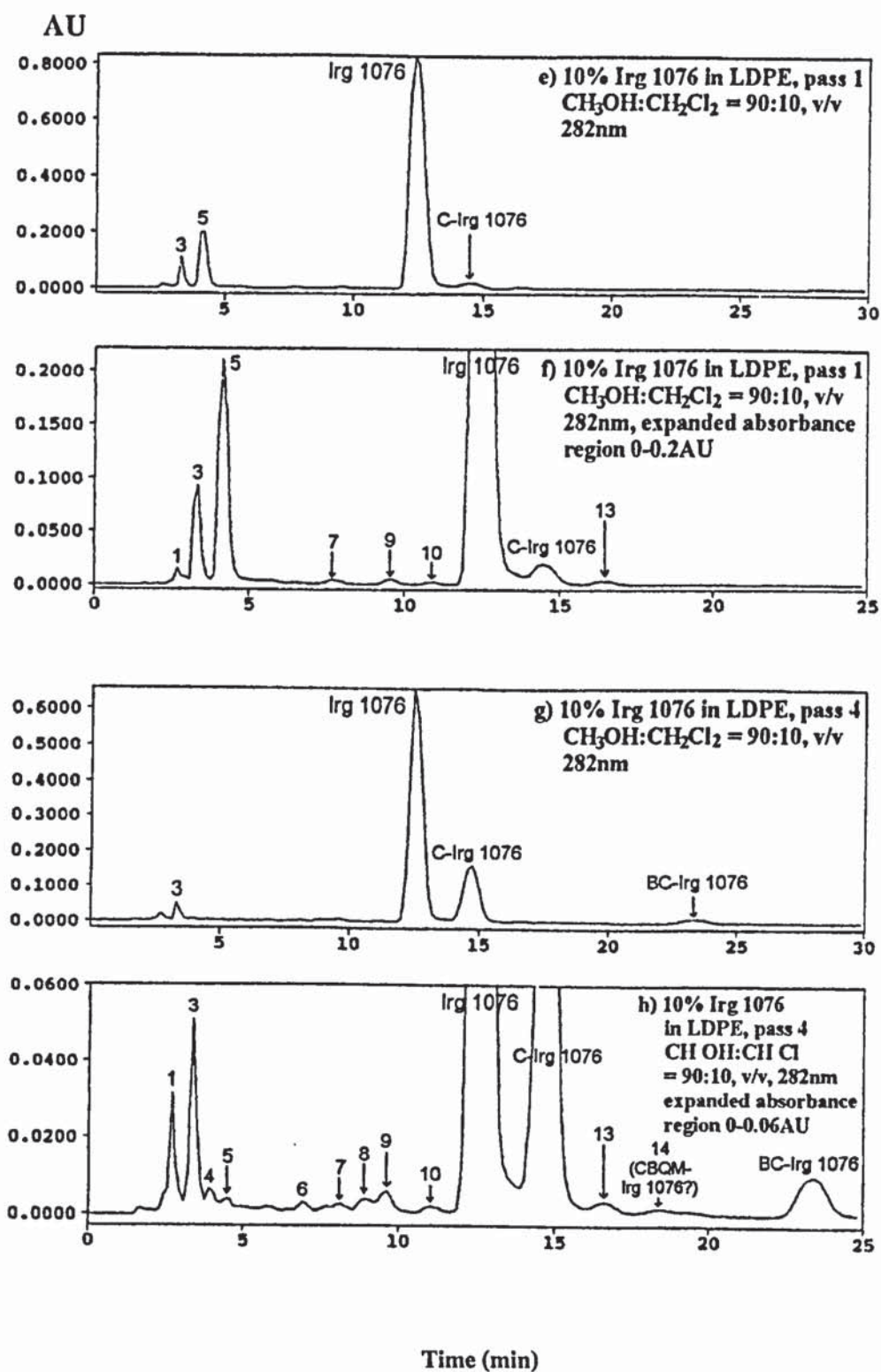


Figure 4.47: HPLC chromatograms of the products extracted from LDPE stabilised with (e-h) 10% Irg 1076, passes 1 (e, f) and 4 (g, h) (single screw extruder, 180°C) (see section 4.2.7, p. 392, and table 4.27, p. 384) Instruments: Philips PU4100 liquid chromatograph and PU4120 diode array detector; Column: Zorbax ODS (4.6mm x 25cm); Flow rate: 1ml.min⁻¹ Eluent: CH₃OH:CH₂Cl₂ = 90:10, v/v

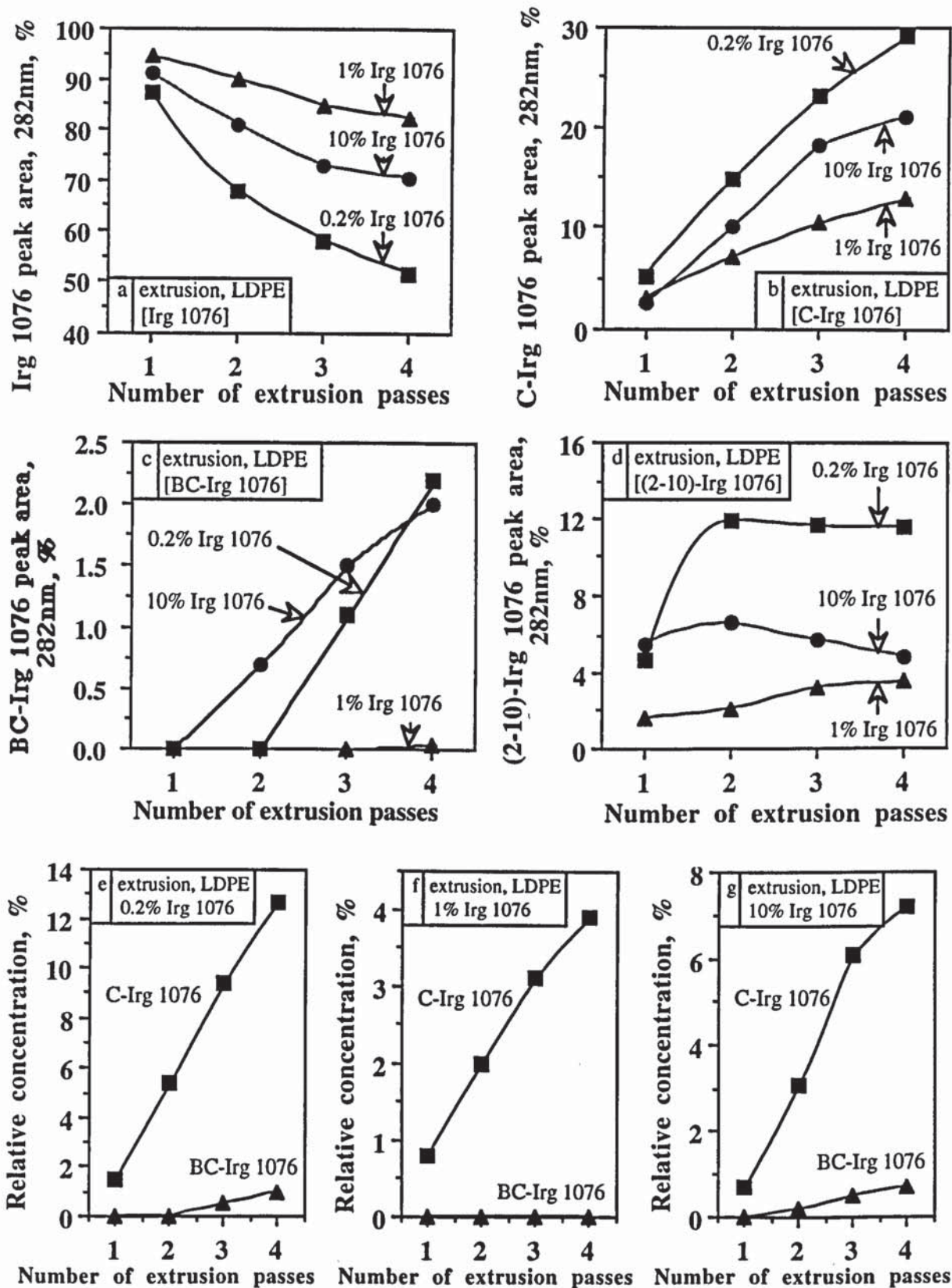


Figure 4.48: Effect of extrusion severity and initial Irg 1076 concentration on the nature and peak areas (282nm) of the transformation products of Irg 1076 in LDPE (a-d) and concentrations of C-Irg 1076 and BC-Irg 1076, relative to Irg 1076 (total 100%) (e-g) (single screw extruder, 180°C) (see tables 4.31-4.32, p. 394)

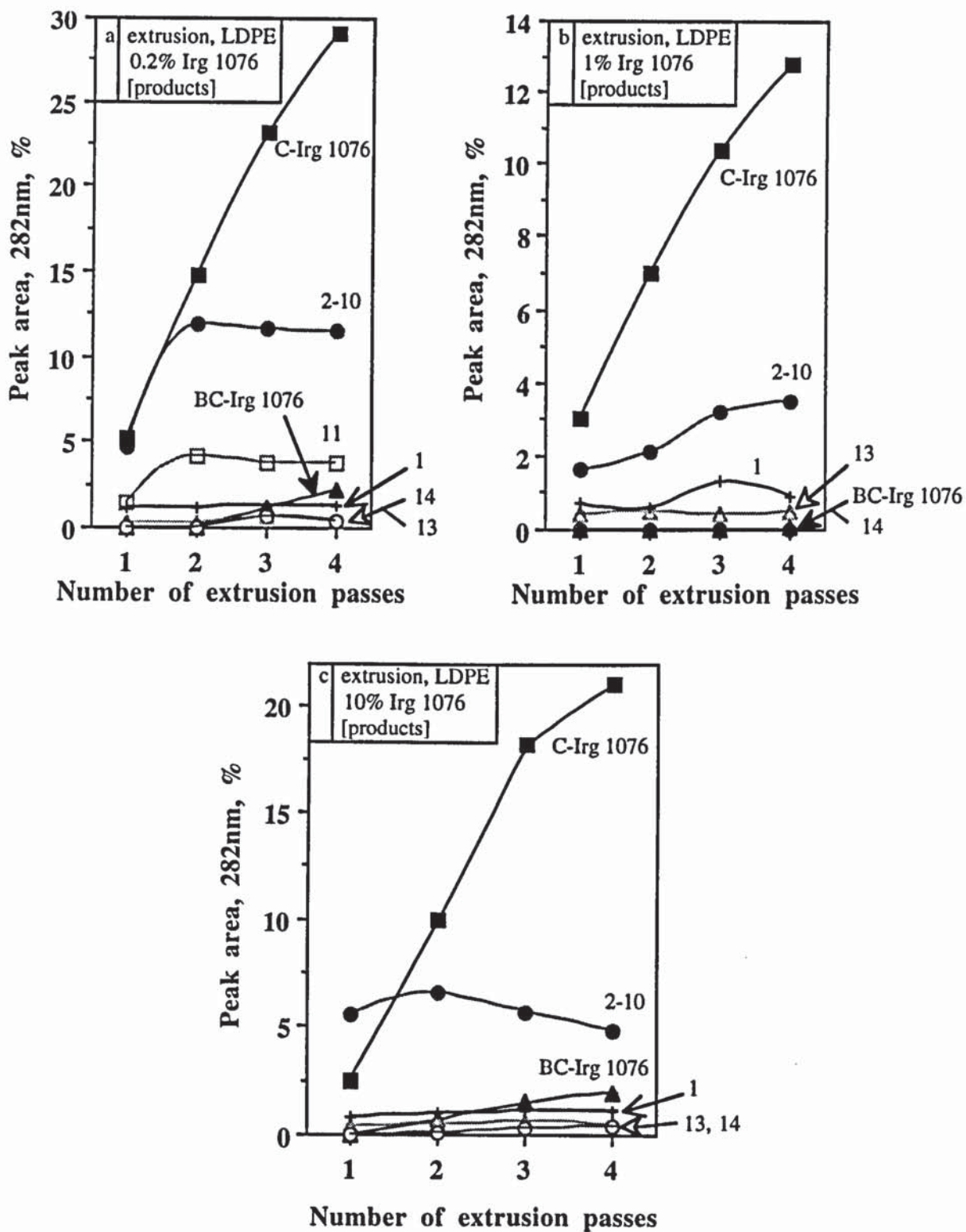


Figure 4.49: Effect of extrusion severity on the peak areas (282nm) and distribution of the transformation products of Irg 1076 in LDPE (single screw extruder, 180°C) (see table 4.31, p. 394)

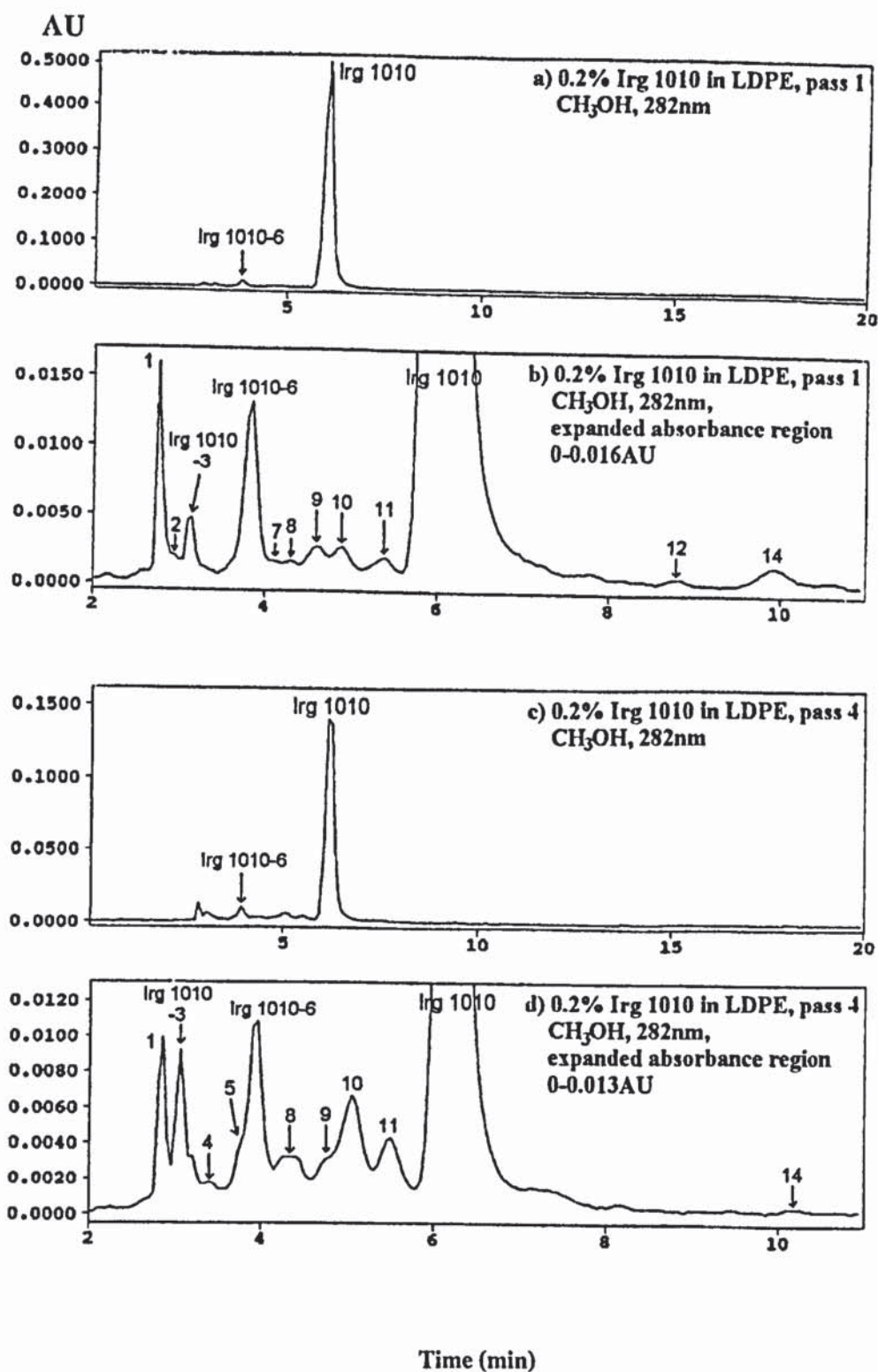


Figure 4.50: HPLC chromatograms of the products extracted from LDPE stabilised with (a-d) 0.2% Irg 1010, passes 1 (a, b) and 4 (c, d) (single screw extruder, 180°C) (see section 4.2.8, p. 395, and table 4.28, p. 385)

Instruments: Philips PU4100 liquid chromatograph and PU4120 diode array detector; Column: Zorbax ODS (4.6mm x 25cm); Flow rate: 1ml.min⁻¹
 Eluent: CH₃OH

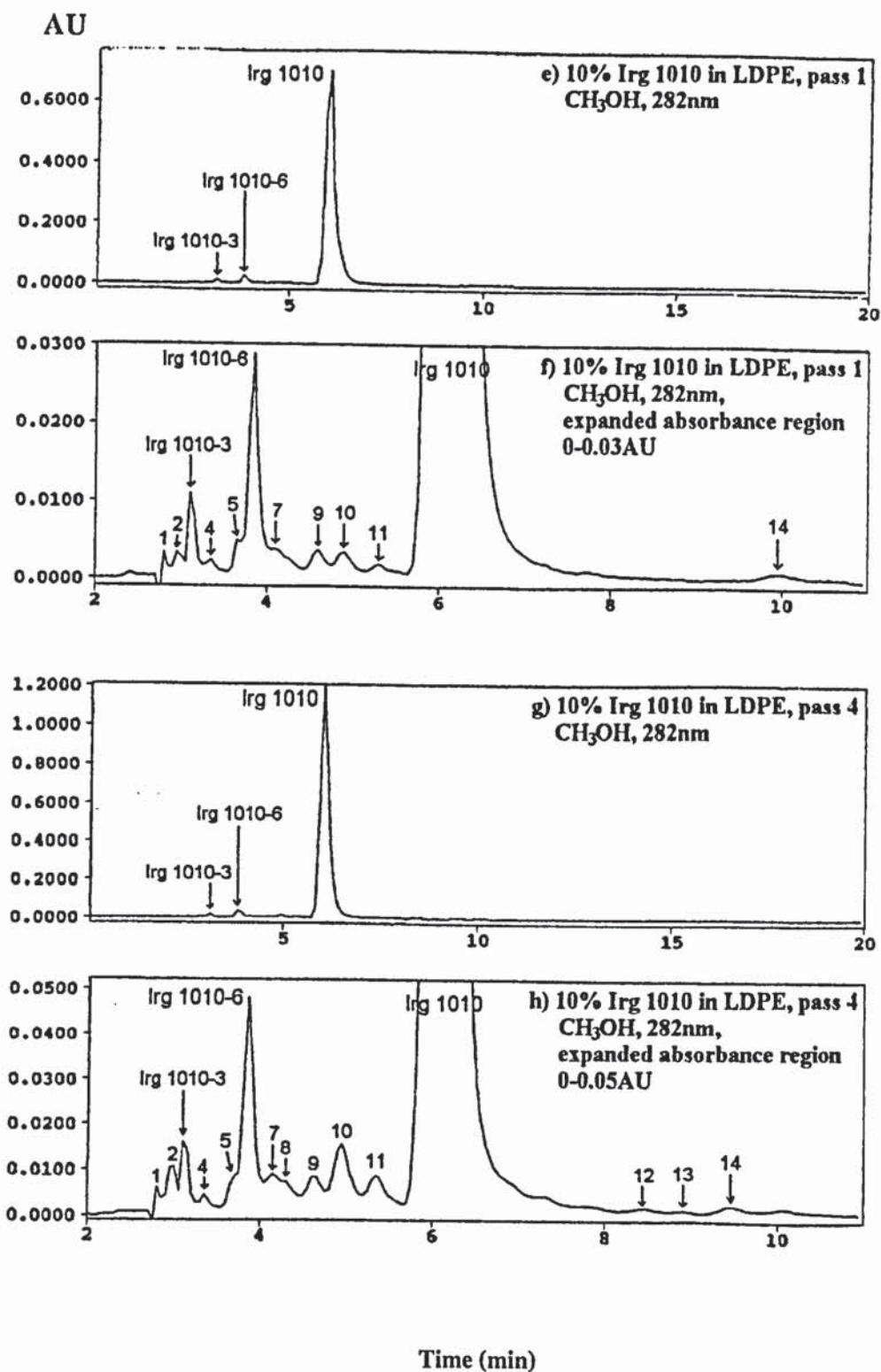


Figure 4.50: HPLC chromatograms of the products extracted from LDPE stabilised with (e-h) 10% Irg 1010, passes 1 (e, f) and 4 (g, h) (single screw extruder, 180°C) (see section 4.2.8, p. 395, and table 4.28, p. 385)

Instruments: Philips PU4100 liquid chromatograph and PU4120 diode array detector; Column: Zorbax ODS (4.6mm x 25cm); Flow rate: 1ml.min⁻¹
 Eluent: CH₃OH

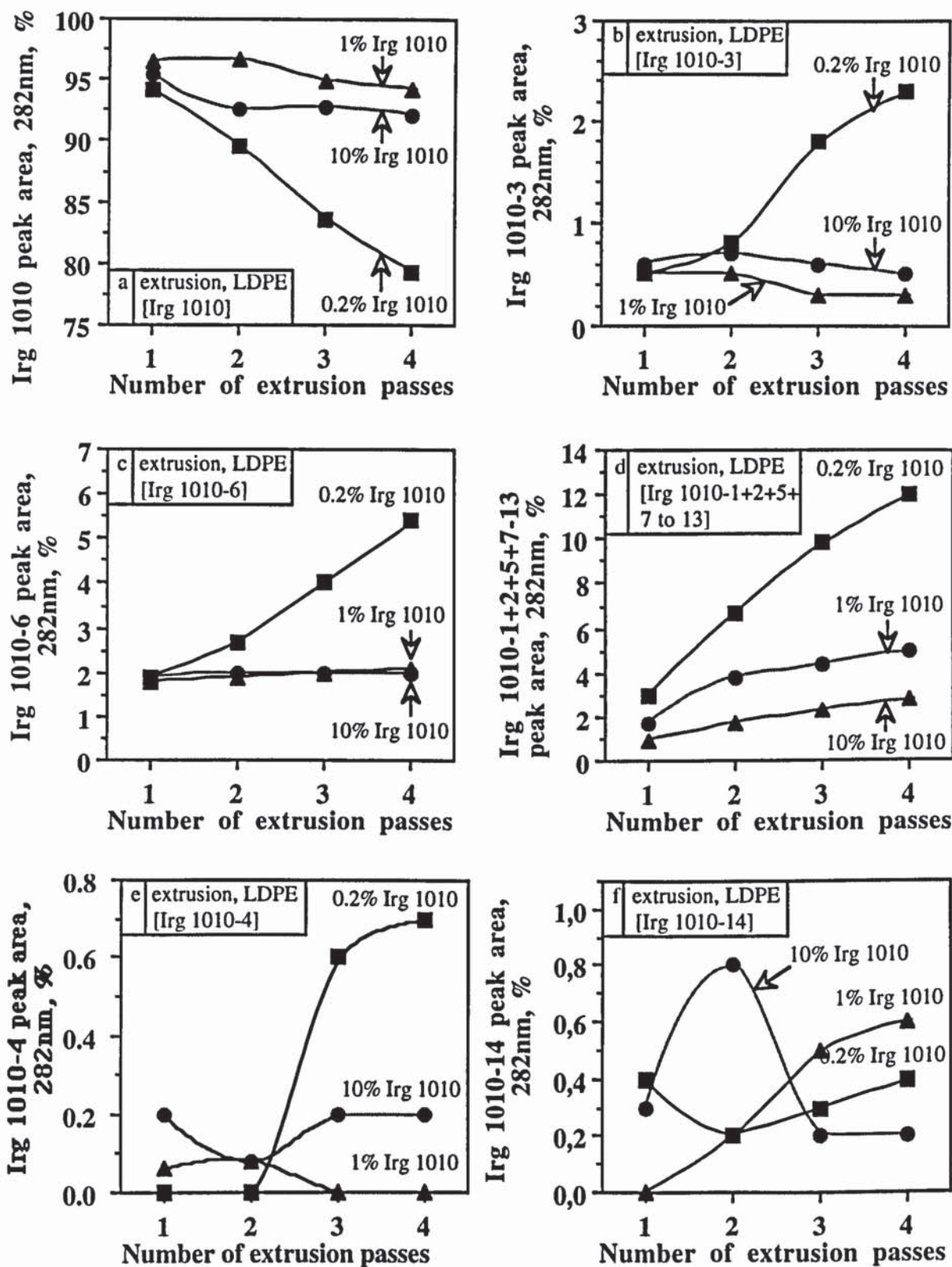


Figure 4.51: Effect of initial Irg 1010 concentration in LDPE and extrusion severity on the nature and the peak areas (282nm) of its transformation products (single screw extruder, 180°C) (see table 4.33, p. 397)

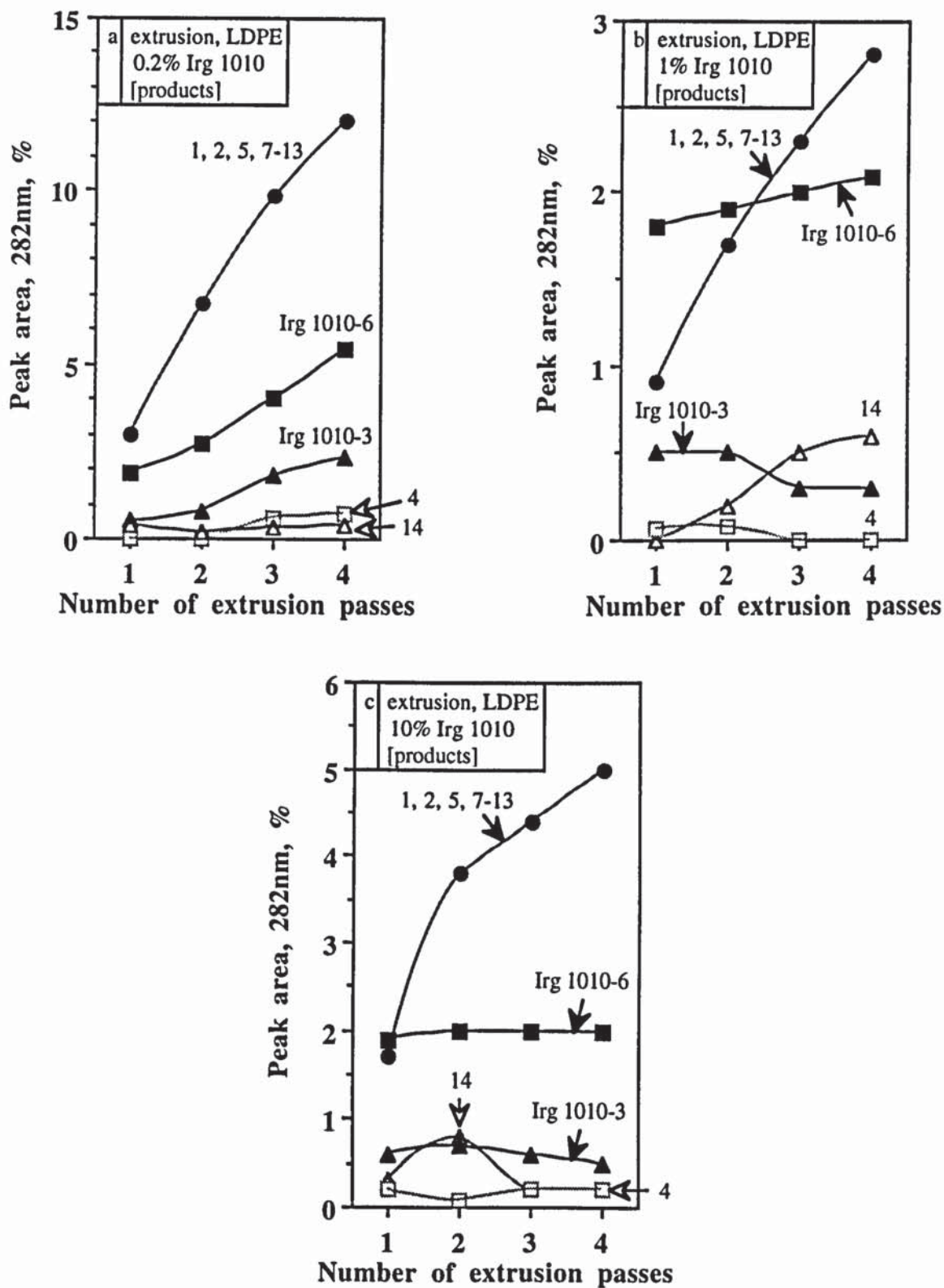


Figure 4.52: Effect of extrusion severity on the nature and distribution of the transformation products of Irg 1010 in LDPE (single screw extruder, 180°C) (see table 4.33, p. 397)

CHAPTER FIVE

**NATURE OF TRANSFORMATION PRODUCTS FORMED DURING THERMAL
AND UV AGEING OF PP STABILISED WITH TOC AND MIGRATION
CHARACTERISTICS OF TOC FROM LDPE FILMS INTO FOOD SIMULANTS**

LIST OF FIGURES-CHAPTER FIVE

Figure	Description	Page
5.1	Changes in the UV spectra of PP films, unstabilised and stabilised with 0.02, 0.05 and 0.1% Toc (CM, 10min) during thermal ageing	464
5.2	Decrease in the relative net absorbance at 290nm of Toc and its transformation products in PP films stabilised with 0.02 to 0.2% Toc and yield of total products extracted from PP stabilised with 0.05% Toc (CM, 10min) during thermal ageing	465
5.3 (a-d)	HPLC analysis of the extracts of PP stabilised with 0.05% Toc (CM, 10min) after thermal ageing at 140°C	485
5.3 (e-h)	HPLC analysis of the extracts of PP stabilised with 0.05% Toc (CM, 10min) after thermal ageing at 140°C	486
5.4	Effect of thermal ageing at 140°C on the concentration of the transformation products of Toc in PP stabilised with 0.05% Toc (CM, 10min)	487
5.5	Changes in the UV spectra of PP films (0.25mm thick), unstabilised and stabilised with 0.2 and 1% Toc (CM, 10min) during UV ageing	469
5.6	Decrease in the relative net absorbance at 290nm of Toc and its transformation products in PP films stabilised with 0.2 and 1% Toc and yield of total products extracted from PP stabilised with .4% Toc (CM,) 10min) during UV ageing	470
5.7 (a-d)	HPLC analysis of the extracts of PP stabilised with 1% Toc (CM, 10min) after UV ageing	488
5.7 (e-h)	HPLC analysis of the extracts of PP stabilised with 1% Toc (CM, 10min) after UV ageing	489
5.8	Effect of UV ageing on the concentration of the transformation products of Toc in PP stabilised with 1% Toc (CM, 10min)	490
5.9	Extent of migration of Toc and its transformation products from LDPE stabilised with 0.2% Toc, pass 1, into various food simulants under different conditions	474
5.10	Rate of migration of Toc and Irg 1076 from LDPE stabilised with 0.2% of each antioxidant, pass 1, into various food simulants	476

5.1 OBJECT AND METHODOLOGY

In chapter three, the melt, thermal and UV stabilisation efficiencies of Toc and its major transformation products (formed during processing of PP and LDPE) were compared with those of conventional hindered phenol antioxidant systems, in PP and LDPE. It was shown that Toc is an excellent melt stabiliser for polyolefins, far better than the hindered phenols Irg 1076 and Irg 1010 (see table 5.1 for structures), especially at low concentrations (e.g. 0.02%). Toc showed lower thermal efficiency during oven ageing in PP films than commercial antioxidants. However, the thermal stabilisation efficiency of Toc increased rapidly with decreasing temperatures (140-100°C), and the latter temperatures are far higher than end-use temperatures for food packaging materials. Therefore it is clear that Toc is also a good thermal stabiliser. Like other hindered phenols, Toc only possesses limited UV stabilisation activity in PP. The introduction of the hindered aryl phosphite U-626 in PP containing Toc lead to even better melt stability of the polymer and improved thermal stability, and in particular, colour retention during processing.

In chapter four, the nature of the transformation products formed during processing of Toc with PP and LDPE under different conditions were identified. It was shown that dimers (DHD, E and SPD, D), trimers (TRI, A, B, C), aldehydes (ALD 1-5) and a quinone (TQ) were formed (see table 5.1 for structures). The major products were themselves tested for their melt, thermal and UV stabilisation efficiencies in PP (chapter three), for a better understanding of the stabilisation mechanism of Toc in polyolefins. It was shown that ALD 1 and TQ had poor stabilisation efficiencies, whereas the dimers and the trimers lead to either similar (SPD, D, TRI, A, B, C) or better (DHD, E) stabilisation. The examination of their transformation products formed during processing in PP lead to the melt stabilisation mechanism of Toc in PP and LDPE.

In this chapter, the nature of the transformation products of Toc formed during thermal and UV ageing of PP films stabilised with Toc were first examined, to elucidate the reason for the lower thermal and, especially, UV stabilisation activities of Toc compared to

commercial antioxidants. PP films (0.25mm thick), stabilised with 0.05 and 1% Toc in an internal mixer (CM, 10min, 200°C) were used for the thermal and UV ageing experiments, respectively. Scheme 5.1 describes the methodology employed for the determination of the nature and concentrations of the transformation products of Toc formed during the ageing experiments. The rate of the oxidation and physical loss of Toc from the films during ageing was examined by UV spectroscopy of the films and extracts of the films. The effect of time of thermal and UV ageing on the nature of the transformation products of Toc was investigated by extracting the products from the polymer films with dichloromethane (see section 2.6), after increasing ageing times, and analysing them by NP-HPLC. The HPLC Rt and UV characteristics of the extracted products were then compared with those of known oxidation products of Toc and the concentration of the transformation products were determined from their HPLC peak areas and extinction coefficients (see section 2.11.1). For each different thermal and UV ageing time, three films were used and extracted together to reduce experimental errors. Errors on the concentrations were calculated from the errors on the peak integration procedure and the extinction coefficients (see section 2.11.1.3) and were found not to exceed 15, 6 and 5%, for concentrations below 10%, between 10-50% and 50-100%, respectively. Table 5.1 shows the structures and UV characteristics of the transformation products of Toc extracted from the films during thermal and UV ageing.

Finally, the migration characteristics of Toc and its transformation products from LDPE films into different food simulants were investigated and compared with those of the commercial hindered phenol Irg 1076. Migration of antioxidants is a major concern in applications involving polymers in direct contact with food and human environment. This concern is compounded by the realisation that very little is known about the nature and the migration behaviour of antioxidant transformation products. Unlike commercial hindered phenols, Toc can be considered as a safe and non-toxic stabiliser. However, the long term stability of the polymer is affected by the extent and rate of migration of the antioxidant from the polymer into the foodstuff. LDPE films (2cm x 9cm, 0.25mm thick), stabilised with 0.2% of each of the antioxidants Toc and Irg 1076 in a single screw extruder (one

pass, 180°C) were immersed in organic (olive oil, iso-octane and heptane) and aqueous food simulants (water, ethanol and diluted acetic acid) under specific conditions, and the extent (static tests) and rate (dynamic tests) of migration of the antioxidants into the solvent was determined by UV spectroscopy of the films (see section 2.12). All the tests were carried out in duplicate and UV measurements were taken at both ends of the films to establish the experimental error. It was found that errors on the extent of migration of the antioxidant did not exceed 10%.

Table 5.1: Chemical structures and UV characteristics of the transformation products formed during thermal (140°C) and UV ageing of Toc in PP films (0.25mm)

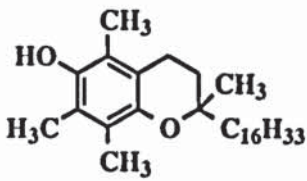
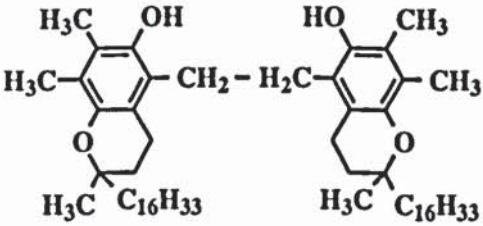
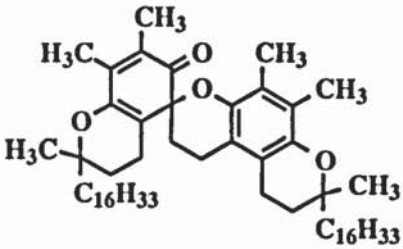
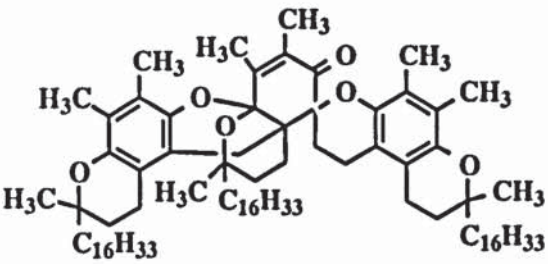
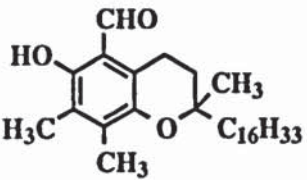
code name	chemical structure and name	MM	λ (max and 290 and/or 275nm) (E, l.g ⁻¹ .cm ⁻¹)
Toc	 <p style="text-align: center;">α-tocopherol</p>	430g	298 (8.6) 290 (8.1) 275 (3.3)
DHD, E (E1, E2, E3, E4)	 <p style="text-align: center;">dihydroxydimer</p>	858g	300 (8.9) 290 (7.9) 275 (3.0)
SPD, D (D1, D2, D3)	 <p style="text-align: center;">spirodimer</p>	856g	301 (5.2) 339 (2.5) 290 (4.3)
TRI, A, B, C (A1, A2, B, C)	 <p style="text-align: center;">trimer</p>	1285	292 (5.12) 290 (4.98)
ALD 1, F	 <p style="text-align: center;">5-formyl-γ-tocopherol</p>	444g	290 (20.5) 282 (19.7) 386 (6.4) 275 (15.2)

Table 5.1 continued

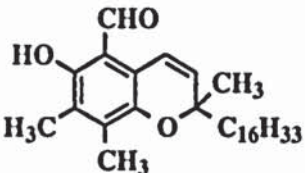
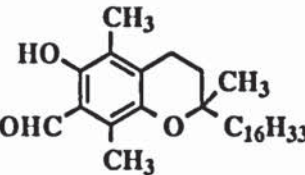
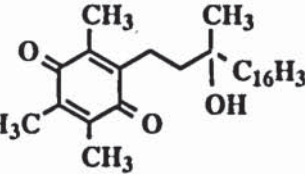
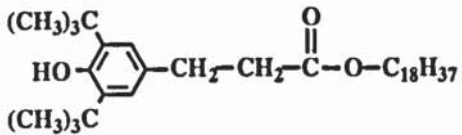
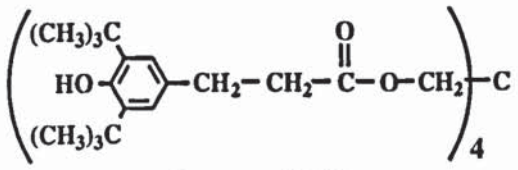
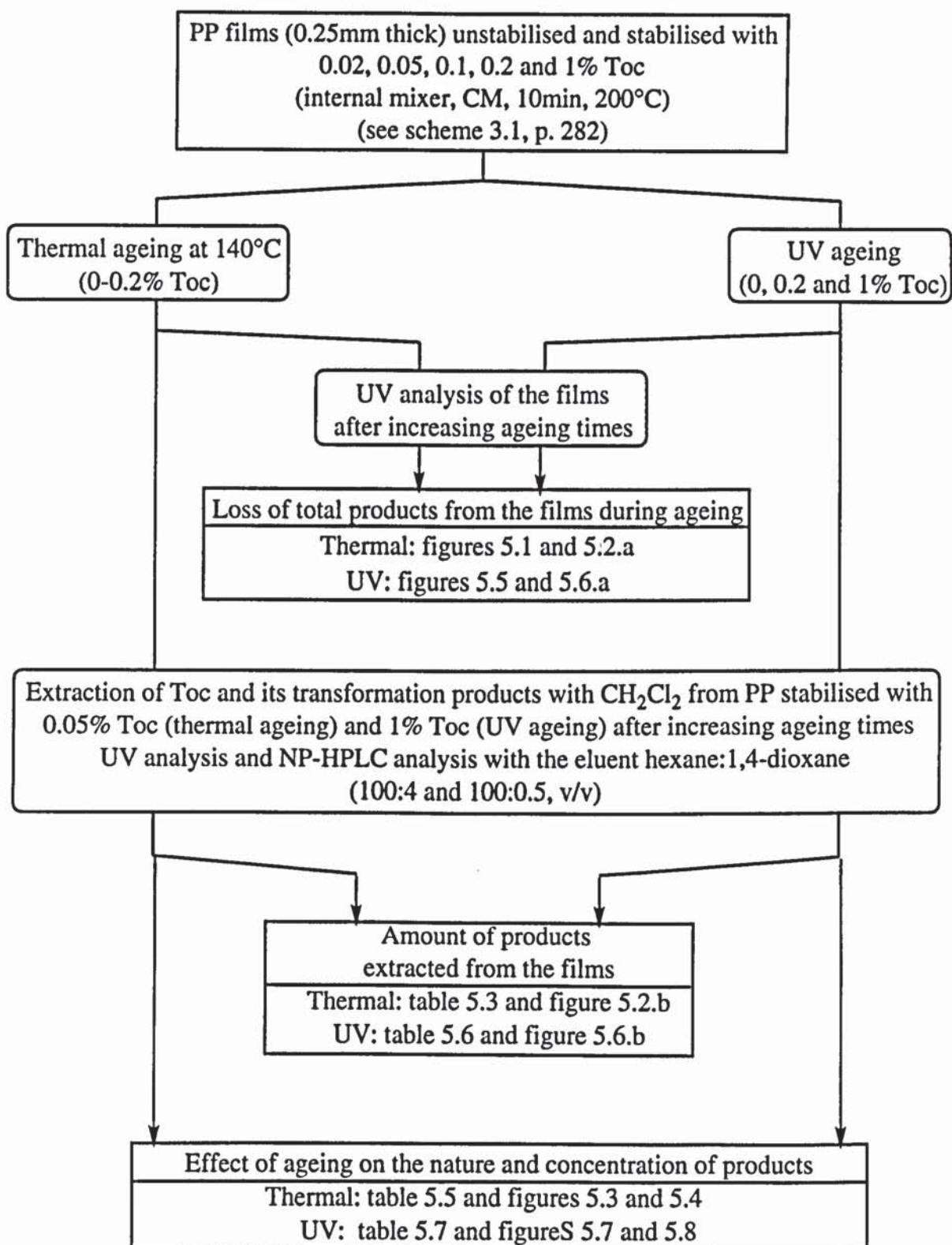
code name	chemical structure and name	MM	λ (max and 290 and/or 275nm) (E, l.g ⁻¹ .cm ⁻¹)
ALD 2, G	 <p>5-formyl-γ-tocopherol-3-en</p>	442g	285 (18.6) 297 (16.7) 404 (4.9) 290 (17.7)
ALD 3, H	 <p>7-formyl-β-tocopherol</p>	444g	283 (16.0) 395 (4.3) 290 (15.6)
ALD 4	unknown	-	280, 380
ALD 5	unknown	-	280, 382
TQ	 <p>α-tocoquinone</p>	446g	260 (39.0) 268 (38.4) 275 (11.9)

Table 5.2: Chemical structures and UV characteristics of the commercial hindered phenols Irganox 1076 and Irg 1010

code name	chemical structure and name	MM	λ_{\max} , nm (E, l.g ⁻¹ .cm ⁻¹)
Irg 1076	 <p>Irganox 1076</p>	530g	282 (3.8) 276 (3.8)
Irg 1010	 <p>Irganox 1010</p>	1177g	282 (6.4) 276 (6.3)



Scheme 5.1: Methodology for the determinations of the loss of total products and of the nature and concentrations of the transformation products formed during thermal and UV ageing of PP stabilised with Toc (internal mixer, CM, 10min, 200°C)

5.2 NATURE OF TRANSFORMATION PRODUCTS OF Toc FORMED IN PP DURING THERMAL AGEING AT 140°C

5.2.1 Physical loss of Toc during ageing

PP films (0.25mm thick), unstabilised and stabilised with various concentrations of Toc (0.02-0.2%) (CM, 10min, 200°C), were placed in single cell Wallace ovens at 140°C under air atmosphere (see section 2.4.2 for procedure and scheme 5.1 for methodology). The extent of loss of the antioxidant and its transformation products was evaluated for all the samples by recording the decrease in their net absorbance at 290nm during ageing, until embrittlement was reached (see section 2.13.1). For example, Figure 5.1 shows the changes in UV spectra of unstabilised PP films and PP films stabilised with 0.02, 0.05 and 0.1% Toc during ageing until embrittlement. Figure 5.2.a reveals the decrease in relative net absorbance at 290nm of Toc and its transformation products in PP films stabilised with 0.02, 0.05, 0.1 and 0.2% Toc during ageing. The products from PP stabilised with 0.05% Toc were extracted after increasing ageing times and the extent of recovery was determined by UV analysis of the extracts, using equation 2.8, p. 108 (see table 5.3). The results obtained were compared with the change in relative net absorbance at 290nm of PP stabilised with 0.05% Toc during ageing (figure 5.2.b).

The UV spectra of unstabilised and stabilised PP films all show a general increase in absorbance over the range 190-400nm with increasing ageing times and, when embrittlement is reached, the increase is more pronounced, especially around 205nm, as shown in figures 5.1.a-d. The UV spectra of PP stabilised with Toc (figure 5.1.b-d) also show a decrease in absorption of the antioxidant and its transformation products, which is suggested to be caused mainly by their loss by volatilisation. The decrease in relative net absorbance is very similar for each initial Toc concentration before embrittlement is reached. After or near embrittlement of the films, no absorbance can be detected by UV spectroscopy, again suggesting that the degradation of PP is mainly caused by physical loss of the antioxidant. This was confirmed by the UV analysis of the extracts of PP stabilised with 0.05% Toc, revealing a decrease in the amount of total products extracted,

m'AO, with time of ageing, as shown in table 5.3 and figure 5.2.b. Figure 5.2.b also reveals that the decrease in amount of products extracted is similar to the decrease in relative absorbance at 290nm.

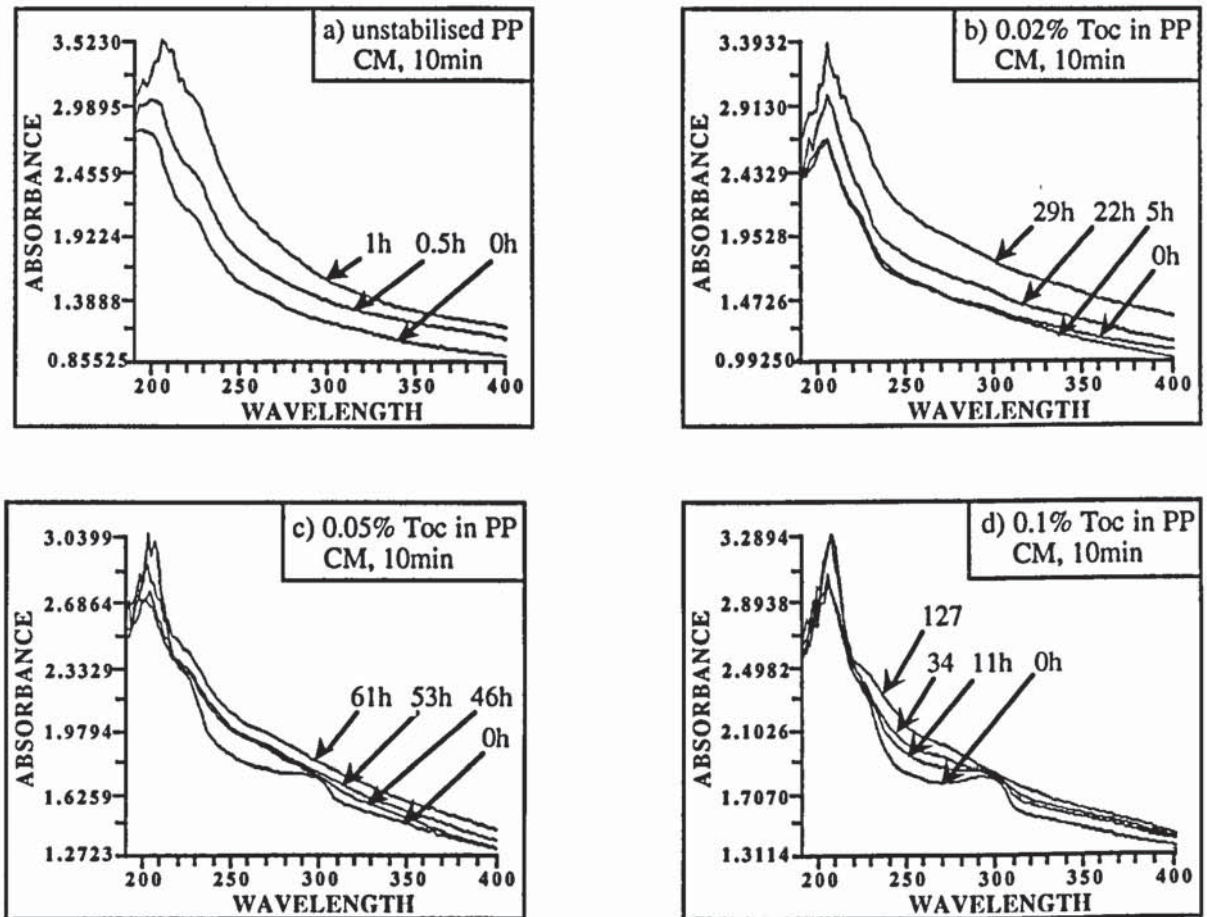


Figure 5.1: Changes in the UV spectra of PP films (0.25mm thick), unstabilised and stabilised with 0.02, 0.05 and 0.1% Toc, in an internal mixer (CM, 10min, 200°C) during thermal ageing at 140°C until embrittlement

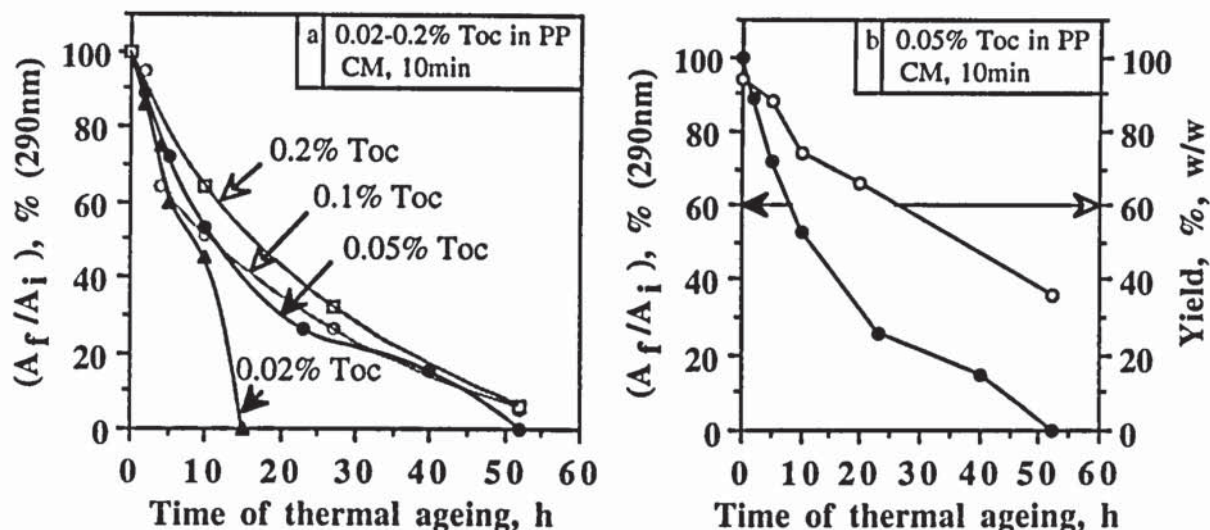


Figure 5.2: Decrease in the relative net absorbance at 290nm of Toc and its transformation products in PP films (0.25mm thick) stabilised with 0.02 to 0.2% Toc (a) and yield of total products extracted from PP stabilised with 0.05% Toc (b) (internal mixer, CM, 10min, 200°C), during thermal ageing at 140°C, measured by UV spectroscopy

Table 5.3: Total concentration of Toc and its transformation products recovered from PP films (0.25mm thick) stabilised with 0.05% Toc (internal mixer, CM, 200°C), after thermal ageing at 140°C, measured by UV analysis of the extracts at 290nm (figure 5.2.b)

Time of ageing, h	absorbance, 290nm	\bar{E} , $\text{l.g}^{-1}.\text{cm}^{-1}$	c_{TQ} , % weight	v, ml	m_i , g	m'_{AO} , % weight	yield of total products, %
0	0.62051	9.0	1.4	2	2.9885	0.047	94
5	0.14539	9.4	2.5	2	0.7213	0.044	88
10	0.19011	9.5	2.3	2	1.0984	0.037	74
20	0.22859	11.3	3.3	2	1.2540	0.033	66
52	0.12985	14.1	7.0	2	1.1132	0.018	36

Where,

\bar{E} = extinction coefficient of the extract ($\text{l.g}^{-1}.\text{cm}^{-1}$)

c_{TQ} = concentration of TQ in the extract (% weight)

v = volume of solvent (l)

m_i = weight of polymer films before extraction (%)

m'_{AO} = weight of extract in the polymer (%)

5.2.2 Nature of transformation products formed during thermal ageing of PP stabilised with Toc

The nature of the products formed during thermal ageing at 140°C of PP films (0.25mm thick) stabilised with 0.05% Toc (CM, 10min, 200°C) were examined by extracting them from the polymer films with dichloromethane (see section 2.6 for procedure) after different ageing times, until embrittlement was reached (52h). The extracts were then analysed by NP-HPLC using the solvent system hexane:1,4-dioxane (100:4 and 100:0.5, v/v) at 275nm (to detect the presence of quinones) and 290nm (see figures 5.3.a-h, p. 485, for typical chromatograms). The HPLC Rt and the UV characteristics of the different products were compared with known oxidation products of Toc and PP (see table 5.4). The concentrations of the products were determined from their HPLC peak areas and extinction coefficients (see section 2.11 for procedure) and table 5.5 shows the results.

Figure 5.4, p. 487, reveals the effect of thermal ageing on the concentration of Toc and its transformation products in PP. Figure 5.4.a shows that the loss of Toc during thermal ageing is fast, with only 15% Toc remaining when embrittlement is reached (52h). The sharp decrease in Toc concentration with time of ageing is initially (0-5min) accompanied by an increase in DHD, E, TRI, A, B, C and ALD 1-3 concentrations (figure 5.4.a-c), with ALD 1 and TRI, A, B, C being the major products. After 5min of ageing, the concentrations of TRI, A, B, C and ALD 1-5 continue to increase, whereas the amount of DHD, E decreases. This suggests that DHD, E and a small amount of Toc undergo further oxidation to TRI, A, B, C and ALD 1-5, respectively, during ageing. However, the increase in the amount of transformation products does not account entirely for the loss of Toc (figure 5.4.a), suggesting that Toc is also lost by volatilisation from the polymer film. After about 30h of ageing, the concentration of TRI, A, B, C also starts to decrease, whereas the concentration of ALD 1-5 remains more or less constant. This suggests that the loss by volatilisation of TRI, A, B, C and ALD 1-5 is slower than that of Toc during ageing and that ALD 1-5 (particularly ALD 1, see figure 5.4.c) are retained the longest.

Table 5.4: HPLC Rt and UV characteristics of transformation products of Toc and LMWP extracted from PP films (0.25mm thick) stabilised with 0.05% Toc (internal mixer, CM, 10min, 200°C) and thermal aged at 140°C (solvent ratios are in hexane:1,4-dioxane, v/v)

compound		Rt, min:sec		λ_{max} , nm
		100:4	100:0.5	
LMWP		3:00, 3:30, 3:50, 4:50	3:20, 3:40, 3:55, 4:30, 6:10	250, 232, (232, 275), 281, 245
TRI	A (A1, A2)	2:30-5:00	9:30, 9:50	292
	B (B1-B4)		15-24	
	C	5:40	30-40	
SPD	D (D1-D3)	3:30-5:00	22-27	301, 339
ALD	1, F	5:10	13:00	239, 290, 282, 386
	2, G	5:00	10:30	250, 285, 297, 404
	3, H	4:50	9:30	283, >390
	4, J	5:10	17:00	281, 379
	5, K		23:00	281, 372
Toc		11:00	45:00	298
DHD	E (E1-E4)	13-17	180	300
TQ		32:00	-	262, 268
Figures (page)		5.3.a-d (486)	5.3.e-h (487)	

Table 5.5: Concentration of products extracted from PP stabilised with 0.05% Toc (internal mixer, CM, 10min, 200°C) and thermal aged at 140°C (figure 5.4, p. 487)

Time of ageing, h	concentration, % weight										Total, %
	Toc	DHD, E	SPD, D	TRI, A, B, C	ALD 1, F	ALD 2, G	ALD 3, H	ALD 4, J	ALD 5, K	TQ	
0	83.4	0	0.5	5.5	2.4	0.4	0.7	0.2	0	1.1	94
5	68.6	4.5	0	7.6	3.5	0.5	1.1	0	0	2.2	88
10	55.8	3.1	0	8.9	3.3	0.4	0.6	0.2	0	1.7	74
20	41.0	1.7	0	11.3	6.1	1.1	2.0	0.7	0	2.1	66
52	15.4	0	0	7.4	6.4	1.0	1.5	0.6	1.2	2.5	36

5.3 NATURE OF TRANSFORMATION PRODUCTS OF TOC FORMED IN PP DURING UV AGEING

5.3.1 Physical loss of Toc during ageing

PP films (0.25mm thick), unstabilised and stabilised with 0.2 and 1% Toc in an internal mixer (CM, 10min, 200°C), were subjected to UV irradiation in an accelerated UV ageing cabinet (see section 2.4.3 for procedure). The extent of loss of the antioxidant and its transformation products during ageing was evaluated by measuring the decrease in their net absorbance at 290nm (see section 2.13.1). Figure 5.5 shows the changes in UV spectra of PP films, unstabilised and stabilised with 0.2 and 1% Toc, during ageing. Figure 5.6.a reveals the decrease in relative net absorbance at 290nm of Toc and its transformation products in PP films stabilised with 0.2 and 1% Toc. The products from PP stabilised with 1% Toc were extracted after increasing ageing times and the amount of products recovered was determined by UV analysis of the extracts, using equation 2.8, p. 108 (see table 5.6). The results obtained were compared with the change in relative net absorbance at 290nm of PP stabilised with 1% Toc during ageing (figure 5.6.b).

Similar to thermal ageing, the UV spectra of unstabilised and stabilised PP (see figures 5.5.a-c) show a general increase in absorbance over the range 190-400nm with increasing ageing times. However, the UV spectra of PP stabilised with Toc reveal that most of the products are lost well before embrittlement (i.e. 201h and 250h for 0.2 and 1% Toc, respectively) is reached. Loss of products by volatilisation is expected to be much slower during UV ageing (temperature of about 35°C) than during thermal ageing at 140°C. Unlike during thermal ageing, the loss of products from the films is dependent on the initial concentrations of Toc, as shown in figure 5.6.a. The decrease in relative net absorbance at 290nm is much faster for 0.2% Toc in PP than 1% Toc in PP, suggesting that the products are physically lost from the polymer films. The decrease in the amount of products extracted from PP stabilised with 1% Toc with time of ageing is similar to the decrease in relative net absorbance at 290nm, as shown in figure 5.6.b.

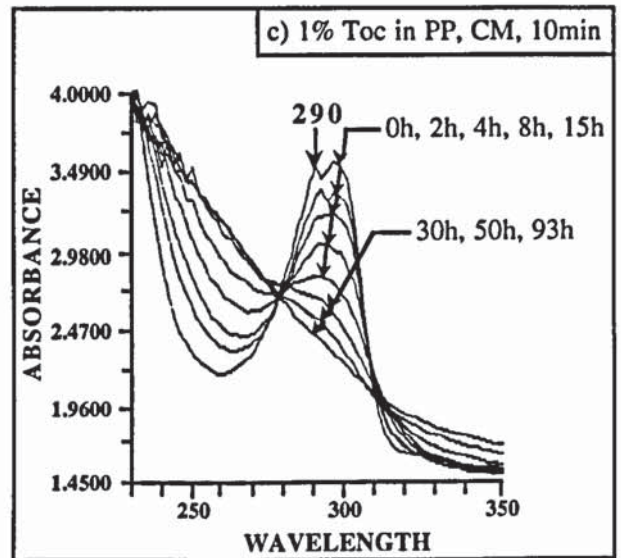
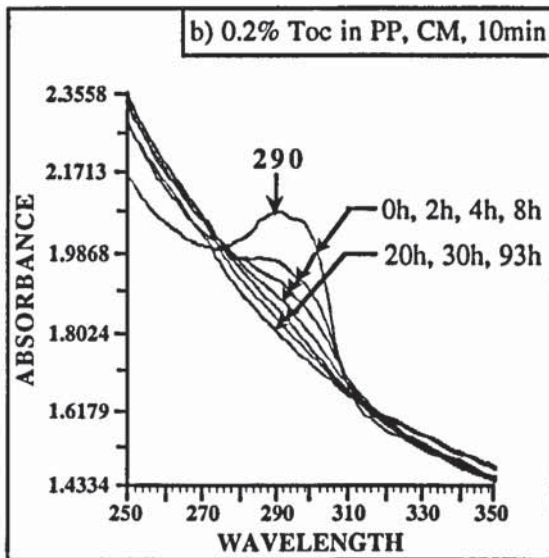
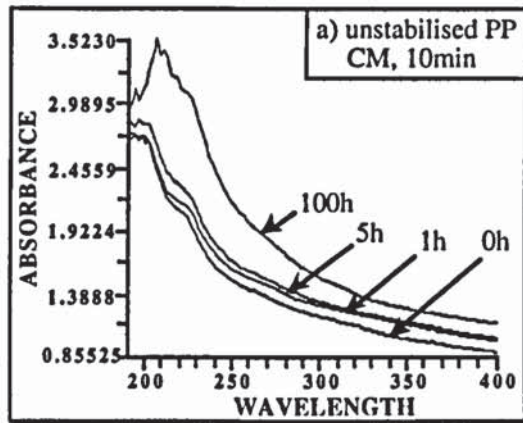


Figure 5.5: Changes in the UV spectra of PP films (0.25mm thick), unstabilised and stabilised with 0.2 and 1% Toc, in an internal mixer (CM, 10min, 200°C) during UV ageing

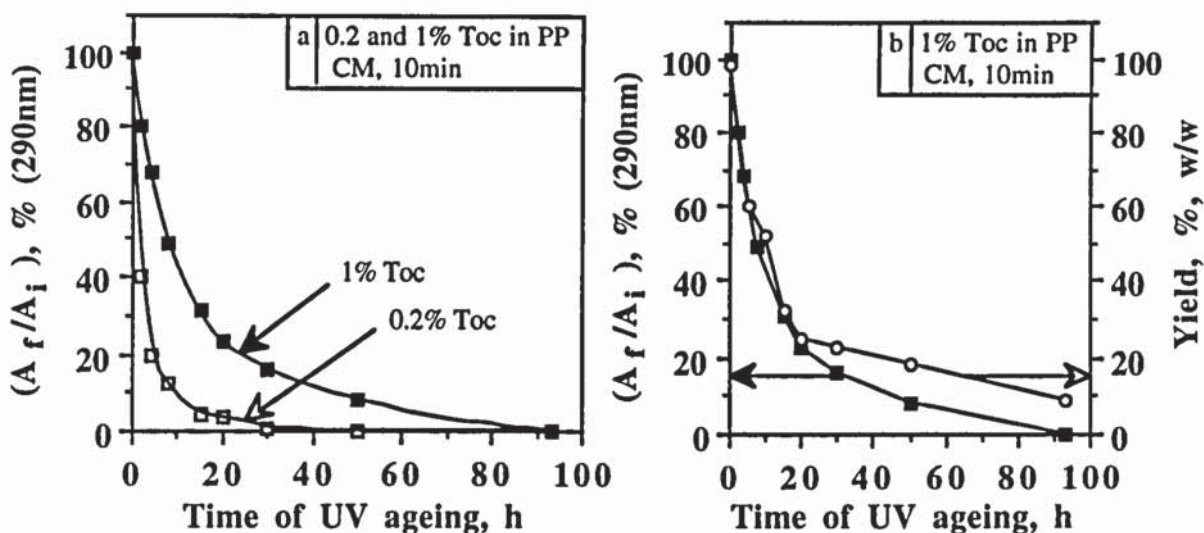


Figure 5.6: Decrease in relative net absorbance at 290nm of Toc and its transformation products in PP films (0.25mm thick) stabilised with 0.2 and 1% Toc (a) and yield of total products extracted from PP stabilised with 1% Toc (b) (internal mixer, CM, 10min, 200°C) during UV ageing, measured by UV spectroscopy

Table 5.6: Total concentration of Toc and its transformation products recovered from PP films (0.25mm thick) stabilised with 1% Toc (internal mixer, CM, 200°C), after UV ageing, measured by UV analysis of the extracts at 290nm (figure 5.6.b)

Time of ageing, h	absorbance, 290nm	\bar{E} , l.g ⁻¹ .cm ⁻¹	cTQ, % weight	v, ml	m _i , g	m'AO, % weight	yield of total products, %
0	0.42541	8.1	0.4	5	0.2700	0.98	98
5	0.24412	8.7	2.1	5	0.2370	0.60	60
10	0.24158	10.2	1.7	5	0.2376	0.51	51
15	0.18541	11.4	1.9	5	0.2617	0.32	32
20	0.18501	12.8	2.1	5	0.2985	0.25	25
30	0.11918	12.0	1.3	5	0.2337	0.22	22
52	0.09482	11.1	0.9	5	0.2381	0.18	18
98	0.05173	10.9	1.1	5	0.2658	0.09	9

Where,

\bar{E} = extinction coefficient of the extract ($\text{l.g}^{-1}.\text{cm}^{-1}$)

c_{TQ} = concentration of TQ in the extract (% weight)

v = volume of solvent (l)

m_i = weight of polymer films before extraction (%)

m'_{AO} = weight of extract in the polymer (%)

5.3.2 Nature of transformation products formed during UV ageing of PP stabilised with Toc

The nature of the products formed during UV ageing of PP films (0.25mm thick) stabilised with 1% Toc in an internal mixer (CM, 10min, 200°C) were examined by extracting them from the polymer films with dichloromethane (see section 2.6 for procedure) after different ageing times. The extracts were then analysed by NP-HPLC using the solvent system hexane:1,4-dioxane (100:4 and 100:0.5, v/v) at 275nm (to detect the presence of quinones) and 290nm (see figures 5.7.a-h, p. 488, for typical chromatograms). The HPLC R_t and the UV characteristics of the different products were compared with known oxidation products of Toc and PP (see table 5.4). The concentrations of the products were determined from their HPLC peak areas and extinction coefficients (see section 2.11 for procedure) and table 5.7 shows the results. Figure 5.8 reveals the effect of UV ageing on the concentration of the transformation products of Toc in PP.

During the first 5 hours of UV ageing, the concentration of Toc decreases rapidly and more than half of the antioxidant is lost after 5 hours (85 → 39%). On the other hand, SPD, D, TRI, A, B, C and ALD 1-4 show a small increase in their concentrations whereas the concentration of DHD, E decreases (see figures 5.8.a-c, p. 490). This suggests that small amounts of Toc and DHD, E undergo oxidation to SPD, D, TRI, A, B, C and ALD 1-4. A similar behaviour was initially observed after 5h of thermal ageing of PP stabilised with 0.05% Toc (figure 5.4, p. 487) but the decrease in Toc concentration with time of ageing was much slower. Indeed, during UV ageing, most of the products are lost when less than half (100h) of the embrittlement time is reached (250h), whereas during thermal ageing

most of the products are lost by embrittlement time, which is caused by the higher stability of PP during UV exposure than thermal ageing. The loss of Toc is suggested to be caused by the formation of photosensitising products leading to the photodecomposition of the antioxidant, rather than volatilisation, like during thermal ageing. After 5 hours of UV ageing, the concentration of SPD, D decreases rapidly, whereas the concentrations of TRI, A, B, C remain more or less constant. The concentrations of ALD 1-4 start to decrease after about 20h of ageing. ALD 1, 2, 3 and 4 all behave in a similar way (figure 5.8.c), their concentrations first increasing during the first 10min of ageing and then decreasing. However, ALD 4 is formed later (at about 20h) and its concentration seems to increase slightly again when 100h of ageing are reached.

Table 5.7: Concentration of products extracted from PP stabilised with 1% Toc (internal mixer, CM, 10min, 200°C) and UV aged (figure 5.8, p. 490)

Time of ageing, h	concentration, % weight									Total, %
	Toc	DHD,E	SPD, D	TRI, A, B, C	ALD 1, F	ALD 2, G	ALD 3, H	ALD 4, J	TQ	
0	84.8	6.1	4.5	1.8	0.5	0	0	0	0.3	98
5	39.0	1.2	9.1	7.1	1.4	1.0	0	0	1.3	60
10	33.5	1.4	4.6	5.5	3.0	0.8	1.5	0	0.8	51
15	17.6	0.4	3.1	5.2	3.0	1.2	1.0	0	0.6	32
20	11.3	0.6	2.2	4.6	3.1	1.5	0.6	0.6	0.5	25
30	9.6	0.4	0.9	6.4	2.4	0.6	0.9	0.5	0.3	22
52	9.2	0.4	0.5	5.1	1.6	0.3	0.6	0.2	0.2	18
98	1.3	0.1	0	6.2	0.6	0	0	0.7	0.1	9

5.4 MIGRATION OF TOC AND IRG 1076 AND THEIR TRANSFORMATION PRODUCTS FROM LDPE FILMS INTO FOOD SIMULANTS

5.4.1 Static migration tests

Migration of antioxidants and their transformation products from food packaging materials into the foodstuff is a major concern because of the unknown toxicological consequences. Furthermore, the long term stability of the polymer is affected by the loss of the antioxidant. Static migration tests were carried out for LDPE films (2cm x 9cm, 0.25mm thick) stabilised with 0.2% Toc in a single screw extruder (one pass, 180°C) (see section 2.12 for procedure). Toc is relatively highly retained (79%) after the first extrusion pass and transformation products include TRI, A, B, C (11%), SPD, D (3%), TQ (3%), ALD 1 (1%), ALD 4 (1%) and DHD, E (1%) (see table 5.1 for structures). The films were immersed into 100ml food simulant for a specific period of time and temperature, according to EC and FDA Directives (see tables 2.67 and 2.68, p. 139). The extent of migration, M , of Toc and its transformation products into various food simulants was determined by measuring their net absorbance before (A_i) and after (A_f) the migration test (see equation 2.31, p. 140) and the results are shown in figure 5.9.

Figure 5.9 shows that the test condition, i.e. migration at 70°C for 2h or 40°C for 10 days, in a given food simulant, did not influence greatly the extent of migration of Toc and its transformation products. M was the highest in the fatty food simulants iso-octane and heptane ($\geq 95\%$) and was relatively high in olive oil, especially when the test condition of 40°C for 10 days was used. On the other hand, M was relatively low in the aqueous food simulants ($\leq 17\%$) and was very low in water ($\leq 2\%$). The migration pattern obtained in the order of decreasing extent of migration was as follows:

iso-octane = heptane > olive oil >> 15% ethanol > 3% acetic acid > water

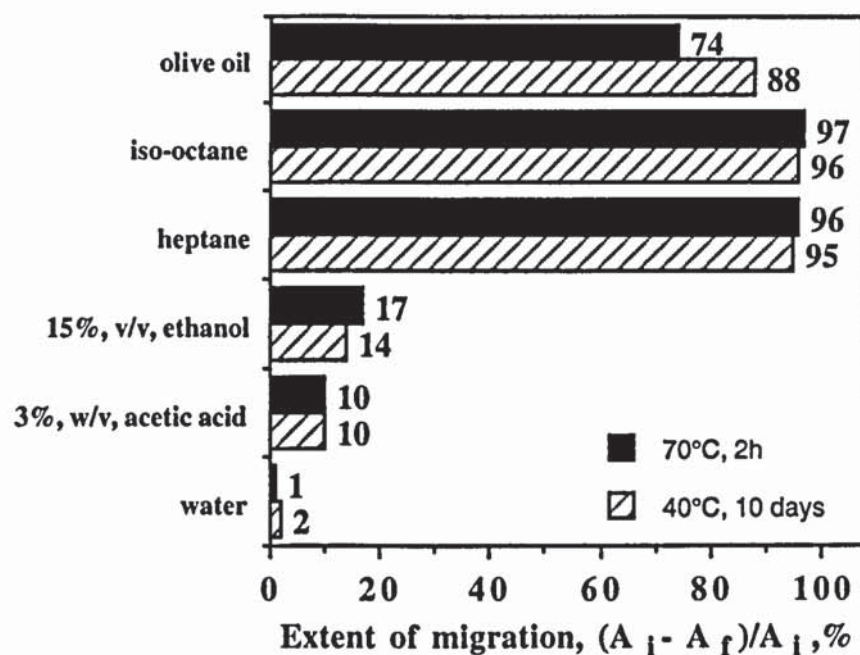


Figure 5.9: Extent of migration of Toc and its transformation products from LDPE stabilised with 0.2% Toc (single screw extruder, one pass, 180°C) into various food simulants under different conditions

5.4.2 Dynamic migration tests

Dynamic migration tests were carried out for LDPE films (2cm x 9cm, 0.25mm thick) stabilised with 0.2% of each of the antioxidants Toc and Irg 1076 (single screw extruder, one pass, 180°C). After the first extrusion pass, it was shown that, like Toc, Irg 1076 was also highly retained (see figure 4.47.a, p. 447) and its major transformation products were found to be the corresponding cinnamate, C-Irg 1076, biscinnamate, BC-Irg 1076, and Irg 1076-11, which is possibly the quinone methide of Irg 1076, QM-Irg 1076 (see table 4.2, p. 332, for structures). The polymer films were immersed into 100ml of each of the food simulants shown in table 5.8 and the rate of migration at 40°C of the antioxidant and its transformation products was followed by UV spectroscopy, until a constant value of M was obtained (see section 2.12 for procedure). Table 5.8 and 5.9 show the results for LDPE stabilised with Toc and Irg 1076, respectively.

Figure 5.10 reveals the rate of migration of each of the antioxidants Toc and Irg 1076 and their transformation products into various food simulants. The migration characteristics of Toc and Irg 1076 are very similar. It is clear, for both antioxidants, that the migration into the fatty food simulants iso-octane and heptane is very fast, most of the products are lost from the film after 1h. On the other hand, the migration into olive oil is much slower, although it was shown to be very high after 2h at 70°C and 10 days at 40°C (see figure 5.9). Finally, as expected, the migration into 3% aqueous acetic acid remains very low.

Table 5.8: Effect of time on the extent of migration, M, of Toc and its transformation products from LDPE films (2cm x 9cm, 0.25mm thick) stabilised with 0.2% Toc (single screw extruder, one pass, 180°C) into various food simulants

time (h:min)	M, %			
	olive oil	iso-octane	heptane	3% acetic acid
0	0	0	0	0
0:15	9.4	56.1	87.2	0.7
0:30	14.8		91.4	
0:35		81.5		
0:45				3.3
1:00	20	91.7	90.8	
1:15				6.0
1:30		94.3		
1:45	26.8			10.7
2:00			94.4	10.7
2:45	30.2			10.7
3:00		94.3	95.5	
3:15	36.9			
3:45	38.3	94.3	95.9	
4:45	41.6			
5:15	44.3			
5:45	50.5			
6:15	56.7			
6:45	56.7			

Table 5.9: Effect of time on the extent of migration, M, of Irg 1076 and its transformation products from LDPE films (2cm x 9cm, 0.25mm thick) stabilised with 0.2% Irg 1076 (single screw extruder, one pass, 180°C) into various food simulants

time (h:min)	M, %			
	olive oil	iso-octane	heptane	3% acetic acid
0	0	0	0	0
0:15	14.5	34.5	81.1	8.3
0:30	21.3	87.5	100	
0:45				9.6
1:00	27.4	97.6	100	
1:15				10.2
1:30	30.2			
1:45				11.6
2:15	32.9			
4:00	45.2	97.6	100	11.6

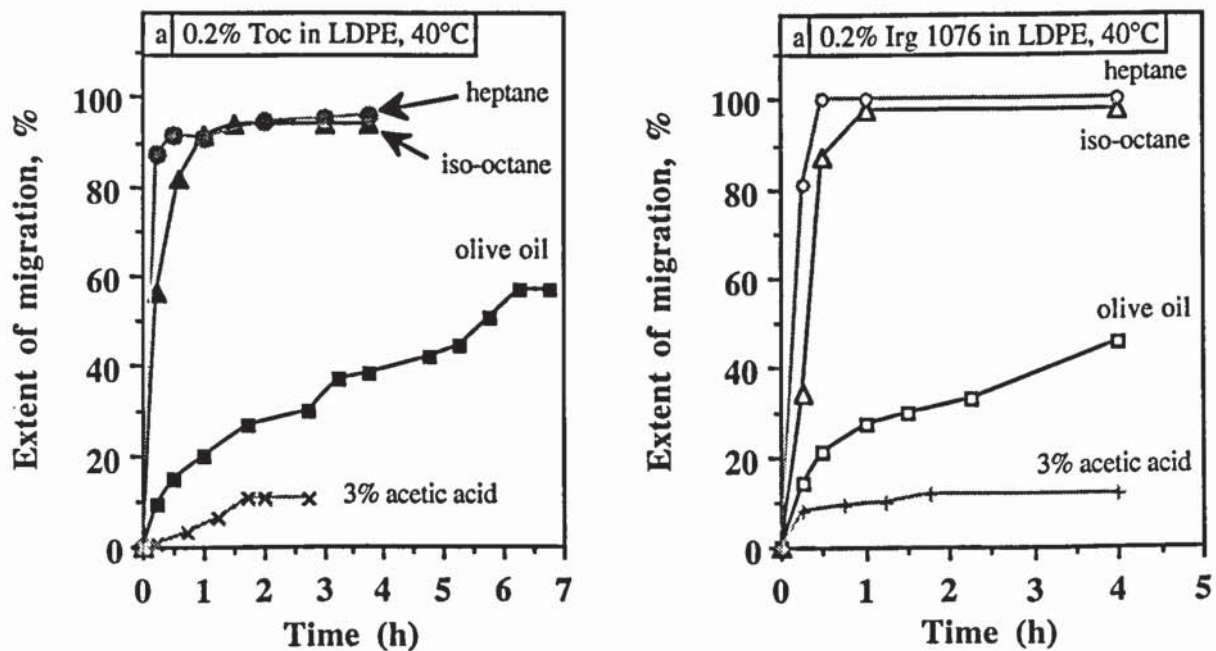


Figure 5.10: Rate of migration of each of the antioxidants Toc (a) and Irg 1076 (b) from LDPE stabilised with 0.2% of each antioxidant (single screw extruder, one pass, 180°C) into various food simulants

5.5 DISCUSSION

5.5.1 Mechanism of stabilisation of Toc in PP during thermal ageing at 140°C

5.5.1.1 Effect of initial Toc concentration in PP on the degradation of the polymer and loss of the antioxidant during ageing

PP films (0.25mm thick), unstabilised and stabilised with 0.02, 0.05, 0.1 and 0.2% Toc in an internal mixer (CM, 10min, 200°C), were subjected to thermal ageing at 140°C in circulating air ovens, and their decrease in relative net absorbance at 290nm during ageing until embrittlement was followed by UV spectroscopy (see figures 5.1-5.2, p. 464-465). The general increase in absorbance over the range 190-400nm with increasing ageing times for both unstabilised and stabilised films is caused by the thermal degradation of PP, i.e. chain scission (figure 5.1). It was shown [103] that during thermal ageing of unstabilised PP at 85°C, the formation of hydroperoxides, ketones, acids, alcohols and esters are responsible for its degradation. These are likely to cause the increase in the UV absorbance of the polymer film during ageing. Hydroperoxides, which are initially formed during processing of the polymer [13-15], are the most important source of initiating radicals, leading to the formation of alkyl and alkoxy radicals (reactions 1.4-1.6 in scheme 1.1, p. 36). Alkyl radicals react rapidly with oxygen to form peroxy radicals (reaction 1.2 in scheme 1.1).

In PP stabilised with Toc, the decrease in the absorbance of the antioxidant with increasing ageing times (figure 5.1.b-d) is mainly caused by its physical loss from the polymer, leading to the degradation of the polymer. Figure 5.2.a shows that the decrease in relative net absorbance of Toc and its transformation products with time of ageing is very similar at all initial Toc concentrations until embrittlement is reached, suggesting that the degradation of the polymer is caused by physical loss of the antioxidant. The physical loss of total products from PP stabilised with 0.05% Toc was followed by UV analysis of the extracts during ageing (see figure 5.2.b and table 5.3, p. 465). It was shown that only 36% of products were retained in the polymer when embrittlement was reached (52h),

confirming that the degradation of the polymer is mainly caused by the physical loss of the antioxidant and its transformation products by volatilisation. Hence, volatilisation of the products is also expected to contribute to the degradation of PP stabilised with the lower and higher concentrations of Toc. This explains the decrease of the thermal stability of PP stabilised with Toc with decreasing initial concentrations of the antioxidant (see figure 3.8, p. 314).

5.5.1.2 Effect of thermal ageing on the nature of the transformation products of Toc

The nature of the products formed from Toc during thermal ageing at 140°C of PP films (0.25mm thick) stabilised with 0.05% Toc in an internal mixer (CM, 10min, 200°C) were identified by comparing their HPLC Rt and UV characteristics with those of known oxidation products of Toc. Figures 5.3 and 5.4, p. 485, show that these are dimers (DHD, E), trimers (TRI, A, B, C), aldehydes (ALD 1-5) and quinones (TQ) of Toc. Initially, during the first 5min of ageing, the loss of Toc is caused by the formation of TRI, DHD, ALD 1-3 and TQ (figure 5.4.a-c). As an effective CB-D antioxidant, Toc reacts rapidly with peroxy radicals $ROO \cdot$ by donating its phenolic hydrogen, as shown in scheme 4.5, reaction a. The mechanism of stabilisation of Toc during the initial stage of thermal ageing is similar to that observed during processing of PP with 0.2% Toc in a CM/N₂ and CM for increasing times (figure 4.28.a, c, p. 437). In both cases the concentrations of TRI (major products), DHD, ALD and TQ increase, whereas the concentration of SPD decreases, with increasing processing or ageing times. DHD are formed via coupling of two Toc-benzyl I radicals (reaction f in scheme 4.5) and TRI are likely to be formed from two consecutive Diels-Alder reactions of QM (reactions d and e in scheme 4.5).

After 5h of thermal ageing, chemical transformations do not account entirely for the loss of Toc (figure 5.4.a), confirming that Toc is also lost by volatilisation from the polymer film. Furthermore, the increase in the concentration of TRI is accompanied by a decrease in DHD concentration (figure 5.4.b). Like during processing of Toc in an OM for increasing times (figure 4.28.e, p. 437), the presence of high concentrations of $ROO \cdot$ after long

thermal ageing times results in the oxidation of DHD to TRI, via SPD (reactions **g**, **h** and **e** in scheme 4.5). After about 30h of ageing, the concentration of TRI also decreases, suggesting that they are also lost from the polymer (figure 5.4.b), whereas the concentrations of ALD 1-5 and TQ remain more or less constant until embrittlement.

The above results suggest that the lower thermal stabilising efficiency of Toc compared to the commercial hindered phenol antioxidants Irg 1076 and Irg 1010 (see figures 3.7.a and 3.8.b, p. 314) is mainly caused by the physical loss by volatilisation of Toc from the polymer film during ageing. Because of the high extent of physical loss of Toc during ageing, the formation in high concentrations of ALD 1 and TQ (figure 5.4.b-c), which have a far lower thermal stabilising activity in PP than Toc and its dimers and trimers (see figure 3.9, p. 315), is unlikely to greatly influence the thermal stabilising efficiency of Toc. Irg 1076 and Irg 1010, which have a higher molecular mass (MM) than Toc (530g and 1177g, respectively, compared to 430g for Toc) are therefore better thermal stabilisers than Toc. On the other hand, the commercial antioxidant BHT, which has a much lower MM than Toc (220g), is a very poor thermal stabiliser (see figure 3.7.b, p. 314), whereas its melt stabilising efficiency is excellent (see figure 3.4 p. 312). However, the thermal stabilising efficiencies of Toc and its transformation products increase rapidly with decreasing temperatures of ageing (figures 3.8 and 3.9), hence Toc is expected to be a good long term stabiliser at normal temperatures of end-use of the polymer article.

5.5.2 Mechanism of stabilisation of Toc in PP during UV ageing

5.5.2.1 Effect of initial Toc concentration in PP on the degradation of the polymer and the loss of total products during ageing

PP films (0.25mm thick), unstabilised and stabilised with 0.2 and 1% Toc in an internal mixer (CM, 10min, 200°C), were subjected to UV ageing in an accelerated UV ageing cabinet, and their decrease in relative net absorbance at 290nm was followed by UV spectroscopy (see figures 5.5-5.6, p. 469). Similar to thermal ageing, the general increase in absorbance over the range 190-400nm with increasing ageing times for both

unstabilised and stabilised films is caused by the thermal degradation of PP (figure 5.5). It was shown [29] that hydroperoxides, which are initially formed during the processing operation, are also formed in high concentrations during photooxidation of unstabilised PP and are mainly responsible for the degradation of the polymer, i.e. formation of alcohol and carbonyl groups.

The decrease in the absorbance of Toc and its transformation products with increasing UV ageing times (figure 5.5.b-c) is similar to that observed during thermal ageing (figure 5.1.c-d, p. 464) and is also caused by their physical loss from the polymer. However, the loss of the antioxidant and its products is expected to be due to chemical transformations rather than volatilisation as the temperature during UV ageing is much lower (about 35°C) than that used during thermal ageing (140°C). Unlike thermal ageing, the decrease in relative net absorbance at 290nm of Toc and its transformation products with time of ageing is much faster at the lower concentration of the antioxidant (figure 5.6.a). Furthermore, the antioxidant and its products are lost well before embrittlement is reached (201h and 250h for 0.2 and 1% Toc in PP, respectively). This is due to the longer stability of PP during UV ageing compared to thermal ageing (embrittlement times of 1h and 100h for thermal and UV ageing, respectively).

The physical loss of total products from PP stabilised with 1% Toc was followed by UV analysis of the extracts during ageing (see figure 5.6.b and table 5.6). It was shown that the decreases in the concentration of the products in the polymer with time of ageing is similar to the decrease in relative net absorbance at 290nm, suggesting that the loss of products in PP stabilised with 0.2% Toc is also similar to their decrease in relative net absorbance. This was reflected by the decrease in embrittlement time with decreasing concentrations of Toc (see figure 3.12, p. 317).

5.5.1.2 Effect of UV ageing on the nature of the transformation products of Toc

The nature of the products formed from Toc during UV ageing of PP films (0.25mm thick) stabilised with 1% Toc in an internal mixer (CM, 10min, 200°C) were identified by comparing their HPLC Rt and UV characteristics with those of known oxidation products of Toc. Figures 5.7 and 5.8, p. 488, show that these are also dimers (DHD, E), trimers (TRI, A, B, C), aldehydes (ALD 1-5) and quinones (TQ) of Toc, like in thermal ageing. The formation of the small concentrations of transformation products of Toc during UV ageing do not account entirely for the sharp decrease in Toc concentration with increasing ageing times (figure 5.8.a). This suggests that, in addition to chemical transformations to the products mentioned above, Toc is also physically lost from the polymer film through photodecomposition, as it is unlikely to be lost by volatilisation. It has been shown [41] that photodecomposition of commercial hindered phenols (e.g. BHT) is caused by the formation of photosensitising products (see scheme 1.6, p. 48) which are responsible for the poor UV stabilisation efficiency of hindered phenols. Photosensitising products result from the formation of peroxy-cyclohexadienones, P-CHD (see scheme, 1.6). The formation of the equivalent P-CHD of Toc (see reactions o and p in scheme 4.5, p. 411) results in the opening of the chroman ring to give TQ (reaction q, scheme 4.5) which could be further destroyed.

The sharp decrease in Toc concentration is initially (0-5h) accompanied by small increases in the concentrations of SPD, TRI (major products), ALD 1-3, TQ and a decrease in the concentration of DHD (figures 5.8.a-b). DHD are oxidised to SPD by donating their two phenolic hydrogens (reactions g and h in scheme 4.5), in the presence of high concentrations of peroxy radicals, ROO •. The formation of TRI is caused by further oxidation of SPD via QM (reaction d, scheme 4.5). On the other hand, during the initial stage of thermal ageing (0-5h), the decrease in Toc concentration was accompanied by an increase in the concentration of DHD, in addition to an increase in TRI, ALD 1-3 and TQ concentrations (figure 5.4.b, p. 488), suggesting that the concentration of ROO • is too low for the further oxidation of DHD. This suggests that the concentration of ROO •, which are

formed initially via the decomposition of hydroperoxides (see reactions 1.10 to 1.13, p. 41), is much higher during the initial stage of UV ageing compared to thermal ageing. This is likely to be caused by the much faster decomposition of the hydroperoxides during UV ageing. However, at later stages of thermal ageing, the decrease in DHD is also observed, indicating the presence of higher concentrations of ROO •.

After 5h of UV ageing, the concentration of Toc continues to decrease rapidly and the antioxidant is nearly lost completely after 98h of ageing (only 1% Toc left) (figure 5.7.a) by photodecomposition. This was accompanied by a general decrease in the concentration of the transformation products, except for the concentration of TRI which remained more or less constant (figure 5.8.b-c). This suggests that SPD, ALD 1-4 and TQ are also photodecomposed.

The above results suggest that the poor UV stabilisation efficiency of Toc is mainly caused by its rapid photodecomposition leading to its physical loss from the polymer.

5.5.3 Migration of Toc and its transformation products from LDPE films into various food simulants

5.5.3.1 Static migration characteristics of Toc

The static migration characteristics of Toc and its transformation products from LDPE films (2cm x 9cm, 0.25mm thick) stabilised with 0.2% Toc into 100ml of various food simulants, under specific conditions were evaluated. After the first extrusion pass, Toc was relatively highly retained (79%) and its transformation products were trimers (TRI, A, B, C), which were the major products (11%), dimers (DHD, E, SPD, D), aldehydes (ALD 1, ALD 4) and a quinone (TQ) (see table 4.12, p. 365 and figure 4.15, p. 425). Static migration tests were carried out under conditions which are specified by EC and FDA directives (see tables 2.67 and 2.68, p. 139). Figure 5.9, p. 474, shows the extent of migration of Toc and its transformation products from the polymer films into fatty (olive oil, iso-octane and heptane), aqueous alcoholic (15%, v/v, aqueous ethanol), aqueous

acidic (3%, w/v, aqueous acetic acid) and aqueous (water) food simulants. Their extent of migration is expected to be governed by two main factors which are the solubility of the antioxidant and its products in the polymer and the food simulant and the rate of additive diffusion. The expected higher solubility of Toc and its products in organic solvents, compared to aqueous solvents, explains the much higher extent of migration of the products in the fatty food simulants compared to the aqueous one. The test condition, i.e. 70°C for 2h or 40°C for 10 days, does not seem to influence greatly the extent of migration the extent of migration of the products, suggesting that either condition can be applied.

It is very likely that not only Toc but also its transformation products, formed during extrusion (e.g. DHD, SPD, TRI, ALD 1, see figure 4.15, p. 225) migrate into the food simulants, specially when fatty food simulants are used, because of the higher extent of migration. The nature and the concentration of products migrating into the different food simulants can be examined by HPLC analysis of the extracts in future work.

5.5.3.2 Dynamic migration characteristics of Toc

Dynamic migration tests were carried out for LDPE films (2cm x 9cm, 0.25mm thick) stabilised with 0.2% of each of the antioxidants Toc and Irg 1076 (single screw extruder, one pass, 180°C), at 40°C and in 100ml of various food simulants. Like Toc, after the first extrusion pass, Irg 1076 was highly retained and its transformation products were its cinnamate, C-Irg 1076, biscinnamate (BC-Irg 1076) and Irg 1076-11, which is possibly the quinone methide of Irg 1076, QM-Irg 1076 (see figure 4.47.a-b, p. 447). The migration characteristics of Toc and Irg 1076 were found to be very similar (figure 5.10, p. 476). The migration into the fatty food simulants iso-octane and heptane was very fast, whereas the migration into olive oil was much slower, although in the latter case, the extent of migration was also shown to be high after the static migration test (figure 5.9). This suggests that the migration in real fatty foods is much slower than in heptane and in iso-octane. Furthermore, at temperatures of end-use, which are usually lower than 40°C, the rate of migration is expected to be slower. However, migration of antioxidants and their

transformation products from their packaging does takes place and leads to the contamination the food.

Although Irg 1076 may have toxicity clearance, its transformation products, e.g. C-Irg 1076 (see figure 4.47.a-b, p. 447), have unknown or uncertain toxicological effects. Furthermore their extent of migration is expected to become higher after multiple extrusion passes, which were shown to lead to higher concentrations of transformation products (figure 4.15, p. 425). The determination of the extent of migration of transformation products of Irg 1076, after single and multiple extrusion passes, into different food simulants is essential for the determination of the safety of the antioxidant when used in food packaging materials. It is clear that the use of the non-toxic antioxidant Toc represents an advantage over commercial hindered phenols. Furthermore, it was shown [80,81,96,98] that dimers (e.g. DHD, SPD), trimers (TRI), aldehydes (ALD 1, ALD 2) and quinones (TQ) of Toc are formed under biological simulated conditions.

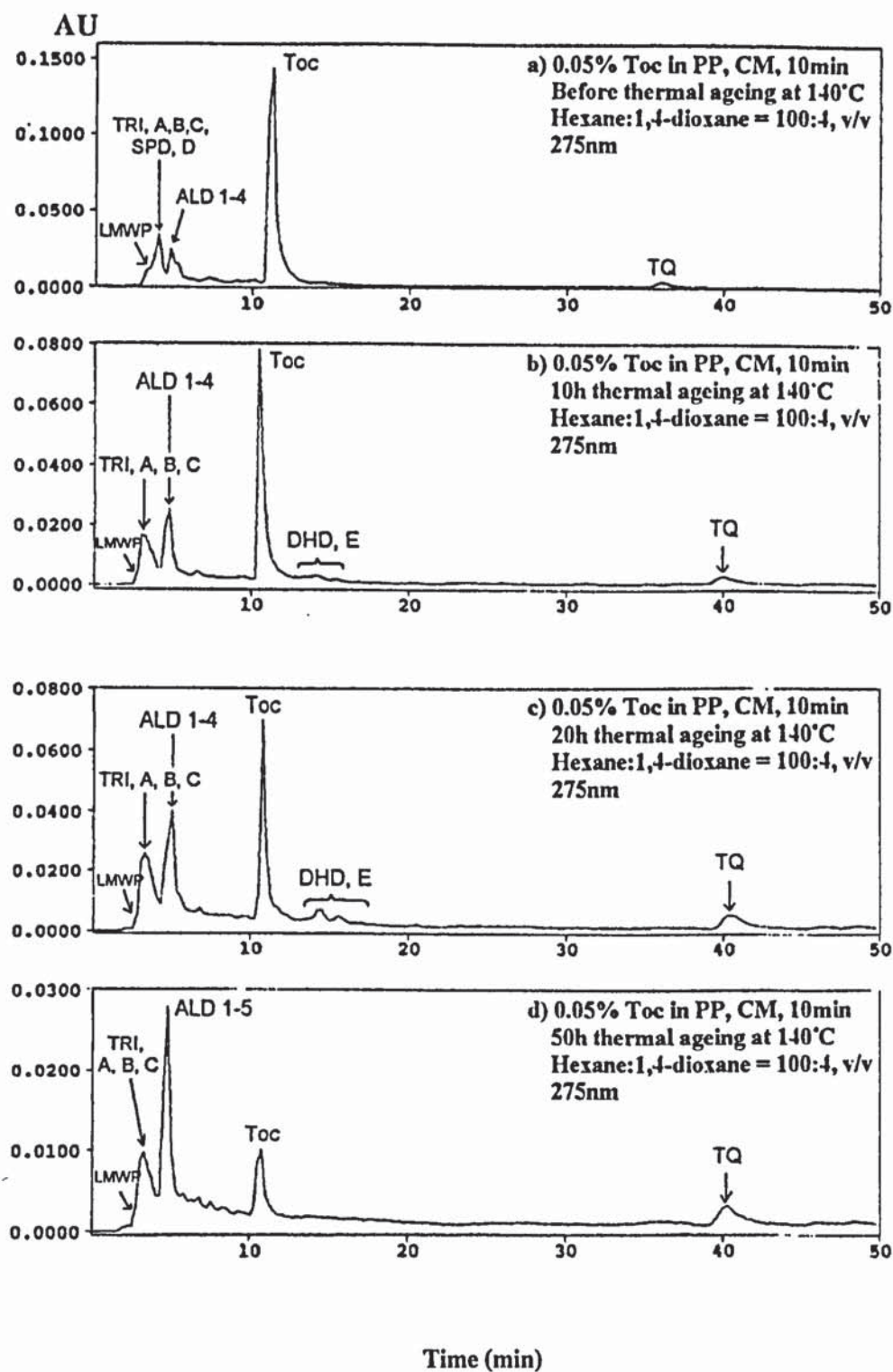


Figure 5.3: HPLC analysis of the extracts of PP stabilised with 0.05% Toc in an internal (a-d) mixer (CM, 10min, 200°C) after thermal ageing at 140°C, in hexane (see table 5.4, p. 467)

Instrument: Philips PU4100 liquid chromatograph and PU4120 diode array detector; Column: Zorbax SIL (4.6mm x 25cm); Flow rate: 1ml.min⁻¹
 Eluent: hexane:1,4-dioxane = 100:4, v/v

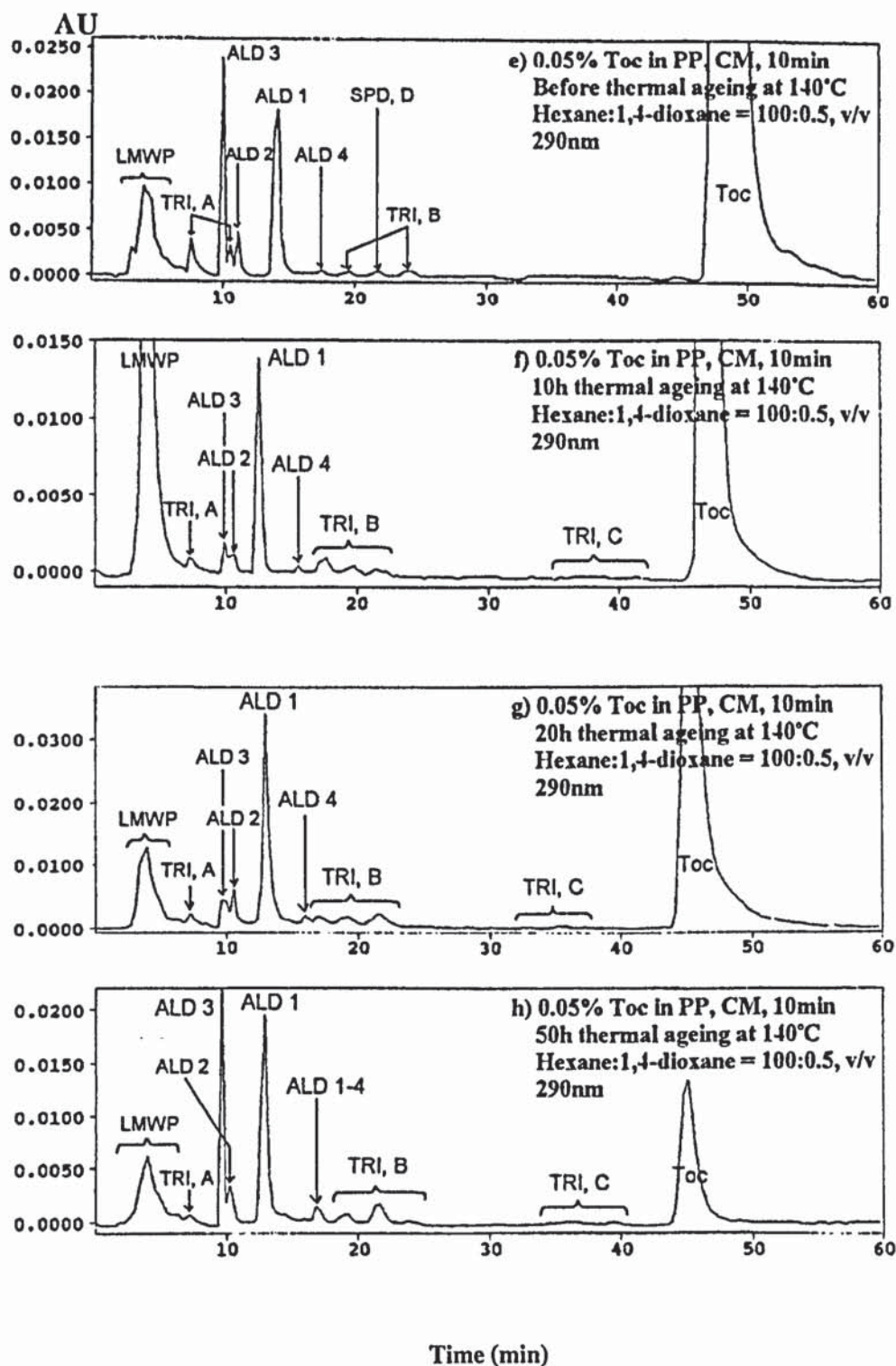


Figure 5.3: HPLC analysis of the extracts of PP stabilised with 0.05% Toc in an internal (e-h) mixer (CM, 10min, 200°C) after thermal ageing at 140°C, in hexane (see (see table 5.4, p. 467)

Instrument: Philips PU4100 liquid chromatograph and PU4120 diode array detector; Column: Zorbax SIL (4.6mm x 25cm); Flow rate: 1ml.min⁻¹
 Eluent: hexane:1,4-dioxane = 100:0.5, v/v

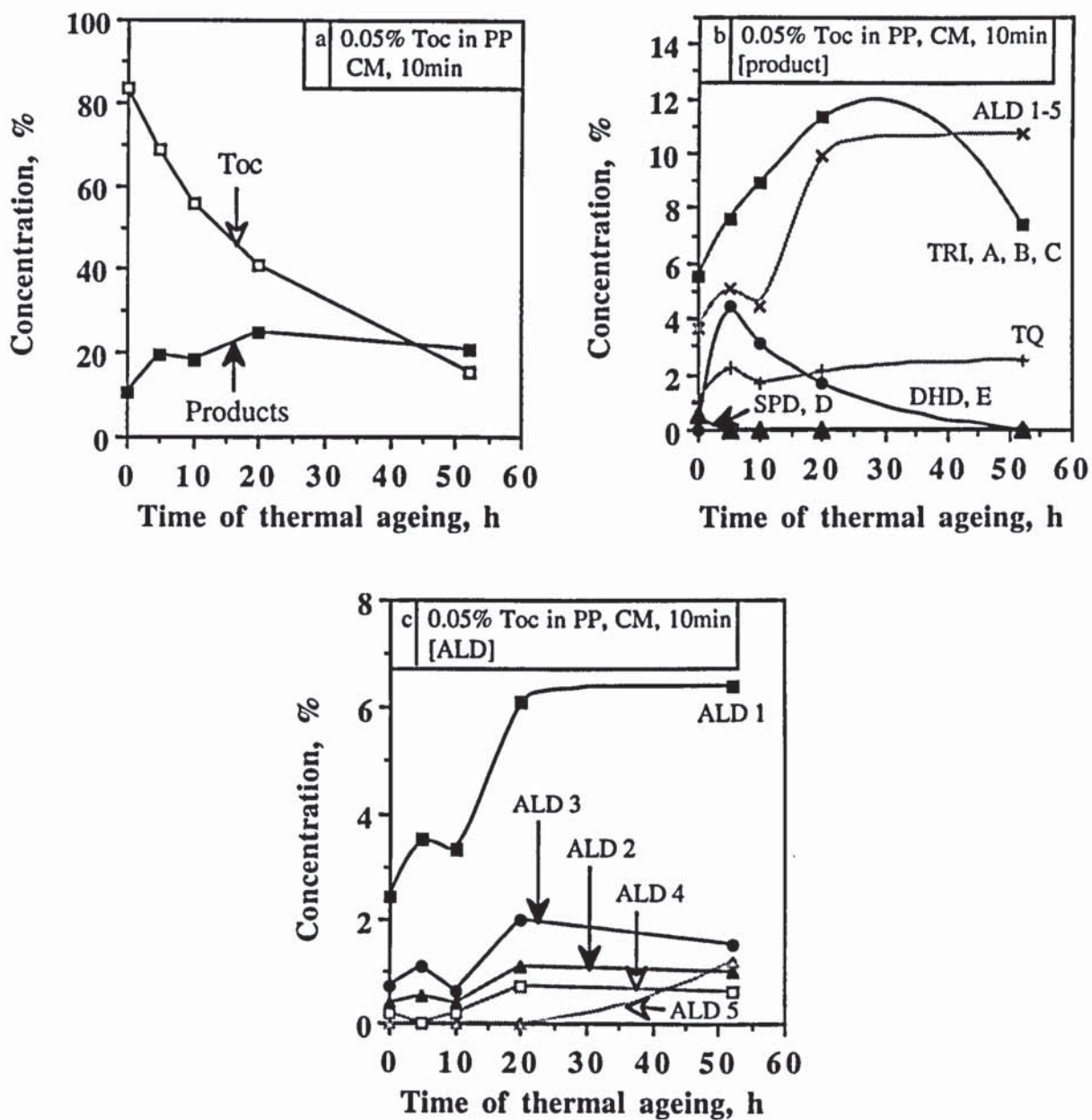


Figure 5.4: Effect of thermal ageing at 140°C on the concentration of the transformation products of Toc in PP stabilised with 0.05% Toc (internal mixer, CM, 10min, 200°C) (see table 5.5, p. 467)

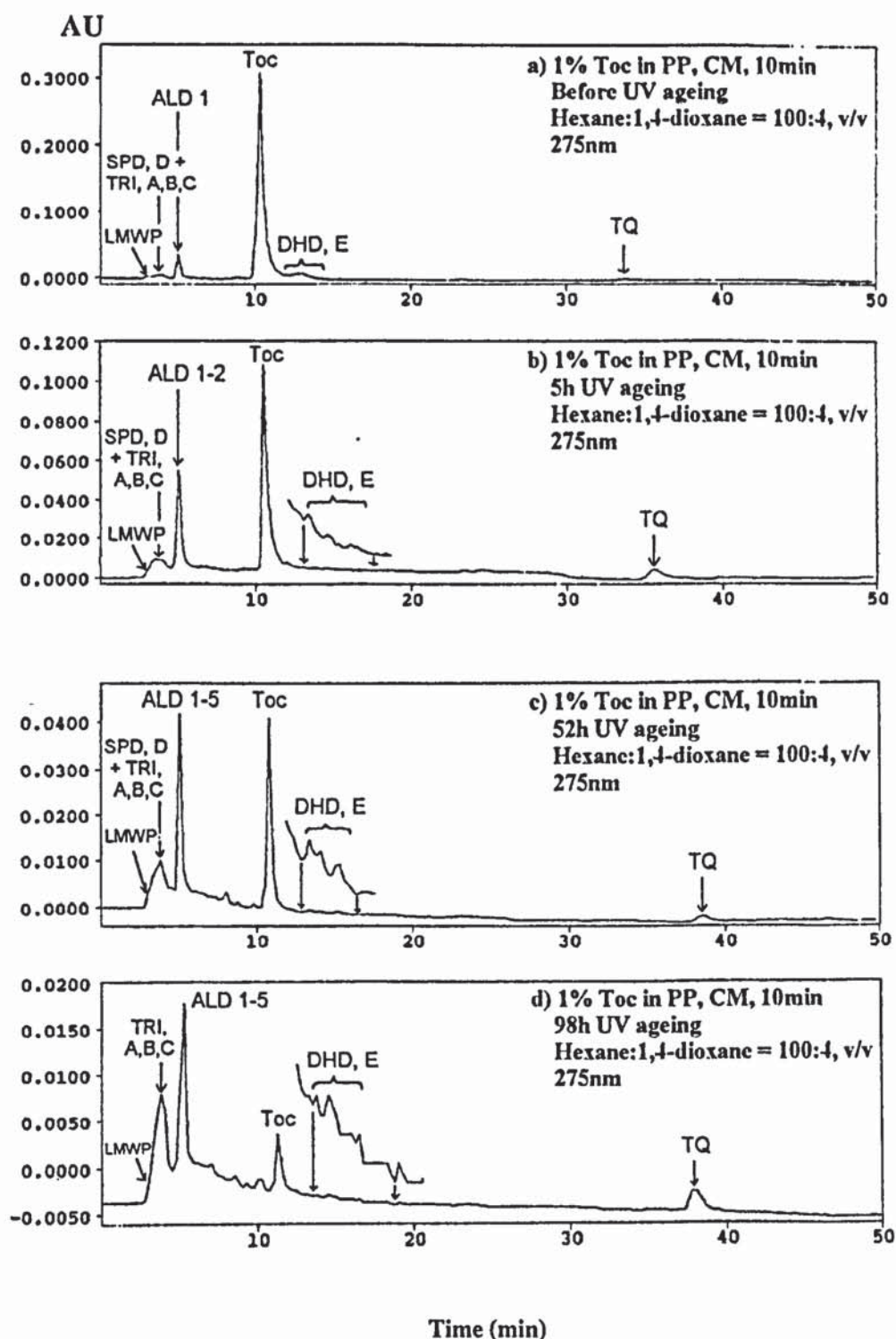


Figure 5.7: HPLC analysis of the extracts of PP stabilised with 1% Toc in an internal (a-d) mixer (CM, 10min, 200°C) after UV ageing, in hexane (see table 5.4, p. 467) Instrument: Philips PU4100 liquid chromatograph and PU4120 diode array detector; Column: Zorbax SIL (4.6mm x 25cm); Flow rate: 1ml.min⁻¹ Eluent: hexane:1,4-dioxane = 100:4, v/v

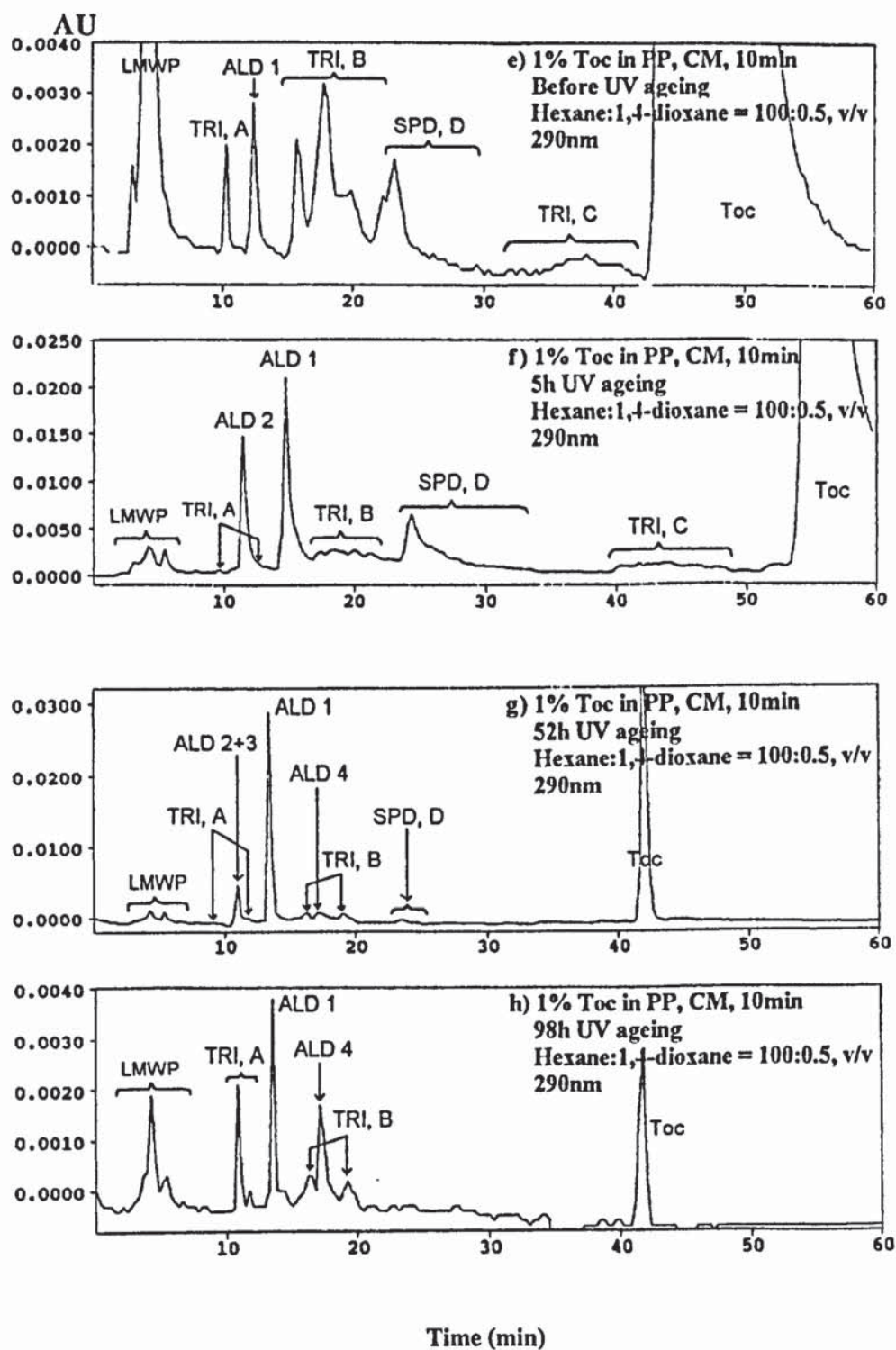


Figure 5.7: HPLC analysis of the extracts of PP stabilised with 1% Toc in an internal (e-h) mixer (CM, 10min, 200°C) after UV ageing, in hexane (table 5.7, p. 472) Instrument: Philips PU4100 liquid chromatograph and PU4120 diode array detector; Column: Zorbax SIL (4.6mm x 25cm); Flow rate: 1ml.min⁻¹ Eluent: hexane:1,4-dioxane = 100:0.5, v/v

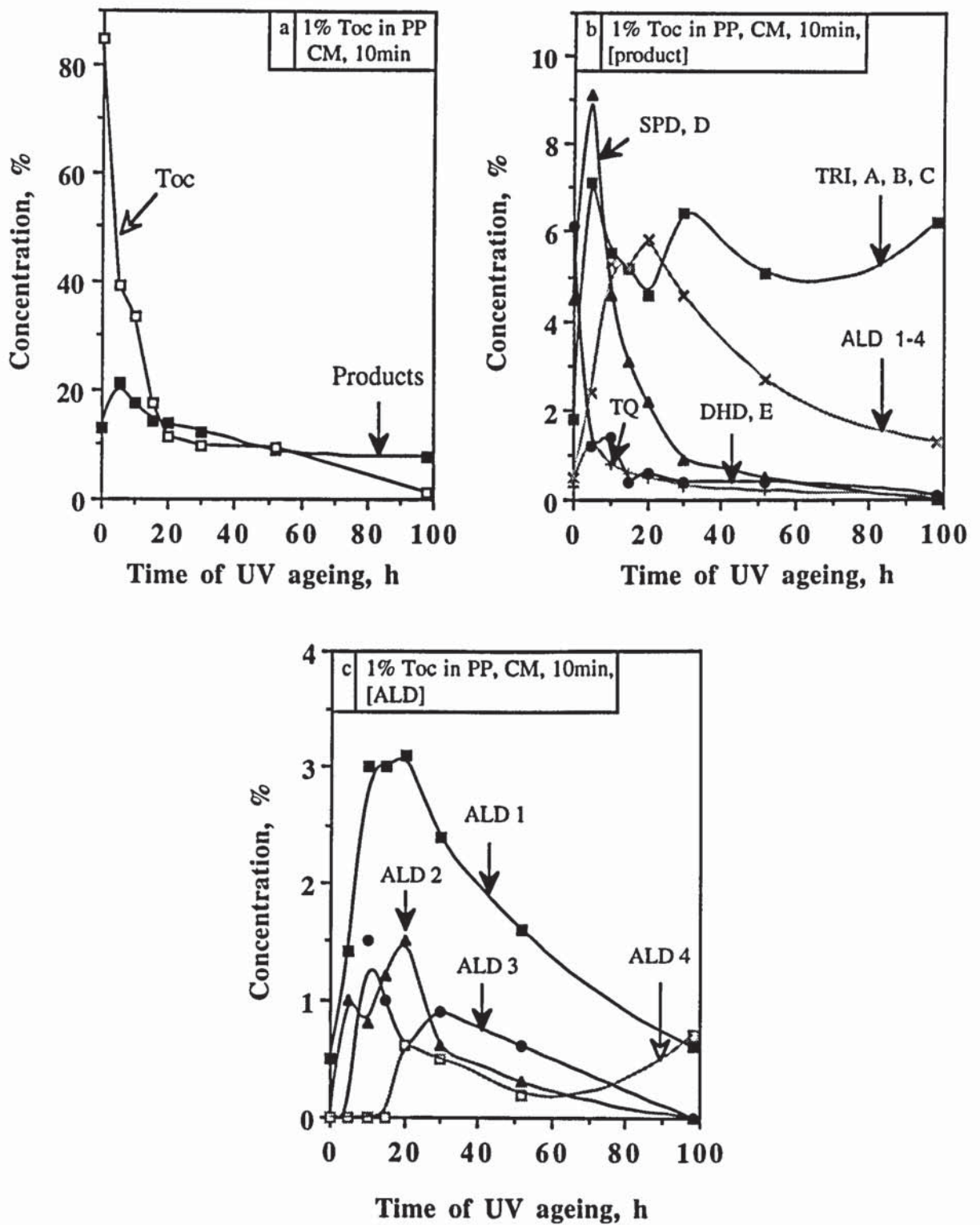


Figure 5.8: Effect of UV ageing on the concentration of the transformation products of Toc in PP stabilised with 1% Toc (internal mixer, CM, 10min, 200°C) (see table 5.7, p. 472)

CHAPTER SIX

CONCLUSION AND RECOMMENDATIONS FOR FURTHER WORK

6.1 CONCLUSION

6.1.1 Stabilisation efficiency of Toc in polyolefins

All-*rac*- α -tocopherol (Toc) is the synthetic form of the natural Vitamin E compound RRR- α -tocopherol, which is an excellent chain-breaking-donor (CB-D) antioxidant for peroxy radicals in living systems. In this work, the excellent CB-D activity of Toc in polyolefins was illustrated by its high efficiency as a processing melt stabiliser in low density polyethylene (LDPE) and polypropylene (PP). Without the addition of stabilisers, the degradation of LDPE and PP during processing is very fast, especially after multiple extrusions and when subjected to long processing times in an internal mixer.

Toc was found to be an excellent melt stabiliser for LDPE and PP and was shown to exhibit far better melt stabilising activity than the commercial hindered phenol antioxidants Irganox (Irg 1076) and Irganox 1010 (Irg 1010), especially at very low concentrations (e.g. 0.02% in PP). The melt stabilising efficiency of 0.02% Toc was equivalent to that exhibited by 0.2% Irg 1010 in PP. The lower melt stabilising activity of Toc in PP at concentrations below 0.02% (i.e. 0.01%) can be attributed to the formation of higher concentrations of transformation products of Toc during processing (see section 6.1.4.2). Although some of these products were shown to possess better (dihydroxydimer of Toc, DHD) or similar (spirodimer, SPD, and trimer, TRI, of Toc) melt stabilising efficiency in PP compared to Toc, the aldehyde 5-formyl- γ -tocopherol, ALD 1, as well as the α -tocoquinone, TQ, have much lower melt stabilisation activities than Toc. Hence, the formation of high concentrations of ALD 1 when very low concentrations of Toc are used is most certainly responsible for the lower stabilising activity of Toc.

Toc also enhances the thermal stability of PP during long term stabilisation tests (thermal ageing), but its thermal stabilisation efficiency is lower than that of the higher molecular mass (MM) hindered phenols Irg 1076 and Irg 1010. However, the stabilising effect of Toc is higher than that offered by the lower MM commercial hindered phenol BHT. This suggests that the volatility of the antioxidant is detrimental to its long-term retention under

atmospheric conditions in polymers. Physical loss of Toc and its transformation products from PP was shown to take place during thermal ageing (140°C), at initial concentrations of 0.02-0.2%. Furthermore, the much lower thermal stability of PP stabilised with very low concentrations of Toc, e.g. 0.01%, was also caused by the initial presence of very high concentrations of ALD 1 and TRI (formed during processing). These were found to have much lower thermal stabilising efficiency than Toc in PP at 120-140°C. However, the stabilising activity of Toc increases dramatically at lower test temperatures (from 140 to 100°C) at concentrations above 0.01%. For example, at a concentration of 0.02% Toc the embrittlement times of PP were 1 day at 140°C, 6 days at 120°C and 34 days at 100°C. This suggests that at normal temperatures of end-use of the polymer article, which are usually far lower than 100°C (e.g. food packaging materials), the thermal stabilising efficiency of Toc at a concentration of 0.02% is high and should be acceptable.

Similar to commercial hindered phenols, the limited UV stabilisation activity of Toc in PP films (0.25mm thick) during ageing in an accelerated UV cabinet is suggested to be caused by its rapid photodecomposition. The physical loss of Toc and its transformation products from PP stabilised with 0.2 and 1% Toc was shown to be very fast during UV irradiation. At very low initial Toc concentration, i.e. 0.01%, the initial presence in high concentration of ALD 1 (formed during processing) is expected to contribute to the much lower photostabilising activity of Toc, compared to those shown at higher concentrations of the antioxidant.

From the above results, it is clear that Toc is an excellent melt stabiliser and good thermal antioxidant in PP when used at very low concentrations (e.g. 0.02%). This concentration is far lower than that required for commercial antioxidants like Irg 1076 and Irg 1010. However, hindered phenols lead to colour development in polyolefins during the processing operation.

6.1.2 Development and prevention of colour during processing of LDPE and PP with antioxidants

The development of colour in LDPE and PP stabilised with Toc, Irg 1076 and Irg 1010 generally increases with increasing concentrations of the antioxidant and was shown to be caused by the formation of transformation products of the hindered phenols, as a consequence of their antioxidant action during processing. The formation of coloured oxidation products such as ALD 1, SPD and TRI of Toc, were shown to be mainly responsible for the discolouration of LDPE and PP stabilised with Toc. In LDPE stabilised with Irg 1076 and Irg 1010, it was suggested that the formation of coloured quinonoid and cinnamate oxidation products are most likely to lead to the discolouration of the polymer. However, at lower concentrations of Toc in PP (e.g. 0.02%), the discolouration was much lower and the melt and thermal stabilities were still high enough. Therefore, for the stabilisation of food packaging materials, when used at low concentrations, Toc seems fully acceptable. However, the introduction of the commercial hindered aromatic phosphite Ultrinox 626 (U-626) in PP containing Toc prevented colour development. This was shown to be caused by the higher retention of the antioxidant (i.e. lower concentrations of transformation products), as a consequence of the antioxidant action of the phosphite (see section 6.1.4.3). Similarly, U-626 and Irgafos 168 (Irgf 168) prevented the discolouration of PP stabilised with Irg 1010.

6.1.3 Effect of hindered aryl phosphite on the melt, thermal and UV stabilising activities of Toc

Hindered aromatic phosphites are normally used in combination with hindered phenols to prevent discolouration of the polymer during processing. Furthermore, the presence of U-626 also improved the melt, thermal and UV stabilising activity of Toc in PP. The melt stability of PP processed with Toc and U-626 was higher than that of similar combinations of Irg 1010 with U-626 or Irgf 168. The melt stability and thermal stability at 120-140°C of PP stabilised with 0.05% Toc + 0.1% U-626 was similar in the former case and higher in

the latter to those of PP stabilised with 0.2% Toc only. This suggests that, at lower concentrations, e.g. 0.01% Toc + 0.02% U-626, combinations of Toc and U-626 would still impart good melt and thermal stabilities to PP. This was shown [8] to be the case during multiple extrusions with PP. The UV stabilising activity of Toc in the presence of U-626 was only improved slightly and was still low compared to commercial UV stabilisers. The improved melt stability of PP containing combinations of U-626 and Toc was shown to be caused by the antioxidant activity of U-626 (see section 6.1.4.3), leading to a higher retention of Toc.

6.1.4 Mechanisms of melt, thermal and UV stabilisation of Toc in LDPE and PP

6.1.4.1 Synthesis, isolation and characterisation of oxidation products of Toc from model systems and polymer extracts

Before investigating the nature of the products formed from Toc during processing with polymers, a number of oxidation products of Toc were synthesised, isolated and characterised from model reactions, using lead dioxide as the oxidising agent. The oxidation of Toc with various concentrations of lead dioxide in hexane lead to the formation of dimers (dihydroxydimer, DHD, and spirodimer, SPD), trimers (TRI) and an aldehyde (5-formyl- γ -tocopherol, ALD 1). These products have also been characterised in the literature. However, optimisation of NP-HPLC conditions lead to the separation and characterisation of the different stereoisomeric structures that exist for the dimers and trimers of Toc, whereas in the literature there is no reference to the existence of most of these isomers. SPD, D (D1, D2, D3, stereoisomers) was obtained as a major product (81%) when the ratio 1:40 in Toc:PbO₂ was used, whereas TRI, A, B, C (A1, A2, B1-B4, C1-C4, stereoisomers) were major products (65%) at a ratio of 1:10. DHD, E (E1-E4) were obtained from the reduction of SPD, D with lithium aluminium hydride in a relatively high yield (56%). The effect of PbO₂ concentration on the nature and concentrations of the oxidation products of Toc was examined and a mechanism of oxidation was suggested (see scheme 4.4, p. 404). It was suggested that TRI are formed via the quinone methide of Toc (QM) and SPD. The latter

was formed via the oxidation of the DHD, and in the presence of QM, the SPD lead to the TRI.

In addition to ALD 1, two other aldehydes of Toc, 5-formyl- γ -Toc (ALD 2) and 7-formyl- β -Toc (ALD 3) were isolated from a provided sample of PP stabilised with 39% Toc processed in a single screw extruder. ALD 1, 2 and 3, as well as dimers (DHD, SPD), trimers (TRI) and α -tocoquinone (TQ, provided) were also shown to be present in LDPE stabilised with 0.2 and 10% Toc (single screw extruder) by isolating and characterising them.

6.1.4.2 Mechanism of melt stabilisation of Toc in LDPE and PP

The nature of the transformation products formed from Toc during multiple extrusions with LDPE in a single screw extruder (180°C) and processing with PP in an internal mixer (200°C), under different conditions, were investigated. Although Toc was evaluated as a melt, thermal and UV stabiliser for polyolefins in the literature, the nature of the products formed from Toc during processing and thermal and UV ageing of the polymer have not been examined. During processing of Toc with LDPE and PP, it was shown that dimers (DHD, SPD), trimers (TRI), aldehydes (ALD 1, 2, 3) and a quinone (TQ) of Toc were formed. In addition, two other aldehydes, ALD 4 and ALD 5, were formed but could not be identified. The nature and concentrations of the transformation products were shown to be highly dependent on the initial Toc concentration, oxygen availability and processing severity. In scheme 4.5, p. 411, a mechanism of melt stabilisation of Toc in LDPE and PP is suggested.

During processing of PP with 0.2% Toc in an internal mixer, it was shown that higher concentrations of oxygen in the mixing chamber, i.e. processing in an open mixer (OM), lead to a higher extent of oxidation of Toc, which is mainly caused by the formation of higher concentrations of ALD 1-5 (mainly ALD 1). However, Toc was still highly retained, even after 30min processing in an OM ($\geq 82\%$). ALD 1, 2 and 3 are formed from the reaction of the tocopheroxyl radical Toc • (formed from the attack of peroxy radicals) with

oxygen. TRI were formed in high concentrations in a closed mixer (CM), closed mixer with prior nitrogen flushing (CM/N₂) and OM, and their concentration increased with processing severity. Higher oxygen concentrations lead to the formation of higher concentrations of peroxy radicals, ROO •, which were shown to affect the concentrations of the dimers (DHD, SPD) of Toc. At lower oxygen concentrations (CM/N₂, CM), both DHD and SPD were present, and the concentration of DHD increased with processing severity, whereas SPD were oxidised to TRI via QM. On the other hand, at higher oxygen concentration (OM), higher concentrations of ROO • lead to the oxidation of DHD to TRI, via SPD.

The mechanism of melt stabilisation of Toc during multiple extrusions in LDPE was very similar to the one observed in PP during processing in a closed (CM/N₂ and CM) internal mixer, at an initial Toc concentration of 0.2%. However the extent of oxidation of Toc was much higher after multiple extrusions (e.g. after 4 passes only 16% Toc was retained) than in the internal mixer after long processing times (e.g. 30min). When higher concentrations of Toc were used (1 and 10%), the retention of Toc was much higher (≥ 76%). However, the melt stabilising activity of Toc was found to be highest at the lower concentration of 0.2%, suggesting that only small concentrations of Toc are required for a good melt stabilisation of LDPE.

In PP stabilised with various concentrations of Toc (0.01-0.2%) in an internal mixer, it was revealed that Toc is highly retained at initial concentrations of 0.02 or above (≥ 76%), whereas Toc was highly oxidised (only 27% retained) at an initial concentration of 0.01%, mainly to ALD 1-4 (23%) and TRI (43%). ALD 1, which was the major aldehyde, was found to be a poor melt stabiliser in PP, whereas TRI were shown to possess similar melt stabilising activity than Toc. This indicates that the formation of ALD 1 is mainly responsible for the much lower stabilising activity of Toc at this low concentration. The similar melt stabilising activity of SPD and TRI in PP, at initial concentrations of 0.2%, was shown to be caused by the formation of DHD in relatively high concentrations (23-29%) during processing, whereas DHD itself is highly retained during processing. The latter was shown to be a better melt stabiliser than Toc.

6.1.4.3 Effect of hindered aryl phosphite U-626 on the melt stabilisation activity of Toc

U-626 acts as a peroxidolytic (PD-S) antioxidant, i.e. decomposes hydroperoxides stoichiometrically in a non-radical process, and has also the ability to scavenge oxygen at high temperatures, leading to the formation of the mono and diphosphates of U-626 during processing with polyolefins (see scheme 4.6, p. 113). The nature and the distribution of the transformation products formed from Toc in PP stabilised with 0.2% Toc + 0.4% U-626 and 0.05% Toc + 0.1% U-626 were similar to those formed during processing of PP with Toc only, suggesting similar mechanisms of melt stabilisation. However, in the presence of the phosphite, the retention of Toc was higher, i.e. lower concentrations of transformation products were formed, which is suggested to be caused by the antioxidant activity of U-626. In PP stabilised with combinations of SPD with U-626 and TRI with U-626, the nature and concentrations of the transformation products formed from the Toc derivatives were very similar to those formed in PP stabilised with the derivatives only, which also suggests similar melt stabilisation mechanisms. The higher retention of Toc in PP in the presence of U-626 lead to higher colour and melt stabilities of the polymer, and is also expected to lead to the observed higher thermal and UV stabilities.

6.1.5 Mechanism of melt stabilisation of Irg 1076 in LDPE

Irg 1076, a widely used CB-D commercial hindered phenol antioxidant in polyolefins, reacted with peroxy radicals formed during extrusion with LDPE (single screw extruder, 180°C), leading to the formation of various oxidation products. Various oxidation products of Irg 1076, formed in model reactions, were characterised in the literature, but the examination of the products formed during processing of Irg 1076 with polyolefins is rather limited. The cinnamate of Irg 1076, C-Irg 1076, was shown to be a major transformation product. The biscinnamate of Irg 1076, BC-Irg 1076, was also formed, but in smaller concentrations. Three other compounds were also shown to contain cinnamate and quinonoid structures. The structures of quinone methide, QM-Irg 1076, and conjugated

bisquinone methide of Irg 1076, CBQM-Irg 1076, were proposed. The other products had very similar UV characteristics to Irg 1076, suggesting that they have intact phenolic groups without any further conjugation.

According to the nature of the transformation products formed and suggested to be formed, a mechanism of melt stabilisation of Irg 1076 in LDPE was proposed (see scheme 4.7, p.418). The peak areas at 282nm (λ_{max} of Irg 1076) of the transformation products were highest in LDPE stabilised with the lower concentration of the antioxidant (0.2%) and lowest in LDPE stabilised with 1% Irg 1076. This was reflected by the higher melt stabilising activity of Irg 1076 at a concentration of 1%, compared to 0.2% and 10%. Although the retention of Irg 1076 in LDPE seemed higher than that of Toc, especially after multiple extrusions, the melt stabilising activity of Toc was much higher. Discolouration of LDPE stabilised with Irg 1076 was most certainly caused by the formation of C-Irg 1076, which is a yellow solid (Irg 1076 is colourless).

6.1.6 Mechanism of melt stabilisation of Irg 1010 in LDPE

Irg 1010 is also a widely used commercial CB-D hindered phenol antioxidant and like for Irg 1076, the investigation of the nature of its transformation products formed during processing with polyolefins is limited. Irg 1010 contains four identical phenolic groups which are similar to Irg 1076. In this work, most of the transformation products formed from Irg 1010 during multiple extrusions with LDPE (single screw extruder, 180°C) were shown to contain one to four sub-units of Irg 1010, suggesting thermal cleavage of Irg 1010 during extrusion. Two of the products, present in small amounts, were shown to contain cinnamate and quinonoid structures. Like in LDPE stabilised with Irg 1076, the extent of oxidation of Irg 1010 was highest at the initial concentration of 0.2% and lowest at the concentration of 1%, which is also in accordance with the higher melt stabilising activity of Irg 1010 at a concentration of 1%.

The retention of Irg 1010 was higher than that of Irg 1076 and Toc, especially after multiple extrusions. However, the melt stabilising efficiency of Irg 1010 was slightly lower than that of Irg 1076 and much lower than that of Toc.

6.1.7 Mechanism of thermal stabilisation of Toc in PP

The reason for the lower thermal stabilising activity of Toc in PP, compared to commercial hindered phenols like Irg 1076 and Irg 1010, was investigated by examining the nature and concentrations of the products formed during thermal ageing at 140°C of PP films stabilised with 0.05% Toc (internal mixer, 10min, 200°C). It was shown that, in addition to chemical transformations (e.g. formation of aldehydes and trimers of Toc), Toc was also physically lost by volatilisation from the polymer during thermal ageing. Volatilisation of the antioxidant was shown to be the major reason for the thermal degradation of the polymer. However, transformation products of Toc account entirely for the loss of Toc at very early stages of thermal ageing. The mechanism of oxidation of Toc during thermal ageing was shown to be very similar to that observed during long processing times and multiple extrusions with PP and LDPE (see scheme 4.5, p. 411). This suggests that, at lower initial Toc concentrations (e.g. 0.01%), the much higher concentrations of transformation products (mainly TRI and ALD 1) formed during processing contribute to a higher extent to the much lower thermal stability of the polymer. It was shown that the thermal stabilising activity of ALD 1 is much lower than that of Toc.

6.1.8 Mechanism of UV stabilisation of Toc in PP

The limited UV stabilising activity of Toc in PP films was also shown to be caused by the very fast physical loss of Toc from the polymer films during UV ageing. This is suggested to be mainly due to the rapid decomposition of the antioxidant, similar to commercial hindered phenols. Transformation products of Toc were also found to be formed during UV ageing of PP stabilised with 1% Toc but these only accounted to a small extent for the loss of Toc. The mechanism of oxidation of Toc during UV ageing was shown to be very similar

to that observed during long processing times in PP (e.g. formation of dimers, trimers, aldehydes). Their distribution suggested high concentrations of peroxy radicals.

6.1.9 Migration characteristics of Toc from LDPE films into various food simulants

The migration characteristics of antioxidants is a major concern in applications involving polymers in direct contact with food and human environment (e.g. food packaging materials). This concern is compounded by the realisation that very little is known about the nature and the migration behaviour of antioxidant transformation products. Migration tests were carried out according to conditions specified by EC and FDA Directives.

It was shown that the extent of migration of both Toc, and the commercial antioxidant Irg 1076, from LDPE films was very high in the fatty food simulants olive oil, iso-octane and heptane, and was quite low in aqueous food simulants (e.g. 3% acetic acid), at 70°C (2h) and 40°C (10 days). It was also revealed that the rate of migration at 40°C of the antioxidants was much lower in olive oil compared to iso-octane and heptane, suggesting that the migration into real fatty foods is even slower. However, migration of antioxidants does take place and leads to the contamination of the food. Furthermore, transformation products of the antioxidants, formed during processing and subsequent use of the polymer article are also expected to migrate. Transformation products of commercial hindered phenols have unknown or uncertain toxicological effects. Hence, the use of the non-toxic biological antioxidant Toc represents a clear advantage over commercial antioxidants like Irg 1076 and Irg 1010, considering that similar oxidation products of Toc than those formed during processing and long-term stabilisation activity tests, were also shown to form under biological simulated conditions, according to the literature. The nature and concentrations of the transformation products of Toc, as well as Irg 1076, that migrate from the polymer films into the different food simulants can be examined by HPLC analysis of the extracts in future work.

6.2 RECOMMENDATIONS FOR FURTHER WORK

For a full understanding of the cause of colour development in LDPE and PP processed with Toc, the effect of each transformation product of Toc on the colour of the polymer after processing can be evaluated. This can be done through calibration curves of the initial product concentration versus the yellowness index of the polymer. An ideal solution for preventing discolouration in food packaging materials would be the use of a natural, or its synthetic analogue, reducing agent which is stable during processing. This could lead to the reduction of products like SPD and TRI to DHD. The latter Toc derivative possesses higher melt and thermal stabilising activities in PP than Toc.

The lower thermal stabilising activity of Toc compared to commercial hindered phenols like Irg 1076 and Irg 1010 is caused, at least in part, by the higher volatility of Toc at the test temperature. The extent of volatilisation of Toc and each of its transformation products from the polymer film should also be evaluated using volatilisation tests (in this work it was done by HPLC and UV analysis of the extracted products after increasing ageing times), for a better understanding of the stabilising activity of Toc. Furthermore, the reason for the higher thermal stabilising efficiency of Toc in the presence of the phosphite U-626 can be further examined by extracting the products after increasing ageing times and comparing them with those formed in the absence of U-626

The migration characteristics of Toc and its transformation products can be further investigated by determining the extent of migration of each of the transformation products of the parent antioxidant from the polymer film into various food simulant. This can be done by HPLC analysis of the migrated products. This experiment is particularly important in the stabilisation of Food packaging materials. Migration tests should also be carried out at lower initial Toc concentrations (e.g. 0.01-0.02%), which are high enough for a good melt and thermal stabilising activity.

LIST OF REFERENCES

1. N. Jushi, "Application of Tocopherol for PP Resin for Food Packaging", Packaging, **9**(46), 49-54, (1988).
2. A. D. Schwoppe, D. E. Till, D. J. Ehntholt, K. R. Sidman and R. H. Whelan, "Migration of BHT and Irganox 1010 from Low-density Polyethylene (LDPE) to Foods and Food-simulating Liquids", Fd. Chem. Toxic., **25**(4), 317-326, (1987).
3. N. C. Billingham and P. D. Calvert, "The Degradation and Stabilisation of Polyolefins- an Introduction", in Degradation and stabilisation of polyolefins, N. S. Allen (ed.), Applied Science Publishers, London, (1983).
4. J. Pospíšil, "Chemical and photochemical behaviour of phenolic antioxidants in polymer stabilization: a state of the art report, Part I", Polym. Deg. Stab., **40**, 217-232, (1993).
5. J. Pospíšil, "Chemical and photochemical behaviour of phenolic antioxidants in polymer stabilization: a state of the art report, Part II", Polym. Deg. Stab., **39**, 103-115, (1993).
6. S. F. Laermer and F. Nabholz, "Use of biological antioxidants as polypropylene stabilisers", Plastics Rubber Process. Applic., **14**, 235-239, (1990).
7. Z. Lin "Evaluation of tocopherols, ascorbic acid and their related compounds as antioxidants for polypropylene", First Annual report of the project sponsored by F. Hoffmann-la Roche and Co, PPP group, Aston University (1988).
8. M. R. Gmünder and T. J. Henman, "Synergistic stabilisation systems for polyolefins based on dl- α -tocopherol", Compounding '93, Brussels, February (1993).
9. T. König, "Synthesis and evaluation of new antioxidants derived from tocopherols and ascorbic acid in polymers and lubricating oils and mechanisms of their antioxidant action", Final report of the project sponsored by F. Hoffmann-La Roche and Co. (1991).
10. J. L. Bolland and P. Ten Have, "Kinetic studies in the chemistry of rubber and related materials", Trans. Faraday Soc., **43**, 201- 210, (1947).
11. J. L. Bolland, "Kinetics of olefin oxidation", Q. Rev. (London), **3**, 1-21, (1949).
12. L. Bateman, "Olefin oxidation", Q. Rev. (London), **8**, 147-167, (1954).
13. G. Scott (ed.), Chapter 4: "Antioxidants: Radical Chain-breaking Mechanisms", in Atmospheric Oxidation and Antioxidants, Elsevier Publishing Company, Amsterdam, (1965).
14. L. Reich and R.S.S. Stivala (eds.), in Autoxidation of Hydrocarbons and Polyolefins, Kinetics and Mechanisms, M. Dekker, New York, (1969).
15. W. L. Hawkins (ed.), in Polymer Stabilization, Wiley-Interscience, New York, (1972).
16. J. A. Howard, W.J. Schwalm and K.U. Ingold, "Absolute Rate Constants for Hydrocarbon Autoxidation" in Oxidation of Organic Compounds-I, Proceedings of the International Oxidation Symposium, San Francisco, California, 28 August-1 September 1967, Adv. Chem. Ser., R. F. Gould (ed.), **75**, pp. 6-23, American Chemical Society, USA, (1968).
17. J. A. Howard, K.U. Ingold and M.S. Symonds, "Absolute rate constants for hydrocarbon oxidation. VIII. The reactions of cumylperoxy radicals", Can. J. Chem., **46**, 1017-1022, (1968).

18. T. J. Henman, Chapter 2: "Controlled cross-linking and degradation", in Degradation and stabilisation of polyolefins, N. S. Allen (ed.), Applied Science Publishers, London, (1983).
19. The late H. Hinsken, S. Moss, J.-R. Pauquet and H. Zweifel, "Degradation of Polyolefins during Melt Processing", Polym. Deg. Stab., **34**, 279-293, (1991).
20. P. P. Klemchuk and P.-L. Horng, "Transformation Products of Hindered Phenolic Antioxidants and Colour Development in Polyolefins", Polym. Deg. Stab., **34**, 333-346, (1991).
21. G. Scott (ed.), Chapter 3: "Oxidation and stabilisation of polymers during processing", in Atmospheric Oxidation and Antioxidants-II, Elsevier Science Publishers, Amsterdam, (1993).
22. N. Grassie and G. Scott (eds.), in Polymer Degradation and Stabilisation, Cambridge University Press, Cambridge, (1985).
23. K. B. Chakraborty and G. Scott, "The effects of thermal processing on the thermal oxidative and photo-oxidative stability of low density polyethylene", Europ. Polym. J., **13**, 731-737, (1977).
24. S. Al-Malaika, "Reactive processing and polymer performance", Polym.-Plast. Technol. Eng., **29(1&2)**, 73-86, (1990).
25. W. O. Drake, J. R. Pauquet, R. V. Todesco and H. Zweifel, "Processing Stabilisation of Polyolefins", Angew. Makromol. Chem., **176/177**, 215-230, (1990).
26. A. Garton, D. J. Carlsson and D. M. Wiles, Chapter 4: "Photo-oxidation mechanisms in commercial polyolefins", in Developments in Polymer Photochemistry-1, N. S. Allen (ed.), Applied Science Publishers, London, (1980).
27. S. Al-Malaika, Chapter 19: "Effects of Antioxidants and Stabilizers", in Comprehensive Polymer Science, G. C. Eastmonds (ed.), Pergamon Press, **6**, 539-578, (1989).
28. D. J. Carlsson, A. Garton and D. M. Wiles, "Initiation of Polypropylene Photooxidation. 2. Potential Processes and Their Relevance to Stability", Macromolecules, **9 (5)**, 695-701, (1976).
29. D. J. Carlsson, A. Garton and D. M. Wiles, Chapter 7: "The photo-stabilisation of polyolefins", in Developments in Polymer Stabilisation-1, G. Scott (ed.), Applied Science Publishers, London, (1979).
30. J. M. Ginhac, J. L. Gardette, R. Arnaud and J. Lemaire, "Influence of Hydroperoxides on the Photothermal Oxidation of Polyethylene", Macromol. Chem., **182**, 1017-1025, (1981).
31. D. Vaillant, J. Lacoste and G. Dauphin, "The Oxidation Mechanism of Polypropylene: Contribution of ^{13}C -NMR Spectroscopy", Polym. Deg. Stab., **45**, 355-360, (1994).
32. P. Vink, Chapter 5: "The photo-oxidation of polyolefins-structural and morphological aspects", in reference 18.
33. G. Scott (ed.), Chapter 5: "Antioxidants: Preventive Mechanisms" in reference 13.
34. S. Al-Malaika and G. Scott, Chapter 7: "Photostabilisation of polyolefins", in reference 18.
35. T. J. Henman, Chapter 2: "Melt stabilisation of polypropylene", in reference 29.
36. G. Scott (ed.), Chapter 1: "Autoxidation and antioxidants: historical perspective", in Atmospheric Oxidation and Antioxidants-I, Elsevier Science Publishers, Amsterdam, (1993).

37. E. T. Denisov, Chapter 2: "Role of alkyl radical reactions in polymer oxidation and stabilisation", in Developments in Polymer Stabilisation-5, Applied Science Publishers, London, (1982).
38. G. Scott (ed.), Chapter 1: "Mechanisms of antioxidant action", in Developments in Polymer Stabilisation-4, Applied Science Publishers, London, (1981).
39. J. Pospíšil, Chapter 1: "Chain-breaking antioxidants in polymer stabilisation", in reference 29.
40. K. B. Chakraborty and G. Scott, "Mechanisms of antioxidant action: Synergism between antioxidants and 'U.V. absorbers' ", Europ. Polym. J., **13**, 1007-1013, (1977).
41. J. Pospíšil, Chapter 3: "Photooxidation reactions of phenolic antioxidants" in Developments in polymer photochemistry-2, N. S. Allen (Ed), Applied Science Publishers, London, (1981).
42. G. Scott (ed.), Chapter 9: "Synergism and antagonism" in Atmospheric Oxidation and Antioxidants-I, Elsevier Science Publishers, Amsterdam, (1993).
43. N. Grassie and G. Scott (eds.), Chapter 5: "Antioxidants and Stabilisers", in Polymer Degradation and Stabilisation., Cambridge University Press, Cambridge, (1985).
44. L. V. Samsonova, L. Taimr and J. Pospíšil: "Antioxidants and stabilisers", Angew. Makromol. Chem., **65** (967), 197-210, (1977).
45. H. J. M. Bartelink, J. Beulen, E. F. T. Duynstee and E. Konijnenberg, "Unstable intermediate in the oxidation of octadecyl 3-(3,5-di-tert-butyl-4-hydroxyphenyl) propanoate (Irganox 1076) ", Chem. Ind., **202-204**, (1980).
46. H. J. M. Bartelink, J. Beulen, G. Biolders, L. Cremers, E. F. J. Duynstee and E. Konijnenberg, "An oxidation product of octadecyl 3-(3,5-di-tert-butyl-4-hydroxybenzyl) propanoate (Irganox 1076)", Chem. Ind., **586-587**, (1978).
47. D. Dilettato, P. J. Arpino, K. Nguyen and A. Bruchet, "Investigation of Low Mass Oligomers and Polymer Additives from Plastics. Part II: Application to polyolefin Soxhlet Extracts", J. High Resolution Chromatogr., **14**, 335-341, (1991).
48. D. W. Allen, M. R. Clench, A. Crowson and D. A. Leathard, "Characterisation of solvent-extractable transformation products of high molecular weight hindered phenols in polypropylene subjected to ionising radiation in air or thermal ageing", Polym. Deg. Stab., **39**, 293-297, (1993).
49. D. W. Allen, M. R. Clench, A. Crowson, D. A. Leathard and R. Saklatvala, "Characterisation of electron beam generated transformation products of Irganox 1010 by particle beam liquid chromatography-mass spectrometry with on-line diode array detection", J. Chromatogr. A., **679**, 285-297, (1994).
50. J. Scheirs, J. Pospíšil, N. J. O'Connor and S. W. Bigger, "Characterisation of conversion products formed during the degradation of processing antioxidants", ACS-book, (1993).
51. E. F. J. Duynstee, "Transformation of antioxidants in polyolefin systems", Proc. 6th International Conference on advances in controlled degradation of polymers, Luzern, 1-4, (1984).
52. F. Gugumus, "Aspects of the stabilization mechanisms of phenolic antioxidants in polyolefins", Angew. Makromol. Chem., **137**, 189-225, (1985).
53. J. D. Vargo and K. L. Olson, "Characterisation of additives in plastics by liquid chromatography-mass spectrometry", J. chromatogr., **353**, 215-224, (1986).

54. J. Lerchova, C. A. Nikiforov and J. Pospíšil, "Antioxidants and stabilisers .LX. Transformations of octadecyl 3-(3,5-di-tert-butyl-4-hydroxyphenyl) propanoate and properties of products", J. Polym. Sci., Polym. Symp., **57**, 249-253, (1976).
55. K. Schwetlick, Chapter 2: "Mechanisms of Antioxidant Action of Phosphite and Phosphonite Esters" in Mechanisms of Polymer Degradation and Stabilisation, Applied Science Publishers London, (1990).
56. K. Schwetlick, T. König, C. Rüger, J. Pionteck and W. D. Habicher, "Chain-breaking Antioxidant activity of phosphite esters", Polym. Deg. Stab., **15**, 97-108, (1986).
57. K. Schwetlick, C. Rüger and R. Noack, "Kinetik und Mechanismus der Zersetzung von Alkylhydroperoxiden durch o-phenylen-phosphite und-phosphate", J. Prakt. Chem., **324** (5), 697-705, (1982).
58. C. Rüger, T. König and K. Schwetlick, "Kinetik und Mechanismus der Cumylhydroperoxidzersetzung durch cyclische Phosphite", J. Prakt. Chem., **326**(4), 622-632, (1984).
59. C. Neri, S. Costanzi, R. M. Riva, R. Farris and R. Colombo, "Mechanism of action of phosphites in polyolefin stabilisation", Polym. Deg. Stab., **49**, 65-69, (1995).
60. W. C. Ray and K. Isenhardt, "Phosphites in polyolefin process stabilisation", Polym. Eng. Sci., **15**(10), 703-704, (1975).
61. T. R. Crompton, in Additive migration from plastics into food., Pergamon press, Oxford, (1979).
62. The Council of the European Communities, Directive 82/711/EEC, No L 297/26-L297-30, 23.10.82.
63. The Commission of the European Communities, Official Journal of European Communities, Directive 93/181/EEC, No L90/22-L90/25, 14.4.93.
64. G. Scott(ed.), Chapter 5: "Macromolecular and polymer bound antioxidants", in Atmospheric Oxidation and Antioxidants-II, Elsevier Science Publishers, Amsterdam, (1993).
65. G. W. Burton and K. U. Ingold, "Vitamin E: Application of the Principles of Physical Organic Chemistry to the Exploration of Structure and Function", Acc. Chem. Res., **19**, 194-201, (1986).
66. E. Niki, Y. Yamamoto, M. Takahashi, E. Komuro and Y. Miyama, "Inhibition of Oxidation of Biomembranes by Tocopherol", Ann. N. Y. Acad. Sci., **570**, 23-31, (1989).
67. J. L. G. Nilsson, G. D. Daves Jr and K. Folkers, "New Tocopherol Dimers", Acta. Chem. Scand., **22** (1), 200-206, (1968).
68. P. Schudel, H. Mayer, J. Metzger, R. Ruegg and O. Isler, "Über die Chemie des Vitamin E. Die Synthese von rac-all-trans- α -und- β -Tocopherol", Helv. Chim. Acta., **XLVI**(VII), 2517-1526, (1963).
69. M. Vecchi, W. Walther, E. Glinz, T. Netscher, R. Schmid, M. Lalonde and W. Vetter, "79. Chromatographische Trennung und quantitative Bestimmung aller acht Stereoisomeren von α -Tocopherol", **73**, 782-789, (1990).
70. V. L. Frampton, W. A. Skinner, P. Cambour and P. S. Bailey, " α -Tocopurple, an Oxidation Product of α -Tocopherol", J. Am. Chem. Soc., **82**, 4632-4634, (1960).
71. G. W. Burton, D. O. Foster, B. Perly, T. F. Slater, I. C. P. Smith and K. U. Ingold, "Biological Antioxidants", Phil. Trans. R. Soc. Lond., **B311**, 565-578, (1985).

72. G. W. Burton, Y. LePage, E. J. Gabe and K. U. Ingold, "Antioxidant Activity of Vitamin E and Related Phenols. Importance of Stereoelectronic Factors", J. Am. Chem. Soc., **102**, 7791-7792, (1980).
73. G. W. Burton, T. Doba, E. J. Gabe, L. Hughes, F. L. Lee, L. Prasad and K. U. Ingold, "Autoxidation of Biological Molecules.4. Maximising the Antioxidant Activity of Phenols", J. Am. Chem. Soc., **107**, 7053-7065, (1985).
74. G. W. Burton and K. U. Ingold, "Vitamin E as an '*in Vitro*' and '*in Vivo*' Antioxidant", Ann. N. Y. Acad. Sci., **570**, 7-22, (1989).
75. E. Niki, J. Tsuchiya, Y. Yoshikawa, Y. Yamamoto and Y. Kamiya, "Oxidation of lipids. XIII. Antioxidant Activities of α -, β -, γ and δ -Tocopherols", Bull. Chem. Soc. Jpn., **59**, 497-501, (1986).
76. K. Mukai, S. Yokoyama, K. Fukuda and Y. Uemoto, "Kinetic Studies of Antioxidant Activity of new Tocopherol Model Compounds in Solution", Bull. Chem. Soc. Jpn., **60**, 2163-2167, (1987).
77. K. Mukai, K. Fukuda and Ishizu "Stopped-flow investigation of antioxidant activity of tocopherols. Finding of new tocopherol derivatives having higher antioxidant activity than α -tocopherol", Chem. Phys. Lipids, **46**, 31-36, (1988).
78. K. Mukai, K. Okabe and H. Hosose, "Synthesis and Stopped-Flow Investigation of Antioxidant Activity of Tocopherols. Finding of New Tocopherol Derivatives Having the Highest Antioxidant Activity among Phenolic Antioxidants", J. Org. Chem., **54**, 557-560, (1989).
79. L. R. C. Barclay, M. R. Vinqvist, K. Mukai, S. Itoh and H. Morimoto, "Chain-Breaking Phenolic Antioxidants : Steric and Electronic Effects in Polyalkyl Chromanols, Tocopherol Analogs, Hydroquinones and Superior Antioxidants of the Polyalkylbenzochromanol and Naphthofuran Class", J. Org. Chem., **58**, 7416-7420, (1993).
80. D. C. Liebler, J. A. Burr, S. Matsumoto and M. Matsuo, "Reactions of the Vitamin E Model Compound 2,2,5,7,8-Pentamethylchroman-6-ol with Peroxyl Radicals", Chem. Res. Toxicol., **6**, 351-355, (1993).
81. R. Yamauchi, K. Kato and Y. Ueno, "Formation of Trimers of α -Tocopherol and its Model Compound, 2,2,5,7,8-Pentamethylchroman-6-ol, in Autoxidising Methyl Linoleate", Lipids, **23**(8), 779-783, (1988).
82. M. Fujimaki, K. Kanamaru, T. Kurata and O. Igarashi, "Studies on the oxidation mechanism of Vitamin E. Part I. The Oxidation of 2,2,5,7,8-Pentamethyl-6-hydroxychroman", Agr. Biol. Chem., **34** (12), 1781-1786, (1970).
83. E. I. Zakharova, K. A.-V. Shuaipov, V. V. Chudinova, S. M. Alekseev and R. P. Evstigneeva, "Products of the transformation of vitamin E and its analogue chroman C1 in oxidizing ethyl linoleate", Bioorg. Khim., **18**(7), 543-551, (1992).
84. W. A. Skinner and P. Alaupovic, "Oxidation Products of Vitamin E and its model, 6-Hydroxy-2,2,5,7,8-pentamethylchroman. V. Studies of the Products of Alkaline Ferricyanide Oxidation", J. Org. Chem., **28**, 2854-2858, (1963).
85. J. L. G. Nilsson and H. Sievertsson, "Interconversion of α -tocopherol and its oxidation products", Acta. Pharm. Suecica, **5**, 517-524, (1968).
86. K. Mukai, N. Tsuzuki, S. Ouchi and K. Fukuzawa, "Electron spin resonance studies of chromanoxyl radicals derived from tocopherols", Chem. Phys. Lipids, **30**, 337-345, (1982).
87. M. Matsuo and S. Matsumoto, "Electron Spin Resonance Spectra of the Chromanoxyl Radicals Derived from Tocopherols (Vitamin E) and Their Related Compounds", Lipids, **18**(1), 81-86, (1983).

88. V. L. Frampton, W. A. Skinner Jr and P. S. Bailey, "The Production of Tocored upon the Oxidation of dl- α -Tocopherol with Ferric Chloride", J. Am. Chem. Soc., **76**, 282-284, (1954).
89. V. L. Frampton, W. A. Skinner, P. Cambour and P. S. Bailey, " α -Tocopurple, an oxidation product of α -Tocopherol" J. Am. Chem. Soc., **82**, 4632-4634, (1960).
90. F. Dallacker, R. Eisbach and M. Holschbach, "Darstellung und Reaktionen von all-rac-5-Formyl- γ -tocopherol", Chemiker-Zeitung, **115**(4), 113-115, (1991).
91. C. Suarna, M. Baca, D. C. Craig, M. Scudder and P. T. Southwell-keeley, "Further Oxidation Products of 2,2,5,7,8-Pentamethyl-6-chromanol, Lipids, **26**(10), 847-852, (1991).
92. I. Kohar, C. Suarna and P. T. Southwell-keely, "Oxidation of the α -Tocopherol Model Compound 2,2,5,7,8-Pentamethyl-6-chromanol, Formation of 2,2,7,8-Pentamethyl-5,6-dione" Lipids, **28**(11), 1015-1020, (1993).
93. W. A. Skinner and R. M. Parkhurst, "Oxidation Products of Vitamin E and Its Model, 7-Hydroxy-2,2,5,7,8-Pentamethylchroman. VIII. Oxidation with Benzoyl Peroxide", J. Org. Chem., **31**, 1248-1251, (1966).
94. W. L. Porter, L. A. Levasseur and A. S. Henick, "An Addition Compound of Oxidised Tocopherol and Linoleic Acid", Lipids, **6** (1), 1-8, (1971).
95. Ishikawa and E. Yuki, "Reaction Products from Various Tocopherols with Trimethylamine Oxide and Their Antioxidant Activities", Agr. Biol. Chem., **39**(4), 851-857, (1975).
96. W. A. Skinner "Vitamin E Oxidation with free radical inhibitors Azobis-isobutyronitrile", Biochem. and Biophys. Res. Comm., **15**(5), 469-472, (1964).
97. R. Yamauchi, T. Matsui, Y. Satake, K. Kato and Y. Ueno, "Reaction Products of α -Tocopherol with a free Radical Initiator, 2,2'-Azobis-(2,4-dimethylvaleronitrile)", Lipids, **24**(3), 204-209, (1989).
98. R. Yamauchi, N. Miyake, K. Kato and Y. Uemo, "Reaction of α -Tocopherol with Alkyl and Alkylperoxyl Radicals of Methyl Linoleate", Lipids, **28**(3), 201-206, (1993).
99. J. Winterle, D. Dubin and T. Mill, "Products and Stoichiometry of Reaction of Vitamin E with alkylperoxy radicals" J. Org. Chem., **49**, 491-495, (1984).
100. D. R. Nelan and C. D. Robeson, "The Oxidation Product from α -Tocopherol and Potassium Ferricyanide and its Reaction with Ascorbic and Hydrochloric Acids", J. Am. Chem. Soc., **84**, 2963-2965, (1962).
101. T. R. Crompton, in Chemical Analysis of Additives in Plastics (2nd edn.), International series of monographs in analytical chemistry, Pergamon Press, Oxford, (1977).
102. Y. Ishikawa, "Yellow Reaction Products from Tocopherols and Trimethylamine Oxide", Agr. Biol. Chem., **38** (12), 2545-2547, (1974).
103. J. Lacoste, D. Vaillant and S. Chmela, "Gamma-, photo- and thermally-initiated oxidation of polyolefins used in packaging", J. Polym. Eng., **15**(1-2), 139-152, (1995/1996)
104. T. Gottstein and W. Grosch, "Model Study of Different Antioxidant Properties of α - and γ -Tocopherol in Fats", Fat. Sci. Technol., **92**(4), 139-144, (1990).
105. Y. L. Ha and A. S. Csallany, "Separation of α -Tocopherol and its Oxidation Products by High Performance Liquid Chromatography", Lipids, **23**(4), 359-361, (1988).

106. H. M. Fales, H. A. Lloyd, J. A. Ferretti and J. V. Silverton, "Optical Resolution of the α -Tocopherol Spirodimer and Demonstration of its Fluxional Nature", J. Chem. Soc. Perkin. Trans., **2**, 1005-1010, (1990).
107. M. Baca, C. Suarne and P. T. Southwell-keeley, "Seperation of the α -Tocopherol Model compound 2,2,5,7,8-pentamethyl-6-chroman from its oxidation products by high performance liquid chromatography" J. Liq. Chromatogr., **14 (10)**, 1957-1966, (1991).
108. R. Yamauchi, T. Matsui, K. Kato and Y. Ueno, "Reaction of α -Tocopherol with 2,2'-Azobis(2,4-dimethylvaleronitrile) Benzene", Agr. Biol. Chem., **53(12)**, 3257-3262, (1989).
109. C. Suarne and P. T. Southwell-Keely, "New Oxidation Products of α -Tocopherol", Lipids, **23(2)**, 137-139, (1988).
110. S. B. Cavitt, H. Sarrafizadeh and P. D. Gardner, "The Structure of o-Quinone Methide Trimer", J. Org. Chem., **27**, 1211-1216, (1962).
111. I. Kohar, M. Baca, C. Suarna, R. Stocker and P. T. Southwell-keely, "Is α -tocopherol a reservoir for α -tocopherolhydroquinone?", Free. Radic. Biol. Med., **19(2)**, 197-207, (1995).

APPENDIX

PUBLISHED WORK

- SI-1:** S. Al-Malaika, H. Ashley and S. Issenhuth, "The Antioxidant Role of α -Tocopherol in Polymers. I. The Nature of Transformation Products of α -Tocopherol Formed during Melt Processing of LDPE", J. Pol. Sci. A, **32**, 3099-3113, (1994)
- SI-2:** S. Al-Malaika and S. Issenhuth, "Processing Effects on Antioxidant Transformation and Solutions to the Problem of Antioxidant Migration" in Polymer Durability-Degradation, Stabilization and Life Time Prediction , R. L. Clough, N. C. Billingham and K. T. Gillen (Eds.), Adv. Chem. Ser., **249**, 425-439, American Chemical Society, (1996)

Page removed for copyright restrictions.